

Dorso-ventral Differentiation and Specification of Mesencephalon in Early Chick Embryos

Dissertation zur Erlangung des
naturwissenschaftlichen Doktorgrades
der Bayerischen Julius-Maximilians-Universität Würzburg

vorgelegt von

Naixin Li

aus Tianjin, V. R. China

Würzburg, 2007

Eingereicht am:14. June 2007

Mitglieder der Promotionskommission:

Vorsitzender:Prof. Dr. Martin Müller

Gutachter: Prof. Dr. Martin Heisenberg

Gutachter: Dr. Andrea Wizenmann

Tag des Promotionskolloquiums:

Doktorurkunde ausgehändigt am:

To My Parents

Table of Contents

| | |
|--|-----------|
| Introduction | 1 |
| Early development of chick central nervous system..... | 1 |
| The formation of the neural tube..... | 1 |
| The differentiation of the neural tube..... | 2 |
| The development of the three embryonic axes..... | 3 |
| Regionalization of the developing CNS..... | 5 |
| Neuronal migration during neurogenesis..... | 7 |
| Dorso-ventral patterning of the central nervous system..... | 8 |
| Determining dorso-ventral cell types in the spinal cord..... | 8 |
| The paired-box transcription factor Pax7..... | 11 |
| Shh in the development of central nervous system..... | 13 |
| A small GTP-binding protein Rab23..... | 15 |
| Methods of gene repression in chick embryos..... | 16 |
| RNA interference..... | 16 |
| Morpholino oligonucleotides..... | 19 |
| Why still working with chick embryos?..... | 20 |
| Aim of the project..... | 21 |
| Materials | 23 |
| Avian embryos..... | 23 |
| Bacterial Strains..... | 23 |
| Clones..... | 24 |
| Plasmids..... | 25 |
| Morpholinos..... | 26 |
| Oligonucleotides..... | 27 |
| Size Standard..... | 28 |
| Enzymes..... | 29 |
| Fluorescent Probes..... | 30 |
| Chemicals..... | 30 |
| Reagents..... | 30 |
| Solutions, Media and Buffers..... | 32 |
| Kits..... | 35 |
| Antibodies..... | 35 |
| Antibodies for Immunohistochemistry..... | 35 |
| Antibodies for RNA <i>in situ</i> hybridisation..... | 36 |
| Genes for RNA probes..... | 36 |
| Apparatus and Instruments..... | 37 |
| Softwares and Websites..... | 38 |

Methods **39**

| | |
|--|----|
| 1. Embryo and tissue preparations..... | 39 |
| 1.1. <i>in vivo</i> manipulations..... | 39 |
| Transplantation..... | 39 |
| <i>In ovo</i> electroporation..... | 41 |
| 1.2. <i>in vitro</i> manipulations..... | 43 |
| Co-culture..... | 43 |
| <i>in vitro</i> aggregation assay..... | 43 |
| 2. Molecular Techniques..... | 44 |
| 2.1. Isolation and determination of plasmid DNA..... | 44 |
| Mini preparation of plasmid DNA..... | 44 |
| Midi/Maxi preparation of plasmid DNA..... | 44 |
| Endotoxin-free plasmid extraction..... | 45 |
| DNA concentration..... | 45 |
| Agarose gel electrophoresis..... | 45 |
| Gel extraction of DNA..... | 45 |
| DNA quantitation..... | 45 |
| 2.2. Isolation and cloning of embryogenetic genes & fragments..... | 46 |
| Isolation of total RNA..... | 46 |
| RT-PCR..... | 46 |
| Polymerase chain reaction..... | 47 |
| Restrictive digestion..... | 48 |
| Dephosphorylation of linearized plasmid DNA..... | 48 |
| Ligation..... | 49 |
| Preparation of competent cells..... | 49 |
| Transformation..... | 49 |
| Selection of colonies..... | 50 |
| Bacterial culture..... | 50 |
| Glycerol stocks..... | 50 |
| DNA sequencing..... | 50 |
| 2.3. <i>In vitro</i> transcription..... | 51 |
| Linearisation of the plasmid..... | 51 |
| Phenol/chloroform extraction..... | 51 |
| DNA precipitation..... | 51 |
| Synthesis of RNA-labelled probes..... | 51 |
| RNA precipitation..... | 52 |
| 3. Histological examinations..... | 52 |
| Dissection, fixation and mounting..... | 52 |
| Whole-mount immunostaining..... | 52 |
| Whole-mount RNA <i>in situ</i> hybridization..... | 54 |
| Vibratome section..... | 55 |
| Cresyl violet staining..... | 55 |
| Hematoxylin and eosin staining..... | 56 |

Results & Discussions **57**

Part I: DV Specification of Chick Midbrain **59**

| | |
|--|----|
| 1. Expression patterns of Pax3/7, nkx6.1 and neural differentiation in the mesencephalon..... | 59 |
| 2. DV Polarity-reversed transplantation..... | 62 |
| Homochronic grafts..... | 62 |
| Heterochronic grafts..... | 68 |
| 3. Influence of floor plate and roof plate on the expression of ventral and dorsal specific genes..... | 70 |
| 4. Adhesion between ventral and dorsal midbrain cells..... | 72 |
| 5. Long-term transplantation..... | 74 |
| 6. Discussion..... | 76 |
| Identity and autonomy along the DV axis..... | 76 |
| Cell adhesion as a mechanism or read-out of DV regionalization..... | 78 |
| Progenitor dispersal..... | 79 |
| Regionalisation as a feature of DV patterning in large structures..... | 79 |

Part II: Function of Pax7 on Midbrain Expansion **81**

| | |
|---|-----|
| 1. Isolation and subcloning of chick <i>Pax7</i> cDNA..... | 81 |
| 2. Influence of Pax7 on the size of mesencephalon..... | 84 |
| Overexpression of Pax7 in dorsal midbrain..... | 84 |
| Misexpression of Pax7 in ventral midbrain..... | 84 |
| Repression of Pax7 in dorsal midbrain..... | 88 |
| 3. Pax7 promotes the neural proliferation in the midbrain..... | 91 |
| Dividing precursor cells in the neural tube..... | 91 |
| More dividing cells by Pax7 overexpression..... | 91 |
| No effect on cell death..... | 94 |
| 4. Analysis of Pax7 on the neural differentiation and specification..... | 95 |
| Neural differentiation normally..... | 95 |
| Induction of Brn3a positive cells but not Isl-1 cells..... | 96 |
| 5. Pax7 - induced Pax3 co-localizes with Nkx6.1..... | 99 |
| 6. Discussion..... | 102 |
| Pax7 is involved in the neuronal proliferation..... | 102 |
| A role of Pax7 on the specification of some dorsal neuronal lineages..... | 104 |
| Cross-regulation between Pax3 and Pax7..... | 106 |
| Pax3/7 action on rapid expansion of the mesencephalon..... | 107 |

Part III: Expression and Function of Rab23 in Chick Nervous System 111

| | |
|--|-----|
| 1. Expression pattern of <i>Rab23</i> in chick embryos..... | 111 |
| Preparation of antisense RNA probes for chick <i>Rab23</i> | 111 |
| <i>Rab23</i> expression early in chick embryos..... | 112 |
| A transient <i>Rab23</i> expression in the notochord at early stages..... | 113 |
| Expression pattern of <i>Rab23</i> in the neural tube..... | 113 |
| 2. Identification and analysis of chick <i>Rab23</i> gene..... | 118 |
| Identification of chick <i>Rab23</i> cDNA..... | 118 |
| Sequential analysis of chick <i>Rab23</i> protein..... | 119 |
| Phylogenetic analysis of <i>Rab23</i> proteins..... | 122 |
| 3. Subcloning and ectopic expression of chick <i>Rab23</i> gene..... | 123 |
| Construction of <i>Rab23</i> expression plasmid..... | 123 |
| Ectopic expression of <i>Rab23</i> <i>in vivo</i> | 123 |
| 4. <i>Rab23</i> specifies dorsal regional identity in early neural tube..... | 126 |
| Induction of dorsal specific genes <i>Pax3/7</i> | 126 |
| No effect on ventral specific gene <i>Nkx6.1</i> | 127 |
| 5. Influence of <i>Rab23</i> on early neurogenesis in dorsal midbrain..... | 131 |
| No obvious effect on the dorsal Islet 1/2 cell subpopulation..... | 131 |
| Specification of <i>Brn3a</i> expressing cells..... | 132 |
| Differentiation of early midbrain neurons normally..... | 134 |
| 6. Analysis of <i>Rab23</i> on neural proliferation..... | 136 |
| 7. Preliminary analysis of <i>Rab23</i> with <i>Shh</i> signalling pathway..... | 138 |
| Expression patterns of <i>Shh</i> and its downstream genes in the mesencephalon..... | 138 |
| Analysis of gene expression in <i>Rab23</i> –transfected midbrains..... | 139 |
| 8. Discussion..... | 142 |
| The tissue - and region - specific expression pattern of <i>Rab23</i> | 142 |
| Asymmetric expression of <i>Rab23</i> and the left-right determination of chick embryo..... | 144 |
| The intracellular vesicular trafficking of <i>Rab23</i> | 145 |
| <i>Rab23</i> is served to establish the dorsal polarity..... | 147 |
| Contribution to the roof plate formation..... | 148 |
| <i>Shh</i> signalling and <i>Rab23</i> | 149 |

Part IV: RNA Interference in Chick Embryos 151

| | |
|---|-----|
| 1. Long-hairpin dsRNA (lhRNA) experiments..... | 151 |
| Preparation of lhRNA constructs for chick <i>Pax7</i> gene..... | 151 |
| Morphological changes of the transfected midbrains..... | 152 |
| Gene expression was reduced in the transfected cells..... | 157 |
| Analysis of other gene expressions..... | 157 |

| | |
|--|----------------|
| 2. Short-hairpin siRNA (shRNA) experiments..... | 160 |
| Preparation of shRNA – Pax7 constructs..... | 160 |
| Transfection of pMES-based shRNA – Pax7 constructs..... | 161 |
| Transfection of p <i>Silencer</i> 1.0-U6 - based shRNA–Pax7 constructs | 167 |
| 3. Antisense DNA oligonucleotides experiment..... | 171 |
| 4. Morpholino oligonucleotides experiment..... | 173 |
| 5. Discussion..... | 175 |
| Gene repression by plasmid-based dsRNA in chick embryos..... | 175 |
| Length of the hairpins..... | 176 |
| A local and temporal gene silencing available for embryogenesis.. | 177 |
| Delivery of dsRNA..... | 178 |
| Antisense-based approaches for gene silencing in chick embryos... | 179 |
| Summary | 181 |
| Zusammenfassung | 183 |
| Literatures | 185 |
| Appendix | 223 |
| A. pMES vector..... | 223 |
| B. pBluescript [®] II KS (+/-) phagemid vector..... | 224 |
| C. pCR [®] 4-TOPO [®] vector..... | 225 |
| D. p <i>Silencer</i> [™] 1.0-U6 siRNA expression vector..... | 226 |
| E. Chick Rab23 cDNA and protein sequence..... | 227 |
| F. Curriculum Vitae..... | 228 |
| G. Publication..... | 229 |
| H. Acknowledgements..... | 230 |

Abbreviations

| | |
|--------------|--|
| <i>Ago2</i> | <i>Argonaute</i> gene |
| AP | anterioposterior |
| APPL | adaptor protein containing PH domain, PTB domain, and Leucine zipper motif 1/2 |
| AS | 2', 5' - oligoadenylate synthetase |
| asRNA | anti-sense RNA |
| bHLH | basic Helix-Loop-Helix |
| bMN | branchial Motor Neuron |
| BMP | Bone Morphogenetic Proteins |
| ccdB | coupled cell division |
| CDK5 | cyclin-dependent kinase |
| cDNA | copy DNA |
| CDS | coding sequence |
| Ci | Cubitus interruptus |
| CK1 α | casein kinase |
| CLSM | Confocal Laser Scanning Microscope |
| CMV-IE | huamn <i>cytomegalovirus</i> immediate early enhancer |
| CNS | central nervous system |
| Cos2 | Costal2 |
| CRD | cystein rich domain |
| Dbx1 | developing brain homeobox transcription factor |
| DCX | doublecortin gene |
| DHH | Dessert hedgehog |
| DE | diencephalons |
| dI | dorsal Interneuron |
| DICER | DNA-independent RNA polymerase |
| <i>Dlx1</i> | <i>Distal-less</i> gene |
| Dpp | Decapentaplegic |
| dsRBD | dsRNA-binding domain |
| dsRNAs | double-stranded RNAs |
| DV | dorsoventral |
| EC | embryonal carcinoma cells |
| ECM | extracellular matrix |
| EGFP | enhanced green fluorescent protein |

| | |
|-------------------|--|
| EGL | external germinal layer |
| <i>En1</i> | <i>Engrailed</i> gene |
| EPEI | ethoxylate polyethylenimine |
| ER | endoplasmic reticulum |
| ES | embryonic stem cells |
| EST | expressed sequence tag |
| FGF | Fibroblast growth factor |
| <i>FKHR</i> | <i>Forkhead-related</i> gene |
| FMRP | the fragile X mental retardation protein |
| <i>FoxA</i> | <i>Forkhead box</i> gene |
| FP | floor plate |
| Fu | the kinase Fused |
| GAP | GTPase-activating protein |
| GDF | growth and differentiation factors |
| GDI | guanine dissociation inhibitor |
| GEF | GDP/GTP exchange factor |
| GFP | green fluorescent protein |
| Gli3 | Glioma-associated oncogene |
| GTP | granosine triphosphate |
| GSK-3 β | Glycogen Synthase Kinase |
| GTPase | guanosine triphosphatase |
| GZ | germinative zone |
| HB9 | homeobox 9 protein |
| HD | homoedomain |
| HH | Hamburger and Hamilton |
| Hip | Hedgehog -interacting protein |
| HNF3 β | Hepatocyte nuclear factor |
| HSPG | Heparin sulfate proteoglycan |
| HTH | helix-turn-helix motif |
| IFN | interferon |
| IFT | intraflagellar transport protein |
| IHH | India hedgehog |
| Irx3 | iroquois homeodomain protein |
| KHCs | kinesin heavy chains |
| KIFs | kinesin superfamily proteins |
| <i>Krox20, 24</i> | Krüppel box genes, <i>egr1/2</i> (early growth response genes) |
| LIM | an acronym derived from 3 genes, <i>lin-11</i> , <i>isl-1</i> and <i>mec-3</i> |
| LIS1 | lissencephaly gene |
| LPM | lateral plate mesoderm |
| INC | interstitial nucleus of Cajal |
| IRES | internal ribosome entry site |
| ISH | <i>in situ</i> hybridization |
| <i>Isl-1/2</i> | Islet genes |
| Kifs | Kinesin family members |
| KS | Koller's sickle |
| lhRNA | long hairpin dsRNA |
| LLF | lateral longitudinal fascicle |
| LNA | locked nucleic acid |
| LR | left-right |
| MCS | multiple cloning site |
| ME | mesencephalon |

| | |
|-------------|--|
| MGE | medial ganglionic eminence |
| MHP | neural hinge point |
| MI | mitotic index |
| miRNAs | microRNAs |
| MLF | medial longitudinal fascicle |
| MNR2 | motor neuron restricted 2 protein |
| mRNA | messenger RNA |
| MHB | midbrain-hindbrain boundary |
| MO | morpholino oligonucleotides |
| MTN | mesencephalic trigeminal neuron |
| Ngn1/2 | neurogenin genes |
| Nkx2.2 | Homeobox protein NK-2 homolog B |
| NPC1 | Niemann-Pick C1 protein |
| NPCs | neural precursor (progenitor) cells |
| NSCs | neural stem cells |
| NTDs | neural tube defects |
| OLP | oligodendrocyte precursor |
| <i>opb</i> | <i>open brain</i> gene |
| ORF | open reading frame |
| Pax3/6/7 | pair-box domain proteins |
| PAZ | named after 3 proteins, Piwi, Argonaute and Zwillig |
| PBS | phosphate buffered saline |
| PCD | programmed cell death |
| <i>Pcl2</i> | <i>Polycomblike 2</i> gene |
| PCR | polymerase chain reaction |
| PD | paired domain |
| PDR | Parkinson's Disease Related |
| PEF | pulsed electric field |
| PFA | paraformaldehyde |
| pH3 | phosphorylated Histone 3 |
| PKA | Protein Kinase A |
| PKR | dsRNA-dependent protein kinase |
| PMZ | posterior marginal zone |
| PNA | peptide nucleic acid |
| POU | Pit-Oct-Unc homeodomain |
| PPD | PAZ-Piwi domain |
| PSM | presomitic mesoderm |
| Ptc1/2 | Patched proteins |
| PTGS | post-transcriptional gene silencing |
| RA | Retinoic acid |
| Rab | <i>Ras</i> -like gene in rat brain |
| Rb | Retinoblastoma gene |
| RdRP | RNA-dependent RNA polymerase |
| RE | rhombencephalon |
| REP1 | Rab escort protein 1 |
| RISC | RNA-induced silencing complex |
| RITS | RNA-induced initiation of transcriptional gene silencing |
| RNAi | RNA interference |
| RNAPs | RNA Polymerases |
| RP | roof plate |
| RT | room temperature |

Abbreviations

| | |
|-------------|---|
| SC | spinal cord |
| S-DNAs | phosphorothioate DNA oligonucleotides |
| SH2/3 | Src- homology domains |
| Shh | Sonic Hedgehog |
| shRNA | short hairpin siRNA |
| siRNAs | small interfering RNAs |
| siRNP | siRNA-protein complex |
| SMART | Simple Modular Architecture Research Tool |
| sMN | somatic Motor Neurons |
| Smo | Smoothed protein |
| SNARE | soluble NSF-attachment protein receptor |
| SSD | sterol-sensing domain |
| stRNA | small temporal RNA |
| SuFu | suppressor of Fused |
| TD | transactivation domain |
| TE | telencephalon |
| TGF β | Transforming Growth Factor |
| UTR | untranslated region |
| <i>VIG</i> | Vasa intronic gene |
| VZ | ventricular zone |
| <i>Wg</i> | Wingless |
| WNT | wingless (<i>Drosophila</i>) and int-1 (mouse) gene |
| ZPA | zone of polarizing activity |

List of Figures

| | | |
|---------|--|----|
| Fig. 1 | Primary neurulation in chick embryo..... | 2 |
| Fig. 2 | Early gastrulation of chick embryo..... | 3 |
| Fig. 3 | The signal pathway for left-right asymmetry in chick embryo..... | 4 |
| Fig. 4 | Establishment and strategies of compartments in CNS..... | 6 |
| Fig. 5 | Neuronal migratory pathways in mammalian neocortex..... | 8 |
| Fig. 6 | Combinatorial codes of transcription factors for the specification of dorsal cell types in neural tube..... | 9 |
| Fig. 7 | Regulation of Sonic hedgehog on combinatorial expression of transcription factors in ventral neural progenitors..... | 10 |
| Fig. 8 | The structure of a Pax protein..... | 11 |
| Fig. 9 | Autoprocessing reaction of Shh..... | 13 |
| Fig. 10 | The signal transduction pathway of Shh..... | 14 |
| Fig. 11 | The expression of neural markers in <i>opb</i> mutants..... | 15 |
| Fig. 12 | The mechanism of RNA interference..... | 18 |
| Fig. 13 | Inhibition of morpholino oligonucleotides on gene function..... | 19 |
| Fig. 14 | The diagram of chick midbrain transplantation..... | 40 |
| Fig. 15 | Identification of quail cells..... | 41 |
| Fig. 16 | <i>In ovo</i> electroporation in chick midbrain..... | 42 |
| Fig. 17 | Classification of aggregates..... | 44 |
| Fig. 18 | Cresyl violet staining and H & E staining..... | 56 |

| | | |
|---------|---|-----|
| Fig. 19 | Expression patterns of <i>Pax3</i> and <i>Nkx6.1</i> in the midbrain..... | 60 |
| Fig. 20 | <i>Pax7</i> expression and neuronal differentiation in the midbrain..... | 61 |
| Fig. 21 | Protein expression of ventral ectopic midbrain grafts..... | 63 |
| Fig. 22 | Gene expression of ectopic midbrain grafts..... | 64 |
| Fig. 23 | Protein expression of dorsal ectopic midbrain grafts..... | 65 |
| Fig. 24 | Quantitative analysis on the expression of ectopic midbrain grafts | 66 |
| Fig. 25 | Gene expression of heterotopic ventral midbrain grafts..... | 67 |
| Fig. 26 | Heterochronic and homochronic midbrain grafts..... | 69 |
| Fig. 27 | Explant cultures of ventral and dorsal midbrain with and without signaling centers..... | 71 |
| Fig. 28 | Fluorescence photomicrographs of aggregates formed by ventral and dorsal midbrain cells..... | 73 |
| Fig. 29 | Protein expression of long-term quail grafts..... | 75 |
| Fig. 30 | Electrophoretic analysis of chick <i>Pax7</i> expression plasmids..... | 82 |
| Fig. 31 | Sequence and structural organization of chick <i>Pax7</i> cDNA..... | 83 |
| Fig. 32 | Morphological change of a <i>Pax7</i> over-expressing midbrain..... | 85 |
| Fig. 33 | Ectopic expression of <i>Pax7</i> in dorsal midbrains..... | 86 |
| Fig. 34 | Ectopic expression of <i>Pax7</i> in ventral midbrains..... | 87 |
| Fig. 35 | Morphological change of <i>Pax7</i> repressed midbrains..... | 89 |
| Fig. 36 | A series of continuous sections of a <i>Pax7</i> repressed midbrain..... | 90 |
| Fig. 37 | Mitotic cells in the developing neural tube..... | 92 |
| Fig. 38 | Mitotic cells in the <i>Pax7</i> -transfected midbrain..... | 93 |
| Fig. 39 | SYTOX staining of a dead cell in the midbrain..... | 94 |
| Fig. 40 | Neuronal differentiation in the <i>Pax7</i> -transfected midbrain..... | 95 |
| Fig. 41 | <i>Isl-1</i> and <i>Brn3a</i> positive cells in the midbrain and spinal cord..... | 97 |
| Fig. 42 | <i>Isl-1</i> and <i>Brn3a</i> positive cells in <i>Pax7</i> -transfected midbrains..... | 98 |
| Fig. 43 | The expression of <i>Pax3</i> and <i>Nkx6.1</i> in <i>Pax7</i> -transfected midbrains and hindbrains..... | 100 |
| Fig. 44 | Expression pattern of <i>Pax7</i> in chick E8.5 midbrain..... | 104 |
| Fig. 45 | Schematic diagram of chick developing midbrain..... | 107 |
| Fig. 46 | Expression comparison of <i>Pax7</i> protein in the spinal cord at stage 16 and 23..... | 108 |
| Fig. 47 | Schematic diagram of the dynamic expressions of <i>Pax3</i> and <i>Pax7</i> in chick developing midbrain at early stages..... | 110 |
| Fig. 48 | Sequential analysis of chick EST clones containing <i>Rab23</i> gene fragments by restrictive digestion..... | 112 |

| | | |
|---------|--|-----|
| Fig. 49 | Dynamic expression pattern of <i>Rab23</i> gene in chick embryos at stage 4 to 7..... | 114 |
| Fig. 50 | <i>Rab23</i> expression in chick midbrain and spinal cord after neural tube formation..... | 116 |
| Fig. 51 | Four DNA fragments for assembly of chick <i>Rab23</i> cDNA..... | 118 |
| Fig. 52 | Schematic structure and multi - sequence alignment of chick <i>Rab23</i> protein..... | 120 |
| Fig. 53 | Sequence comparison of <i>Rab23</i> proteins..... | 121 |
| Fig. 54 | Phylogenetic tree of <i>Rab23</i> proteins..... | 122 |
| Fig. 55 | Electrophoretic analysis of chick <i>Rab23</i> expression plasmid..... | 124 |
| Fig. 56 | Ectopic expression of <i>Rab23</i> in chick midbrain and hindbrain..... | 125 |
| Fig. 57 | The expression of <i>Pax7</i> in the <i>Rab23</i> - transfected midbrains, hindbrains and spinal cords..... | 128 |
| Fig. 58 | The expression of <i>Pax3</i> and <i>Nkx6.1</i> in the <i>Rab23</i> - transfected midbrains and hindbrains..... | 130 |
| Fig. 59 | Islet 1/2 expressing cells in the <i>Rab23</i> - transfected midbrain..... | 131 |
| Fig. 60 | <i>Brn3a</i> expressing cells in the <i>Rab23</i> - transfected neural tubes..... | 133 |
| Fig. 61 | Neuronal differentiation in <i>Rab23</i> - transfected midbrains and hindbrains..... | 135 |
| Fig. 62 | Mitotic cells in <i>Rab23</i> - transfected midbrains..... | 137 |
| Fig. 63 | Electrophoretic display of RNA-labelled probes for several genes on the <i>Shh</i> signalling pathway..... | 139 |
| Fig. 64 | Expression patterns of <i>Shh</i> , <i>Ptc1/2</i> , <i>Smo</i> and <i>Gli3</i> in chick whole embryo and midbrain..... | 140 |
| Fig. 65 | Gene expressions in the <i>Rab23</i> – transfected midbrains and hindbrains..... | 141 |
| Fig. 66 | Morphological asymmetry of Hensen’s node..... | 144 |
| Fig. 67 | Schematic diagram of the pMES – based lhRNA construct for chick <i>Pax7</i> gene..... | 153 |
| Fig. 68 | The selected sequences for lhRNA – <i>Pax7</i> constructs..... | 154 |
| Fig. 69 | Ligation of gene fragments for hairpin dsRNA transcription..... | 155 |
| Fig. 70 | Digestion of the lhRNA – <i>Pax7</i> constructs by <i>EcoRI</i> | 155 |
| Fig. 71 | Digestion of the lhRNA – <i>Pax7</i> constructs by <i>XbaI</i> | 156 |
| Fig. 72 | Percentages of the reduced midbrains upon lhRNA- <i>Pax7</i> transfection..... | 156 |
| Fig. 73 | Protein expression of the midbrain transfected with lhRNA- <i>Pax7</i> construct..... | 158 |

| | | |
|---------|---|-----|
| Fig. 74 | Quantitative analysis of protein repression in the dorsal cells by lhRNA-Pax7 constructs..... | 159 |
| Fig. 75 | The annealed shRNA inserts for cloning into the pMES vector.... | 161 |
| Fig. 76 | Sequential analysis of the shRNA – Pax7 constructs..... | 162 |
| Fig. 77 | Protein expression of the midbrains transfected with pMES-based shRNA – Pax7 constructs..... | 164 |
| Fig. 78 | Protein expression in the dorsal cells transfected with pMES-based shRNA – Pax7 constructs..... | 165 |
| Fig. 79 | Quantitative analysis of protein repression in the dorsal cells by pMES-based shRNA – Pax7 constructs..... | 166 |
| Fig. 80 | Protein expression of the midbrains transfected with pSilencer-based shRNA – Pax7 constructs..... | 168 |
| Fig. 81 | Protein expression in the dorsal cells transfected with pSilencer-based shRNA – Pax7 constructs..... | 169 |
| Fig. 82 | Quantitative analysis of protein repression in the dorsal cells by pSilencer-based shRNA – Pax7 constructs..... | 170 |
| Fig. 83 | The protein expression in the midbrain transfected with antisense DNA oligonucleotides..... | 171 |
| Fig. 84 | Quantitative analysis of protein repression by antisense DNA oligonucleotides..... | 172 |
| Fig. 85 | The protein expression in the midbrains transfected with antisense morpholinos against Pax7 gene..... | 173 |
| Fig. 86 | Quantitative analysis of protein repression by antisense morpholinos against Pax7 gene..... | 174 |
| Fig. 87 | Map of the pMES vector..... | 219 |
| Fig. 88 | Map of pBluescript® II KS (+/-) phagemid..... | 220 |
| Fig. 89 | Map of pCR®4-TOPO® vector..... | 221 |
| Fig. 90 | Map of pSilencer™ 1.0-U6 siRNA expression vector..... | 222 |
| Fig. 91 | Sequence and structure of siRNA insert..... | 222 |
| Fig. 92 | Characteristics of the cDNA sequence of chick <i>Rab23</i> gene..... | 223 |

List of Tables

| | | |
|---------|--|----|
| Tab. 1 | The early stages of chick and quail embryos..... | 24 |
| Tab. 2 | Chick EST clones..... | 24 |
| Tab. 3 | Morpholino oligonucleotides..... | 26 |
| Tab. 4 | PCR/RT-PCR primers..... | 27 |
| Tab. 5 | Primers for DNA sequencing..... | 27 |
| Tab. 6 | Antisense DNA oligonucleotides..... | 28 |
| Tab. 7 | shRNA oligonucleotides..... | 28 |
| Tab. 8 | Polymerases and DNA/RNA modifying enzymes..... | 29 |
| Tab. 9a | Restriction endonucleases from MBI Fermentas..... | 29 |
| Tab. 9b | Restriction endonucleases from New England Biolabs..... | 29 |
| Tab. 10 | Spectral characteristics of the fluorescent probes..... | 30 |
| Tab. 11 | Chemical reagents..... | 30 |
| Tab. 12 | Kits used for molecular experiments..... | 35 |
| Tab. 13 | Characteristics of the primary antibodies..... | 35 |
| Tab. 14 | Characteristics of the secondary antibodies..... | 36 |
| Tab. 15 | Relevant genes for <i>in situ</i> hybridisation..... | 36 |
| Tab. 16 | Technical equipments..... | 37 |
| Tab. 17 | The setting of the Sutter Puller..... | 42 |
| Tab. 18 | The setting of the Pulse Stimulator..... | 42 |
| Tab. 19 | Whole-mount immunostaining protocols..... | 53 |
| Tab. 20 | Whole-mount RNA <i>in situ</i> hybridization protocol..... | 54 |

| | | |
|---------|---|-----|
| Tab. 21 | The percentage of ventral explants expressed <i>Nkx6.1</i> | 70 |
| Tab. 22 | The percentage of dorsal explants expressed <i>Pax3</i> | 70 |
| Tab. 23 | The Pax7-transfected midbrains in size..... | 85 |
| Tab. 24 | The Pax7-repressed and GFP control midbrains in size..... | 88 |
| Tab. 25 | The Rab23 - transfected midbrains, hindbrains and spinal cords with Pax3/7 misexpression or <i>Nkx6.1</i> repression..... | 127 |
| Tab. 26 | Numbers of Brn3a expressing cells in Rab23 - transfected neural tubes..... | 134 |
| Tab. 27 | Numbers of reduced midbrains by the transfection of pMES-based shRNA - Pax7 constructs..... | 163 |
| Tab. 28 | Numbers of reduced midbrains by the transfection of pSilencer-based shRNA - Pax7 constructs..... | 170 |

Introduction

Early Development of the Chick Central Nervous System

The Formation of the Neural Tube

The normal function of the nervous system requires that neurons be precisely wired together. Only precisely ordered networks guaranty that neurones can rapidly and precisely communicate with their synaptic target. Only with a precisely ordered network the diverse functions of the NS from - cognition to movements - are possible. These networks arise during embryonic development, when an intricate and unerring pattern of neuronal subtypes and axonal connections is generated.

The central nervous system (CNS) arises from the neural plate - a cytologically homogeneous sheet of epithelial cells that forms the dorsal surface of the gastrula-stage embryo. The peripheral nervous system, glia, pigment cells and facial cartilage arises from ectodermal placodes and neural crest cells that form the lateral fringes of the plate at the border to the ectoderm. Anteriorly the neural tube undergoes so-called primary neurulation, while the part caudal to twenty-seventh somite pair undergoes so-called secondary neurulation. The process of primary neurulation in birds is similar to that in amphibians, reptiles, and mammals (Gallera, 1971). During primary neurulation, the neural plate subsequently rolls up along its anterioposterior axis to form a tube. The neural folds migrate toward the middle and eventually fuse to form the neural tube beneath the overlying ectoderm (Fig. 1). The two open ends of the neural tube left there are called the anterior and posterior neuropores (Schoenwolf, 1991; Keller *et al.*, 1992; Jacobson and Moury, 1995; Smith and Schoenwolf, 1997). The secondary neurulation, which takes place at the posterior end of the neural plate involves the making of a medullary cord and hollowing into a neural tube subsequently (Catala *et al.*, 1995; Catala, 2002).

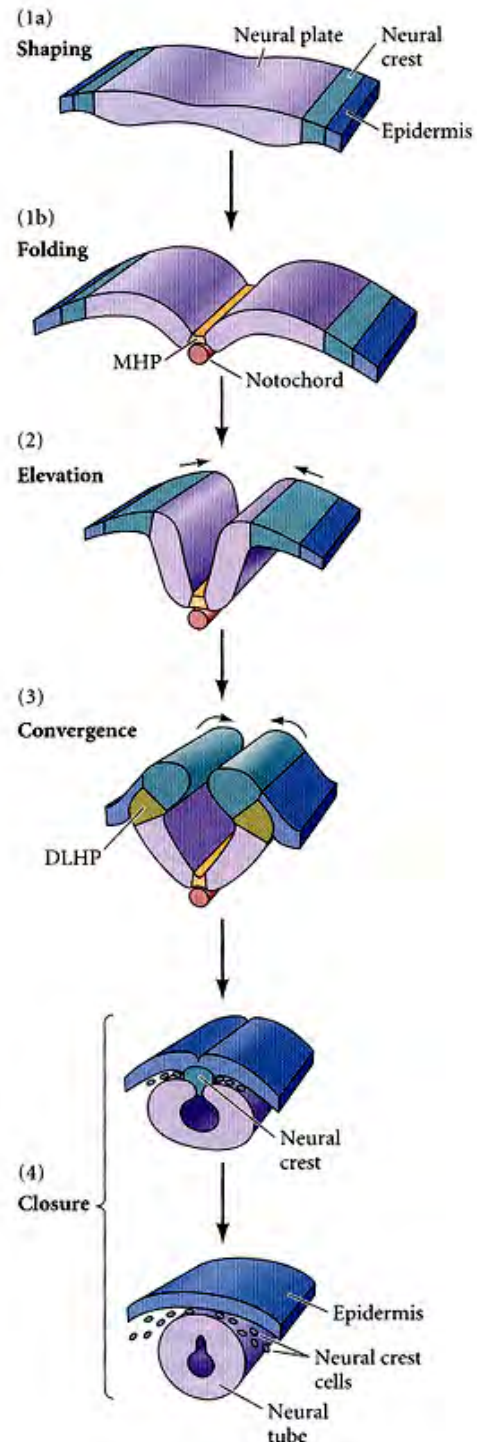
The Differentiation of the Neural Tube

The neural tube is originally a one-cell-layer germinal neuroepithelium composed of rapidly dividing neural stem cells. These cells receive signals from the surrounding tissues (mesoderm and endoderm) and later also from signalling centers within the neural tube, which help to generate the different regions (see below), cell types, cytoarchitectonic arrangements (layers or nuclei) and neuronal connections. Thus, a functional network is finally formed. This involves symmetric and asymmetric cell division of neural stem cells, cell migration, differentiation into different neuronal cell types, growth of axons and dendrites followed by synaptogenesis, cell death and the refinement of neuronal connections.

The neural tube develops into the central nervous system (CNS) at three different levels, more or less simultaneously. On a gross anatomical level, the neural tube bulges and constricts and thus, forms different regions of the brain and spinal cord. At the tissue level, the neuroepithelial cells of the neural tube rearrange themselves to form functional regions. Finally, on a cellular level, the neuroepithelial cells differentiate into the numerous types of nerve cells (neurons) and supportive cells (glia) (Gilbert, 2000).

Figure 1: Primary neurulation in chick embryo

(1a, 1b) The elongated cells of neural plate begin to fold as the medial neural hinge point (MHP) cells anchor to notochord. (2) The neural folds are elevated as presumptive epidermis continues to move toward the dorsal midline. (3) Convergence occurs as the dorsolateral hinge point (DLHP) cells become wedge-shaped and epidermal cells push toward the center. (4) The neural folds are brought into contact with one another, and the neural crest cells link the neural tube with the epidermis. The neural crest cells then disperse, leaving the neural tube separate from the epidermis. (After Gilbert, 2000.)



The neural tube balloons into three primary vesicles, prosencephalon (forebrain), mesencephalon (midbrain) and rhombencephalon (hindbrain), when the anterior and posterior neuropores close. The prosencephalon becomes subdivided into the anterior telencephalon, which will eventually form the cerebral hemispheres and striatum and amygdala, and the more caudal diencephalon forming the thalamic and hypothalamic brain regions. The mesencephalon is subdivided along its dorsoventral axis into a bulging tectum dorsally and tegmentum ventrally. The rhombencephalon, which subdivides into seven rhombomeres along its anteroposterior axis and gives anteriorly rise to the cerebellum.

The Development of the Three Embryonic Axes

During the development of the embryo, the establishment of the anterioposterior (AP), the dorsoventral (DV) and left-right (LR, or medial lateral, ML) axes occur gradually. All three axes begin to be established at early cleavage stage and are refined during late development.

The anterioposterior axis is specified by gravity in that the radially symmetrical blastoderm is converted into a bilaterally symmetrical structure. When the ovum passes through the hen's reproductive tract, the rotation in the shell gland results in the lighter components of the yolk pushing up one side of the blastoderm, which becomes the posterior of the embryo, and the formation of the primitive streak begins from the posterior marginal zone (PMZ) (Fig. 2, Eyal-Giladi *et al.*, 1994; Wolpert *et al.*, 1998). The epiblast and middle layer cells in the anterior portion of Koller's sickle (KS) become Hensen's node, the avian equivalent of the amphibian dorsal blastopore lip, whereas the posterior portion of Koller's sickle contributes to the primitive streak posteriorly (Dias and Schoenwolf, 1990; Bachvarova *et al.*, 1998).

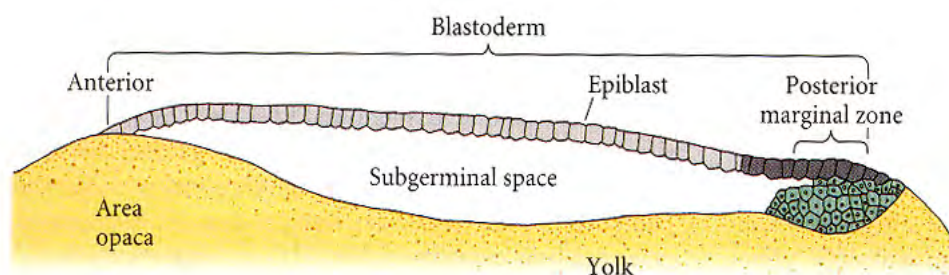


Figure 2: Early gastrulation of chick embryo

Disc-shaped epiblast covers the narrow subgerminal space filling with acidic fluid. The posterior marginal zone locates at the posterior of the epiblast. The posterior marginal zone contains cells that act as the equivalent of the amphibian Nieuwkoop center. (After Gilbert, 2000.)

The dorsoventral (back-belly) axis is established when the cleaving cells of the blastoderm as a barrier allow water and sodium ions transport from the basic (pH 9.5) albumin above the blastodisc into the acidic (pH 6.5) subgerminal space. Thus, the epiblast side facing the basic albumin becomes dorsal; while the other side facing the acidic subgerminal space fluid becomes ventral (Stern and Canning, 1988). The cells from Hensen's node secrete BMP antagonists, such as Follistatin (Towers *et al.*, 1999),

Noggin (Lamb *et al.*, 1993; Smith *et al.*, 1993), Chordin (Sasai *et al.*, 1994), and Nodal proteins (Jones *et al.*, 1995), dorsalize the ectoderm and mesoderm and induce neuralization of the ectoderm, while BMPs seem to have the ventralizing, neural-inhibitory action (Schultheiss *et al.*, 1997; Hsu *et al.*, 1998; Connolly *et al.*, 2000; Faure *et al.*, 2002).

The left-right axis is determined last using a complicated system of gene interactions (activation and repression) to ensure asymmetric gene expression patterns and thus asymmetric organogenesis, like the generation of heart and spleen on the left side of the body, while the liver is created on the right side. In chick embryo, as the primitive streak reaches its maximum length, Sonic hedgehog starts to express on the left side of the Hensen's node and triggers the left-right asymmetry (Fig. 3). Two downstream genes - *pitx2* and *snail* - play crucial roles on directing the asymmetry of the embryonic structures (Levin *et al.*, 1995; Patel *et al.*, 1999; Rodriguez Esteban *et al.*, 1999; Yokouchi *et al.*, 1999; Gilbert, 2000).

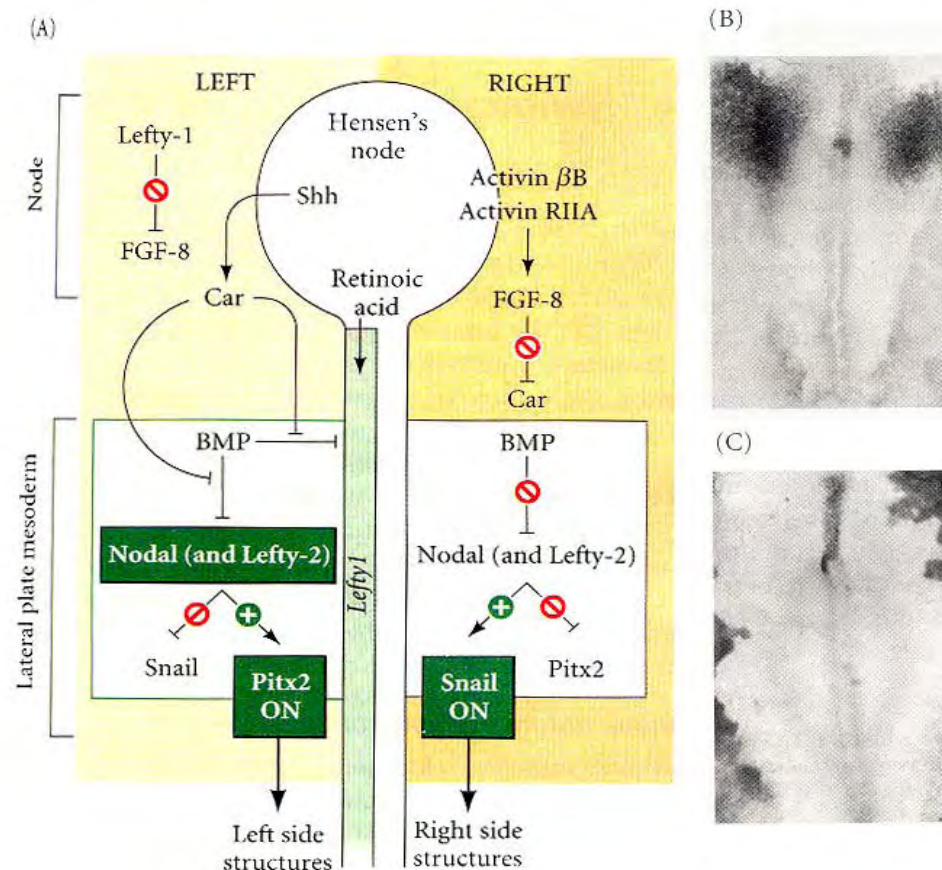


Figure 3: The signal pathway for left-right asymmetry in chick embryo

(A): On the left side of Hensen's node, *Sonic hedgehog* (*Shh*) and *lefty-1* are expressed. *Lefty-1* blocks *fgf8* expression, while *Shh* activates the expression of *caronte* (*car*). Retinoic acid (RA) permits the expression of *Lefty-1* along the ventral midline. *Caronte* blocks bone morphogenetic proteins (BMPs), which could block the expression of *nodal* and *lefty-2*. In the presence of *Nodal* and *Lefty-2*, *Pitx2* is activated in the primordial of various organs and specifies the side to be left. In the right side of Hensen's node, *activinβ* initiates to be expressed along with *activin receptor IIa*. They activate *FGF8*, a protein that blocks the expression of *caronte*. In the absence of *Caronte*, the repression of *nodal* and *lefty-2* by *BMP* allows *snail* gene (*cSnR*) instead of *pitx2* to be activated in this side. (B, C) Ventral views of *Shh* (B) and *activin receptor IIa* mRNAs (C) *in situ* hybridisation. (A from Gilbert, 2000; photographs B and C from Levin *et al.*, 1995.)

Regionalisation of the Developing CNS

The neural tube is regionalized along its AP axis into forebrain (Rubenstein and Beachy, 1998; Rubenstein *et al.*, 1998), midbrain, hindbrain and spinal cord (Schoenwolf *et al.*, 1989; Eagleson and Harris, 1990; Guthrie, 1996; Lee and Jessell, 1999). This regionalisation can be seen at a morphological level by the formation of constrictions of the neural epithelium. No such morphological constrictions are visible along the DV axis early in development. The regional organizing centers, both outside and within the developing neural plate or neural tube, are important to generate this early pattern of central nervous system and thus, influence the identity of neuronal cell types (Edlund and Jessell, 1999; Weinstein and Hemmati-Brivanlou, 1999). Analyses of cell fates after experimental rotation of the neural plate (Jacobson and Moury, 1995; Simon *et al.*, 1995) have indicated that regional fate is determined along the AP axis before and independently of fate restriction on the DV axis. Within the neural epithelium, signals from the anterior neural plate regionalize the forebrain (Houart *et al.*, 1998; Rubenstein *et al.*, 1998), signals from the midbrain-hindbrain boundary (MHB) regulate regional identity in the midbrain and anterior hindbrain (Simeone, 2000; Wurst and Bally-Cuif, 2001), and signals from mesodermal tissue play an important role in AP specification of the hindbrain (Lumsden and Krumlauf, 1996; Gavalas and Krumlauf, 2000). Many of the morphological boundaries of the neural tube appear to demarcate domains with distinct specification and correlate with the boundaries of expression of transcription factors (Fig. 4 A and B). These domains with distinct regional specification have to remain homogenous and to maintain their sharp interfaces to able to keep the pattern of cell type specification precisely defined. However, during growth and morphogenesis extensive cell mixing can occur due to the spreading of clonally related cells or by cell division and intercalation. Independent of the degree of cell mixing it can cause local scrambling between adjacent territories.

Two different strategies are known to maintain internal subdivisions of a cellular population (Fig. 4 C). The definition and information about these strategies derives mostly from studies in *Drosophila* (Lawrence *et al.*, 1996; Mann and Morata, 2000; Pasini and Wilkinson, 2002; Blair, 2003). One is the formation of compartments, defined by interfaces that cells do not cross (a, b). Fate-mapping techniques have shown that compartments are formed from polyclonal groups of cells that are unable to mix with cells from neighbouring compartments (Fraser *et al.*, 1990; Wizenmann and Lumsden, 1997). Each compartment is thought to act as a discrete developmental unit which sets aside to differentiate along its own particular developmental pathway (Pasini and Wilkinson, 2002). Due to their function and mechanism of formation, all compartment boundaries are gene expression boundaries. However, only some compartment boundaries correspond to morphological boundaries, such as rhombenmeres. A secondary mechanism relies on locally inductive signals, which specify the cells that cross the domain boundary to the identity of their new neighbours (c), so called territories (Theisen *et al.*, 1996; Jungbluth *et al.*, 2001).

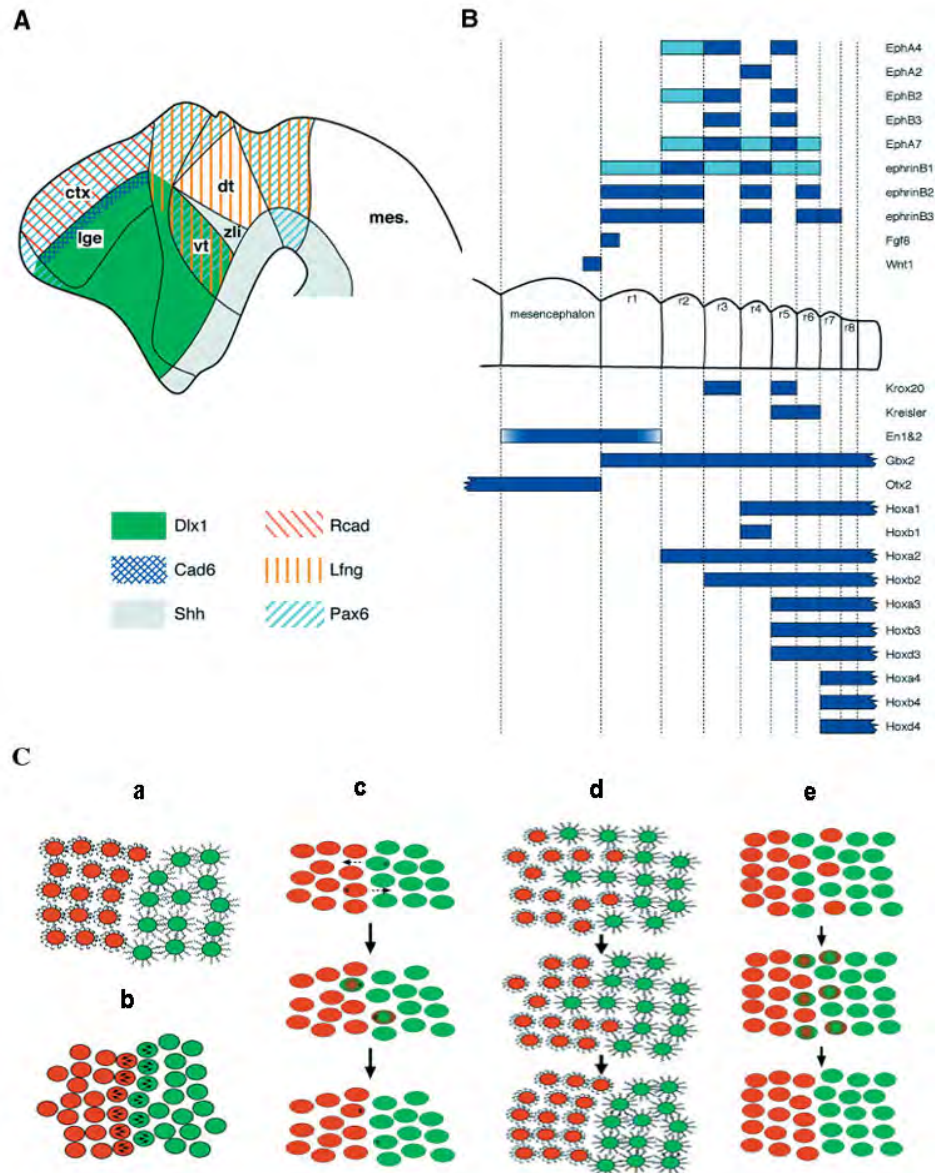


Figure 4: Establishment and strategies of compartments in CNS

A: In the telencephalon, the expression domains of the two transcription factors, Pax6 and Dlx1, are largely complementary with a sharp border at the cortico-striatal boundary. Two cadherins, Rcad and Cad6, are expressed in the ctx and in the lge respectively. In the diencephalon, the expression of Lunatic fringe (Lfng), a modulator of Notch activity, is widespread but is excluded from the zli, which expresses Sonic hedgehog (Shh). B: The midbrain–hindbrain boundary is positioned by the interface between the expression domains of the transcription factors Otx2 and Gbx2 and is maintained by a network of transcription factors and signalling molecules (including En1, En2, Wnt1, Fgf8). In the hindbrain, the rhombomeres correspond to the expression domains of transcription factors (Kr, Krox20, Hox). EphrinB proteins and their receptors (EphB subfamily and EphA4) are expressed in even- and odd-numbered rhombomeres respectively. Light blue, low levels of gene expression; dark blue, high levels of gene expression; shaded blue, gradients of gene expression. C: Strategies of establishment and maintain a sharp interface of adjacent cell populations with distinct identity. a-c: Two general mechanisms can maintain sharp interfaces. Restricted cells intermingle across the interface due to differential homophilic adhesion (a) or mutual repulsion (b), or cells switch their identities cross the interface to that of new neighbours (c). d, e: The boundary between two initially fuzzy territories can be sharpened by local cell sorting (d) or cell-identity switching to the majority population (e) to generate homogenous territories.

Abbreviations: ctx, cortex; dt, dorsal thalamus; lge, lateral ganglionic eminence; mes, mesencephalon; r1– r8, rhombomeres 1 to 8; vt, ventral thalamus; zli, zona limitans intrathalamica. (Modified after Pasini and Wilkinson, 2002.)

Locally acting inductive signals and a plasticity of cell identity are necessary for this strategy. These two mechanisms underlie the transformation of an initial fuzzy interface between domains into sharp territories by sorting and segregating of the cells in both sides (d) or by transforming the cell identity by local signals (e). Recent evidence suggests that both strategies are used in the developing CNS to establish and maintain sharp domains of regional specification (Pasini and Wilkinson, 2002).

Neuronal Migration during Neurogenesis

The neuronal development also involves migration of neural precursors and differentiated neurones. Neuronal migration occurs after regionalization along DV axis sets forth a plan for cell fate specification. As specific classes of cells come to reside in definite layers or nuclei. The integrity of multiple molecular mechanisms seem to be critical for neuronal migration, such as cell cycle control (cdk5, Gupta and Tsai, 2003), cell-cell (neuron-glia) adhesion (Baird *et al.*, 1992; Goldman *et al.*, 1996), the action of transcription factors (Reelin, Curran and D'Arcangelo, 1998), neurotransmitter release (Fueshko *et al.*, 1998), growth factor availability (Anton *et al.*, 1997), and platelet-activation factor degradation (Hattori *et al.*, 1994). Two important proteins in microtubule network - LIS1 (Cahana *et al.*, 2001) and DCX (doublecortin, Sossey-Alaoui *et al.*, 1998) – have been verified to be involved in human cortical disorganizations. In the early embryos, morphogenetic movements of neural precursor cells (NPCs) establish brain vesicles and boundaries to form the compact ventricular zone (VZ) in cerebrum and external germinal layer (EGL) in cerebellum. After mitosis, the postmitotic cells undergo direct migrations and establish the neuronal layers and nuclei. In the postnatal period, a wave of secondary neurogenesis produces huge numbers of interneurons, which migrate in a long way and destine to the cerebellar cortex, the hippocampus and the olfactory bulb.

Two basic migratory pathways are adopted by postmitotic neurons in the central nervous system. Radial migration is the predominant pattern in the developmental mammalian cortex (Fig. 5A), where the postmitotic neurons migrate from the germinative zone (GZ) across a radial glial scaffold, which is provided by radial glia (Rakic, 1972; 1995). The scaffold is refined through neuronal contact, and once the migration is completed, the radial glial cells transform into satellite astrocytes and are positionally locked by the formation of specific axon-target interactions (Baird *et al.*, 1992; Feng *et al.*, 1994; Feng and Heintz, 1995). The laminar structure of the cortex begins to set forth with neuronal migration and neurogenesis (Easter *et al.*, 1993). In the cerebellum, the precursors of granule cells appear in the dorsal ridge - the rhombic lip, and migrate on the surface of the cerebellar anlage across the lip. Tangential migration is the other important manner that neurons move across the glial fiber system (Fig. 5B, Altman, 1969; O'Rourke *et al.*, 1992; 1997). The migrating neurons follow growing axons, using either each other or dispersing in a rather individual manner to reach their final positions. This movement do not respect the regional boundaries (Gray and Sanes, 1991; Letinic and Rakic, 2001).

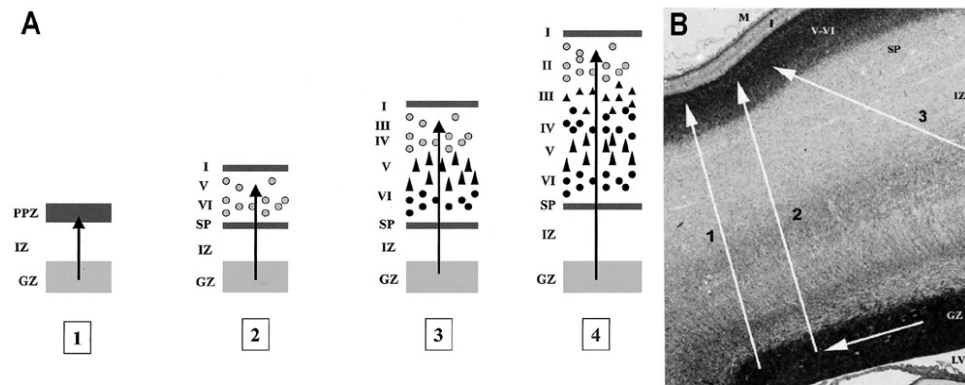


Figure 5: Neuronal migratory pathways in mammalian neocortex

(A): 1. The postmitotic neurons migrate through IZ to form PPZ or named preplate (PP). 2. Subsequently produced neurons migrate into the PPZ, and split it into the marginal zone (MZ, Layer I) and subplate (SP). 3. Successive waves of migration pass the SP and stop under Layer I, forming successively cortical layers VI, V, IV, III. 4. Layer II forms last. Arrows indicate the neuronal migratory pathways, and light gray circles represent migrating neurons while black circles and triangles represent postmigratory neurons. (B): Coronal neopallial section at 15 wk of gestation showing a schematic representation of the different migratory pathways adopted by neurons. 1: Radial migration along radial glial scaffold from the subventricular GZ. 2: Tangential migration in the GZ followed by a radial migration. 3: Tangential migration in zone IZ of neurons originating from the ganglionic eminence.

Abbreviations: I, cortical layer I or molecular layer; II to VI, cortical layers II to VI; GZ, germinative zone; IZ, intermediate zone (prospective white matter); LV, lateral ventricle; M, meninges; PPZ, primitive plexiform zone; SP, subplate. (From Gressens P, 2000.)

Dorso-ventral Patterning of the Central Nervous System

Determining Dorso-ventral Cell Types in the Spinal Cord

Patterning of neuronal cell types in the neural tube appears to be organized on a Cartesian grid of positional information corresponding with both AP and DV axes. For dorso-ventral patterning in the neural tube, two sets of inductive signals that control the identity of neural cell types derive from two distinct groups of non-neural cells — the surface ectoderm and notochord, which specify two secondary signalling centres — the floor plate (FP) and the roof plate (RP), respectively. The signals from the notochord and floor plate are required for the generation of ventral cell types, which appear to be mediated by a secreted protein *Sonic hedgehog* (Shh), while the specification of dorsal neural cell fates requires the action of “dorsalizing” signals like members of the Wnt and Bmp family of secreted proteins (Yamada *et al.*, 1991; Ericson *et al.*, 1992; Liem *et al.*, 1997; Jessell, 2000; Chenn and Walsh, 2002; Muroyama *et al.*, 2002; Timmer *et al.*, 2002; Helms and Johnson, 2003; Maden, 2006; Sommer, 2007; Zechner *et al.*, 2007). Additional signals involving members of fibroblast growth factor (FGF) family also contribute to the proliferation and differentiation of dorsal neuronal cell types (Chandran *et al.*, 2004; Wilson and Maden, 2005). Such signals direct cell fates by inducing the expression of intrinsic proteins, notably transcription factors, which act in turn to regulate the expression of surface receptors and components of signal transduction that provide axons and growth cones to form precise target connections (Bang and Goulding, 1996; Lee and Jessell, 1999; Lee

et al., 2000; Altmann and Brivanlou, 2001; Caspary and Anderson, 2003). Most of the investigation on the developing dorsoventral polarity of the central nervous system is based on the mouse and chick embryonic spinal cord. The neurons in the mature spinal cord serve two major functions topologically: cutaneous and proprioceptive sensory input in the dorsal half and motor output ventrally (Brown, 1981).

In the dorsal spinal cord (Fig. 6), the non-overlapping expression domains of pro-neural genes define progenitor cell types with positional identities. The bHLH transcription factors encoded by these genes are required for the neuronal specification (Gowan *et al.*, 2001). Gain and loss of function studies show a cross repressive interactions between several of the bHLH factors (Bermingham *et al.*, 2001; Wildner *et al.*, 2006). The homeodomain transcription factors expressed in these neural progenitors have central roles in defining their region-specific identity. The dorsal progenitor cells give rise to six types of postmitotic dorsal interneurons (dl1–dl6) which express specific homeodomain transcription factors (Gross *et al.*, 2002; Muller *et al.*, 2002). The laminar organization (5 layer, I-V) of the mature dorsal spinal cord results then from the orchestrated neuronal migration and rearrangement of cellular patterns (Nornes and Carry, 1978; Lee and Jessell, 1999; Jessell, 2000).

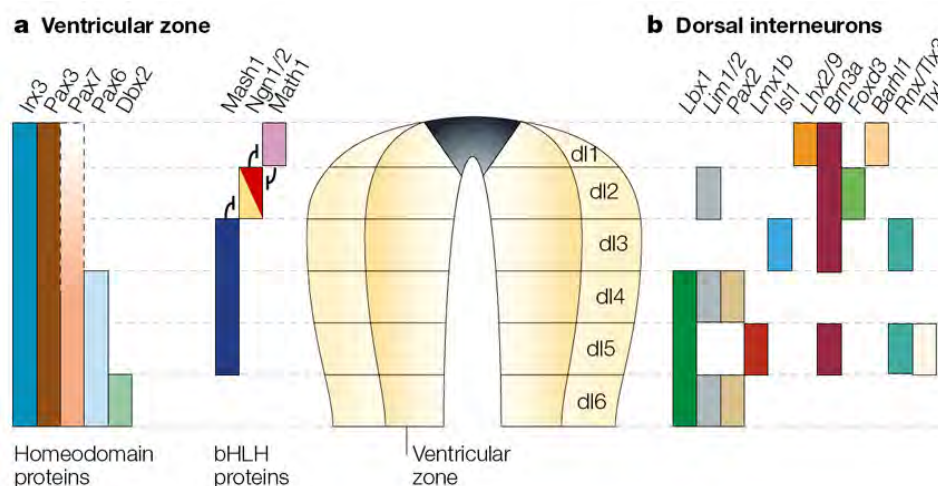


Figure 6: Combinatorial codes of transcription factors for the specification of dorsal cell types in the neural tube

a) Schematic diagram of the transcription factors expressed in the ventricular zone of the dorsal neural tube. The expression domains of some gene pairs are regulated by mutually repressive interactions (indicated by bars on the chart). bHLH proteins define progenitor cell types in the dorsal neural tube. *Math1* is expressed in the precursors of the dorsal-most cells (dl1) adjacent to the roof plate, *Ngn1/2* are expressed in the next ventral band of cells (dl2), and *Mash1* is expressed in the precursors of dl3–dl5 cells. These progenitor cells differentiate to give six types of postmitotic dorsal interneurons (dl1–dl6) on the basis of the homeodomain proteins. b) Schematic diagram of the genes expressed in the differentiating and differentiated dorsal interneurons that emerge from each progenitor domain. (From Caspary and Anderson, 2003.)

In the ventral spinal cord, neurons are induced by a long range ventral to dorsal gradient of Sonic Hedgehog (Yamada *et al.*, 1991; Chiang *et al.*, 1996; Ericson *et al.*, 1997). Two- to three-fold change of Shh concentration results in the generation of five classes of ventral neuronal progenitors - p3, pMN, p2, p1 and p0 from ventral to dorsal, respectively (Fig. 7A, Marti *et al.*, 1995b; Roelink *et al.*, 1995; Ericson *et al.*, 1996).

The five distinct ventral progenitor domains are established by controlling the expression of combinatorial homeodomain proteins (Sander *et al.*, 2000), which act as critical intermediaries in the control of neuronal cell fate determination (Fig. 7B). These homeodomain proteins are divided into two classes on the basis of their expressions and the regulation by Shh (Ericson *et al.*, 1997; Briscoe and Ericson, 1999; Sander *et al.*, 2000; Briscoe and Ericson, 2001). The expressions of Class I proteins (Pax7, Dbx1, Dbx2, Irx3 and Pax6) are repressed at a distinct concentration of Shh, and delineate ventral boundaries of progenitor domains. Conversely, the expressions of Class II proteins, such as Nkx2.2 and Nkx6.1, are activated in response to Shh signalling, and define the dorsal limits of progenitor domains. Gain- and loss-of-function studies indicate the cross-repressive interactions between complementary pairs of Class I and Class II proteins that share the same progenitor domain boundary (Ericson *et al.*, 1997; Sander *et al.*, 2000). Several Shh - dependent or - independent signalling pathways are also implicated in the specification of ventral cell fates, such as Retinoids, Nodal, BMPs and Rab23 (Barth *et al.*, 1999; Pierani *et al.*, 1999; Muller *et al.*, 2000; Eggenschwiler *et al.*, 2001).

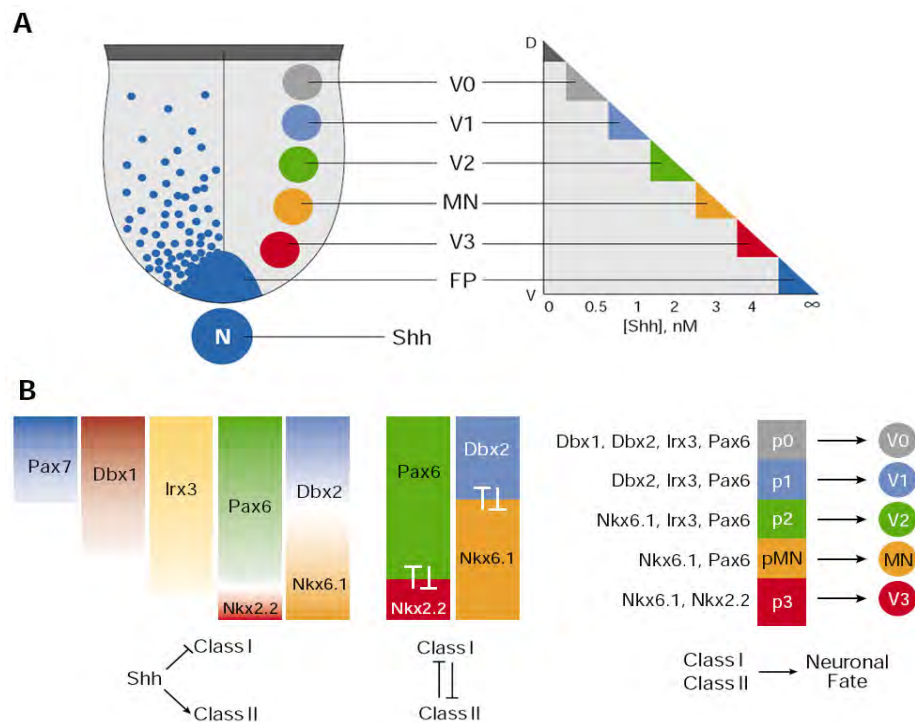


Figure 7: Regulation of Sonic hedgehog on combinatorial expression of transcription factors in ventral neural progenitors

(A) Five distinct ventral neuronal subtypes arise from an equivalent number of progenitor domains in the ventricular zone of the ventral spinal cord. Progressively more dorsal progenitor domains are exposed to a decreasing concentration of sonic hedgehog protein. (B) The concentration gradient of Shh regulates the ventral expression domains of a series of transcription factors in ventral progenitor (p) cells. Three aspects are crucial to this system: Shh either represses (class I genes) or induces (class II genes) expression at different concentration thresholds (left). Progenitor gene-expression domains are refined and maintained by negative cross-regulatory interactions between those proteins that share a boundary (centre). The combinatorial expression of different homeodomain proteins in distinct progenitor domains determines the generation of neuronal subtype (right).

Abbreviations: D, dorsal; Dbx, developing brain homeobox transcription factor; FP, floor plate; Irx, iroquois homeodomain protein; MN, motor neuron; N, notochord; Nkx, Nkx homeodomain protein; Pax, Paired homeodomain protein; V, ventral; V0–V3, ventral interneurons 0–3. (From Jacob and Briscoe, 2003.)

Thus, elaborate interactions of transcription factors bring about the variety of neuronal subtypes, which finally assemble into functional neural circuits in the spinal cord. For instance, MNs are further divided into longitudinally organized columns, and subsequently, group into motor pools to innervate a distinct muscle with the actions of LIM proteins and other transcription factors (Tsuchida *et al.*, 1994; Pfaff *et al.*, 1996; Lin *et al.*, 1998; Arber *et al.*, 1999; Saueressig *et al.*, 1999; Thaler *et al.*, 1999; Kania *et al.*, 2000).

The Paired-box Transcription Factor Pax7

The *Pax* gene family encodes a group of transcription factors that play crucial roles in embryonic development. Pax proteins are defined by the presence of a DNA-binding domain - the paired domain (PD, 128 - amino acid), which is first found in a protein encoded by a segmentation gene *paired* in *Drosophila* PDR (Bopp *et al.*, 1986). Nine Pax members have been identified in mammals, and divided into four classes, Pax1/9 Pax2/5/8 Pax3/7 and Pax4/8, dependent on structural domains (PD, OP and HD), sequence similarity and conserved function (Gruss and Walther, 1992; Noll, 1993). Homologues are also found in worms, frogs, fish and birds (Goulding *et al.*, 1994; Chisholm and Horvitz, 1995; Seo *et al.*, 1998; Holland *et al.*, 1999). Crystal structures (Xu *et al.*, 1995; 1999) indicate that the PD consists of two subdomains structurally resembling helix–turn–helix (HTH) motif, which is common in all homeodomains. Hence, at a structural point of view the PD can be regarded as two covalently associated HDs connected by a flexible linker (Fig. 8). Both HDs and PD exhibit sequence specific DNA-binding activities (Czerny *et al.*, 1993; Underhill and Gros, 1997). All Pax proteins, except for 1/9, are expressed in the developing and adult nervous system (Deutsch *et al.*, 1988; Neubuser *et al.*, 1995). Diverse Pax proteins act as regulators of organogenesis or key factors in maintaining pluripotency of stem cell populations during development, either by binding to DNA enhancer or by modifying transcriptional activity of downstream genes (Treisman *et al.*, 1991; Stoykova and Gruss, 1994; Mansouri *et al.*, 1999; Chi and Epstein, 2002). Some of them show a dose-dependent transcriptional activity: transcription occurs at low concentration, whereas higher level decreases the activity (Glaser *et al.*, 1994).

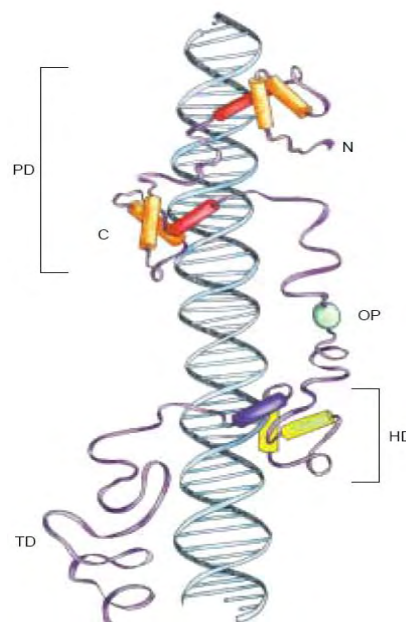


Fig. 8. The structure of a Pax protein

The paired domain (PD) has an amino (N) - and a carboxyl (C) terminal subdomain, each of which is composed of three α -helices. The third one (red) is in contact with the major groove of DNA. An octapeptide motif (OP, green) is followed by a homeodomain (HD) and a C-terminal transactivation domain (TD) at the end. Various Pax proteins contain some or all of these domains. (From Chi and Epstein, 2002.)

In the developing embryos, Pax7 is expressed in the precursor cells of neural tube, head neural crest, eye primordium and somites (Kawakami *et al.*, 1997; Seale *et al.*, 2001). In the central nervous system, the expression of Pax7 is first detected in the alar plate after the closure of the neuroepithelium and lasts even after the birth (Jostes *et al.*, 1990; Kawakami *et al.*, 1997). However, homozygous knockout mice do not show an obvious phenotype in the nervous system, only malformations in facial skeletal structures are visible, suggesting a role at cephalic neural crest development (Mansouri *et al.*, 1996) and satellite cell differentiation (Seale *et al.*, 2000). Pax7 and Pax3 double mutant mice (Mansouri and Gruss, 1998) show severe exencephaly, spina bifida (SB) and defects in commissural neurons in the spinal cord, implying that dI1 and dI2 cells do not differentiate appropriately, although both of Pax proteins appear insufficient to trigger the differentiation of definitive dorsal cell types (Lee and Jessell, 1999). Pax3 is another Pax member expressing in the same region of mesencephalon with Pax7 (Goulding *et al.*, 1991). The Pax3 mutant mice, *Spotch*, show exencephaly and defects in myogenesis and neural crest cell differentiation (Epstein *et al.*, 1991; Franz and Kothary, 1993; Tremblay *et al.*, 1996; Conway *et al.*, 1997). Both Pax3 and Pax7 misexpression can cause fate change of the alar plate of the presumptive diencephalon to that of the mesencephalon (Matsunaga *et al.*, 2001). Therefore, these suggest a functional redundancy of both Pax proteins, and the phenotype of Pax7^{-/-} mice in the nervous system is thought to be alleviated by Pax3 expression.

Previous work suggests that Pax7 plays a role in setting up the dorsal polarity in the developing neural tube, and it is used as a dorsal specific gene in neurogenesis. In chick mesencephalon, Pax7 expression defines the territory of the tectum (Matsunaga *et al.*, 2001) with the help of Shh (Watanabe and Nakamura, 2000). However, Pax7 expression is well correlated with the rapidly enlarged tectum (Nomura *et al.*, 1998), and a large ectopic tectum is induced by Pax7 in the diencephalon (Matsunaga *et al.*, 2001), suggesting a possible function of Pax7 on proliferation and differentiation of dorsal cell populations, which is still unknown. Some results hint that a cross-regulation mechanism between them might be there to balance their expressions (Borycki *et al.*, 1999). Interesting, a number of alternate transcripts of Pax7 have been isolated in vertebrates (Ziman and Kay, 1998). Only one transcript initiates neural cell differentiation (Ziman *et al.*, 2001), whereas the others are thought responsible for directing embryonic cells along a myogenic lineage to form the skeletal muscles (Relaix *et al.*, 2004). Pax7 gene is thought to be activated by BMPs secreted from ectodermal cells before neural plate formation, and suppressed ventrally by Shh (Liem *et al.*, 1995; Lee and Jessell, 1999). Recently studies suggest that Pax7 seems to regulate *ephrin-A2* in a cell autonomous manner (Thomas *et al.*, 2004) and affect the expressions of *En* (Araki and Nakamura, 1999; Thomas *et al.*, 2004) and *Wnt* genes indirectly (Wagner *et al.*, 2000). Pax3 is involved in the subcellular redistribution of cell adhesive molecules (Mansouri *et al.*, 2001; Wiggan *et al.*, 2002). However, the cellular and molecular processes regulated by Pax7 in the nervous system and the mechanisms directing morphogenesis still remain largely unknown.

Shh in the Development of Central Nervous System

Sonic hedgehog (Shh) is a member of the secreted hedgehog (Hh) family involved in intercellular communication. Shh protein, initially described in *Drosophila* (Nusslein-Volhard and Wieschaus, 1980; Mohler and Vani, 1992), exerts essential roles for many embryogenic processes in vertebrates and invertebrates through a combination of short- and long-range manner. In vertebrates, Shh is involved in LR asymmetry, neural tube patterning, neural precursors proliferation, neuron and glial cell survival, and some aspects of organogenesis (Johnson and Tabin, 1995; Hammerschmidt *et al.*, 1997; Chuang and Kornberg, 2000; McMahon, 2000; Hatini and DiNardo, 2001; Ingham and McMahon, 2001; Bijlsma *et al.*, 2004). Misregulation of Shh signalling in human is associated with congenital malformations of the CNS (spina bifida, holoprosencephaly), head (cleft palate), limb (syn- and polydactyly), and with a predisposition for developing a variety of cutaneous (basal cell carcinoma) and neural tumors (medulloblastoma, glioblastoma) (Roessler *et al.*, 1996; Ming *et al.*, 1998; Hahn *et al.*, 1999; Odent *et al.*, 1999; Ruiz i Altaba *et al.*, 2002; Cohen, 2003; Ruiz i Altaba *et al.*, 2004).

The active, secreted form of Shh is a 19 kD N-terminal protein (Shh-N) with a cholesterol moiety via post-translational autocatalytic cleavage of a 46 kD precursor protein (Fig. 9). Cholesterol-modified Shh is anchored to the cell membrane, and further modified to become soluble, diffusible and multimeric (Zeng *et al.*, 2001; Feng *et al.*, 2004).

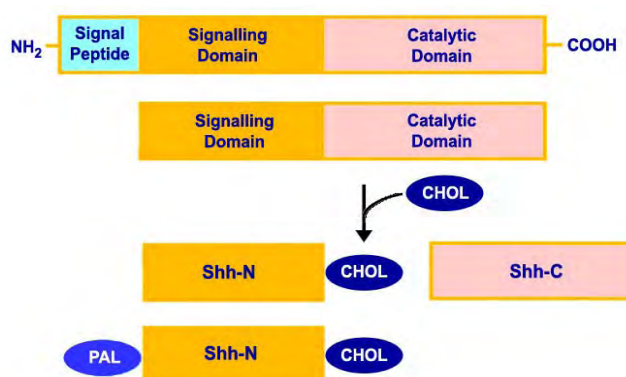


Fig. 9. Autoprocessing reaction of Shh

Shh precursor protein is composed of a N-terminal signalling domain (Shh-N) and a C-terminal catalytic domain (Shh-C) that causes autocleavage of the protein, resulting in a covalent addition of an ester-linked cholesterol moiety (CHOL) at the C-terminal end of the signaling portion; the catalytic portion diffuses away. An amide-linked amino-terminal palmitate (PAL) is critical for signaling activity. (Modified after Cohen 2003.)

For the early development of the central nervous system, Shh begins to be generated from two ventral midline signalling centres in the neural tube - the notochord and the floor plate - at early stages (Marti *et al.*, 1995a), and acts as a morphogen for the dorsoventral patterning of the forebrain (Ericson *et al.*, 1995; Kohtz *et al.*, 1998; Rubenstein *et al.*, 1998; Rallu *et al.*, 2002), midbrain (Ye *et al.*, 1998; Watanabe and Nakamura, 2000; Agarwala *et al.*, 2001; Ishibashi and McMahon, 2002) and the spinal cord (Echelard *et al.*, 1993; Jessell, 2000; Briscoe *et al.*, 2001; McMahon *et al.*, 2003) in mammals and birds. Especially, gain and loss-of-function studies display that Shh plays a key role on the specification of ventral neural cell types in the spinal cord. Shh is thought to be necessary and sufficient to specify distinct ventral neuron precursors at specific positions in a

concentration-dependent mechanism (Roelink *et al.*, 1994; Marti *et al.*, 1995b; Ericson *et al.*, 1996; Briscoe *et al.*, 2000; Cohen, 2003). At the late stages, Shh is still capable of roles in the nervous system, such as oligodendrocyte differentiation (Poncet *et al.*, 1996; Orentas *et al.*, 1999; Davies and Miller, 2001; Nery *et al.*, 2001) and eye development (Ekker *et al.*, 1995; Macdonald *et al.*, 1995; Chiang *et al.*, 1996; Zhang and Yang, 2001). Studies on the signalling pathway of the Shh show that two transmembrane receptors, Patched (Ptc) and smoothened (Smo), are responsible for triggering the activation of its intricate signal transduction (Fig. 10, Alcedo *et al.*, 1996; Marigo *et al.*, 1996). In mammals, two isoforms of Ptc receptor encoded by *Ptc1* and *Ptc2* genes have been isolated (Carpenter *et al.*, 1998; Pearse *et al.*, 2001). Through a cascade of signalling transduction, the transcription factor Ci/Gli as the final effector acts on the chromosome DNA to active transcription of target genes (Ruiz i Altaba, 1998; Palma and Ruiz i Altaba, 2004).

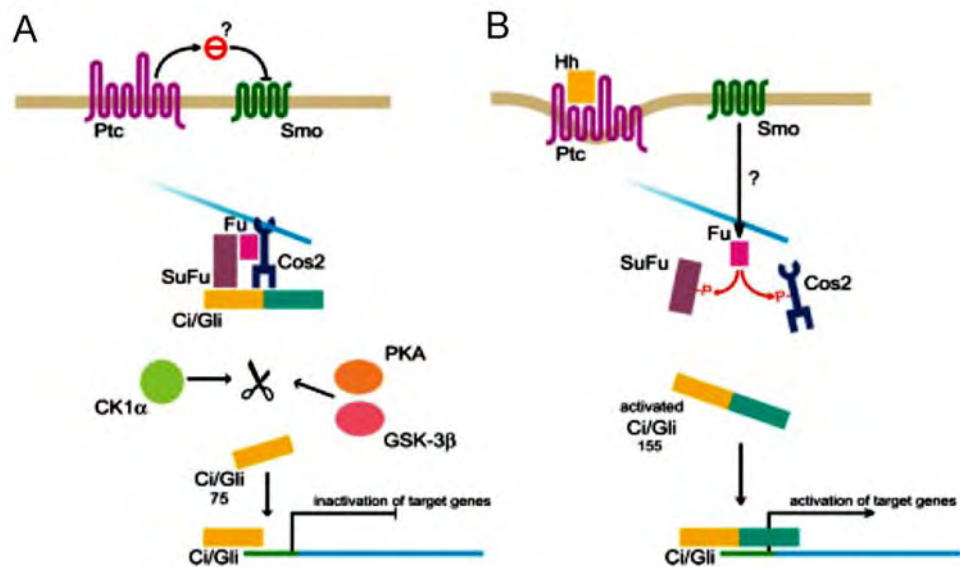


Figure 10: The signal transduction pathway of Shh

A: In the absence of Hedgehog ligand, Ptc inhibits Smo by some kind of inhibitory molecule, which could be cholesterol derivate (Beachy *et al.*, 1997; Frank-Kamenetsky *et al.*, 2002). Within the cells, Fu, Cos2, SuFu and Ci/Gli form a tetrameric microtubule-bound complex (Robbins *et al.*, 1997; Stegman *et al.*, 2000; Wang *et al.*, 2000; Nybakken *et al.*, 2002). The 155 kD large Ci/Gli protein is kept inactive and phosphorylated by PKA, GSK-3 β , CK1 α (and *Drosophila* Shaggy), and cleaved to generate a 75 kD N-terminal fragment, containing the zinc-finger DNA-binding domain (Chen *et al.*, 1999; Jia *et al.*, 2002; Price and Kalderon, 2002; Lum *et al.*, 2003). Ci/Gli75 is translocated into the nucleus and binds target genes, resulting in blockage of the transcription (Ingham and McMahon, 2001; Monnier *et al.*, 2002). B: In the presence of Hedgehog ligand, Hh binds to Ptc receptor and its subsequent internalisation alleviates the Ptc-mediated inhibition on Smo. Then Smo acts in the tetrameric complex through unknown mechanisms leading to phosphorylation of SuFu and Cos2, thus cause Ci/Gli to loosen from the complex. Thereby the full-length Ci/Gli protein is translocates into the nucleus and activates transcription of Hedgehog target genes at proper DNA consensus position (Ruiz i Altaba, 1998). Blue stripe, microtubule; taupe band, cell membrane. Scissors indicate cleavage of Ci/Gli protein. p depicts the phosphorylation states of a protein. Stop sign represents the hypothesized small inhibitory molecule pumped out of the cell by Ptc.

Abbreviations: Ci, Cubitus Interruptus; CK1 α , Casein Kinase 1 α ; Cos2, Costal2; Fu, the kinase Fused; Gli, Glioma-associated oncogene; GSK3 β , Glycogen Synthase Kinase 3 β ; Hh, hedgehog; PKA, Protein Kinase A; Ptc, Patched; Smo, Smoothened; SuFu, Suppressor of Fused. (From Bijlsma *et al.* 2004.)

A Small GTP-binding Protein Rab23

Transport vesicles are essential for cells to function normally, in that they are used to distribute proteins and other molecules to appropriate locations intracellularly. Small GTP-binding proteins (GTPases) play crucial roles on the formation and movement of these vesicles. Rab proteins are a large family of monomeric *ras*-related GTPases, which are guanine nucleotide-binding trimeric proteins that reside in the plasma membrane. In eukaryotic cells, more than 60 Rab members have been reported till now. All of them contain ≈ 200 amino acids and are activated by replacement of GDP with GTP (Lewin, 2000; Zerial and McBride, 2001).

Recently one of small GTP-binding proteins - Rab23 is proposed to be a negative regulator for Shh and influences neural patterning in the spinal cord (Eggenchwiler *et al.*, 2001), and thus it may also function in the rest parts of the neural tube. *opb* mutants (open brain, an autosomal recessive mutation) exhibit defects in the neural tube closure, resulting in spina bifida (Gunther *et al.*, 1994; Sporle *et al.*, 1996; Sporle and Schughart, 1998). The *opb* gene encoding Rab23 protein is mapped in Chromosome 1 in mouse and Chromosome 6 in human (Gunther *et al.*, 1997; Eggenchwiler *et al.*, 2001; Marcos *et al.*, 2003). Eggenchwiler *et al.*'s work (Eggenchwiler and Anderson, 2000; Eggenchwiler *et al.*, 2001) shows that in the deficiency of Rab23 some dorsal cell types are absent and special proteins for ventral cell types, including Shh, expand into dorsal neural tube (Fig. 11). Such manifestations in neural tube are characteristics of overactive Shh signalling. Interestingly, *opb/Shh* double knockout mice not only rescue the size of embryos, but also show a reasonably normal positioning of ventral cells, such as floor plate cells and V3 interneurons, in comparison to *Shh* mutants, but the dorsal phenotype is still visible. These data suggest Rab23 and Shh play opposing roles in

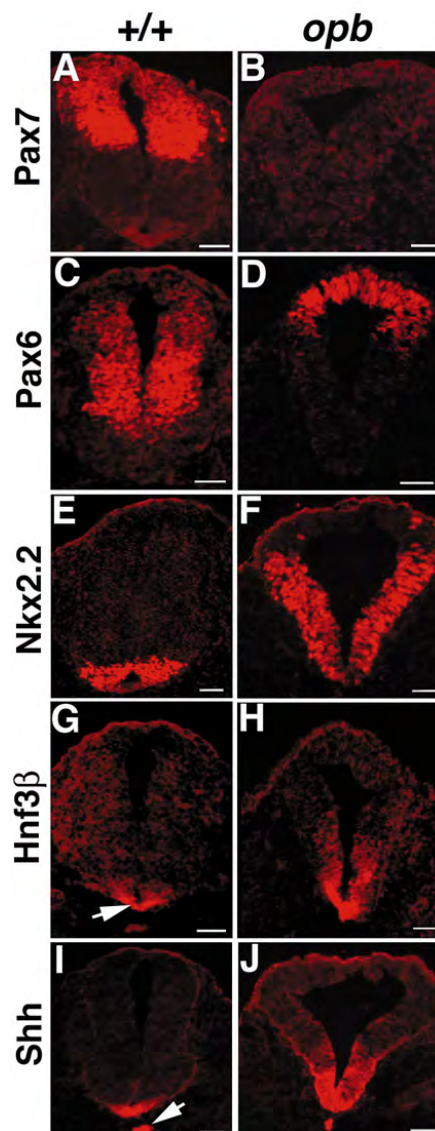


Figure 11: The expression of neural markers in *opb* mutants.

Wildtype (+/+) and *opb* E10.5 murine neural tubes with immunofluorescent staining are shown in transverse sections. In *opb* mutant, Pax7 is not found (B); Pax6 is expressed highest in the most dorsal cells, but not in lateral cells (D); Nkx2.2 expression expands to dorsal region (F); Hnf3 β and Shh display an expanded domain besides floor plate (H, J). (Photographs from Eggenchwiler and Anderson, 2000.)

dorsoventral patterning of the spinal cord: Rab23 is required for the induction of dorsal neural cell types, while Shh is required for ventral cells, and further Rab23 seems to silence the Shh signalling pathway dorsally.

Rab proteins act as GTPases for GDP-GTP exchange and function in the secretion of proteins and intracellular endocytosis, suggesting that Rab23 might be involved in the vesicular transport of particular molecules that play an important role in neural patterning. Studies have shown that GEFs catalyse the exchange of GDP for GTP on cytosolic Rab proteins and result in conformational changes of Rab proteins that thus can bind to vesicles. After vesicle fusion occurs, the hydrolysis of the bound GTP to GDP triggers the release of Rab proteins that are maintained inactive by GDI till undergo another cycle (Lodish *et al.*, 2000; Paduch *et al.*, 2001). In this process, Rab proteins serve as ‘receptors’ for motor proteins to regulate membrane traffic by determining the specificity of transport vesicle docking and fusion along with cognate SNAREs, and its absolute amount controls the rate of vesicle fusion (Hua and Scheller, 2001; Hammer and Wu, 2002). Vesicle transport is achieved with the help of specific microtubule - or actin - based motor proteins on cytoskeletal tracks. In the long-range vesicle transport, microtubule motors drive vesicles with cytoplasmic dynein towards the minus ends of microtubules located adjacent to the nucleus, whereas with kinesin towards either minus or plus ends distributed near the peripheral cortex (Bray, 1992). Following the long-range transport on microtubules, vesicles undergo local movements on F-actin towards the barbed end of the actin filament at the cell cortex, that are powered by members of myosin superfamily (Kuznetsov *et al.*, 1992; Wu *et al.*, 2000). It has been reported the interplay of the microtubule and actin motors and myosin V with several Rab members, such as Rab 1, 5, 6, 9, 11 and 33b (Echard *et al.*, 1998; Zheng *et al.*, 1998; Nielsen *et al.*, 1999; Schlierf *et al.*, 2000; Wilson *et al.*, 2000; Bahadoran *et al.*, 2001; Lapierre *et al.*, 2001; Barbero *et al.*, 2002). However, so far the might function of Rab23 on vesicular transport has not been reported.

Methods of Gene Repression in Chick Embryos

RNA Interference

In the past few years, RNA interference (RNAi) has emerged as a research tool for sequence-specific down-regulation of gene expression, allowing much more rapid characterisation of the function of known genes. Introduction of double-stranded RNA (dsRNA) can induce the degradation of its specific complementary mRNA targets posttranscriptionally. The first hints of the existence such a gene silencing phenomenon referred to as “cosuppression” emerged from the genetic modified plants in the late 1980s (Napoli *et al.*, 1990; van der Krol *et al.*, 1990). Soon after, a similar phenomena were observed in the filamentous fungus *Neurospora crassa* (named “quelling”, Romano and Macino, 1992; Cogoni *et al.*, 1996), the nematode worm *Caenorhabditis elegans* (Guo and Kemphues, 1995; Fire *et al.*, 1998) and fruit fly *Drosophila melanogaster* (Kennerdell and Carthew, 1998; Hammond *et al.*, 2000). It is considered as an

evolutionarily ancient mechanism to protect organisms against viruses and to restrict the movement of transposable elements, since many RNA viruses make dsRNA intermediates in their life cycle (Waterhouse *et al.*, 2001; Hannon, 2002). Fire and his coworkers investigating the effect of dsRNA in *C. elegans* coined the name – RNAi for small pieces of dsRNA that lead to mRNA degradation. However, the gene repression by direct introduction of dsRNA was unsuccessful in mammalian cells, because a powerful interferon (IFN) response caused sequence-nonspecific mRNA degradation of many genes and rapid cell death through activation of dsRNA-dependent protein kinases PKR and 2', 5' - AS (Clemens and Elia, 1997; Stark *et al.*, 1998; Williams, 1999; Alexopoulou *et al.*, 2001; Jackson *et al.*, 2003; Persengiev *et al.*, 2004). Nevertheless, short dsRNA (< 30-nt) was unable to induce the IFN response (Elbashir *et al.*, 2001a; Harborth *et al.*, 2001), expanding this genetic approach for gene repression of interest in biological and medical fields, such as cancer, AIDS, and hepatitis (Fire, 1999; Hannon, 2002; Novina *et al.*, 2002; Caplen, 2004; Downward, 2004).

The elucidation of the RNAi machinery is mainly based on studies with *C. elegans* and *Drosophila* (Fig. 12, Hutvagner and Zamore, 2002b; Zamore, 2002). RNAi is typically initiated by the ATP - dependent, processive cleavage of long dsRNAs into 21 – 23 nt fragments - small interfering RNAs (siRNAs) by Dicer (Zamore *et al.*, 2000; Elbashir *et al.*, 2001a), a dsRNA-specific endonuclease of RNase III family (Bernstein *et al.*, 2001). Dicer-generated siRNAs are then incorporated into RNA-protein complex (siRNP), also named the RNA-induced initiation of transcriptional gene silencing complex (RITS, Verdel *et al.*, 2004). When unwinding the double-stranded siRNA, siRNP becomes active RNA-induced silencing complex (RISC, Hammond *et al.*, 2000), which carries out the destruction of mRNAs as an effector. With little or without ATP, the RISC recognizes a target mRNA complementary to the guide strand of the siRNA and cleave it across the middle position of the siRNA (Elbashir *et al.*, 2001c; Nykanen *et al.*, 2001). Each RISC at least contains a single-stranded siRNA, a ribonuclease, and Ago2 (Elbashir *et al.*, 2001c; Nykanen *et al.*, 2001). Ago2, a member of PPD family involving in germ cell and stem cell generation, is required for the RNA cleavage (Hammond *et al.*, 2001). The ribonuclease in RISC (named 'Slicer') has not been identified yet, however, it should be distinct from Dicer (Yang *et al.*, 2000; Bernstein *et al.*, 2001; Elbashir *et al.*, 2001b). Recent studies suggest that *Drosophila* Dicer 1 and 2 are also components of RISC, and Dicer 2 assembles into the complex with the siRNA (Lee *et al.*, 2004; Pham *et al.*, 2004).

Interestingly in worms, RNAi can not only spreads throughout the entire animal but also be inherited through multiple generations (Grishok *et al.*, 2000). Gene screening in plants, fungi, and worms identifies a family of proteins, RNA-dependent RNA polymerases (RdRPs, Cogoni and Macino, 1999; Dalmay *et al.*, 2000; Mourrain *et al.*, 2000; Sijen *et al.*, 2001), which might mediate the amplification of either dsRNAs or siRNAs. Some evidences suggest that the RdRPs can synthesize new dsRNA using the guide siRNAs (primary siRNAs) as primers and target mRNAs as templates. Thereby, Dicer converts these auto-synthesized dsRNA into new siRNAs (secondary siRNAs), which are released to additional rounds

of synthesis or target destruction (Hamilton and Baulcombe, 1999; Catalanotto *et al.*, 2002; Han and Grierson, 2002). Although RNA-templated RNA synthesis is detected in *Drosophila* embryo lysates (Lipardi *et al.*, 2001; Nykanen *et al.*, 2001), RdRP homologues have not been identified in flies or humans. This could explain the fact that the gene repression in human cells recovers in 4 to 6 days after a siRNA treatment (Holen *et al.*, 2002). Unprimed or prime-independent synthesis of dsRNA from ‘aberrant’ RNA by RdRP is thought to trigger cosuppression in plants (Napoli *et al.*, 1990).

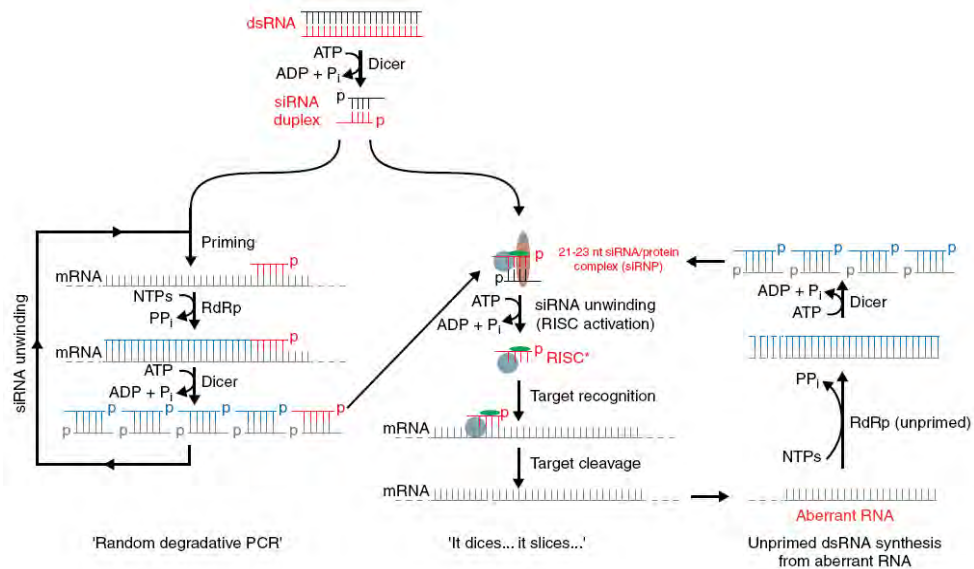


Figure 12: The mechanism of RNA interference

In this model, the sequential action of Dicer (to generate siRNAs) and ‘Slicer’ (to cleave the target RNA) are considered the primary route for target destruction. Amplification of the siRNAs is postulated to occur by either ‘random degradative PCR’ or unprimed synthesis from aberrant RNA — that is, the copying of the target RNA or a cleavage product of the target RNA by RdRp to generate a dsRNA substrate for Dicer, thereby creating new siRNAs. In the random degradative PCR scheme, the mRNA is envisioned to be primed by a siRNA guide strand. Conversion of aberrant RNA to dsRNA is drawn primed-independently.

Abbreviations: dsRNA, double-stranded RNA; RdRP RNA-dependent RNA polymerase; RISC, RNA-induced silencing complex; siRNA, small interfering RNA. (From Hutvagner and Zamore, 2000b.)

Recently, a large number of small RNA molecules called miRNAs expands the field of RNAi in practice (Lagos-Quintana *et al.*, 2001; Lee and Ambros, 2001; Rajewsky, 2006; Scherr and Eder, 2007; Wang *et al.*, 2007). miRNAs represent a class of endogenous siRNA-like noncoding RNAs with the same size of siRNA, and coordinate many aspects of cellular function including development, differentiation, proliferation and apoptosis (Reinhart *et al.*, 2000; Hutvagner and Zamore, 2002a; Mendell, 2005). Another RNase III, Drosha clips pri-miRNAs in the nucleus into ~70-nt pre-miRNAs, that are then exported from the nucleus and cleaved again by Dicer into mature ~22-nt miRNAs (Lee *et al.*, 2003). Deletion of Dicer homologues in *C. elegans* and *Arabidopsis*, for example, disrupts their development due to the defect of short temporal RNAs (stRNAs, Ray *et al.*, 1996a; Ray *et al.*, 1996b; Jacobsen *et al.*, 1999; Grishok *et al.*, 2001; Ketting *et al.*, 2001; Knight and Bass, 2001).

Morpholino Oligonucleotides

Antisense DNA oligonucleotides bind to mRNA and can prevent synthesis of the protein. They are used as a genetic approach to down-regulate gene expression in cells and animals in the past two decades. A typical antisense DNA oligonucleotide consists of 18 - 25 nucleotides, which binds to complementary sequence from a target mRNA of interest and destroy it, and are dramatically successful in some instances (Zamecnik and Stephenson, 1978; Nieto *et al.*, 1994; Srivastava *et al.*, 1995; Runyan *et al.*, 1999). However, the results are often inconsistent *in vivo* due to rapid dispersal and degradation themselves, and nonspecific and toxic side-effects. Novel chemically modified nucleotides, such as phosphorothioate oligos (S-DNAs), RNase H-independent 2'-*O*-methoxyethyl oligos (2'-*O*-MOE), peptide nucleic acids (PNA), locked nucleic acid (LNA), offer reasonable resistance to nucleases and enhance their target affinity (Matsukura *et al.*, 1987; Baker *et al.*, 1997; Kumar *et al.*, 1998; Larsen *et al.*, 1999; Tyler *et al.*, 1999; Malchere *et al.*, 2000; Pooga and Langel, 2001; Sazani *et al.*, 2002; Turner *et al.*, 2006; Boffa *et al.*, 2007). They offer reasonable resistance to nucleases and exhibit good efficacy in cell-free translation systems. However, they still suffer from serious flaws (Summerton and Weller, 1997; 1999). Morpholino oligonucleotides (named morpholinos) are introduced as an alternative method for gene repression since 2000 and proved advantages to other DNA oligos. They interrupt mRNA translation by steric blocking of the translation initiation complex (Fig. 13), unlike RNase-H-dependent antisense DNA oligos. They exhibit a high affinity for RNA and efficiently invasion into stable secondary structures of mRNAs. Especially, non-toxicity, minimal side-effects and sequence specificity provide reliable results in cell cultures and embryos (Heasman, 2002). Morpholinos can be delivered into the cytosol or nucleus by scraping the culture cells or through an ethoxylate polyethylenimine (EPEI) complex (Morcos, 2001). Up to now, morpholinos have been successfully used in a range of organisms, including sea urchin, ascidian, zebrafish, frog, chick, mouse and human (Lacerra *et al.*, 2000; Nasevicius and Ekker, 2000; Audic *et al.*, 2001; Coonrod *et al.*, 2001; Howard *et al.*, 2001; Kos *et al.*, 2003).

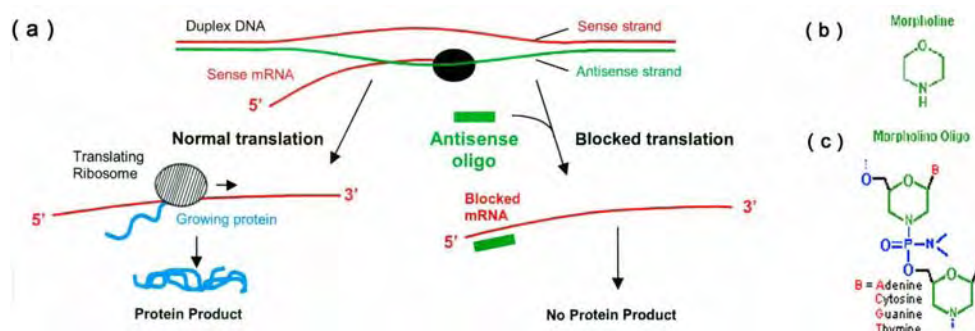


Figure 13: Inhibition of morpholino oligonucleotides on gene function

(A) Translation was blocked due to mRNA bound to morpholino oligonucleotides. (B) Structure of morpholino ring. (C) A short segment of morpholino oligo composed of two morpholino subunits. Morpholinos have four different subunits, each of which contains one of the four genetic Bases (Adenine, Cytosine, Guanine, and Thymine) linked to a 6-membered morpholino ring. 18 to 25 subunits of these four subunit types are joined in a specific order by non-ionic phosphorodiamidate intersubunit linkages to give a morpholino oligo. (Photographs modified after Gene Tools, LLC.)

Why Still Working With Chick Embryos?

The avian embryo is a classic model used widely in developmental biology to investigate questions of vertebrate development since the beginning of comparative and experimental embryology. The easy and cheap accessibility of the embryo for *in ovo* and *ex ovo* experiments all around the year make it an ideal animal model to work with. New Cultures and Petri dish cultures of the entire embryos make it possible to watch and manipulate *in vivo* at gastrulation or neurulation stage. Tissue transplantation and ablation allow to studying the influence of time and surround on cells and tissue. Quail – chick grafting and fluorescent labelling of cell lineages have generated a wealth of information on cell migration and lineage relationships during chick embryogenesis. To investigate specific molecules transplantation of secreting cells or soaked beads engrafting could be applied. (Le Douarin, 1973; Couly *et al.*, 1993; Clarke and Tickle, 1999; Lee *et al.*, 2001; Schoenwolf, 2001; Tumpel *et al.*, 2002). The use of chicken embryos as a model system has led to many significant discoveries of developmental processes, such as the role of the apical ectodermal ridge in the developing limb (Summerbell and Lewis, 1975), the migration and differentiation of neural crest cells (Le Douarin and Teillet, 1973), and the role of the notochord for the establishment of neural patterns (Teillet and Le Douarin, 1983). However, the use of chick embryos still suffers from some limitations due to the absence of established methods for genetic manipulation, for example, targeted or chemical mutagenesis and transgenic analysis are not routinely available in chick embryo.

Only recently new approaches could compensate this disadvantage. A modified electroporation using a low voltage enables to deliver DNA into tissues, animals and living embryos. In chick embryos this *in ovo* electroporation can be used to introduce or overexpress specific genes into a definite region (Muramatsu *et al.*, 1997; Itasaki *et al.*, 1999). The ectopic expression of a target gene in transfected cells can last a few days and several generations. However, loss-of-function approaches are still achieved difficultly. siRNAs (small interfering RNAs) and morpholino oligonucleotides can block protein translation in many species *in vivo*. Both antisense-based methods could also be introduced into chick cells or embryos in same way (Bourikas and Stoeckli, 2003; Katahira and Nakamura, 2003; Kos *et al.*, 2003; Pekarik *et al.*, 2003). Specifically for my work was that the obvious difference of the structures between dorsal and ventral midbrains, lamina in dorsal and nucleus in ventral, the similarity to mammalian development and the easy access together with the new approaches available makes the chick mesencephalon an ideal model system to investigate the dorso-ventral (DV) patterning of the neural tube.

Aim of The Project

The development of the central nervous system is a notable process during the life of every creature. Although the complexity of the nervous system of different species exhibits obvious distinctions, the formation of the central nervous system follows similar ways, such as the neural induction, the neural tube formation, the compartmental demarcation, the neuronal cell type generation, and the neuronal migration. Functional domains in nervous system consist of a variety of neurons with their functional connection. For a single neuron, its specific fate and function are determined by a large amount of exogenous and intrinsic signals during the development, and its location provide positional information along anterioposterior and dorsoventral axes.

The dorsal and ventral regions in the central nervous system function differently, and show significant differences on gene expression since early embryonic stage. However, the dislocated cells always demonstrate a migratory tendency prone to the original position in transplantation experiments. This suggests that it might exist a distinction on the physical properties of both cells. Several questions are investigated here: when midbrain precursor cells are determined to commit to a ventral or dorsal fate, when a specific gene is expressed independently in those cells if morphogenes lose their influences on that gene, and if determined cells have already possessed specific cell properties, in that one cell population should not mix for while with their different neighbours.

An expansion of some brain regions happens before neurogenesis began, not only in avian embryos but also in mammals. However, this expansion does not occur in the spinal cord. Clearly essential for this expansion is a precise coordination of gene expression pattern formation and neuronal proliferation. Thus, a single model with opposing gradients of organizer molecules along the DV axis might be insufficient for DV patterning in neural tube. Additional mechanisms could convey positional identity to early precursor pools laying in a considerable distance to the midline structures. Chick midbrains are used as a model, due to being one of the faster growing brain region, and easy accessible for *in vivo* manipulations like transplantations and for gene misexpression with *in ovo* electroporation. Position-marked proteins, such as transcription factors encoded by *pax* and *nkx* genes, are used to find the answer based on cell proliferation and differentiation.

With the time, more genes related with DV specification of nervous system have been identified, like Rab23, Gli3. Their function in the DV processing and their signalling pathway need to be investigated further. Because the transgenic or mutant avian embryos or cell lines are difficult to obtain till now, molecular techniques for gene repression have been tried in chick embryos, such as RNA interference, morpholinos.

Materials

Avian Embryos

Experiments were performed with chick and quail embryos. Fertilized Ross hen eggs (*Gallus gallus*) and Japanese quail eggs (*Coturnix coturnix japonica*), obtained from the “Bayrische Landesanstalt für Kleintierzucht in Kitzingen”, Germany, were stored at room temperature (18°C) and incubated at 37°C and 65% relative humidity in a climate chamber or an incubator. Chicken embryos after laying were staged (HH) according to the protocol of Hamburger and Hamilton (1951), they gave a detail description of each stage and marked their important changes in morphogenesis (Tab. 1). Quail embryos develop faster and are born 3-4 days shorter than chick embryos, their development is described by Zacchei (1961) & Senut and Alvarado-Mallart (1986).

Bacterial Strains

E. coli strains were used in transformation experiments. Competent *XLI-Blue MRF'* cells (Stratagene, Amsterdam) were used to transform supercoiled plasmids. Highly efficient *JM 109* cells ($>10^8$ cfu/ μ g, Promega, Mannheim) were used for transformations of newly subcloned genes. *SURE*[®]2 supercompetent cells (Stratagene, Amsterdam), which can easily accept the plasmids constructed to transcribe hairpin dsRNA, were used in RNAi experiments. Above of these strains allow blue-white color selection of transformed clones. *One Shot*[®] *TOP10* chemically competent cells (Invitrogen life technologies, Karlsruhe), got with TOPO TA Cloning[®] kit for Sequencing, were used specially for the transformation of pCR[®]4-TOPO[®] vector.

Table 1: The early stages of chick and quail embryos

Hamburger & Hamilton classified chick embryos in stages according to their morphogenesis and incubation time at 37°C. Stages 7 - 14 are based primarily on the numbers of somite pairs. Zacchei staged quail embryos (1961). E: embryonic day.

| Chick (HH) | Incubation | Description | Quail stage |
|------------|--------------------|---------------------------------------|-------------|
| 1 | | <i>Pre-streak</i> | |
| 2 | 6 – 7 h | <i>Initial streak</i> | |
| 3 | 12 – 13 h | <i>Intermediate streak</i> | |
| 4 | 18 – 19 h | <i>Definitive streak</i> | |
| 5 | 19 – 22 h | <i>Head-process</i> | |
| 6 | 23 – 25 h | <i>Head fold</i> | |
| 7 | 23 – 26 h | <i>1 somite</i> | |
| 8 | 26 – 29 h | <i>4 somites</i> | |
| 9 | 29 – 33 h | <i>7 somites</i> | 7 – 8 |
| 10 | 33 – 38 h | <i>10 somites</i> | 8 – 10 |
| 11 | 40 – 45 h | <i>13 somites</i> | |
| 12 | 45 – 49 h | <i>16 somites</i> | |
| 13 | 48 – 52 h | <i>19 somites</i> | 13 |
| 14 | 50 – 53 h | <i>22 somites</i> | |
| 15 | 50 – 55 h | <i>Limb primordia</i> | |
| 16 | 51 – 56 h | <i>Tail bud distinct</i> | |
| 17 | 52 – 64 h | <i>Epiphysis</i> | |
| 18 | E 3 | <i>Allantois distinct</i> | 16 – 17 |
| 21 | E 3 ^{1/2} | <i>Eye pigmentation faint</i> | |
| 23 | E 4 | <i>Wing/leg buds as long as width</i> | 18 |
| 24 | E 4 ^{1/2} | <i>Toe plate distinct</i> | |
| 26 | E 5 | <i>Toe plate demarcation</i> | 20 |

Clones

Chick EST clones (MRC geneservice, Cambridge) were selected as templates to transcribe RNA probes for detecting mRNAs of *Pax7*, *Rab23* and *smoothed (smo)* in chick embryos (Tab. 2). These gene fragments are isolated from different embryonic or adult chick tissues and subcloned into pBluescript II KS+ vector (Boardman *et al.*, 2002).

Table 2: Chick EST clones

| Clones Nr. | Length of Inserts (bp) | Genes |
|-------------|------------------------|--------------|
| ChEST23i17 | ~ 700 | <i>Pax7</i> |
| ChEST329n14 | ~ 850 | <i>Pax7</i> |
| ChEST861p22 | ~ 900 | <i>Pax7</i> |
| ChEST545g23 | ~ 800 | <i>Rab23</i> |
| ChEST885j22 | ~ 750 | <i>Rab23</i> |
| ChEST925k6 | ~ 850 | <i>Rab23</i> |
| ChEST75d14 | ~ 1050 | <i>Rab23</i> |
| ChEST772o6 | ~ 1100 | <i>Rab23</i> |
| ChEST89m23 | ~ 850 | <i>Smo</i> |
| ChEST826i17 | ~ 650 | <i>Smo</i> |

Plasmids

6 plasmids were used in the studies.

pMES Vector

pMES vector was used as an expression vector for cloning chick *Pax7* and *Rab23* in this study. One interest gene with an EGFP (enhanced green fluorescent protein) reporter can be transcribed at same time from a single bicistronic mRNA, which is achieved by an internal ribosome entry site (IRES) of the *Encephalomyocarditis Virus* (ECMV), situated between a MCS and an EGFP coding region. EGFP is a recombinant version of the *Aequorea victoria* green fluorescent protein that is enhanced for high-level expression in mammalian cells (Bierhuizen *et al.*, 1997). The expression level of EGFP is proportional to that of the gene of interest, in that it can define the extent of transfected region. Efficient ubiquitous expression in chick is achieved by the use of a *Cytomegalovirus* (CMV) enhancer fused to a chicken β -actin promoter and a rabbit β -globin 3'UTR that includes the Poly (A) motif. The vector backbone is taken from pCAX, a pCAGGS derivative vector. The pMES is composed of 5,538 bp and includes an ampicillin resistance gene (Swartz *et al.*, 2001). Genes for cloning into the MCS are required start and stop codons. A schematic map of the pMES vector is shown in Fig. 87. This vector was a kind gift from Dr. Christine Krull (University of Missouri-Columbia, USA).

pBluescript[®] II KS (+/-) Phagemid Vector

pBluescript[®] II KS (+/-) phagemid vectors (Stratagene) are used common in molecular biology. To make the templates of RNA probes for in situ hybridization, partial CDS of a gene is inserted into the MCS. pBluescript II KS vectors (Fig. 88) contain T3 and T7 RNA polymerase promoters for *in vitro* transcription, an ampicillin-resistant gene and a *lacZ* promoter for clones' selection. It is a 2961 basepair phagemid derived from pUC19. The KS designation indicates the polylinker is oriented from *KpnI* to *SacI*.

pCR[®]4-TOPO[®] Vector

pCR[®]4-TOPO[®] vectors (3957bp) are used for fast cloning of *Taq* polymerase-amplified PCR products (Fig. 89). TOPO TA Cloning[®] Kit for DNA Sequencing including linearized pCR[®]4-TOPO[®] vector, was ordered from Invitrogen life technologies, Karlsruhe. This linearized vector has a single 3' deoxythymidine (T) overhang in cloning site, which is cleaved by Topoisomerase I from *Vaccinia* virus after 5'-CCCTT in one strand (Shuman, 1991). This allows the vector accept PCR products with single 3' deoxyadenosine (A) end, which can be achieved by the nontemplate-dependent terminal transferase activity of *Taq* polymerase (Shuman, 1994). This vector contains ampicillin and kanamycin resistance genes. Moreover, the *ccdB* gene, a lethal *E. coli* gene, is disrupted by insertion of PCR fragments, which permits growth of only positive recombinants upon transformation in *One Shot[®] TOP10* cells.

pDrive Cloning Vector

pDrive cloning vectors (QIAGEN, Hilden) was used to clone partial CDS of *Patched1* (*Ptc1*) from chick embryos. Linearized vector is composed of 3.85kb and has a U overhang at each end for insertion of a PCR product, which has an opposite A residue. The MCS is flanked by T7 and SP6 RNA polymerase promoters, and Ampicillin and Kanamycin resistant genes are contained in this vector. M13 forward and reverse primers can be used for sequencing the inserts.

pCA β -GFP Vector

pCA β -GFP vectors (~ 5.45kb) were used as a co-injection vector with morpholino oligos or p*Silencer*TM1.0-U6 siRNA expression vector to define the transfected region. This vector is derived from pCAGGS vector, with mGFP6 inserted into *Bam*HI & *Xho*I sites of the polylinker downstream from CAG promoter/CMV-IE enhancer, and the mGFP6 can produce a brighter green fluorescence in eukaryotic cells. It contains a rabbit β -globulin 3' poly (A) sequence. This vector was a kind gift from Dr. Jonathon Guilthorpe (King's College, London, UK).

p*Silencer*TM 1.0-U6 siRNA Expression Vector

p*Silencer*TM 1.0-U6 siRNA expression vector is designed for transcription of siRNA in mouse cells (Sui *et al.*, 2002) and obtained from Ambion (Austin, TX). It is a 3.24kb vector, containing sequence elements for cloning and bacterial replication, i.e. f1 origin, Cole1 origin, Ampicillin resistance gene, and MCS (Fig. 90). A mouse U6 RNA Polymerase III promoter is cloned into the *Kpn*I and *Apa*I sites to drive the transcription of siRNAs (Miyagishi and Taira, 2002). *Apa*I and *Eco*RI sites adjacent to the U6 promoter is used for double-stranded siRNA insert. In this study selected DNA fragments transcribed to siRNA for chick *Pax7* gene were inserted here.

Morpholinos

Morpholino antisense oligonucleotides (Gene Tools, LLC, Philomath) were used to knockdown *cPax7* and *cRab23* in chick embryos (Tab. 3). They are 25 mers complementary to the 5' UTR or the initial sequences of target genes. Due to the high GC % content in 5' UTR of *cPax7*, the oligo sequences are a little far from start codon. All of them are designed by Dr. Shannon Knuth (Gene Tools, LLC).

Table 3: Morpholino oligonucleotides

| Morpholinos | Sequence (5' -3') | Location | Genes |
|-------------|----------------------------|----------|---------------|
| Rab23-MO1 | CACCTCCATGTCCTTCTTCCAACATC | -1 ~ +24 | <i>cRab23</i> |
| Rab23-MO2 | GCAGCTCAGGTGACTCTCTGGCTTA | -20 ~-5 | <i>cRab23</i> |
| Pax7-MO1 | TGCGGAGCGGGTCACCCCGAACCC | -50 ~-26 | <i>cPax7</i> |
| Pax7-MO2 | GCTCTCTCTCGTGTCCGGTAGCTGA | -98 ~-74 | <i>cPax7</i> |

Oligonucleotides

PCR and RT-PCR primers were used for cloning from DNA templates or messenger RNAs (Tab. 4), and some primers were designed especially for DNA sequencing (Tab. 5). Antisense DNA oligonucleotides complementary to initial sequence of interest genes were used in RNAi experiments (Tab. 6). Several pairs of oligonucleotides were designed to transcribe shRNAs in RNAi experiments (Tab. 7). All of primers are ordered from MWG Biotech, Ebersberg and SIGMA-ARK, Steinheim.

Table 4: PCR/RT-PCR primers

| Name | Sequence (5' –3') | GC % | T _m (°C) | RE | f/r |
|---------|-----------------------------------|------|---------------------|--------------|-----|
| p7-5s1 | CGGAATTCGCGATCCGGCCCTGCGTCATCTC | 64.5 | 74.8 | <i>EcoRI</i> | f |
| p7-5as1 | GCTCTAGAGCCCGGATTCCAGCTGAACATC | 57.6 | 73.2 | <i>XbaI</i> | r |
| p7-5as2 | GCTCTAGAGCTCCGAACTTGATTCTGAGCACTC | 52.9 | 71.9 | <i>XbaI</i> | r |
| p7-5as3 | GCTCTAGAGCGGTTCCCTTTGTCGCCAGGAT | 59.4 | 73.3 | <i>XbaI</i> | r |
| p7-3s1 | GCTCTAGAGCCGGGAAGAAAGAGGACGACGAG | 59.4 | 73.3 | <i>XbaI</i> | r |
| p7-3s2 | GCTCTAGAGCGGACCGCTGGCTGAAGGAC | 65.5 | 73.7 | <i>XbaI</i> | r |
| p7-3as1 | CGGAATTCGCGGGCACGCCGTTACTGAA | 62.1 | 72.3 | <i>EcoRI</i> | f |
| cp7f1 | ATTCTAGACGGGGTTCGGGGGTGAC | 60.0 | 67.9 | <i>XbaI</i> | f |
| cp7r1 | GTGGATCCAAGTTGCTGGAGTGGGTTG | 55.6 | 68.0 | <i>BamHI</i> | r |
| cp7f2 | ATTCTAGAGCCTTCAGCTACCGGACACG | 53.6 | 68.0 | <i>XbaI</i> | f |
| cp7r2 | GTGGATCCAGATCCTGGAAGCTGGTAGT | 53.6 | 68.0 | <i>BamHI</i> | r |
| opbf1 | CGCTCTAGATCGGATTGATAGATTTCGTGA | 44.8 | 65.3 | <i>XbaI</i> | f |
| opbr1 | ATCCCGGGTCCCATAGGCACAAGATTT | 51.9 | 66.5 | <i>Cfr9I</i> | r |
| opbf2 | CGCTCTAGATGAGCTGCAGAGATGTTGG | 53.6 | 68.0 | <i>XbaI</i> | f |
| opbr2 | ATCCCGGGTCCCAAGCAGCCTAAG | 62.5 | 67.8 | <i>Cfr9I</i> | r |
| opbr3 | CGCGGATCCCATAGGCACAAGATTT | 52.0 | 64.6 | <i>BamHI</i> | r |
| opbr4 | ACCAAGCAAAGGATCCCATAGGCACAA | 50.0 | 64.8 | <i>BamHI</i> | r |
| cp7c2f1 | GCTCTAGAGCGAAGGGGAGAATC | 56.0 | 66.3 | <i>XbaI</i> | f |
| cp7c2r1 | GGGGTACCCACCTCAGCCTTATC | 62.5 | 67.8 | <i>KpnI</i> | r |
| cp7c2f2 | GCTCTAGAGCTCAACGACATCATGAAG | 48.1 | 65.0 | <i>XbaI</i> | f |
| cp7c2r2 | GGGGTACCCCTTGTACAGTAGGTG | 58.3 | 66.1 | <i>KpnI</i> | r |

Blocks in yellow indicate the recognitive sequences of restriction enzymes (RE) listed in right column.

Table 5: Primers for DNA sequencing

U6m1 and U6m2 primers locate in the mouse U6 promoter of p*Silencer* 1.0-U6 siRNA expression vectors.

| Primer | Sequence (5' –3') | T _m (°C) |
|-------------|------------------------|---------------------|
| pMESfo1 | TCATGCCTTCTTCTTTTCTACA | 57.6 |
| pMESre1 | GCCAGGTTTCCGGGCC | 59.4 |
| pMESfo3 | TTCGGCTTCTGGCGTGTGA | 58.8 |
| pMESre4 | GTTTCCGGGCCCTCACATT | 58.8 |
| T3 | ATTAACCCTCACTAAAG | 45.5 |
| T7 | AATACGACTCACTATAG | 45.5 |
| M13 forward | GTAAACGACGGCCAGT | 48.0 |
| M13 reverse | CAGGAAACAGCTATGAC | 48.0 |
| U6m1 | GGAAACTCACCTAAC | 49.0 |
| U6m2 | TTACATGATAGGCTTG | 48.5 |

Table 6: Antisense DNA oligonucleotides

Each of antisense DNA oligonucleotides is composed of 19 - 21 nucleotides in length, complementary to the mRNA sequences of *cPax7*, *cPax3* or *cRab23* respectively. One DNA oligo for each gene contains ATG start codon binding site.

| Antisense oligo | Sequences (5' -3') | Location | Genes |
|-----------------|-------------------------------|-------------|---------------|
| cP3Di1 | CCCCGGCCAGCGTGGT CATCG | -2 ~ +19 | <i>cPax3</i> |
| cP3Di2 | ATGCCGTGGTGCGCCATCT | +182 ~ +200 | <i>cPax3</i> |
| cP7Di1 | CCCGGGGAGCGCTGC CATAG | -2 ~ +18 | <i>cPax7</i> |
| cP7Di2 | ATGCCGTGGTGCGCCATCT | +182 ~ +200 | <i>cPax7</i> |
| cOpbDi1 | GTCTTCTCCAA CATCTCTGC | -6 ~ +15 | <i>cRab23</i> |
| cOpbDi2 | ATCGCTGAATCATACTGGAC | +66 ~ +85 | <i>cRab23</i> |

Table 7: shRNA oligonucleotides

The sequences for shRNA oligonucleotides are selected immediately downstream of an AA dinucleotides in the ORF of target genes (Elbashir *et al.*, 2002). In the forward oligonucleotides, the 19 nt sense siRNA sequence is linked to the reverse complementary antisense by a 9 nt loop (TTCAAGAGA). 5-6 Ts are added to the 3' end; In the reverse oligonucleotides, the *EcoRI* (AATT) and *Apal* (GGCC) restriction sites are added to the 5' and 3' ends respectively (refer to Fig. 91). Each pair of forward and reverse oligonucleotides annealed to form double-stranded DNAs, which were inserted into p*Silencer* 1.0-U6 siRNA expression vectors. The pairs of oligonucleotides with *EcoRI* and *BamHI* sites were used for cloning into the pMES. All of these oligonucleotides were used in RNA interference for chick *Pax7*.

| Oligos | Sequences |
|--------|--|
| s121f | 5' - CCTCGGAGGGGTTTTCATCA -loop- TGATGAAAACCCCTCCGAG -TTTTTTAG-3' |
| s121sr | 3' -CCGGG GAGCCTCCCCAAAAGTAGT -loop- ACTACTTTTGGGGAGGCTC -AAAAATCTTAA-5' |
| s492f | 5' - CGAAAGAGGAAGAGGAGGAC -loop- GTCCTCCTCTCCTCTTTC -TTTTTTAG-3' |
| s492r | 3' -CCGGG CTTTCCTCTCTCCTCTG -loop- CAGGAGGAGAAGGAGAAAG -AAAAATCTTAA-5' |
| s549f | 5' - CGCACAGCATAGATGGCATC -loop- GATGCCATCTATGCTGTGC -TTTTTTAG-3' |
| s549r | 3' -CCGGG GCTGTCTATCTACCGTAG -loop- CTACGGTAGATACGACACG -AAAAATCTTAA-5' |
| s1206f | 5' - CAATCAGGTGATGAGCATC -loop- GATGCTCATCACCTGATTG -TTTTTTAG-3' |
| s1206r | 3' -CCGGG GTTAGTCCACTACTCGTAG -loop- CTACGAGTAGTGGACTAAC -AAAAATCTTAA-5' |
| m121f | 5' -AATTC CCTCGGAGGGGTTTTCATCA -loop- TGATGAAAACCCCTCCGAG -TTTTTTAG-3' |
| m121r | 3' - GAGCCTCCCCAAAAGTAGT -loop- ACTACTTTTGGGGAGGCTC -AAAAATCCTAG-5' |
| m492f | 5' -AATTC GAAAGAGGAAGAGGAGGAC -loop- GTCCTCCTCTCCTCTTTC -TTTTTTAG-3' |
| m492r | 3' - GCTTTCCTCTCTCCTCTG -loop- CAGGAGGAGAAGGAGAAAG -AAAAATCCTAG-5' |
| m549f | 5' -AATTC GCACAGCATAGATGGCATC -loop- GATGCCATCTATGCTGTGC -TTTTTTAG-3' |
| m549r | 3' - GCGTGTCTATCTACCGTAG -loop- CTACGGTAGATACGACACG -AAAAATCCTAG-5' |
| m1206f | 5' -AATTC CAATCAGGTGATGAGCATC -loop- GATGCTCATCACCTGATTG -TTTTTTAG-3' |
| m1206r | 3' - GTTAGTCCACTACTCGTAG -loop- CTACGAGTAGTGGACTAAC -AAAAATCCTAG-5' |

Size Standard

All used size standards are ordered from MBI Fermentas, St. Leon-Roth, Germany. Before using, 1 part DNA ladder was mixed with 2 parts Loading buffer and 7 parts TE buffer (pH8.0) to reach final concentration of 50µg/ml.

GeneRuler™ 1kb DNA ladder (0.5mg/ml)
 GeneRuler™ 100bp DNA ladder plus (0.1mg/ml)
 Loading Dye Solution 6x

Enzymes

Polymerases and Modifying Enzymes

Table 8: Polymerases and DNA/RNA modifying enzymes

| Items | Companies |
|---|---------------------------------|
| <i>Taq</i> DNA Polymerase (5U/μl) | MBI Fermentas, St. Leon-Rot |
| <i>Pfu Turbo</i> [®] DNA Polymerase (2.5U/μl) | Stratagene |
| SuperScript [™] II RNase H Reverse Transcriptase (200U/μl) | Invitrogen |
| M-MuLV Reverse Transcriptase (20U/μl) | MBI Fermentas |
| Alkaline Phosphatase, Calf Intestinal (CIP) (10U/μl) | New England BioLabs, Schwalbach |
| T4 DNA Ligase (5U/μl) | MBI Fermentas |
| Quick T4 DNA Ligase | New England BioLabs |
| T3/T7/SP6 RNAPolymerase (20U/μl) | MBI Fermentas |
| DNase I, RNase-free (10U/μl) | Roche Diagnostics, Mannheim |
| RNase A (10mg/ml) | Boehringer Mannheim |
| RNase H (10U/μl) | Peqlab, Erlangen |
| RNase Inhibitor (40U/μl) | MBI Fermentas |

Table 9a: Restriction endonucleases from MBI Fermentas

| Enzyme | Sequence (5' - 3') | Buffer |
|-----------------|--------------------|------------------------------------|
| <i>Apa</i> I | GGGCC ↓ C | B ⁺ |
| <i>Bam</i> HI | G ↓ GATCC | <i>Bam</i> HI ⁺ |
| <i>Bgl</i> II | A ↓ GATCT | O ⁺ |
| <i>Bsu</i> 15I | AT ↓ CGAT | Y ⁺ /TANGO [™] |
| <i>Cfr</i> 9I | C ↓ CCGGG | <i>Cfr</i> 9I ⁺ |
| <i>Eco</i> 32I | GAT ↓ ATC | R ⁺ |
| <i>Eco</i> RI | G ↓ AATTC | <i>Eco</i> RI ⁺ |
| <i>Hind</i> III | A ↓ AGCTT | R ⁺ |
| <i>Hpa</i> II | C ↓ CGG | Y ⁺ /TANGO [™] |
| <i>Kpn</i> I | GGTAC ↓ C | <i>Kpn</i> I ⁺ |
| <i>Mls</i> I | TGG ↓ CCA | R ⁺ |
| <i>Mlu</i> I | A ↓ CGCGT | R ⁺ |
| <i>Nor</i> I | GC ↓ GGCCGC | O ⁺ |
| <i>Pst</i> I | CTGC ↓ AG | O ⁺ |
| <i>Pvu</i> II | CAG ↓ CTG | G ⁺ |
| <i>Sac</i> I | GAGCT ↓ C | <i>Sac</i> I ⁺ |
| <i>Sma</i> I | CCC ↓ GGG | Y ⁺ /TANGO [™] |
| <i>Xba</i> I | T ↓ CTAGA | Y ⁺ /TANGO [™] |
| <i>Xho</i> I | C ↓ TCGAG | R ⁺ |

Table 9b: Restriction endonucleases from New England BioLabs

| Enzyme | Sequence (5' - 3') | Buffer |
|----------------|--------------------|-------------|
| <i>Eco</i> NI | CCTNN ↓ NNNAGG | NEB 4 |
| <i>Eco</i> RV | GAT ↓ ATC | NEB 3 + BSA |
| <i>Hae</i> III | GG ↓ CC | NEB 2 |
| <i>Sma</i> I | CCC ↓ GGG | NEB 4 |
| <i>Xba</i> I | T ↓ CTAGA | NEB 2 + BSA |
| <i>Xcm</i> I | CCANNNNN ↓ NNNNTGG | NEB 2 |
| <i>Xma</i> I | C ↓ CCGGG | NEB 4 + BSA |

Fluorescent Probes

All of fluorescent probes are purchased from Molecular Probes Europe, Leiden, Netherlands. Their excitation and emission spectra are listed below (Tab. 10).

CellTracker™ CMTMR and CMFDA

CMTMR (orange, $C_{32}H_{28}ClN_3O_4$) and CMFDA (green, $C_{25}H_{17}ClO_7$) are fluorescent chloromethyl derivatives, that diffuse freely across the membranes of living cells, but once inside the cell, these probes undergo a glutathione S-transferase-mediated reaction, producing a membrane-impermeant, aldehyde-fixable conjugates. They can be inherited by daughter cells, but not transferred among adjacent cells in a population (Boleti *et al.*, 2000).

DAPI

DAPI is a blue fluorescent multicyclic dye utilized frequently as a DNA-specific probe for flow cytometry, chromosome and plasmid DNA visualization (Haugland *et al.*, 1996). It selectively binds to AT clusters of dsDNA, and even brighter than Hoechst dyes.

SYTOX® Orange Nucleic Acid Stain

SYTOX® Orange is a high-affinity nucleic acid stain that easily penetrates cells with compromised plasma membranes and does not cross the membranes of live cells. The fluorescence can be enhanced > 500-fold upon nucleic acid binding, in that the SYTOX Orange stain may work as a single-step dead-cell indicator.

Table 10: Spectral characteristics of the fluorescent probes

| Cell Tracers | Ex(nm) | Em(nm) |
|---|--------|--------|
| CMTMR (5-(and-6)-(((4-chloromethyl)benzoyl)amino)tetramethylrhodamine | 540 | 566 |
| CMFDA (5-choloromethylfluorescein diacetate) | 492 | 516 |
| DAPI (4',6-diamidino-2-phenylindole) | 358 | 461 |
| SYTOX Orange Nucleic Acid stain | 547 | 570 |

Chemicals

Reagents

Table 11: Chemical reagents

| Items | Companies |
|-------------------------------|-----------------------|
| Acetic Acid | AppliCAM/Sigma |
| Adenosin-5'Triphosphate (ATP) | Sigma |
| Agarose, ultra pure | Invitrogen, Karlsruhe |
| Albumin-Bovine | Sigma |

| | |
|---|-----------------------------------|
| Ammonium peroxydisulfate (APS) | Merck KGaA, Darmstadt |
| Ampicillin (50 mg/ml) | Roth, Karlsruhe |
| Aqua-Poly/Mount | Polysciences, Eppelheim |
| Bacto Agar | Hartenstein, Wuerzburg |
| Bacto Yeast extract | Difco, Augsburg |
| BCIP (5-Bromo-4-chloro-3-indolyl phosphate) | La Roche |
| Bicarbonate (Na(CO ₂) ₂) | Invitrogen |
| Boehringer Blocking Reagent (BBR) | Boehringer Mannheim |
| Bromphenolblue | Sigma |
| Boric acid | Sigma |
| BSA | Sigma |
| Bovine dermal Collagen | Cellon S.A, Luxembourg |
| β-Mercaptoethanol (β-ME) | Merck |
| Calciumchlorid (CaCl ₂) | Merck, Darmstadt |
| Chloroform (CHCl ₃) | Roth, Karlsruhe |
| Citric Acid Trisodium Salt | Merck |
| Cresyl-violet Acetate | Sigma |
| Deoxycholate | Sigma-Aldrich Chemie |
| Diaminobenzidine (DAB) | Sigma |
| Diazabicyclo(2.2.2.)octan (DABCO) | Merck |
| Diethyldicarbonat (DEPC) | Merck |
| DIG RNA labeling mix, 10x | Roche Diagnostics, Mannheim |
| Dimethylformaldehyd (DMF) | Sigma |
| Dimethylsulfoxide (DMSO) | Merck, Sigma |
| Dispase I | La Roche |
| Dithiothreitol (DTT) | Sigma |
| DNase, RNase-free | GIBCO BRL, Karlsruhe |
| dNTP mix, 10mM | MBI Fermentas/Invitrogen |
| Entellan | Merck |
| Eosin Yellowish | Polysciences, Eppelheim |
| Ethanol (EtOH, 95%) | AppliCAM |
| Ethidium bromide (10 mg/ml) | Boehringer, Mannheim |
| Ethylenediaminetetraacetic acid (EDTA) | Sigma |
| Fast Green FCF | Sigma |
| Fast Red | Sigma-Aldrich Chemie, Deisenhofen |
| Fetal Calf Serum (FCS) | Invitrogen |
| FITC RNA labeling mix, 10x | Roche, Mannheim |
| Formaldehyde (37%) | Merck |
| Formamide | Roth, Karlsruhe |
| Gelatine | Merck |
| Glucogen | Boehringer |
| Glucose | Sigma |
| Glutarialdehye (25%) | Sigma |
| Glycerol | Merck |
| Glycine | Roth, Karlsruhe |
| Goat Serum (GS) | Invitrogen life technologies |
| Hydrochloric acid (HCl) | AppliCAM |
| Hematoxylin (Gill's No.2) | Polysciences, Eppelheim |
| Heparin (50mg/ml) | Sigma |
| Histo-clear | Fisher Chemicals |
| Hydrogen-Peroxidase (H ₂ O ₂ , 30%) | Merck, Fluka |
| Igepal | Sigma |
| Insulin | Sigma |
| Isopropyl-1-thio-β-D-Galactoside (IPTG) | Peqlab, Erlangen |

| | |
|--|---------------------------------|
| Isopropanol | AppliCAM |
| LB Broth Basis (Lennox L Broth Base) | Invitrogen, Life Technologies |
| Lithiumchloride (LiCl) | Merck |
| Maleic acid | Sigma-Aldrich |
| Methanol (MeOH) | Roth/Merck |
| Magnesiumchloride (MgCl ₂) | AppliCAM |
| Natriumchloride (NaCl) | Merck |
| Natriumacetate (NaAc) | Merck |
| NBT (4-Nitroblue tetrazolium chlorid solution) | La Roche |
| Paraformaldehyde (PFA) | Sigma |
| Pefabloc | Roth, Karlsruhe |
| Polyethylenglycol (PEG) 4000 | Roth, Karlsruhe |
| Penicillin /Streptomycin (P/S) | Gibco BRL, Karlsruhe |
| Phenol | Roth, Karlsruhe |
| Phenol/Cloroform | Roth, Karlsruhe |
| Potassium acetate (KAc) | Sigma |
| Potassiumchloride (KCl) | Sigma |
| Potassiumdihydrophosphate (KH ₂ PO ₄) | Merck |
| 2-propanol | Merck |
| Progesterone | Sigma |
| Putrescome | Sigma |
| SDS (ultra pure) | Roth, Karlsruhe |
| Sodium acetate | Merck |
| Sodium hydroxide (NaOH) | Merck |
| Sodium Selenium | Sigma |
| Sodiumdihydrophosphate (Na H ₂ PO ₄) | Merck |
| Sodiumhydrophosphate (Na ₂ HPO ₄) | Merck/Sigma |
| Transferrin | Sigma |
| Tri-jodothyroxine | Sigma |
| Thimerosal | Merck |
| Thionine | Sigma |
| Thyroxine | Sigma |
| Tris-(hydroxymethyl)-aminomethane base | Roth, Karlsruhe |
| Trizma Hydrochloride | Sigma |
| Triton-X 100 | Sigma |
| tRNA yeast stock | Roche Diagnostics, Mannheim |
| Tween-20 (Polyoxyethylenesorbitan Monolaurate) | Sigma-Aldrich Chemie, Steinheim |
| X-Gal (5-Brom-4-Chlor-3-indolyl-β-D-Galactosid) | Peqlab, Erlangen |

Solution, Media and Buffers

1. Media for Bacteria

LB (Luria-Bertani) Medium

10 g Bacto/Trypton
 5 g Bacto-Yeast Extract
 10 g NaCl
 add H₂O to final volume of 1 l

LB-Ampicillin Agar Plates

14 g LB-Broth Basis
 10 g Bacto-agar
 50 mg Ampicillin
 add H₂O to final volume of 1 l

(cooling to 55-60°C before the antibiotics was added.)

Medium A

1.1 ml 2M Glucose
 2.0 ml 1M MgSO₄
 196.9 ml LB Medium
 to final volume of 200 ml

Medium B

1.8 ml Glycerol (99%)
 0.6 g PEG 4000
 0.06 ml 1M MgSO₄
 add LB to final volume of 5 ml

2. Media & Solution for Embryo and Tissue Preparation

F12 Media (Gibco BRL)

L15 (Leibovitz) Media (Gibco BRL)

Dulbecco's Modified Eagle's Medium (DMEM) (Gibco BRL)

BME Basal Meium (10x) (Gibco BRL)

HBSS (Ca⁺-free) (Gibco BRL)

PBS (phosphate buffer saline, 1x)

137 mM NaCl
3 mM KCl
10 mM Na₂HPO₄
2 mM KH₂PO₄
adjust to pH 7.4

10xTyrode's Solution

73.6 g NaCl
39.6 g Dextrose
2ml 5M MgCl₂
3.28 g KCl
25 g Taurine
6.54 g Creatine
5.5 g sodium pyruvate
1.4 g NaH₂PO₄
20 g NaHCO₃
1.2 g CaCl₂
add H₂O to final volume of 1 l

Howard's Ringer Solution

7.2 g NaCl
0.17 g CaCl₂
0.37 g KCl
adjust to pH 7.2
add H₂O to final volume of 1 l

SATO's mix (50x)

500 mg BSA
80 mg Putrescine
26 µg Sodium Selenium
5.5 g Glucose
500 mg Transferrin
25 mg Insulin
300 µg Progesterone
2 mg Thyroxine
1.5 mg Tri-jodothyroxine
add H₂O to final volume of 100ml

Cresylviolet colour solution (200ml)

184 ml 0.1M sodium acetate
16 ml 0.1M acetic acid
5 ml 1% thionine
5 ml 1% cresylviolet

3. Solutions for DNA preparation

Solution I (Resuspension solution)

900 mg Glucose
1.25 ml 2M Tris-HCl (pH 8.0)
2 ml 0.5M EDTA (pH 8.0)
1 ml RNase
add H₂O to final volume of 100 ml

Solution III (Neutralization Solution)

60 ml 5M Kac (pH 4.8)
11.5 ml Acetic acid (cold)
add H₂O to final volume of 100 ml

Solution II (Lysis Solution)

10 ml 20% SDS
20 ml 2N NaOH
add H₂O to final volume of 100ml

TE (pH 8.0)

250 µl 2M Tris-HCl (pH 8.0)
100 µl 0.5M EDTA (pH 8.0)
add dH₂O to final volume of 50 ml

4. Buffers for Agarosegel electrophoresis

10xTAE (Tris-Acetate-EDTA)

96.8 g Tris base
22.84 ml Acetic acid
40 ml 0.5M EDTA
adjust to pH 7.5
add H₂O to final volume of 2 l

10xTBE (Tris-Borate-EDTA)

215.6 g Tris base
90 g boric acid
15 g EDTA
adjust to pH 8.0
add H₂O to final volume of 2 l

1% Agarosegel

1 g Agarose
100 ml TAE/TBE
3 µl Ethidium bromide (EB)
(add EB when it cooled down to 55-60°C)

5. Solutions for RNA *in situ* hybridization

DEPC-treated H₂O (dH₂O)

0.1% DEPC in H₂O

DEPC-treated PBS (dPBS)

0.1% DEPC in PBS

PBT

0.1% Tween-20 in dPBS

MAB

100 mM Maleic acid
150 mM NaCl
adjust to pH 7.5

MABT

0.1% Tween-20 in MAB

10xTBS (Tris-buffered Saline)

25 ml 1M Tris-HCl (pH 7.5)
8 g NaCl
0.2 g KCl
add d H₂O to final volume of 100 ml

TBST

0.1% Tween-20 in 1xTBS

NTMT (pH 9.5/8.0)

1 ml 5M NaCl
2.5 ml 2M Tris-HCl (pH 9.5/8.0)
1.25 ml 2M MgCl₂
50 µl Tween-20
add H₂O to final volume of 50 ml

20xSSC

175.3 g NaCl
88.2 g Citric Acid Trisodium Salt
adjust to pH 4.5
add H₂O to final volume of 2 l

Detergent Solution

1.5 ml 5M NaCl
2.5 ml 20% Igepal
5.0 ml 10% SDS
5.0 ml 5% Deoxycholate
2.5 ml 1M Tris-HCl (pH 8.0)
100 µl 0.5M EDTA (pH 8.0)
add dH₂O to final volume of 50 ml

Hybridization Solution

25 ml Formamide
12.5 ml 20x SSC (pH 4.5)
10 ml 10% SDS
250 µl tRNA
1 g Boehringer Blocking Reagent
50 µl Heparin
add dH₂O to final volume of 50 ml

Solution X

25 ml Formamide
5 ml 20x SSC (pH 4.5)
5 ml 10% SDS
add H₂O to final volume of 50 ml

6. Solutions for immunohistochemistry

Blocking Reagent (Fluorescein-Thyramin)

10 ml FCS
20 ml 2% Boehringer Blocking Reagent
30 µl Triton-100
add H₂O to final volume of 100 ml

AB Solution

10% FCS
0.1% Triton-X100
0.01% Thimerosal
dissolved in 1xPBS

Fluorescein

Stock solution: 200 mM in DMSO
Working solution: 20 mM

Thyramin

Stock solution: 2 M in DMSO
Working solution: 20mM

Blocking solution

1% DMSO
1% FCS
1% BSA
0.5% Triton-100
dissolved in PBS

PTW

0.1% Tween-20 in PBS

d-Biotin

Stock solution: 100 mM in 1N NaOH
Working solution: 100 µM in PBS

Color solution (FT)

20 mM Fluorescein
20 mM Thyramin

7. Solutions for vibratome section

Gelatin-Albumin embedding solution

10% Gelatine (in PBS)
10% Albumin (in PBS)

Kits

Table 12: Kits used for molecular experiments

| Kits | Companies |
|---|---|
| QIAprep® Spin Miniprep Kit | Qiagen GmbH, Hilden, Germany |
| QIAfilter™ Plasmid Maxi Kit | Qiagen GmbH |
| GenElute™ HP Plasmid Midiprep Kit | Sigma-Aldrich Chemie, Steinheim |
| GenElute™ HP Plasmid Maxiprep Kit | Sigma-Aldrich Chemie |
| endoFree™ Plasmid Maxi Kit | Qiagen GmbH |
| QIAquick PCR Purification Kit | Qiagen GmbH |
| QIAquick Gel Extraction Kit | Qiagen GmbH |
| DNA Extraction Kit | MBI Fermentas, St.Leon-Rot |
| RNeasy Mini Kit | Qiagen GmbH |
| PeqGOLD TriFast™ | PeqLab, Erlangen |
| Quick Ligation™ Kit | New England Biolabs, Schwalbach |
| TOPO TA Cloning® Kit for Sequencing | Invitrogen life technologies, Karlsruhe |
| Silencer™ Express siRNA Expression Cassette Kits | Ambion, Austin, US |
| VECTASTAIN® Elite ABC Kit (mouse IgG) | Vector Laboratories, Peterborough, UK |
| ABI PRISM™ BigDye™ Terminator Cycle Sequencing Ready Reaction Kit | PE Applied Biosystems, Welterstadt |

Antibodies

Antibodies for Immunohistochemistry

Table 13: Characteristics of the primary antibodies

| Antibodies | Host | Dilution | Staining | Companies | References |
|----------------------|--------|----------|------------------------|--------------|------------------------------------|
| α -Brn3a (IgG1) | mouse | 1:50 | Brn3a protein | Chemicon | (Xiang <i>et al.</i> , 1995) |
| α -En1 (IgG1) | mouse | 1:20 | engrailed protein | DSHB | (Ericson <i>et al.</i> , 1997) |
| α -Eph A4 | mouse | 1:1 | EphA4 receptor | Zymed Lab. | (Becker <i>et al.</i> , 1995) |
| α -ephrin A5 | mouse | 1:1 | ephrinA5 ligand | Zymed | (Davy and Robbins, 2000) |
| α -GFP (IgG) | rabbit | 1:500 | S65T-GFP; RS-GFP; EGFP | MoBiTec | (Jedrusik and Schulze, 2001) |
| α -pH3 (IgG) | rabbit | 1:200 | phos-Histone H3 | Upstate | (Juan <i>et al.</i> , 1999) |
| α -HNF3β (IgG1) | mouse | 1:10 | TK, labels RP | DSHB | (Ericson <i>et al.</i> , 1996) |
| α -Islet1 (IgG2b) | mouse | 1:25 | MNs, neural crest | DSHB | (Ericson <i>et al.</i> , 1992) |
| α -Lim2 (IgG1) | mouse | 1:3 | Lim1+2 protein | DSHB | (Tsuchida <i>et al.</i> , 1994) |
| α -Nkx2.2 (IgG2b) | mouse | 1:10 | Nkx2.2 protein | DSHB | (Ericson <i>et al.</i> , 1997) |
| α -Pax3 (IgG) | rabbit | 1:500 | Human Pax3 | Active Motif | (Tsukamoto <i>et al.</i> , 1994) |
| α -Pax6 (IgG1) | mouse | 1:10 | Pax6 protein | DSHB | (Ericson <i>et al.</i> , 1997) |
| α -Pax7 (IgG1) | mouse | 1:10 | Pax7 protein | DSHB | (Ericson <i>et al.</i> , 1996) |
| QCPN (IgG1) | mouse | 1:5 | Quail cell nuclei | DSHB | (Selleck and Bronner-Fraser, 1995) |
| RMO270 (IgG2a) | mouse | 1:500 | NF-160kD | Zymed | (Verberne <i>et al.</i> , 2000) |
| α -Smad3 (IgG) | rabbit | 1:100 | Human Smad3 | Active Motif | (Liu <i>et al.</i> , 1997) |
| α -Shh-1 (IgG1) | mouse | 1:5 | Shh protein | DSHB | (Ericson <i>et al.</i> , 1996) |
| α -β-Tubulin (IgG2b) | mouse | 1:400 | β-Tubulin III | Sigma | (Banerjee <i>et al.</i> , 1990) |

DSHB - Developmental Studies Hybridoma Bank, Iowa, USA

Mo Bi Tec – Molecular Biologische Technologie, Göttingen, Germany

Table 14: Characteristics of the secondary antibodies

All of the 2nd antibodies are produced from goats, and against the F(ab')₂ fragment of IgG. Alexa Fluor[®] antibodies are ordered from Molecular Probe Europe, Leiden, Netherlands. Cy2-/Cy3-/AMCA-/AP-conjugated AffiniPure Antibodies are from Jackson Immuno Research Laboratories, Inc., West Grove, PA, USA. FITC-/TRITC-conjugated IgG subtype antibodies come from southern Biotechnology Association, Inc., Birmingham, AL, USA.

| Antibodies | Dilution | Properties |
|---|----------|---------------------------------------|
| Alexa Fluor [®] 488 anti-mouse IgG (H+L) | 1:200 | Green fluor (A-495nm, E-519nm) |
| Alexa Fluor [®] 546 anti-mouse IgG (H+L) | 1:200 | Orange fluor (A-556nm, E-573nm) |
| AMCA-Conjugated AffiniPure anti-mouse IgG | 1:100 | Blue fluorescence (A-350nm, E-450nm) |
| AP-Conjugated AffiniPure anti-mouse IgG | 1:500 | Alkaline phosphatase |
| AP-Conjugated AffiniPure t anti-rabbit IgG | 1:500 | Alkaline phosphatase |
| Cy2-Conjugated AffiniPure anti-mouse IgG | 1:100 | Green fluorescence (A-492nm, E-510nm) |
| Cy2-Conjugated AffiniPure anti-rabbit IgG | 1:100 | Green fluorescence (A-492nm, E-510nm) |
| Cy3-Conjugated AffiniPure anti-mouse IgG | 1:200 | Red fluorescence (A-550nm, E-570nm) |
| Cy3-Conjugated AffiniPure anti-rabbit IgG | 1:200 | Red fluorescence (A-550nm, E-570nm) |
| FITC-Conjugated anti-mouse IgG1 | 1:300 | Green fluorescence (A-488nm, E-520nm) |
| TRITC-Conjugated anti-mouse IgG1 | 1:300 | Red fluorescence (A-555nm, E-582nm) |
| TRITC-Conjugated anti-mouse IgG2a | 1:300 | Red fluorescence (A-555nm, E-582nm) |
| TRITC-Conjugated anti-mouse IgG2b | 1:300 | Red fluorescence (A-555nm, E-582nm) |

FITC - fluorescein isothiocyanate

TRITC - tetramethylrhodamine isothiocyanate

Antibodies for RNA *in situ* Hybridisation

Anti-Digoxigenin-AP and Anti-Fluorescein-AP Fab fragments (Roche Dagnostics, Mannheim, Germany) are used in ISH. They are AP (Alkaline Phosphatases)-conjugated goat antibodies and dilute to 1:2000 for use.

Genes for RNA Probes

RNA probes were labelled with digoxigenin- (Dig) or Fluorescein- (FITC) UTPs by *in vitro* transcribed (T7, T3 or SP6-RNA polymerases) from the following clones (Tab. 15) that contain a partial sequence of the genes listed below.

Table 15: Relevant Genes for RNA *in situ* hybridisation

| Genes | Size | Vector | From |
|----------------|---------|--------------|---|
| <i>BMP-7</i> | 0.7 kb | pSK | Anthony Graham (Kings College, London, UK) |
| <i>Brn-3a</i> | 1.2 kb | pSK | A. Graham (Kings College) |
| <i>Chordin</i> | 0.49 kb | pMT23 | Kevin Lee (Columbia University, NY, USA) |
| <i>Isl-1</i> | 1.4 kb | pBluescript | Thomas Jessell (Columbia University, NY, USA) |
| <i>Lim1</i> | 2.1 kb | | T. Jessell (Columbia University) |
| <i>Nkx6.1</i> | 1.1 kb | pSK | John L.R. Rubenstein (San Francisco, CA, USA) |
| <i>Pax3</i> | 0.54 kb | pKS | Britta Eickholt (Kings College) |
| <i>Pax6</i> | | pBSKS+ | Andrew Lumsden (Kings College) |
| <i>Ptc1</i> | 0.94 kb | pDrive | Farshid Seif (Wuerzburg, Germany) |
| <i>Ptc2</i> | 0.47kb | pBSKS II (+) | Naixin Li (Wuerzburg, Germany) |
| <i>Shh</i> | 0.38 kb | pCR II | Frank Schubert (Guy's hospital, London) |

Apparatus and Instruments

Apparatus for Embryo and Tissue Preparation

Sellotape and thick plastic canvas tape
 Syringes and needles
 Needle holders
 Petri dishes
 Egg stools, cut from water pipe insulation
 Pure tungsten wire
 Fine watchmarker forceps
 Scalpel blade and handle
 Curved, sharp-pointed scissors
 Vannas spring scissors
 Ultrafine scissors
 Stainless steel spatula, 5-8mm wide tip
 Scalpel Handle
 Sealing wax
 Haemocytometer
 Glass capillary
 Platinum electrode

All of them are ordered from company A. Hartenstein GmbH, Wuerzburg, World Precision Instruments (WPI), Berlin, Fine Science Tools, Heidelberg, and VWR International GmbH, Darmstadt, Germany.

Technical Instruments

Table 16: Technical instruments

| Items | Model | Companies |
|------------------------|------------------------------|---------------------------------------|
| Air compressor | Model 3-Minor | JUN-AIR A/S, Norresundby, Denmark |
| CCD Camera | RT color Spot | Diagnostic Instruments, Inc. |
| | Pixera PVC 100C | Digital Imaging systems, Egham, UK |
| Centrifuge | Sorvoll® RC 5B superspeed | Beckman Instrument |
| | Heraeus® Biofuge® pico | Kendro Laboratory, Langenselbold |
| | Small Centrifuge Micro 12-24 | Andreas Hettich GmbH, Tuttlingen |
| Climate Chamber | | Genheimer GmbH, Hettstadt |
| Confocal microscope | Leica TCS SP | Leica Microsystems |
| Epifluo. Microscope | Leica KL FLIII | Leica Microsystems |
| Fluorescent microscope | Leica DM RA | Leica Microsystems |
| Fluorescent source | ebq 100 | Carl Zeiss Germany, Oberkochen |
| Gel electrophoresis | Horizon® 11.14 | Life Technologies |
| Incubator | Flächenbrüter Modell 3000 | Brutmaschinen-Janeschitz, Hammelburg, |
| | Heraeus® function line | Kendro Laboratory Products Ltd, Swiss |
| Microinjector | Narishige IM 300 | Intracel Ltd. |
| Micromanipulator | | Leitz, Wetzlar |
| Micropipette Puller | Model P-2000 | Sutter Instrument Co. |
| Pulse Stimulator | Intracel TSS10 | Intracel Ltd. |
| Safety Cabinet | Heraeus® HERAsafe HSP | Kendro Laboratory |
| Stereomicroscope | Stemi 1000 & 2000C | Carl Zeiss Germany, Oberkochen |
| Thermocycler | Gene Amp PCR System 2400 | Perkin-Elmer |
| Thermomixer | Compact | Eppendorf |
| Vibratome | Leica VT 100 S | Leica Microsystems |

Softwares and Websites

Softwares

ACDSee 3.22
Adobe Acrobat 6.0
Adobe Photoshop 7.0
Adobe Illustrator 10.0
HyperCam 1.70
HyperSnap-DX 3.63
IrfanView 3.75
Microsoft® Word 9.0
Microsoft® Excel 2000
Microsoft® PowerPoint® 2000 SR-1
EndNote 6.0
Amira 3.0
Chromas 1.45
DNAstar 5.06
Advanced SPOT (Diagnostic Instruments, Inc.)
Pixera VCS 1.1.0

Websites

<http://www.ncbi.nlm.nih.gov/>
<http://www.chick.unist.ac.uk/>
<http://www.ambion.com/>
<http://www.gene-tools.com/>
<http://smart.embl-heidelberg.de/>
<http://www.bork.embl-heidelberg.de/STRING/>
<http://motif.genome.ad.jp/>
<http://www.ebi.ac.uk/>
<http://www.expasy.ch/>
<http://links.bmn.com>
<http://www.promega.com/tbs/default.htm>
<http://www.fermentas.com/>
<http://www.google.de/>

Methods

1. Embryo and Tissue Preparation

1.1. *In vivo* Manipulations

Transplantation

Dorsal midbrain into ventral region and vice versa

Fertile hens' eggs were incubated horizontally in a humidified atmosphere at 37°C to the required stage. Embryos were staged according to Hamburger and Hamilton (Tab. 1), and divided into two groups, 1) the host and 2) the donor. Hosts were prepared as follows: after withdrawal of 2 ~ 3 ml albumin, the upper part of eggshell was opened to gain access to the chick embryos. A mixture of India ink (Pelican Fount India, Hannover) with Tyrode's solution (1:5) was injected beneath blastodermal region to allow its visualization. The vitelline membrane was opened over the midbrain and the site to receive the graft was prepared in the dorsal or the ventral part of the midbrain by cutting out a graft-sized piece of tissue, leaving floor or roof plate intact. Donors were collected in Howard's Ringer solution, and the midbrains were then cleanly dissected from the surrounding mesoderm after 10 - 15 minutes incubation with Dispase 1 (1 mg/ml in L-15 medium, La Roche). After being washed in sterilized phosphate buffered saline (PBS), the isolated midbrains were stained with an orange CellTracker dye (CMTMR, Molecular Probe in L-15 medium) as described (Wizenmann and Lumsden, 1997), washed twice with L-15 and kept on ice till needed. The grafts were cut with tungsten needles from a medial position within dorsal or ventral region of midbrains, excluding floor or roof plate (Fig. 14), and then transferred to the prepared recipients using a pipette and orientated with tungsten needles. After adding several drops of Ringer solution, the eggshells were sealed with tissue tape and the embryos were incubated for 18 - 24 hours. The grafted embryos were fixed in 4% paraformaldehyde (PFA in PBS, pH 7.4) and kept overnight at 4°C until further analysis.

Roof plate transplantation

Roof plate (RP) transplantations were performed as described above in ‘Dorsal midbrain into ventral region and vice versa’ with the difference that the graft was a strip of labelled roof plate.

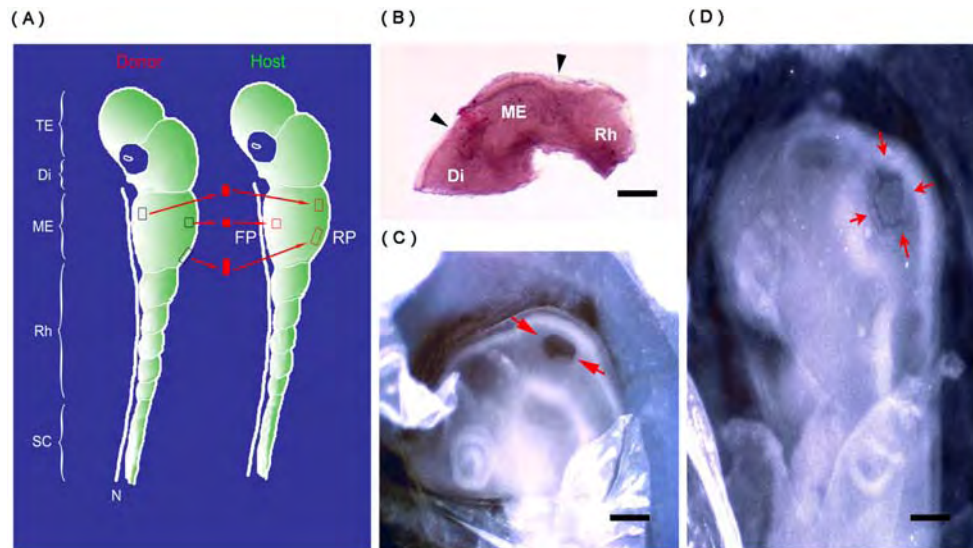


Figure 14: The diagram of chick midbrain transplantation

(A) Schematic diagram of the basic approach of midbrain transplantation in chick embryos. A piece of labelled tissue (red) from a wanted region of a donor midbrain was transferred to seal the prepared window in the host midbrain, without interrupting roof or floor plate. Three types were done: ventral to dorsal, dorsal to ventral, and dorsal to dorsal. Green represents the expression of Pax3/7. (B - D) An example of transplantation from ventral to dorsal at stage HH13. (B) A dissected donor midbrain (marked by arrowheads) with CMTMR labeling is showed in red. (C) A window (arrows) was prepared in one side of the host dorsal midbrain, whereas the other side was left intact. (D) A ventral graft cut from the labelled donor midbrain was transferred to the opened window (arrows) in the host.

Abbreviations: Di, Diencephalon; FP, floor plate; ME, Mesencephalon; N, Notochord; Rh, Rhombomere; RP, roof plate; SC, Spinal cord; TE, telencephalon. Scale bar: 100µm. (A modified after Dr. Andrea Wizenmann.)

Beads transplantation

Heparin-coated beads (Sigma) were prepared by washing twice in L15 medium (Life Technologies) and then incubated in 10 µl of 0.1 µg/µl BMP2 (kind gift of Prof. Seebald) or BMP7 (R&D Systems) for 1 hour. For control experiments, beads were incubated in L15 medium. The beads were crushed with a pipette tip into smaller pieces before implantation into neural tube; bead fragments were held in place in the neural tube more stably than intact spherical beads, which tended to extrude into the lumen during development. Chicken embryos were incubated to stages 8 - 9, “windowed” for manipulation and prepared for bead implantation by making an incision with a sharpened tungsten needle in the neural tube at the required level, i.e. intermediate mesencephalon. A bead fragment was then inserted into the incision with a sharpened tungsten needle. Operated eggs were closed and incubated for 24 - 36 hours, till approximately stage 15 of development, prior to further analysis by *in situ* hybridisation. Accuracy of the axial level of bead implantation was confirmed by referring to the negative controls.

Quail-chick chimeras

Quail embryos were staged according to chick criteria (Tab. 1) and used as donors (Cobos *et al.*, 2001). Isochronic quail to chick transplantations were performed as described for chick transplantation, and the chick hosts can develop continuously *in ovo*. Quail cells can be distinguished clearly from chick cells either by Feulgen-Rossenbeck staining or immunostaining with QCPN, a quail-specific antibody (Fig. 15).

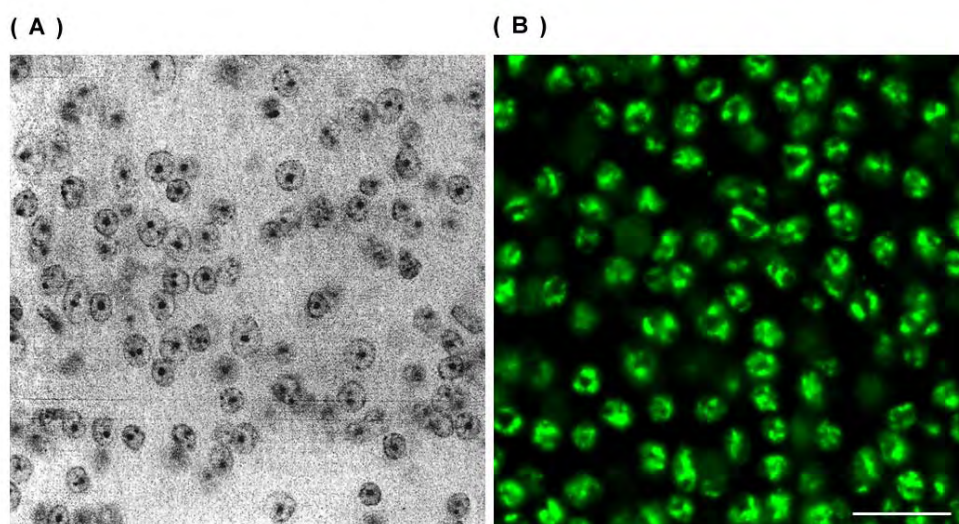


Figure 15: Identification of quail cells

(A) A quail cerebellum section in Feulgen-Rossenbeck staining. Quail Purkinje cells show an obvious centronuclear mass of heterochromatin. (B) A flat-mount quail midbrain at stage 17 in immunostaining with QCPN antibody. Chromosomes of quail cells are visualized in a brilliant green fluorescence with a secondary antibody - Cy2 anti-mouse IgG (Jackson Immuno Research Laboratories Inc.). QCPN, a mouse anti-quail monoclonal IgG1 (Developmental Hybridoma Bank, Iowa). Scale bar: 25 μ m. (Photograph A from Alvarado-Mallart *et al.*, 1990)

In ovo Electroporation

In ovo electroporation is a safe and effective way to introduce exogenous genes into chick embryos for the analysis of their regulation, function and expression (Sakamoto *et al.*, 1998; Itasaki *et al.*, 1999). Electroporation applies a pulsed electric field (PEF) to create transient reversible aqueous pathways (pores) in lipid bilayer membranes (Prausnitz *et al.*, 1995). Through these pores, negative-charged DNAs or RNAs move toward the anode and enter the living cells, while the other side (cathode) constitutes an untransfected control. Translation of a transfected gene can be detected in 2 hours after an electroporation. In this study, it is used for the overexpression of Rab23 and Pax7 as well as for transcription of dsRNA in vector-based RNAi experiments.

Chick embryos were cultured till stage 9 - 11 (Fig. 16). At this stage, the neural epithelium consists of a single layer of cells, of which all are exposed to the DNA confined to the lumen. Chicken eggs were “windowed” for manipulation and prepared for electroporation by making an incision with a sharpened tungsten needle in the vitelline membrane at the required level. Plasmid DNA (2 – 5 μ g/ μ l) was mixed with 1/20 fast green (Sigma) for the visualization of the injected DNA. Microneedles for

injection, with a tip diameter of ~ 5 μm, were pulled from borosilicate glass capillaries (A. Hartenstein, 100 mm x 0.9 mm) by a Sutter Micropipette Puller. The setting refer to Tab. 17. Before and after electroporation a few drops of sterile, cold Tyrode's solution were added. The platinum electrodes were fixed on a micromanipulator and placed parallel along the anteriorposterior (AP) axis of the midbrain with a distance of 5 mm (Nakamura and Funahashi, 2001). The tip of the microcapillary was inserted into the lumen at the midbrain level, and the DNA was injected using a microinjector (Narishige IM300, Intracel) at 10 - 15 psi pressure (1 psi = 12 bar). 3 ~ 5 pulses were generated by an Intracel Pulse Stimulator. The setting of parameters refer to Itasaki' work (1999; Tab. 18). After electroporation, the window in the eggshell was sealed with Scotch tape and the injected embryos were incubated at 37°C for 16 to 28 hours till approximately stage 14 ~ 16.

After complete neural tube closure (stage 10), injected DNA was nicely confined to the ventricle. Moreover, chick embryos showed a higher survival rate (90 - 100%) compared to younger ones. In our hands fast green did not affect the efficiency of transfection.

Table 17: The setting of the Sutter Puller

| Parameters | Values |
|------------|--------|
| Heat | 350 |
| Pull | 100 |
| Velocity | 50 |
| Delay | 200 |

Table 18: The setting of Pulse Stimulator

| Parameters | Values |
|------------|-------------|
| Frequency | 50 Hz |
| Delay | 50 ms |
| Width | 50 ms |
| Voltage | 8 – 25 V |
| Pulse | 3 – 5 times |

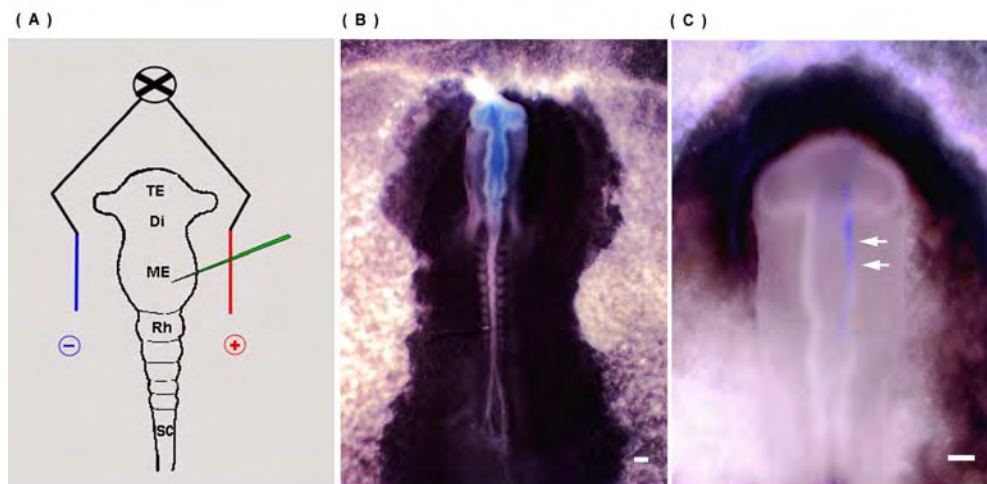


Figure 16: *In ovo* electroporation in chick midbrain

(A) Schematic diagram of *in ovo* electroporation in chick midbrains. Platinum electrodes were placed parallel to the anteriorposterior axis of chick embryo at the midbrain level. Plasmid DNA (in green) was injected into the lumen with the help of a microinjector, and then it was transferred into midbrain unilaterally (positive pole) by application of electric pulses. (B) An example of an electroporated embryo at stage 10. The DNA mixture remained blueish in the lumen of the neural tube. (C) The transfected side (arrows) of the midbrain was still tinted for a few minutes. The left side was intact.

Abbreviations: Di: Diencephalon; ME: Mesencephalon; Rh: Rhombomere; SC: Spinal cord; TE: telencephalon. Scale bar: 100μm. (Schematic diagram A modified after Katharina Köppen-Schomerus.)

1.2. *In vitro* Manipulations

Co-culture

Defined regions of the midbrain for collagen gel co-culture were dissected from chick embryos at different stages by sharpened tungsten needles (Lumsden and Davies, 1983). The tissues were cultured in the following combinations: 1) dorsal or ventral midbrain without roof or floor plate, 2) dorsal or ventral midbrain with roof or floor plate attached, and 3) dorsal midbrain with floor plate and ventral midbrain with roof plate. Rat-tail collagen was mixed thoroughly with 10% BME medium (10 x, Invitrogen) and 20 μ l/ml of 7.5 % bicarbonate (Invitrogen), and immediately, a drop of collagen mix was placed into one well of a 4 - well plate, the tissues were added and arranged using pipettes in such a way that the pieces bordered each other. 500 μ l of F-12 medium with 2 % Sato-mix and 1 % Penicillin/Streptomycin (P/S, Invitrogen) was added into each well in several minutes after the collagen was given. The plates were transferred to an incubator with 37°C, 5 % CO₂ and 50 % relative humidity. The cultures were fixed after 48 h by adding 1/10 vol. of 37 % formaldehyde, and kept at 4°C until further staining or analysis.

In vitro aggregation assay

The assay and data analysis procedure have been described previously (Wizenmann and Lumsden, 1997). Briefly, 8 - 15 midbrains of the same developmental stage were dissected out and pooled for one experiment. The mesenchyme was completely removed and midbrains were divided into ventral and dorsal halves, removing floor and roof plate to avoid contamination. Isolated ventral and dorsal midbrains were labelled with different CellTracker dyes (CMFDA and CMTMR, 10 mM in F-12 medium; Molecular Probes) as described. After incubation in Ca-free HBSS medium the tissue was dissociated into single cell suspensions by gently pipetting up and down using coated pasteur pipettes. I did never use Trypsin since the cell surface molecules were wanted to be intact. Dorsal and ventral cell populations were mixed with equal cell numbers (2.5×10^5 /ml) in F-12/Sato medium, and incubated on a horizontal shaker for 3 ~ 4 hrs at 65 rpm, 37°C and 5 % CO₂ condition. The cultures were fixed by adding 1/10 of 37 % formaldehyde for 1 hr. This suspension was then shortly centrifuged to reduce the volume of the fixative, and then placed on a glass slide and embedded in Mowiol. The aggregates were analysed by confocal microscopy (Leica TCS Sp).

The aggregates were classified 'segregated' and 'mixed' (Fig. 17) and calculated the segregation ratio in each experiment. The percentage of 'segregated' aggregates in comparison to the total number of aggregates of one well was expressed as segregation ratio. Experiments with high numbers of dead cells, weak aggregation, incomplete or ambiguous fluorescent labeling was excluded from the analysis.



Figure 17: Classification of aggregates

Aggregates are classified as 'segregated' when they nearly consist of only one cell population or show distinct clusters of the two cell populations. A cluster is defined as an association of at least eight cells come from the same population (showing the same fluorescent emission). (Schematic diagram from Dr. Andrea Wizenmann)

2. Molecular Techniques

2.1. Isolation and Determination of Plasmid DNA

Mini preparation of plasmid DNA

Mini-plasmid preparation from bacterial cells based on alkaline lysis was performed (modified after Sambrook *et al.*, 1989). Briefly, 2 ml overnight bacterial cultures in LB medium were shortly centrifuged, the pellet was resuspended in 150 μ l chilled solution I and dissolved completely by vortexing. 150 μ l of fresh solution II and 150 μ l of ice-cold solution III were added one after the other and thoroughly mixed. After minutes on ice, the solution was centrifuged at top speed for 5 minutes, and the supernatant containing plasmid DNA was transferred into a new Eppendorf tube. 1 ml chilled 100 % Ethanol was added, mixed, incubated at room temperature 2 minutes and centrifuged for 30 minutes. The supernatant was discarded. The pellet was washed twice with 1 ml of 70 % ethanol. After aspirated in air for 5 - 10 minutes, the pellet was dissolved in 20 μ l of sterile H₂O or TE (pH 8.0) and stored at -20°C . The prepared plasmid DNA was used to be linearized for *in vitro* transcriptions or to be analysed to determine the sequence of the insert in a recombinant clone.

An alternative procedure was used for QIAprep[®] Spin Miniprep Kit (Qiagen, Hilden). Up to 20 μ g purified plasmid DNA can be extracted following manufacturer's instructions.

Midi-/Maxi preparation of plasmid DNA

To obtain a high amount of purified plasmid DNA (up to 1500 μ g) from *E.coli* bacteria, QIAfilter[™] Plasmid Maxi Kit (Qiagen, Hilden) and GenElute[™] HP Plasmid Midi-/Maxiprep Kits (Sigma-Aldrich Chemie, Steinheim) were applied according to their manufacturer's handbooks. On account of the final DNA concentration extracted by GenElute Maxiprep Kit was lower (0.3 - 0.5 μ g/ μ l) for electroporation, the plasmid DNA was further concentrated by a salt precipitation (see below).

Endotoxin-free plasmid extraction

To minimize the effects of endotoxin on transfected cells (Cotten *et al.*, 1994), plasmid DNAs were prepared using Qiagen endoFree™ Plasmid Maxi Kit according to manufacturer's handbook. The amount of endotoxin released from *E. Coli* was largely decreased (<0.1 EU/μg plasmid DNA). These non-toxic plasmid DNAs were used for *in ovo* electroporation.

DNA concentration

At room temperature, 300 μl of 3.0 M sodium acetate and 2.1 ml of isopropanol were added to 3ml DNA solution (eluted by GenElute Maxiprep Kit), and mixed well by inversion. The mixed solution was then centrifuged at $\geq 15,000 \times g$ at 4 °C for 30 minutes. The supernatant was removed, and the pellet was rinsed in 1.5 ml of 70 % ethanol and centrifuged twice for 10 minutes. After the residual ethanol had evaporated, a suitable volume (50 – 100 μl) of Elution Solution or dH₂O was added to achieve a final DNA concentration of 2 – 5 μg/μl.

Agarose gel electrophoresis for DNA

Agarose gel electrophoresis was used to separate DNA fragments with a size between 0.5 kb and 10 kb. Depending on the length of the DNA, 1 ~ 2 % agarose was prepared either in 1 x TAE or TBE buffer. Ethidium bromide (EB, 0.2 μg/ml) was added when the agarose solution had cooled down beyond 50 °C, and the mixture was poured into a prepared gel chamber. After polymerization, the gel was loaded with DNA samples, which were mixed with 1:1 loading buffer. The gel was run at 100 volts in 1 x TAE or TBE buffer till the buffer dye reached the end of the gel and analyzed under UV light (320 nm). To be able to estimate the size of the DNA fragments, 1 kb or 100 bp DNA-ladders (MBI Fermentas) were used as size standards.

Gel extraction of DNA

Gel slices containing the DNA band of interests (70 bp to 10 kb) was cut out of TBE agarose gel with a sharp scalpel under UV light, and transferred into an Eppendorf tube. The DNAs can be extracted with QIAquick Gel Extraction Kit (Qiagen), or recovered by silica powder using DNA Extraction Kit (MBI Fermentas), following their manufacturer's protocols, respectively.

DNA quantitation

The DNA concentration was determined by a spectrophotometer (Eppendorf). 2 μl of the probe was diluted in 78 μl dH₂O in a disposable cuvette (Eppendorf) and the absorption was measured at a wavelength of 260 nm and 280 nm. The absorption of '1' at 260 nm corresponds to a concentration of 50 μg/ml double-stranded DNA. The ratio of absorbance at A_{260}/A_{280} shows the contamination of the DNA and should ideally be 1.5 ~ 2.0. The quality of DNA can be checked by agarose gel electrophoresis.

2.2. Isolation and Cloning of Embryogenetic Genes & Fragments

Isolation of total RNA

PeqGOLD TriFAST™ (peqLab, Erlangen) was used to isolate total RNAs in my study. This kit has an advantage that RNA, DNA and protein can be extracted at same time. 3 - 10 dissected neural tubes or midbrains at wanted stages were collected in a 1.5 ml vial under sterile conditions and homogenized in 1 ml TriFAST™ solution by pipetting. After 5 minutes at room temperature, the homogenate was added 0.2 ml of chloroform and centrifuged for 5 minute at 12,000 x g. The interphase and phenol phase was kept at 4 °C for further isolation of DNA and protein, respectively. The supernatant containing total RNA was transferred to a new vial. 0.5 ml of isopropanol was added, mixed well, and centrifuged for 10 minutes at 4 °C. The RNA pellet was washed twice in 1ml of 75 % ethanol and dried in air. The semi-dry RNA pellet was dissolved in 20 – 50 µl of RNase-free H₂O or 0.5 % SDS dH₂O. The total RNA was used directly for RT-PCR or stored at – 80 °C.

As an alternative RNeasy Mini Kit (Qiagen) was also used to isolate total RNA following the manufacturer's protocol.

The concentration of RNA was measured at 260 nm using a photometer (refer to 'DNA quantitation'). The absorption of '1' corresponds to a concentration of 37 µg/ml RNA. Pure RNA should have an absorbance ratio of 1.8 to 2.0 at A_{260}/A_{280} .

For RNA electrophoresis, all solutions were made fresh under sterile, RNase-free condition. The procedure was performed as for DNA. To avoid secondary structure, RNA probes were heated at 80 °C for 10 minutes before loading on the gel.

cDNA synthesis

Embryonic genes or gene fragments were synthesized via RT-PCR in two steps: the first strand cDNA synthesis and the double-stranded cDNA synthesis. Two reverse transcriptases (RT), SuperScript™ II RNase H RT (Invitrogen) and M-MuLV RT (Moloney Murine Leukemia Virus, MBI Fermentas), were used to synthesize first strand cDNA from isolated embryonic mRNA. 20 µl of reaction solution was made as follows: 1 – 5 µg total RNA and 1 µl oligo (dT) primer (500 µg/ml) were mixed in sterile water to final volume of 12 µl, heated for 10 minutes at 70°C and then quickly chilled on ice. 4 µl 5 x first strand buffer, 2 µl 0.1 M DTT and 1 µl 10 mM dNTP mix were added, gently mixed, and incubated for 2 minutes at 42°C. Either 1 µl of Superscript II (200 U/µl) was added and the mixture was incubated for 50 minutes at 42°C or 2 µl M-MuLV reverse transcriptase (20 U/µl) was added, and incubated for 60 minutes at 37°C.

No reverse transcriptase was added to the negative control. Heating at 70°C for 10 - 15 minutes inactivated the reaction. The mRNA template was removed with RNase H (peqLab) at 37°C for 20 minutes. Thus obtained first strand cDNA served as template for PCR to obtain double-stranded cDNA with gene-specific primers (Tab. 4).

The following reagents were added as below:

| | |
|--------|------------------------------------|
| 10 µl | 10 x PCR buffer |
| 3 µl | 50 mM MgCl ₂ |
| 2 µl | 10 mM NTP mix |
| 1 µl | amplification primer 1 (10 µM) |
| 1 µl | amplification primer 2 (10 µM) |
| 1 µl | <i>Taq</i> DNA polymerase (5 U/µl) |
| 2 µl | first strand cDNA |
| 80 µl | sterile distilled water |
| <hr/> | |
| 100 µl | |

The PCR was performed in a thermocycler from Perkin Elmer (GeneAmp; PCR System 2400). The settings for the cycles refer to 'Polymerase Chain Reaction'. After purification, the cDNA solution was kept at - 20 °C.

Polymerase Chain Reaction

Polymerase chain reaction (PCR) allows the production of more than 10 million copies of a target DNA sequence (genomic DNA or cDNA). To amplify specific genes or gene fragments, oligonucleotide primers (Tab. 4) were designed using the software DNASTAR. Optimal primer pairs consist a forward and reverse primer with 18 - to 25 - mer. Linker primers (for Linker PCR) were designed to fit specific restriction sites of the vector for cloning, in that the recognitive sequences of a desired restriction enzyme was added to the 5' end of the primers. Recombinant thermostabile *Taq* DNA polymerase (MBI Fermentas) from the eubacteria *Thermus aquaticus* was used in a routine PCR. In 50 µl of PCR solution, the following reagents were added and mixed well.

| | |
|--|------------------------------------|
| 5 µl | 10 x PCR buffer |
| 2 µl | 10 mM dNTP mix |
| 3 µl | MgCl ₂ (25 mM) |
| 1 µl | forward primer (10 pmol/µl) |
| 1 µl | reverse primer (10 pmol/µl) |
| 1 µl | template DNA (0.1 - 1 µg) |
| 0.5 µl | <i>Taq</i> DNA polymerase (5 U/µl) |
| <hr/> | |
| adjust to 50 µl with sterile deionized water | |

The optimal final concentration of MgCl₂ was determined empirically (1.0 - 2.5 mM). All reagents were kept on ice during preparation.

Pfu Turbo[®] DNA polymerase (2.5 U/µl, Stratagene) was used for high-fidelity PCR in my study to clone *Pax7* and *Rab23* cDNA. This DNA polymerase is produced from a hyperthermophilic marine archaeobacteria *Pyrococcus furiosus* and possesses a 3' to 5' exonuclease activity.

The PCR reaction was set as following steps: An initial denaturation at 95°C for 1 - 2 min, followed by 25 - 35 amplification cycles. Each cycle comprised three steps: 1) Denaturation step, 30 seconds at 95°C, 2) Primer annealing step for 30 - 60 seconds, the temperature usually 5°C lower than the melting temperature (T_m) of the primer-template DNA, and 3) The extending step for 1 - 2 min at 72°C. The time was adjusted by 1 min per kb of the sequence. After the last cycle, the final extending step at 72°C for 5 - 10 min allowed the newly PCR products to fill-in the protruding ends.

PCR products were checked on a gel and purified either with a QIAquick PCR purification kit (Qiagen) or via a Gel Extraction.

Restrictive digestion

The restrictive digestion of transformed plasmids can serve either as a fast means to check if genes or gene fragments are inserted, or to linearize a vector for *in vitro* transcriptions for example, or to isolate the wanted DNA sequence from a vector for further subcloning. All of restriction endonucleases and their buffers were received from MBI Fermentas and New England BioLabs (Tab. 9a, 9b).

A restriction digest was performed as follows:

| | |
|---|--|
| 2 μ l | 10 x RE-specific buffer |
| 1 μ l | Restriction endonuclease (10 U/ μ l) |
| 0.1 - 1 μ g | template DNA |
| <hr/> | |
| adjust to 20 μ l with sterile deionized water | |

The reaction was incubated in a water bath at the optimal temperature (mostly 37 °C) for 2 to 3 hrs. Double digestions were performed in one step if the action conditions (temperature and buffer) of both enzymes allowed (refer to website <http://www.fermentas.com/>). Otherwise, two digest were carried out one after the other, with a phenol/chloroform extraction in between. Restriction endonucleases were inactivated by heating at 65 °C for 10 minutes, and the digested DNAs were checked on a gel.

Dephosphorylation of linearized plasmid DNA

Due to covalent termini of the linearized vectors, prior to ligation, they need to be dephosphorylated at 5' - phosphate residues to inhibit self-circularisation. This reaction is catalysed by calf intestine alkaline phosphatase (CIAP, MBI Fermentas). In short, 250 ng of linearized vector DNA was mixed with 1 u/ μ l CIAP and 1/10 volume of 10 x dephosphorylation buffer in dH₂O, and incubated for 30 minutes at 37°C. The reaction was stopped by heating at 85°C for 15 minutes. These dephosphorylated DNAs were then purified with phenol/chloroform and precipitated with ethanol.

Ligation

The ligation was catalyzed by T4 DNA Ligase (MBI Fermentas). For linearized vectors with cohesive ends, the following reagents were gently mixed (do not use a pipette).

| | |
|--|-------------------------|
| 50 ng | linearized vector DNA |
| x µg | insert DNA |
| 2 µl | 10 x T4 ligation buffer |
| 0.5 µl | T4 DNA ligase (5 u/µl) |
| adjust to 20 µl with dH ₂ O | |

The ratio of the reaction concentration of insert DNA (pmol) to linearized vector DNA is 2 - 5:1, and the amount of inserted DNA (µg) is calculated according to the formula:

$$X (\mu\text{g}) = \mu\text{g}_{\text{vector}} \times \text{bp}_{\text{insert}} / \text{bp}_{\text{vector}} \times (2 \sim 5)$$

The mixture was incubated for 2 hours at room temperature (25°C) or overnight at 14°C. The ligase was inactivated by heating at 65 °C for 10 minutes. The mixture was kept on ice or frozen till the transformation.

Quick Ligation™ Kit (New England BioLabs) was also used. It enables the ligation fulfill within 5 minutes at room temperature. TOPO TA Cloning® Kit (Invitrogen) allows PCR products amplified with *Taq* polymerase directly clone into pCR®4-TOPO® vectors, which is achieved by topoisomerase I from the *Vaccinia virus* instead of T4 DNA ligase. Moreover, 1/3 recommended volume (manufacturer's instruments) of each reagent was enough to perform in a reaction (after Simpson Lab).

Preparation of competent cells

Competent *E. coli XLI Blue* cells were prepared as described (Nishimura *et al.*, 1990). 100 ml medium A was added into 1 ml overnight cultured LB medium with *XLI Blue* cells (Stratagen). Bacteria were cultured at 37°C and 300 rpm till mid-log phase (OD₆₀₀ = 0.35). The bacterial solution was centrifuged at top speed for 10 minutes at 4°C (Backmann Sorvoll® RC 5B). The pellet was resuspended in 1 ml cold medium A and 5 ml newly prepared medium B, and mixed well. The bacteria were aliquoted, frozen in liquid nitrogen and stored at -80°C.

Transformation

Transformation was performed after Sambrook *et al.* (1989) using heat-shock. In short, competent cells (50 µl) from a desired host strain were thawed on ice and mixed with 1 µl β-mercaptoethanol. 1 – 2 µl of the plasmid or ligation solution (1 – 10 ng DNA) was added and mixed gently by tapping the vial, then kept on ice for 20 - 30 minutes. The cells were incubated at 42°C for 45 seconds and rapidly chilled on ice for 2 minutes. These cells were grown in 400 µl LB at 37°C and 300 rpm for 1 hour, and then concentrated to 100 µl (at 3000 rpm for 30 ~ 60 seconds), plated onto a LB-ampicillin agar plate, and incubated overnight at 37°C. X-Gal and IPTG were streaked onto agar plates prior to transformation if the plasmids allowed for white-blue colour selection.

Transformation of *One Shot*[®] *TOP10* chemically competent cells for pCR4-TOPO vector was performed as the specific protocol from Invitrogen life technologies Inc.

Selection of colonies

Picked colonies were checked either by restriction digests after mini plasmid preparations or direct PCR using transformed bacteria instead of plasmid DNA. The PCR products without an insert can be used here as negative control. DNA sequencing (see below) serves as an expensively alternative approach to confirm the colonies.

Bacterial cultures

To isolate plasmid DNA, bacterial colonies were picked or taken from a glycerol stock and cultured in LB medium, containing an appropriate antibiotic for selection (mostly ampicillin 50 µg/ml, diluted 1:1000), with vigorous shaking (~300 rpm) at 37°C. Chick EST clones were streaked again to obtain a pure colony before use.

Glycerol stocks

800 µl medium from overnight bacterial cultures (log phase) were thoroughly mixed with 200 µl of 100 % autoclaved glycerol, and stored at – 80 °C for use in the future.

DNA sequencing

DNA sequencing is developed by Fred Sanger (1977) and can determine each deoxynucleotide of a DNA chain. Once a labelled dideoxy nucleotide triphosphate (ddNTP) is incorporated into a growing chain, the synthesis of DNA terminates at that point. Thus, a set of single-stranded DNAs with one nucleotide difference in length is achieved.

ABI PRISM[™] BigDye[™] Terminator Cycle Sequencing Ready Reaction Kit (PE Applied Biosystems, Welterstadt) was used according to the manual of the Sequencing Kit. In short, 2 – 4 µl of terminator ready reaction mix (depending on the length of the DNA to be sequenced), 200 ng plasmid DNA, 3.2 pmol of a single primer (Tab. 5) were mixed with deionized water to final volume of 20 µl. Totally 25 cycles were performed to synthesize the single-stranded DNAs. The setting is at 96°C for 10 sec., 50°C for 5 sec., and 60°C for 4 min. PCR products were purified with ethanol and the pellet was dissolved in 20 µl of template suppression reagent (TSR) in a sequencing-specific tube. The DNA sequencing was run by the CEQ 2000 sequencer, and the data analyses was carried out with the software itself. For plasmids containing hairpin structure or stable secondary structure, 5 % DMSO (1 µl) was added to the PCR reaction mixture. Most of DNA sequencing are performed by Ellen Fecher (Zoology I, Würzburg). A part of samples were sent to MWG Biotech AG, Ebersberg.

2.3. *In vitro* Transcription

Linearisation of the plasmid

Prior to transcription of antisense RNA probes, plasmids were linearized with restriction endonucleases (RE). Briefly, 20 µg of plasmid DNA was digested with 3 µl of particular restriction enzyme (10 U/µl) in a volume of 100 µl for 2 hours at 37°C. The reaction was stopped at 65 ~ 80°C for 20 minutes. The linearized plasmid DNA was purified by phenol/chloroform extraction under a ventilated hood.

Phenol/chloroform extraction

The DNA solution was increased to a total volume of 200 µl with distilled water. A same volume of phenol/chloroform (Roth, Karlsruhe) was added, thoroughly mixed by vortexing, and centrifuged at top speed for 5 minutes. The supernatant was collected and same procedure repeated with 200 µl of chloroform instead of phenol/chloroform. The DNA was then precipitated with ethanol.

DNA precipitation

1/10 volume of 3M NaAc was mixed with the DNA before adding 2 ~ 3 volume of 100 % ethanol. The mixture was centrifuged for 30 minutes, followed by two washes with 70 % ethanol. The supernatant was removed and the pellet was aspirated for 10 minutes at room temperature. The DNA was resuspended in 20 µl of RNase-free water and stored at -20°C. DNA concentration (2 µl) was checked on a 1 % TAE agarose gel.

Synthesis of RNA-labelled probes

Labelled RNA probes were synthesized by RNA polymerases (SP6, T7 or T3) using either digoxigenin- (DIG) or fluorescein- (FITC) UTPs in RNase-free condition. Linearized plasmid DNAs containing specific promoters for bacteriophage RNA polymerases were served as templates. The synthesis is preformed according to MBI Fermentas instructions.

Briefly, the following reagents were mixed gently in an Eppendorf tube, and incubated for 2 hours at 37°C.

| | |
|--|---|
| 1 µl | linearized plasmid DNA (1 µg) |
| 4 µl | 5 x transcription buffer (Promega) |
| 2 µl | 0.1 M DTT (Promega) |
| 2 µl | dNTP-mix (10 mM; FITC- or DIG-conjugated) |
| 0.5 µl | RNase-inhibitor (40 U/µl) |
| 1 µl | T7- or T3-polymerases (10 U/µl) |
| <hr/> | |
| adjust to 20 µl with RNase-free H ₂ O | |

After the finish of the reaction, 2 µl RNase-free DNase I (10 U/µl, Roche Diagnostics) was added and incubated for another 15 minutes at 37°C to remove the DNA template.

RNA precipitation

The RNA solution was adjusted to 100 μ l with RNase-free H₂O. Excess dNTPs were removed using the RNAeasy Kit from Qiagen or precipitating the RNA with LiCl. The later reagent was used as following: 1 μ l glycogen (Boehringer) was added to the transcription solution and mixed by tapping; and then 1/10 volume of 4 M LiCl and 2 - 3 volumes of 100 % ethanol were added. The mixture was centrifuged for 30 minutes and washed with 70 % ethanol. After aspirated at room temperature for 5 - 10 minutes, RNA was dissolved in 50 - 100 μ l RNase-free water or Tris buffer (pH 8.0). The RNA concentration can be analysed on a 1% TBE agarose gel and quantified by photometer.

3. Histological Examinations

Dissection, fixation and mounting

When chick embryos were incubated to the required stages, eggshells were disinfected with 70 % ethanol and opened on the top, and the embryos with yolk and albumin were poured into a 9 cm Petri dish. Embryos were removed with a pair of scissors and carefully transferred into another Petri dish in sterile PBS on ice. Embryos younger than stage HH9 were directly transferred from the egg into Petri dishes using a spatula. Under a stereomicroscope (Leica, Stemi 2000C), the vitelline membrane was peeled from the embryo, and a small hole was cut in the forebrain to avoid antibody or RNA-probe trapping in further procedures.

The embryos were usually fixed in 4% paraformaldehyde (PFA in PBS, pH 7.4) and kept at 4°C at least for 2 hours. For *in situ* hybridisation, embryos should not be stored over 2 weeks.

After the embryos had been labelled, midbrains and/or other parts of CNS were freed from surrounding mesenchyme, cut along roof or floor plate and mounted so-called “open book” preparations on a slide in PBS/glycine (1:9). To avoid fading in fluorescing specimens the PBS/glycine contained DABCO or Aqua-Poly/Mount (Polysciences) was employed. Entellan (Merck) was used to fix the cover slips.

Whole-mount immunostaining

To identify the localization and function of molecules immunohistochemical staining were employed. Chick whole embryo labelling can be performed well up to stage 22. Most antibodies were used after the protocol 1 in Tab 19. In protocol 2 the VECTASTAIN[®] Elite ABC Kit (mouse IgG, Vector Laboratories) was served for staining of QCPN, EphA4 and ephrinA5 proteins. Labelling of phospho-Histone 3 (pH3) required the use of a blocking solution (containing 1% DMSO). The dilution of the antibodies was according to the instruction of the company or the relevant references (Tab. 13, 14). Once a fluorescence-coupled secondary antibody was employed, the specimens should be kept off the light.

Table 19: Whole-mount immunostaining protocols

| |
|---|
| <p>Protocol 1</p> <ul style="list-style-type: none"> • Fix embryos in 4% PFA overnight at 4°C • Block in AB solution 3x 60min at RT ➤ (DAB staining) Block endogenous peroxidase with 0.1% H₂O₂ in PBS overnight at 4°C • Wash in PBS 3x 60min at RT • Incubate with primary antibody in AB solution for 2-4 days at 4°C • Wash in PBS 6x 60min at RT • Incubate with secondary antibody in AB solution overnight at 4°C • Wash in PBS 6x 60min or at RT or overnight at 4°C ➤ (DAB staining) Wash in 100mM Tris (pH 7.4) 2x 30 min ➤ (DAB staining) Add inactive DAB (5mg/10ml) in Tris 3 hours at 4°C, keep dark ➤ (DAB staining) Add active DAB (with 3μl/10ml H₂O₂) in cold Tris 5-15min at RT ➤ (DAB staining) wash in tap water to stop color reaction • Flat mount in PBS/glycerol (plus DABCO) or Aqua-Poly/Mount, seal with Entellan |
| <p>Protocol 2</p> <ul style="list-style-type: none"> • Fix embryos in 4% PFA overnight at 4°C • Wash in AB solution 3x 60min at RT • 50% methanol 5min • 100% methanol plus 3% H₂O₂ 30min • 50% methanol 5min • Wash in PBS/0.2-0.5% Triton 3x 30min • Block in blocking reagent (horse serum) 2 hours at RT • Incubate with primary antibody in blocking reagent overnight at 4°C • Wash in PBS/0.2-0.5% Triton 3x 60min - (Block the endogenous Avidin in PBS with 100mM d-Biotin 60min at RT) - (Wash in PBS 3x 60min) • Incubate with biotin-coupled secondary antibody in blocking solution overnight at 4°C • Wash in PBS with 0.2-0.5% Triton-x 100 3x 60min • Preincubate in 2.5ml PBS containing each drop of solution A and B, 30min at RT • Incubate in ABC 60 min at RT • Wash in PBS 3x 60min • Incubate with DAPI (1:100) in PBS 30min at RT • Wash in PBS 2x 30min at RT • Incubate with Fluorescein-Thyramin (2.7μl) plus 1μl H₂O₂ in PBS 30min at RT ➤ (DAB staining) Add inactive DAB (5mg/ml) in 100mM Tris 3 hours at 4°C, keep dark ➤ (DAB staining) Add active DAB (with 3μl/10ml H₂O₂) in cold Tris 5-15min at RT ➤ (DAB staining) wash in tap water to stop color reaction • Flat mount in PBS/glycerol plus DABCO or Aqua-Poly/Mount, seal with Entellan |

For double staining, embryos were re-fixed in 4 % PFA after the first antibody staining, and then incubated with another primary and secondary antibody produced in a different species. Images were captured and analyzed using a Leica microscope (Leica D-RM) with a Sport RT camera (Diagnostic Instruments Inc.) or a confocal microscope (CLSM, Leica TCS Sp).

Whole-mount RNA *in situ* hybridization

Whole-mount RNA *in situ* hybridization (ISH) of chick embryos was performed as described (Henrique *et al.*, 1995) and shown in Tab. 20. Most of antisense probes (Tab. 15) have been used previously.

Table 20: Whole-mount RNA *in situ* hybridisation protocol

| Procedures | Time | Temp |
|--|------------|-------|
| Dissect embryos in sterile and DEPC-treated PBS | | |
| Fix in 4 % PFA | o/n | 4°C |
| Wash embryos in PBT | 2 x 5 min | RT |
| 25% MeOH in PBT | 5 min | RT |
| 50% MeOH in PBT | 5 min | RT |
| 75% MeOH in PBT | 5 min | RT |
| 100% MeOH in PBT (can store up to three weeks) | 60 min~o/n | -20°C |
| 100% MeOH in PBT | 5 min | RT |
| 75% MeOH in PBT | 5 min | RT |
| 50% MeOH in PBT | 5 min | RT |
| 25% MeOH in PBT | 5 min | RT |
| Wash embryos in PBT | 2 x 5 min | RT |
| 6% Hydrogen peroxidase (H ₂ O ₂) in PBT | 60 min | RT |
| Wash embryos in PBT | 3 x 5 min | RT |
| Detergent mix | 3 x 20 min | RT |
| Fix in 4% PFA with 0.2% Glutaraldehyde | 20 min | RT |
| Wash embryos in PBT | 3 x 5 min | RT |
| Pre-hybridize in hybridisation solution (prewarm at least 60min at 70°C) | 60 min~o/n | 70°C |
| Hybridize with 0.5~1.0 µg/ml RNA probe in hybridisation solution | o/n | 70°C |
| Wash embryos in solution X (prewarm 15 min at 70°C) | 4 x 30 min | 70°C |
| Wash embryos in MABT | 3 x 5 min | RT |
| Block in MABT with 20% GS plus 2% BBR | 2 hrs | RT |
| Add antibody (1:2000~3000) in block mix | o/n | 4°C |
| Wash embryos in MABT | 3 x 5 min | RT |
| Wash embryos in MABT | 5 x 60 min | RT |
| Wash embryos in MABT (or 2 nights) | o/n | 4°C |
| Wash in NTMT (pH 9.5) | 3 x 10 min | RT |
| Incubate in NTMT with 3.5µl NBT and 3.5µl BCIP per 2~3ml | | RT |
| Wash in PBT or TBST, until no longer coloured by reaction by-products | o/n | 4°C |
| Stop colour reaction with 4% PFA or PBS/EDTA | | |
| Store in 4% PFA or 50% glycerol in PBS | o/n | 4°C |

For double *in situ* hybridizations the protocol was modified as follows. FITC- and DIG-labelled RNA probes were hybridized at the same time. After the first color reaction for DIG-labeled probes, embryos were re-fixed in 4 % PFA and washed in PBS with 0.1 M glycine (pH 2.2) for 15 minutes to destroy the alkaline phosphatase (AP). Blue embryos were washed again with MABT, and incubated with anti-FITC-AP antibody. Fast red was used to give a red colour for the Fitc-labelled RNA (1 tablet

per 2 – 3 ml developed in NTMT, pH 8.0). Flat-mounts or vibratome sections helped to check the location of the mRNA of the interest genes.

Vibratome section

The fixed embryos were embedded in 10 % gelatine-albumin (gel-alb) solution at least for 2 hours, till the neural tubes were filled with embedding solution (modified after the ‘semifree-floating’ method described by (Herzog and Brosamle, 1997). 0.5 ml (10 % v/v) glutaraldehyde (25 %) was mixed with 5 ~ 6 ml of gel-alb to accelerate its polymerisation. 5 ml of the mix solution was loaded into a plastic embedding mold (Polysciences), and the embryo was added quickly and covered with the rest of the mix. This step should be performed within 30 seconds before the gel-alb-glutaraldehyde mix hardens. For fluorescent immunostaining, 10 % v/v formaldehyde (37 %) with 0.2 % glutaraldehyde mix replaced the 10 % glutaraldehyde. After the gel-albumin had polymerised (at 4°C overnight), the blocks were fixed in 4 % PFA for 1 - 2 days.

The blocks were trimmed to a convenient size and adhered to the specimen platform in the desired orientation. The tissue sections were cut with a vibratome (Leica VT 100S) in PBS. 20 ~ 50 µm thick sections were mounted onto albumin (BSA) coated slides with several sections on one slide and embedded in Glycerol /PBS. These sections were stained with cresyl violet-thionine or hematoxylin & eosin to reveal the tissue structure.

Vibratome sections can also be immunostained while being attached to the slides. For that 1 % STA-ON solution (Surgipath Europe Ltd., Peterborough, UK) was used to attach the sections on the slide. The staining procedure is same as described in Tab. 19, only the washing and incubation steps were shortened. Sections were photographed under a fluorescence microscope (Leica, DM RA) with a Spot camera (RT colour supply, Diagnostic Instruments, Inc.) or the confocal microscope (CLSM, Leica TCS SP).

Cresyl violet staining

In the nervous system, cresyl violet -a cell body (Nissl) stain- is used to label both neurons and glia (Fig. 18A). Sections were stained in glass chambers at room temperature as described (Hirsch *et al.*, 1998). The protocol is shown as below:

| | |
|-----------------------------------|---------|
| 95% EtOH | 15 min |
| 70% EtOH | 1 min |
| 50% EtOH | 1 min |
| tap water | 2 min |
| cresylviolet color solution | 5 min |
| tap water | 1 min |
| 50% EtOH | 1 min |
| 70% EtOH (2 drops of acetic acid) | 2 min |
| 95% ETOH | 1 min |
| 100% ETOH | 2x1 min |
| Histoclear | 5 min |

In short, an initial alcohol treatment removed the lipids (fats) from the sections. Then the following decreasing alcohol baths allowed the tissue to be stained well by the water-based stain. The sections were submerged in 0.025 % cresylviolet plus 0.025 % thionine colour solution. Acetic acid was used to remove excess stain and the tissues was then dehydrated and made transparent by a clearing agent (Histo-clear, Fisher Chemicals). The slices were mounted in DPX mounting medium (Fisher Scientific company, Loughborough, UK) and analysed by light microscope.

Hematoxylin and eosin staining

Hematoxylin and eosin (H&E) staining is a routine method in histology to stain cell nuclei blue-black by hematoxylin, while cytoplasm or collagen stains in pink by eosin (Fig. 18 B, C). Eosin staining also can be used alone as counterstain to antibody DAB labelling. The protocol below was modified after Rosen Laboratory (Baylor college of medicine, Houston, TA).

1. Wash sections in water
2. Stain in hematoxylin (Gill's No 2) for 3-5 min.
3. Bring 'blue slide' into tap water
4. Decolorize in 1% acid alcohol for a few sec.~1min.
5. Wash in tap water
6. Counterstain in eosin for 2~3 min.
7. Wash in tap water
8. Dehydrate in 95% ethanol 3x 1min
9. Clear in Histo-clear 3x 1 min
10. Mount in DPX

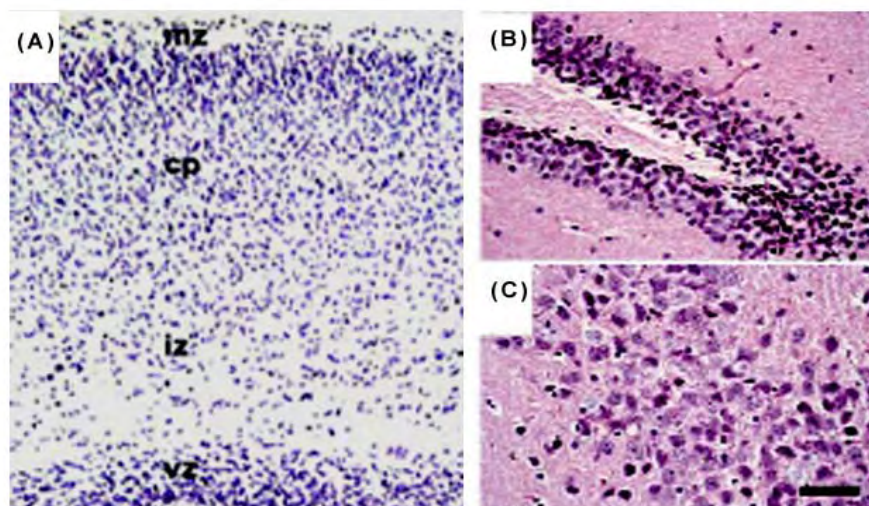


Figure 18: Cresyl violet staining and H & E staining

(A) A coronal section of E18.5 mice cerebrum in cresyl violet staining. (B, C) Coronal sections through the hippocampus of 8 - month mice in Haematoxylin & eosin staining (B, dentate gyrus; C, CA2 region). (Photograph A: Janssen *et al.*, 2003; B, C: Dragatsis *et al.*, 2000).

Abbreviations: cp, cortical plate; iz, intermediate zone; mz, Marginal zone; vz, ventricular zone. Scale bar 50µm.

Results and Discussions

The results are divided into four independent parts, which all connect under the theme of this work – specification and differentiation of the DV axis of the chick mesencephalon. In the first part on ‘DV specification of the chick midbrain’, tissue transplantation and different staining procedures are largely employed. These results suggest that progressive specification of the midbrain DV axis is accompanied by progressively reduced cell mixing between dorsal and ventral precursors, leading to a partial regionalization of midbrain tissue into autonomous units of precursor cell populations. During the early development of the nervous system, precursor cells express specific transcription factors, which guide them to differentiate into different cell types. In the nervous system, an important homeodomain protein - Pax7 emerges at around the closure of the neural tube, and is broadly expressed in the dorsal neural tube and defines the dorsal territory. To investigate the functions for the development of the dorsal midbrain, and interactions of Pax7 with other transcription factors like Pax3, or Brn3a, overexpression and repression of Pax7 are performed. These experiments show that Pax7 seems to regulate cell proliferation in the dorsal midbrain but has no influence on neuronal specification. A member of small GTP proteins - Rab23 is suggested to be involved in the patterning of the dorsal spinal cord in mice. Here illustrates that the expression of Rab23 initiates at very early stage in chick embryos and shows a neural-specific pattern, and it indeed affects some dorsal genes expression. Further the relationship between Rab23 and Shh signalling is investigated via Rab23 overexpression. In the last part, different knockdown approaches are tried and analysed in chick embryos. Comparison of different antisense-based methods suggests that short hairpins siRNA is most efficiently to knockdown gene expression in chick.

Part I:

DV Specification of Chick Midbrain

The chick midbrain is subdivided into functionally distinct ventral and dorsal domains, tegmentum and optic tectum. In the mature tectum, neurons are organized in layers, while they form discrete nuclei in the tegmentum. Dorso-ventral (DV) specification of the early midbrain should thus play a crucial role for the organization of the neuronal circuitry in optic tectum and tegmentum. To investigate regional commitment and establishment of cellular differences along the midbrain DV axis, the commitment of gene expression patterns was examined in isolated ventral and dorsal tissue *in vivo* and *in vitro*, and their cell mixing properties were checked as well. The results suggest that progressive specification of the midbrain DV axis is accompanied by progressively reduced cell mixing between dorsal and ventral precursors, leading to a partial regionalization of midbrain tissue into autonomous units of precursor cell populations.

1. Expression Patterns of Pax3/7, Nkx6.1 and Neural Differentiation in the Mesencephalon

To investigate cell fate determination in the midbrain, the expression patterns of *Pax3* and *Nkx6.1* genes and the Pax7 protein in the mesencephalon were examined firstly.

At stage 11, *Pax3* and Pax7 expressions are detected lateral to the roof plate in the alar plate (Fig. 19 A, D, 20 A). By stage 14, this expression had extended to cover the entire alar plate of the midbrain (Fig. 19 B, C, E, F, and Fig. 20 B - D), which will give rise to the tectum. *Pax3* and Pax7 expression show a similar distribution in the midbrain both are expressed in the alar plate, but only Pax7 is also expressed in the roof plate (Fig. 19 G, H). Interestingly, *Pax3* expression decreases largely after around stage 24, whereas Pax7 continues to be expressed strongly in the tectum during development into adult stages (Fig 20 I, J, Puellas and Rubenstein, 1993; Kawakami *et al.*, 1997). *Nkx6.1* occupies a thin strip adjacent to the floor plate at stage 11 (Fig. 19 A, see the arrowheads, and 19 D). Later in development expression expands more laterally and occupies most of the ventral midbrain by stages 15 (Fig. 19 B, C, E, F). Double staining demonstrates that a small gap exists between *Pax3* and *Nkx6.1* expression

at stage 15 and 17 (Fig. 19 B, C, E, F). Although the regions of *Nkx6.1* and *Pax3* and *Pax7* expression do not abut, at the stages studied here, the majority of ventral and dorsal cells can be characterized by the expression of one or the other gene. Therefore, these complementary patterns of expression were used to define dorsal and ventral identity in subsequent experiments.

Neurofilament specific antibody - RMO-270 was used to gauge the differentiation of midbrain neurons in early development. The first midbrain neurons are born either side of the roof plate at stage 14, (Fig. 20 E), corresponding to the proposed origin of mesencephalic trigeminal nucleus (MTN, Chedotal *et al.*, 1995; Hunter *et al.*, 2001). In ventral midbrain, neurons of the nucleus oculomotorius express neurofilament at stage 16 (Fig. 20 F). At stage 19, most cells in the neuroepithelium remain unstained (Fig 20 H), and at HH24 (embryonic day 4.5), the mantle zone is still relatively thin (Fig. 20 I, J).

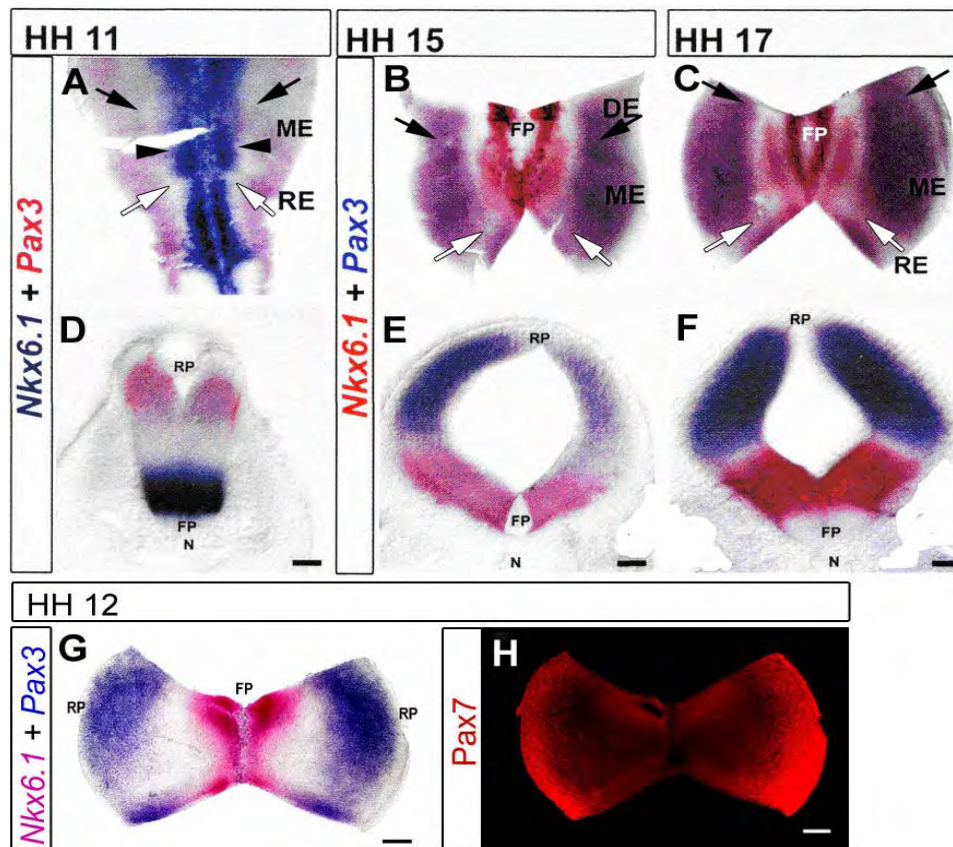


Figure 19: Expression patterns of *Pax3* and *Nkx6.1* in the midbrain

A, - C, G and H are 'open book' preparations of different developmental stages with anterior to the top. D, E, and F are coronal sections of the midbrain with dorsal up. Stages are indicated at the top of pictures, labelled genes at the left. *Pax3* is expressed in the alar plate of the midbrain, but not in the roof plate. *Nkx6.1* is expressed in the basal plate except for the floor plate (A – G). At stage 11 (A, D), a gap exists between *Nkx6.1* and *Pax3*, which almost disappeared by stage 15 (B, E). Both genes are expressed in ventricular and mantle layer (D - F). A midbrain with double staining shows that both *Pax3* (blue) and *Pax7* (red fluorescence) are expressed a similar pattern in dorsal region (G, H). The arrows in the flat mounts indicate the mesencephalic boundary with diencephalons (black) and rhombencephalon (white). The arrowheads in A indicate the lateral extension of *Nkx6.1* expression at stage 11.

Abbreviations: FP, floor plate; DE, diencephalon; ME, mesencephalon; N, notochord; RE, rhombencephalon; RP, roof plate. Scale bars: 100µm.

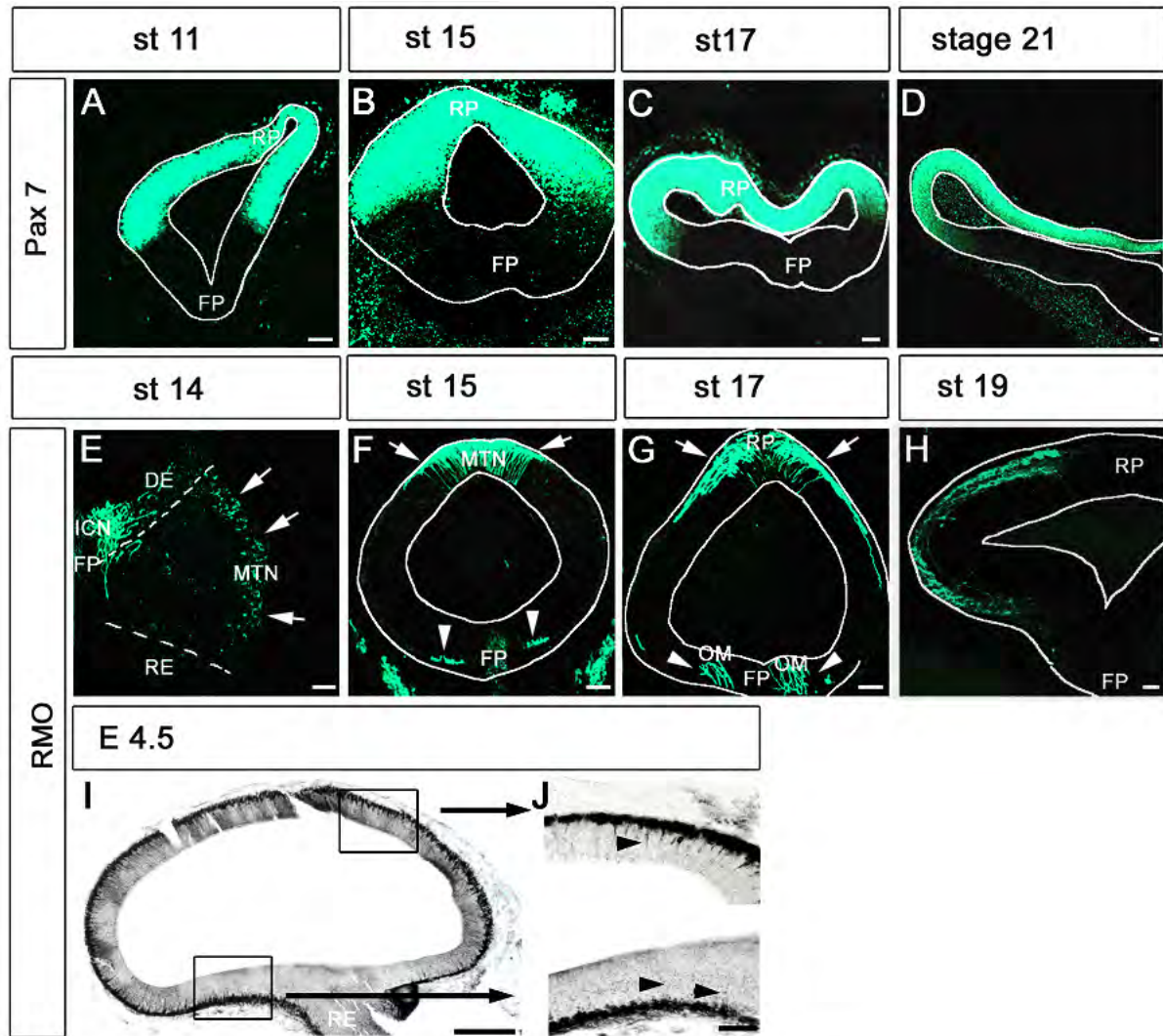


Figure 20: Pax7 expression and neuronal differentiation in the midbrain

A –D, F–J: Coronal midbrain sections (dorsal up, ventral down). E: open book preparation of one half midbrain (dorsal to the right, ventral to the left, anterior to the top).

A –D: Pax7 is expressed in the ventricular and mantle zone of alar plate and roof plate in early developmental stages (2D displays only one half of the midbrain).

E – J: Neurofilament staining (RM0-270 antibody) depicts differentiated neurons in the midbrain at different stages.

E: The first neurons in the midbrain appear along the roof plate at stage 14 forming the mesencephalic trigeminal nucleus (MTN; arrows). The neurons ventrally belong to the interstitial nucleus of Cajal (INC) and originate in the diencephalon.

F: By stage 16 the ventral neurons of the nucleus oculomotorius (OM, arrowheads) have differentiated. Dorsally, MTN neurons have formed axons growing ventrally (arrows).

G: At stage 17, more neurons differentiated and ventral OM neurons formed axons (arrowheads).

H: Stage 19 displays neurons and axons throughout the entire dorsal mantle layer of the midbrain (green fluorescence; brackets indicate mantle zone and ventricular zone).

I: A parasagittal section through a midbrain at E4.5. The mantle layer with differentiated neurons (visualized in black) is still small compared to the ventricular region with progenitor cells.

J: A magnification of the indicated ventral and dorsal regions in I. Differentiated neurons migrate from the ventricular to mantle layer (arrowheads).

Abbreviations: FP, floor plate; DE, diencephalons; INC, interstitial nucleus of Cajal; ME, mesencephalon; MTN, mesencephalic trigeminal nucleus; OM, nucleus oculomotorius; RE, rhombencephalon; RP, roof plate. Scale bars: 100µm.

2. DV Polarity-Reversed Transplantation

Tissues from dorsal and ventral midbrain were grafted into ventral and dorsal midbrain, respectively, in order to analyze the potential of maintaining the original gene expression pattern. Well-integrated grafts were screened for the expression of dorsal markers 16 hr after surgery. In grafts exceeding a certain cell number, developmental potentials could change due to community effect (reviewed by: Gurdon *et al.*, 1993a; Gurdon *et al.*, 1993b; Buckingham, 2003). Therefore, the explants were kept small and constant in size to avoid the influence of these variations on the outcome of transplantation. The results of these grafting experiments are summarized in Fig. 24 and 26.

Homochronic Grafts

At stage 11, both dorsal (n = 4) and ventral midbrain grafts (n = 14) were able to adopt the characteristics of neighboring tissue as defined by expression of *Nkx6.1* or *Pax3/Pax7*, respectively. The first indication of regional commitment was seen at stage 12, when 3 ventral grafts (n = 17) failed to develop a dorsal-specific marker after heterotopic transplantation. Fig. 21 A - F show two examples of ventral transplants grafted at stage 11, which express *Pax7*, a dorsal marker. The ventral midbrain tissue has integrated fully: cells are able to migrate away from the transplant, while axons extend ventrally from donor tissue (not shown). Fig. 23 A - F show dorsal grafts located at the dorso-ventral border of the midbrain. The grafts still express *Pax7*, when dorsally located; however, they stopped expressing *Pax7* in their ventral extension. In Fig. 22A, a dorsal graft is depicted expressing the ventral marker gene *Nkx6.1*.

The ability of grafted tissue to adopt the molecular identity of surrounding tissue decreases progressively as the midbrain matures. At stages 13 and 14, 75% of the dorsal tissue transplanted ventrally adopted a ventral fate (75 %; n = 16, and 73%; n = 11, respectively). Similarly, only 50% of the ventral grafts transplanted dorsally (57 %; n = 69 and 47 %; n = 21, respectively) expressed dorsal markers. By stage 15, only 30% of grafts remained plastic (36%; n = 14, and 28%; n = 25, respectively), falling to 15% by stage 16 (14%; n = 7 and 12%; n = 8, respectively). Fig. 21 G - L shows dorsal midbrain in which ventral transplants grafted at stage 17 fail to express *Pax7*. Fig. 22 B depicts a ventral midbrain graft that has maintained expression of *Nkx6.1* in a *Pax3*-positive territory. In Fig. 23 G - I a dorsal transplant grafted at stage 17 is shown still expressing *Pax7* although in a ventral *Pax7*-negative surround. By contrast to midbrains transplanted at earlier stages, only very few of these later grafts showed cell mixing into neighboring territory or extended axons (not shown). By stage 18, no dorsal or ventral graft was able to activate ventral or dorsal specific gene expression, respectively (n = 2; Fig. 24 A, B). In addition, midbrain cells rarely expressed a dorsal and ventral gene simultaneously (3%) in about 50 % of ventral and dorsal grafts at the time analyzed.

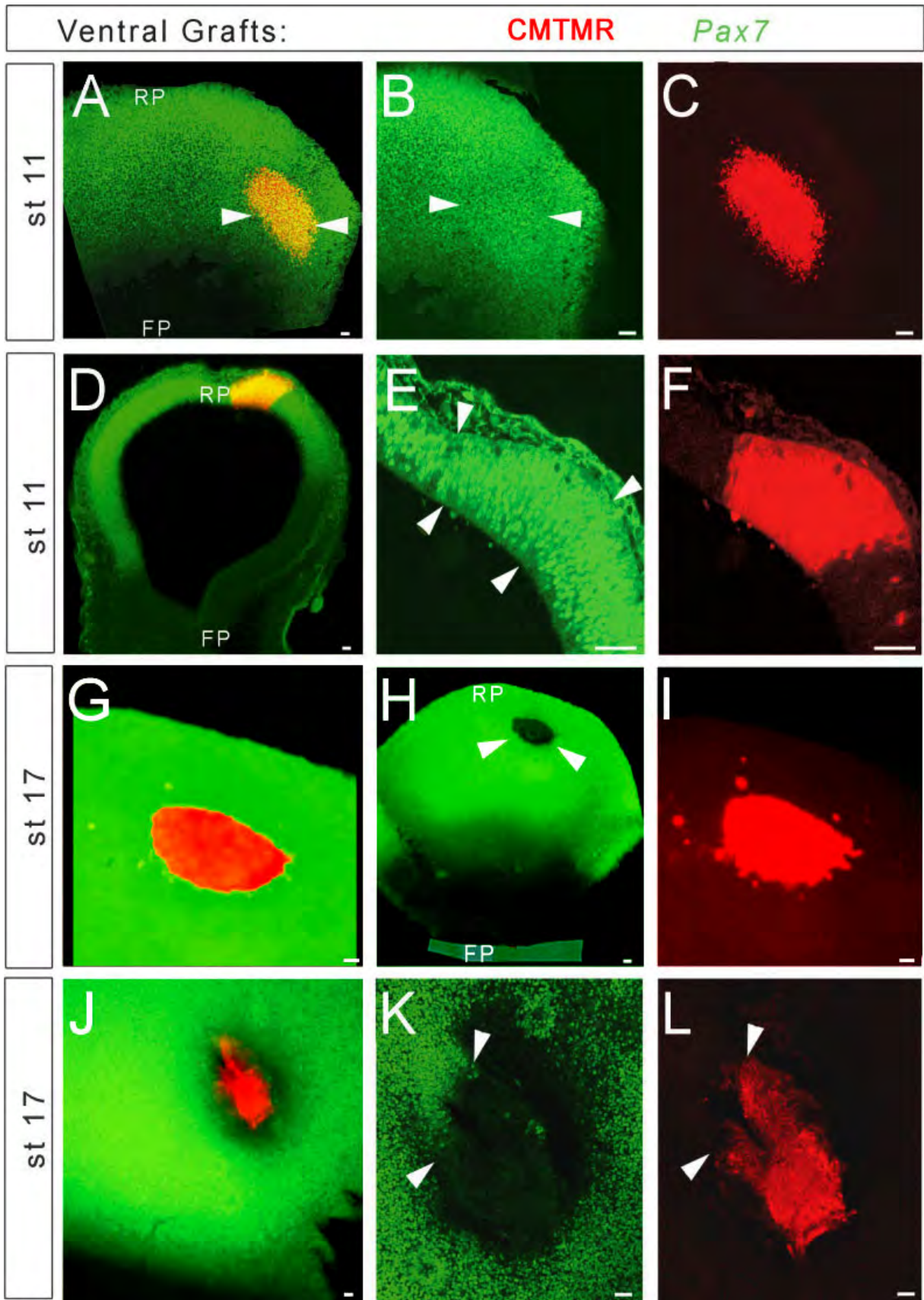


Figure 21: Protein expression of ventral ectopic midbrain grafts

Figure 21: Protein expression of ventral ectopic midbrain grafts

“Open book” preparations (A - C, G - L; anterior to the left, posterior to the right, dorsal up, ventral down) and coronal sections (D - F; dorsal is up, ventral down) of midbrain. The midbrain is stained with an antibody against Pax7 (green fluorescence) and the grafts are labelled with orange Cell Tracker dye (CMTMR, red fluorescence). Stages of grafting are indicated at the left. A - F were fixed at stage 17, G - L at stage 19.

A: Dorsal midbrain is outlined by the expression of Pax7 and displays a ventral graft (indicated by arrowheads). The grafted ventral cells appear yellow because they express Pax7 and CMFDA.

B: Higher magnification of A. Clearly, ventral graft cells (location indicated by arrowheads) express Pax7 protein.

C: Same panel as in B, but ventral midbrain graft labelled with CMFDA.

D: A ventral midbrain graft near the roof plate appears yellow due to the expression of Pax7 and CMFDA.

E: Magnification of D showing Pax7 expression of the graft. Arrowheads indicate the graft borders.

F: Same panel as in E showing the ventral midbrain graft labelled with CMFDA.

G: Cells of this ventral graft show in red (labelled with CMFDA) and not yellow as in A and D when the cells are double labelled with Pax7 (green).

H: A lower magnification of G shows that the cells in the graft (outlined by arrowheads) do not express Pax7.

I: Same panel as in G showing the ventral graft (CMFDA).

J - L: Another ventral midbrain graft transplanted at stage 17. The graft cells do not express Pax7 (L). The arrowheads in K indicate the border between graft and dorsal midbrain. L shows the CMFDA - stained cells of the ventral graft in K.

Abbreviations: FP, floor plate; RP, roof plate. Scale bars: 100µm.

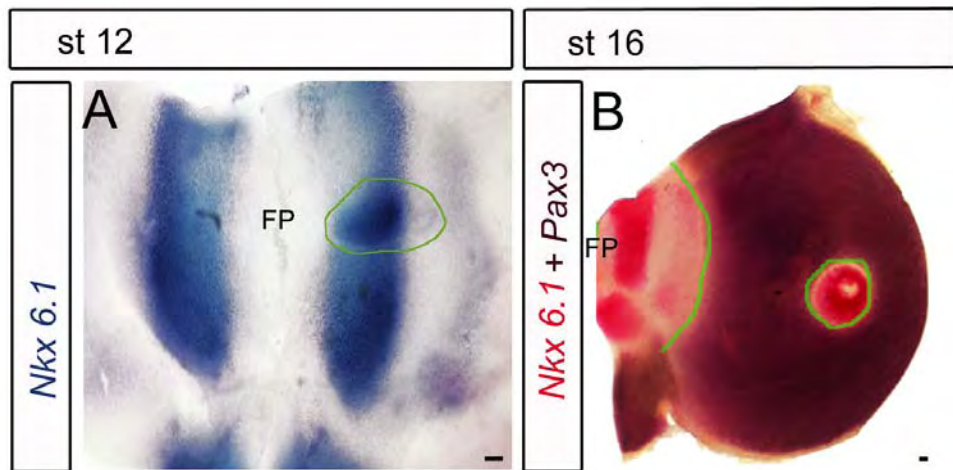


Figure 22: Gene expression of ectopic midbrain grafts

The stage of transplantation is indicated at the top, Genes used for staining at the left.

A: A dorsal graft in a ventral surround expresses *Nkx6.1* (blue staining), a ventral marker gene. The graft is outlined in green.

B: A ventral graft (outlined in green) still expressing *Nkx6.1* (red staining) in a dorsal surround expressing *Pax3* (purple staining).

Abbreviations: FP, floor plate. Scale bars: 100µm.

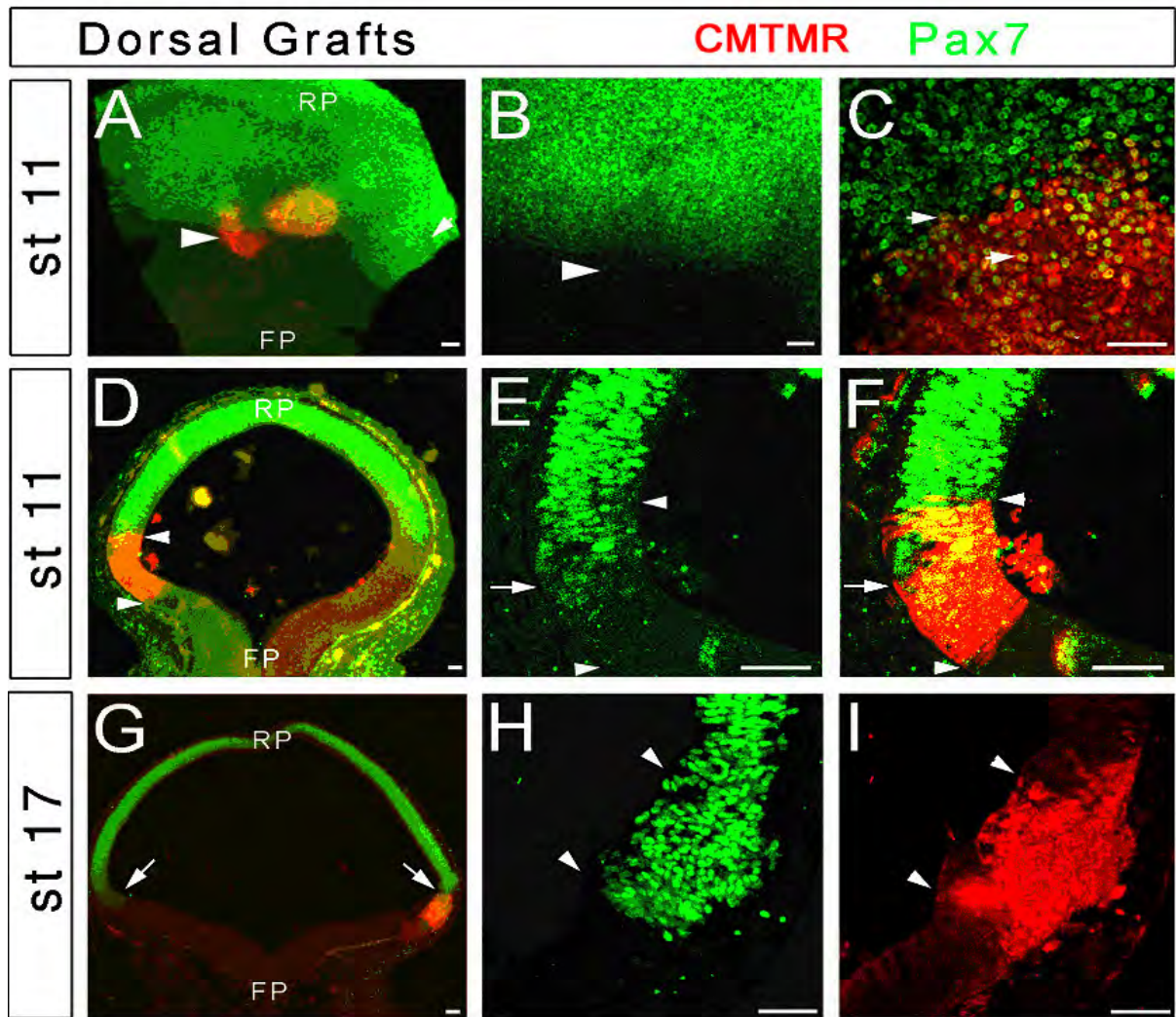


Figure 23: Protein expression of dorsal ectopic midbrain grafts.

“Open book” preparations (A-C; anterior left, dorsal up) and coronal sections (D – I; dorsal up) of midbrain. Pax7 is labelled with green fluorescence. The grafts are labelled with CMTMR (red fluorescence). Grafts from stage 11 (indicated at the left) were fixed at stage 17, and stage 17 grafts at stage 19.

A: Of the two dorsal midbrain grafts (CMFDA labelled) at the DV border, one has lost most of its Pax7 expression (only in red fluorescence, arrowhead) ventrally.

B: Magnification of A, showing a normal Pax7 border that does not extend ventrally as does the left dorsal graft in A (arrowhead).

C: Magnification of B around the arrowhead in B. Note that toward the bottom fewer cells express both Pax7 and CMFDA (yellow fluorescence).

D: A section through dorsal midbrain graft at the DV border. Dorsally (upper arrowhead), the graft appears yellow due to the expression of Pax7 and CMFDA. Ventrally (lower arrowhead), the graft cells express only CMFDA.

E: Magnification of D. Arrowheads indicate the dorsal and ventral graft borders, the border of Pax7 expression is indicated by a small arrow.

F: Same panel as in E showing the CMFDA-labelled graft and Pax7 staining. Graft borders (arrowheads) and the border of Pax7 (arrow) are indicated.

G: A coronal section of a dorsal midbrain graft (yellow fluorescence) still expressing Pax7 in a ventral surround. The two arrows indicate the DV border of Pax7 expression.

H: Magnification of G displaying the Pax7 staining of the transplant (indicated by arrowheads).

I: Same panel as in H displaying the dorsal graft labelled with CMFDA.

Abbreviations: FP, floor plate, RP, roof plate. Scale bars: 100µm.

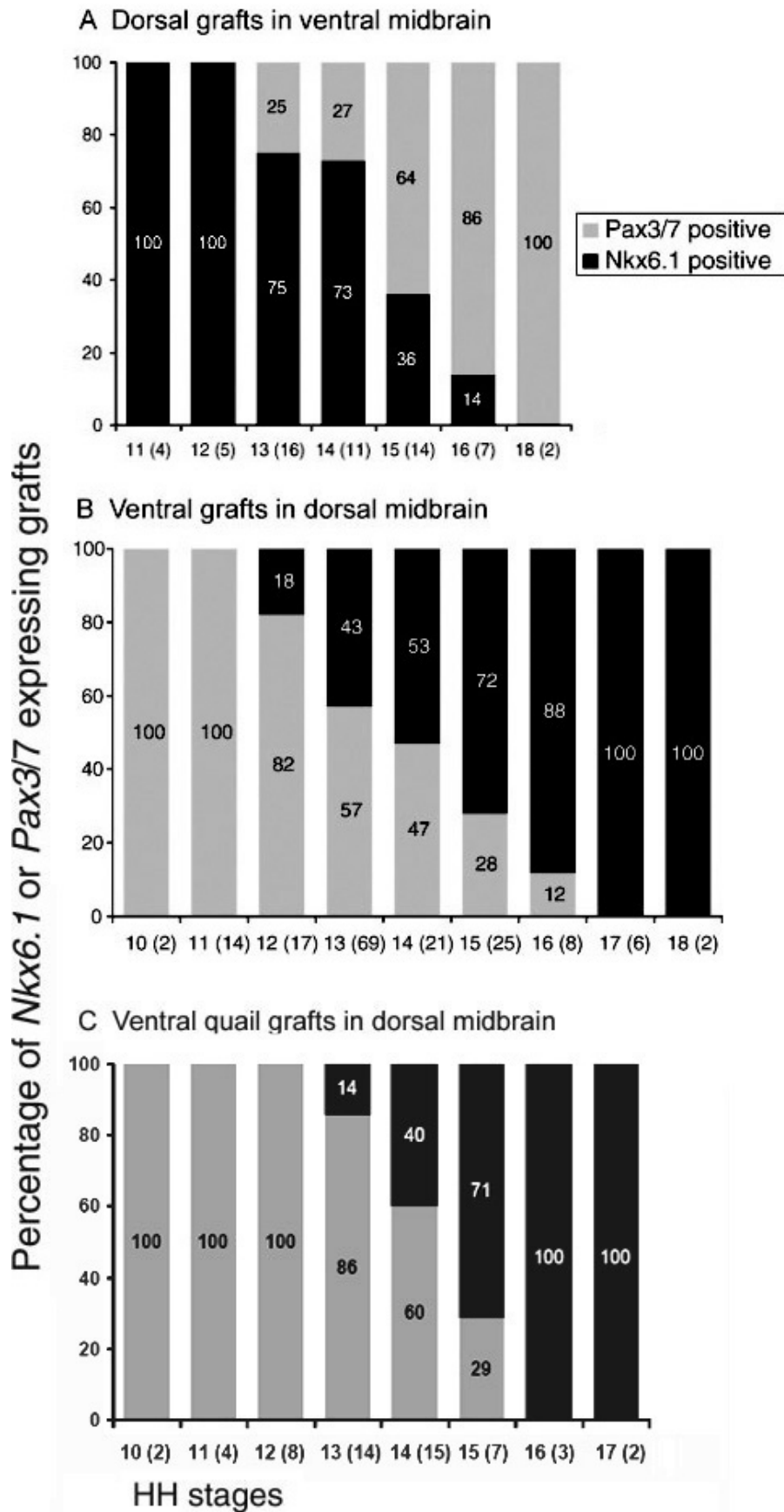


Figure 24:
Quantitative analysis of the gene expression of ectopic midbrain grafts

A: The percentage of dorsal midbrain grafts in a ventral surround, which express the ventral marker *Nkx6.1*. Clearly, dorsal grafts lose gradually their ability to change their original gene expression of *Pax3* to *Nkx6.1* over time.

B: The graph shows the percentage of ventral transplants that expressed a dorsal marker (*Pax3* or *Pax7*) after transplantation at different stage stages.

Comparable to dorsal grafts, over 80% of the ventral grafts lost their ability to change their original gene expression at stage 16.

C: Percentage of ventral quail grafts in dorsal chick midbrain that expressed dorsal markers. Note that quail grafts already cease to express dorsal markers at stage 16, one stage earlier than chick ventral grafts.

The numbers of embryos are indicated in the brackets behind the stages of the abscissa.

To prepare for the quail-chick chimera, the commitment of gene expression in quail embryonic neural tubes was tested firstly. The development of quail embryos is closely matched with chick at early stages (Tab. 1). However, due to an endogenous acceleration at later stages quails hatch 3 – 4 days earlier than chicks (Senut and Alvarado-Mallart, 1987). Grafts of quail tissue into chick have successfully been used in neurobiology (Alvarado-Mallart and Sotelo, 1984; Wakamatsu *et al.*, 1997). In this study, immunohistochemistry and RNA *in situ* hybridisation showed that expression patterns of Pax3/7 and Nkx6.1 in quail midbrains were same as chick embryos at early corresponding stages (data not shown).

Grafts of quail ventral midbrains in chick dorsal regions showed that prior to stage 12 the transplants exclusively expressed the dorsal markers Pax3 or Pax7 (Fig. 24 C, 25 A, B). The maintenance of Nkx6.1 expression in dorsal surrounds was first detected at stage 13 (n = 1/14). The ratios of ventral grafts expressing dorsal genes fell to 60% at stage 14 (n = 9/15; Fig. 25 C, D), and to 30% at stage 15 (n = 2/7). By stage 16, ventral quail cells were unable to express a dorsal marker in dorsal chick midbrain (n = 3 at stage 16, and n = 2 at stage 17). Thus, the transition from a labile to a committed cell state also occurs in the quail-chick chimera as homotopic transplantation. In addition, Pax3/7-non-expressing quail grafts (about 50%) always displayed repression of these genes in neighbour chick cells (Fig. 25 C, D). This might be due to the grafts closely to floor plate or higher Shh level in the quail neural tube.

These results indicate that the dorsoventral identity of midbrain cells acquire progressively commitment along with the DV position over stages 12 - 17, and become refractory to the influence by neighboring tissue of heterotopic grafts. To some extents, these changes reflect endogenous programs of maturation as indicated by inter-species grafts between quail and chick.

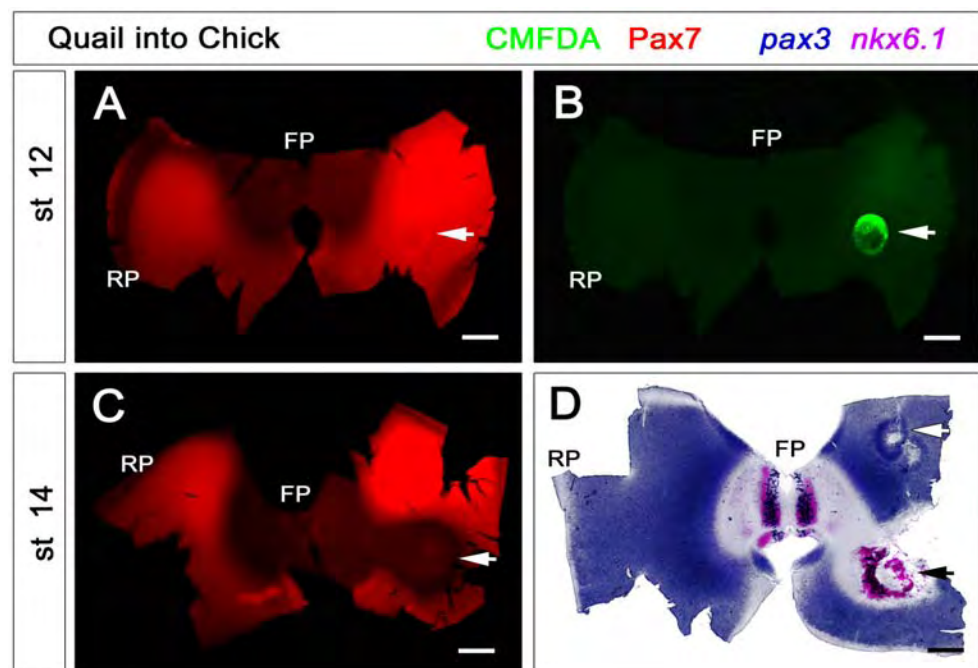


Figure 25: Gene expression of heterotopic ventral midbrain grafts

Heterochronic Grafts

Since the previous results could be due to a different competence of graft or host at the various stages, heterochronic grafting was performed.

Dorsal tissue from a stage 16 donor grafted into ventral midbrain of a stage 11 host showed a higher ability to adopt to the molecular identity of ventral midbrain, compared with the stage 16 homochronic grafting experiments (50% compared with 14%, $n = 8$; Fig. 26 A). However, tissue grafts derived from stage 17 or 18 embryos never adopted ventral-specific gene expression ($n = 7$ and 4 , respectively, Fig. 26 A). Half of the ventral tissue grafts from stage 16 ($n = 4$) and 17 ($n = 4$) did still adopt a dorsal molecular identity after transplantation into stage 11 or 10 embryos compared with 12% or 0% of the homochronic ventral grafts, respectively (Fig. 26 B). However, stage 18 ventral tissues ($n = 4$) failed to express dorsal makers in stage 11 embryos (Fig. 26 B). Taken together, at stage 18 ventral and dorsal tissue grafted into younger hosts did not change their molecular identity anymore.

In addition, we studied the fate of ventral stage 14 and 13 grafts in older and younger host embryos (Fig. 26 C, D). In homochronic ventral grafts at stage 13 and 14, around halves of transplants failed to express the dorsal marker Pax7 (Fig. 26 C, D). The heterochronic transplantations showed that about 20% more stage 13 ventral grafts adopted a dorsal fate in younger host embryos compared with homochronic grafts (stage 11: 83 %, $n = 6$; stage 12: 71 %, $n = 7$; Fig. 26 C). Stage 14 ventral grafts in younger hosts also displayed higher percentages of dorsal fates (stage 12: 67 %, $n = 3$; stage 13: 50 %, $n = 4$; Fig. 26 D). Around 65% of the grafts maintained their molecular identity in host tissue two stages older than the transplant (60 % and 67 %, respectively; Fig. 26 C, D). Overview of ventral grafts at stage 10 to 18 displays that the transplants are refractory to dorsal fates with the development in a dorsal surround (Fig 26 E). This finding suggests that ventral or dorsal midbrain of older hosts shows less inductive abilities than midbrain tissues of hosts at early stages.

Figure 25: Gene expression of heterotopic ventral midbrain grafts

'Open book' preparations of quail-chick chimera midbrains. The midbrain transplantations from quail to chick were performed at stages 12 (A, B) and 14 (C, D) and incubated for 24 hrs. Quail tissues were labelled with a CellTracker dye CMFDA (green fluorescence in B). Pax7 protein was visible by immunohistochemistry with an antibody (red fluorescence in A, C). Pax3 (blue in D) and *Nkx6.1* (red) mRNAs were detected by *in situ* hybridisation with RNA probes.

A, B: A quail ventral graft (arrow) had integrated into chick dorsal midbrain and expressed Pax7 in this new location.

C: A stage-14 quail ventral graft (arrow) did not express Pax7 in dorsal midbrain. The surrounding chick cells did not express Pax7 as well.

D: In a chick dorsal midbrain, one ventral graft expressed *Nkx6.1* continuously (black arrow), the other changed to express Pax3 (white arrow). The gene expression of grafts was not related to their positions along anterioposterior axis.

Abbreviations: FP, floor plate, RP, roof plate. Scale bars: 100µm.

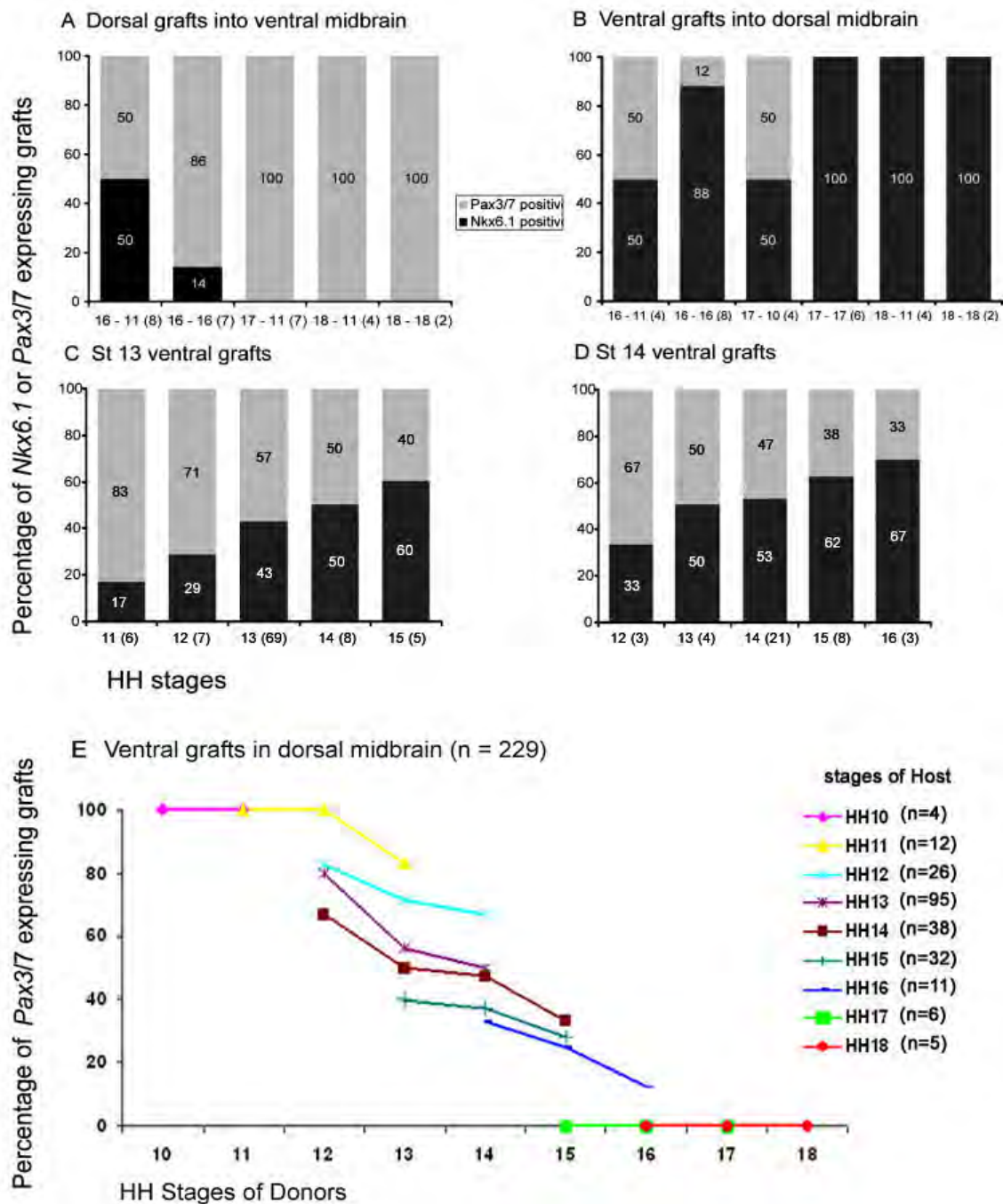


Fig. 26. Heterochronic and homochronic midbrain grafts

A: The percentage of dorsal midbrain grafts in a younger ventral surround, which express the ventral marker *Nkx6.1*. Clearly, stage 17 and 18 dorsal grafts show no ability to change their original gene expression anymore.

B: The graph shows the percentage of ventral transplants that started to express a dorsal marker (*Pax3* or *Pax7*) in younger host embryos. Comparable to heterochronic dorsal grafts, no stage 18 ventral transplants adopted a dorsal fate.

C: Percentages of stage 13 ventral grafts in dorsal midbrain of different stages. Compared with homochronic transplantation, 20 % more grafts activated a dorsal-specific gene expression in younger hosts, whereas in hosts of two stages older than the graft, 20 % fewer grafts adjusted to coincide with the new surround.

D: Stage 14 ventral grafts in older embryos show the same changes of gene expression as stage 13 grafts in C. More and fewer grafts adjusted to a new surround in younger and older hosts, respectively, compared with homochronic grafts. The number of embryos is indicated in the brackets behind the stages of the abscissa.

E: The percentage of ventral grafts expressing *Pax3* or *Pax7* in dorsal midbrains at different stages (from 10 – 18). Hosts of different stages are marked in coloured line. The numbers of embryos are indicated in the brackets behind the stages of hosts.

3. Influence of Floor Plate and Roof Plate on the Expression of Ventral and Dorsal Specific Genes

To investigate, whether the positional identity of ventral or dorsal midbrain tissue is autonomous or dependent on midline-derived signals, explants from dorsal and ventral midbrain were cultured for 18 - 20 hr with or without roof plate or floor plate, respectively, and then examined for the expression of a dorsal (*Pax3*) or ventral (*Nkx6.1*) marker. Prior to stage 16, in the absence of floor plate tissue, ventral explants (stages 8, 10 or 12) failed to maintain *Nkx6.1* expression (Tab. 21, Fig. 27). These explants did also not adopt a dorsal identity (Table 21). Similarly, before stage 16, the expression of *Pax3* in dorsal explants (stages 10 and 12) was lost in the absence of roof plate and no ventral identity was adopted (Tab. 22, Fig. 27). Furthermore, co-culture experiments of ventral midbrain with roof plate tissue or dorsal midbrain with floor plate tissue demonstrated that dorsal and ventral tissue from stage 16 midbrain is refractory to ectopic ventralizing or dorsalizing signals, respectively (Tab. 21, 22). At earlier stages, 90 – 100 % of ventral or dorsal midbrain co-cultures adopted dorsal or ventral identity, respectively (Tab. 21, 22). The 10% not expressing the expected gene when co-cultured with one of the two signaling centers are certainly caused by the difficulty to isolate roof plate and floor plate at that stages, which results in isolating areas lateral to roof or floor plate.

TABLE 21. Number (x) of Ventral Midbrain Explants From Different Stages Expressing *Nkx6.1* or *Pax3* Without Floor Plate (-FP), With Floor Plate (+FP), or Cultured With Roof Plate (+RP) Is Shown in Comparison to the Total Number of Explants (n)

| Stage | <i>Pax3</i> (x/n) | | <i>Nkx6.1</i> (x/n) | | |
|-------|-------------------|-----|---------------------|-------|------|
| | -FP | +RP | -FP | +FP | +RP |
| 8 | 0/13 | 2/2 | 0/9 | 6/6 | 0/2 |
| 10 | 0/8 | 4/6 | 0/20 | 11/12 | 2/15 |
| 12 | 0/14 | — | 0/6 | 2/2 | — |
| 16 | — | — | 6/7 | — | 3/3 |
| 19 | — | — | 14/14 | 19/20 | 7/7 |
| 20/21 | — | — | 9/10 | 7/7 | — |

TABLE 22. Number (x) of Dorsal Midbrain Explants From Different Stages Expressing *Pax3* or *Nkx6.1* Without Roof Plate (-RP), With Roof Plate (+RP) or Cultured With Floor Plate (+FP) Is Shown in Comparison to the Total Number of Explants (n)

| Stage | <i>Nkx6.1</i> (x/n) | | <i>Pax3</i> (x/n) | | |
|-------|---------------------|-----|-------------------|-------|-------|
| | -RP | +FP | -RP | +RP | +FP |
| 8 | 0/11 | — | 0/5 | 6/6 | — |
| 10 | 0/9 | 3/3 | 0/6 | 10/11 | 0/4 |
| 12 | 0/11 | — | 0/9 | 8/8 | — |
| 16 | — | — | 5/5 | — | 2/2 |
| 19 | — | — | 13/15 | 8/9 | 15/16 |
| 20/21 | — | — | 7/7 | 6/7 | — |

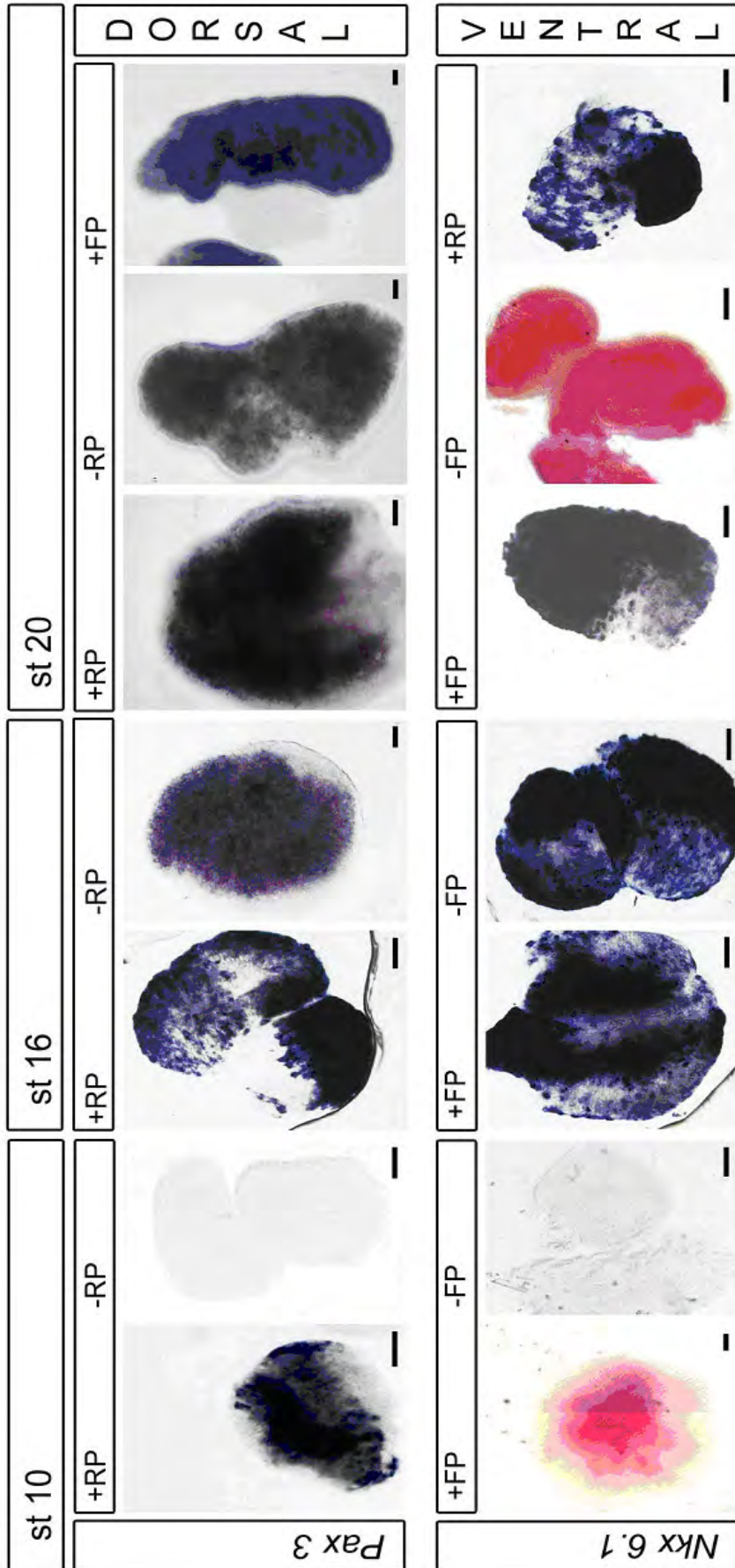


Figure 27: Explant cultures of ventral and dorsal midbrain with and without signaling centers

The stage at which the midbrain tissue was cultured is indicated in the panels above the pictures. Dorsal midbrain tissue (upper panel of pictures) was stained with Pax3, ventral midbrain explants (lower panel of pictures) with Nkx6.1. Culturing with roof plate (+RP) or floor plate (+FP) or without the two signalling centres (-RP, -FP) is indicated above each picture.

At stage 10, neither Pax3 nor Nkx6.1 were expressed in dorsal or ventral explants without the signalling centres. Dorsal and ventral explants expressed Pax3 or Nkx6.1 without roof plate or floor plate, respectively by stage 16. At stage 20 dorsal and ventral midbrain explants maintained the expression of their original gene although they were co-cultured with the opposite signalling centre, floor or roof plate, respectively.

Scale bars: 100µm.

4. Adhesion Between Ventral and Dorsal Midbrain Cells

Regional specification is reflected to some extent by cell surface changes that can be revealed by cell adhesion assays. An *in vitro* short-term cell aggregation assay (Wizenmann and Lumsden, 1997) was employed to examine specific adhesive properties of dorsal and ventral midbrain at different stages. Briefly, dissociated cells from dorsal and ventral midbrain were labeled with different fluorescent dyes, mixed in certain combinations, and allowed to segregate for 3 - 4 hr. Resulting aggregates were analyzed by microscopy and classified as either segregated or mixed to determine a “segregation ratio” (Fig. 17). Control aggregation cultures, where either identical ventral cells or identical dorsal cells labeled with two contrasting dyes were recombined, revealed a baseline segregation ratio of 14 % (n = 2,374) at stage 19 and 13 % at stage 22 (n = 2,088; Fig. 28 D and E).

Combining separately labelled ventral and dorsal cell populations revealed a progressive differentiation of aggregation characteristics from stage 17 - 22. At stage 17, ventral/dorsal cell mixtures showed a low segregation ratio of 12 % (n = 1320; Fig 28 A, E), close to the baseline level described above. With the chick development, the segregation ratio was determined as 36 % at stage 19 (n = 996), 62% (n = 1024) at stage 20 (Fig. 28 B, E), and 80 % (n = 1119) at stage 22 (Fig. 28 C, E). The segregation ratios at stage 19 to 22 were significantly higher than that of controls and stage 17 (X^2 ; $p \leq 0.01$).

Figure 28: Fluorescence photomicrographs of aggregates formed by ventral and dorsal midbrain cells

Ventral and dorsal midbrain cells at stage 17 (A), stage 20 (B), and stage 22 (C, D) were labelled with different Cell Tracker dyes.

A: Aggregates from stage 17 composed of cells from ventral (red fluorescent) and dorsal (green fluorescent) midbrain that intermingle freely.

B: Cell aggregates from stage 20 show that dorsal (red fluorescent) and ventral midbrain cells (green fluorescent) segregate from each other.

C: Aggregates formed by midbrain cells at stage 22. Clearly, ventral (red) and dorsal (green) cells segregate from each other.

D: Aggregates formed by stage 22 ventral midbrain cells labelled with red and green fluorescence that intermingle freely.

E: Quantitative analysis of aggregates formed at different stage stages. The histogram depicts the segregation ratio of aggregates (percentage of segregated vs. mixed aggregates) formed by ventral and dorsal midbrain cells at different stages (orange bars). Ventral and dorsal midbrain cells show different segregation ratios at stage 17, 19, 20, and 22. These segregation ratios are significantly different from each other (X^2 ; $p \leq 0.01$). At stage 19 and 22 the segregation ratio between ventral and dorsal midbrain is significantly different from that of control aggregates (green bars) consisting of only ventral or dorsal cells. Note, the segregation ratio of stage 17 and controls are very similar. The number of aggregates is indicated in the brackets behind the stages.

Scale bars: 100 μ m.

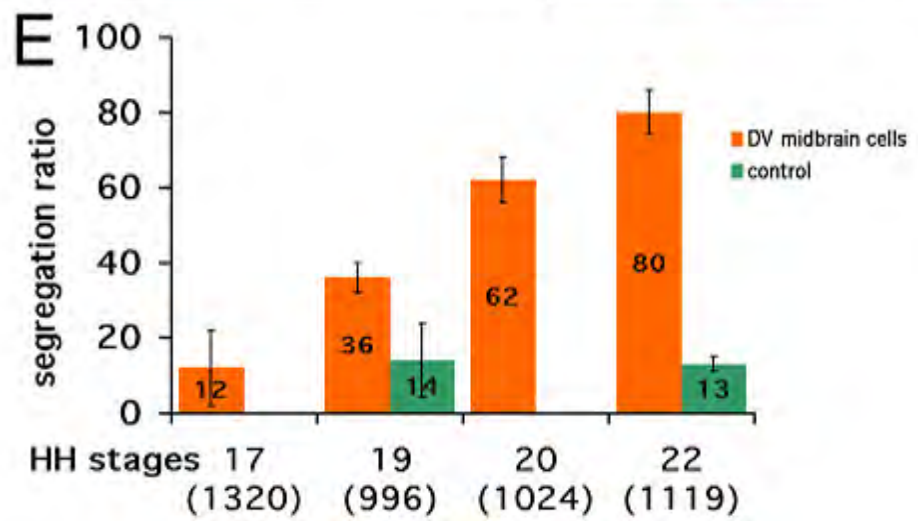
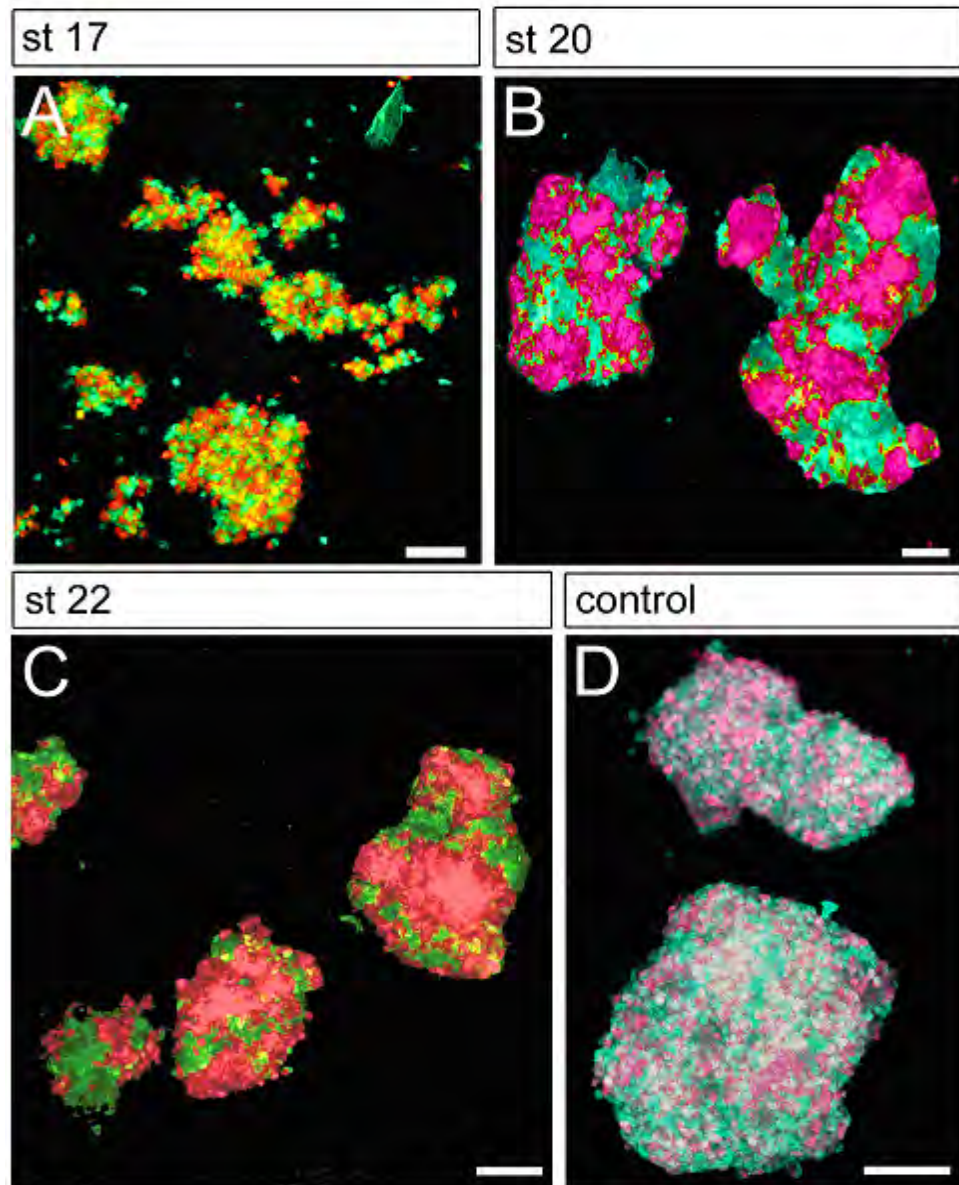


Figure 28: Fluorescence photomicrographs of aggregates formed by ventral and dorsal midbrain cells

5. Long-term Transplantation

To investigate the architectonal fate of the ventral or dorsal grafting cells, DV polarity-reversal transplantation was performed with a dorsal or ventral quail tissue into chick midbrain, and incubated till embryonic day 5.5, 7, 8.5 or 13. The chick-quail chimeric midbrains were cut into coronal sections, and stained with H&E and cresyl violet (Fig. 29 A, B), which allow clear views on the cellular layers in the tectum and nucleus in tegmenta (LaVail and Gowan, 1971). The long-term ventral grafts showed a coincident result (Fig. 29 I) with quail ventral grafts incubated for a short period (Fig. 24 C). At stage 12, all of the ventral grafts (n = 4) exclusively expressed Pax7 in dorsal surround. This ability to express Pax7 was gradually decreased in the grafts at the following stages (stage 13: 86 %, n = 7; stage 14: 67 %, n = 12; and stage 15: 50 %, n = 8). By stage 16, Pax7 expression was not detected in any ventral graft (stage 16, n = 2; stage 17, n = 3). In another hand, the long-term dorsal grafts lost to express Pax7 in ventral midbrain at stage 12, and gradually strengthened to maintain their dorsal-specific gene expression with the time (data not shown).

At the view on histological structures, nearly all of the ventral grafting cells in dorsal midbrain preferred to accumulate together, and interrupted the laminar layering of the tectum at least partially (Fig. 29 A - D). Whatever these cells expressed Pax7 or not, they were separated with surrounding host cells. This suggests that the ventral fate of these grafting cells is still plastic in an ectopic surround, but they seem to develop differently with original dorsal cells in molecular cell properties and architectonal cell arrangements. At this point, dorsal grafting cells only revealed a good integration into the ventral midbrain due to lack of cellular structures in tegmentum (Fig. 29 G, H). In addition, a few of dorsal and ventral grafts showed that quail cells were integrated into both dorsal and ventral regions (Fig. 29 G, H). This could be due to the grafts situated at the DV border of the host midbrains.

Figure 29: Protein expression of the long-term quail grafts

A - F: A quail ventral midbrain tissue was grafted into chick dorsal midbrain at stage 13 and fixed at E 8.5. G, H: A ventral quail graft was performed at stage 14 and fixed at E 7. Dorsal is up. A - D, and G - H are consecutive coronal sections of midbrains. A dorsal-specific gene - Pax7 was identified by immunostaining with an antibody (C, E, G). Quail cells were visualized by a quail-specific antibody - QCPN (D, F, H).

A, B: A ventral graft (arrows) was integrated into the tectum. Cellular structures of the tectum were illustrated by hematoxylin and eosin (A) and cresyl violet staining (B). Note: At this stage the laminar layers have already formed.

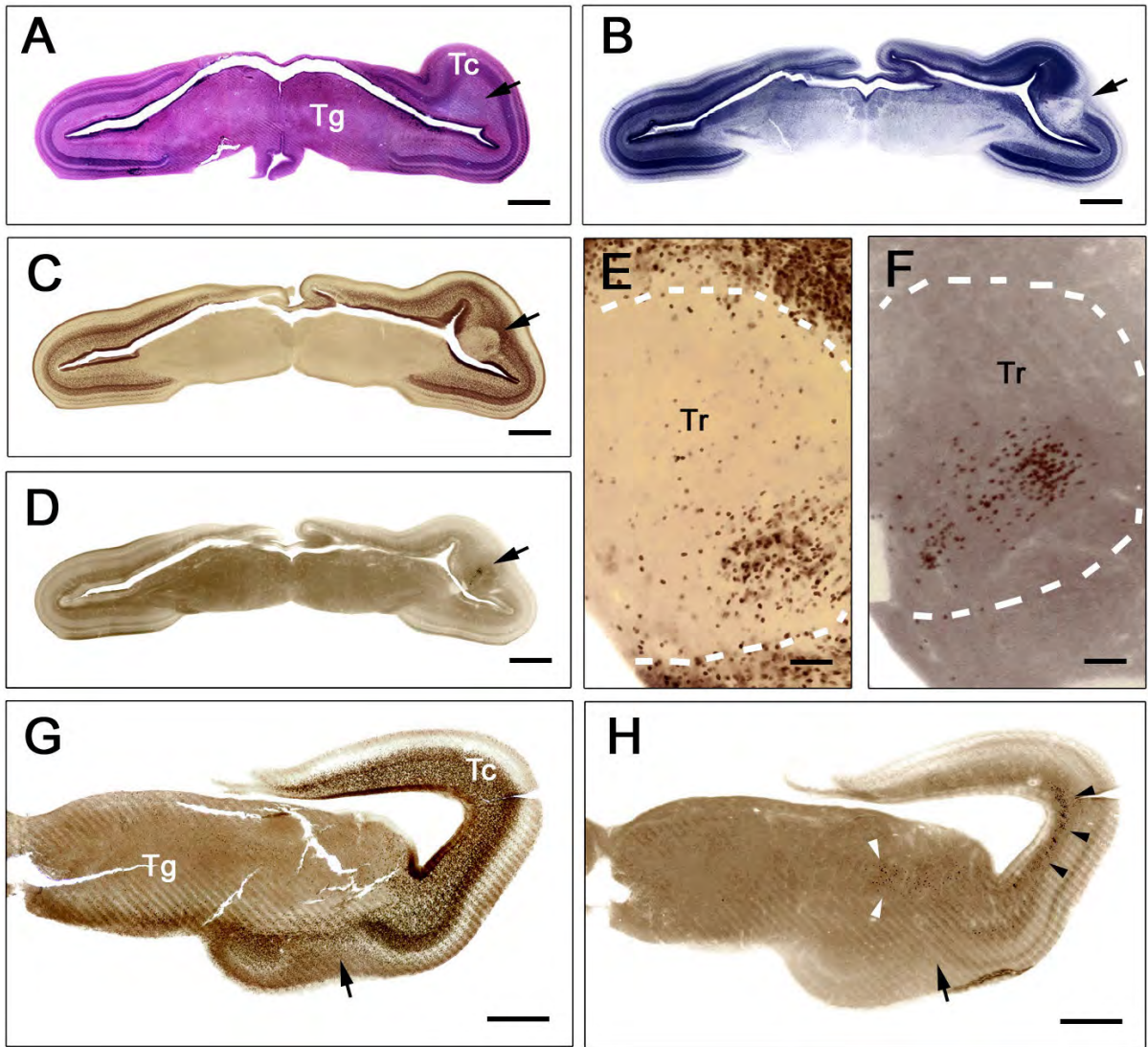
C, E: Some of Pax7-expressing cells (dark brown) were detected within the ventral graft. Laminar structure of the tectum was disrupted by the graft. E is a magnification of C. Note: Pax7 was expressed in diverse cellular layers and subventricular zone of the tectum.

D, F: Quail cells (dark brown) were visible in the graft. They seem to be the cell population expressing Pax7 in C. F is a magnification of D. Dashed lines delimit the graft boundary.

G, H: Some of the dorsal quail cells (white arrowheads in H) stopped to express Pax7 within the tegmentum, whereas other cells (black arrowheads) in the tectum still expressed Pax7. The layering of the tectum was also disrupted.

I: The percentage of quail ventral grafts expressing Pax7 in chick dorsal midbrain at different stages. The embryos were fixed from E5.5 to E13. Clearly, the ventral grafts lose the ability to express Pax7 over time. The number of embryos is indicated in the brackets behind the stages of the abscissa.

Abbreviation: Tc, tectum; Tg, tegmentum; Tr, transplant. Scale bars: A - D, G, H, 1mm; E and F, 100µm.



Quail ventral grafts into chick dorsal midbrain

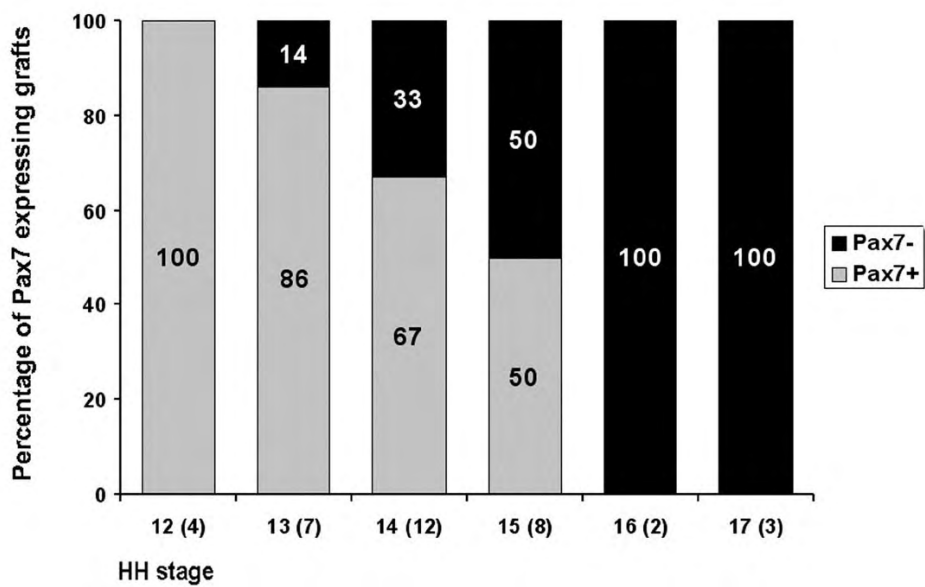


Figure 29: Protein expression of long-term quail grafts

6. Discussion

This study demonstrates a progressive commitment to autonomous gene regulation along the DV axis of the chick midbrain between stages 12 and 18. Within this period, the DV specificity in gene expression becomes independent of midline organizers. The results also show that, autonomous gene regulation is more or less established by stage 17, and a progressive differentiation of adhesion properties in ventral and dorsal midbrain cells is set up between stages 17 and 22.

Identity and Autonomy along the DV Axis

Two experimental strategies were used in this study to challenge the autonomy of gene expression of midbrain tissue along the DV axis, *in vivo* grafting and *in vitro* tissue cultures. Heterotopic grafting has been successfully used by several groups to approach the problem of commitment of specific areas of encephalic vesicles: Gardner and Barald (1991), Alvarado-Mallart and co-workers (Alvarado-Mallart and Sotelo, 1984; Martinez and Alvarado-Mallart, 1989; Martinez *et al.*, 1991) and Nakamura and co-workers (Nakamura *et al.*, 1986; Nakamura and O'Leary, 1989; Matsuno *et al.*, 1991; Itasaki and Nakamura, 1992; Matsuno and Nakamura, 1993; 1994; Itasaki and Nakamura, 1996; Ichijo, 1999) looked at forebrain and midbrain regions. Lumsden and co-workers investigated the hindbrain (Guthrie and Lumsden, 1991; Guthrie *et al.*, 1992; Guthrie *et al.*, 1993; Simon and Lumsden, 1993; Simon *et al.*, 1995; Wingate and Lumsden, 1996), to name a few. Grafting experiments suggest a progressive increase in the ability of grafts to maintain their original identity after stage 12 such that midbrain precursor pools are committed to either a dorsal or ventral fate by stage 17. This finding suggests that the sensitivity to inductive signals is reduced in grafts from later stages and has disappeared by stage 17. Whereas grafts transplanted into younger hosts showed a higher capacity to adopt the molecular identity of the new environment, by stage 18, heterotopic ventral or dorsal grafts were unable to activate dorsal -or ventral - specific gene expression, respectively. Grafts (stage 13 and 14) transplanted into older hosts showed a slightly lower capacity to adopt the molecular identity of the new environment compared with their grafting into younger hosts but comparable to homochronic grafts. Thus, the sensitivity of stage 13 or 14 grafts toward inductive signals does not change much in hosts of different stages but the signals from the host change in their inductive ability. The difference in the molecular sensitivity of grafts in older versus younger embryos may then be explained in two ways. With the midbrain being smaller at younger stages, the concentration gradient of differentiation factors along the DV axis secreted by surrounding tissue may be steeper than at older stages. Thus, in older host embryos, a graft transplanted into a medial dorsal or ventral position of the neural tube will see lower levels of a given factor than at an equivalent position in a younger host embryo. Alternatively, it seems possible that inductive signals are produced at

higher levels in younger than in older embryos, as has been suggested for the AP axis (Itasaki *et al.*, 1991). The exact position of the graft in older embryos might influence the molecular identity of the graft. In fact, although more attention was paid as to where the grafts were positioned, some of the dorsal grafts in particular were found more ventrolateral than expected (Fig. 24). This finding would mean that the percentage of grafts changing their molecular identity would be higher when grafts are more closely located near the floor or roof plate. However, at least 70% of all the transplants evaluated were found in a medial position with regard to dorsal or ventral midbrain. Finally, at stage 18, the dorsal - or ventral - specific gene expression of midbrain tissue appeared fixed, no matter at which position the transplant was placed. It suggests that the cell fates have been determined before that stage, and then following its own autonomous regulation to develop. Chick-quail chimeras showed a same tendency of DV specification in gene expression, except for labile cell fate stopped one stage earlier, due to the fast development in quails. Long-term follow-up of these chimeras suggests the new DV properties of the ectopic midbrain cells adopt before stage 17 are irreversible or at least last for a long period. However, interestingly that the transformed dorsal cells from ventral grafts did not integrate into tectal layers, although they have already expressed dorsal marker as their neighbour cells. Because the grafts were integrated into the hosts very well, the development of the properties in these cells differently with normal dorsal midbrain cells is the most reasonable explanation. The intrinsic identities of these cells, such as physical property, have been determined when transplanted, and influence their differentiation or specification ways at later stages. Except for the location of the transplant along DV axis, the volume of the graft is possibly an influence factor. The cells from small piece are easier to migrate into the ectopic surround, and the genes are expressed in accordance with their new neighbours, whereas the cells in larger grafts keep to be tethered together. This work need to be further investigated.

The heterochronic and homochronic grafting experiments over stages 13 – 18 indicate that the DV identity of midbrain tissue becomes progressively independent from the influence of neighboring tissue. For ventral spinal cord, it has been reported that cell - autonomous differentiation proceeds in a graded manner with respect to the exact position on the DV axis (Ericson *et al.*, 1996). Thus, ventrally located motorneuron precursors become independent of a ventral signal (Briscoe *et al.*, 2000) later in development than the more dorsally located interneuron precursors (Ericson *et al.*, 1996). The ventral progenitors of the spinal cord remain sensitive to the ambient Shh concentration at the time they leave the cell cycle (Ericson *et al.*, 1996). The progressive commitment of midbrain to a dorsal or ventral fate might suggest differences in sensitivity to inductive signals, depending on the origin and final location of the grafts. However, the process described is unlikely to be linked to the first stages of differentiation, as demonstrated for dorsal and ventral neuron pools in the spinal cord (Briscoe *et al.*, 2000). The genes assayed are expressed in ventricular progenitor cells and not in differentiating neurons. In addition, the proportion of definitive neurons in the midbrain remains low throughout our experimental period.

To directly test the autonomy of gene expression in different tissues, explant cultures of dorsal and ventral tissues independent of midline structures were used. Gene expression in midbrain tissue becomes autonomous from signals derived from roof plate and floor plate at stage 16, two stages earlier than exhibited autonomy by heterochronic grafting. This discrepancy in the observed onset of autonomy can be explained by the different experimental approaches. Whereas explants develop in isolation, grafts may be influenced by differently specified surrounding tissue, delaying an observable onset of gene expression autonomy. When compared with earlier work, these results show that commitment along the DV axis of the midbrain is fixed a day later than the AP axis of the midbrain (Itasaki *et al.*, 1991).

Cell Adhesion as a Mechanism or Read-out of DV Regionalization

Using short term aggregation assays (Gotz *et al.*, 1996; Wizenmann and Lumsden, 1997), dorsal and ventral midbrain cells are shown to develop progressively different adhesive properties between stages 17 and 22, shortly after autonomy of DV gene expression is established. This finding suggests that the acquisition of a degree of DV identity in precursor pools precedes a measurable change in cell surface properties between progenitors. This timing could either reflect a degree of DV commitment in terms of a heterogeneity of membrane associated molecules or, indeed, provide a mechanism whereby the relative values of a positional coordinate system are stabilized, as in *Drosophila* (Lawrence *et al.*, 1999), within a neuroepithelium that is rapidly expanding in DV extent.

However, differential adhesion alone does not argue for the compartmentation of the DV axis of the midbrain, as exemplified in the rhombomeric organization of the AP axis of the hindbrain (Wizenmann and Lumsden, 1997). Compartment formation would reflect a progressive restriction on the movement of precursor cells or the establishment of boundaries, which can be definitively assessed by performing intracellular lineage labeling experiments between stages 18 – 22. Differential adhesion along the DV axis of the midbrain rather might stabilize relative positional values for a certain time to ensure correct positional identities of cells.

One might argue that extensive cell mixing in aggregate cultures, especially at early stages, could be due to reduced stability of the molecular identity of cells. However, this explanation seems rather unlikely, because short-term (4 hr maximum) aggregation cultures were performed. As seen in the transplantation experiments, changes in gene expression require approximately 16 hr in culture.

In contrast to the aggregation assays, the cells of grafts from stage 17 or older embryos rarely mixed with their new environment. This restriction in cell mixing appears to be active at least two stages before it is observed in cell aggregation cultures. A possible explanation for this finding is that cell migration from the graft into host tissue may be prevented by secreted repulsive factors, which are not present in cell aggregation experiments.

(Cell adhesion and migration are in general different processes.) Furthermore, the integration of a transplant takes some time, during which transplanted cells will continue to differentiate and, thus, lose their migration potential.

Progenitor Dispersal

Clonal analysis of retroviral or dye-labelled progenitor cells have shown that the dispersal of progenitor cells decreases as development proceeds in the chick spinal cord (Stern *et al.*, 1991; Leber and Sanes, 1995; Erskine *et al.*, 1998), the hindbrain (Hemond and Glover, 1993; Clarke *et al.*, 1998), and the mammalian cerebral cortex (Luskin *et al.*, 1988; Walsh and Cepko, 1993). The dispersal of clones was not analyzed, but the progressively different adhesion properties of dorsal and ventral midbrain hint to a progressively restricted dispersal of cells in the ventricular zone of early midbrain. This finding suggests a remarkable similarity between brain regions and spinal cord in restricting neuroepithelial cell mixing progressively. Clarke and coworkers (Clarke *et al.*, 1998; Erskine *et al.*, 1998) analyzed further the dispersal along the DV axis and found that the dispersal of early progenitor cells in the hindbrain and spinal cord was different along the DV axis. Mid-lateral clones spread more widely in the DV axis in comparison to clones at the ventral and dorsal extremes. This finding suggests a gradient of dispersal along the DV axis, where the dispersal of medially, located progenitors is restricted later in development than at the dorsal and ventral midlines. Cell aggregation experiments or transplantation experiments cannot reveal such differences, but this organization may well be true in the midbrain and other brain regions. Erskine *et al.* (1998) show further that in the spinal cord the DV pattern of Pax3 expression is not maintained by restriction of cell mixing at stage 14. This explanation coincides with our results. Dorsal and ventral midbrain grafts still change their original gene identity at that stage of development. In addition ventral and dorsal cell populations show a low segregation ratio at stage 17 and at stage 14 might even mix completely. However, as diverse as the different brain regions and the spinal cord may be, they appear to use progressive restriction in neuroepithelial cell mixing as a way of building region-specific patterns to generate unique neural structures.

Regionalization as a Feature of DV Patterning in Large Structures

The concept of regionalization along the anteroposterior axis has been established by wealth of experimental data (Lumsden and Krumlauf, 1996). Autonomy of gene expression, differential adhesion and restrictions on precursor mixing are facets of axial subdivision that are variously displayed to a greater or lesser extent during regionalization. In this study, dorsoventral patterning of the midbrain demonstrates some of the features associated with the regionalization of the anteroposterior axis. At a time when differentiated neurons are relatively sparse, the midbrain has distinct dorsal and ventral precursor pools, which show developmental autonomy

and cell surface differences. It is hypothesized that these experimentally demonstrable properties reflect a stabilization of DV patterning cues within progenitors that allows dividing cells to maintain positional identity independent of increasing distances between midline organizers. In addition, regional identity and integrity is maintained by restriction on precursor mixing. It is even possible that boundaries between dorsal and ventral could form that would separate these territories into real compartments. However, this possibility remains to be demonstrated.

The ability of the DV axis precursor pools to be organized into regions might be anticipated in any part of the forebrain where a rapid expansion of the neuroepithelial surface precedes overt differentiation. It would be predicted that the activity of early neural tube organizers might remain imprinted on the DV axis only in the form of a series of committed precursor pools, whereas fine-grain pattern is organized by local tissue interactions at later stages within each developing region.

Part II:

Function of Pax7 on Midbrain Expansion

During the development of chick nervous system, the neural tube is closed at stage 10 and classified as alar plate and basal plate along DV axis, which follow different ways to generate dorsal and ventral neurons, respectively. The alar plate of the midbrain undergoes strong proliferation, and accelerates from embryonic day 3 (E3) onward to form an enlarged optic tectum. Dorsal-specific genes Pax3/7 are expressed in entire alar plate and define the territory of the tectum formed at later stages (Jostes *et al.*, 1990; Mansouri *et al.*, 1994; Kawakami *et al.*, 1997; Nomura *et al.*, 1998; Matsunaga *et al.*, 2001). Interestingly, Pax7 is also expressed in neural precursor cells of ventricular zone (Kawakami *et al.*, 1997), where postmitotic neurons are continuously generated. This proposes a suggestion that Pax7 might be involved in dorsal cell proliferation of midbrain or other parts of the neural tube, as a counterpart to Shh for ventral cell proliferation. To explore the function of Pax7 on neural precursor cells and DV patterning of the neural tube, over-expression and repression of Pax7 were performed in chick midbrains at early stages.

1. Isolation and Subcloning of Chick Pax7 cDNA

To retrieve the full-length chick *Pax7* gene, total RNAs were extracted from E3 midbrains and neural tubes to synthesize chick Pax7 cDNA by RT-PCR using designed primer pairs cp7f1/r1 (Tab. 4). PCR products (1665 bp) were directly ligated with linearized pCR[®]4-TOPO[®] vectors and transformed *One Shot*[®] competent cells (Fig. 30 A). The expected plasmids contain an insert of 1.7 kb (Fig. 30 B), which was cut out and subcloned into a chick-specific expression vector – pMES and transformed *XLI-Blue* competent cells. The clones containing full-length Pax7 cDNA were confirmed by mini-PCR (Fig. 30 C), restriction digest (Fig. 30 D) and DNA sequencing. The constructed Pax7-expressing plasmid – cPax7-GFP – isolated from clones p7m1 and p7m5 had an identical insert, and was used to overexpress Pax7 in the following experiments.

The sequence of chick Pax7 cDNA (2132 bp) is published in NCBI GenBank database, (<http://www.ncbi.nlm.nih.gov>; accession number: D87838) and contains four conserved domains (Fig. 31): the paired domain (PD), the homeodomain (HD), the octapeptide (OP) and the transactivation domain (TD). Chick Pax7 protein is composed of 524 amino acids, and shows in a high homology with mouse (97.2%, NM_011039) and human Pax7 proteins (91.4%, NM_002584). It has a C - terminal deletion (22 aa) and extension (32 aa) compared to human Pax7 (Schafer *et al.*, 1994). Sequencing of chick Pax7 cDNA isolated in this study revealed a trinucleotide (CAG) at + 321 (arrowheads in Fig. 31 A) but not a hexanucleotide (GTTTAG) at + 450 within the paired-box encoding region, suggesting a close similarity to Pax7d, one of the four alternate transcripts in human, which is expressed in the neurogenic line (Kay and Ziman, 1999; Ziman *et al.*, 2000; 2001).

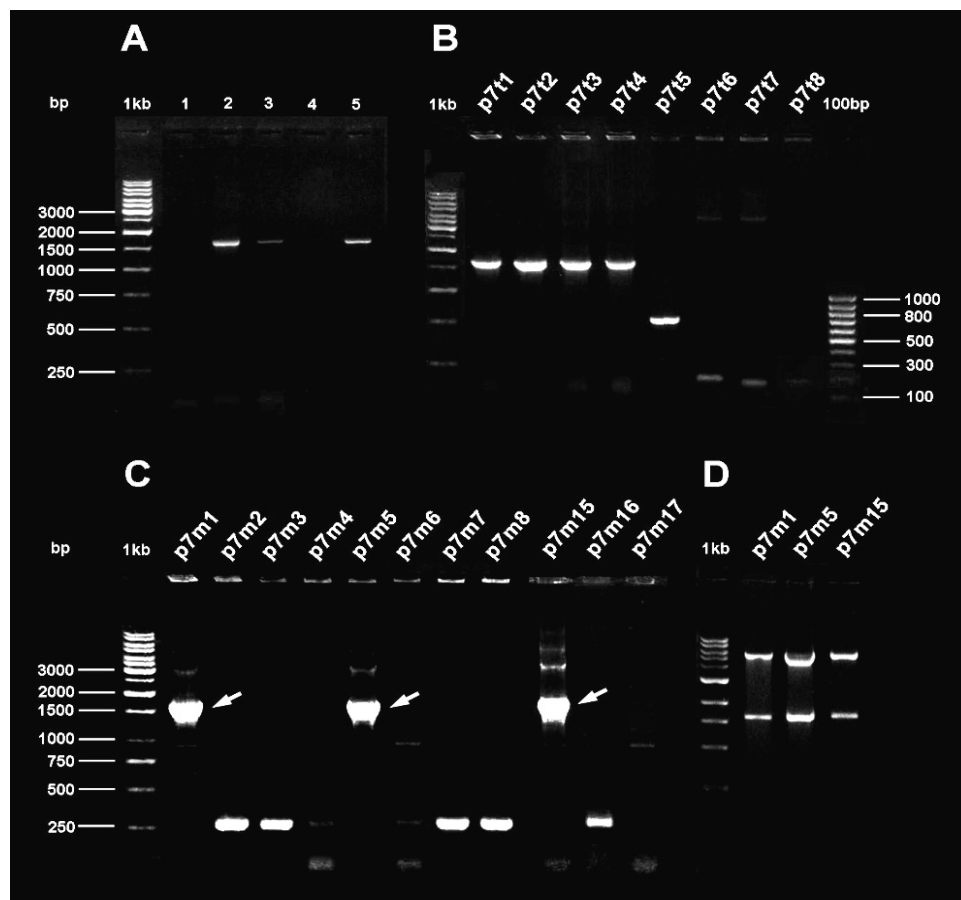


Figure 30: Electrophoretic analysis of chick Pax7 expression plasmids

A: RT-PCR products from the total mRNAs extracted from chick E3 midbrains (Lane 1 - 3) and neural tubes (lane 4, 5). DNA fragments of about 1700 bp were synthesized using primer pair cp7f1/r1 (lane 2, 3 and 5), but not using primers cp7f2/r2 (lane 1, 4). Note: RNase H was not used in lane 3.

B: Mini-PCR revealed that clones p7t1 – 4 (from lane 5 in A) contained a TOPO vector with a wanted insert. Plasmids from clone p7t5 – 8 only contained an insert with a wrong size.

C: The insert DNA (from lane 1 in B) was subcloned into pMES vector. Mini-PCR from 3 clones (p7m1, 5, 15) showed a right-sized DNA band (arrows) with primer pair (pMESfo3/re4). Note: The PCR product from the original pMES vector is about 250 bp.

D: Double digest of plasmids from the three clones with *Xba*I/*Bam*HI resulted in a DNA fragment of 5500bp, which corresponds to the linear pMES vector, and a 1700bp product, the full-length chick Pax7 cDNA. 1kb and 100bp DNA ladders were used as size standards.

A

```

1  CCGGAGCGCCCGCTCAGGCCGGTGTGACATAGCCCGAAAACITTCGAGGGATTTCTGCCGCGGGCTGGGAGACCGCGAAAGCCTTCA 90
91  GCTACCGGACACGAGAGAGAGCCCGACGCTCTCTCGGCTCTCCCGGGTTCGGGGGTGACCCGCTCCGCACGGAGCCGCTCCGCGCCCGCC 180
181  CCGCTATGCGCAGCGCTCCCGGGACGGTACC CGCGGATGATGCGCCCGCGCCGGGCGCAGAACTACCCGCGCACCGGCTTCCCTTTGGAAG 270
      +1
      1  M A A L P G T V P R M M R P A P G Q N Y P R T G F P L E V 29
271  TGTCCACCCCGCTGGGCCAGGGCCGGTGAACCACTCGGAGGGGTTTCATCAACGGGCGCCACTGCCCAACCCATCCGCCATAAGA 360
      PD
30  S T P L G Q G R V N Q L G G V F I N G R P L P N H I R H K I 59
361  TCGTGGAGATGGCTCACCACGGCATCCGGCCCTGCGTGATCTCCAGGCAGCTGAGGGTCTCCACGGCTGCGTTTCCAAAATCCTCTGCA 450
60  V E M A H H G I R P C V I S R Q L R V S H G C V S K I L C R 89
451  GGTACCAAGAGACGGGCTCCATCCGGCCCGGGCCATCGGGGCGAGCAAGCCAGGCAGGTTGCGACTCCCGACGTGGAGAAGAAATCG 540
90  Y Q E T G S I R P G A I G G S K P R Q V A T P D V E K K I E 119
541  AGGAATACAAGAGGGAGAACCCTGGGATGTTGAGTGGGAGATCCGGGACAGGCTGCTGAAGGACGGACACTGCGACCGCAGCACTGTGC 630
120  E Y K R E N P G M F S W E I R D R L L K D G H C D R S T V P 149
631  CCTCAGTGAGTTGATAGCCGTGTGCTACGCATCAAAATCGGGGAAGAAAGAGGAGGAGCTGCGACAAGAAGAGGAGAGCGGGG 720
150  S V S S I S R V L R I K F G K K E E E E D C D K K E E D G E 179
      OP
721  AGAAGAAGCCCAAGCAGCATAGATGGCATCCTGGGCGACAAAGGGAACAGGCTGGATGAAGGCTCCGATGTCGAATCAGAACCAGACC 810
180  K K A K H S I D G I L G D K G N R L D E G S D V E S E P D L 209
      HD
781  TGCCTTTGAGAGCAAGCAGCGCCGACGGCCACTTTCACTGCCGAGCAGCTGGAGGAGCTGGAGAAGCCCTTTGAGAGGACCCACT 900
210  P L K R K Q R R S R T T F T A E Q L E E L E K A F E R T H Y 239
901  ACCCGACATCTACCCAGGGAGGAGCTGGCACAGAGAACCAGCTCACCGAGGCCCGTGTTCAGGTGTGGTTGAGCAACCAGCAGCAGCA 990
240  P D I Y T R E E L A Q R T K L T E A R V Q V W F S N R R A R 269
991  GATGGCGCAAGCAGCGCGGTGCAACCACTCGCAGCATTCAACCATCTGCTGCCAGGGGGATTCCACCACCAGGGAAATGCCAACTCTGC 1080
270  W R K Q A G A N Q L A A F N H L L P G G F P P T G M P T L P 299
1081  CCCCGTACCAGCTGCCAGACTCCACCTACCCAAACCACCACCTTTCCCAAGATGGAGGCAGCACCCTGCACAGACCCAGCCCTTGCCAC 1170
300  P Y Q L P D S T Y P T T T I S Q D G G S T V H R P Q P L P P 329
1171  CATCCACCATGACCAGGGAGGGCTCCTGCGCCCGCTGCAGCCACTCCAGCTCTGCCTATGGGGCCCGACAGCTTCTCCAGCTACT 1260
330  S T M H Q G G L A A A A A A D S S S A Y G A R H S F S S Y S 359
1261  CAGACAGCTTCATGAATGCTGCAGCTCCTGCCAACCATGAATCCTGTTAGCAATGGCCTCTCTCCGAGAAGCAGGGTGCCTCAAAACA 1350
360  D S F M N A A A P A N H M N P V S N G L S P Q K Q G A Q N K 389
1351  AGATGCAGTGTCCAGGTGGAACCTCACCATAGCCTTGAACAATCAGGTGATGAGCATCCTGAGCAACCCAGCGGGTCTCTCCGAGC 1440
390  M Q C S R W N L T I A L N N Q V M S I L S N P S G V P P Q P 419
1441  CCCAGGCTGACTTCTCCATCTCTCCTTTCACGGTGGCCTGGACACCACCAACTCCATCTCTGCCAGCTGCAGCCAGCGGAGTGACTCCA 1530
420  Q A D F S I S P L H G G L D T T N S I S A S C S Q R S D S I 449
1531  TCRAAGTCCGTGGACAGCCCTCCCGACCTCGCAGTCTACTGTCTCCACCTACAGCACCACCAGTTACAGCGTGGACCCGGTGGCTGGCT 1620
450  K S V D S L P T S Q S Y C P P T Y S T T S Y S V D P V A G Y 479
1621  ACCAGTATGGGCGATATGGACAACTGCTGTTGATTATTTGACCAAGAACGTGAGCCTGTCCACGCGCGCAGGATGAAGCTGGGAGAAC 1710
480  Q Y G Q Y G Q T A V D Y L T K N V S L S T Q R R M K L G E H 509
1711  ATTCCGGCGTCTGCGGGCTCCTACCAGTAGAGACAGGCCAAGCTTACTGAGAGGTCGACTGTGCCAACACCCTCCAGCAACTTGG 1800
510  S A V L G L L P V E T G Q A Y * 524
1801  TACCCTGGAGAAACTACCAGCTCCAGGATCTGCTGTACCCAAGACCCTACTCCTTCCCAACTCCCTTCCACCTCGCATCAACTTGT 1890
1891  GGAAGGAAGACGGGAAAGATGGGGAGGGCTCTCCAAGAACTCCAGCTCCTCCAGGGCGCTCAGAGGAAGCCTGGCCATGACCTGAA 1980
1981  TTCTGTGGCCAGAGACAATAGGTTGGGTACATTTATTAACCCGAGTTCATGCCTCCTCTACTGGCCATGTGTCTGCCATGCTAAAGACC 2070
2071  TTCATTGATCTAGTAGTTGGCATAGTCAAAGCCAAATGATCTTTTTTCTTTTCTTTTGT 2132
    
```

B

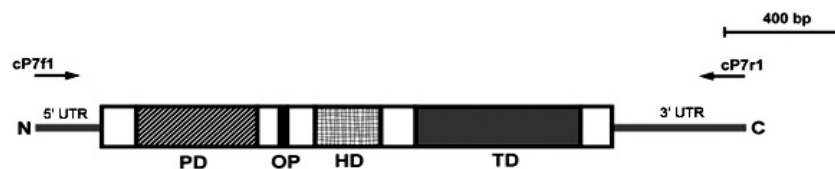


Figure 31: Sequence and structural organization of chick Pax7 cDNA

A: cDNA sequence and the deduced amino acid sequence of chick Pax7 gene. The Pax7 cDNA includes 1575 bp of the coding region with 5' and 3' UTRs. The start and stop codons are underlined. The amino acid is shown in the single code letter under the cDNA sequence, and the stop is marked by an asterisk. The conserved paired domain (PD, 124 aa), octapeptide (OP, 8 aa), homeodomain (HD, 60 aa) as well as the transactivation domain (TD, 149 aa) are boxed in gray. A trinucleotide (CAG) is included and a hexanucleotide (GTTTAG) is excluded at the two splice sites (arrowheads).

B: Schematic illustration of the structures of chick Pax7 cDNA. Primer pair cP7f1/r1 used to amplify the full coding region is illustrated with direction.

2. Influence of Pax7 on the Size of Mesencephalon

Overexpression of Pax7 with cPax7-GFP plasmid and down-regulation of Pax7 with dsRNA-Pax7 construct were performed in chick embryonic midbrains at stages 8 to 14. The transfected embryos showed a high survival rate over 95 % at 24 - 72 hours after electroporation (n = 228, 283 in ectopic Pax7 expression and Pax7 repression group, respectively) as GFP control (n = 55) electroporated with pMES at the same stages. For both constructs, a GFP reporter, transcribed from a single bicistronic mRNA simultaneously, was used to define the transfected region. The GFP expression was detected as short as 6 hours after an electroporation and still visible at 36 hours. All of transfected embryos were examined in morphology as well as the expression of Pax7 by whole-mount immunostaining. A secondary staining for GFP protein was performed in some embryos to display the transfection clearly.

Overexpression of Pax7 in Dorsal Midbrain

Overexpression of Pax7 in dorsal midbrain at stage 9 - 12 showed a clear phenotype. About one - third of the studied embryos (35.5%, n = 154) displayed a larger half midbrain in the transfected side compared to the untransfected side in a midbrain (Tab. 23, Fig. 35 C). However, only 6 out of 54 enlarged midbrains were directly recognized within the embryos (Fig. 32). Of the remaining 48 midbrains, the thickness or the width of the midbrain in both sides was analyzed under microscope. The measurement of the width of a half midbrain is based on the distance between roof and floor plates (Fig. 43 G). In general, the transfected side was 10 ~ 20 % thicker than the unaffected side in a midbrain (Fig. 33 G). Only 3 % of transfected embryos (n = 5, Tab. 23) showed a smaller ipsilateral midbrain, which might be due to the electroporation when the cathode electrode was placed too near. The analysis revealed that the influence of Pax7 overexpression depended on the stages of the embryos when the electroporation was performed. At stage 9/10, about 60% of embryos showed a larger midbrain (n = 10/16 and n = 22/38, respectively), and only 20% at stage 12 (n = 7/33). At the cell level, the immunostaining displayed a strong Pax7 expression in the transfected cells compared to normal/wild-type dorsal cells (Fig. 33). Neurite outgrowth was distinguishable in these transfected cells by GFP expression (Fig. 33 C - E and H - J), which was spread in the whole cells, in cytoplasm and the nucleus, whereas Pax7 protein specifically localized in the nucleus. This suggests that neurons are continuously generated from neural precursor cells with overdose of Pax7. In addition, some cells directly locating at the ventricular layer did not express Pax7 (arrowheads in Fig. 33 H - J), might be dividing cells (Purves *et al.*, 2001).

Misexpression of Pax7 in Ventral Midbrain

To investigate the influence of Pax7 in ventral midbrain, cPax7-GFP was also electroporated into the basal plate at different stages (Fig. 33 G, 34). Ectopic Pax7 expression was detected in the transfected ventral cells,

which does not originally express Pax7 at all. However, only 6 out of 74 ventrally Pax7 - misexpressed embryos showed an enlarged midbrain (Tab. 23, Fig. 35 C). In comparison to the GFP-transfected midbrains (n = 3/55, Tab. 24), this was not significantly different (X^2 ; $p > 0.05$). In addition, ectopic Pax7 expression was strong in transfected ventral cells at 24 hours (Fig. 34 A - C). However, at 36 hours, Pax7 misexpression was largely decreased although GFP expression was strong in these cells (Fig. 34 D - F). In contrast, ectopic Pax7 expression in transfected dorsal cells was still robust at this time (data not shown).

Table 23: The Pax7 - transfected midbrains in size

| Stages | Dorsal | | | Ventral | | |
|--------|--------|----|---|---------|---|---|
| | n | + | - | n | + | - |
| 8 | - | - | - | 7 | 1 | 0 |
| 9 | 16 | 10 | 1 | 13 | 3 | 2 |
| 10 | 38 | 22 | 1 | 25 | 1 | 1 |
| 11 | 57 | 15 | 3 | 17 | 1 | 0 |
| 12 | 33 | 7 | 0 | 8 | 0 | 1 |
| 14 | - | - | - | 4 | 0 | 0 |
| Sum | 154 | 54 | 5 | 74 | 6 | 4 |

The numbers of enlarged (+) and reduced (-) midbrains in comparison to the total number of midbrains (n) with dorsally or ventrally Pax7 transfection at different stages, depending on the thickness and the width of the midbrain along DV axis in both sides.

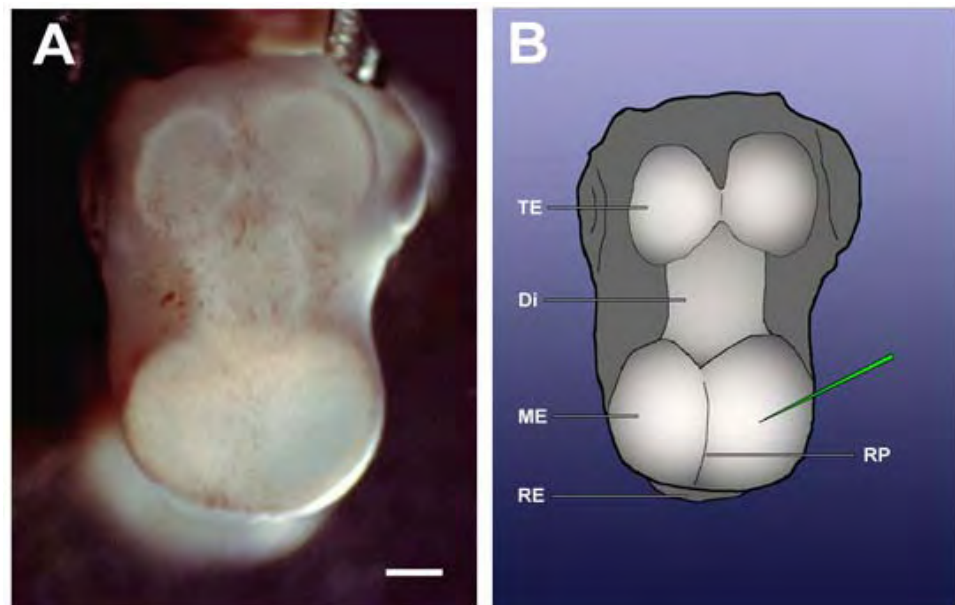


Figure 32: Morphological change of a Pax7 over-expressing midbrain

A: The dorsal midbrain of a stage - 11 chick embryo was transfected with Pax7, and fixed at stage 26. The brain was viewed from the top. Anterior is up. The transfected half midbrain (the right side) was enlarged in comparison to the intact side (left). B: Schematic graph of the brain in A. The green needle represents the position of electroporation.

Abbreviations: Di, diencephalon; ME, mesencephalon; RE, rhombencephalon; RP, roof plate; TE, telencephalon. Scale bar: 500µm.

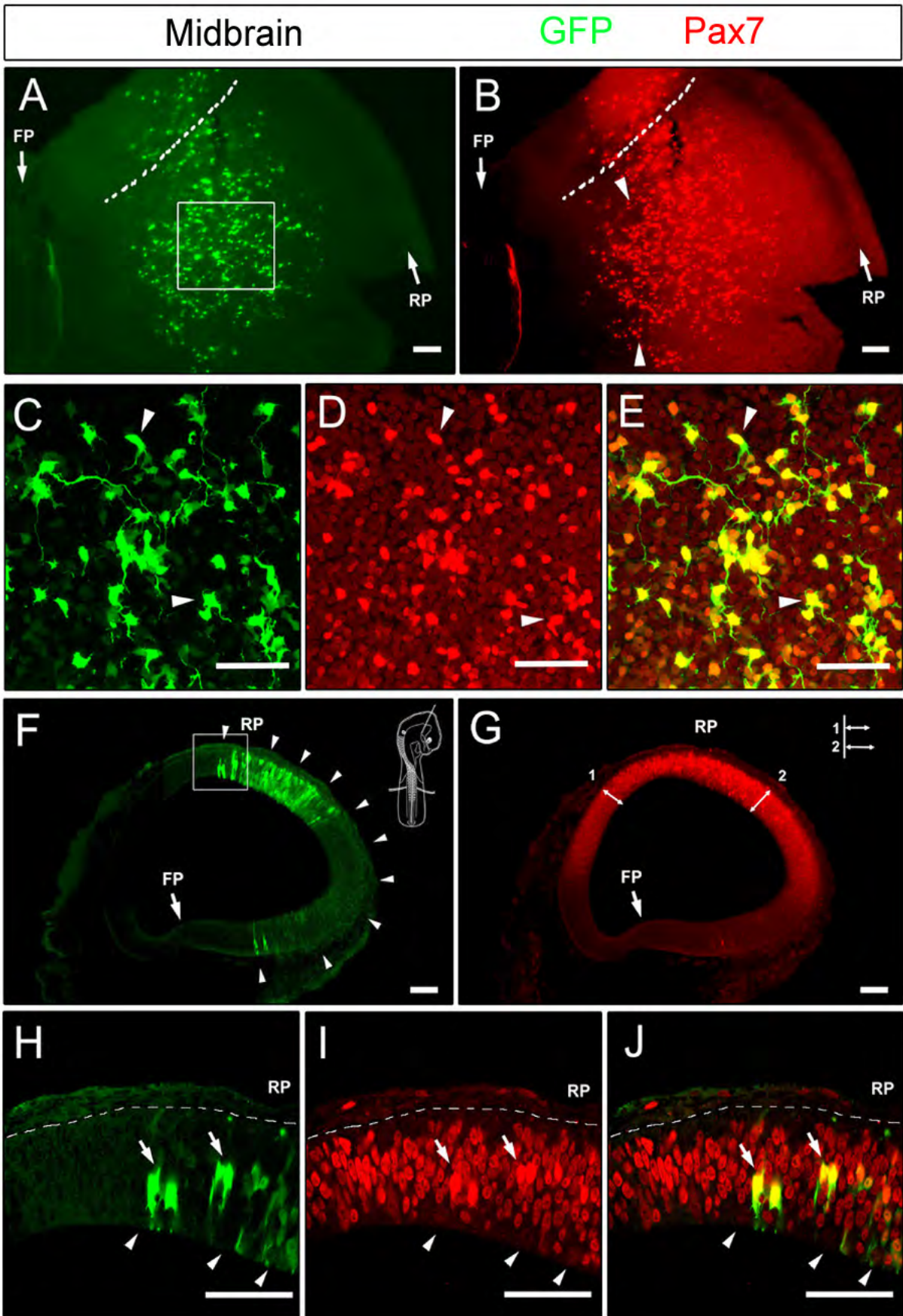


Figure 33: Ectopic expression of Pax7 in dorsal midbrains

Figure 33: Ectopic expression of Pax7 in dorsal midbrains

The midbrains were transfected with Pax7 at stage 11 and fixed at stage 17. The fluorescence immunostaining of Pax7 (red) and GFP (green) was performed. A – E: ‘Open-book’ preparation of the midbrain with anterior to the up. F – J: Coronal midbrain sections (30µm). Dorsal is up.

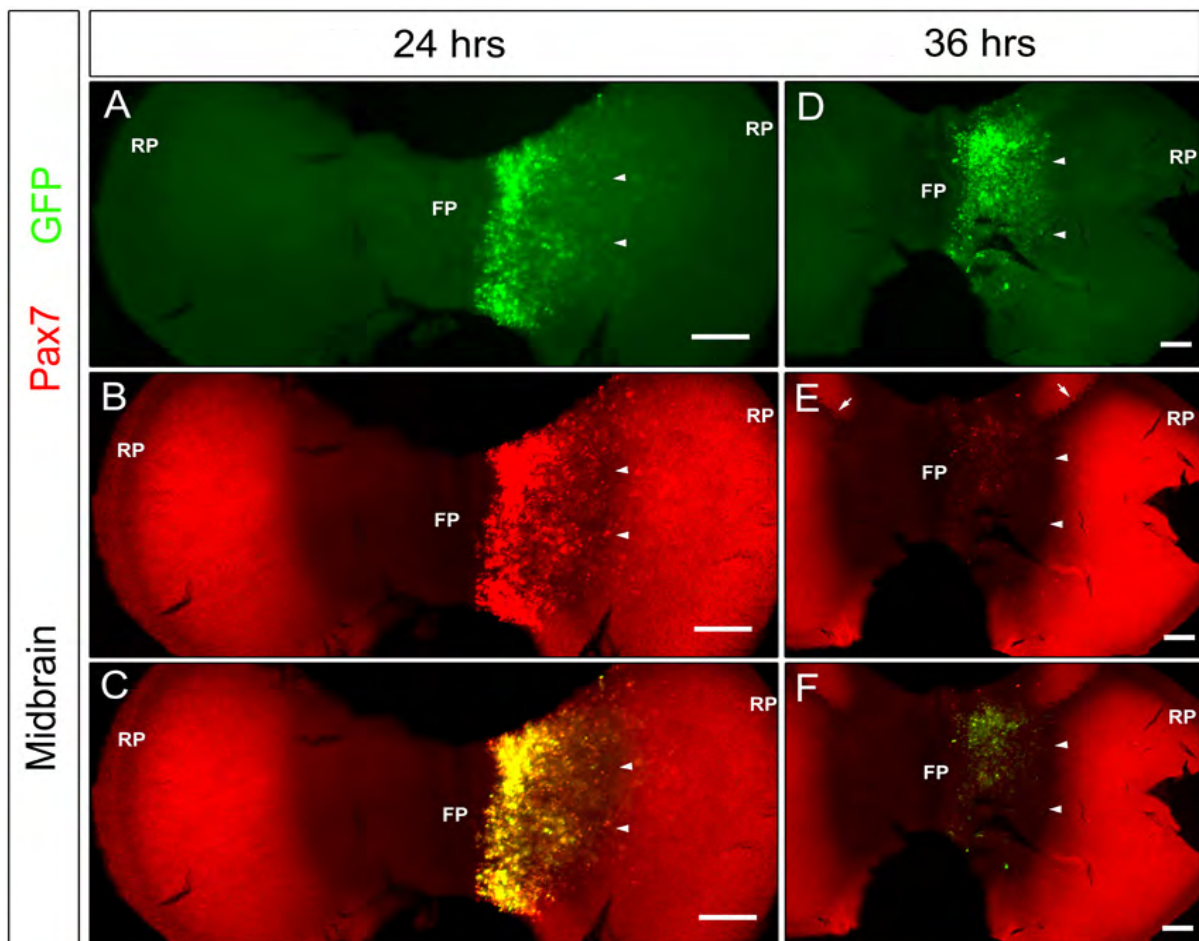
A, B: The GFP-expressing midbrain cells (A) correlated with a strong Pax7 expression (B). The endogenous Pax7 was relative weaker and marked the DV border of the midbrain (arrowheads in B). Arrows indicate the roof plates and floor plates. Dotted lines mark the border between diencephalon and mesencephalon.

C - E: Magnification of the indicated area in (A) was showed in GFP expression (C), Pax7 expression (D) and double staining (E). Cells with double fluorescence appeared in yellow (E). Note: The nuclei of the transfected cells appeared in yellow, while their cytoplasm and neurites are green fluorescent. The arrows indicate such transfected cells.

F, G: A coronal midbrain section showing GFP (F) and Pax7 expression (G). The level of the section is shown in the index figure (F). The transfection covered the right midbrain from dorsal to ventral (arrowheads in F). Arrows indicate the position of the floor plate. The numbers 1 and 2 represent the thickness of the midbrain epithelium in the control and operated sides, respectively.

H - J: Magnification of the indicated area in (F) with GFP expression (H), Pax7 expression (I), and double staining (J). Dotted lines mark the boundary between the neural tissue and the covering mesenchyme. The green cells showed a strong Pax7 expression (arrows). Some cells (arrowheads) in the ventricular layer did not express Pax7.

Abbreviations: FP, floor plate; RP, roof plate. Scales: 100µm.

**Figure 34: Ectopic expression of Pax7 in ventral midbrains**

The ventral midbrains were transfected with Pax7 at stage 11, and fixed at 24 (A - C) and 36 hours (D - F). ‘Open-book’ preparations of the midbrains were shown in GFP expression (green in A, D), Pax7 expression (red in B, E) and double staining (yellow in C, F). Anterior is up. The ventrally misexpression of Pax7 was largely decreased at 36 hours (E) compared to the midbrains at 24 hours (B). Arrows indicate the boundary between diencephalon and mesencephalon. The DV border of the midbrain (arrowheads) and roof and floor plates are marked.

Abbreviations: FP, floor plate; RP, roof plate. Scales: 100µm.

Repression of Pax7 in Dorsal Midbrain

To explore the influence of Pax7 deficiency in the midbrain, *in ovo* electroporation of a pMES-based lhRNA construct for Pax7 gene into chick dorsal midbrains was performed at stage 8 to 14. This RNAi construct contains a long-hairpin dsRNA structure sequence-specific for chick pax7 gene, and can block the translation of Pax7 protein. The knockdown effect of this construct on Pax7 protein in chick midbrains refers to Part IV in details (Fig. 72, 73). Control midbrains were electroporated with original pMES vector, which only produced GFP protein.

Pax7 repression in dorsal midbrains resulted in smaller midbrains at the transfected side in half of all analyzed embryos (55 %; n = 283, Tab. 24, Fig. 35 C). Among 156 reduced midbrains, 105 of them (67 %) were easily recognized by the appearance of the midbrains (Fig. 35). Of the remaining 51 midbrains, the thickness and the width of the midbrain along DV axis in both sides were analyzed as in Pax7 misexpression experiments. The Pax7 - repressed midbrains were largely reduced in the dorsal of the transfected side, while the ventral region was symmetrical (Fig. 36). Statistical evaluation indicated that the morphological change is related to the stages of the embryos when transfected (Tab. 24). Before stage 9, about 3/4 midbrains were smaller in size due to Pax7 repression (77 %; n = 18 and 76 %; n = 38, respectively). The ratio was decreased to 50 % at stage 10 – 12 (59 %; n = 97, 56 %, n = 62; and 43 %, n = 40, respectively), and less effect of Pax7 repression was seen after stage 13 (23 %, n = 13 and 0 %, n = 15, respectively). In comparison to the control midbrains with GFP expression (7 %; n = 4/55, Tab. 24, Fig. 35 C), the ratio of small midbrains by Pax7 repression at stage 8 –12 was significant high (X^2 ; $p < 0.01$).

Table 24: The Pax7-repressed and GFP-control midbrains in size

| Stages | Pax7 repression | | | GFP expression | | |
|--------|-----------------|---|-----|----------------|---|---|
| | n | + | - | n | + | - |
| 8 | 18 | 0 | 14 | 6 | 1 | 1 |
| 9 | 38 | 1 | 29 | - | - | - |
| 10 | 97 | 1 | 58 | 20 | 1 | 1 |
| 11 | 62 | 0 | 35 | 17 | 1 | 2 |
| 12 | 40 | 0 | 17 | 12 | 0 | 0 |
| 13 | 13 | 0 | 3 | - | - | - |
| 14 | 15 | 0 | 0 | - | - | - |
| Sum | 283 | 2 | 156 | 55 | 3 | 4 |

The numbers of enlarged (+) and reduced (-) midbrains were evaluated by calculating the thickness of midbrain epithelium and the DV distance between roof plate and floor plate of the midbrain. GFP expression was achieved by transfection of original pMES plasmid, which is a chick expression vector without any insert but a functioning GFP after an IRES. Pax7 expression was largely reduced by a construct - dspax7-GFP-a, which is based on pMES with a long-hairpin dsRNA insert specific for chick Pax7 gene.

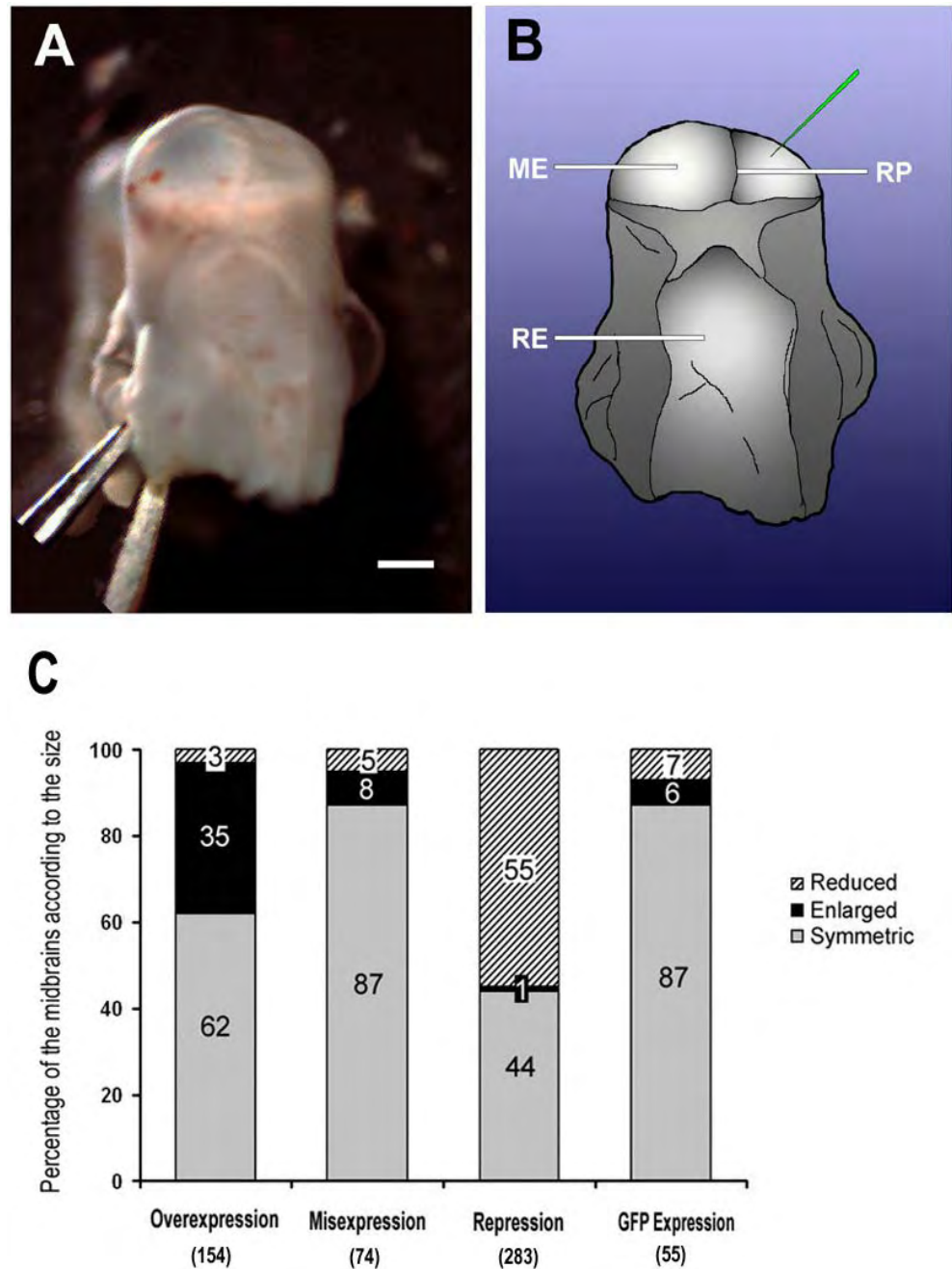


Figure 35: Morphological change of Pax7 - repressed midbrains

A, B: A chick midbrain was transfected with lhRNA-Pax7-GFP-a41 construct at stage 10 and fixed at 72 hrs. The brain is viewed from posterior. B is a schematic diagram of A. The green needle indicates the operated side of the midbrain (right), which is smaller than the intact side (left).

C: Quantitative analysis of the transfected midbrains with Pax7 overexpression dorsally, misexpression ventrally, repression dorsally and GFP expression. The percentage of enlarged midbrains in Pax7 - overexpressed embryos is the highest among all four groups, whereas the percentage of reduced midbrains in Pax7 - repressed embryos is the biggest one. The results of Pax7 misexpression in ventral midbrains are similar to that of the GFP expression group. The number of embryos is indicated in the brackets under each group.

Abbreviations: ME, mesencephalon; RE, rhombencephalon; RP, roof plate. Scale bar: 500µm.

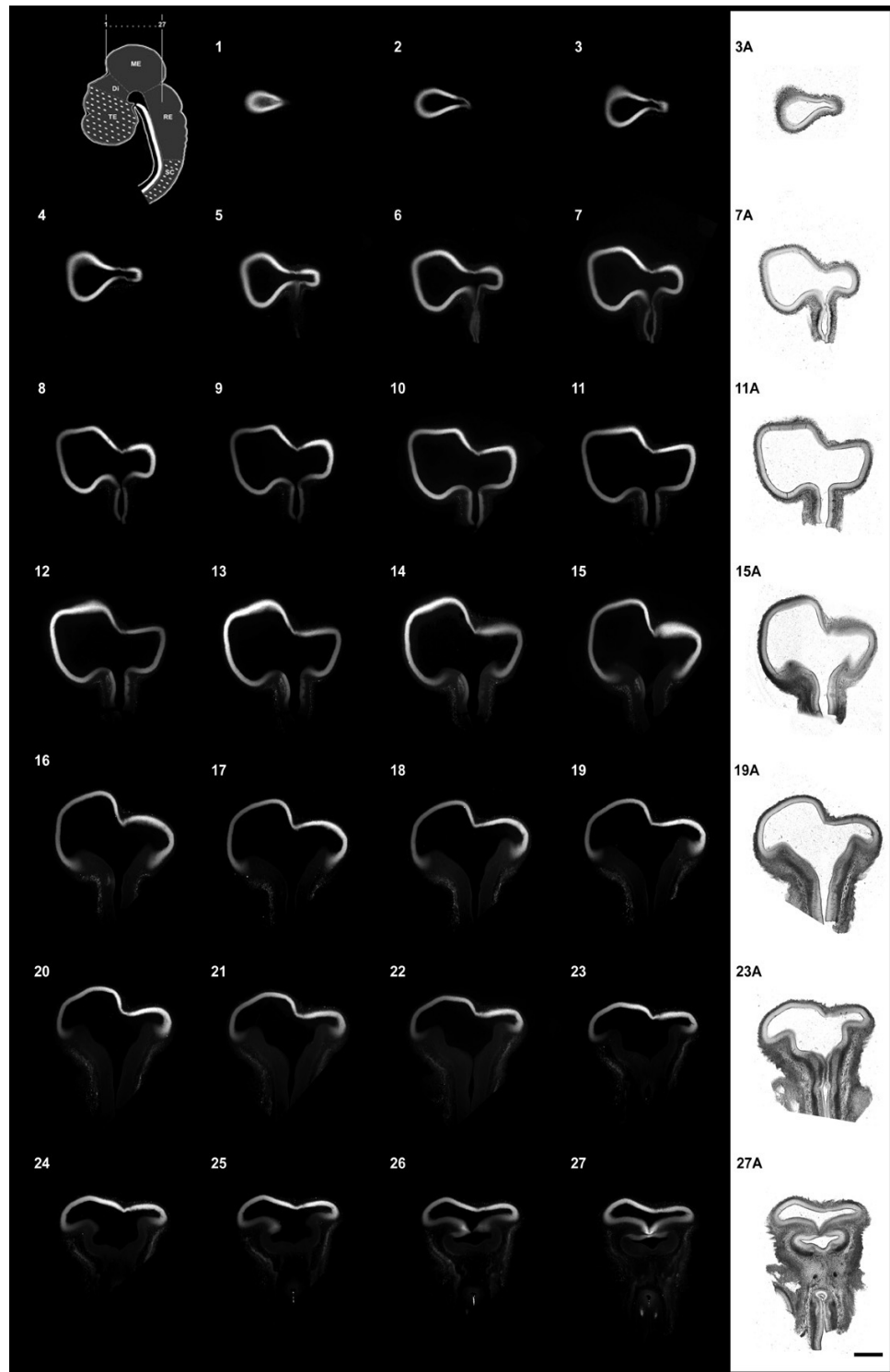


Figure 36: A series of continuous sections of a Pax7 repressed midbrain

A stage - 9 chick embryo was transfected in the right midbrain with a long - hairpin dsRNA construct for Pax7 gene (lhRNA-Pax7-GFP-a41), and fixed at 72 hours. 27 coronal midbrain sections with a distance of 80µm in between are shown from anterior to posterior (indicated in the index figure). Dorsal is up. The telencephalon and spinal cord were removed (dotted regions in the index figure). The Pax7 expression was examined by immunohistochemistry. The transfected side (right) of the dorsal midbrain did not bulged as the control half (left). The sections 3, 7, 11, 15, 19, 23 and 27 are also photographed under transmitted light, and shown in the right column.

Abbreviations: ME, mesencephalon; RE, rhombencephalon; SC, spinal cord; TE, telencephalon;. Scale bar: 250µm.

3. Pax7 Promotes the Neural Proliferation in the Midbrain

Morphological changes in the midbrain by Pax7 overexpression and repression should be coincided with the more or less cells generated there, raising the question if the Pax7 is involved in the neural proliferation, or cell differentiation and specification. Especially, the effect of Pax7 protein is obvious when the transfection is performed before stage 13, and at that time majority of the chick midbrain cells are neural precursor cells or progenitor cells (NPCs, Fig. 20). These precursor cells can exit cell cycle after several times of division and become postmitotic. They differentiate into neurons or glial cells (astrocytes or oligodendrocytes) depending on the environmental cues they receive (Hatten, 2002; Levitan and Kaczmarek, 2002). To investigate the proliferative property of the neural precursors, dividing cells (mitotic cells) should be examined.

Dividing Precursor Cells in the Neural Tube

A mitosis marker - pH3 (phosphorylated Histone 3) was used to visualize dividing precursor cells in chick neural tube, either by a fluorescent immunostaining or DAB staining (Fig. 37). pH3 can label the condensing chromosomes of the mitotic cells in vertebrates, when these cells undergo division at M- and late G2-phases of cell cycle (Hendzel *et al.*, 1997; Van Hooser *et al.*, 1998; Wei *et al.*, 1999).

In the midbrain, dividing precursor cells were detected in both dorsal and ventral regions at different stages (stage 14: Fig. 37 A; stage 20: Fig.37 B), but only located in the ventricular layer facing the lumen (Fig. 37 C, D). The percentage of labelled mitotic cells (mitotic index, MI) in stage-14 chick midbrain was $3.04 \% \pm 0.41 \%$ ($n = 4$). High resolution revealed the labelled chromosomes of dividing cells in diverse morphology (arrowheads in Fig. 37 G), suggesting these cells lie in different sub-stages of M-phase (Levitan and Kaczmarek, 2002). Mitotic cells were also detected in other regions of the developmental nervous system (forebrain; Fig. 37 E, spinal cord; Fig. 37 F, hindbrain not shown).

More Dividing Cells by Pax7 Overexpression

Transfection of Pax7 in dorsal and ventral midbrains was performed at stage 8 - 14, and followed by an immunostaining against pH3. The transfected neural precursor cells still underwent cell proliferation, in that a few cells displayed in double staining of GFP and pH3 (Fig. 38 A - D). Coronal sections showed these cells were located in the ventricular layer as normal pattern (Fig. 38 E). Control dorsal and ventral midbrains were transfected with pMES vector at stage 10 and fixed at stage 15/16. Statistical evaluation indicated that more dividing cells were detected in a defined region of the transfected side than in a same-sized area of the untransfected side within the same midbrain (Fig. 38 F). Transfection in dorsal midbrain at stage 10 showed 8.4 % of more dividing cells in the transfected side (354 ± 36 , $n = 7$) than the untransfected side (326 ± 32).

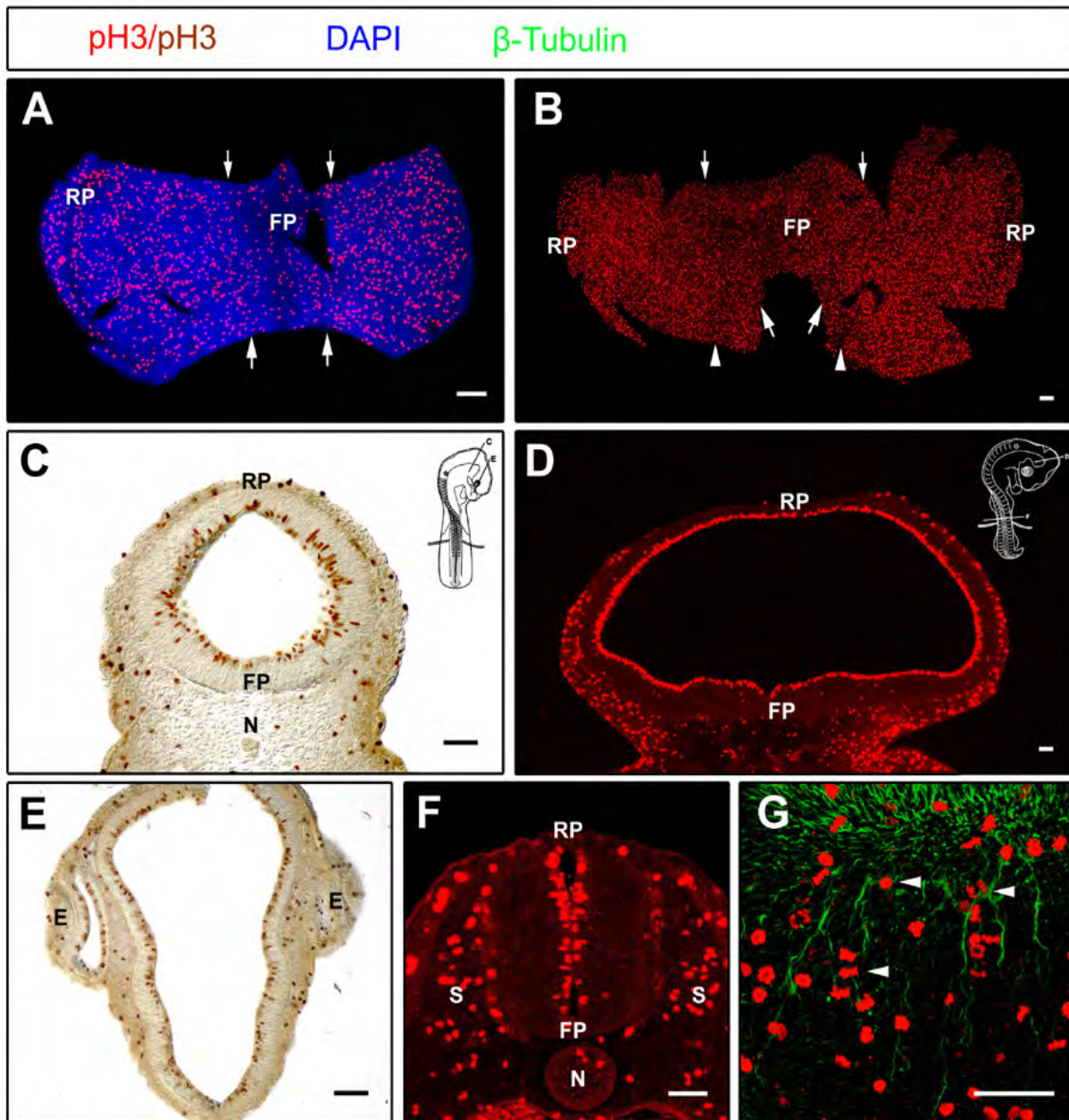


Figure 37: Mitotic cells in the developing neural tube

A, B and G: 'open-book' preparations of chick midbrains. Anterior is up. C - F: Coronal sections (30µm) of midbrains (C, D) and spinal cord (F) with dorsal to the up, and forebrain (E) with anterior to the up. Their levels are shown in the index figures in C and D. The dividing cells were visualized by fluorescent immunostaining (red) or DAB (brown) with an antibody against pH3.

A, B: Chromosome-condensing cells (red) were detected in the entire midbrains at stage 14 (A) and 20 (B), including roof and floor plates. The DV borders of the midbrains are indicated by arrows. Arrowheads (B) mark the midbrain - hindbrain boundary. The midbrain cells were counterstained with DAPI (blue in A).

C, D: pH3-positive cells exclusively located in the ventricular layer of the midbrains at stage 14 (C) and 20 (D). A few of mesenchymal cells surrounding the midbrain epithelium were stained as well.

E, F: pH3-positive cells also located in the ventricular layer of the forebrain (E, stage 14) and spinal cord (F, stage 20). Some pH3-positive cells were also found in the somites and notochord.

G: High resolution of a stage-14 midbrain. Arrowheads indicate diverse morphologies of the pH3-labelled chromosomes. The filaments in the midbrain was counterstained with β - tubulin (green).

Abbreviations: E, eye disc; FP, floor plate; N, notochord; pH3, phosphorylated Histone 3; RP, roof plate; S, somite. Scale bar: 100µm.

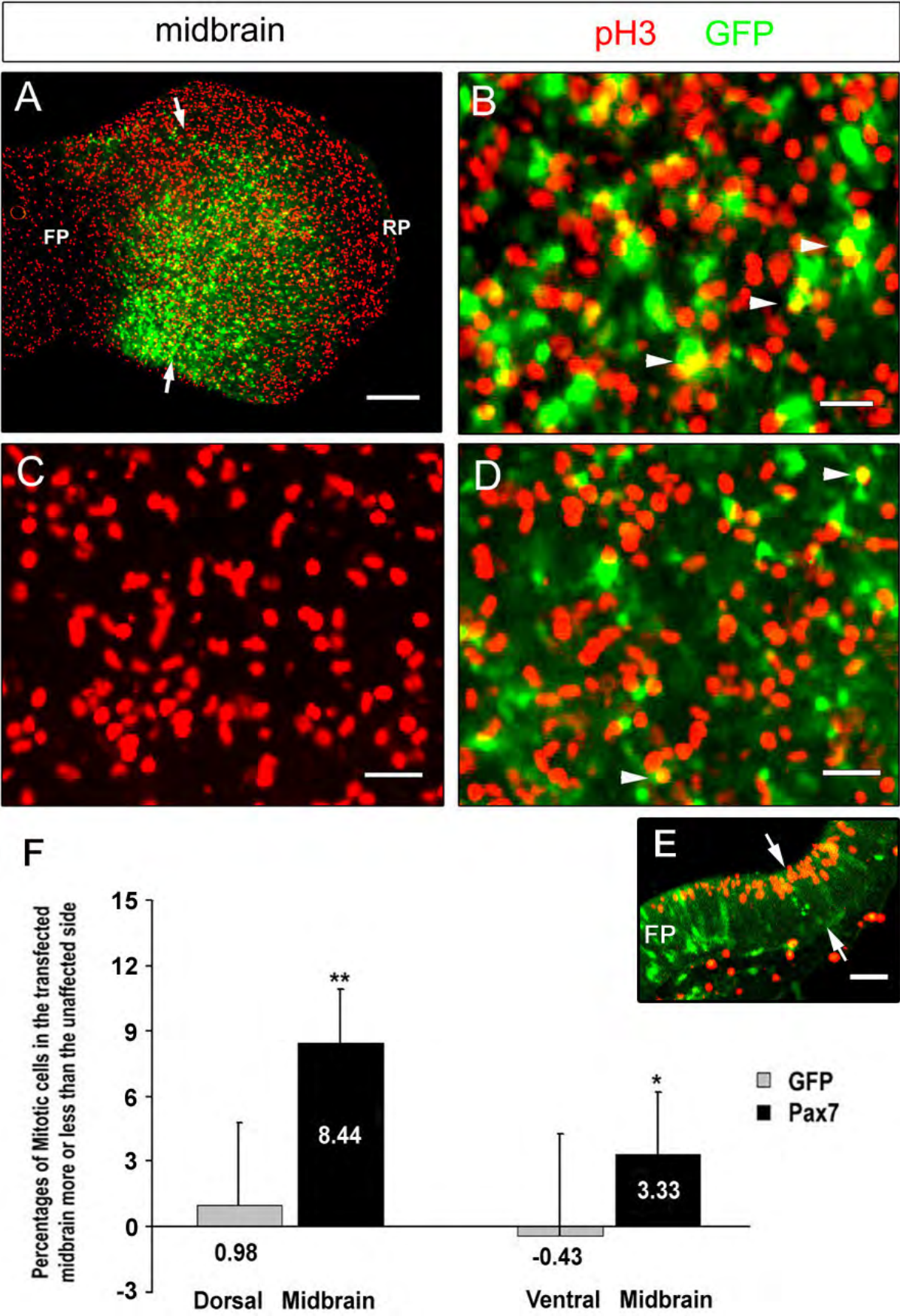


Figure 38: Mitotic cells in the Pax7-transfected midbrain

However, only 3.3 % of more dividing cells was shown in transfected ventral midbrain (222 ± 21 , $n = 6$) compared to the untransfected side (214 ± 20). The mitotic cells in GFP expression midbrain did not show an obvious difference between the transfected and untransfected sides ($< 1\%$), in both dorsal (144 ± 10 : 146 ± 11 , $n = 5$) and ventral region (122 ± 10 : 120 ± 10 , $n = 4$). The differences of mitotic cells between Pax7 transfection and GFP control midbrains are significant (*t*-test; $P < 0.001$ in dorsal, $P < 0.05$ in ventral). The analysis on stage 11 transfected midbrains showed similar results (data not shown).

No Effect on Cell Death

To investigate cell death in the transfected midbrains, SYTOX orange stain was used as a dead-cell indicator (Fig. 39). This nucleic acid binding dye easily penetrates dead cells with compromised plasma membranes, but not cross the membranes of living cells (Burnett and Beuchat, 2002; Petersen and Dailey, 2004). Chick embryos were immersed in the staining solution (1:500 in PBS) for 10 minutes immediately after they were dissected out from the eggs, and followed by fixation in 4% PFA. Referring to the normal developing midbrains, Pax7 transfected midbrains at stage 10 to 14 did not result in significant changes on the number of the dead cells ($n = 11$). The repression of Pax7 by RNAi also did not increase the dead cells on the operative region, although some of embryos exhibited a smaller midbrain ($n = 12$).

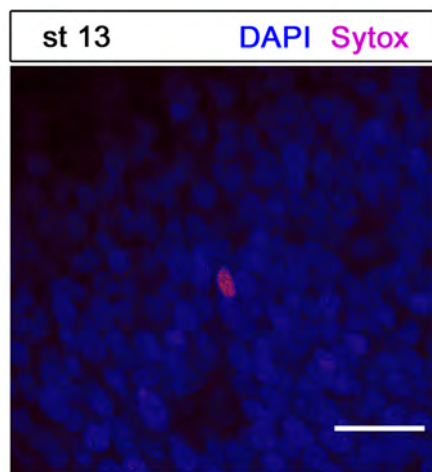


Figure 39: SYTOX staining of a dead cell in the midbrain

The midbrain cells were labelled with DAPI (blue). SYTOX staining shows dead cell in orange. Scale bar: 25 μ m.

Figure 38: Mitotic cells in the Pax7-transfected midbrain

Chick midbrains were transfected with cPax7-GFP at stage 10 and fixed at stage 18. A – D: 'Open-book' preparation of midbrains, anterior is up. E: coronal section of a part transfected midbrain, dorsal is up. Staining of GFP (green) and pH3 (red) were performed. A: A half transfected midbrain. pH3 - positive cells were detected in the GFP - expressing region. Arrows indicate the DV border of the midbrain.

B, D: Higher resolution of a dorsal (B) and ventral (C) transfected midbrain area. Anterior is up, and ventral is left. Double staining of GFP and pH3 showed in yellow (arrowheads).

C: An untransfected ventral area of the same midbrain with D.

E: A coronal section of a transfected midbrain showed that pH3 - positive cells were located in the ventricular layer. Arrows indicate the DV border of the midbrain.

F: Quantitative analysis of mitotic cells in Pax7-transfected midbrain. GFP control midbrains were transfected with pMES at stage 10 and fixed at stage 15/16. Mitotic cells in a region of the transfected side was counted and compared to a same - sized area of the untransfected side within a midbrain. At least 200 cells on 2 sections of each midbrain were analysed. Statistics showed more mitotic cells in dorsal and ventral region of the pax7-transfected side, which showed significant differences with GFP control midbrains (two-tailed paired *t*-test, $P < 0.001$ and $P = 0.048$, respectively).

Abbreviations: FP, floor plate; RP, roof plate. Scale bars: 250 μ m in A; 25 μ m in B - E.

4. Analysis of Pax7 on the Neural Differentiation and Specification

Neural Differentiation Normally

Due to Pax7 is expressed not only in neural precursor cells but also postmitotic neurons in the neural tube (Kawakami *et al.*, 1997; Matsunaga *et al.*, 2001), the relationship of Pax7 with neuronal differentiation also need to be elucidated. A few of Pax7-transfected midbrains were stained with RMO270, a specific neurofilament antibody used previously, which can detect the first neurons in the midbrain (MTN) as early as stage 14 (Chedotal *et al.*, 1995). Results showed that Pax7 overexpression did not significantly change the spatial and temporal differentiation pattern for neurons in the dorsal (Fig. 40, n = 8) and ventral midbrains (data not shown, n = 3). For an individual cell, the Pax7-transfected midbrain cells had developed their neurites (Fig. 33), indicating that cell differentiation did go on in neural precursor cells. The Pax7-repressed midbrains by dspax7-GFP also suggest that the differentiation is continuously proceeding (data not shown, n = 6).

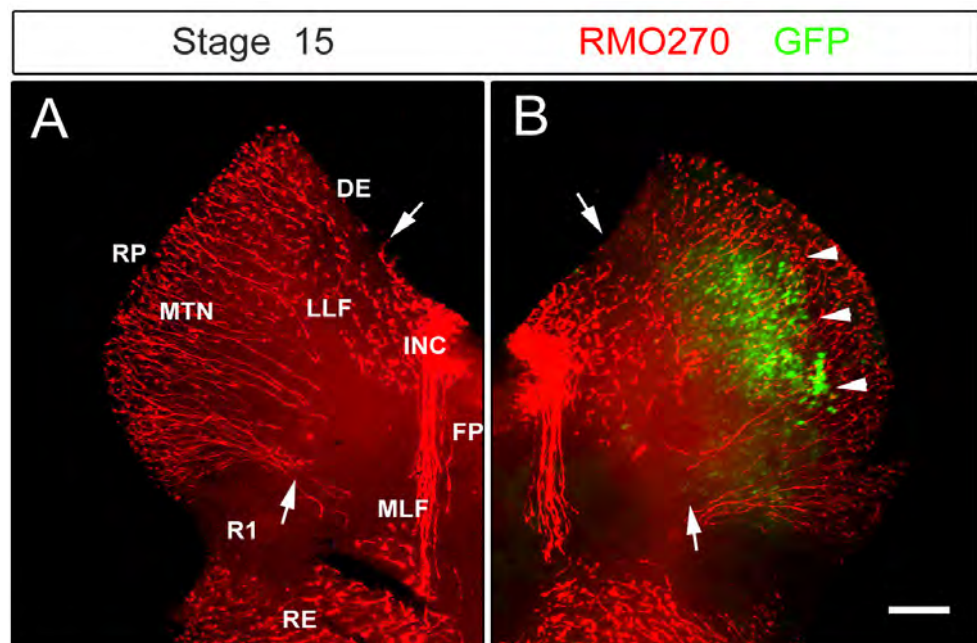


Figure 40: Neuronal differentiation in the Pax7-transfected midbrain

'Open book' preparation of the midbrains. Dorsal is left. Immunostaining against neurofilament was performed with a specific antibody - RMO-270 (red). Arrows indicate the DV border of the midbrain.

A: A lateral view of a half chick midbrain at stage 15. MTN neurons originate in the dorsal mesencephalon and send their axons first ventrally and then posteriorly pioneering the LLF. The MLF from the interstitial nucleus of Cajal descended along the floor plate. No neurons were detected in the MHB of anterior rhombomere 1.

B: A half midbrain transfected with Pax7 at stage 9 and fixed at stage 15. The axon growth from dorsal mesencephalic neurons was not disturbed in the transfected area (arrowheads), which was indicated by GFP expression (green).

Abbreviations: DE, diencephalons; FP, floor plate; INC, interstitial nucleus of Cajal; LLF, lateral longitudinal fascicle; MLF, medial longitudinal fascicle; MTN, mesencephalic trigeminal nucleus; R1, rhombomere 1; RE, rhombencephalon; RP, roof plate. Scale bar: 100µm.

Induction of Brn3a Positive Cells, but not Isl-1 Cells

To investigate the effect of Pax7 on specification of early postmitotic neurons, two transcription factors, Isl-1 and Brn3a, were selected as early neuronal markers in this study. Isl-1, a LIM homeodomain transcription factor, is identified as the earliest marker for postmitotic motor neurons (MNs) in the ventral spinal cord and hindbrain. Isl-1 expression appears soon after the final mitotic division of the precursor cells at around stage 14 and is regulated by inductive signals from the floor plate and notochord (Fig. 41 B, Ericson *et al.*, 1992; 1995; Varela-Echavarría *et al.*, 1996). Later in development Isl-1 also labels a population of neural crest cells in the alar plate in the spinal cord (Avivi and Goldstein, 1999). In the midbrain, the ventral and dorsal postmitotic neurons were first detected by neurofilament (RMO270) staining at stage 14 (Fig. 20 E). These dorsal mesencephalic neurons are born on both sides of the roof plate, corresponding to the proposed origin of mesencephalic trigeminal nucleus (MTN, Chedotal *et al.*, 1995; Hunter *et al.*, 2001). The ventral neurons are located on either side of the floor plate, belonging to the nucleus oculomotorius (OMN), which provides innervation to four extraocular muscles (EOM, Chilton and Guthrie, 2004). Immunostaining showed that Isl-1 was expressed in these two subpopulations in the midbrain (Fig. 41 A).

Brn3a (also known as Brn3.0) is a POU - domain transcription factor expressed in differentiated sensory neurons of cranial nerves and dorsal root ganglia (DRG), as well as specific interneurons of the CNS (Fedtsova and Turner, 1995; Xiang *et al.*, 1996; Eng *et al.*, 2001; 2003). In chick midbrain and spinal cord, Brn3a - expressing neurons arise as Isl-1 positive cells on both sides of the roof plate round stage 15 (Fig. 41 C, D). However, Brn3a positive cells label only the most dorsally located Isl-1 positive cells. The Brn3a/Isl-1 positive cells differ in their properties from the rest of the dorsally located Isl-1 positive cells (Fedtsova and Turner, 1997, Ledderose, Diplomarbeit). In the ventral midbrain, Brn3a-positive cells appeared by stage 19.

The chick embryos were transfected with Pax7 at stage 9 - 12 and fixed at 16 - 28 hours, followed by fluorescent staining with an antibody against Isl-1 or Brn3a. When the embryos were fixed before stage 14, Isl-1 or Brn3a positive cells were never detected in the transfected midbrain or untransfected control side (Isl-1: Fig. 42 A, B, n = 7; Brn3a not shown, n = 3). Since the stage 14, the expression patterns of both proteins in the transfected side were indistinguishable from the control side in a midbrain (Isl-1: Fig. 42 C, D, n = 19; Brn3a not shown, n = 10). Isl-1 positive cells were found in the dorsal and ventral region along both sides of the roof plate and floor plate, respectively. Statistical analysis displays more cells with Isl-1 and Brn3a expression in a transfected region compared to that of a same-sized area in the untransfected side of the same midbrain (Fig. 42 E). Fixation at stage 15/16, 2.80 % (\pm 5.63 %) and 1.79 % (\pm 4.64 %) more Isl-1 positive cells was detected in dorsal (n = 11) and ventral region (n = 9) of transfected midbrains, respectively. However, these increases of Isl-1 cells do not show significant differences with GFP control midbrains (dorsal: 1.66 ± 1.83 %, n = 7; ventral: 1.32 ± 3.44 %, *t*-test, P > 0.05).

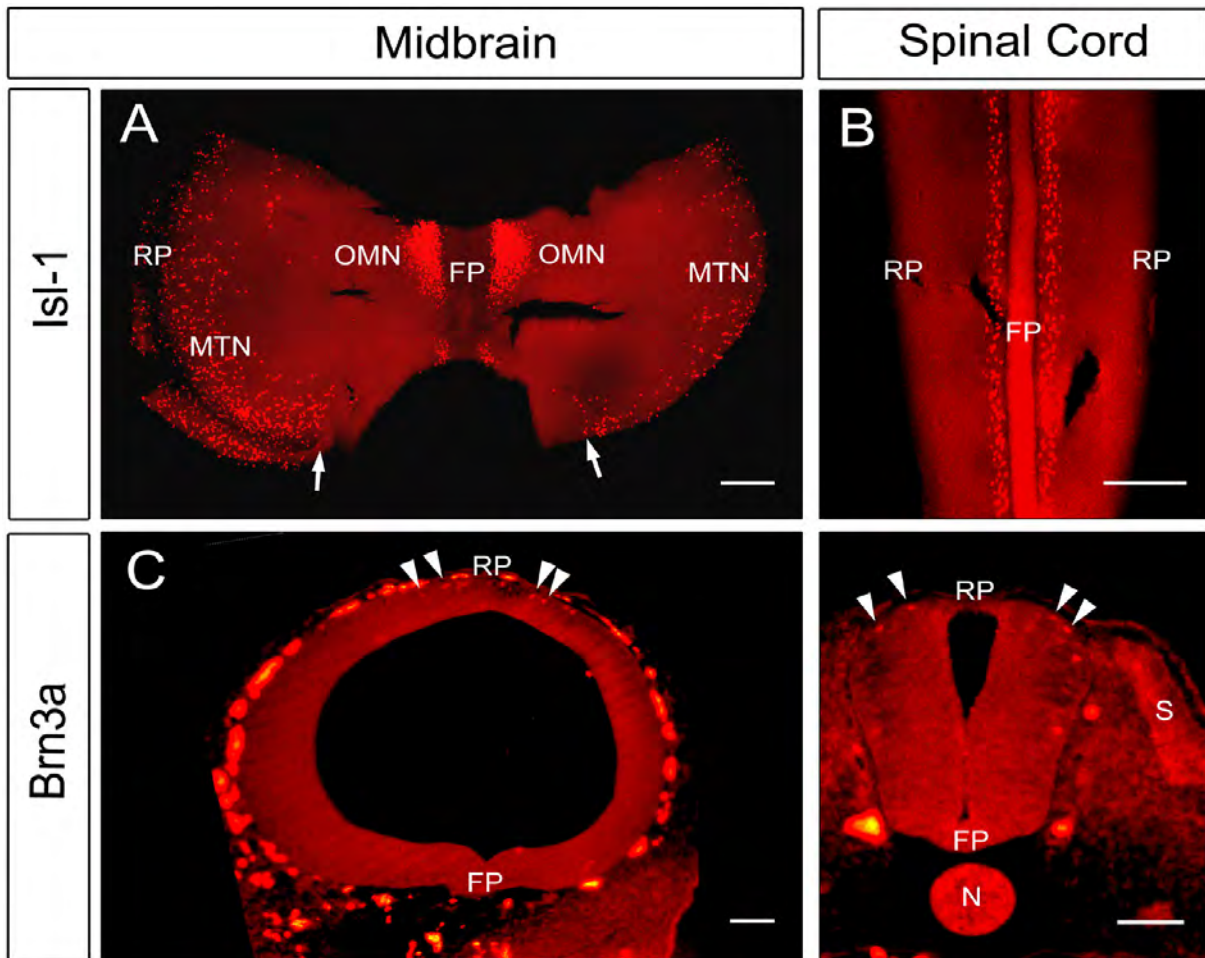


Figure 41: Isl-1 and Brn3a positive cells in the midbrain and spinal cord

The chick embryos were fixed at stage 15 (A – C) and 19 (D). The midbrains (A, C) and spinal cords (B, D) are shown in ‘open-book’ preparation (A, B) or coronal section (C, D). Fluorescent immunostaining for Isl-1 and Brn3a was performed.

A, B: In midbrain (A), Isl-1 positive cells (red) were detected ventrally in both rostral regions near floor plate corresponding to the nucleus oculomotorius, and dorsally on both sides of the roof plate corresponding to the proposed origin of mesencephalic trigeminal nucleus. Isl-1 expressing cells were also detected in the ventral spinal cord (B) as well as in hindbrain except anterior rhombomere 1 (data not shown). The floor plate was disguised by notochord. The arrows indicate the midbrain-hindbrain boundary (MHB).

C, D: The midbrain (C) and spinal cord (D) showed Brn3a positive cells (red) in both alar plates close to the roof plate. Brn3a cells (arrowheads) only located in the outer layer of the neural tube, same as Isl-1 cells (data not shown). Brn3a cells can be detected in ventral neural tube by stage 19 (data not shown).

Abbreviations: FP, floor plate; HB, hindbrain; MTN, mesencephalic trigeminal nucleus; N, notochord; OMN, nucleus oculomotorius; RP, roof plate; S, somite. Scale bar: 100µm.

Figure 42: Isl-1 and Brn3a positive cells in Pax7-transfected midbrains

A, B: The midbrain was transfected with Pax7 at stage 9, fixed at stage 13, and displayed in coronal section. Isl-1 positive cells were not detected in the transfected region (green in A) as well as Brn3a cells (data not shown).

C, D: The embryo was transfected at stage 10 and fixed at stage 16. The expression pattern of Isl-1 positive cells in dorsal region (arrowheads) did not show an obvious significant difference on both transfected and untransfected sides, which is same for Brn3a (data not shown).

E: Quantitative analysis of Isl-1 and Brn3a cells in the Pax7 - transfected midbrains. All embryos were performed at stage 10 and fixed at 15/16 stages. Pax7 overexpression in the dorsal midbrain results in more Isl-1 and Brn3a positive cells in a transfected region compared to a same-sized area of the untransfected side in a midbrain. The change of Brn3a positive cells was significantly different with GFP transfection (two-tailed paired *t*-test; $P = 0.0044$), but not Isl-1 cells ($P = 0.69$). Pax7 transfection did not obviously affect the ventral Isl-1 cells ($P = 0.97$). Each analyzed group consisted of 5 - 14 embryos and at least 500 cells. GFP transfection with pMES vector was performed here as control.

Abbreviations: FP, floor plate; N, notochord; RP, roof plate. Scale bar: 100µm.

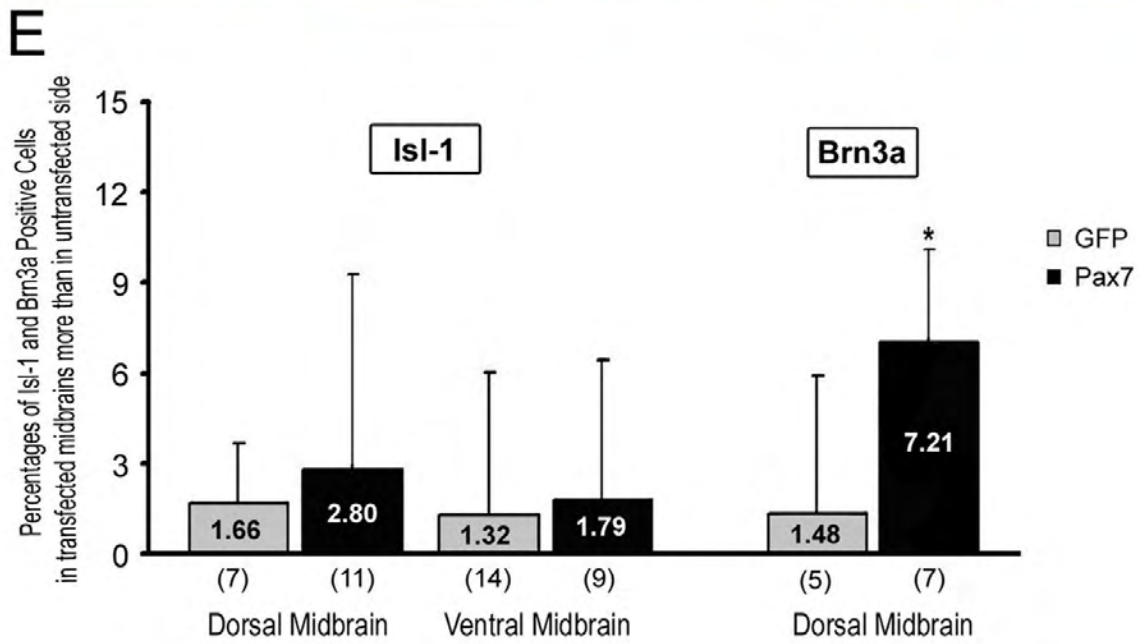
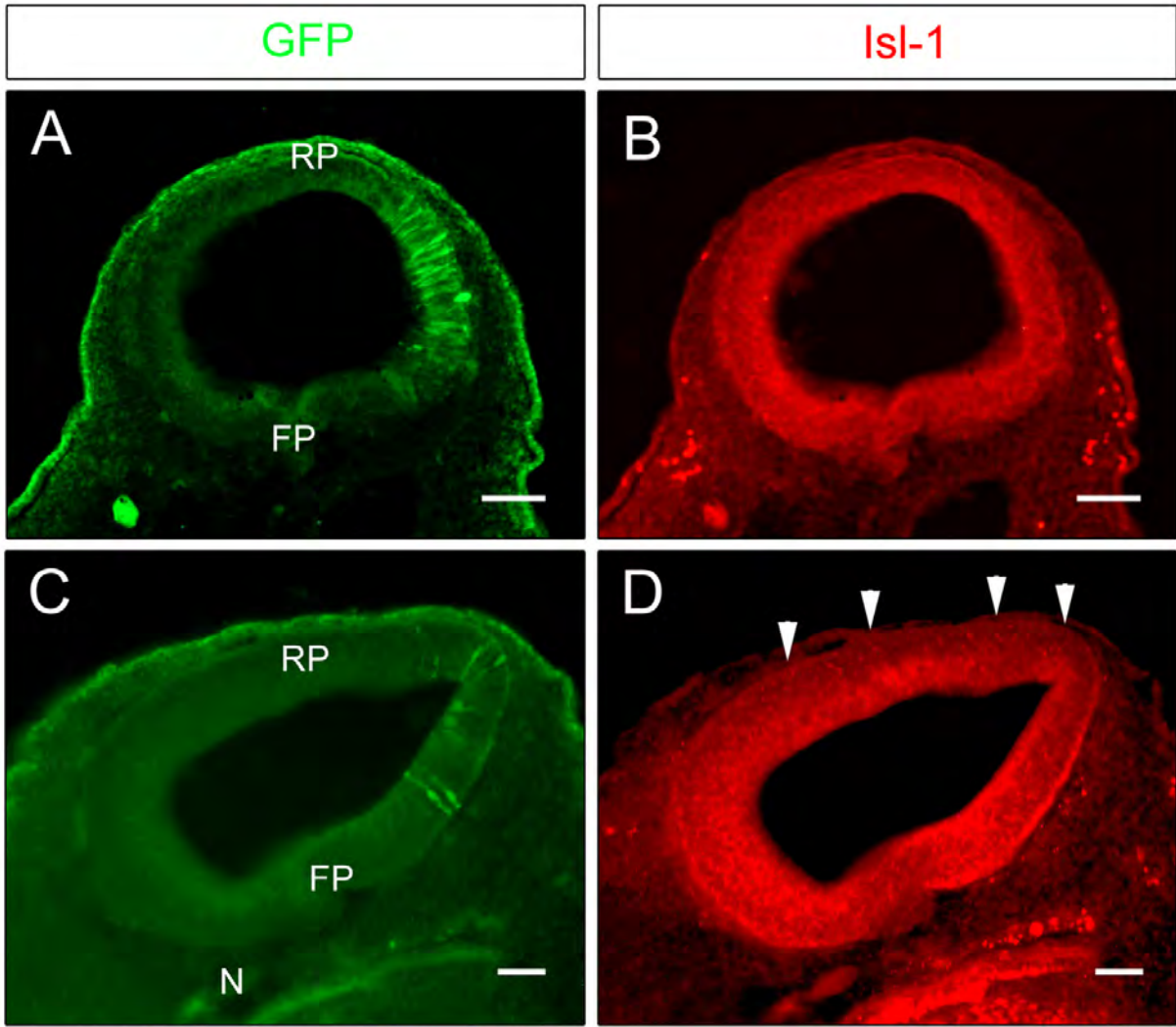


Figure 42: Isl-1 and Brn3a positive cells in Pax7-transfected midbrains

Pax7 overexpression in dorsal midbrains resulted in more Brn3a positive cells (7.21 ± 3.78 %, $n = 7$) in a transfected region than in a same-sized area of untransfected side, which was significantly different with GFP transfection (1.48 ± 4.41 %, $n = 5$, *t*-test, $P < 0.05$). For the ventral Brn3a cells emerge late in the midbrains, the analysis on these cells have not proceeded in this study.

5. Pax7 - induced Pax3 Co-localizes with Nkx6.1

The process of dorso-ventral patterning of the neural tube leads to precursor cells expressing transcription factors specific for their ventral and dorsal location (Altmann and Brivanlou, 2001; Caspary and Anderson, 2003; Jacob and Briscoe, 2003). Two transcription factors, Pax3, specific for dorsal cells and Nkx6.1, specific for ventral cells, were analyzed in Pax7-transfected midbrains to test the influence of Pax7 on the cell fates of neural precursors. The expression patterns of both genes have been described in chick midbrains (Lee and Jessell, 1999; Briscoe *et al.*, 2000; Matsunaga *et al.*, 2001). In short, Pax3 localizes close to the roof plate at stage 11, and then begins to extend to the entire alar plate towards stage 14 (Fig. 19). Nkx6.1 expression occupies a thin strip adjacent to the floor plate at stage 11 and expands more laterally till stage 15. At stage 15 only a small gap is left between the expressions of these two genes. This small gap broadens with further development again. In this study, both genes were examined by *in situ* hybridization with RNA probes.

Analysis of Pax7-transfected midbrains at different stages from 9 – 12 showed that ectopic Pax3 mRNA was induced by exogenous Pax7 in dorsal cells compared to the intact cells with a normal Pax7 level (Fig. 43 A - F, $n = 15/15$). This ectopic Pax3 expression was detected as early as 16 hours after an electroporation (Fig. 43 A) and at least sustained till 36 hours (Fig. 43 B, C). Misexpression of Pax3 mRNA was also detected in ventral transfected midbrains ($n = 8/8$), not only in the gap between the Pax3 and Nkx6.1 expression regions (Fig. 43 A - C, I, J), but also more ventrally in Nkx6.1 - expressing region (Fig. 43 G) and near/in the floor plate (Fig. 43 H). This ectopic Pax3 expression induced by exogenous Pax7 was also observed in other parts of neural tube, such as the rhombencephalon (Fig. 43 K - N) and spinal cord (data not shown). These ectopic Pax3-expressing cells showed a high coordination with GFP expression (Fig. 43 E, F, I, J, and M, N), suggesting that the induction of Pax3 by Pax7 occurs in a cell-autonomous manner. Interestingly, the ventral marker, Nkx6.1 continued to be expressed in the transfected ventral midbrain and hindbrain, displaying a co-localization pattern with ectopic Pax3/7 (Fig. 43 G - N). This suggests that Pax3/7 is not capable to repress Nkx6.1 expression directly. However, it is not excluded if a ventral cell can express both Pax3 and Nkx6.1 simultaneously due to the resolution of visibility for double *in situ* hybridisation. Fluorescent immunostaining with antibodies would be necessary to clearly separate the two staining (Fig. 43 H, I, K, M). Taken together, these data propose that Pax7 can allow ventral cells to have dorsal properties, but does not display an influence on the expression of a ventral-specific gene – Nkx6.1.

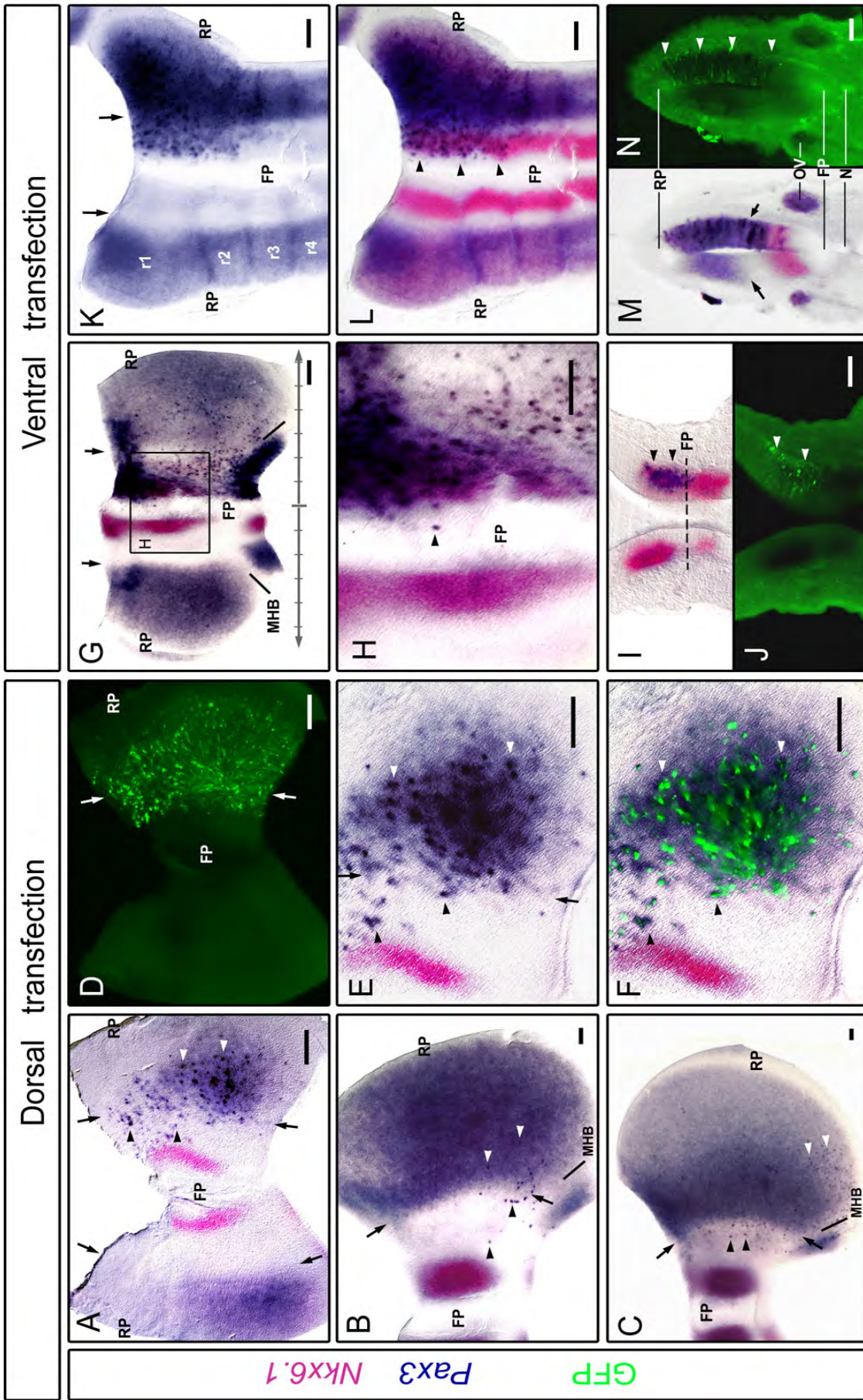


Figure 43: The expression of Pax3 and Nkx6.1 in Pax7-transfected midbrains and hindbrains

Figure 43: The expression of Pax3 and Nkx6.1 in the Pax7-transfected midbrains and hindbrains

The embryos were transfected with Pax7 at stage 9 (A, D – F), 10 (B, C) and 11 (G - N), and fixed at 16 ~ 36 hours. A – H, and K, L are 'open-book' preparations of midbrains and hindbrains, respectively. Anterior is up. I, J and M, N are coronal sections of a midbrain and a hindbrain (30µm). Dorsal is up. Pax3 (blue) and Nkx6.1 mRNAs (red) were hybridized with RNA probes in all embryos. Some embryos were performed by an immunostaining for GFP protein (green). Arrows indicate the ventral boundary of the Pax3-expressing region.

A - C: The transfected midbrains (in the right side) were fixed at 16 hrs (stage 14, A), 24 hrs (stage 18, B) and 36hrs (stage 21, C). In dorsal region, the strongly Pax3 - expressing cells (white arrowheads) were detected due to Pax7 overexpression (referring to D). Pax3 – misexpressed cells (black arrowheads) were also detected in ventral area devoid of endogenous Pax3 expression. At stage 14, the expression of endogenous Pax3 is relative weak compared to older embryos. Nkx6.1 was expressed in the ventral region near floor plate. The boundaries between mesencephalon and rhombencephalon are marked (B, C).

D: GFP expression of the midbrain in A. The Pax7-transfected area covered the entire midbrain along the DV axis. in the right side,

E and F: High resolution of the right midbrain in A. F is an overlay of the images of Pax3/Nkx6.1 and GFP expressions. The strongly Pax3 - expressing cells in dorsal region (white arrowheads in E) corresponded with GFP expression (F). Some Pax3 positive cells with GFP expression (black arrowheads) localized in the gap between Pax3 and Nkx6.1 expression regions.

G: A transfected embryo was fixed at stage 18. Compared to the left midbrain (control side) with a normal Pax3 expression pattern, many ectopic Pax3-expressing cells (dark blue) were seen in the ventral region of the transfected side (right), including the Nkx6.1/Pax3 expression gap and the original Nkx6.1-expressing region (red). The ventrally expressed Nkx6.1 was still detected in its presumed location on the transfected side as the control side. The scale under the midbrain illustrates the width of each half along DV axis in 100µm/bar. The midbrain - hindbrain boundaries are marked.

H: Magnification of the indicated area in G displayed Pax3-positive cells (arrowhead) were located in/close to the floor plate.

I and J: The ventral midbrain was transfected with Pax7 in the right side (green in J). The ventral midbrain section showed ectopic Pax3 was located in the Nkx6.1-expressing area (I). The position of the floor plate is marked by dotted line.

K: A rhombencephalon with Pax7 transfection in the right side. In the rhombomeres 1 to 3 of the transfected side, the territory of Pax3 expression expanded into the ventral region.

L: Pax3/Nkx6.1 double staining of the same hindbrain in K. Arrowheads indicate the actual ventral boundary of Pax3 expression, which covered the region of Nkx6.1 expression. The Nkx6.1 expression in operated side seemed to be unchanged compared to the control side.

M and N: A coronal section through the otic vesicle of the myelencephalon with Pax3/Nkx6.1 mRNA (M) and ectopic GFP expression (N). The ectopic expression of Pax3 was found in the hindbrain (right) from dorsal to ventral (M), corresponding to the Pax7 transfection (arrowheads in N). No significant repression of Nkx6.1 in the ventral region was found.

Abbreviations: FP, floor plate; MHB, midbrain-hindbrain boundary; N, notochord; OV, otic vesicle; r1 to r4, rhombomeres 1 to 4; RP, roof plate. Scale bar: 100µm.

6. Discussion

This study demonstrates that Pax7 overexpression in chick mesencephalon at early stages resulted in an enlargement of the midbrain and Pax7 repression in dorsal region resulted in a reduction in size as expected. In both cases, the observed effects depended on the time when Pax7 gene or shRNA-Pax7 were transfected into the developing neural tube. The enlargement of the midbrain by dorsally Pax7 overexpression was coordinate with an increase of dividing precursor cells. Pax7 overexpression or reduction did not influence the temporal and spatial patterning of neuronal differentiation, but increase the number of some neuronal subpopulations. In addition, Pax7 was able to induce another dorsal – specific marker Pax3 in dorsal and ventral cells of the midbrain and hindbrain in a cell autonomous manner. In contrast, the expression pattern of ventral gene Nkx6.1 was not affected by the misexpression of both Pax3 and Pax7.

Pax7 is Involved in the Neuronal Proliferation

The function of Pax7 on early midbrain development was examined via gain-of-function and loss-of-function approaches at stage 8 to 14, before the neural precursor cells started to differentiate. The present study reveals that a role of Pax7 protein plays on the midbrain development, regulating neuronal proliferation in dorsal region. Especially, the temporal effect of ectopic Pax7 on the midbrain in size is related with the normal expression pattern of Pax7. Higher percentage of enlarged midbrains by Pax7 overexpression was observed at stage 9 and 10, a time when Pax7 was initially expressed in the neural tube after the closure of the neural epithelium (Kawakami *et al.*, 1997; Nomura *et al.*, 1998). This ratio was quickly decreased after stage 12 when Pax7 expression nearly covered in the entire dorsal region. The Pax7 repression experiments displayed a significant difference when performed before and after stage 13. Previous experiments of DV polarity-reversed transplantation reveal that since stage 12 DV regional commitment and autonomous gene regulation initiate to be set up in the midbrain. Consistent with the idea that Pax7 is responsible for the formation and maintenance of optic tectum and different subdivisions of diencephalon (Puelles and Rubenstein, 1993; Stoykova and Gruss, 1994; Kawakami *et al.*, 1997; Nomura *et al.*, 1998; Matsunaga *et al.*, 2001) similar to the role of Pax6 in regionalizing the dorsal telencephalon (1996; Stoykova *et al.*, 1997; 2000; Toresson *et al.*, 2000; Yun *et al.*, 2001), these data suggest that Pax7 exerts to promote the proliferative activity of precursor cells in dorsal midbrain before the regional identities have been committed.

However, the cell proliferation of ventral midbrain precursors seemed not to be changed by Pax7 misexpression. This different effect of ectopic Pax7

in ventral and dorsal midbrain could be due to a weaker Pax7 expression in the ventral, assuming that the Pax7 might influence the rate of cell proliferation very likely in a dose dependent manner. A famous example for a dose - dependent effect on the size of developing tissue by a pair ruled gene is the Pax6 effect on eye development. Heterozygous Pax6 mutants exhibit microphthalmia, homozygous aniridia (Grindley *et al.*, 1995; Hill *et al.*, 1999). Overexpression of Pax6 leads to bigger eyes (Schedl *et al.*, 1996). This weaker expression of ectopic Pax7 in ventral midbrain might be achieved by the repression of Shh or others secreted from notochord and/or floor plate (Ericson *et al.*, 1996; Nomura *et al.*, 1998; Watanabe and Nakamura, 2000; Fedtsova and Turner, 2001). Thus, the already existing Pax7 expressed in the dorsal midbrain could enhance cell proliferation more than in the ventral midbrain. Recently studies suggest that in the ventral neural tube, Shh/Gli signalling pathway acts on the proliferation and survival of progenitor cells via G1 phase of cell cycle and the expression of the anti-apoptotic factor Bcl2 (Charrier *et al.*, 2001; Jeong and McMahon, 2005; Cayuso *et al.*, 2006).

A number of studies suggest Pax7 might function via Wnt signalling to promote the proliferation and survival of neural precursors at least in dorsal regions of the caudal neural tube (Megason and McMahon, 2002; Panhuysen *et al.*, 2004). Wnt3/4 are largely decreased or absent in the dorsal spinal cord of Pax3/7 double mutants (Mansouri and Gruss, 1998). However, the dorsal midline Wnts, Wnt1 and Wnt3a, expressing in a DV concentration gradient, illustrate mitogenic activity with the proliferation rate highest dorsally in hindbrain (Ikeya *et al.*, 1997) and spinal cord (Muroyama *et al.*, 2002). This may very well reflect the situation in the midbrain. Another possibility of neuronal proliferation and differentiation by Pax7 regulation is reasoned from a recently study, a Mesi transcription factor expression is restricted to dorsal mesencephalic vesicle and affected by both Pax3/7 genes (a Dorothea Schulte' paper in prepared). How the actual regulation takes place is less well understood yet and interesting to further investigate.

At the later development, Pax7 expressing cells are found in different laminae of the optic tectum and some nuclei of the ventral midbrain (Fig. 44, LaVail and Gowan, 1971; Kawakami *et al.*, 1997; Thomas *et al.*, 2006). Particularly, strongly expressed Pax7 is located in the ventricular zone of the tectum, where a source of postmitotic neurons is non-stop generated (McKay, 1997; Gage, 2000; Levitan and Kaczmarek, 2002). This provides a sign of Pax7 to maintain the proliferative activity of neural precursors in dorsal midbrain. An involvement of Pax7 in maintaining proliferation and preventing differentiation has already been urged in another cell lineage, muscle precursor cells, (Olguin and Olwin, 2004; Oustanina *et al.*, 2004; Zammit *et al.*, 2006), as Pax7 deficiency resulting in muscle satellite cell death (Seale *et al.*, 2000; Relaix *et al.*, 2004; 2005; 2006). Taken together, above observations suggest that Pax7 is required to maintain and promote cell proliferation in neural precursor cells in dorsal midbrain.



Figure 44: Expression pattern of Pax7 in chick E8.5 midbrain

A: A coronal section (80 μ m) of one half midbrain at E8.5 (stage 37) showed Pax7 expression was located at diverse cellular layers of the tectum. No expression was detected in the tegmentum. Dorsal is up.

B: Magnification of the indicated area in A. Pax7 positive cells mainly localized at the widest SGFS layer, the retino-recipient site for the retinal axons, and other two deeper laminae, SGC and SAC. Strongly expressed Pax7 was also detected in the ventricular zone of the entire tectum.

Abbreviations: SAC, stratum album centrale; SGC, stratum griseum centrale; SGFS, the stratum griseum fibrosum; SGP, stratum griseum periventricularis; SO, the stratum opticum (the layer of retinal axon fibers); VZ, ventricular zone. Scale bar: 250 μ m.

A Role of Pax7 on the Specification of Some Dorsal Neuronal Lineages

During the development of the nervous system, an enormous amount of neurons is generated, consisting of separate subpopulations dependent on their precise positions, which is reflected by combinational codes of a series of transcription factors. The interplay of morphogenes such as Shh and BMPs regulates this spatial expression pattern to create sharp boundaries along the DV axis. Significant progress has been made in understanding the molecular mechanism of the developing spinal cord to specify neuronal identity (Ericson *et al.*, 1992; Roelink *et al.*, 1994; Tsuchida *et al.*, 1994; Liem *et al.*, 1995; Ericson *et al.*, 1996; Piccolo *et al.*, 1996; Tanabe and Jessell, 1996; Lee *et al.*, 1998; McMahon *et al.*, 1998; Lee and Jessell, 1999; Briscoe *et al.*, 2000; Liem *et al.*, 2000; Briscoe and Ericson, 2001; Timmer *et al.*, 2002). The dorsal-specific transcription factor Pax7 is expressed in the differentiating neurons as well as neural precursors in the dorsal neural tube and required to define the territory of the optic tectum, suggesting a role on neuronal identity in dorsal midbrain. To understand the neuronal differentiation and specification in the midbrain, overexpression and repression of Pax7 was performed in dorsal midbrains in this study.

In this study, not a spatial and temporal deviation on neuronal differentiation was achieved by Pax7 overexpression or reduction in the dorsal mesencephalon at early stages. Consistent with the normal differentiation of ventral neurons misexpressing Pax7, this recommends

that Pax7 is not necessary for the neuronal differentiation in the midbrain. Analysis on the early neurons with Brn3a expression revealed a marked increase of the expressing cells in dorsal midbrain upon Pax7 overexpression. The Brn3a (Pou4f1) transcription factor, first detected around stage 15 in dorsal midbrain (Fedtsova and Turner, 1995; Eng *et al.*, 2004), is required for the survival of trigeminal ganglion neurons and activation of a number of neuronal genes (McEvelly *et al.*, 1996; Xiang *et al.*, 1996; Huang *et al.*, 1999; Eng *et al.*, 2001; Fedtsova and Turner, 2001; Eng *et al.*, 2003; 2004). However, Pax7 did not cause a distinguishable change on another differentiated cell subpopulation with Isl-1 expression in the dorsal or ventral midbrain. Isl-1 expression even rises earlier than Brn3a in the spinal cord (Karlsson *et al.*, 1990), and is known to be the first motor neuron (MN) marker and required for MN generation (Pfaff *et al.*, 1996; Varela-Echavarria *et al.*, 1996; Muller *et al.*, 2003b). The difference of Isl-1 and Brn3a cells might reflect the situation in the spinal cord. Brn3a and Isl-1 cells belong to different subpopulations of dorsal interneurons dependent on the location along DV axis, Brn3a covering dl1 to dl3 region, and Isl-1 only in dl3 region (Fedtsova and Turner, 1997; Lee and Jessell, 1999; Caspary and Anderson, 2003), and they receive different inductive signals (Ericson *et al.*, 1992; 1995; Fedtsova and Turner, 1997; Latchman, 1998; Dutton *et al.*, 1999; Lee *et al.*, 2000; Fedtsova and Turner, 2001). For instance, Wnt3a derived from roof plate induces expression of dl1 and dl2 markers, but not Isl-1 cells (Muroyama *et al.*, 2002). Thus, the slightly increase on cell count of Isl-1 interneurons by Pax7 overexpression might be due to more postmitotic neurons generated. Moreover, although more Brn3a positive cells were generated, the location of these cells was still unchanged as Isl-1 cells observed. Taken together, this study proposes that Pax7 can promote to generate some subtype of early neurons in the dorsal midbrain. *In vitro* experiments have already demonstrated an inductive role of Pax7 on some neuronal cell lineages, such as Pax7 and Pax6 can induce P19 embryonic carcinoma cells become neurons and astrocytes (McBurney *et al.*, 1982; Pruitt, 1992; Jonk *et al.*, 1994; Ziman *et al.*, 2001; 2003; Thomas *et al.*, 2004). However, Retinoic acid (RA) – induced neurons from NTera2 human embryonal carcinoma cells display a ventral neuron identities (Houldsworth *et al.*, 2002; Przyborski *et al.*, 2003), as the presence of *Nkx6.1*, but not *Pax7* or the dorsal regulator BMP4 (Andrews, 1984; Andrews *et al.*, 1986; Lee and Andrews, 1986; Younkin *et al.*, 1993; Hartley *et al.*, 1999; Megiorni *et al.*, 2005). This implies that a neuron develops to a dorsal or ventral fate very likely following different ways.

For the ventral midbrain, a subset of early ventral neurons expressing *Nkx6.1* was checked here. Ventral – specific transcription factor *Nkx6.1* is expressed in specific subpopulation of sMN and interneuron V2 of the spinal cord (Rudnick *et al.*, 1994; Jensen *et al.*, 1996; Qiu *et al.*, 1998; Sander *et al.*, 2000). Mutant mice demonstrated developmental defects of branchial motor neurons (bMN) concerning their migration and axonal projections (Muller *et al.*, 2003a), whereas the misexpression of *Nkx6.1* in the dorsal spinal cord induced a sMN phenotype (Briscoe *et al.*, 2000). This study did not show a significant *Nkx6.1* repression as expected by Pax3/7 misexpression in ventral midbrain and hindbrain. Double *in situ*

hybridization could not clearly show if such a ventral midbrain cell expressed both Nkx6.1 and Pax3/7 together. Fluorescent immunostaining would be a good way to solve this question when the specific antibodies are available. Matsunaga's work (2001) has found that another ventral-specific transcription factors Lim 1 is suppressed by Pax7 misexpression in the ventral midbrain, however, only effect on the broader stripe of expression that is more lateral to the floor plate. This could mean that Pax7 alone is not enough to induce dorsal cell types and/or that Shh expression is too strong in this area and overrules ectopic Pax7 expression (Watanabe and Nakamura, 2000). In the spinal cord Shh expression is necessary for the development of motoneurons at later time (Liem *et al.*, 2000). Thus, it very well could be that a high concentration of Shh in the ventral midbrain counteracts Pax7 effects. This might be the case for Nkx6.1 expression in my study. It has to be further tested by examining the development of midbrains.

Cross-regulation between Pax3 and Pax7

Pax3 and Pax7 belong to the same Pax subfamily, and share extensive overlapping domains of expression in the nervous system and somite regions (Jostes *et al.*, 1990; Goulding *et al.*, 1991; 1994). In the dorsal neural tube, they show a similar expression pattern except for the lack of Pax3 in the roof plate (Kawakami *et al.*, 1997; Matsunaga *et al.*, 2001). Defects in muscular and neural tube of the mutant mice (Epstein *et al.*, 1991; Franz and Kothary, 1993; Mansouri *et al.*, 1996; Conway *et al.*, 1997; Mansouri and Gruss, 1998) and phenotypes of the misexpressed neural tubes (Wada *et al.*, 1997; Mansouri *et al.*, 2001) suggest a functional redundancy of Pax3 and Pax7. Thus, the single mutant phenotypes are not severe as Pax3/7 double mutant due to one can compensates a partial function of the other, which protects the embryo from individual gene inactivation. In another hand, the possible interaction between them was further investigated. This study demonstrated that misexpression of Pax7 in the dorsal or ventral midbrain resulted in ectopic Pax3 transcription in a cell autonomous manner at early stages. The reverse effect of Pax3 on Pax7 has already been examined by Borycki (1999). His study shows that Pax3 represses endogenous Pax7 expression in cultured cells, and the expression of Pax7 is upregulated in the dorsal neural tube and somite regions in Pax3-deficient (*Spotch*) mice. These findings suggest that a cross-regulatory mechanism exists between the two closely related transcription factors. In shortly, Pax3 downregulates Pax7 expression and Pax7 upregulates Pax3 expression in a dose-dependent manner. Evidences from the two single mutant mice also demonstrate that each one of the two genes is not required for the expression of the other (Mansouri *et al.*, 1996; Borycki *et al.*, 1999). Some other studies imply the expression of Pax3 and Pax7 could to be initiated in the nervous system through different signaling pathways. Pax3 might be induced by some FGF members, like Fgf8, which is shown to be necessary and sufficient for expression of Pax3 and other genes in nasal region, but not for Pax7 expression (Firnberg and

Neubuser, 2002). While *Pax7* is possibly initiated by BMPs or GDFs expressed in ectodermal cells (Liem *et al.*, 1995; Lee and Jessell, 1999).

The present work confirmed the result from Matsunaga's work (2001). Misexpression of *Pax7* in the ventral midbrain results in the formation of the dorsal, laminar tectal structures, accompanied with ectopic expression of *Pax3* and suppression of *Pax6* and *Lim1* expression. Thus, these ventral cells expressing *Pax7* acquire a dorsal fate. Interestingly, Matsunaga (2001) experienced a difference in the strength of the induce *Pax3* expression. Only after 96 h a robust *Pax3* expression can be detected. However, a strong *Pax3* expression was already visible at 16 h after a *Pax7* transfection in this study. This might be due to some slight differences of the expression vectors used in the two studies. Or, it could be due to the difference in plasmid concentration. DNA solution used here was 2 – 5 $\mu\text{g}/\mu\text{l}$, higher than 1 $\mu\text{g}/\mu\text{l}$ in Matsunaga's experiments. This might be reflected by a dose – dependent function of *Pax3* on *Meis2* (a paper from Dorothea Schulte, in preparation).

Pax3/7 Action on Rapid Expansion of the Mesencephalon

During the development of central nervous system, some regions of brain vesicles rapid expand into a visible swelling. Chick optic tectum as such a represent model is analysed here. The alar plate undergoes strong proliferation and accelerates from embryonic day 3 (E3) onward to form a lateral extension in the optic tectum (Fig. 45). Less cell proliferation takes place in ventral area to produce many nuclei related to motor function (Senut and Alvarado-Mallart, 1987; Watanabe and Nakamura, 2000).

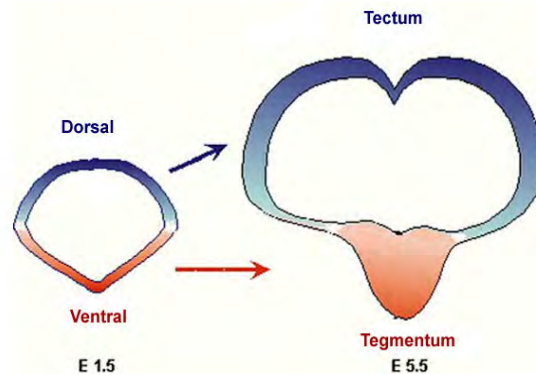


Figure 45: Schematic diagram of chick developing midbrain

Increased differentiation in the midbrain starts in the basal plate where *Shh* regulates the ventral cell fates. In the alar plate cells continuously proliferate to form large optic tectum. In the E5.5, the tectum has started to subdivide into two hemispheres at the dorsal midline. The alar plate is represented in blue, while the basal plate in red.

In the alar plate of the mesencephalon, the paired-type transcription factors *Pax3* and *Pax7* were both expressed strongly at around stage 20 (E3.5), a time of accelerated extension initiated in the dorsal midbrain (Matsunaga *et al.*, 2001). The results of this study suggest that *Pax7* is required to promote and/or maintain the proliferative activity of neural precursor cells in dorsal midbrain. Some evidences propose that *Pax3* may - at least partially - contribute to the midbrain expansion at this fast developmental period as well. It has shown that *Pax3* is able to stimulate the transcription of an anti-apoptotic gene *Bcl-x1*, and disruption of *Pax3* expression results in an obvious impaire on *MyoD* activation accompanied by a marked

increase of programmed cell death (PCD, Maroto *et al.*, 1997; Borycki *et al.*, 1999; Margue *et al.*, 2000). In several malignant tumors, such as melanoma, antisense *Pax3* treatment results in tumor cell apoptosis at a large scale (Schulte *et al.*, 1997; Mansouri, 1998; Schafer, 1998; Margue *et al.*, 2000; Scholl *et al.*, 2001). This suggests the effect of Pax3 to prevent cell death may very well function on neural cell lineages. Thus, the expansion of dorsal midbrain is due to more neural precursor cells generation and less cell death, which is achieved by a proper threshold activity of both factors via a dynamic cross-regulative feedback between them, resulting in an increased count of the cells. Although *Pax3* is shown to be decreased markedly from stage 24 onwards in the dorsal midbrain (Kawakami *et al.*, 1997), the expansion of the tectum has already formed at that time. Or, this proposes the enlargement of the dorsal midbrain becomes slow. The expression of the two paired-box proteins are prevailing from diencephalon to the spinal cord in dorsal region of the early neural tube (Jostes *et al.*, 1990; Goulding *et al.*, 1991), however, the swelling of other dorsal regions is not so much prominent as the tectum. This could be explained thus, that the effect of Pax3/7 on cell increase might correlate with the protein amounts. For instance, the expression of Pax7 seems to become weaker in the spinal cord since stage 19/20 compared to the expression in the dermamyotome (Fig. 46), while this expression is maintained at a higher level in dorsal midbrain till stage 30. Although there is evidence in the literature and in this study suggest that this is the case, so far it has not been investigated thoroughly. Another possibility might be that some particular co-factors present in the midbrain but not in other parts of the neural tube. Meis2a for example is reported to be a co-factor for homeodomain proteins restricted to the dorsal mesencephalon, but absent from the diencephalon and metencephalon (Zhang *et al.*, 2002, Dorothea Schulte's paper in preparation).

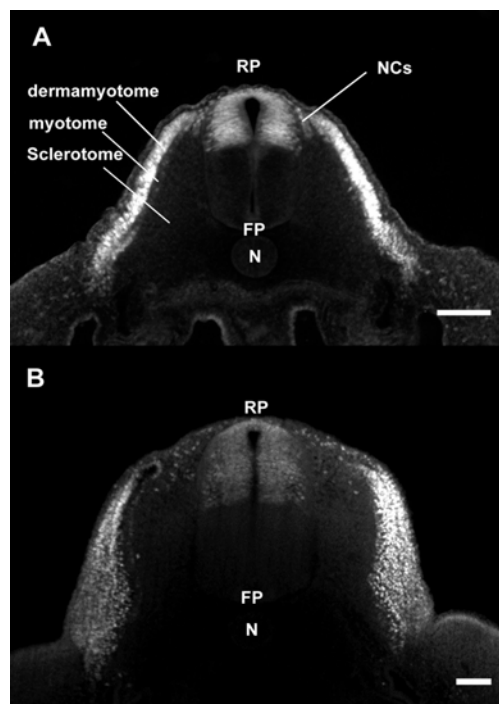


Figure 46: Expression comparison of Pax7 protein in the spinal cord at stage 16 and 23

Chick embryos were fixed at stage 16 (A) and 23 (B). Transversal sections (50µm) through the anterior spinal cord are illustrated here. Dorsal is up.

A: The expression of Pax7 was located in the dorsal region of the spinal cord with a sharp ventral boundary. The expression level in spinal cord was similar to that in the dermamyotome. The lumen was visible in the dorsal region.

B: The spinal cord section showed a weaker Pax7 expression with a narrow ventricle compared to the expression in the dermamyotome.

Abbreviations: FP, floor plate; N, notochord; NCs, neural crest cells; RP, roof plate. Scale bar: 100µm.

The influence of Pax3/7 genes on the cell proliferation is only one process to shape the mesencephalon. Actually, many other molecules are involved in the development of the mesencephalon as well, with or without evidences of a relation to Pax3/7. Diverse growth factors and morphogenes, such as FGFs, Shh and Wnt members, are known to be required for patterning and progressive commitment of brain regions. Among the FGF members, which modify the fates of precursor cells via Fgf - homeodomain interaction (Arsenijevic *et al.*, 2001; Vaccarino *et al.*, 2001; Ohkubo *et al.*, 2004), Fgf8 is a good candidate in the mesencephalon. It has been shown that disruption of *Fgf8* causes the absence of a portion of the midbrain and the cerebellum (Meyers *et al.*, 1998), and ectopic expression induces the growth of midbrain or cerebellar tissue in the diencephalon (Crossley *et al.*, 1996; Nakamura and Watanabe, 2005). Fgf8 also seems to influence the induction of specific dorsal interneurons at later development (Tanaka *et al.*, 2001). Pax2/5 and En are also thought to be contributed to initiate and maintain the tectum development via consisting of a positive feedback loop with Fgf8 to keep organizing activity (Song *et al.*, 1996; Araki and Nakamura, 1999; Funahashi *et al.*, 1999; Okafuji *et al.*, 1999; Shamim *et al.*, 1999; Liu and Joyner, 2001). The function of En genes were demonstrated by En2 misexpression and En1/2 double mutant mice, as the neural tissue should express En to differentiate into the tectum (Araki and Nakamura, 1999; Liu and Joyner, 2001). The expression of Pax3 and Pax7 only commences after En expression in the mesencephalon (Song *et al.*, 1996; Kawakami *et al.*, 1997; Matsunaga *et al.*, 2001). In addition, Pax3 protein is suggested to be required for the closure of the neural tube closure, since *Pax3* mutant mice show a neural tube defect of spina bifida (Franz and Kothary, 1993; Borycki *et al.*, 1999; Juriloff and Harris, 2000), which can be rescued by Pax3 overexpression (Li *et al.*, 1999).

In summary, these results point towards a model for the rapid expansion of the dorsal midbrain at early stages via a balanced expression level of Pax3 and Pax7 transcription factors (Fig. 47). At first, *Pax3* gene is activated in the neural plate by Fgf8 and/or other factors, and subsequently expressed in the alar plate of the midbrain. Soon after the neural tube closure with the help of Pax3, Pax7 starts to be activated in the alar plate by some molecules that might be different to *Pax3* induction. The expressions of both genes are controlled by signals from floor plate or midbrain-hindbrain boundary. From stage 16 onwards, Pax3 and Pax7 are both expressed independently, but regulated each other at a large scale by the reciprocal feedback between them. A balanced high level of their expression then leads to a rapid expansion of the dorsal midbrain, which might be mediated by some factors like Wnt or Fgf members. At a certain amount, Pax7 protein promotes cell division and Pax3 blocks cell apoptosis. The midbrain expansion might slow down since the expression of Pax3 is decreased at stage 24. Since stage 31, Pax3/7 expressing postmitotic neurons migrate radially towards the pial side to settle in different laminar layers of the tectum, and Pax7 very likely maintains the proliferative activity of neural precursor cells in the ventricular zone to generate neurons continuously.

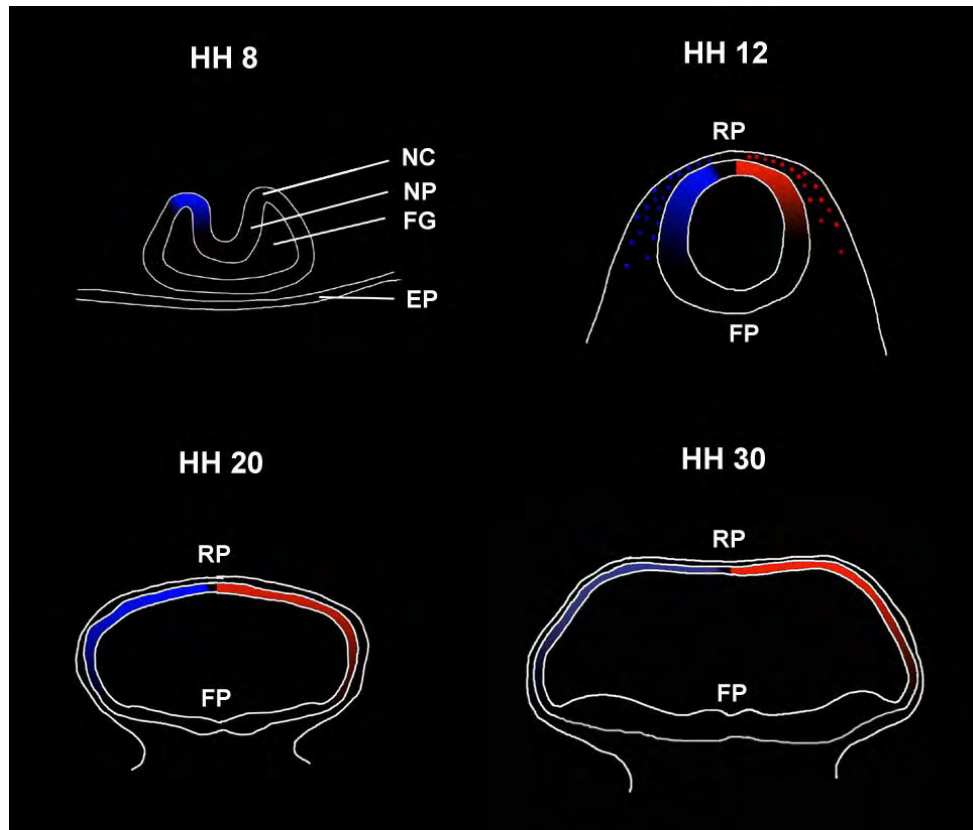


Fig47: Schematic diagram of the dynamic expressions of Pax3 and Pax7 in chick developing midbrain at early stages

At early development, Pax3 is initially expressed in the neural precursor cells of the presumed mesencephalic region in the neural plate at about stage 8 (HH 8). The neural crest cells express Pax3 too. Since stage 10 (HH 12), a time when the neural tube closes, Pax7 starts to be activated in the alar plate of the mesencephalon. Pax3 expression is spread laterally within the alar plate except for the roof plate. With the development (HH 20), the expressions of the two Pax genes is spread to the entire alar plate and become strong. The dorsal midbrain undergoes a rapid expansion during this period. Since stage 24 (HH 30), the expression of Pax3 becomes decreased, whereas Pax7 expression is still strong in the dorsal midbrain till the laminar structures form. The expression of Pax3 is illustrated in blue on the left midbrain, and Pax7 expression is red on the right.

Abbreviations: EP, epidermis; FG, foregut; FP, floor plate; HH, Hamburger and Hamilton; NC, neural crest; NP, neural plate; RP, roof plate.

Part III: Expression and Function of Rab23 in Chick Nervous System

Rab23, a small G protein, was first identified in *opb* mutant and thought to be involved in the dorsoventral patterning of murine neural tube as a negative regulator of *Sonic hedgehog* signaling (Gunther *et al.*, 1994; 1997; Kasarskis *et al.*, 1998; Eggenschwiler and Anderson, 2000; Eggenschwiler *et al.*, 2001). To know its expression pattern in chick embryos, *in situ* hybridization with RNA probe specific for chick *Rab23* gene was performed at different embryonic stages. Isolation and overexpression of this gene were also performed to explore the function of Rab23 in chick nervous system.

1. Expression Pattern of *Rab23* in Chick Embryos

Preparation of Antisense RNA Probes for Chick *Rab23*

Using the coding region of mouse *Rab23* cDNA (Olkkonen *et al.*, 1994) as a query, five chick EST clones (Tab. 2) with higher sequential similarities in BBSRC chick EST Database Bank (<http://www.chick.unist.ac.uk/>) were ordered from MRC geneservice, Cambridge. After analysis of the sequence by restrictive digestion (Fig. 48) and DNA sequencing, three of the five ChEST clones (545g23, 885j22 and 925k6) were used to synthesize antisense RNA probes for the detection of chick *Rab23* mRNA via RNA *in situ* hybridization. In short, the isolated plasmids (based on pBluescript II KS + vector) were linearized with *SacI*, and the Dig – labelled antisense RNA probe was transcribed with T3 RNA polymerase, while the Fitc – labelled sense RNA probes was produced with *EcoRI* and T7 polymerase and used as negative control.

The hybridisation with all three antisense RNA probes showed a same expression pattern, which ensured to be specific for *Rab23* mRNA. The

RNA probe from ChEST clone 885j22 produced a stronger signal and less background. This RNA probe was revealed by sequence alignment to be complementary to a large part of the coding region close to the 5' end (refers to p2 in Fig. 51), and used to detect chick Rab23 in the following experiments. Sense transcripts from all 3 clones did not show any signal (Fig. 50 S, T).

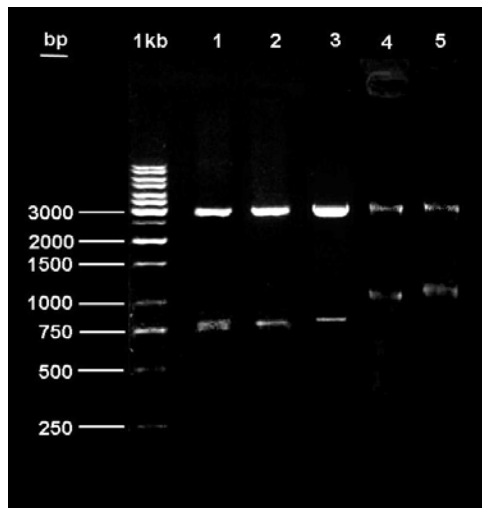


Figure 48: Sequential analysis of chick EST clones containing *Rab23* gene fragments by restrictive digestion

Five chick EST clones were digested with *EcoRI* and *NotI*. The expected bands are a 3kb band, corresponding to the pBluescript II KS + vector, and a small band of *Rab23* gene fragments in around 800, 750, 850, 1050 and 1100 base pairs, respectively. Lanes 1 to 5 are chEST clone 545g23, 885j22, 925k6, 75d14 and 772o6. 1kb DNA ladder was used here as a size standard.

***Rab23* Expression Early in Chick Embryos**

Rab23 mRNA was checked by *in situ* hybridization in chick embryos at stage 4 to 23 and embryonic day 6 (E6). The results showed that the expression of *Rab23* mRNA was first detected in chick embryos at stage 4 during gastrulation (Fig. 49), when the primitive streak is at its full extension from posterior to anterior (\cong 1.88 mm). At this stage, *Rab23* expression was located in Hensen's node and the entire primitive streak along the primitive groove (Fig. 49 A). This expression was sustained there till stage 7 when the node and the primitive streak started to regress posteriorly (Fig. 49 B, C, D). However, *Rab23* seems to be stronger in the posterior part of the primitive streak. Transverse sections of these early chick embryos showed that *Rab23* was initially expressed in the epiblast (epidermis) and the new forming mesoderm in these embryonic structures (Fig. 49 E - G), whereby *Rab23* - positive cells were more basally located in the epidermis (Fig. 49 H and L). At stage 7, *Rab23* was mainly expressed in the underlying mesoderm in the caudal embryos (Fig. 49 S and T). In the brain region, *Rab23* was found in the mesoderm and the entire neural plate (Fig. 49 D, R, U).

An interesting finding was that between stage 4 and 7 *Rab23* was asymmetrically expressed in Hensen's node and the anterior primitive streak with a stronger bias to the right lip (Fig. 49 A - D, F, G, J, K, N, O, Q, S, T, V). At these stages, Hensen's node showed an asymmetric morphology with a steep right boundary at stage 4 and a significant burge on the right side at stage 7 (Fig. 49 F, J, N, S), which was also mentioned in other previous studies (Viebahn, 2001; Dathe *et al.*, 2002). The

expression was much stronger in the anterior right region of Hensen's node at stage 4 to 6 (Fig. 49 A – C, Q) and in the posterior right region of Hensen's node at stage 7 (Fig. 49 D, V). *Rab23* expression in Hensen's node and the primitive streak was not obviously enhanced from stage 4 to 7 (Hensen's node, Fig. 49 F, J, N, S; primitive streak, Fig. 49 G, K, O, T), while the expression in neural plate strengthened with the time (Fig. 49 D, P, U, and Fig. 50).

Rab23 was also expressed in the somite, since this embryonic structure commenced to form at stage 7 (Fig. 49 D, V). From stage 15 onwards (Fig. 50 N – Q), the expression was gradually restricted to the dorsal region of the somite (dermamyotome).

A Transient *Rab23* Expression in the Notochord at Early Stages

Rab23 mRNA was also detected in the head process (Fig. 49 B, C, I, L, Q), an embryonic midline region rostral to Hensen's node, which is pushed up by the anterior movement of the ingressing cells through Hensen's node. The chordamesoderm beneath the neural plate in this region will form anterior notochord and prechordal plate at later stages (Psychoyos and Stern, 1996a). High resolution indicated that *Rab23* expression was located in these mesodermal cells (Fig. 49 P, U). However, *Rab23* expression in the notochord was only visible up to stage 13 (Fig. 50 M).

Expression Pattern of *Rab23* in the Neural Tube

Rab23 was expressed in the neural plate since the onset of neural precursor cells at stage 6 (Fig. 49 C, M, P). These column – shaped neural precursor cells are specified from the epidermis localized anterior to Hensen's node. As the neural folds were elevated, *Rab23* expression in the neural plate became stronger (Fig. 49 D, R). However, no expression of *Rab23* was seen in neural crest or presumptive epidermis (Fig. 49 R, U).

As the formation of brain vesicles at stage 8 to 13, *Rab23* expression was located in the whole neural tube along anterioposterior axis (Fig. 50 A, E, I, M, Q). 'Open book' preparations and transverse sections of midbrain and spinal cord at stage 11/13 showed that *Rab23* was expressed along the entire dorso-ventral axis with a weaker expression in the floor and roof plates (Fig. 50 A, B, E, I, J, M). This expression restricted to the dorsal region gradually over the next five stages (Fig. 50 B – D, F, J – L, N). At stage 21, the *Rab23* expression was only detected in the alar plate except for a narrow stripe of the roof plate (Fig. 50 G, O), and this pattern was still seen up to embryonic day 6 (Fig. 50 H, P, and data not shown).

In addition, *Rab23* was also detected in the eye disc, very likely in the layer of the retinal ganglion cells, whereas the sclera and surrounding mesenchyme were devoid of *Rab23* expression (stage 23, Fig. 50 R).

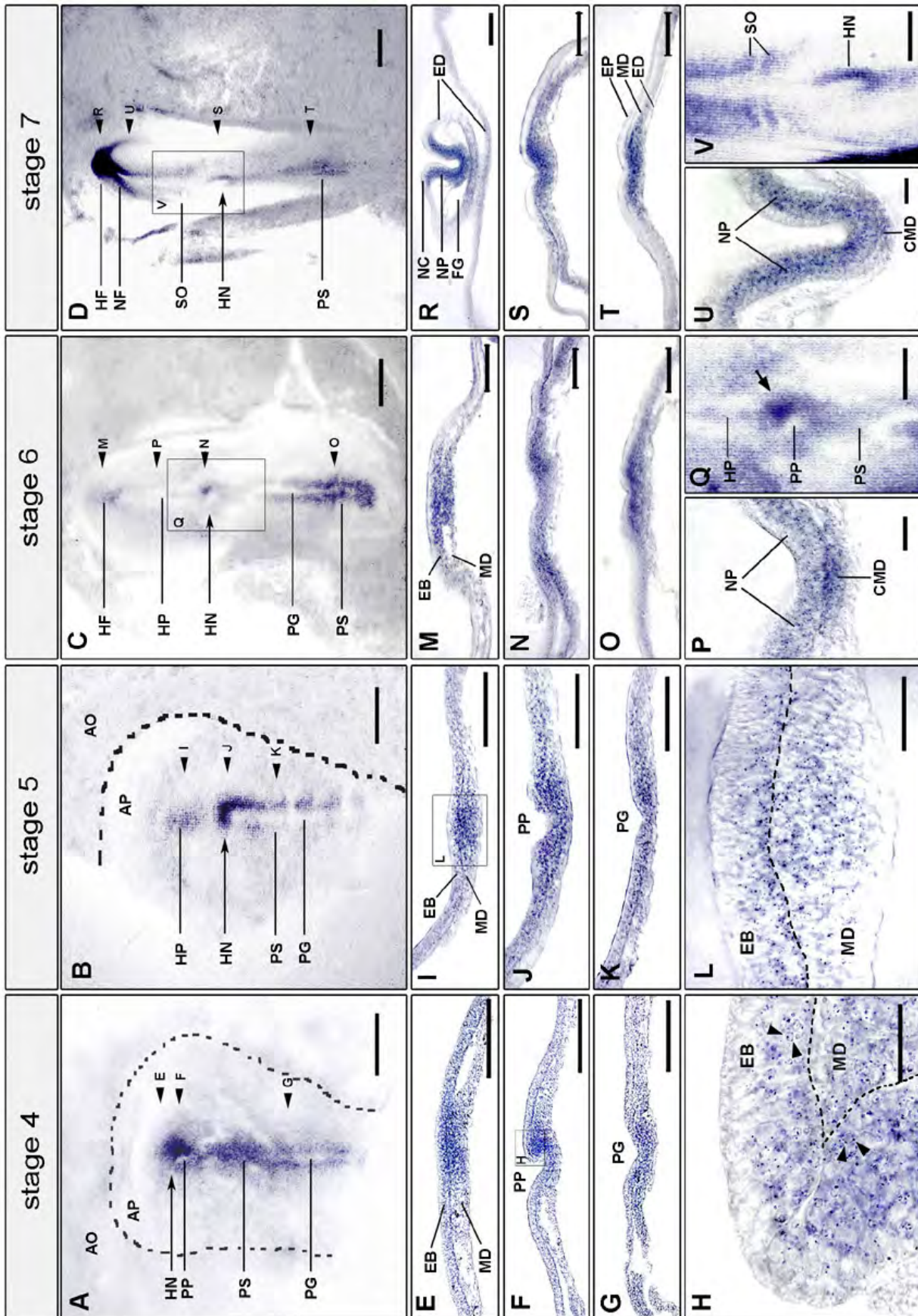


Figure 49: Dynamic expression pattern of *Rab23* gene in chick embryos at stage 4 to 7

Figure 49: Dynamic expression pattern of *Rab23* gene in chick embryos at stage 4 to 7

Chick embryos at stage 4 to 7 were labelled with antisense RNA probes for *Rab23* gene. A - D, Q, V, Dorsal views of the entire embryos. Anterior is up. E - P, R - U, Transverse sections (20µm) of the embryos in A - D, respectively. Dorsal is up. The cut level of each section is indicated in A - D by black arrows with the corresponding figure letter. Stages of the chick embryos are indicated at the top.

A: At stage 4, the expression of *Rab23* mRNA was detected in Hensen's node and the primitive streak with a significant stronger expression on the right lip of Hensen's node (see also F). The border between area opaca and pellucida is indicated.

B: At stage 5, *Rab23* gene started to be detected in the head process. The expression in Hensen's node and the primitive streak was still shown in an asymmetrical pattern as stage 4 in A (see also J and K).

C: At stage 6, *Rab23* expression was detected in the forming head fold. The expression in Hensen's node was still visible in the anterior right region (see also N and Q). The posterior primitive streak expressed *Rab23* strongly.

D: At 2-somite stage (stage 7), the expression of *Rab23* was much stronger in the neural fold than in the node and streak region. The *Rab23* expression in Hensen's node became unfocused except for a weak signal on the right side. In addition, somitic mesoderm showed *Rab23* expression (see also S).

E - H: Transverse sections of a stage 4 chick embryo. *Rab23* mRNA was detected in both ectoderm and mesoderm along the embryonal midline (E), including Hensen's node (F) and the primitive streak (G). The right lip of Hensen's node exhibited a strong *Rab23* expression pattern with a sharp boundary in morphology. H is a magnification of the indicated area in F, showing that the *Rab23* was expressed in the basal layer of the infolded epiblast (epidermis) as well as the underlying mesoderm. Arrowheads depict *Rab23* mRNA signals within a cell. The fractured line indicates the boundary between the ectoderm and mesoderm.

I - L: Transverse sections of the stage 5 embryo in B. Densely labelled *Rab23* positive cells were shown in the head process (anterior mesoderm). *Rab23* expression in Hensen's node (J) and the primitive streak (K) was still stronger on the right side. L is a magnification of the head process region in I, which indicates *Rab23* expression in both mesoderm and basal epidermis.

M - P: Transverse sections of the stage 6 embryo in C. The expression of *Rab23* in the head fold region (M) was located in the mesoderm and ectoderm (epidermis). The asymmetrical expression pattern of *Rab23* was sustained mainly in the mesoderm of Hensen's node (N) and the primitive streak regions (O). Expression in the ectoderm was nearly lost. P showed that neural plate cells began to express *Rab23* in addition to the underlying chordamesoderm (presumable notochord).

Q: A magnification of the indicated area around Hensen's node in C. A strong *Rab23* expression was showed in the anterior right region of Hensen's node (arrow). Anterior and posterior midline structures (head process and primitive streak) expressed *Rab23* as well.

R - U: Transverse sections of the stage 7 embryo in D. R and U depict a strong *Rab23* expression in the neural plate. *Rab23* expression was not visible in neural crest cells or epidermis cells. However, the expression was detected in the presumed notochord (chordamesoderm, U). The expression of *Rab23* was still found in Hensen's node with a stronger right bias (S). Hensen's node was still morphologically asymmetric. T indicated a dense *Rab23* expression in the midline mesoderm of the primitive streak region, but fewer signals in the epidermis.

V: A detailed graph of the indicated area in D. Two new forming somites exhibited a *Rab23* expression. The asymmetric expression of Hensen's node was followed by the primitive streak, which still expressed *Rab23*. The Hensen's node became a long shape along the AP axis at this stage.

Abbreviations: AO, area opaca; AP, area pellucida; CMD, chordamesoderm; EB, epiblast; ED, endoderm; EP, epidermis; FG, foregut; HF, head fold; HN, Hensen's node; HP, head process; MD, mesoderm; NC, neural crest; NF, neural fold; NP, neural plate; PG, primitive groove; PP, primitive pit; PS, primitive streak; SO, somite. Scale bar: A - D, 500 µm; E - G, I - K, M - O, Q, R - T, V, 100 µm; H, L, P, U, 25 µm.

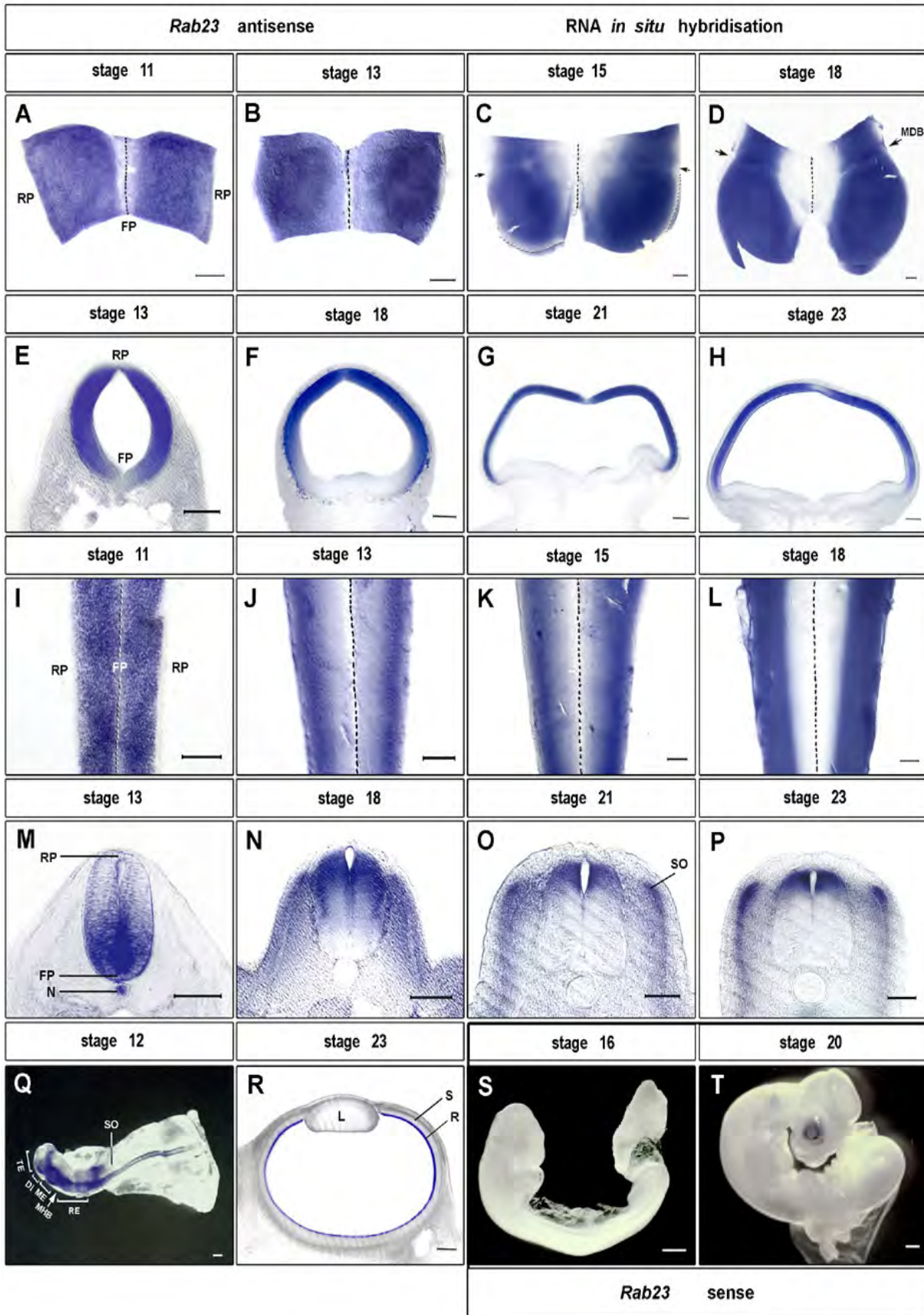


Figure 50: *Rab23* expression in chick midbrain and spinal cord after neural tube formation

Figure 50: Rab23 expression in chick midbrain and spinal cord after neural tube formation

A – R: Chick embryos were labelled by *in situ* hybridisation with antisense RNA probe for *Rab23* gene. S and T: with sense RNA probe for *Rab23*. The midbrains (A – D) and the spinal cords (I – L) are made in ‘open-book’ preparations with anterior to the up. The midbrains (E – H) and the spinal cords (M – P) are shown in transverse sections (50 μm), and dorsal is up. Q, S and T show the whole embryos. R is a parasagittal section through the diencephalon at the eye level. Black and white dash lines indicate the position of the floor plate and roof plate, respectively.

A - D: In chick midbrain, *Rab23* mRNA was strongly expressed in the entire neuroepithelium at stage 11 (A) and 13 (B). Within the next five stages (C, D) the expression gradually restricted to the dorsal region. Meantime, the narrow stripe of the roof plate did not express *Rab23* any more. The arrows point out the mesencephalon-diencephalon boundary.

E - H: Transverse sections through midbrain showed the same DV expression pattern as the flat mounts in A - D. From stage 18 onwards *Rab23* was exclusively expressed in the entire dorsal midbrain except for the roof plate (G, H), but not in the ventral region. Note: *Rab23* expression in the dorsal midbrain at least could sustain till E6 (data not shown).

I - L: The ‘open-book’ preparations of the anterior spinal cord displayed a *Rab23* expression pattern similar to the midbrain (A – D). *Rab23* expression localized in the entire spinal cord along DV axis at stage 11 (I) and gradually disappeared in the ventral from stage 13 to 18 (J - L).

M - P: Transverse sections through the posterior spinal cord at different stages confirmed the dynamic expression pattern of *Rab23* in flat-mount preparations of I - L. A gradient expression pattern of *Rab23* in the spinal cord along DV axis retreated more dorsally with the time (N – P). In addition, *Rab23* was also detected in the notochord at stage 13 (M) and disappeared later. The expression pattern in the somites was consistent with its DV pattern in spinal cord (O, P).

Q: A whole stage 12 embryo labelled with *Rab23*. The expression of *Rab23* was seen in the entire neural tube from telencephalon to the end of spinal cord. *Rab23* expression in posterior somites was visible.

R: Parasagittal section through the diencephalon at the level of the eye at stage 23. The retina lining the inner wall of the eye expresses *Rab23*, while the sclera, which deviates from neural crest, was depleted of *Rab23* expression.

S and T: Hybridisation with the sense RNA probes for *Rab23* disclosed no staining in chick embryos at different stages. The grey-colored eye disc at later stage (stage 20, T) revealed the formation of the pigmental epithelium.

Abbreviations: Di, diencephalon; FP, floor plate; L, lens; MDB, mesencephalon-diencephalon boundary; ME, mesencephalon; MHB, midbrain-hindbrain boundary; N, notochord; R, retina; RE, rhombencephalon; RP, roof plate; S, sclera; SO, somite; TE, telencephalon. Scale bar: A - R, 100 μm ; S, T, 500 μm .

2. Identification and Analysis of Chick *Rab23* Gene

Identification of Chick *Rab23* cDNA

Using mouse *Rab23* cDNA sequence (PubMed, NM_008999) as a query in the BBSRC Chick EST Database Bank (<http://www.chick.umist.ac.uk/>), eleven candidates were assembled into four DNA fragments with highest homology, 026299.1, 035898.2, 035898.1, and 321099.1, named as p1 - p4 (p - partial), respectively. These fragments were assembled into a DNA sequence of 1706 nucleotides (Fig. 51).

Analysis of the assembled cDNA by DNASTAR revealed an open reading frame (ORF) of 714 bp including a start codon and a stop codon (Fig. 92). DNA sequence alignment using the J. Hein method showed this ORF is about 80 % of sequential similarity to the coding region of the human and murine *Rab23* genes (AB034244 and NM_08999, both 714 bp). The amino acid sequence (237 aa, 26.8 kD) deduced from this ORF also showed high similarities with human (88.2 %) and murine (84.9 %) *Rab23* proteins using Clustal method (Fig. 53). Additionally, two AU - rich elements (ATTTA) were identified in the 3' UTR, which might be involved in mRNA degradation. Thus, the 1706 bp DNA sequence described here should be the full-length chick *Rab23* cDNA including 5' and 3' UTR, and it was further verified by the expression of subcloned plasmid using this ORF in the following experiments (Fig. 56).

BLAST analysis of the chicken genome using the cDNA sequence as a query (<http://www.ncbi.nlm.nih.gov/genome/seq/GgaBlast.html>) revealed that the chick *Rab23* gene consisted of seven exons (six coding exons) and was located on chromosome 3 in chick.

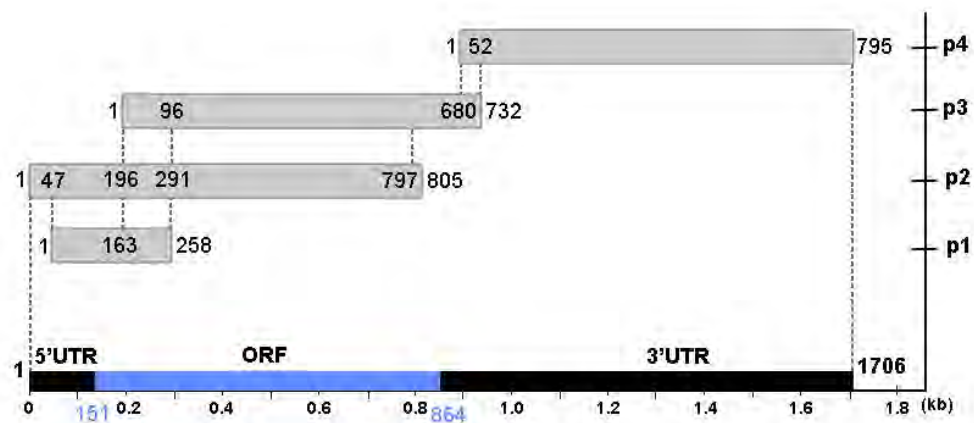


Figure 51: Four DNA fragments for assembly of full-length chick *Rab23* cDNA

Four DNA fragments (p1 - p4) for chick *Rab23* cDNA were aligned each other. The direction of 5' to 3' end is shown from left to right. The corresponding positions between them are numerated and marked by dashed lines. The assembled chick *Rab23* cDNA sequence is a length of 1706 bp (black bar) with correction of some nucleotides. The blue bar represents the open reading frame (714 bp), starting at position 151 and ending at 864 in this sequence. 5' and 3' UTR are indicated on both sides.

Sequential Analysis of Chick Rab23 Protein

The deduced amino acid sequence of chick Rab23 reveals characteristic features of small G proteins involved in GTP binding and hydrolysis (Fig. 52, 92). It contains an effector domain (marked in blue) and four highly conserved domains (marked in yellow) corresponding to the five polypeptide loops (G1 – G5) of G protein, respectively (Bourne *et al.*, 1991; Paduch *et al.*, 2001). The effector domain in G2 loop (the effect loop or switch I region) is the interacting site for effectors and GTPase-activating protein (GAP). It corresponds to the amino acids (aa) 32 – 46 and conforms to the Rab consensus T-I-G-[VI]-[DE]-F (Jurnak, 1985; Valencia *et al.*, 1991; Spoerner *et al.*, 2001). The first highly-conserved domain is the ATP/GTP-binding site motif A (aa 16 – 23) in G1 loop (also called P - loop), which is a Glycine-rich domain (CRD) and responsible for the binding alpha- or beta - phosphate group of the nucleotide. The consensus pattern is [AG]-x(4)-G-K-[ST] (Saraste *et al.*, 1990). The second conserved domain (aa 63 – 69) in G3 loop (also named switch II region) provides two important residues - Aspartic acid (D) and Glycine (G), for the binding of Mg²⁺ and for gamma-phosphate. The consensus sequence is DxxG (Amor *et al.*, 1994). Switch I and II regions surround the gamma-phosphate group of the nucleotide (Paduch *et al.*, 2001). Their stretches undergo structural changes upon GTP binding and hydrolysis. The switch III region is absent in this small G protein (Gilman, 1987). The third one (aa 119 – 124) locates in G4 loop, which is also called the recognition loop. The consensus sequence NKxD contains Lysine (K) and Aspartic acid (D) residues directly interacting with the nucleotides (Zhong *et al.*, 1995; Sprang, 1997). The fourth one (aa 149 – 154) lies in G5 loop, which is a recognition site for guanine base. The consensus sequence is [RE]-x-S-V (Sprang, 1997). A conserved Cys - containing motif (CSIP) locates in the C - terminus. The sequence pattern is generally known as CAAX box (A – aliphatic aa) in Ras-like proteins, which provides a prenyl - group binding site for the posttranslational prenylation modification by the attachment of either a farnesyl or geranyl-geranyl group to a cysteine residue when these proteins are required for the membrane association (Yamane *et al.*, 1990; Newman and Magee, 1993). A striking feature of the Rab23 sequence is the exceptional length of the C - terminal tail, which is significantly longer than that of other Rab members (Fig. 52). This hypervariable C - terminal domain of Rab proteins is thought to be crucial for specific membrane association as a targeting signal (underlined in Fig. 92, Chavrier *et al.*, 1991). Chick Rab23 protein also shares sequences with other GTP - related proteins, such as GTP binding domain of elongation factor Tu (EF - Tu, aa 63 - 94, Stark *et al.*, 1997), a hypothetical ATP - binding protein (aa 14 - 171, Zarembinski *et al.*, 1998), ATP - binding region A of Sigma - 54 interaction domain (Morett and Segovia, 1993), ADP - ribosylation factor (Arf, aa 45 - 97, Kahn *et al.*, 1991), nucleolar GTP - binding protein 1 (NOG1, aa 113 - 124, Park *et al.*, 2001), Ras binding domain (aa 11 - 171, Paduch *et al.*, 2001).

Sequence comparison of Rab23 protein in diverse species (Fig. 53) and chick Rab23 with other closely - related Rab proteins (Fig. 52) revealed a high homology. All five polypeptide loops (G1 – G5) containing the

different binding site regions are highly conserved among vertebrates and invertebrates (Fig. 53).

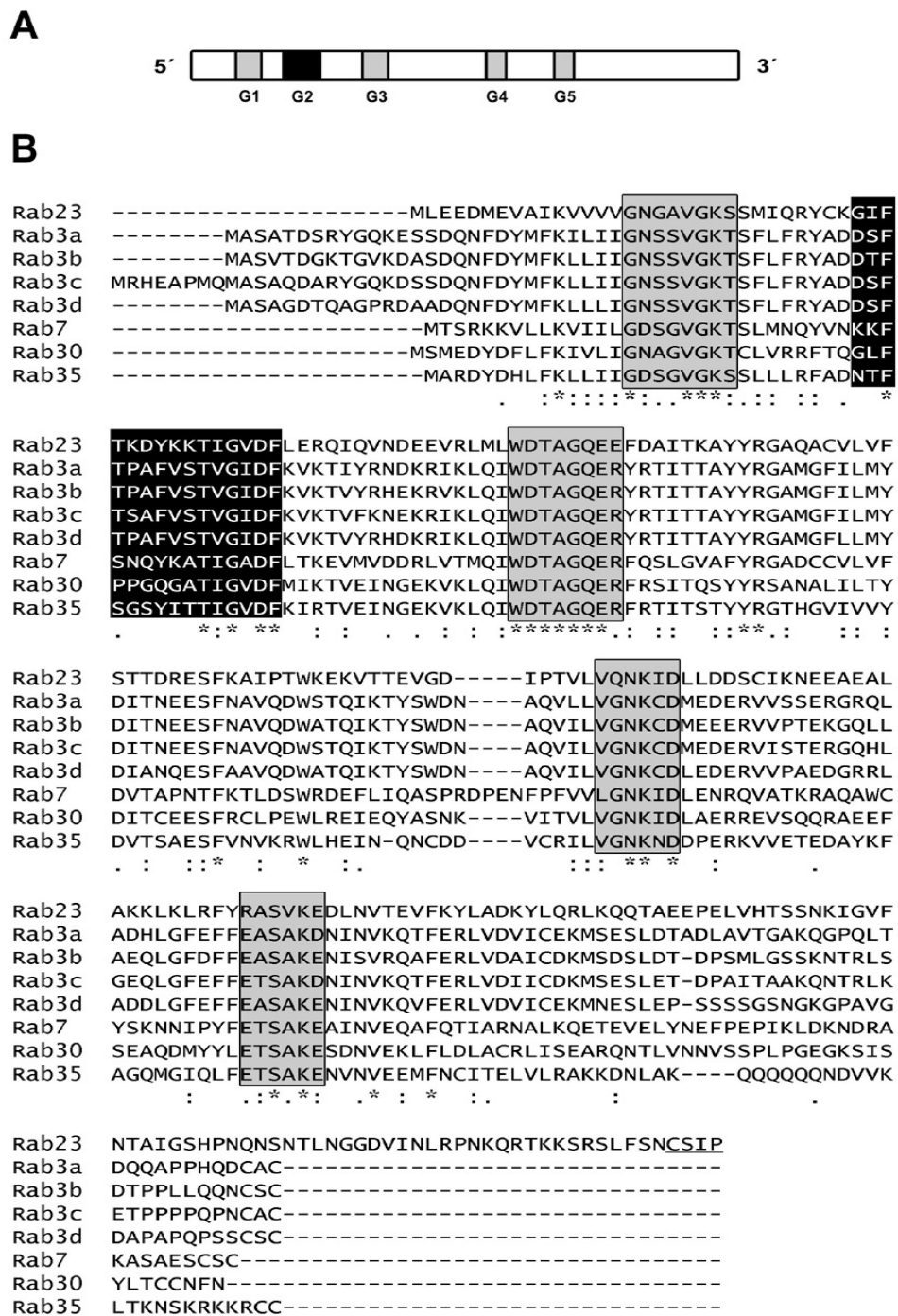


Figure 52: Schematic structure and multi-sequence alignment of chick Rab23 protein

A: Schematic diagram of the basic structure of chick Rab23 protein (237aa). Four highly-conserved domains (in gray) and the effector domain (in black) are located in five polypeptide loops (G1 – G5), respectively.

B: Multiple sequence alignment of chick Rab23 protein with other closely-related Rab members from mouse or human by CLUSTAL W (1.81) (<http://motif.genome.ad.jp/>). The post-translational modification domain is underlined. Accession numbers: Rab3a, rno:25531; Rab3b, hsa:5865; Rab3c, hsa:115827; Rab3d, hsa:9594; Rab7, hsa:7879; Rab30, hsa:27314; Rab35, hsa:11021. Identical residues are marked by (*), and the conservative substitutions are marked by (.) or (:).

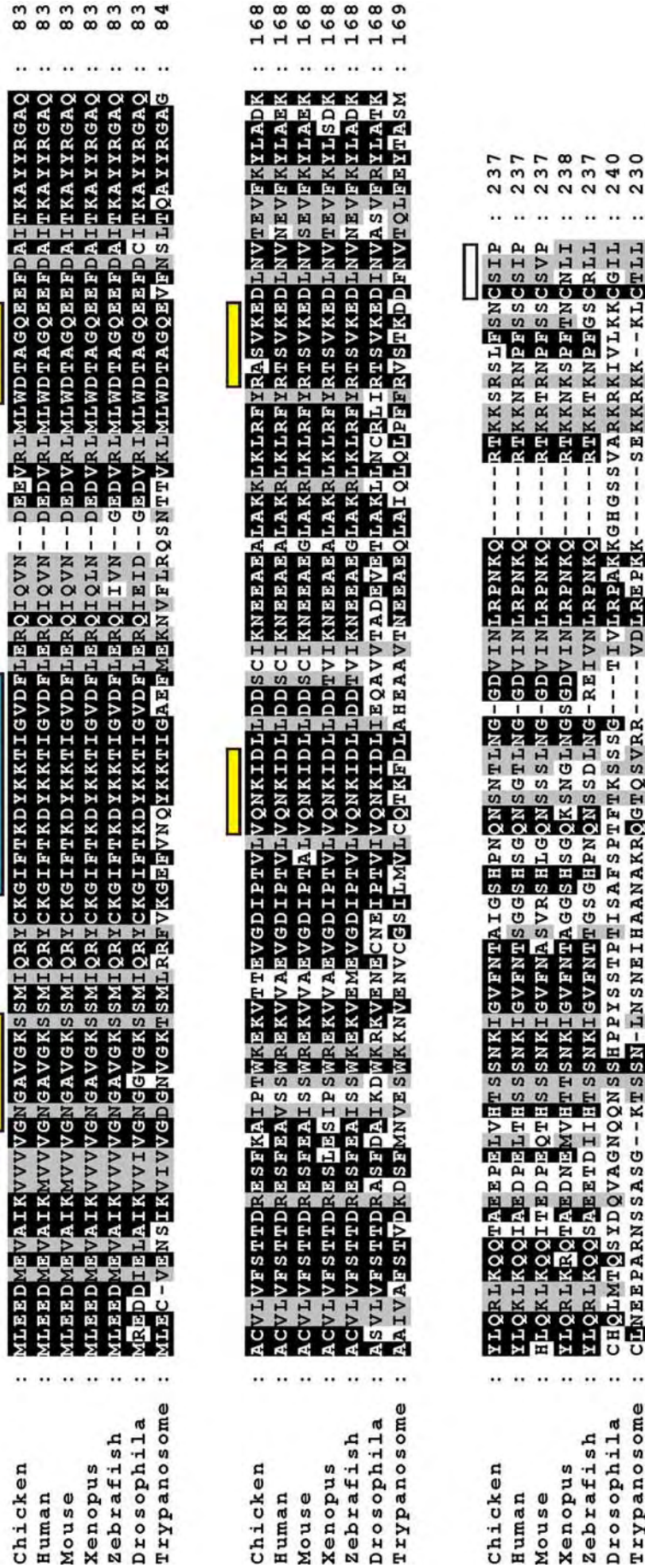


Figure 53: Sequence comparison of Rab23 proteins

The multiple alignment of Rab23 protein was processed among different species. The sequences from chick, mouse, human, Xenopus and zebrafish are used Rab23 proteins, whereas the sequences from the rest species (Drosophila and trypanosome) are used their closely related Rab members. Identical residues are white on black, conservative substitutions are black on gray. The matched amino acid is marked by black or gray. The highly conserved domains are marked in yellow, and the effector domain in blue and post-translational modification domain in boxed. Accession numbers are given in the legend of figure 54 (constructed by Dr. Jean-Nicolas Wolff).

Phylogenetic Analysis of Rab23 Proteins

A Phylogenetic tree of all known Rab23 proteins (Human, Rat, Mouse, Chick, Dog, Zeberafish) and closely related Rab proteins sequences in Mosquito, Drosophila, Trypanosome, Nematode is disclosed in Fig. 54. Only the open reading frames of these sequences were used. The phylogenetic analysis confirmed the identity of the chick sequence as a bona fide Rab23 protein with orthologues in mammals, fish, amphibians and insets.

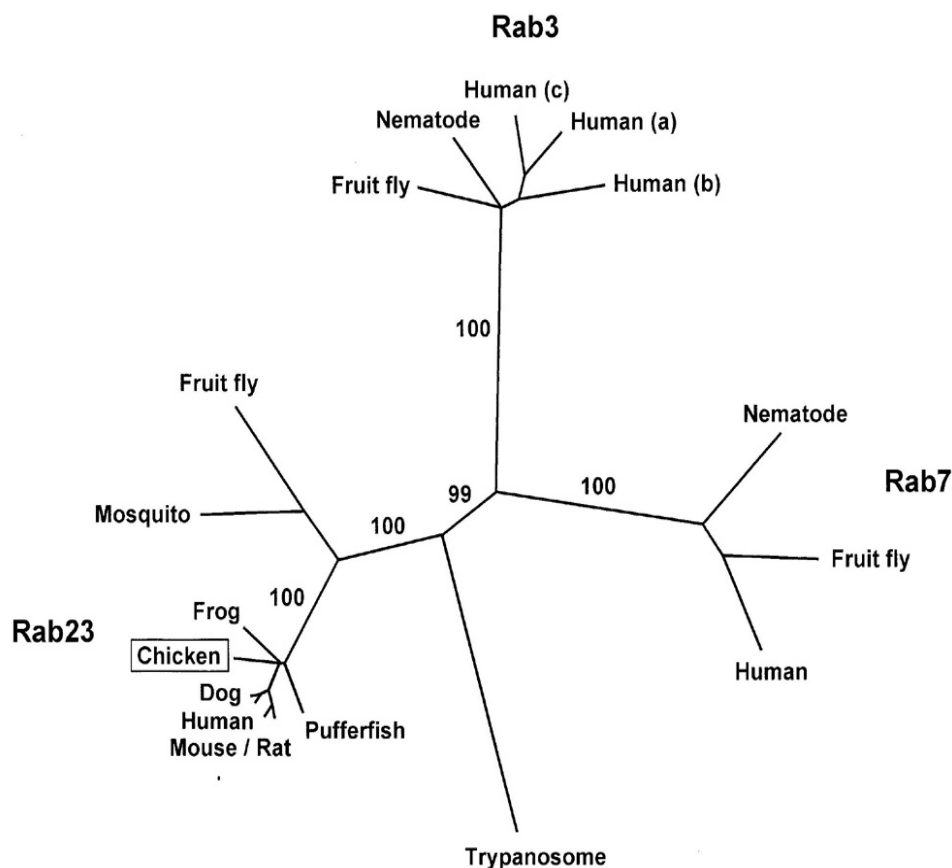


Figure 54: Phylogenetic tree of Rab23 proteins

Analysis was performed on an alignment of 192 amino-acids using the neighbour-joining method (Saitou and Nei, 1987, 1000 pseudosamples, bootstrap values are given). This topology was also supported by other methods of analysis (data not shown). Branches with less than 50 % support have been collapsed. Accession numbers: *Anopheles gambiae* (African malaria mosquito) XP_309942; *Canis familiaris* (dog) XP_538975; *Drosophila melanogaster* (fruit fly) NP_649574; *Gallus gallus* (chicken) XP_419896; *Homo sapiens* (human) NP_899050; *Mus musculus* (house mouse) AAH25578; *Pan troglodytes* (chimpanzee) XP_527422; *Rattus norvegicus* (Norway rat) XP_346034; *Tetraodon nigroviridis* CAG09432; *Xenopus laevis* (African clawed frog) AAH75188; *Trypanosoma cruzi* (trypanosome) AAC32778. Rab7: *Caenorhabditis elegans* (nematode) NP_496549; *Drosophila melanogaster* (fruit fly) NP_524472; *Homo sapiens* (human) AAA86640. Rab3: *Caenorhabditis elegans* (nematode) AAK68195; *Drosophila melanogaster* (fruit fly) BAD07037; *Homo sapiens* (human) NP_002857(a), D34323 (b), AAK08968 (c). (Constructed by Dr. Jean-Nicolas Volff).

3. Subcloning and Ectopic Expression of Chick *Rab23* Gene

Construction of Rab23 Expression Plasmid

To misexpress Rab23 in chick nervous system, the chick Rab23 cDNA needs to be constructed into an effective expression plasmid. The expected chick Rab23 sequence for cloning includes the entire open reading frame and a partial 5' and 3' UTR linked nearby. In short, total RNAs were isolated from chick embryonic neural tissues at first. A DNA product with the wanted size was obtained by RT - PCR (Fig. 55 A) with primer pairs containing recognitive sequences of restriction endonucleases (Tab. 4), and ligated into pCR 4 - TOPO vector and transformed *E. coli* cells. Sequential analysis of the selected clones was processed by direct PCR and restrictive digestion with restriction enzymes (Fig. 55 B, C). The constructed plasmids assumed containing the chick *Rab23* cDNA were followed to confirm by DNA sequencing. Then, the released inserts from these plasmids by double digestion of *XbaI/BamHI* were subcloned into a chick specific expression vector – pMES, and analyzed by PCR, enzymatic digestion and DNA sequencing (Fig. 55 D, and data not shown). Details of the performance refer to the Methods part. Both Rab23 expression plasmids from the clones r3-m36 and r4-m10 were shown to contain the same sequence of chick Rab23 cDNA.

Ectopic expression of Rab23 *in vivo*

To know the efficiency of Rab23 expression plasmid, both constructed plasmids mentioned above were electroporated into chick embryos at stage 10 and the Rab23 mRNA was checked by RNA *in situ* hybridisation at 12 – 36 hours (Fig. 56). The effect of the transfection was monitored by an immunostaining against GFP, which is a co-expressing reporter by these plasmids. The results showed a stronger level of *Rab23* mRNA was located in the transfected region due to the addition of ectopic *Rab23*, compared to normal expression (wild-type) on the control side of the same neural tube (midbrain, Fig. 56 A, B; hindbrain, Fig. 56 C, D). This ectopic *Rab23* expression was already detected in the neural tube at 12 hours after an electroporation, and could last till 36 hours. Close views indicated that the transfected cells (neural precursor cells at stage 10) expressed Rab23 and GFP simultaneously (Fig. 56 E, F), and further underwent the differentiation after the transfection (Fig. 56 F). The control midbrains electroporated with pCA β -GFP never resulted in an increase of Rab23 expression (data not shown). Thus, this suggests that the ectopic Rab23 transcription was activated by both constructed plasmids. However, the protein level of Rab23 was not examined in this study due to lack of the specific antibody for Rab23 protein at the moment. In the following study, the constructed plasmid cRab23-GFP from the clone r3-m36 clone was used in chick embryos.

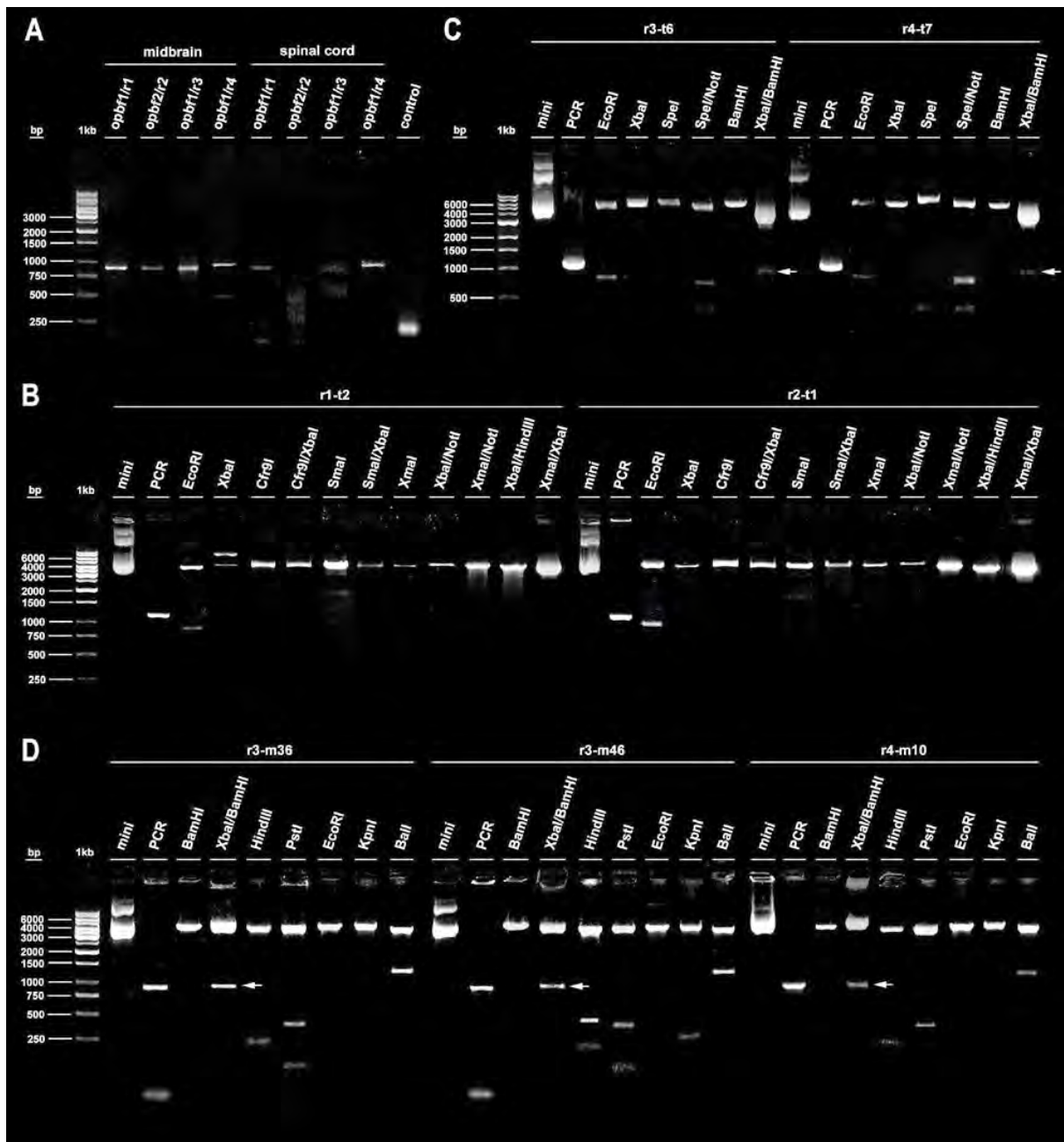


Figure 55: Electrophoretic analysis of chick *Rab23* expression plasmid

A: Chick *Rab23* cDNA was amplified with four primer pairs from total RNAs that isolated from E3 chick midbrain and spinal cord. The expected PCR product is a size of about 850 - 900 bp. Control PCR (with a primer pair p7-5s1/p7-5as1) only yielded a short product of 226bp. The primer pairs are indicated at the top of each lane.

B, C: Four transformed clones (pCR 4 - TOPO vector) as represents for each PCR product from chick midbrain in A were analysed by a direct PCR and enzymatic digestion with different restriction endonucleases, r1-t2, r2-t1, r3-t6 and r4-t7 for the primer pairs opbf1/r1, opbf2/r2, opbf1/r3 and opbf1/r4, respectively. The PCR product of about 1100 bp (with T3/T7 primers) suggests that *Rab23* cDNA was inserted, whereas the plasmid without an insert yielded a fragment of less 200 bp (data not shown). Digestion by *EcoRI* resulted in a slightly smaller product (since the *EcoRI* recognitive site lies adjacent to the insert, but the locations of T3/T7 primers are further away). Double digestion of r1 and r2 clones with *XbaI* and *Cfr9I* (*SmaI* or *XmaI*) did not release the insert (B), whereas *XbaI/BamHI* digestion of r3 and r4 clones resulted in the expected fragments (ca. 900 bp, indicated by arrows), which were used for the further work.

D: The sequences of three *Rab23* subcloned plasmids (pMES vector) with the released inserts from clones r3-t6 and r4-t7 were analysed by direct PCR and enzymatic digestion. PCR (with primer pairs pMESfo3/re4) and *XbaI/BamHI* digestion resulted in a fragment around 900 bp (indicated by arrows), suggesting chick *Rab23* cDNA had successfully inserted. 1 kb DNA ladder was used here as a size standard.

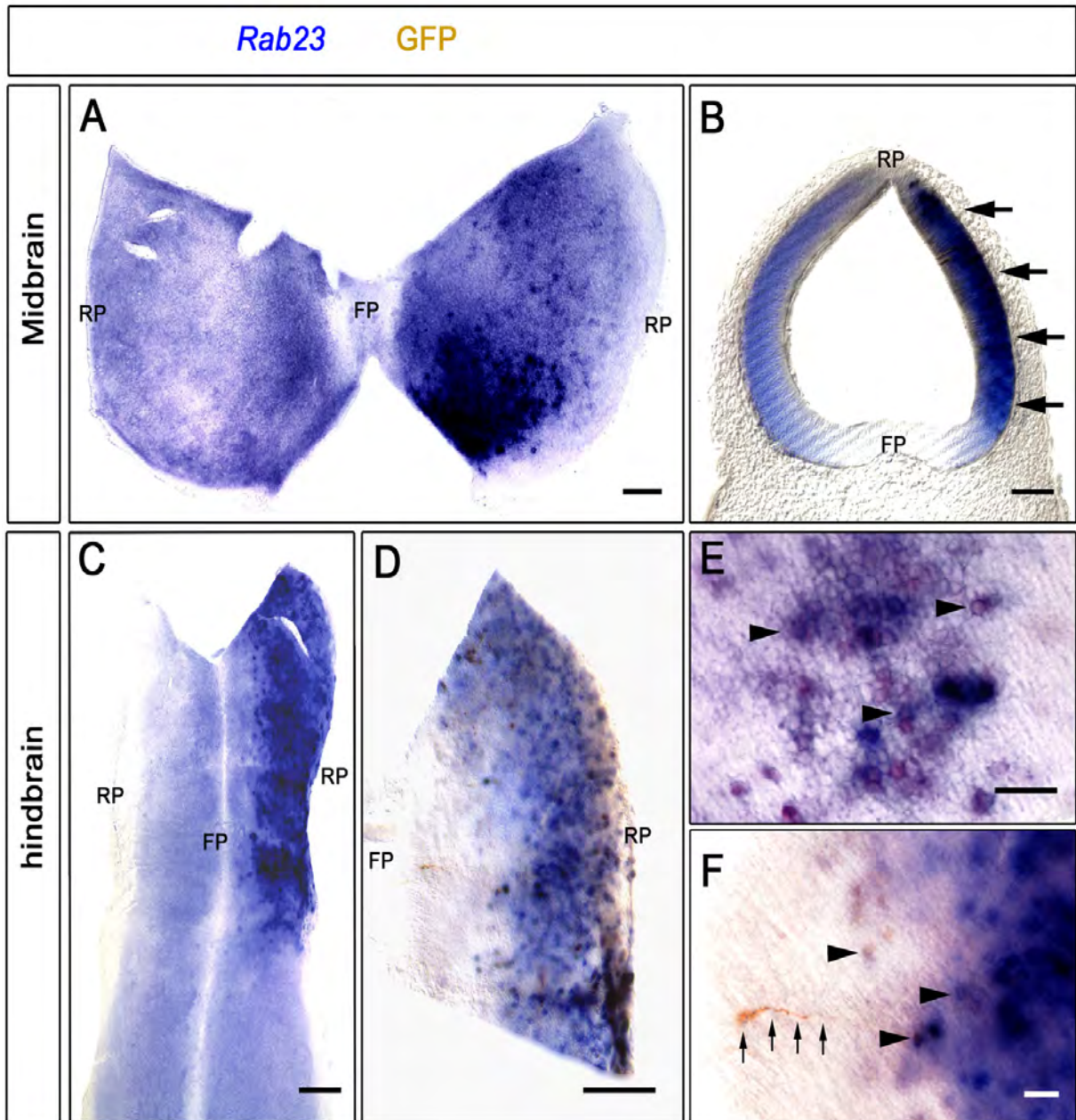


Figure 56: Ectopic expression of *Rab23* in chick midbrain and hindbrain

Stage - 10 chick embryos were electroporated with constructed *Rab23* expression plasmids isolated from the clone *r3-m36* (A, C, E) and *r4-m10* (B, D, F) and fixed at stage 14/15. A, C – F are 'open-book' preparations with anterior is up. B is a coronal section (30 μ m) of a midbrain with dorsal to the up. *Rab23* mRNA (blue) was visualized by RNA *in situ* hybridisation. An Immunostaining of GFP (brown) was performed to demonstrate the transfection region (B, D – F). Roof plate and floor plate are marked.

A – D: Transfection of *Rab23* expression plasmids resulted in a stronger expression (right side) in the midbrains (A, B) and hindbrains (C, D). GFP expression was co-located with ectopic *Rab23* (B, D). Arrows in B indicate the transfected region.

E, F: High resolution of transfected hindbrain regions showed the transfected neural cells exhibited both *Rab23* and GFP expression. Arrowheads point to such cells. The small arrows in F delineate an axon with a growth cone, which originates from a transfected cell.

Abbreviations: FP, floor plate; RP, roof plate. Scale bars: A – D, 100 μ m; E, F, 25 μ m.

4. Rab23 Specifies dorsal regional identity in early neural tube

To investigate the function of Rab23 gene for dorsoventral patterning of the central nervous system, chick Rab23 was misexpressed in different regions of early neural tube. The Rab23 expression plasmid - cRab23-GFP - was transfected into the dorsal or ventral areas of the midbrain, hindbrain and spinal cord at stages 9 - 14 and incubated for 20 or 36 hours. Pax3, Pax7 and *Nkx6.1*, regionally expressed in distinct cell populations along the DV axis, were used here as dorsal and ventral marker genes, respectively (Briscoe *et al.*, 2000; Matsunaga *et al.*, 2001). Their expression patterns were evaluated by RNA *in situ* hybridisation and immunostaining. The effect of the transfection was monitored by an antibody against GFP, a co-expressing protein by this plasmid.

Induction of Dorsal Specific Genes Pax3/7

As Rab23 was misexpressed in the dorsal midbrain (n = 9), hindbrain (n = 7) and spinal cord (n = 2) at stage 9/10, a strong Pax7 expression was detected in the transfected area compared to the normal expression level of the surrounding in all the cases (Tab. 25, Fig. 57 A, B). High resolution revealed that the ectopic Pax7 always coincided to be expressed in GFP expressing cells (Fig. 57 C, D), suggesting that the ectopic Pax7 expression was elicited in these cells by Rab23 misexpression. The expression of another dorsal gene - *Pax3* - was also strengthened in the transfected dorsal cells after Rab23 overexpression (Tab. 25, Fig. 58 A - D, midbrain, n = 4, hindbrain, n = 4). When the transfection of Rab23 was performed in ventral regions at this stage, both Pax genes were induced to express ectopically as well (Tab. 25, Fig. 57 and 58; midbrain, n = 14/16; hindbrain, n = 9/10; and spinal cord, n = 2/2). A difference between the ectopically induced Pax7 and *Pax3* is that the expression level of Pax7 was much obvious compared to the *Pax3*. Particularly, in ventral region the GFP expressing cells were all shown in an ectopic Pax7 expression simultaneously, however, only a few transfected cells expressed *Pax3* (Fig. 57 E - G, Fig. 58 A - D).

However, when the electroporation of cRab23-GFP at one stage late, only 2 out of 7 dorsal transfected midbrains were found the ectopically induced Pax7 (Tab. 25). For another dorsal gene - *Pax3*, the ectopic expression was hardly determined in dorsal midbrains (Tab. 25, Fig. 58 E, F, n = 1/5). Close views indicated that the ventral boundary of *Pax3* domain in the transfected side was not straight as the control side when the transfection covered the DV boundary (Fig. 58 E - H). The situation was similar in the hindbrains (Tab. 25; Pax7: n = 0/3; *Pax3*: n = 1/4) and spinal cords (*Pax3*: n = 0/2). When the transfection was performed at stage 12 or later (Tab. 25), ectopic Rab23 never induced *Pax3* or Pax7 in the dorsal or ventral regions of the midbrains (Pax7: Fig. 57 H - K; *Pax3*: Fig. 58 I and J; dorsal/ventral, n = 15/19), hindbrains (Pax7: Fig. 57 L - N; *Pax3*: Fig. 58 K and L; d/v, n = 3/7) or spinal cords (Pax7: Fig. 58 O - Q; d/v, n = 4/4).

Take together, these findings suggest that Rab23 can induce or facilitate the expression of Pax3/7 in the neural tube, but this effect stops by stage 12. Thus, consistent with the neural defects in *opb* mutant mice (Eggenchwiler and Anderson, 2000; Eggenchwiler *et al.*, 2001), it is suggested that Rab23 is required and necessary for Pax7 expression at early development, and involves in the specification of dorsal regional identity.

No Effect on Ventral Specific Gene *Nkx6.1*

In another hand, to know if Rab23 can effect the specification of ventral neural identity as a negative regulator, a ventral - specific gene *Nkx6.1* was checked after the Rab23 transfection (Tab. 25, Fig. 58). *Nkx6.1* expression has shown previously to be located in a discrete region near the floor plate and ventrally to the Pax3/7 expression in the entire neural tube (Fig. 19). The results of the ventral transfection at the investigated stages from 9 to 14 displayed that ectopically expressed Rab23 did not result in an obvious change of *Nkx6.1* expression in the midbrain (Fig. 58 A, E, I; n = 18) or other regions of the neural tube (hindbrain: Fig. 58 C, K, n = 14; and spinal cord, n = 9). Thus, this suggests Rab23 very likely did not exert a direct effect on the specification of ventral neurons. In addition, the individual ventral cells expressing *Pax3* localized in the continuously expressed region of *Nkx6.1* (black arrowheads in Fig. 58 D) after Rab23 transfection suggesting that Rab23 at least can not inactive *Nkx6.1* expression via Pax3/7. However, to clearly elucidate the possible influence of Rab23 on the ventral neural identities, other ventral – specific gene are necessary to be checked.

Table 25: The Rab23 - transfected midbrains, hindbrains and spinal cords with Pax3/7 misexpression or *Nkx6.1* repression

| Stages | Pax3/7 misexpression (x/n) | | | | | | Nkx6.1 repression (x/n) | | |
|--------|----------------------------|-----|-----|---------|-----|-----|-------------------------|-----|-----|
| | Dorsal | | | Ventral | | | Ventral | | |
| | MB | HB | SC | MB | HB | SC | MB | HB | SC |
| 9 | 6/6 | 6/6 | - | 7/7 | 5/5 | - | 0/4 | 0/4 | 0/1 |
| 10 | 7/7 | 5/5 | 2/2 | 7/9 | 4/5 | 2/2 | 0/3 | 0/3 | 0/2 |
| 11 | 3/12 | 1/7 | 0/2 | 0/13 | 0/7 | 0/2 | 0/5 | 0/2 | 0/2 |
| 12 | 0/9 | 0/2 | 0/4 | 0/10 | 0/5 | 0/4 | 0/3 | 0/3 | 0/4 |
| 13 | 0/2 | - | - | 0/3 | 0/1 | - | 0/1 | 0/1 | - |
| 14 | 0/4 | 0/1 | - | 0/6 | 0/1 | - | 0/2 | 0/1 | - |

Note: Number (x) of the Rab23 transfected midbrain (MB), hindbrain (HB) and spinal cord (SC) with Pax3/7 misexpression or *Nkx6.1* repression in the total number (n).

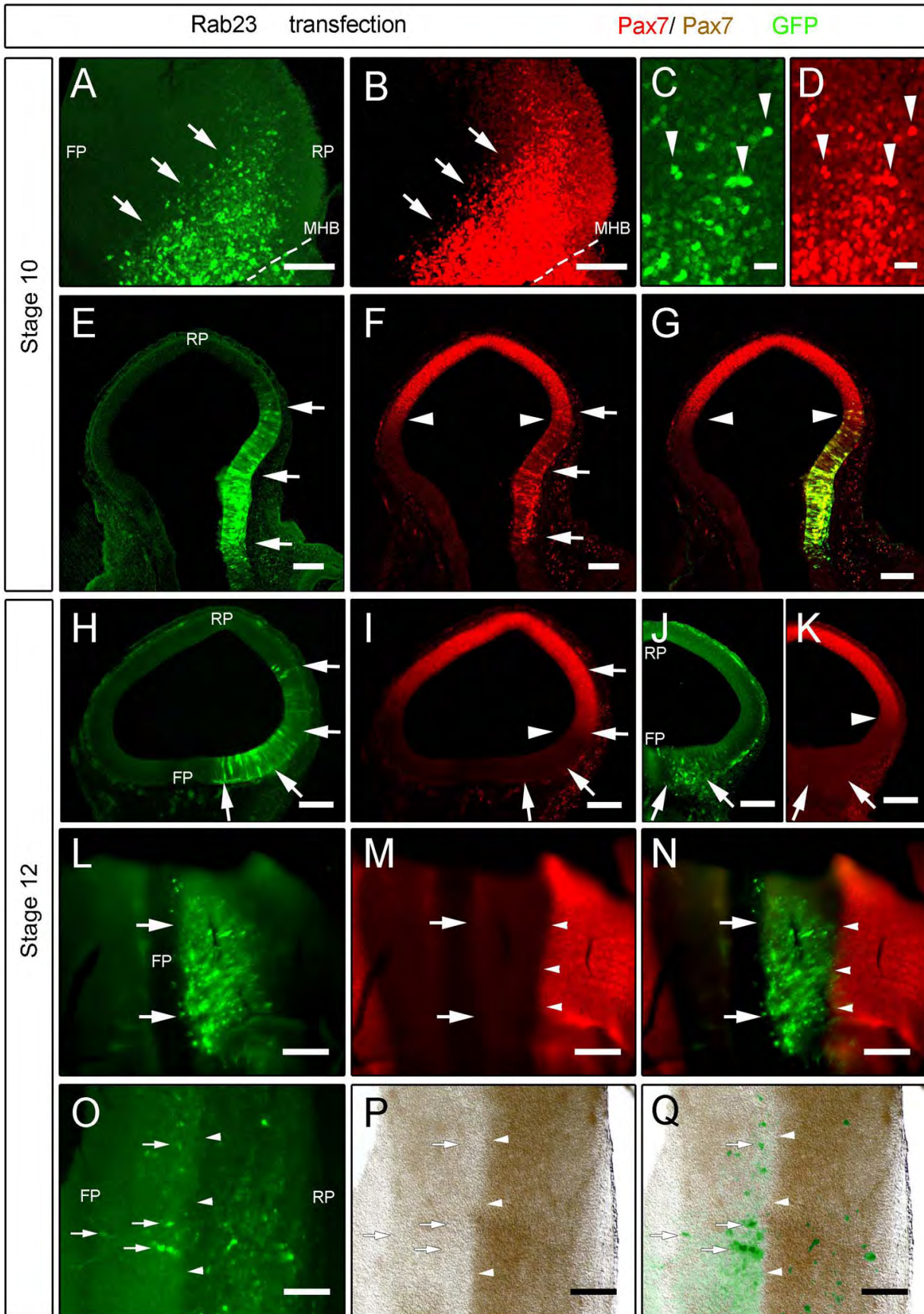


Figure 57: The expression of Pax7 in the Rab23 - transfected midbrains, hindbrains and spinal cords

Figure 57: The expression of Pax7 in the Rab23 - transfected midbrains, hindbrains and spinal cords

Chick embryos were transfected with cRab23-GFP at stage 10 and 12 and fixed at 24 hrs (A – K, O – Q) or 36 hrs (L – N). A – D, L – Q: 'open-book' preparations of the midbrain (A – D), hindbrain (L – N) and spinal cord (O – Q). Anterior is up. E – K: Coronal sections (30µm) of the midbrains, dorsal to up. Pax7 protein is shown by immunostaining in red fluorescence in all pictures except for P and Q with DAB color (brown). The transfection was visualized by immunostaining with an antibody against GFP (green fluorescence). The stages of the transfected embryos are marked in the left. Roof plate and floor plate are also indicated.

A – D: at stage 10, transfection of Rab23 in the dorsal midbrain and hindbrain (indicated by arrows in A) resulted in a strong expression of Pax7 (B). Magnifications of the dorsal transfected area showed that almost all of GFP expressing cells (C) expressed Pax7 (D) simultaneously. Arrowheads represent such cells. The midbrain – hindbrain boundaries are indicated by dotted line.

E – G: Ectopic Pax7 expression (arrows in F) was detected in the transfected region (E) of ventral midbrain (right side). The transfected dorsal cells also expressed a strong Pax7. G is an overlay of E and F with double staining in yellow. Arrowheads point to the dorsoventral boundary of the midbrain.

H – K: Transfection of Rab23 at stage 12 (arrows in H, J) did not induce to express Pax7 ectopically in the dorsal and ventral regions (I) of the midbrain or in the floor plate (K). Arrowheads point to the dorsoventral boundary of the midbrain.

L – N: Transfection of Rab23 in the ventral hindbrain (close to the floor plate; arrows in L) did not result in ectopic Pax7 expression (K), which is clearly viewed in the overlay of F. A few dorsal cells expressing GFP did not display a stronger Pax7 expression in comparison to wild-type dorsal cells. Arrowheads indicate the sharp ventral boundary of the Pax7 expression domain.

O – Q: The Rab23 - transfected cells in spinal cord (green fluorescence in O) did not reveal an ectopic Pax7 expression (brown in P). Q is an overlay of O and P. The arrows point to such transfected ventral cells. Some transfected cells stretched out an axon (O). Arrowheads indicate the sharp ventral boundary of the Pax7 expression domain. Dorsal is right.

Abbreviations: RP, roof plate; FP, floor plate. Scale bars: A – E, H – P, 100µm; F and G, 25µm.

Figure 58: The expression of Pax3 and Nkx6.1 in Rab23 - transfected midbrains and hindbrains

The embryos were transfected with *Rab23* at stage 10 - 12 and fixed at 20 or 36 hours. The expression of *Pax3* (blue) and *Nkx6.1* (red) were evaluated by RNA *in situ* hybridisation. The transfection was visualized by GFP immunostaining (green fluorescence). All pictures are shown in 'open-book' preparations with anterior to the up. The stages of the transfected embryos are marked in the left. Roof plate and floor plate are also indicated.

A, B: Transfection of Rab23 in the midbrain at stage 10 (right side in A) resulted in a stronger *Pax3* expression compared to the control side (left). In the region of the midbrain - hindbrain boundary (arrows), *Pax3* was also detected in the transfected side. The ventral boundary of *Pax3* expression domain in transfected side (white arrowheads) did not look so straight as the control side (black arrowheads). *Nkx6.1* is expressed in the ventral region. B is a magnification of the marked area in A. Arrowheads represent some transfected dorsal cells with strong *Pax3* expression.

C, D: *Pax3* is strongly expressed in the anterior part of the transfected hindbrain (rhombomere 1, right side in C). D is a magnification of the indicated area in C. Ectopic *Pax3* was detected not only in the dorsal cells but also in a few ventral cells, located in the gap between *Pax3* and *Nkx6.1* expression domains (white arrowheads) and in the *Nkx6.1* expression domain (black arrowheads). The ventral expression of *Nkx6.1* seemed not to be affected. In addition, the ventral boundary of *Pax3* expression domain of the transfected side was not straight (arrows).

E, F: *Pax3* expression (right side in E) was slightly stronger in the transfected region of the dorsal midbrain (F) compared to the control side (left), and its ventral boundary (arrowheads) was smeared. The boundaries of mesencephalon with diencephalons (white arrows) and rhombencephalon (black arrows) were marked.

G, H: Magnifications of the marked area in F showed that the some ventral midbrain cells did express a weak *Pax3* upon Rab23 transfection (arrowheads). The ventral boundary of the *Pax3* expression domain is marked by a dotted line.

I, J: Transfection in ventral area and floor plate of a midbrain (green in J) at stage 12 did not result in ectopic expression of *Pax3* (I). *Nkx6.1* expression domain was not changed by Rab23 misexpression. Arrows indicate the midbrain-hindbrain boundary. Some transfected cells extended long axons (arrowheads).

K, L: Transfection in ventral hindbrain at stage 12 (arrows in L) did not result in an ectopic expression of *Pax3*. The expression pattern of *Nkx6.1* was not interrupted by Rab23 transfection. Arrowheads indicate the boundary between *Nkx6.1* expression domain and floor plate.

Abbreviations: DI, diencephalon; FP, floor plate; ME, mesencephalon; r1 - r3, rhombomeres, RE, rhombencephalon; RP, roof plate. Scale bars: A, C, E, F; I - L, 100 µm; B, D, G, H 25 µm.

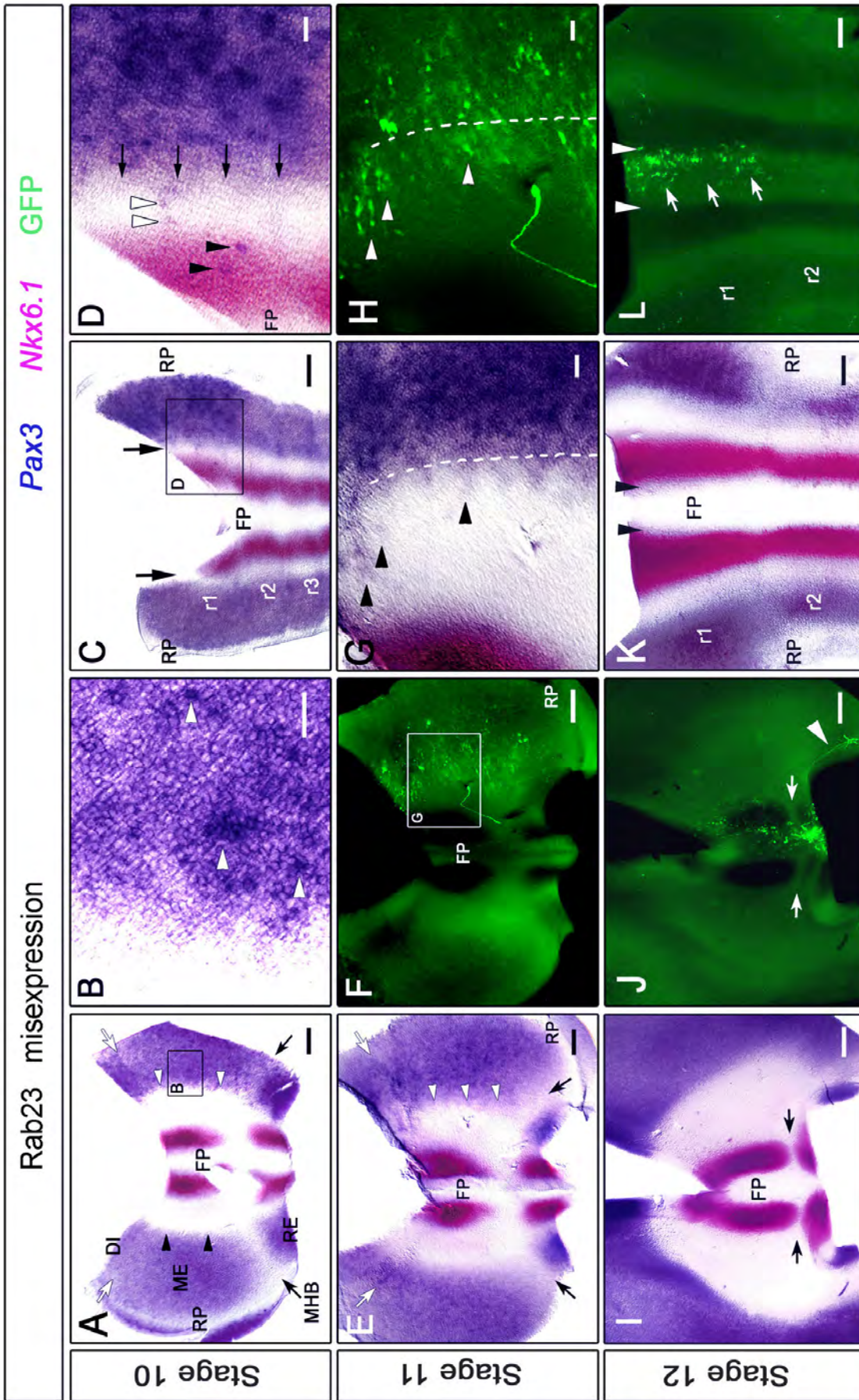


Figure 58: The expression of Pax3 and Nkx6.1 in the Rab23 - transfected midbrains and hindbrains

5. Influence of Rab23 on Early Neurogenesis in Dorsal Midbrain

In *opb* murine neural tubes, the dorsal located cells never display a dorsal neural identity any more according to gene analysis and the cells expressing ventral genes expand dorsally (Gunther *et al.*, 1994; Sporle *et al.*, 1996; Eggenschwiler and Anderson, 2000; Eggenschwiler *et al.*, 2001), suggesting an essential role on neural patterning along DV axis. However, the possible function of Rab23 on the neurogenesis of the dorsal cells has not been investigated. Two early motor neuron subtypes in the dorsal midbrain – Isl-1/2 and Brn3a positive cells – were examined in the following experiments. The first neurons in the dorsal midbrain arise at around stage 14 adjacent to the roof plate and form the mesencephalic trigeminal nucleus (MTN, Ericson *et al.*, 1992; 1995a; Varela-Echavarria *et al.*, 1996; Hunter *et al.*, 2001) and can be detected by an antibody against medium weight neurofilament - RMO-270 (Fig. 20 I – J). These early neurons all express the Lim transcription factor Islet 1/2 (Fig. 41 A, B, Ericson *et al.*, 1992), but only the most dorsal cells expressed Brn3a, a POU – domain transcription factor (Fig. 41 C, D, Hunter *et al.*, 2001).

No obvious effect on the Dorsal Islet 1/2 Cell subpopulation

Dorsal midbrains were transfected with cRab23-GFP at stage 9 to 12 and fixed at stage 16 - 18. The results showed Islet 1/2 expressing cells were first detected in the transfected area of the dorsal midbrain at around stage 14 as the control side, and the location of these cells was not shifted due to Rab23 overexpression (Fig. 59, n = 3). Although some dorsal transfected cells expressed Isl-1/2 simultaneously, quantitative analysis did not reveal a significant increase or decrease of Islet positive cells between the transfected and control sides in a midbrain (n = 7; P > 0.01).

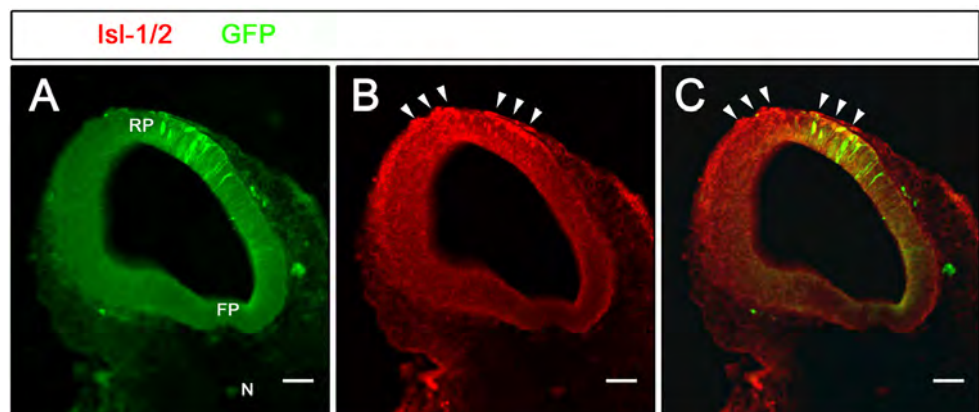


Figure 59: Islet 1/2 expressing cells in the Rab23 - transfected midbrain

The midbrain was transfected with cRab23-GFP at stage 12, fixed at stage 17 and shown in transversal sections (30 μ m). Dorsal is up. Isl-1/2 proteins were stained with an antibody (red), and the transfection was visualized by GFP staining (green in A). Islet 1/2 expressing cells were located in the both sides of dorsal region lateral to the roof plate (arrowheads in B). An overlay (C) of A and B demonstrated the Islet expressing cells were not highly coincided with the Rab23 overexpression. Double staining was shown in yellowish.

Abbreviations: FP, floor plate; N, notochord; RP, roof plate. Scale bar: 100 μ m.

Specification of Brn3a Expressing Cells

Brn3a (Brn3.0) is expressed in postmitotic neurons of some specific CNS nuclei, as well as dorsal root ganglia (DRG, Fedtsova and Turner, 1995; 1997). In chick dorsal midbrain, Brn3a expressing neurons appear in MTN lateral to the roof plate at stage 15, whereas Brn3a positive cells are detected in the ventral midbrain by stage 19 (Fedtsova and Turner, 2001). Stages 9 to 11 embryos were electroporated with cRab23-GFP and incubated till they reached stage 14 or older. When fixation at stage 14, Brn3a positive cells were never found in the transfected midbrain ($n = 4$). Brn3a expression was first detected in the presumed location of the transfected midbrain by stage 15 (Fig. 60), as the normal expression pattern. A few dorsal cells with strongly expressing ectopic Rab23 also expressed Brn3a simultaneously (Fig. 60 A – I). However, Rab23 transfection did not induce Brn3a expression in the roof plate or the lateral region of the midbrains (Fig. 60 A – C and J – L). Quantity analysis indicated that more Brn3a expressing cells were generated in the transfected dorsal region of the neural tube compared to an equivalent area in the control side (Tab. 26, Fig. 60 P). In the midbrain, when fixed at stage 16 – 18, Rab23 transfection resulted in 8.73 % ($n = 3$), 9.55 % ($n = 5$) and 6.25 % ($n = 7$) more dorsal Brn3a cells, respectively, whereas comparison of Brn3a cells when performed at stage 9 – 11 showed 10.86 % ($n = 2$), 9.08 % ($n = 10$) and 2.88 % ($n = 3$) more cells than an equivalent control area, respectively. Compared to pMES transfection (1.48 %, $n = 5$), the stage 9 and 10 transfection showed significant increases of positive cells (t -test, $P < 0.05$,). Rab23 transfection in dorsal spinal cord also resulted in more Brn3a positive cells (stage 16: 7.04 %, $n = 3$; stage 17: 6.04 %, $n = 4$; and stage 18: 2.66 %, $n = 3$; Fig. 60 G – I). Moreover, Brn3a positive cells could be detected in the transfected dorsal hindbrain at stage 17/18 (Fig. 60 D – F, $n = 4$). However, None of Brn3a expressing cells were found in ventral area of transfected midbrain, hindbrain or spinal cord before stage 19 (Fig. 60 M – O; Tab. 26; $n = 8$).

Table 26: Numbers of Brn3a expressing cells in Rab23 - transfected neural tubes

| Location | | Stage 16 | | | Stage 17 | | | Stage 18 | | |
|-------------|---|----------|--------|--------|----------|--------|--------|----------|---------|---------|
| | | n | C | T | n | C | T | n | C | T |
| Midbrain | D | 3 | 45 ± 3 | 48 ± 3 | 5 | 58 ± 7 | 64 ± 9 | 7 | 65 ± 12 | 69 ± 12 |
| | V | - | - | - | 3 | 0 | 0 | 1 | 0 | 0 |
| Hindbrain | D | - | - | - | 2 | 0 | 4 ± 1 | 2 | 0 | 3 ± 1 |
| | V | - | - | - | 2 | 0 | 0 | - | - | - |
| Spinal cord | D | 3 | 34 ± 6 | 37 ± 6 | 4 | 39 ± 6 | 41 ± 6 | 3 | 36 ± 3 | 37 ± 4 |
| | V | 2 | 0 | 0 | 1 | 0 | 0 | 1 | 0 | 0 |

The midbrain, hindbrain and spinal cord were transfected with cRab23-GFP in the dorsal (D) and ventral region (V) at stage 9 – 11, and fixed at stage 16 - 18. Numbers of Brn3a expressing cells in the transfected area (T) and in an equivalent area of the control side (C) were counted. The number (n) in each item is given.

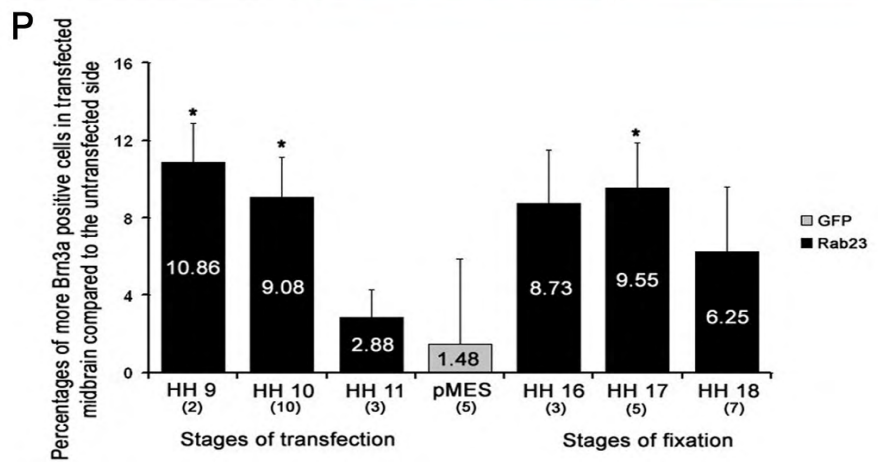
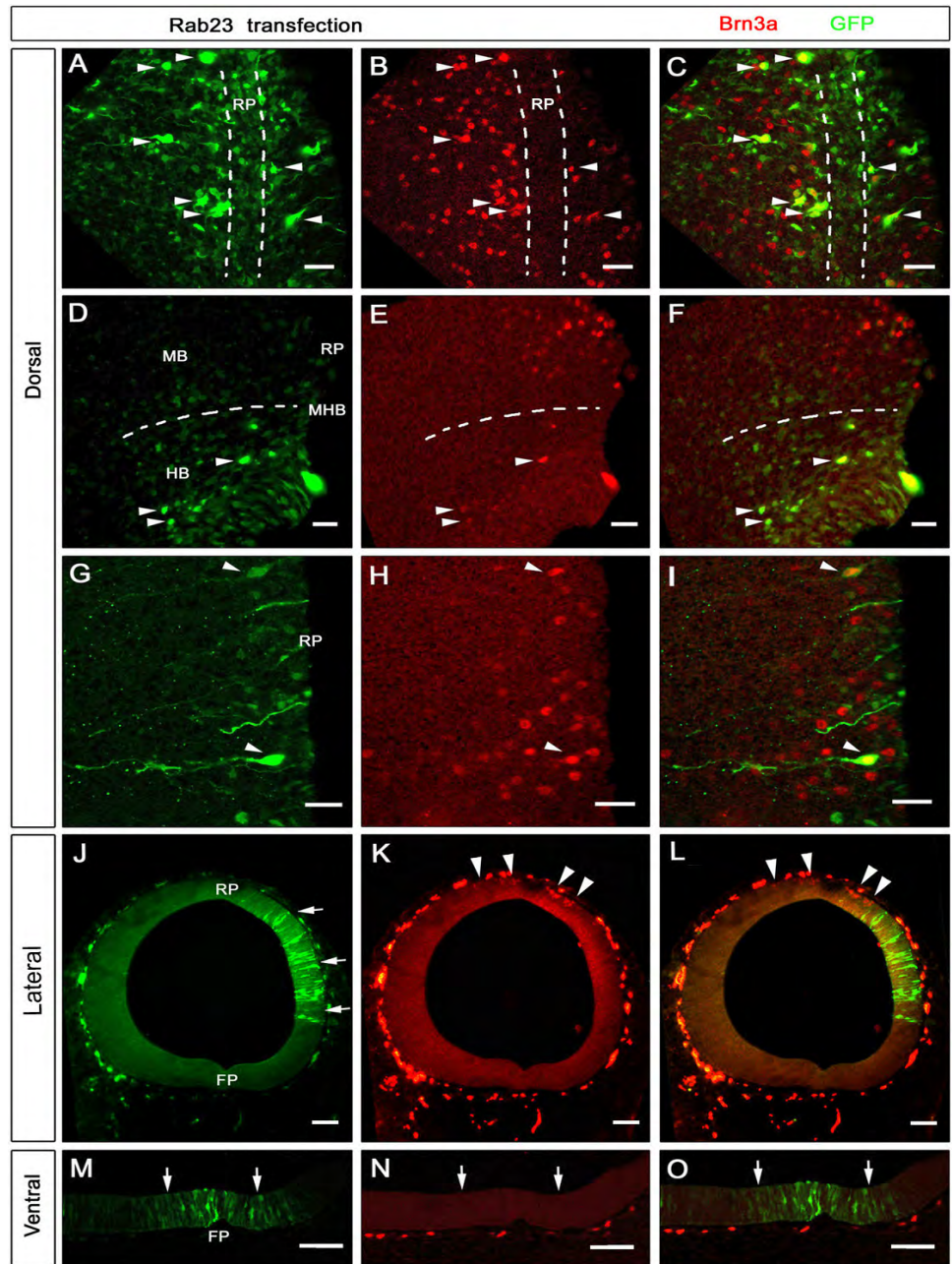


Fig. 60: Brn3a expressing cells in the Rab23 - transfected neural tubes

Fig. 60: Brn3a expressing cells in the Rab23 - transfected neural tubes

Embryos were transfected with cRab23-GFP at stage 10 and fixed at stage 17. The early motor neurons were stained with an antibody against Brn3a (red fluorescence), and the transfection was visualized by GFP staining (green fluorescence). A – I are 'open-book' preparations of midbrain (A – C), hindbrain (D – F) and spinal cord (G – I), and anterior is up; J – O are coronal sections (30 μ m) of midbrains, and dorsal is up.

A – C: Ectopic Rab23 (green in A) was transfected into both sides of the dorsal midbrain. Brn3a expressing cells (B) were detected in transfected dorsal area but not the roof plate. The overlay (C) of A and B showed a few strongly GFP expressing cells expressed Brn3a simultaneously (yellowish, arrowheads). The dotted lines mark the territory of the roof plate.

D – F: Transfection of Rab23 (D) resulted in a weak expression of Brn3a in some hindbrain cells (arrowheads in E), which expressed GFP at high level. F is an overlay of D and E. Dotted line indicates the midbrain - hindbrain boundary. Note: None of Brn3a positive cells are detected in the wild-type hindbrain at this stage.

G – I: A transfected spinal cord (G) showed that some Brn3a positive cells (arrowheads in H) was coincided with a strong ectopic Rab23 expression. I is an overlay of G and H. A few of transfected cells extended long axons.

J – L: Transfection in the lateral area of a midbrain (arrows in J) did not result in ectopic Brn3a expression (K). The Brn3a cells (arrowheads) were still located in the most dorsal region lateral to the roof plate. L is an overlay of J and K.

M – O: Rab23 was transfected into the most ventral area including the floor plate (M). None of Brn3a expressing cells was detected in the location (arrows in N) where the ventral Brn3a cells are presumed to generate at later stages. O is an overlay of M and N. Note: Brn3a positive cells were seen in the surrounding mesenchyma (N).

P: Quantitative analysis of the Brn3a positive cells in the Rab23 – transfected dorsal midbrains. Rab23 transfection in the dorsal midbrain resulted in more Brn3a positive cells in a transfected region compared to a same-sized area of the untransfected side in a midbrain. The changes of Brn3a positive cells were significantly different with GFP transfection (two-tailed paired *t*-test; $P = 0.0038$ and 0.0013) when transfected at stage 9/10, but not at stage 11 ($P = 0.63$). Analysis on cell count also showed an increase of positive cells in the dorsal transfected midbrain when fixed at stage 16 – 18 ($P = 0.11$, 0.0068 , and 0.058 , respectively). Each group consisted of 2 - 10 embryos and at least 100 cells. GFP transfection of pMES vector at stage 10 was used here as control. The number of embryos in each item is indicated in the parentheses.

Abbreviations: FP, floor plate; HB, hindbrain; MB, midbrain; MHB, midbrain-hindbrain boundary; RP, roof plate. Scale bars: A – I, 25 μ m; J – O, 100 μ m.

Differentiation of Early Midbrain Neurons Normally

The Brn3a and Islet 1/2 expressing neurons together account for a majority but not all of the postmitotic neurons in the spinal cord (Fedtsova and Turner, 1997). To know the effect of Rab23 on the early neuronal differentiation in general, RMO270, an antibody against phosphorylated neurofilament, was used to label the neurites of all postmitotic neurons (Wilson *et al.*, 2003). At stage 14, the first mesencephalic neurons exit the cell cycle and are born on either side lateral of the roof plate corresponding to the proposed origin of mesencephalic trigeminal nucleus (MTN, Fig. 20 E). In the ventral midbrain, neurons initiate to express neurofilament in the nucleus oculomotorius (OM) at a similar stage. They are located in the outer layer (mantle zone) of the midbrain. These differentiated neurons expand to the entire dorsal midbrain at stage 19/20 (Fig. 20 E - H), but most mesencephalic cells are still dividing. At stage 23 (E 4.5) the mantle zone is still relatively thin (Fig. 20 I and J).

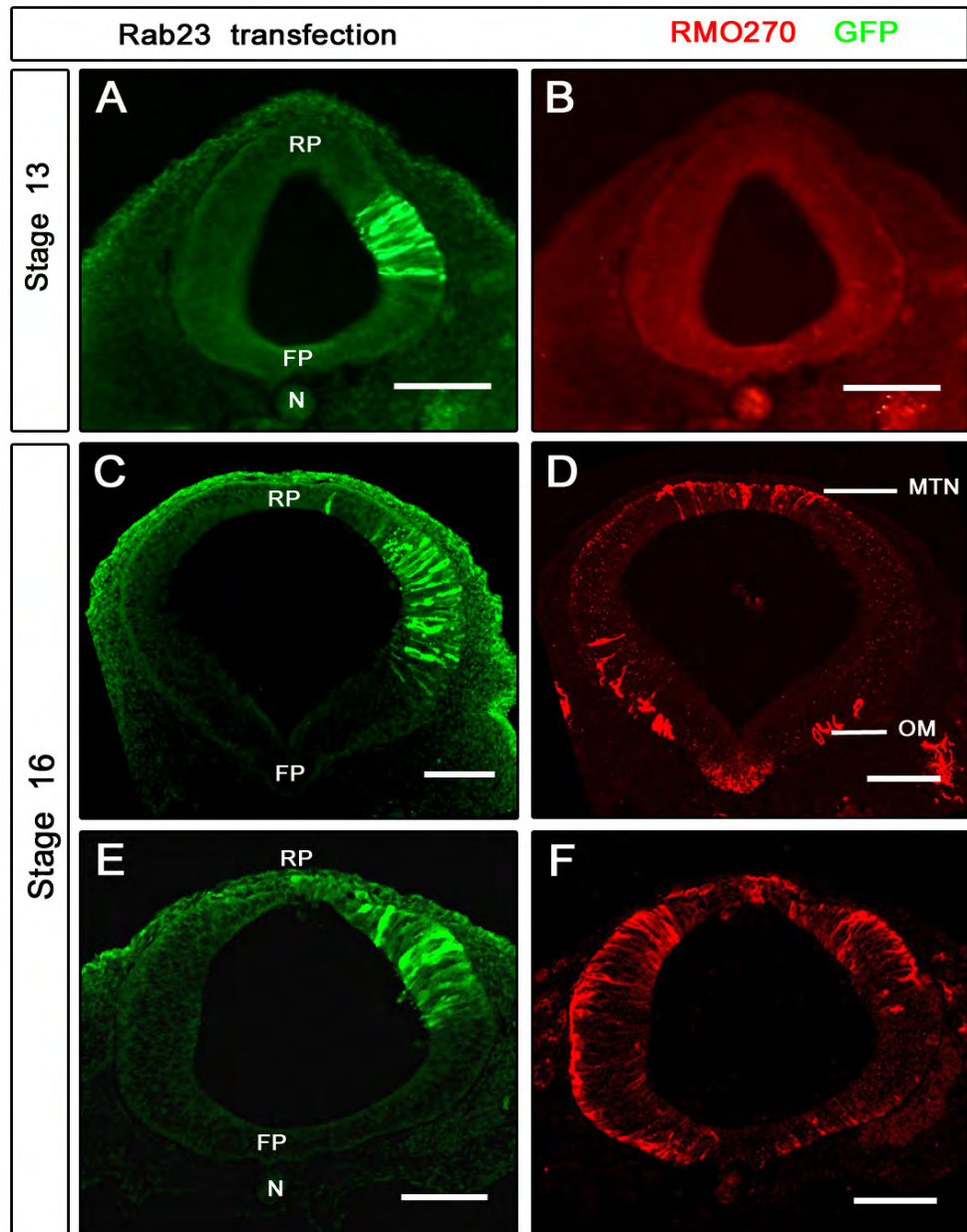


Figure 61: Neuronal differentiation in Rab23 - transfected midbrains and hindbrains

Chick embryos were transfected with cRab23-GFP at stage 9 and fixed at stage 13 (A, B) or stage 16 (C – F). The differentiated neurons were labelled with an antibody against medium weight neurofilament (RMO270; red fluorescence), and the transfection was monitored by GFP (green fluorescence). Transversal sections (30 μ m) of the transfected midbrain (A - D) and hindbrain (E, F) are illustrated. Dorsal is up. Roof plate, floor plate and notochord are marked.

A, B: When the embryos fixed at stage 13, no differentiated neurons (B) were detected in both transfected (green in A) and control sides of the transfected midbrain.

C, D: Early mesencephalic neurons were found in the dorsal and ventral regions lateral to the midline, presumed to form the mesencephalic trigeminal nucleus and nucleus oculomotorius, respectively. These differentiated cells resided in the mantle zone (D). No an obvious difference of the neuronal differentiation between the transfected (right side in C) and control sides (left) was seen.

E, F: Transfection of Rab23 (green in E) in the hindbrain did not result in a significant change on the neuronal differentiation (F) compared to the control side (left).

Abbreviations: FP, floor plate; MTN, mesencephalic trigeminal nucleus; N, notochord; OM, nucleus oculomotorius; RP, roof plate. Scale bar: 100 μ m.

The embryos were transfected with cRab23-GFP at stage 9/10 and fixed at stage 13 - 20. The transfected midbrains fixed after stage 15 indicated that the differentiation of the neural precursor cells was not affected due to ectopic Rab23 expression (Fig. 61 C, D, n = 6). Two mesencephalic neuronal subpopulations (MTN and OM) were originated from the dorsal or ventral domain in the transfected side as the control side. Flat-mount preparations of the transfected midbrains did not show a significant change on the amount of the neurofilaments or the assembled fascicles (data not shown). The neuronal differentiation in the transfected hindbrain (Fig. 61 E, F; n = 4) and spinal cord (n = 2) were also identical to the control side. Additionally, when fixed at stage 13, the transfected midbrain did not contain any differentiated neurons in both transfected and control sides (Fig. 61 A, B, n = 3).

6. Analysis of Rab23 on Neural Proliferation

To investigate whether Rab23 plays a role on the proliferation and specification of dorsal neural cells besides an up-regulation of Pax7, the dorsal and ventral midbrains were transfected with cRab23-GFP at stage 9 - 12, and checked the dividing precursor cells by the visualization of phosphorylated Histone 3 (pH3), a mitosis marker. pH3 labels the condensing chromosome of the mitotic cells in vertebrates, which are undergoing division at M- and late G2-phases of cell cycle (Hendzel *et al.*, 1997; Van Hooser *et al.*, 1998; Wei *et al.*, 1999). The mitotic neural progenitor/precursor cells (NPCs) are scattered in the ventricular zone (VZ) of the entire neural tube at early stages (Fig. 39). A few of embryos were simultaneously electroporated with pMES vector as controls and visualized by GFP immunostaining.

Rab23 misexpression in ventral and dorsal midbrain showed a few of transfected neural precursor cells underwent dividing (Fig. 62 A, B), however, the majority of transfected cells were pH3 negative. The analysis on the proliferation (Fig. 62 C) of dorsal midbrain showed more dividing cells per defined area in the Rab23 misexpressed region than an equivalent area of the control side (at stage 19/20, n = 12; 88 ± 5 vs. 86 ± 5) in about 2 %. However, this increase of the mitotic cells upon Rab23 transfection was not significant in comparison with those of GFP transfected controls (n = 8, 0.98 %; $P > 0.05$; two-tail paired *t*-test). In the ventral midbrain, the difference of mitotic cells per area between the ectopic Rab23 expressed region and control region was less than 1 % (n = 13; 52 ± 4 vs. 51 ± 4), which was not obvious compared to GFP transfection embryos (n = 10, -0.43 %; $P > 0.05$). The proliferation rate was also demonstrated higher in the dorsal midbrain than in the ventral region. Misexpression of Rab23 in the hindbrain and spinal cord neither show a significant increase on the proliferating cells compared to the control (data not shown). Thus, this suggests that Rab23 does not have a significant effect on the cell cycle of the neural precursor cells.

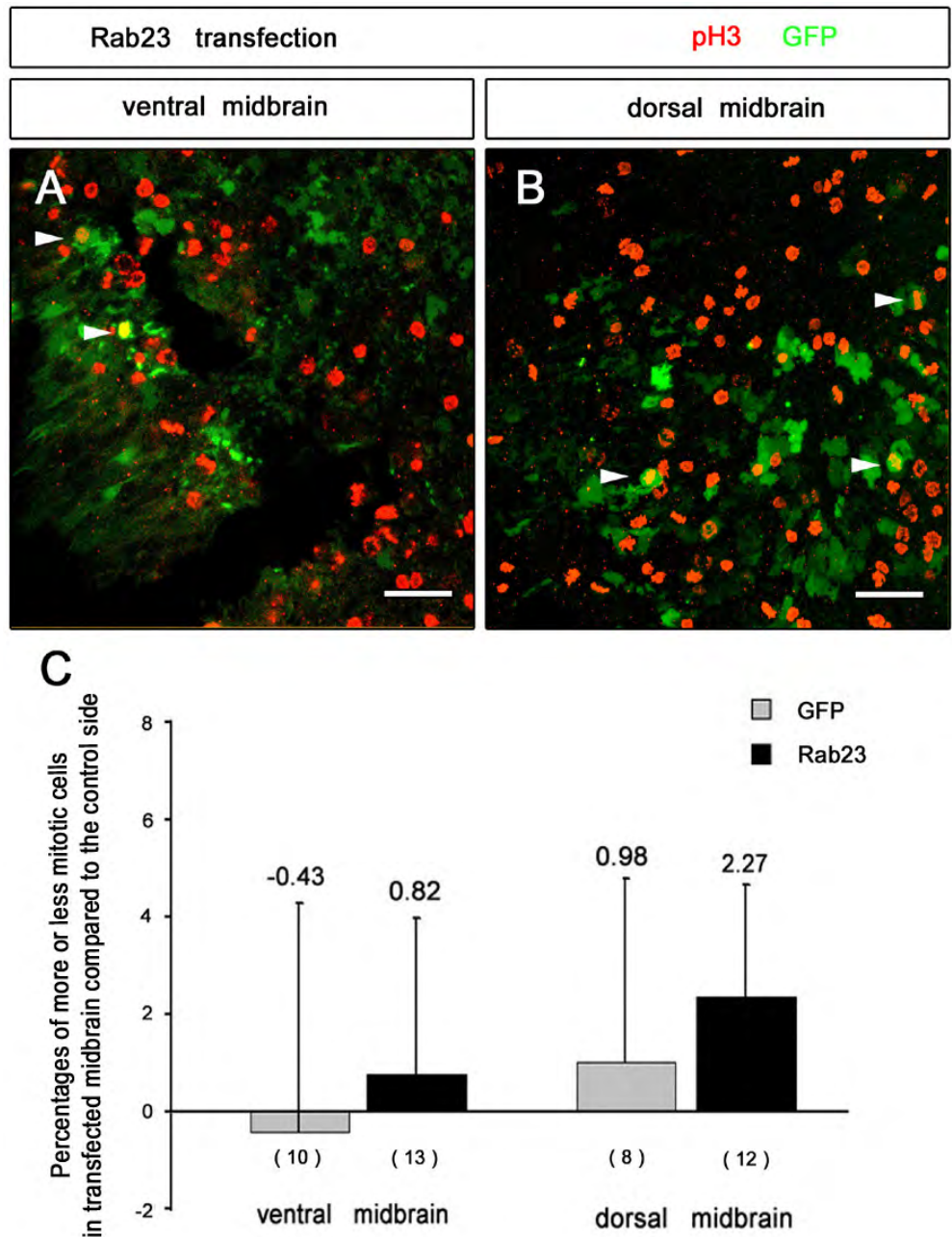


Figure 62: Mitotic cells in Rab23 - transfected midbrains

A and B: Chick embryos were transfected with cRab23-GFP at stage 10 and incubated for 36 hours (stage 19). The mitotic neural precursor cells were labelled with pH3 (red fluorescence), and the transfection of Rab23 was visualized by GFP staining (green fluorescence). 'Open-book' preparations of the ventral (A) and dorsal (B) midbrain in high resolution demonstrated that a few of transfected cells were stained by pH3 simultaneously (yellowish by double staining; indicated by arrowheads). Anterior is up, and dorsal to the right.

C: Quantitative analysis of the mitotic cells in the midbrain with ectopic Rab23 expression, which were transfected at stage 10 and dissected at stage 19/20. The control embryos were electroporated with GFP (pMES) at stage 10 and incubated for 24 hours. The graph showed more mitotic cells in per defined area of the transfected midbrain compared to an equivalent area of control side. However, the increase of mitotic cells in the Rab23 - transfected dorsal and ventral midbrain was not significant in comparison with those of GFP transfection controls (*t*-test, $P > 0.05$). At least 100 cells on 2 sections of each midbrain were analysed. The number of embryos in each item is indicated in the parentheses.

7. Preliminary Analysis of Rab23 with Shh Signalling Pathway

During the development of the spinal cord, Shh is necessary for the specification of ventral neural cell fates, including motor neurons, several classes of interneurons, and the floor plate (Ericson *et al.*, 1997; Watanabe and Nakamura, 2000; Briscoe and Ericson, 2001). Rab23 acts as a cell autonomous negative regulator of the mouse Shh signalling pathway (Eggenchwiler and Anderson, 2000; Eggenchwiler *et al.*, 2001). To investigate the relationship of the Rab23 with Shh signalling pathway in nervous system, the expression patterns of *Shh* and important genes of the downstream, including the two transmembrane receptors *Patched* (*Ptc1/2*) and *smoothened* (*Smo*, Alcedo *et al.*, 1996; Marigo *et al.*, 1996; Murone *et al.*, 1999; Pearse *et al.*, 2001), and the zinc finger transcription factor *Gli3* (Ruiz i Altaba, 1998) were first checked by RNA *in situ* hybridisation in chick midbrain.

Expression Patterns of Shh and Its Downstream Genes in the Mesencephalon

The antisense RNA probes for detecting *Shh* and *Gli3* genes were well used in previous hybridisation (Tab. 15). The RNA - labelled probe for *Ptc1* was transcribed *in vitro* following Dr. F. Seif. The antisense RNA for *Ptc2* gene was directly isolated from chick neural tube (a primer pair cptc2f1/r1 in Tab. 4) and cloned into pBluescript II KS vector. Chick *Smo* antisense was transcribed from chick EST clone 826i17 (Tab. 2). These antisense RNA probes were labelled with either digoxigenin- (DIG) or fluorescein- (FITC) UTPs (Fig. 63).

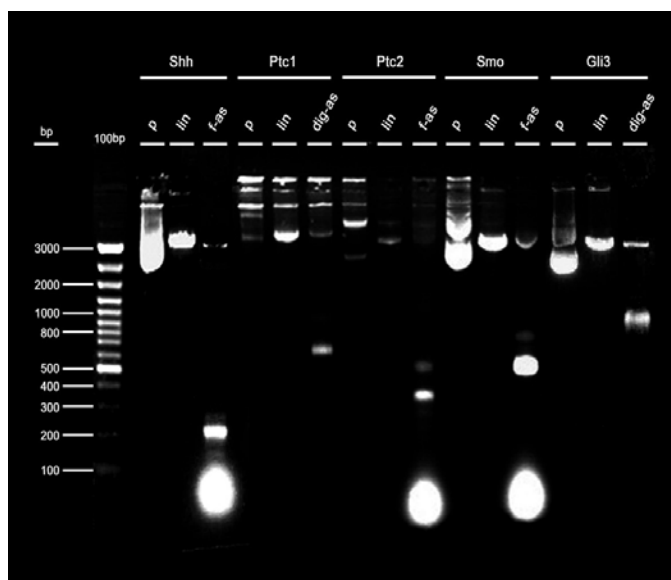


Figure 63: Electrophoretic display of RNA - labelled probes for several genes on the Shh signalling pathway

The plasmid containing chick *Shh* and the downstream genes, *Patched 1* and *2*, *Smoothened*, *Gli3* were linearized by identical enzymes and transcribed *in vitro* into antisense RNA -labelled probes. The probes for *Shh*, *Ptc2* and *Smo* were labelled with FITC, whereas the *Ptc1* and *Gli3* probes with Dig. These antisense probes for *Shh*, *Ptc1*,

Ptc2, *Smo* and *Gli3* genes were 0.38kb, 0.94kb, 0.47kb, 0.7kb and 1.2kb, respectively. 100bp DNA plus ladder was used here as a size standard.

Abbreviations: dig-as, digoxigenin-labelled antisense RNA; f-as; fitc-labelled antisense RNA; Gli3, Glioma-associated oncogene; lin, linearized DNA; p, isolated plasmid DNA; Ptc, patched; Shh, Sonic hedgehog; Smo, smoothened.

Whole-mount hybridisation was performed with the above RNA-labelled probes to detect the expression of these genes in chick midbrains at different stages (Fig. 64). In short, *Shh* was expressed in the notochord and the most-ventral domain including the floor plate, whereas *Ptc1* and *Ptc2* were expressed as stripes in both sides apart from the floor plate in a distance, except for a stronger signal on *Ptc2* in this study. Their expressions seemed to localize closely to the *Shh* expression domain. (Echelard *et al.*, 1993; Carpenter *et al.*, 1998; Pearse *et al.*, 2001; Frank-Kamenetsky *et al.*, 2002). *Smo* was detected nearly in the entire midbrain with less or no signal in the dorsal and ventral midlines. *Gli3* was only strongly expressed in the dorsal midbrain (Litingtung and Chiang, 2000; Wijgerde *et al.*, 2002).

Analysis of Genes expression in Rab23 – transfected Midbrains

The ventral or dorsal chick midbrains were transfected with cRab23-GFP at stage 9/10 and fixed after 18 hours or later. At first, the results showed that the ventrally expressed *Shh* was not significantly downregulated upon Rab23 misexpression as expected (Fig. 65 A, B, n = 8), and the transfected midbrain also showed in a normal size and shape. This is very likely to suggest that Rab23 does not repress *Shh* expression via a direct interaction. Then, the expression patterns of several components downstream of *Shh* signal were checked further (Cohen, 2003; Jacob and Briscoe, 2003). The expressions of the two transmembrane receptors – *Ptc1/2* and *Smo* – were not affected by ectopic expression of Rab23 in the midbrain before stage 11 (Fig. 65 C – H, n = 4 in each). However, an important downstream transcription factor, *Gli3* (a Ci/Gli member) was largely repressed by Rab23 in the dorsal midbrain (Fig. 65 I, J, n = 2/3), suggesting Rab23 could be involved in the *Shh* signalling pathway at a downstream level of *Shh*. Thus, some transcription factors, such as class II proteins for *Shh* signal, were checked as well. *Nkx2.2* transcription factor, a specific marker for ventral V3 neurons in the spinal cord, was also expressed in the most ventral region of the midbrain. However, Rab23 misexpression did not activate or repress *Nkx2.2* expression (Fig. 65 K, L, n = 3) as another NKX gene - *Nkx6.1* in the ventral midbrain, which has been examined previously (Fig. 58 C, D, I, K). In addition to look the effect of Rab23 at expansion, the expression of *Hnf3 β* , a floor plate marker, did not shown to be down - regulated by the ectopic Rab23 expression in the floor plate (Fig. 65 M, N, n = 3). Due to the location of the Rab23 in the midbrain and spinal cord, BMP signals might interact with Rab23. Several BMP members, such as BMP4, BMP7 and GDF7, were selected to analyze here, however, no significant changes of their expression patterns were seen in the dorsal midbrain upon Rab23 misexpression (data not shown). Moreover, one BMP antagonist – chordin, located in the ventral region, and *Smad3*, a TGF- β closely - related gene, did not display any significant change in the Rab23 – transfected midbrains compared to the control side (Fig. 65 O – R, n = 3 in each). However, the relationship between Rab23 with BMP signalling still need to be further investigated via the effect of BMPs misexpression on Rab23 protein.

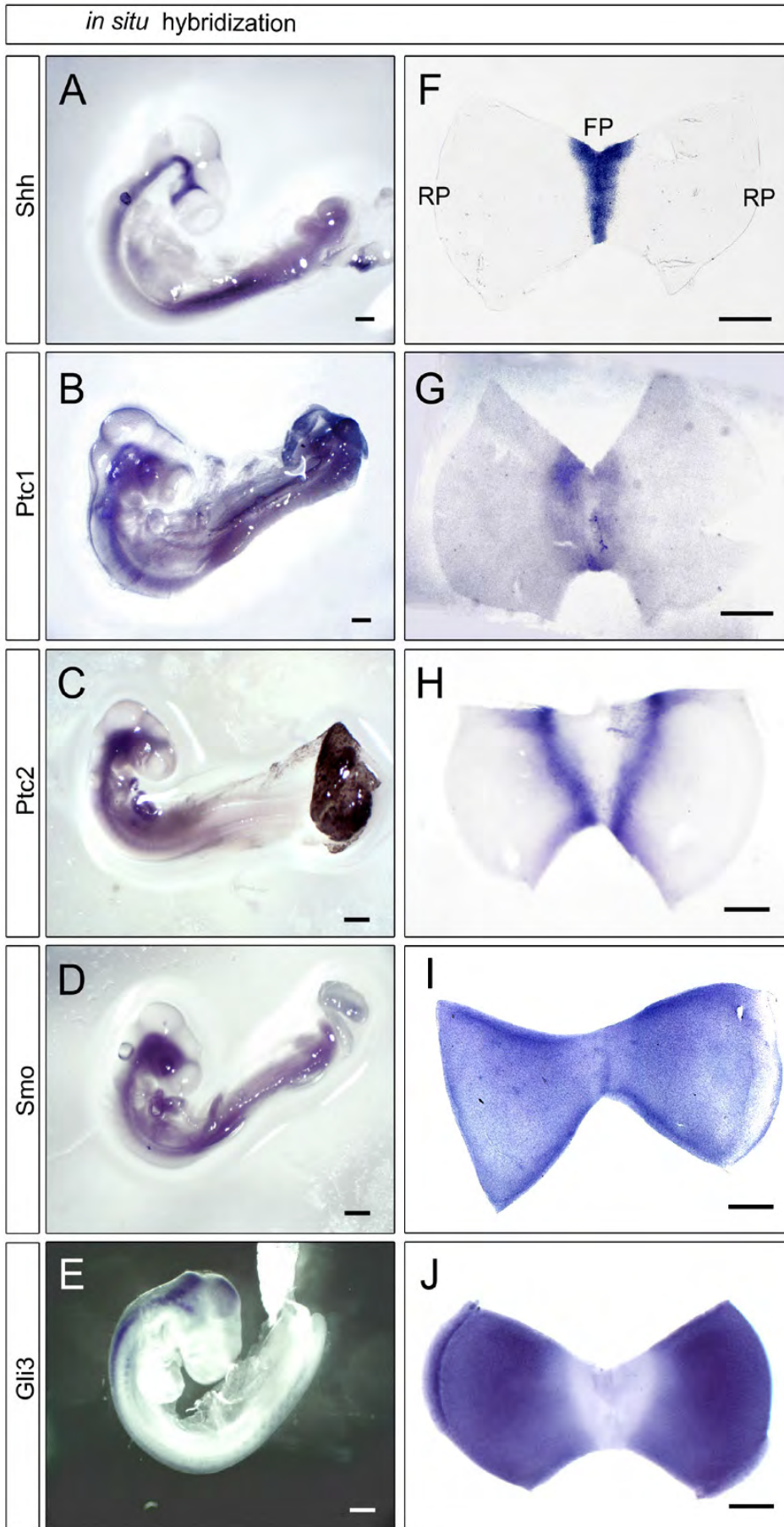


Figure 64: Expression patterns of *Shh*, *Ptc1/2*, *Smo* and *Gli3* in whole chick embryo and midbrain

A – E: Overviews of the chick whole embryos at stage 18 - 20 with *in situ* hybridisation of *Shh*, *Ptc 1*, *Ptc 2*, *Smo* and *Gli3*. The labelled genes are indicated in the left of the panels. *Shh* (A) and *Ptc 1/2* (B, C) were expressed in the ventral neural tube. *Smo* (D) was visible in both dorsal and ventral neural tube. *Gli3* (E) was detected in the dorsal region of the neural tube.

F - J: 'Open-book' preparations of the midbrains at stage 15 or 16. *Shh* was only expressed in the floor plate of the midbrain (F). *Ptc1* mRNA was detected weakly on both sides of the floor plate in the ventral midbrain (G). *Ptc2* was strongly expressed in the ventral midbrain with a distance away from the floor plate (H). *Smo* was detected in the whole midbrain along DV axis with a weak signal in the dorsal and ventral midlines (I). *Gli3* was only strongly expressed in the dorsal midbrain (J).

Abbreviations: FP, floor plate; Gli, Glioma-associated oncogene; Ptc, patched; RP, roof plate; Shh, Sonic hedgehog; Smo, smoothed. Scale bar: 100µm.

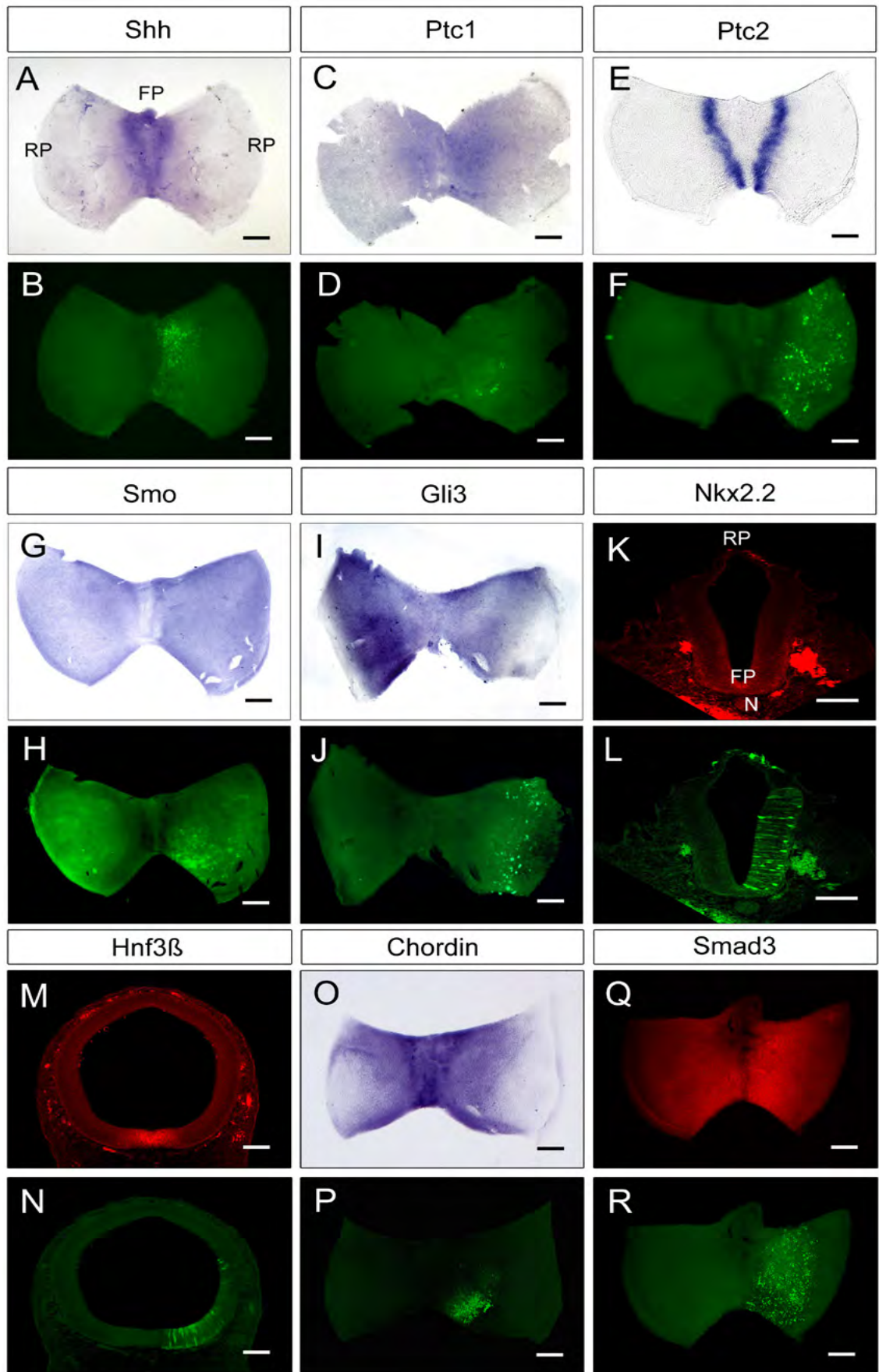


Figure 65: Gene expressions in the Rab23-transfected midbrains and hindbrains

Figure 65: Gene expressions in the Rab23 - transfected midbrains and hindbrains

Chick embryos were electroporated with cRab23-GFP in the right side at stage 9/10, and fixed at stage 15/16. A - J and O - R are 'open-book' preparations of the midbrains, and anterior to the up. K - N are transverse sections (30 μ m) of the midbrain (M, N) and hindbrain (K, L). Dorsal is up. The expressions of *Shh*, *Ptc1*, *Ptc2*, *Smo*, *Gli3* and *Chordin* were detected with antisense RNA probes by *in situ* hybridisation. Nkx2.2, Hnf3 β and Smad3 proteins were stained by special antibodies and shown in red fluorescence. The transfection of Rab23 was visualized with an antibody against GFP (green fluorescence). Roof plate and floor plate are indicated.

A - J: The expressions of Shh (A, B), Ptc1/2 (C - F) and Smo (G, H) have not shown significant changes between the transfected (right) and control sides (left) of the midbrains. However, the transfection of Rab23 resulted in a significant repression of Gli3 expression in the dorsal midbrain (I, J).

K - L: Normally Nkx2.2 protein is expressed in the most ventral neural tube. Here showed that the ectopic Rab23 (green in L) did not induce its expression in the hindbrain.

M, N: The expression of Hnf3 β only localizes in the floor plate of the neural tube as the development. No any change of its expression was detected in the transfected midbrain compared to the control side.

O, P: BMP antagonist chordin is normally expressed in the ventral region of the midbrain. Rab23 misexpression did not result in a significant change of its expression in the midbrain.

Q, R: A TGF- β relative molecule, Smad3, is mainly expressed in the ventral neural tube. Rab23 transfection did not affect its expression in the midbrain.

Abbreviations: FP, floor plate; N, notochord; RP, roof plate. Scale bar: 100 μ m.

8. Discussion

This study presented that *Rab23* gene was already expressed in chick embryo during early gastrulation, and appeared in Hensen's node and the primitive streak with a left - right asymmetric expression pattern. In the nervous system, Rab23 expression was detected in the entire neural plate since progenitor (precursor) cells had been specified to be neural identity, and gradually restricted to the dorsal neural tube at the following stages. Additionally, a transient expression of Rab23 was also seen in the pre - notochord tissue (chordamesoderm) and the consequently formed notochord till stage 13. The transfection of Rab23 before stage 11 could induce dorsal specific genes (Pax7/3) in the both dorsal and ventral regions of the midbrain, hindbrain and spinal cord, whereas the ventral gene Nkx6.1 was not influenced by ectopic Rab23. The specification of some early dorsal neuronal subtypes (Brn3a⁺ cells) was affected by Rab23, however, the neural proliferation and the general differentiation in the midbrain demonstrated not be significantly influenced by Rab23. In the last, the relationship between Rab23 with Shh signal and its downstream components was investigated via Rab23 misexpression in the dorsal or ventral midbrain, and some transcription factors, floor plate marker and BMP signaling members and antagonist were checked as well.

The Tissue - and Region - Specific Expression Pattern of Rab23

Analysis on the dynamic expression of *Rab23* mRNA showed it emerged very early in the chick embryo. During the gastrulation *Rab23* was first

detected in the epidermis and mesoderm at the region of the primitive streak and Hensen's node. With the neural plate forming, *Rab23* was expressed in these specified neural precursor (progenitor) cells of the neural ectoderm layer. The visualization of this expression was enhanced at the rostral region when the neural plate folded, and spread to the entire consequently formed neural tube. However, no signal was detected in the neural crest cells nearby. Transversal sections indicated that *Rab23* was initially expressed throughout the neural tube along DV axis, and became confined to the dorsal region except for the roof plate by around stage 18. In addition, *Rab23* was also detected in the somite. This expression pattern of *Rab23* in chick embryos is correlated to the expression in mice, where Rab23 is present in most tissues at low level but at high level in the spinal cord, somites, limb buds and cranial mesenchyme (Eggenschwiler *et al.*, 2001). Mouse *Rab23* is also initially expressed throughout the neural tube but localizes to the dorsal region excluding the roof plate at embryonic day 10.5 (E 10.5, Caspary and Anderson, 2003). However, the expression in the cranial mesenchyme or limb buds was not observed in chick embryos at the analysed stages. Mouse E 10 correlates roughly with stage 18 to 23 in chick, thus, Rab23 might appear later in the limb buds and cranial mesenchyme or chick Rab23 might possess different properties in these structures. At the cell level in adult mouse brain, Guo *et al.* (2006) shows that Rab23 is predominantly found in cell bodies of neurons rather than in glial cells, such as astrocytes and oligodendrocytes. This tissue - or cell type - specific expression pattern of Rab23 has been observed in Rab3s, Rab15 and Rab17 (Baldini *et al.*, 1992; Elferink *et al.*, 1992; Lutcke *et al.*, 1993), whereas other Rab members are expressed broadly and function in ubiquitous transport processes (Takai *et al.*, 1992). Sequential analysis of chick Rab23 demonstrated to share a large portion with all four isoforms of Rab3 protein (Rab3a, b, c and d), which are expressed abundantly in the neural tissue (Geppert *et al.*, 1994).

Rab23 was also detected in the eye, exclusively in the retinal layer, which might reflect a function of this gene in the eye development not only in mouse (Gunther *et al.*, 1994) but also in chick. Several other Rab members were expressed in the retinal layer, such as Rab3a, -6, -8, -11 and -27 (Deretic *et al.*, 1995; Grabs *et al.*, 1996; Shetty *et al.*, 1998; Moritz *et al.*, 2001; Marcos *et al.*, 2003). A Rab relevant protein, REP1 (Rab escort protein 1), is described to play an essential role in the prenylation process for Rab proteins in photoreceptor cells. Lack of REP1 results in vesicular traffic defect of the choroids, leading to choroideremia (CHM) and retinal degeneration (Seabra *et al.*, 1993; Hayakawa *et al.*, 1999; Alory and Balch, 2000). However, the role of Rab proteins in retinal cells is still unclear.

As in mouse embryo chick *Rab23* mRNA expression was similar to that of Gli3 (Schweitzer *et al.*, 2000). Gli3 in chick embryos was initially restricted to the anterior portion of the neural plate similar to Rab23. In the mouse and chick embryos, Gli3 was initially expressed throughout the neural plate and subsequently becomes restricted to the dorsal neural tube, where it negatively regulates the Shh signalling pathway (Patten and Placzek, 2000; Persson *et al.*, 2002; Meyer and Roelink, 2003; Blaess *et*

al., 2006), like Rab23 (Eggenschwiler *et al.*, 2001). Both genes were necessary for the specification of dorsal neuronal cell types by suppressing Shh signalling in the dorsal neural tube (Gunther *et al.*, 1994; Ruiz i Altaba, 1998; Eggenschwiler and Anderson, 2000; Litingtung and Chiang, 2000; Eggenschwiler *et al.*, 2001; 2006). The malformation of axial skeleton reported in *opb* mutant mice (Sporle *et al.*, 1996; Sporle and Schughart, 1998) and the gene function analysis of Gli3 (Mo *et al.*, 1997) also suggest a possibly relationship between them.

Asymmetric Expression of Rab23 and the Left - Right Determination of Chick Embryo

In chick embryos, Hensen's node lies at the tip of the primitive streak and is thought to be the avian organizer, corresponding to the dorsal blastopore lip in *Xenopus* (Spemann's organizer, Waddington and Schmidt, 1933). It can be well - defined by a set of molecular properties, such as *gooseoid*, *cNot*, *Chordin*, *Otx2*, *Dickkopf1*, *Lim1*, *Hnf3 β* in specific spatiotemporal patterns (Streit *et al.*, 1998; Chapman *et al.*, 2002). The left - right (LR) body axis of chick embryo is thought to be determined by a cascade of genes that are expressed in or near the Hensen's node in an asymmetric fashion including *Activin β B*, *ActR IIA*, *Shh*, *Fgf8*, *BMP4*, *Car*, *Lefty*, *Nodal* and *Pitx2* (Levin *et al.*, 1995; Levin *et al.*, 1997; Pagan-Westphal and Tabin, 1998; Boettger *et al.*, 1999; Capdevila *et al.*, 2000; Monsoro-Burq and Le Douarin, 2001; Rodriguez-Esteban *et al.*, 2001; Hackett, 2002; Raya and Izpisua Belmonte, 2004). However, this LR difference seems not to be conserved in other species (Matzuk *et al.*, 1995; Chiang *et al.*, 1996; Hamada *et al.*, 2002; Hirokawa *et al.*, 2006). *Sonic hedgehog* is thought to be the key signal conveying the left - right information from the node to lateral plate mesoderm (LMP, Pagan-Westphal and Tabin, 1998; Gilbert, 2000). Gene expression indicate that *Shh* and *Fgf8/Bmp4* are symmetrical in the node at stage 4, only with a weaker expression of *Fgf8* in the node compared to the

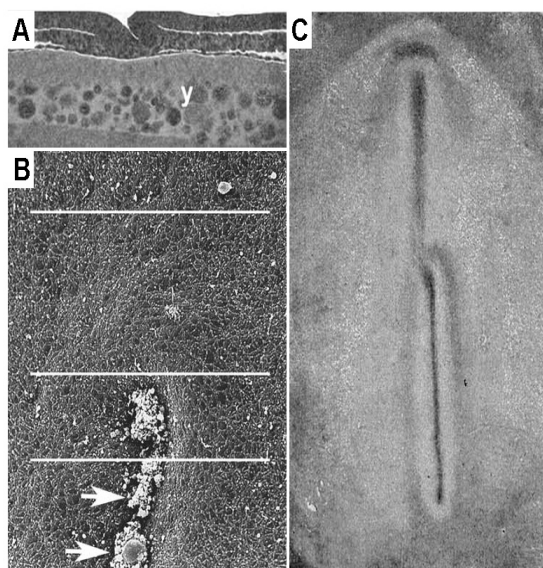


Figure 66: Morphological asymmetry of Hensen's node

A: Transverse section at stage 4. The right lip of the Hensen's node is higher than the left. The yolk sac (y) is underlying the blastodisc.

B: Hensen's node at stage 4 with scanning electron microscopy. A crozier-like structure is visible with bulges more prominent on the right and anterior side. Cell debris (arrows).

C: An embryo at stage 6. The definitive body axis is shifted to the left compared to the axis of the primitive streak. Photographs A and C from (Hertwig, 1902); B from Dathe *et al.* 2002.

primitive streak. They begin to express asymmetrically in the node at late stage 5, *Shh* in the left side of the node and *Fgf8/Bmp4* in the right (Levin *et al.*, 1995; Pagan-Westphal and Tabin, 1998; Monsoro-Burq and Le Douarin, 2001; Dathe *et al.*, 2002). The *Ptc* (1 and 2) receptors are also expressed in the left-side lateral to the node at this stage similar to the *Shh* expression pattern (Pagan-Westphal and Tabin, 1998; Pearse *et al.*, 2001). This left-right polarity is suggested to be responsible for the laterality of organ formation at later stages, such as unidirectional loop of the heart, gut and other visceral organs (Levin *et al.*, 1995; Boettger *et al.*, 1999). This study indicated that the *Rab23* asymmetric expression in the node and the primitive streak initiated at stage 4, earlier than the asymmetric onset of *Shh*. Although a morphological asymmetry of the node was observed at this stage (Fig. 66, Dathe *et al.*, 2002), the left - right inductive function of the node has not formed yet (Psychoyos and Stern, 1996b; Pagan-Westphal and Tabin, 1998). This suggests a very likely role of Rab23 on the onset of left-right polarity in the chick embryos.

The right-sided expression of *Fgf8* was induced by *Bmp4* via chick *Mid1* (Levin *et al.*, 1995; Levin *et al.*, 1997; Monsoro-Burq and Le Douarin, 2001; Granata and Quaderi, 2003). Asymmetrically expressed *Bmp4* inhibited *Shh* expression in the right side of the node, thereby restricting *Shh* expression to the left side of the node (Monsoro-Burq and Le Douarin, 2001). *Pcl2* gene (*Polycomblike 2*) was also shown to be a direct downstream target of the *Bmp4* pathway to suppress *Shh* through direct transcriptional effects, in the right side of the node (Wang *et al.*, 2004). Asymmetric *Rab23* expression in the node also came up one stage earlier than *Pcl2*. *Rab23* has been suggested to be a negative regulator of *Shh* signalling pathway, and it might communicate with *Bmps* in the dorsal neural tube (Eggenchwiler *et al.*, 2001). The upregulation of *Bmp4* by Activin A only occurred in a restricted area around the node (Monsoro-Burq and Le Douarin, 2001). Thus, it speculated the early asymmetric pattern of *Rab23* could have a function to set up the left-right orientation of the node or break the left-right symmetry of gene expression in the node.

The Intracellular Vesicular Trafficking of Rab23

Like all Rab GTPases studied so far function in some aspect of intracellular vesicular trafficking (Hua and Scheller, 2001; Paduch *et al.*, 2001; Hammer and Wu, 2002), *Rab23* protein too, has all of the structural hallmarks of this family receptors and localizes in the plasma/endosomal membrane and endocytic vesicles (Evans *et al.*, 2003), suggesting a vesicular transportation should be happened on *Rab23*. Each Rab protein links to specific microtubule - or actin - based motor proteins of cytoskeletal tracks to act in either long-range or local vesicular movement (Pfeffer, 1992; Zerial and McBride, 2001; Hammer and Wu, 2002). For *Rab23*, Kinesin family members (Kifs) are suggested to be very likely the linked motor proteins. In general, Kifs move different cargos like vesicles and organelles towards either minus or plus end of microtubules near the peripheral actin - rich cortex via the interaction of their conserved motor

domains on microtubules (Kull, 2000). All five classes of Kifs have been isolated in mice, and Kif1, Kif3 and Kif5 express almost exclusively in the nervous system (Aizawa *et al.*, 1992). Among them, Kif5c is described to be a similar expression pattern in chick embryos as Rab23 (Dathe *et al.*, 2004). It is first detected in Hensen's node and the primitive streak during gastrulation, and located within neuronal and mesodermal tissues but not neural crest at later stages. The expression initiates in the entire neural epithelium and restricts to the dorsal neural tube gradually. Interestingly, Kif5c also shows an asymmetric expression pattern around Hensen's node at stage 4, displaying a strong bias on the right side as described on Rab23. The co-localization and the asymmetric expression in the node of Rab23 and Kif5c prompt a suggestion that a mutual action between them might be involved in the LR determination. Unfortunately, analysis on the role of Kif5c in the nervous system is not available in mutant mice (Kanai *et al.*, 2000), which might be due to the redundancy of the three Kif5 members (Kif5a, Kif5b and Kif5c). The neuronal kinesin subfamily Kif3 is another candidate. Kif3a and Kif3b are reported to be essential for the proper formation of the cilia (Nonaka *et al.*, 1998; Marszalek *et al.*, 1999; Takeda *et al.*, 1999), and loss of the cilia or ciliary movement result in murine LR randomization (Chen *et al.*, 1998; Okada *et al.*, 1999; Supp *et al.*, 1999; Murcia *et al.*, 2000; Tanaka *et al.*, 2005). Kif3c is not only a heterodimeric partner for Kif3a expression in the central and peripheral nervous systems, but also thought to drive anterograde axonal transport. The three Kif3 members very likely form a kinesin motor complex together (Muresan *et al.*, 1998; Navone *et al.*, 2001). Due to the redundancy of the three Kif3 members in neural tissues (Navone *et al.*, 2001; Yang *et al.*, 2001), their exact function on the neurogenesis is difficult to be discovered from the mutant mice (Takeda *et al.*, 1999). Thus, although the onset of LR asymmetry in chick is thought to be different with mouse embryo, the expression pattern of Rab23 similar to Kif3 and Kif5 members in Hensen's node and neural tube advocates mutual interactions between them to transport vesicles, which are worthwhile to be studied further.

Besides the possible function on LR determination, Rab23 is suggested to be a negative regulator of Shh signalling pathway (Eggenschwiler *et al.*, 2001). Although the Rab23 trafficking vesicles or proteins have not been identified so far, some evidences still suggest that Rab23 is likely to regulate the intracellular trafficking of vesicle - associated components in Shh signalling pathway as Rab5/APPL (Miaczynska *et al.*, 2004). Shh receptor *Patched* (Ptc) could be the case for Rab23. Ptc has a topology reminiscent of G-protein-coupled receptors and co-localizes with Rab23 in the endosomes (Alcedo *et al.*, 1996; Murone *et al.*, 1999; Evans *et al.*, 2003). However, analysis on Rab23 overexpression and GTP - or GDP - restricted mutants seems not to support this ideal (Evans *et al.*, 2003; Guo *et al.*, 2006). Rab23 also might regulate the trafficking of Tectonic, a secreted protein described recently, along the exocytic pathway (Reiter and Skarnes, 2006). This protein acts as a positional negative regulator of Shh signalling pathway at a downstream level of Ptc receptor. This investigation is still moving onwards.

Rab23 is Served to Establish the Dorsal Polarity

Lack of Rab23 protein in *opb* mice results in defects of the developing nervous system, including the failure of neural tube closure, exencephaly, the absence of dorsal cell types in the caudal neural tube and dorsal extension of ventral specific genes (Gunther *et al.*, 1994; Eggenschwiler and Anderson, 2000; Eggenschwiler *et al.*, 2001). Hence, misexpression of Rab23 in ventral neural tube could cause the down-regulation of ventral genes and the upregulation of dorsal genes. Two Pax genes (*Pax3/7*) specific for dorsal cells in the neural tube were analysed in this study (Jostes *et al.*, 1990; Goulding *et al.*, 1991; Chalepakis and Gruss, 1995; Kawakami *et al.*, 1997; Matsunaga *et al.*, 2001). In fact, Rab23 misexpression did induce ectopic Pax3 and Pax7 expressions not only in the dorsal but also in ventral neural tube (midbrain, hindbrain and spinal cord). Consistent with the absence of Pax7 in *opb* mutants (Nomura *et al.*, 1998; Thomas *et al.*, 2004), this suggests that Rab23 is required for triggering Pax3/7 transcription to define the territory of the dorsal region, such as the optic tectum (Matsunaga *et al.*, 2001). The weak ectopic Pax3 expression compared to Pax7 expression might be due to the induction of Pax3 by Rab23 is indirect. Thus, it will take a long time to induce Pax3 by ectopic Rab23, might via Pax7 protein, which can induce Pax3 expression ventrally as described previously. Or, Pax3 expression in the ventral would not become stronger due to the Shh suppression (Watanabe and Nakamura, 2000). This ectopic Pax3/7 expression was only seen till stage 11 when the transfection of Rab23 was performed, suggesting other signals should be also involved in this process, possibly Fgf8 or BMPs expressed in the ectodermal cells (Liem *et al.*, 1995; Lee and Jessell, 1999; Firnberg and Neubuser, 2002). This may well be that after stage 11 the cells do not respond to the activity of these signals (Arkell and Beddington, 1997; Patten and Placzek, 2000; Placzek *et al.*, 2000), might be due to the regional commitment in the midbrain begins to be established since stage 12 (Li *et al.*, 2005). Bmp signals from the roof plate and surface ectoderm are required for the expression of dorsal genes (Liem *et al.*, 1995; Lee *et al.*, 2000; Liem *et al.*, 2000) and the specification of dorsal cell types in the neural tube (Tanabe and Jessell, 1996; Lee *et al.*, 1998; Lee and Jessell, 1999; Millonig *et al.*, 2000; Timmer *et al.*, 2002; Chizhikov and Millen, 2005). These BMP signals are blocked by Bmp antagonists expressed in the notochord and the floor plate (Amthor *et al.*, 1996; Graham and Lumsden, 1996; McMahan *et al.*, 1998; Dale *et al.*, 1999; Liem *et al.*, 2000). Thus, a likely scenario might be that Rab23 sets up a proper circumstance via down-regulating Shh signalling, which facilitates BMP to specify dorsal neurons. Nevertheless, these results provide evidence that Rab23 can cell - autonomously specify the dorsal neural identity in the early development, might with/without the help of Shh suppression.

In addition, more dorsal Brn3a positive cells were specified in the midbrain lateral to the roof plate upon Rab23 transfection, but no any significant influence on dorsal Isl-1/2 cells. Brn3a co-expresses with Islet in the dorsal cells, but not all Islet positive cells express Brn3a, thus, two different cell subpopulation are suggested as described (Fedtsova and

Turner, 1997, Ledderose, Diplomarbeit). This difference is more likely on account of their inductive/regulative signals, for *Islet* genes mainly from the roof plate (Ericson *et al.*, 1992; 1995a; Pfaff *et al.*, 1996; Varela-Echavarría *et al.*, 1996; Dutton *et al.*, 1999; Lee *et al.*, 2000), whereas Brn3a expression is down-regulated by the signals from the ventral midline and isthmus (Fedtsova and Turner, 1995; Xiang *et al.*, 1996; Fedtsova and Turner, 1997; Latchman, 1998; Huang *et al.*, 1999; Eng *et al.*, 2001; Fedtsova and Turner, 2001; Eng *et al.*, 2003; Eng *et al.*, 2004). Thus, a dorsalized circumstance facilitated by Rab23 is required for Brn3a transcription, and Brn3a cells located in the most dorsal region also hints a dose or gradient dependent way to induce Brn3a. The present study showed that Rab23 misexpression did not cause any change on the neuronal differentiation and proliferation in the midbrain and hindbrain. Taken together, these data suggest Rab23 is served to establish the dorsal polarity in the neural tube to specify the dorsal neuronal identity.

However, the reduction of ventral gene *Nkx6.1* was not seen in the midbrain upon ectopic Rab23 transfection. This result could be explained by non-sufficient amounts of ectopic Rab23 protein to affect highly abundant Shh signalling required for *Nkx6.1* induction. Or, it might be possible that *Nkx6.1* is induced by another pathway. The second interpretation comes from the results of *Shh/Gli3*, *Smo/Gli3* and *Shh/Opb* compound knockouts (Litington and Chiang, 2000; Eggenschwiler *et al.*, 2001; Persson *et al.*, 2002; Wijgerde *et al.*, 2002; Ruiz i Altaba *et al.*, 2003). In these knockout mice, *Nkx* genes are still generated in the ventral despite a lack of Shh or Shh signalling. However, the correct stratification of the ventral cell types is lost suggesting that Shh signalling is essential to organize ventral cell type patterning but not necessary to induce *Nkx* genes.

Contribution to the Roof Plate Formation

The dorsalizing signals emanating from the dorsal neural plate and the margin area of surface ectoderm specify the roof plate (RP) at the dorsal midline, a group of specialized neuroepithelial cells (Altman and Bayer, 1984; Yamada *et al.*, 1991; Dickinson *et al.*, 1995; Selleck and Bronner-Fraser, 1995; LaBonne and Bronner-Fraser, 1999), where several BMPs are expressed as inductive signals for dorsal cells after the neural tube closure (Lyons *et al.*, 1995; Arkell and Beddington, 1997; Dudley and Robertson, 1997; Liem *et al.*, 1997; Lee *et al.*, 1998; Solloway *et al.*, 1998; 2000; Timmer *et al.*, 2002; Liu *et al.*, 2004). *In vivo* study demonstrates that diverse dorsal interneuron subtypes generate in response to different levels of Bmp signalling. Additional Wnt and Fgf signals in the roof plate also contribute to the proliferation and differentiation of dorsal neurons (Wilson *et al.*, 2001; Chenn and Walsh, 2002; Garcia-Castro *et al.*, 2002; Muroyama *et al.*, 2002; Millen *et al.*, 2004). The characteristics of the roof plate is shown to be absent in *opb* mutant neural tube, mimicking the phenotype of roof plate ablation (Gunther *et al.*, 1994; Eggenschwiler and Anderson, 2000; Lee *et al.*, 2000). Neither BMP signals (Bmp6 nor Bmp7) nor Wnt signals (Wnt1 and Wnt3a), which are important to specify the

dorsal cells (McMahon and Bradley, 1990; Takada *et al.*, 1994; Muroyama *et al.*, 2002), are expressed in the dorsal neural tube of the *opb* mutants and roof plate ablated mice. However, dorsal spinal cord of *opb* mutant still retains some ability to generate *Msx1/2*, a Bmp downstream component (Vainio *et al.*, 1993; Liem *et al.*, 1995; Takahashi *et al.*, 1996; Barlow and Francis-West, 1997), only narrowly in the most dorsal area of the neural tube (Gunther *et al.*, 1994; Eggenschwiler and Anderson, 2000). This dorsally restricted expression of *Msx* might be due to the signals from overlying surface ectoderm, like *Bmp7*, which can be detected in the surface ectoderm overlying the dorsal neural tube in *opb* mutant. Bmp signalling and *Msx1* have shown to possess an ability to induce roof plate cell fate at early stage 10 – 12, however, this induction was lost after stage 14 (Liu *et al.*, 2004). The regional specific gene expression in the midbrain is dependent of the activity of the midline organizers — the roof and floor plates till stage 16 (Li *et al.*, 2005). Some transcription factors, like *Math1*, also fail to be detected in the dorsal neural tube of *opb* mice as in roof plate missing neural tube (Lee *et al.*, 1998; Eggenschwiler and Anderson, 2000; Lee *et al.*, 2000). In *opb-wt* chimeras, both the wild - type cells and adjacent mutant cells in the dorsal region express *Msx1/2* implying that *Rab23* does not influence *Msx1/2* expression in a cell-autonomous manner. In addition, *Rab23* can induce *Pax3* protein, which is suggested to be required for the closure of the neural tube closure (Franz and Kothary, 1993; Borycki *et al.*, 1999; Li *et al.*, 1999; Juriloff and Harris, 2000). Thus, *Rab23* very likely exerts a role on the roof plate formation with the signals from surface ectoderm. Taken together, these data suggest that neural precursor cells initiate to adopt a dorsal identity with a cell-autonomous requirement of *Rab23*, and since stage 12 a permissive dorsal circumstance established by *Rab23* allows BMPs or other signals from roof plate to specify diverse dorsal cell subtypes. Although misexpression of *Rab23* has not displayed a direct influence on *BMP4*, *BMP7* and *GFP7* as expected (data not shown), if the early expressed BMPs can in turn regulate *Rab23* need more experiments to test.

Shh Signalling and Rab23

During the CNS development, *Shh* plays a role as morphogen for the specification of ventral neuronal cells in the spinal cord and brain by controlling the expression of combinatorial homeodomain proteins (Ericson *et al.*, 1995b; Marti *et al.*, 1995; Chiang *et al.*, 1996; Ericson *et al.*, 1996; 1997; 1997; Briscoe and Ericson, 1999; Briscoe *et al.*, 1999; Sander *et al.*, 2000; Briscoe and Ericson, 2001; Schubert *et al.*, 2001; Pattyn *et al.*, 2003). The transduction of *Shh* signal is mediated by specific receptors through the membrane into the nucleus to modulate gene expression (Ingham and McMahon, 2001; Bijlsma *et al.*, 2004). *Rab23* and *Shh* mutant spinal cords suggest a negative regulation of *Rab23* on *Shh* signalling pathway (Eggenschwiler *et al.*, 2001). In this study, a direct downregulation of *Rab23* on *Shh* signal was not observed in the midbrain upon *Rab23* mixexpression, as well as *Ptc1/2* and *Smo*, two transmembrane receptors located on the *Shh* signalling pathway (Kinzler *et*

al., 1988; Ruiz i Altaba, 1998; Murone *et al.*, 2000; Stegman *et al.*, 2000; Wang *et al.*, 2000; Nybakken *et al.*, 2002). However, Gli3 expression was largely down-regulated by ectopic Rab23, in consistent with a suggestion that Rab23 may acts more distally in regulating hedgehog signalling, at a level of downstream of Smo and upstream of Gli2/Gli3 repressor. Double mutants of *Rab23/Gli2*, *Rab23/Gli3* and *Rab23/Smo* display that both Gli genes can mediate Shh signalling and the loss of Gli2 nearly rescues the Rab23 phenotype. (Motoyama *et al.*, 2003; Bai *et al.*, 2004; Lei *et al.*, 2004; Tyurina *et al.*, 2005). Loss of Smo, however, seems not to prevent an activation of the Shh pathway resulting from the Rab23 mutation (Eggenchwiler *et al.*, 2006). Mutation of some IFT members shows many aspects of neural patterning similar to Rab23 phenotype, and these vesicle – related proteins are crucial for the function of Gli proteins (Huangfu and Anderson, 2005; Liu *et al.*, 2005). The observation of early chick embryos in this study showed a transient expression of Rab23 in pre-notochord tissue underlying the neural plate and in the consequently formed notochord, suggesting a co - expression of Shh and Rab23 in the notochord at these stages. With the development, Rab23 retreats from the notochord and ventral region to free the activity of Shh signalling in the ventral region. At the same time, Rab23 contribute to form roof plate and facilitate the activities of Bmps in the dorsal region. The neural cells are specified to possess either dorsal or ventral identities by Rab23 or Shh, respectively, and further adjusted to be distinct cell types depending on their positions in the neural tube along dorsoventral axis.

Part IV:

RNA Interference in Chick Embryos

For it is difficult to obtain transgenic or mutagenic avian embryos or cells for embryogenetic research, RNA interference (RNAi) was tested here as a strategy to silence gene expression in chick embryos. Double-stranded RNA (dsRNA) has been exploited in vertebrates to induce the degradation of the mRNA of target genes recently (Hutvagner and Zamore, 2002; Tijsterman *et al.*, 2002; Zamore, 2002; Mittal, 2004), however, less was known on chick embryos *in vivo*. In this study, chick *Pax7*, a dorsal - specific gene, was used as the target. Diverse dsRNA constructs containing long (ca. 200 – 300 nt) or short (19 nt) hairpin sequences were produced with different vectors, and electroporated into chick midbrains *in ovo*. The effect of these constructs on *Pax7* expression at the protein level was evaluated by immunostaining with an antibody against *Pax7*. In addition, other approaches to repress gene expression by antisense DNA oligonucleotides and antisense morpholinos were also checked and compared their effects to dsRNA constructs. The control midbrains were transfected with pMES vector and only GFP was expressed there.

1. Long - hairpin dsRNA (lhRNA) Experiments

Preparation of lhRNA constructs for Chick *Pax7* Gene

The sequence of chick *Pax7* cDNA (Fig. 31, Kawakami *et al.*, 1997) was acquired from the NCBI GenBank database (accession no: D87838, <http://www.ncbi.nlm.nih.gov>). To make the long – hairpin dsRNA (lhRNA) constructs (Fig. 70), at first, several gene fragments (hundreds of nucleotides) were synthesized using the coding region of chick *Pax7* gene as the template (1575 bp, Fig. 67 A). In short, five gene fragments were obtained by RT - PCR using linker - primers (linkers: *Xba*I and *Eco*RI; Table 4) from the isolated total RNAs of E3 chick neural tubes (Fig. 67 B). These fragments were digested by *Xba*I and then ligated by different combinations of a short fragment with a longer one (Fig. 68). The longer

fragment contains the complementary sequence of the entire short one and a part of linked un-matched sequence. Thus, the ligated DNAs contained complementary sequences at the 5' prime and 3' prime ends, and the RNA transcripts from them should automatically fold into hairpin dsRNAs with the un-matched part as the loop in between. After the recovery from the agarose gel, these ligated DNAs were digested by *EcoRI*, and then inserted into the MCS of pMES vector (Fig. 69), which can co-express a GFP protein simultaneously. For using one recognition site, the insert can be cloned with different directions. To distinguish them, the inserts with the longer fragment located at 5' end are named dsA, dsB and dsC, whereas the inserts with reverse direction as dsA⁻, dsB⁻ and dsC⁻, respectively. *SURE*[®]2 supercompetent cells (Stratagene, Amsterdam) were used for the transformation, since this *E. coli* strain easily accept these special constructs for dsRNA transcription. The expected clones were selected by "Mini"-PCR, restrictive digestion (a example with *EcoRI* in Fig. 71) and confirmed by DNA sequencing. Totally, 26 clones containing the lhRNA constructs for chick Pax7 gene were obtained in this process, 15 with dsA/dsA⁻ insert, 4 with dsB/dsB⁻, and 7 with dsC/dsC⁻. Six of them were isolated as the representatives for different constructs and electroporated into chick dorsal midbrains at early stages 8 to 14. lhRNA-Pax7-GFP-a40 and -a41 constructs contained the insert of dsA and dsA⁻, respectively. lhRNA-Pax7-GFP-b25 construct contained the dsB⁻ insert. lhRNA-Pax7-GFP-c51 had the dsC, whereas -c58, -c65 had the dsC⁻. The effect of these lhRNA constructs was analysed by immunostaining for Pax7 protein.

Morphological Changes of the Transfected Midbrains

As a developmental gene, Pax7 display a role on the dorsal polarity in the neural tube (Jostes *et al.*, 1990; Mansouri *et al.*, 1994; Kawakami *et al.*, 1997; Nomura *et al.*, 1998; Matsunaga *et al.*, 2001) as well as on neuronal and satellite cell proliferation (Olguin and Olwin, 2004; Oustanina *et al.*, 2004; Thomas *et al.*, 2006; Zammit *et al.*, 2006). The transfection of all six pMES - based lhRNA constructs for Pax7 gene mentioned above revealed a morphological change on the midbrain as expected (Tab. 24, Fig. 35, A, B). The embryos developed into a small dorsal midbrain on the transfected side compared to the intact control side. The midbrain sections suggest the reduction in size mainly in the dorsal, while ventral region was similar in size on both sides (Fig. 36). Statistical analysis of lhRNA-Pax7-GFP-a41 transfection indicated that about 55 % of embryos showed a reduced transfected midbrain (n = 156/283, Tab. 24, Fig. 35 C), and this morphological change was related to the stages of the embryos when transfected (Tab. 24, Fig. 72). The ratios of reduced midbrains are about 75 % before stage 9, 50 % at stage 10 – 12, and less than 25 % at stage 13 and later. In comparison to the GFP control midbrains with pMES transfection (7%; n = 4/55, Tab. 24, Fig. 35 C), the ratios of small midbrains with lhRNA-Pax7 transfection at stage 8 – 12 were significant high (χ^2 ; p < 0.05). In addition, over 95% of embryos survived and developed well till 72 hours, except for a few having a smaller eye.

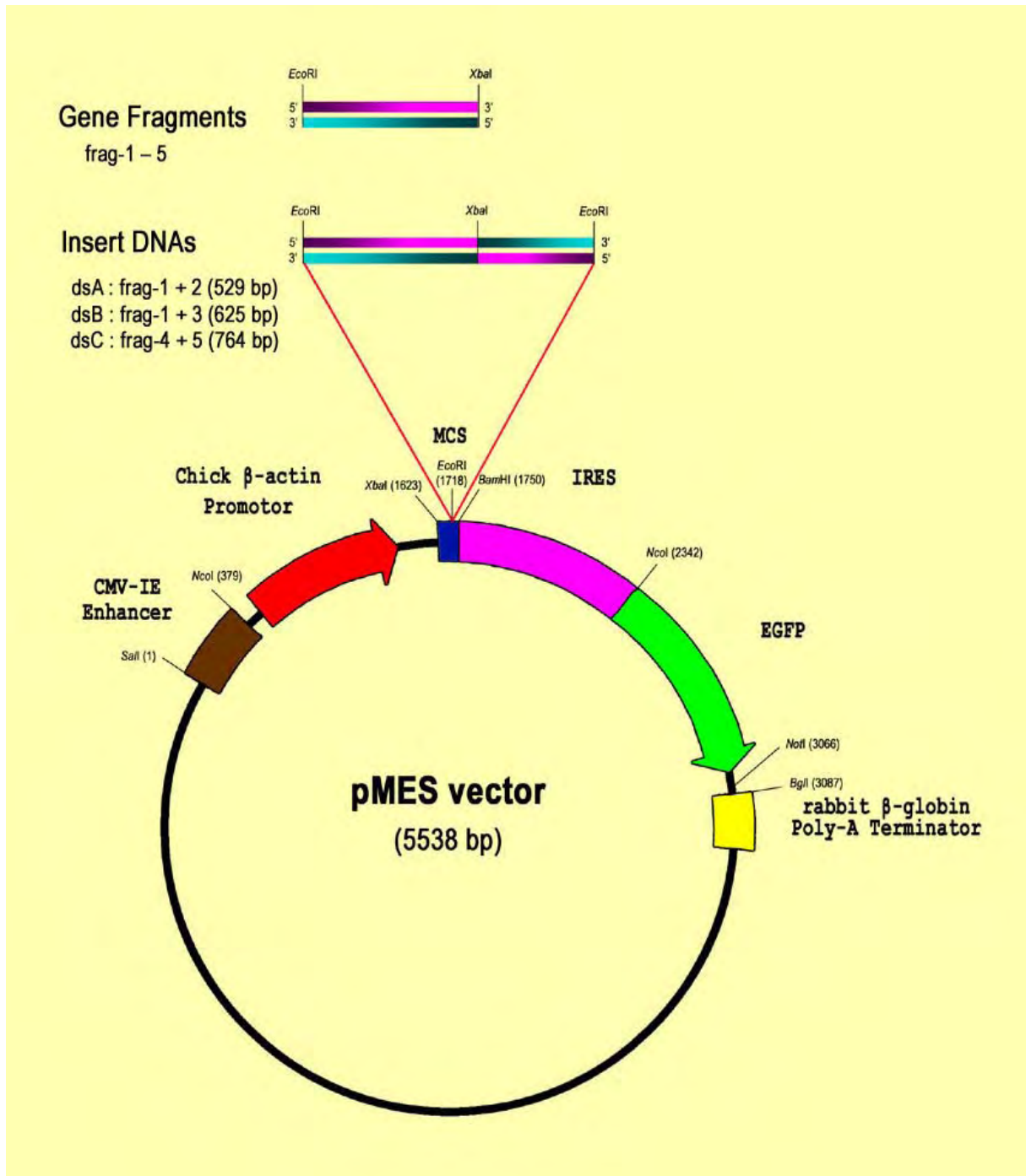


Figure 67: Schematic diagram of the pMES – based lhrRNA construct for chick Pax7 gene

At first, several gene fragments (frag-1 – 5, about 200 - 300 nt) selected from chick Pax7 coding region are amplified by RT-PCR with designed linker primer pairs. After digested by XbaI, these gene fragments are ligated by different combinations to form the insert DNAs (dsA, dsB and dsC), which shows a complementary sequence in 5' and 3' ends and a part of un-matched sequence in between. Thus, the RNA transcribed from this insert should fold in the complementary part at the end and leave the un-matched middle part as the loop. The heterogeneous ligated products were digested by another restriction endonuclease - EcoRI, and then cloned into the MCS of the linearized pMES vector by the same enzyme. This will produce two type constructs containing a same insert but in different directions. The constructs will give rise to a long-hairpin dsRNA for Pax7 gene and an EGFP mRNA simultaneously from a single bicistronic mRNA, which is achieved by an IRES situated between MCS and EGFP coding region. Chick β-actin promoter and CMV-IE enhancer are located at the upstream of the MCS, and rabbit β-globin poly-A terminator lies at the downstream of EGFP coding region.

Abbreviations: CMV-IE, human Cytomegalovirus immediate early enhancer; EGFP, enhanced green fluorescent protein; IRES, internal ribosomal entry site; lhrRNA, long-hairpin dsRNA; MCS, multiple cloning site.

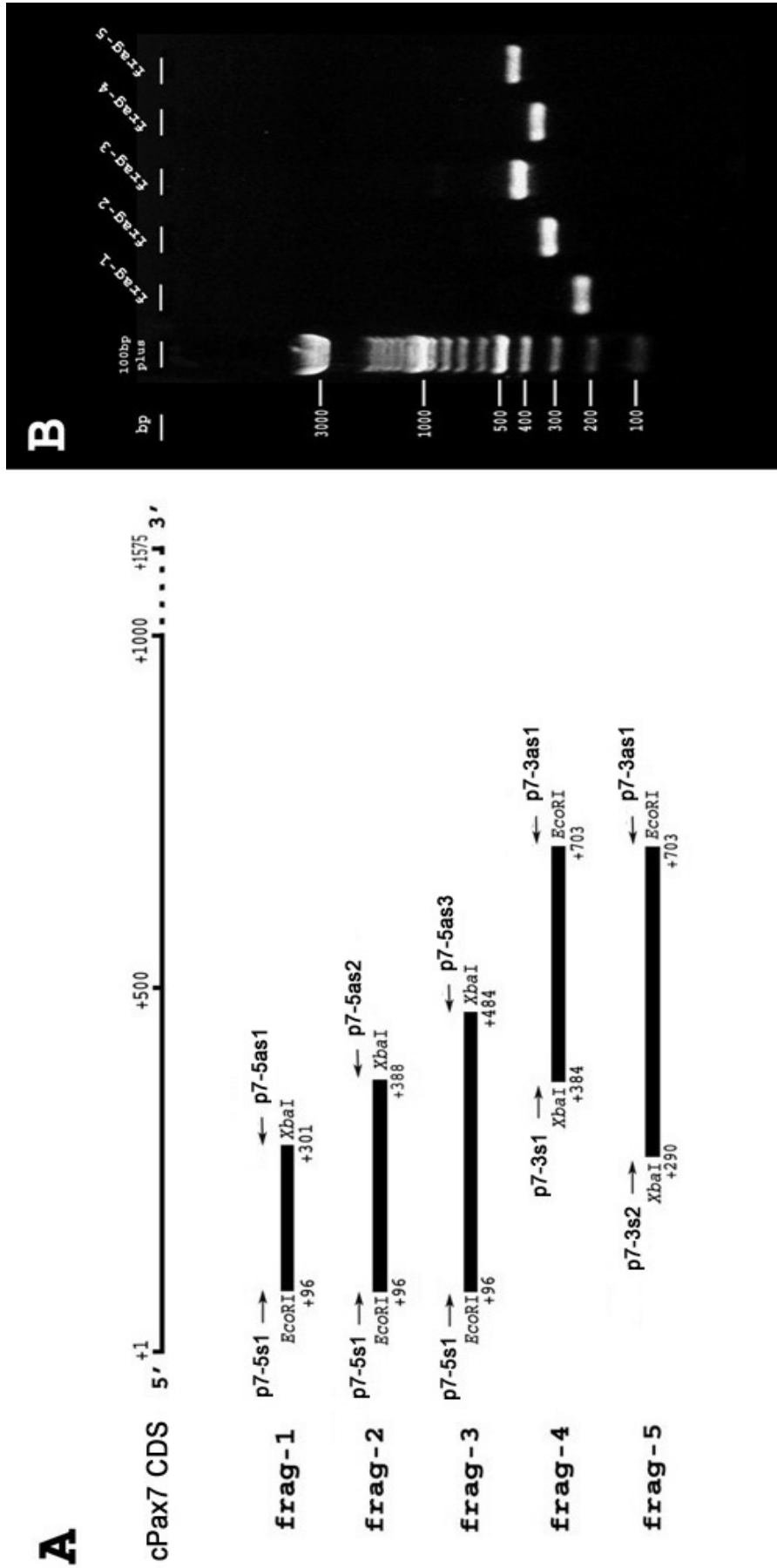


Figure 68: The selected sequences for lhrRNA – Pax7 constructs

A: Schematic diagram of the locations and sizes of the selected sequences within the coding region of chick Pax7 gene. Five gene fragments are 226 bp, 313 bp, 409 bp, 340 bp and 434 bp, respectively. The start and end positions of each fragment in the Pax7 coding region and the linker - primers used for RT-PCR are indicated. The primers p7-5s1 and p7-3as1 contain the recognitive sequence for EcoRI, and the rest primers contain an XbaI site. The coding sequence of chick Pax7 is illustrated in 5' – 3' direction from left to right.

B: Five PCR products amplified by RT - PCR from E3 chick neural tube tissues were checked in agarose gel. 100bp DNA plus ladder is used as a size standard.

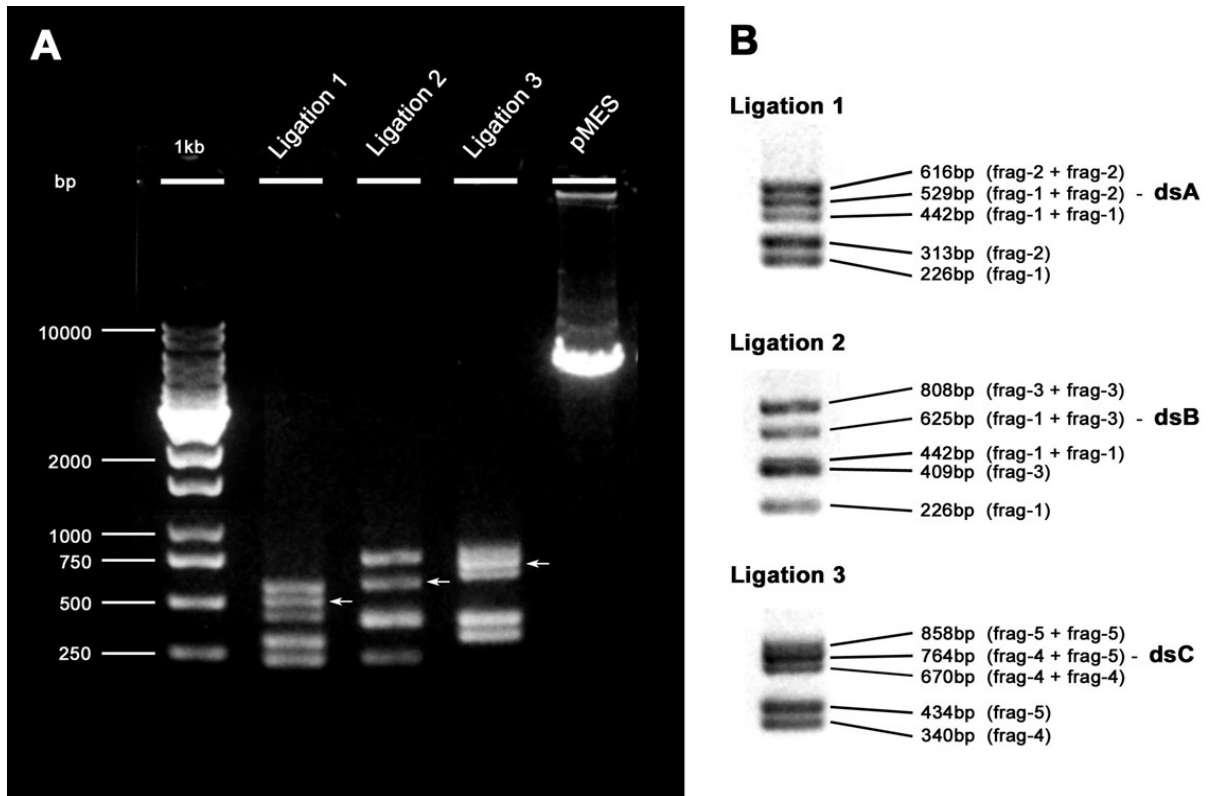


Figure 69: Ligation of gene fragments for hairpin dsRNA transcription

A: Five gene fragments digested by *Xba*I were ligated with different combinations. The three ligations 1 - 3 were performed with frag-1/2, frag-1/3 and frag-4/5, respectively, and displayed five products in each. The arrows indicate the expected heterogeneous DNA products, which are assumed to form hairpin dsRNAs after transcription. The linearized pMES vector by *Eco*RI shown in the right lane was used to accept the three ligated products digested by the same enzyme. 1kb DNA ladder was used here as a size standard.

B: Detail views on the results of the ligations in A. Among the five products in each ligation, 2 small ones are original gene fragments, and 3 larger ones are the ligated DNAs. The heterogeneous ligated products are marked as dsA, dsB and dsC, respectively.

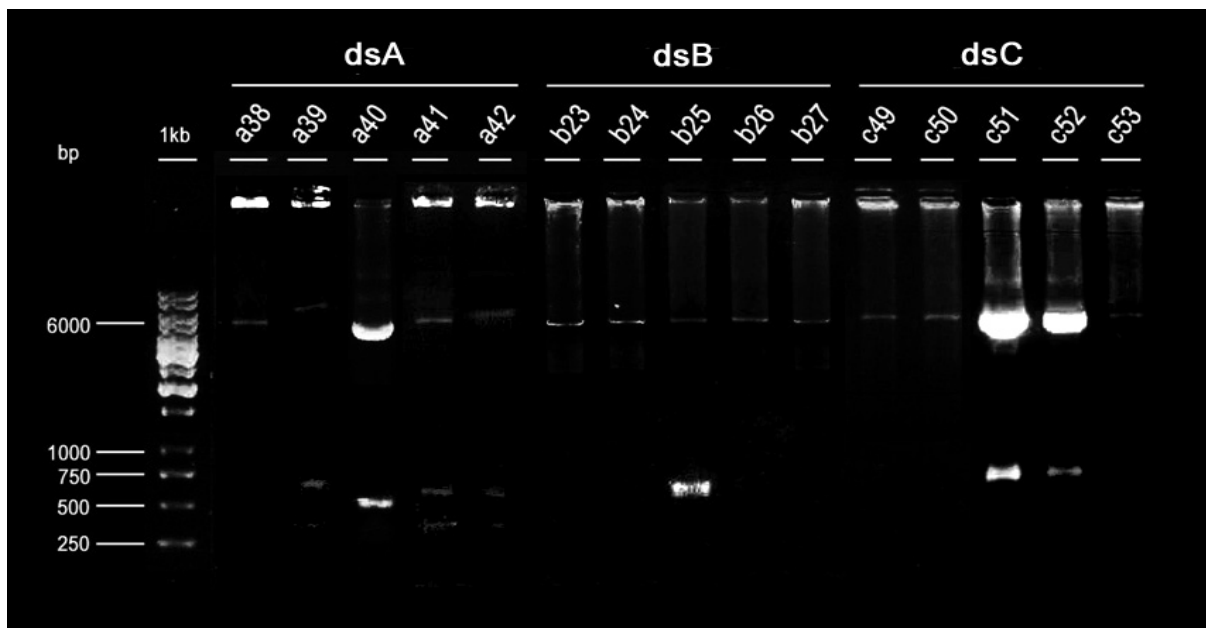


Figure 70: Digestion of lhRNA – Pax7 constructs by *Eco*RI

Figure 70: Digestion of lhRNA – Pax7 constructs by *EcoRI*

Examples of the pMES-based lhRNA constructs for Pax7 gene were digested by *EcoRI*. Several constructs (a39, a40, a41, a42, b25, c51 and c52) released the insert with an expected size (dsA, dsB or dsC). The different results of a40 with the rest 3 constructs (a39, a41 and a42) suggest that the insert (dsA) was cloned in different direction. The large product was presumed to be the pMES vector. 1kb DNA ladder was used as a size standard.

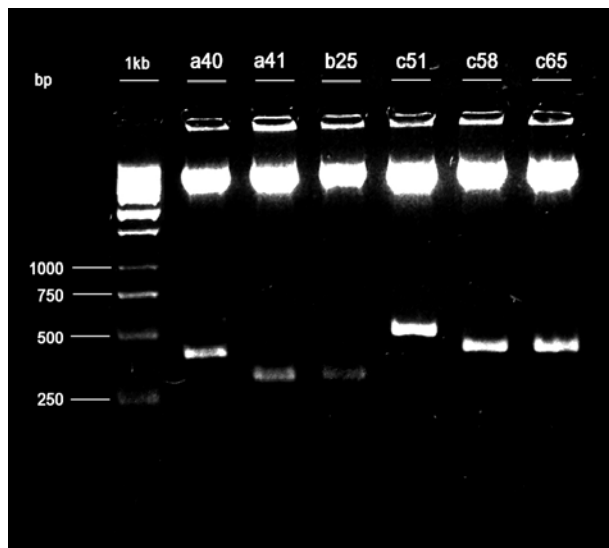


Figure 71: Digestion of lhRNA – Pax7 constructs by *XbaI*

Six selected lhRNA - Pax7 constructs were digested by *XbaI*. Due to a second *XbaI* site was located at the 5' MCS of pMES vector in addition to the *XbaI* site in the insert, thus, the direction of the insert could be determined by the sizes of the digested products. Both lhRNA-Pax7-GFP constructs a40 and a41 contain a same insert (dsA), with a difference that the longer fragment (frag-2) at the 5' end of the MCS in a40, but at 3' end in a41. The insert (dsB) in b25 construct is composed of frag-1 and frag-3

from 5' to 3' end. In the dsC insert of c51, the frag-5 is located at the 5' end, however, this fragment lies at the 3' end in c58 and c65 constructs. 1kb DNA ladder was used as standard.

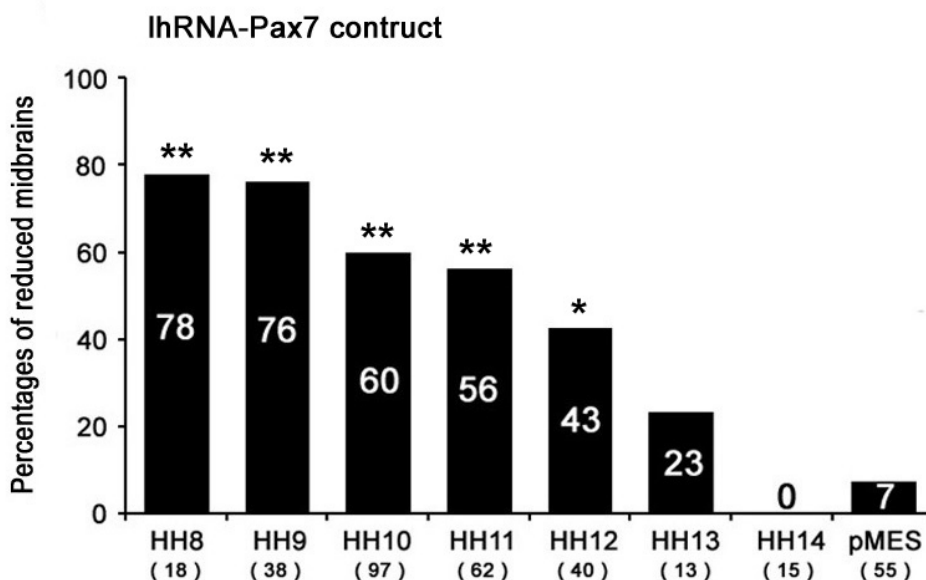


Fig. 72: Percentages of the reduced midbrains upon lhRNA-Pax7 transfection

The dorsal midbrains were transfected with lhRNA-Pax7-GFP-a41 construct at different early stages. The percentages of the reduced midbrain on the transfected side were decreased with the time. At stage (HH) 8 and 9, about 75 % of transfected midbrains were showed in a smaller size. At stage 10 –12, and 13 the ratios were about 50 % and 25 %, respectively. No morphological change on the midbrain was seen at stage 14. The control midbrains were transfected with pMES vector at stage 8 –12, resulting in GFP expression. The statistic analysis revealed the effect of the lhRNA-Pax7 was significant higher than the GFP controls (X^2 -test, $P < 0.01$ or 0.05). The number of the total transfected midbrains at each stage is indicated in the brackets.

Gene Expression was reduced in the Transfected Cells

The effect of these pMES-based lhRNA-Pax7 constructs was evaluated by an immunostaining of Pax7 protein, and the transfected area was visualized by EGFP directly, which was co-expressed by these constructs simultaneously. However, for some samples incubated over 48 hours post a transfection, GFP signal was strengthened by a second immunostaining following Pax7. About 50 % of the transfected midbrain showed a prevailing weak expression of Pax7 in the transfected area compared to the opposing control side (Fig. 73 A - D). The strong Pax7 repression was only seen in some transfected areas of a few midbrains (Fig. 73 B). Close views displayed that the Pax7 protein was largely suppressed in a few transfected midbrain cells, but not in all GFP expressing cells (Fig. 73. E - G). Statistical analysis (Fig. 74 A) indicated that the lhRNA-Pax7 constructs containing dsA insert (a40, n = 6, and a41, n = 13) suppressed Pax7 expression in about 5 % of total transfected midbrain cells similar as the dsB - inserted construct (b25, n = 7), but nearly double as the dsC - inserted ones under the same condition (c51, n = 11; c58, n = 5, and c65, n = 7). The hairpin dsRNAs produced by the dsA and dsB inserts were assumed to be same in the double-stranded part, but different only in the loops. The effect on Pax7 suppression was also similar by the constructs with same insert no matter what direction they are (a40/a41 and c51/c58/c65). Thus, these suggested lhRNA constructs did suppress gene expression, and the effect is dependent on the hairpin composition, especially the double-stranded part. The percentages of Pax7 - suppressed cells by the six lhRNA-Pax7 constructs were all significant high compared to the GFP control midbrains transfected with pMES vector (0.08 %, n = 16, *t*-test, all *P* < 0.001), however, no significant differences were found among them (*F*- test, *P* > 0.05).

In addition, the effect of protein repression by lhRNA-Pax7 constructs at different concentrations was also checked in the midbrains (Fig. 74 B). The results showed that 4 - 6 µg/µl of a41 construct (5.14 %, n =13) resulted in four - time of Pax7 – repressed cells compared to the 1 - 2 µg/µl transfection (1.21 %, n = 12, *t*-test, *P* < 0.05). A concentration of the construct less than 1 µg/µl (0.46 %, n = 9) revealed a significant lower percentage compared to the 4 – 6 µg/µl transfection (*P* < 0.01), but still slightly higher than the ratio of GFP controls (*P* < 0.05). This indicates that the low concentration of lhRNA construct is difficult to elicit protein suppression.

Analysis of Other Gene Expressions

A specific dorsal (*Pax3*) and ventral (*Nkx6.1*) neural gene were used here to investigate the possible influence by a reduced Pax7 protein on the DV patterning in the neural tubes (Goulding *et al.*, 1991; Qiu *et al.*, 1998). In all transfected midbrains (n = 24), *Pax3* and *Nkx 6.1* mRNAs visualized by RNA *in situ* hybridization did not display an obviously change on both expression patterns compared to the intact control side (data not shown).

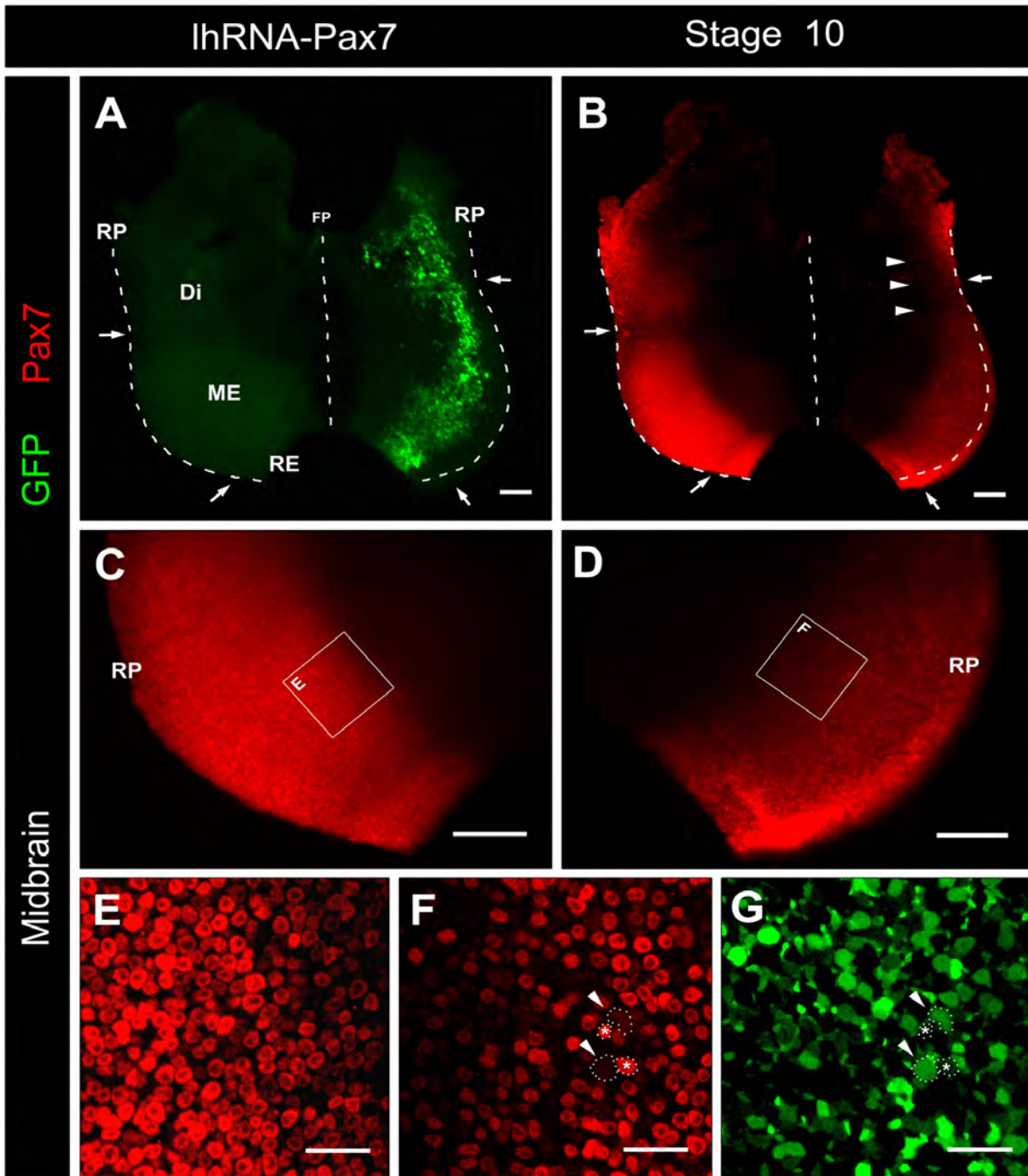


Figure 73: Protein expression of the midbrain transfected with lhRNA - Pax7 construct

A stage - 10 chick midbrain transfected with the construct lhRNA-Pax7-GFP-a41 was fixed at 24 hours, and viewed in 'open-book' preparations. Anterior is up. Pax7 protein (red) was visualized by immunostaining, and the transfected region and cells were defined by the co-expressed GFP (green).

A - D: The Pax7 expression in the transfected region (right in B) was relative weak in general compared to the control side (left), which is viewed clearly in the high resolution (D). Strong repression of Pax7 was only seen in some transfected area (indicated by arrowheads in B). C is a magnification of the left midbrain in B. The roof and floor plates are indicated by dotted lines, and the arrows point to the boundaries of mesencephalon with diencephalon and rhombencephalon.

E - G: Magnifications (F, G) of the transfected areas in D showed the Pax7 was largely repression in a few transfected dorsal cells (indicated by arrowheads), whereas their neighbour cells (asterisk) with less or no GFP signal are still expressed Pax7 as normal. E is a magnification of the indicated area in C as control.

Abbreviations: Di, diencephalon; ME, mesencephalon; RE, rhombencephalon; RP, roof plate; FP, floor plate. Scale bar: A - D: 100 μ m; E - G: 25 μ m.

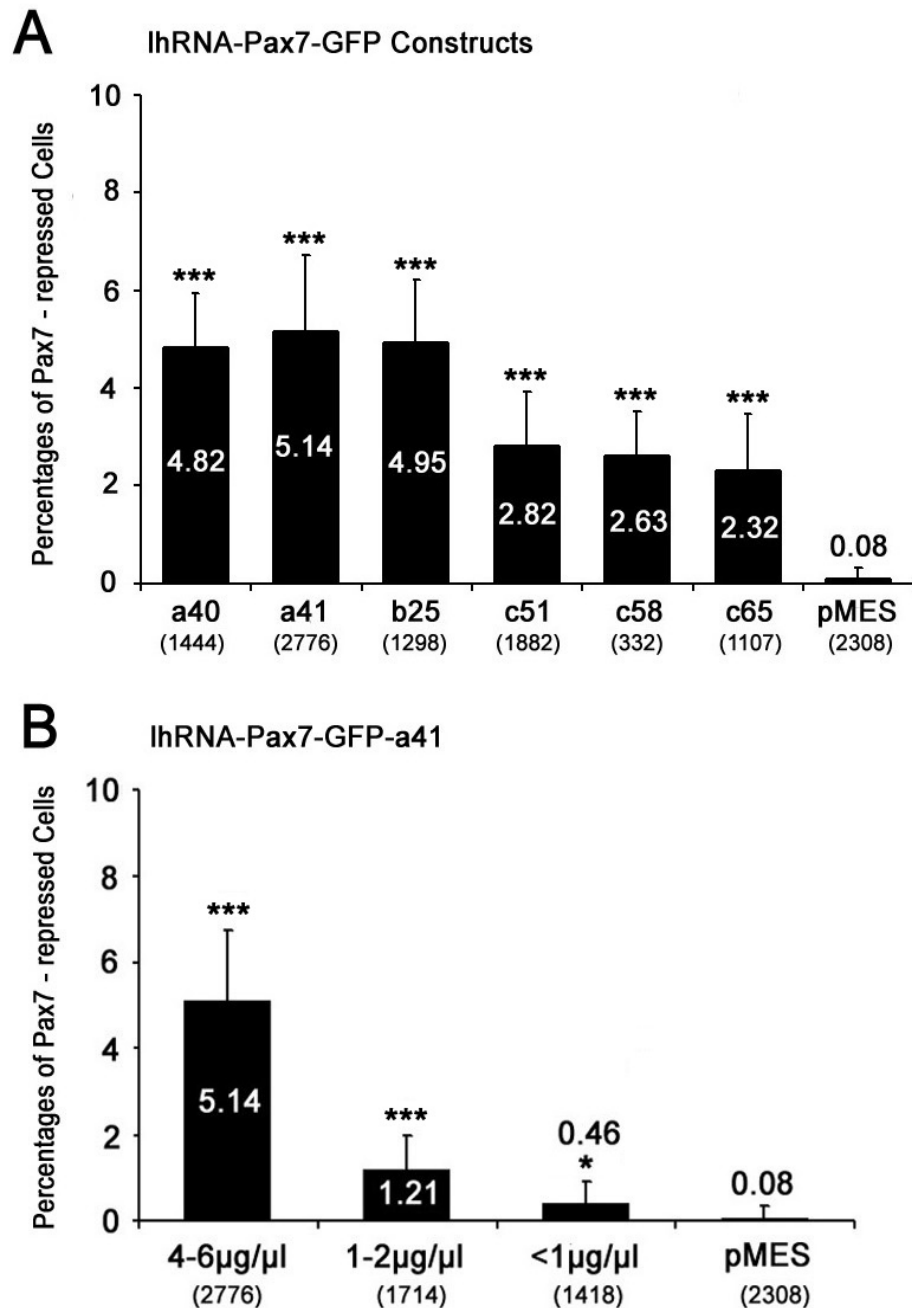


Figure 74: Quantitative analysis of the protein repression in the dorsal cells by lhRNA-Pax7 constructs

A: The midbrains were transfected with six lhRNA-Pax7 constructs at stage 10 and fixed in 24 hours. The constructs fall into 3 groups according to the insert, dsA (a40, a41), dsB (b25) and dsC (c51, 58, c65). The percentages of Pax7 - repressed dorsal cells among the total transfected cells were calculated. For each construct, 5 to 17 embryos were analyzed. The percentages of Pax7 - repressed cells by the constructs containing the dsA and dsB were nearly double as the dsC construct. Transfection with the six constructs all showed a higher percentage of Pax7 - repressed cells compared to GFP control midbrains with pMES vector (*t*-test, $P < 0.001$). However, no significant difference was found among them (*F*-test, $P > 0.10$). The number of the total transfected cells is indicated in the brackets.

B: Dorsally transfection with lhRNA-Pax7-GFP-a41 construct at different concentrations showed the 4 - 6 µg/µl DNA ($n = 13$) resulted in the highest percentage of Pax7-repressed cells among the 3 groups, and the ratio was decreased at low concentration. The percentages of 4 - 6 µg/µl and 1 - 2 µg/µl DNA were significantly higher than the pMES controls (*t*-test, $p < 0.001$), but < 1 µg/µl group only showed a slightly higher ($P < 0.05$).

To evaluate the possible role of Pax7 on the neurogenesis, which was not achieved by mutants (Mansouri and Gruss, 1998), the expression of *Pax6*, *Brn3a* and *Lim1* mRNA, and Isl-1, Lim2 proteins were investigated. All of these genes did not show significant changes in the midbrains due to the transfection of lhRNA-Pax7 constructs (data not shown). In addition, the expressions of inductive signals, such as BMP4, BMP7 (Liem *et al.*, 1995; Nguyen *et al.*, 2000), were not affected as well (data not shown).

2. Short-hairpin siRNA (shRNA) Experiments

In the past few years, RNAi approach was used to repress gene expression in diverse plants and invertebrates, but it was still less successful in mammalian cells. This might be due to that long dsRNA can cause a powerful interferon (IFN) response, resulting in sequence-nonspecific mRNA degradation of many genes and rapid cell death through activation of dsRNA-dependent protein kinases PKR or other molecules (Clemens and Elia, 1997; Stark *et al.*, 1998; Williams, 1999; Alexopoulou *et al.*, 2001; Jackson *et al.*, 2003; Persengiev *et al.*, 2004). However, the IFN response can not be evoked by short dsRNA molecules of less than 30 - nt (Elbashir *et al.*, 2001; Harborth *et al.*, 2001; Chesnutt and Niswander, 2004). Therefore, short hairpin siRNA constructs for Pax7 gene were also produced and transfected into chick midbrains. The efficiencies of them on gene knockdown were compared to the long-hairpin dsRNA constructs tested previously.

Preparation of shRNA – Pax7 Constructs

To construct the short-hairpin siRNA (shRNA), four specific 19 - nt sequences were selected from the Pax7 coding region using an Ambion program (http://www.ambion.com/techlib/misc/siRNA_finder.html). They were located immediately downstream of an AA dinucleotides (Elbashir *et al.*, 2002), starting at the position +121, +492, +549 and +1206, respectively. The first and the last sequence were located within the paired domain and transactivation domain, respectively. Using four 19-nt sequences as queries, identical sequences in other genes were not found by a BLAST program (<http://www.ncbi.nlm.nih.gov/BLAST/>). The shRNA insert was achieved by annealing a pair of forward and reverse oligonucleotides (Fig. 75). The forward one is composed of a 19-nt sense sequence, the reverse complementary antisense sequence with 5 - 6 Ts, and a 9 - nt loop (TTCAAGAGA) in between (Fig. 91). The reverse oligonucleotides is the complementary sequence to the forward one. Thus, the RNA transcribed from this shRNA insert should fold to become a 'stem - loop' structure comprising a 19-nt double-stranded stem and a 9 - nt loop with 2 Us at the 3' end.

For cloning into different vectors, two sets of shRNA inserts with specific recognition sites at both ends were prepared (Tab. 7). The shRNA inserts containing *EcoRI* and *ApaI* restriction sites were used to clone into p*Silencer*TM 1.0-U6 siRNA expression vector (Ambion). In this vector (Fig. 90), the unique *ApaI* site is adjacent to the mouse U6 promoter, which is located at upstream of the MCS, and the second G of the *ApaI* site is predicted to start the RNA transcription (Sui *et al.*, 2002). To clone into the pMES vector, the shRNA inserts with a *Bam*HI site at the 3' end were used. Both shRNA inserts were transformed into *SURE*^{®2} supercompetent cells, and the clones were checked and selected by mini PCR with specific primers or restrictive digestion (Fig. 76), and confirmed by DNA sequencing. Representative shRNA constructs containing different inserts were isolated with endotoxin-free kit and used in the following *in ovo* electroporation.

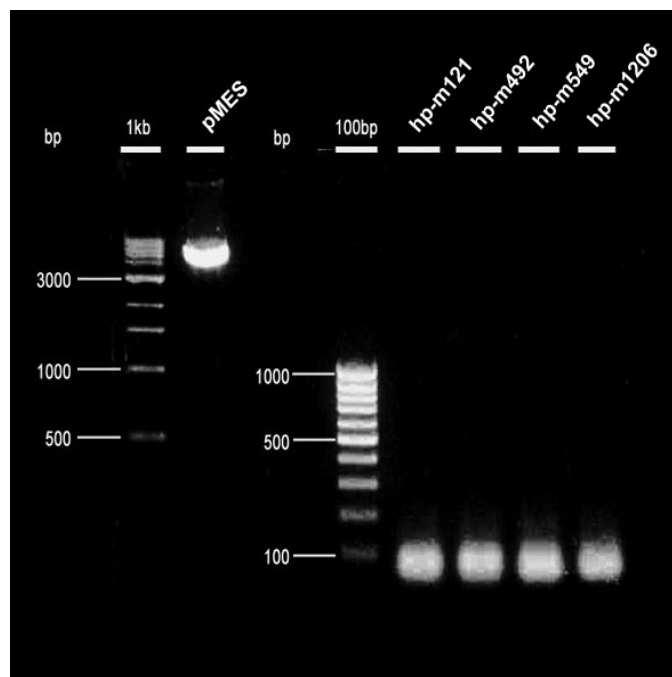


Figure 75: The annealed shRNA inserts for cloning into the pMES vector

Four pairs of forward and reverse shRNA oligonucleotides (m121f/r, m492f/r, m549f/r and m1206f/r) were annealed to form double-stranded shRNA inserts – hp-m121, -m492, -m549 and -m1206, which are all 57 base pairs. The pMES vector (ca. 5.5 kb, in the left lane) was prepared by a double digestion with *EcoRI* and *Bam*HI for accepting the above shRNA inserts.

100 bp and 1 kb DNA ladders were used as size standards.

Transfection of pMES - based shRNA – Pax7 Constructs

The four pMES-based shRNA – Pax7 constructs, m121, m492, m549 and m1206, contained different short sequences of chick Pax7 gene. 1 - 2 $\mu\text{g}/\mu\text{l}$ of each construct was used to electroporate into chick midbrains at stages 9 - 12. After 24 - 36 hours incubation, the embryos were fixed and stained with an antibody against Pax7 protein. The transfection was visualized by the co-expressed GFP. In appearance, less reduced midbrains were observed in the transfected embryos compared to the pMES - based long - hairpin dsRNA constructs (Tab. 27). Only eight m549 - transfected (11 %, n = 71) and one m1206 - transfected embryos (4 %, n = 23) displayed a smaller midbrain, whereas the rests look like normal. Further, the effect of the shRNA construct on Pax7 was checked at protein level.

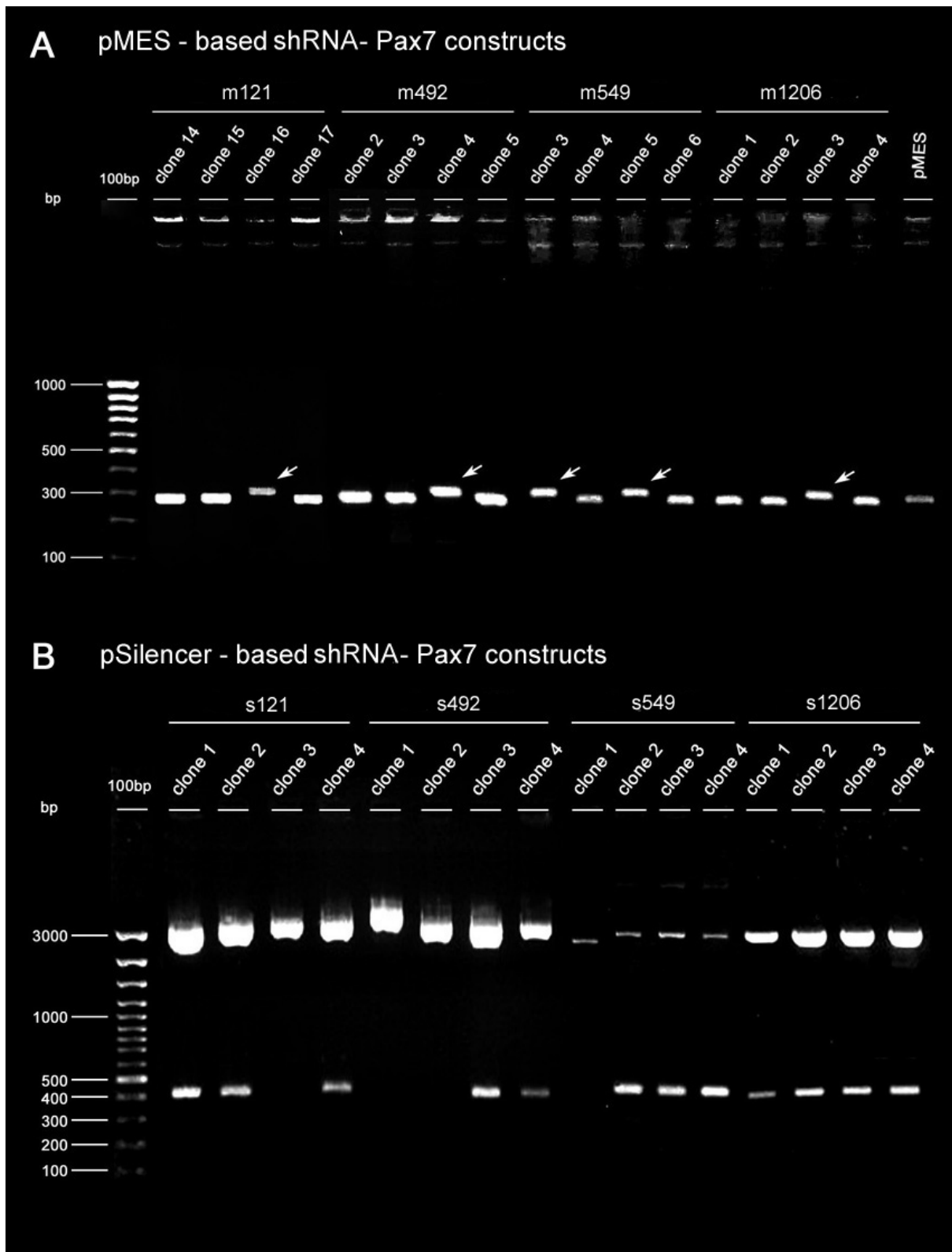


Figure 76: Sequential analysis of the shRNA – Pax7 constructs

A: Sequential analysis of the pMES - based shRNA – Pax7 constructs by mini PCR. Four types of constructs contained different shRNA sequences but in same size. The constructs containing shRNA inserts (indicated by arrows) showed a longer PCR product as expected, whereas the empty vectors produced a short one exactly as the pMES vector in the right lane. 100bp DNA ladder was used as a size standard.

B: Among the p*Silencer* 1.0 - U6 – based shRNA – Pax7 constructs, the s549 clones were checked by PCR, whereas the rests were evaluated by restrictive digestion with *Bam*HI. The expected produce is about 400 bp.

The immunostaining of Pax7 displayed that the transfections of four pMES – based shRNA constructs all did not cause a clear Pax7 repression in the midbrains as assumed (Fig. 77). Only a few midbrains transfected with the m549 (n = 5/32) and m1206 constructs (1/5) seemed to express Pax7 at a lower level in the transfected region compared to the intact control side (Fig. 77 H, K). Close views of these transfected midbrains (Fig. 78 D - F) showed some transfected dorsal cells did not express Pax7 any more. This Pax7 repression was largely correlated with a strong GFP expression, suggesting that more shRNA - Pax7 constructs m549 or m1206 were electroporated into these cells. However, Pax7 - repressed cells were hardly found in the m121 and m492 - transfected midbrains, even in strongly GFP expressing cells (Fig. 78 A – C), similar as the GFP control midbrains transfected with pMES vector (Fig. 78 G – I). The effects of m549 and m1206 constructs were also observed in the hindbrains and spinal cords (data not shown). Statistical evaluation in the midbrains transfected with the four shRNA constructs at stage 9 (Fig. 79 A) revealed that m549 transfection caused more dorsal cells stop to express Pax7 (3.27 %, n = 18) than the m1206 transfection (1.26 %, n = 5), and both ratios of the Pax7 – repressed cells were apparently different from the GFP controls (0.08 %, n = 16; *t*-test, *P* < 0.001 and 0.01). However, in the m121 and m492 - transfected midbrains less Pax7 – repressed cells were found (0.32 %, n = 5, and 0.37 %, n = 8) and the ratio is not significantly different with GFP controls yet (*P* > 0.05).

The effects of the transfection using different DNA concentrations and performed at different stages were also analyzed and compared. The results of m549 construct showed that the percentages of Pax7-repressed cells were only slightly decreased from stage 9 towards 12 (3.27 %, 2.85 %, 2.82 %, and 2.58 %, n = 18, 6, 5, and 3, respectively, Fig. 79 B), and all were significantly different from GFP controls (*t*-test, *P* < 0.001), however, no apparent differences among them (*F*-test, *P* > 0.05). The statistic analysis also indicated high DNA concentration resulting in more Pax7 - repressed cells (5.8 µg/µl, 8.27 %, n = 4; 1 – 2 µg/µl, 3.27 %, n = 18; *t*-test, *P* < 0.001; Fig. 79 C).

Table 27: Numbers of reduced midbrains by the transfection of pMES-based shRNA - Pax7 constructs

| shRNA – Pax7 Constructs | Reduced Midbrain (x/n) | | | | |
|----------------------------|------------------------|--------|--------|--------|--------|
| | HH 9 | HH 10 | HH 11 | HH 12 | SUM |
| m121 | 0 / 18 | 0 / 9 | 0 / 6 | 0 / 10 | 0 / 43 |
| m492 | 0 / 25 | 0 / 5 | 0 / 8 | - | 0 / 38 |
| m549 | 5 / 33 | 2 / 18 | 1 / 13 | 0 / 7 | 8 / 71 |
| m1206 | 0 / 13 | 1 / 7 | 0 / 3 | - | 1 / 23 |

The number (x) of chick embryos having a reduced ipsilateral midbrain after the transfection of four pMES - based shRNA – Pax7 constructs at stage (HH) 9 to 12 among the total number of the transfected embryos (n).

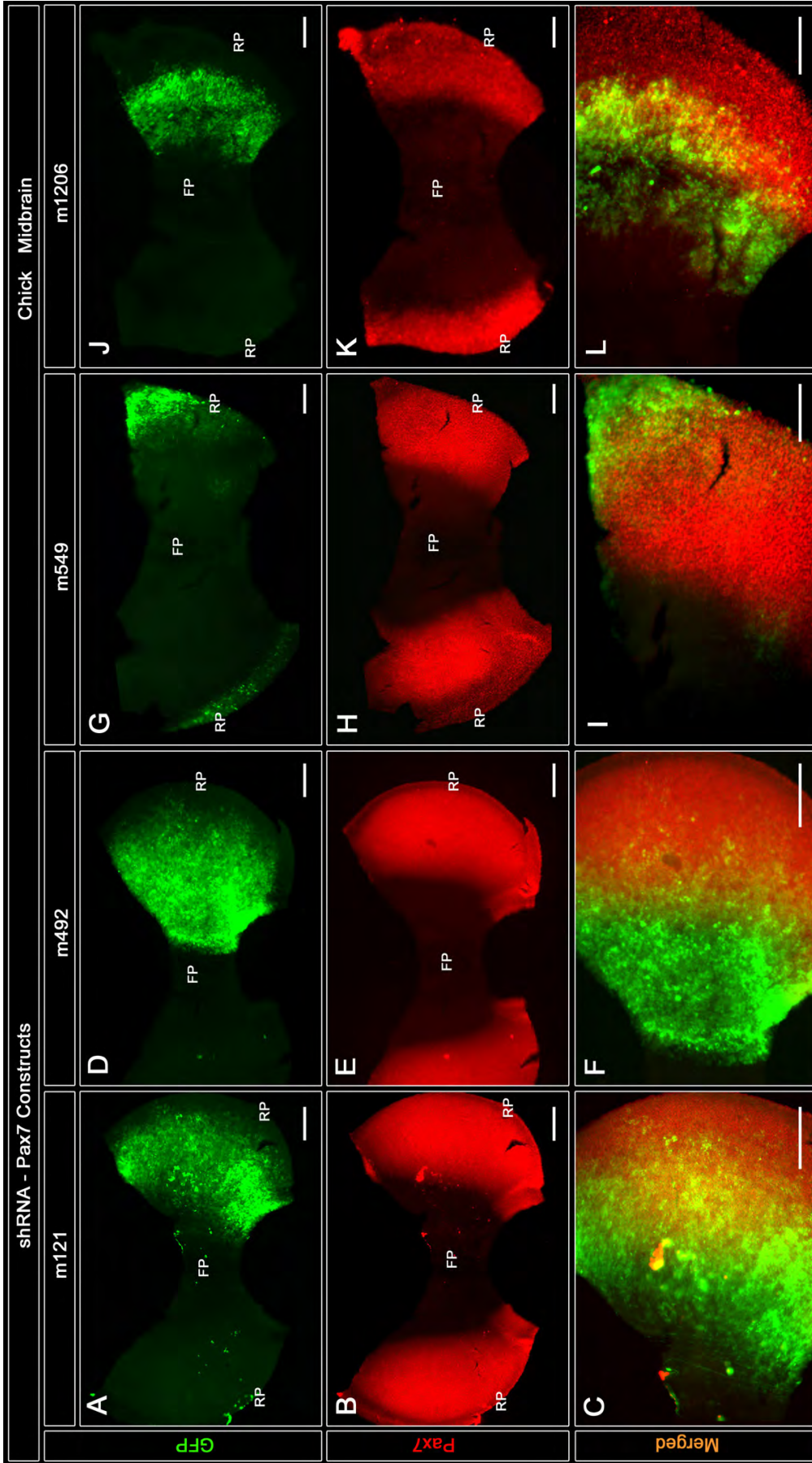


Figure 77: Protein expression of the midbrains transfected with pMES - based shRNA - Pax7 constructs

Chick embryos were transfected with four different pMES - based shRNA - Pax7 constructs at stage 9 and fixed in 24 hours. The Pax7 protein (red) was visualized by fluorescent immunostaining, and the transfection was indicated by the co-expressed GFP (green). The expression of Pax7 did not show significant changes in the midbrains transfected with m121 (A - C) and m492 (D - F). However, the m549 (G - I) and m1206 (J - L) transfected areas within the dorsal midbrains looked to express Pax7 weakly. C, F, I and L are the merged figures of the transfected side in AVB, D/E, G/H and J/K, respectively, in high resolution. Roof and floor plates are indicated. Abbreviations: FP, floor plate; RP, roof plate. Scale bar: 100µm.

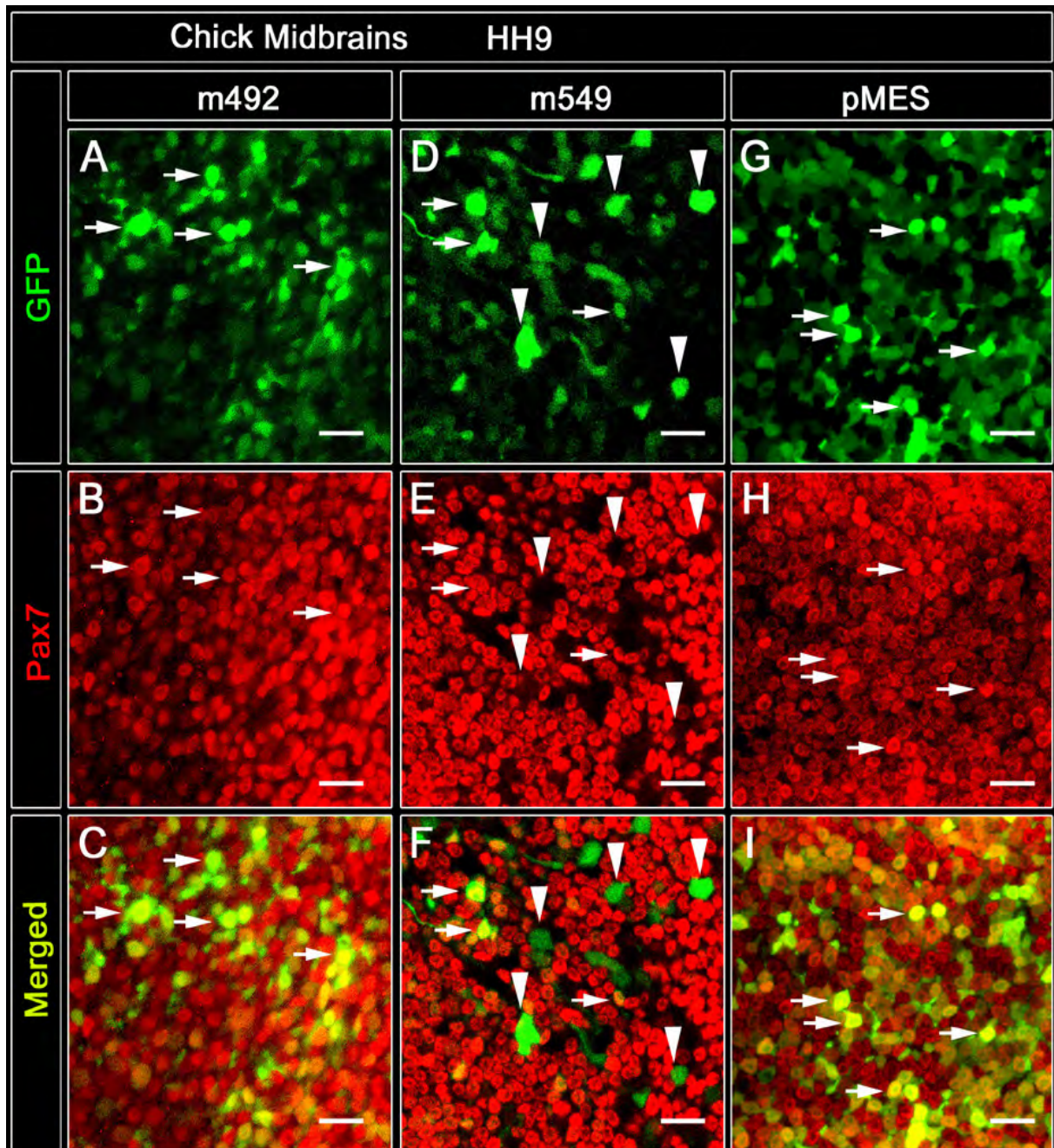


Figure 78: Protein expression in the dorsal cells transfected with pMES-based shRNA – Pax7 constructs

All chick midbrains were transfected with the pMES vector and the pMES-based shRNA – Pax7 constructs m492 and m549 at stage 9, fixed in 24 hours. The ‘open-book’ preparations of the midbrains were shown in high resolution. Anterior is up and dorsal to the right. The Pax7 protein (red) was illustrated by an immunostaining, and the transfected cells were determined by the co-expressed GFP (green).

A – C: A midbrain transfected with the m492 construct indicated that nearly all of the transfected cells (green in A) expressed Pax7 as a normal level (B) compared to their neighbor cells. Arrows represents such cells, even they co-expressed GFP strongly at the same time. Double staining of Pax7 and GFP was shown as yellow color in merged figure C.

D – F: The m549 - transfected midbrain revealed that Pax7 expression was repressed in a few transfected cells, which almost expressed GFP strongly (arrowheads). However, most of cells in the transfected area still expressed Pax7. Arrows point to the cells with double staining. The axons sending from neurons were also seen. F is the merged figure of D and E.

G – I: The pMES – transfected midbrain showed that no matter what level of GFP the Pax7 expression was similar in all cells. Arrows point to the strongly GFP – expressed cells.

Scale bar: 25µm.

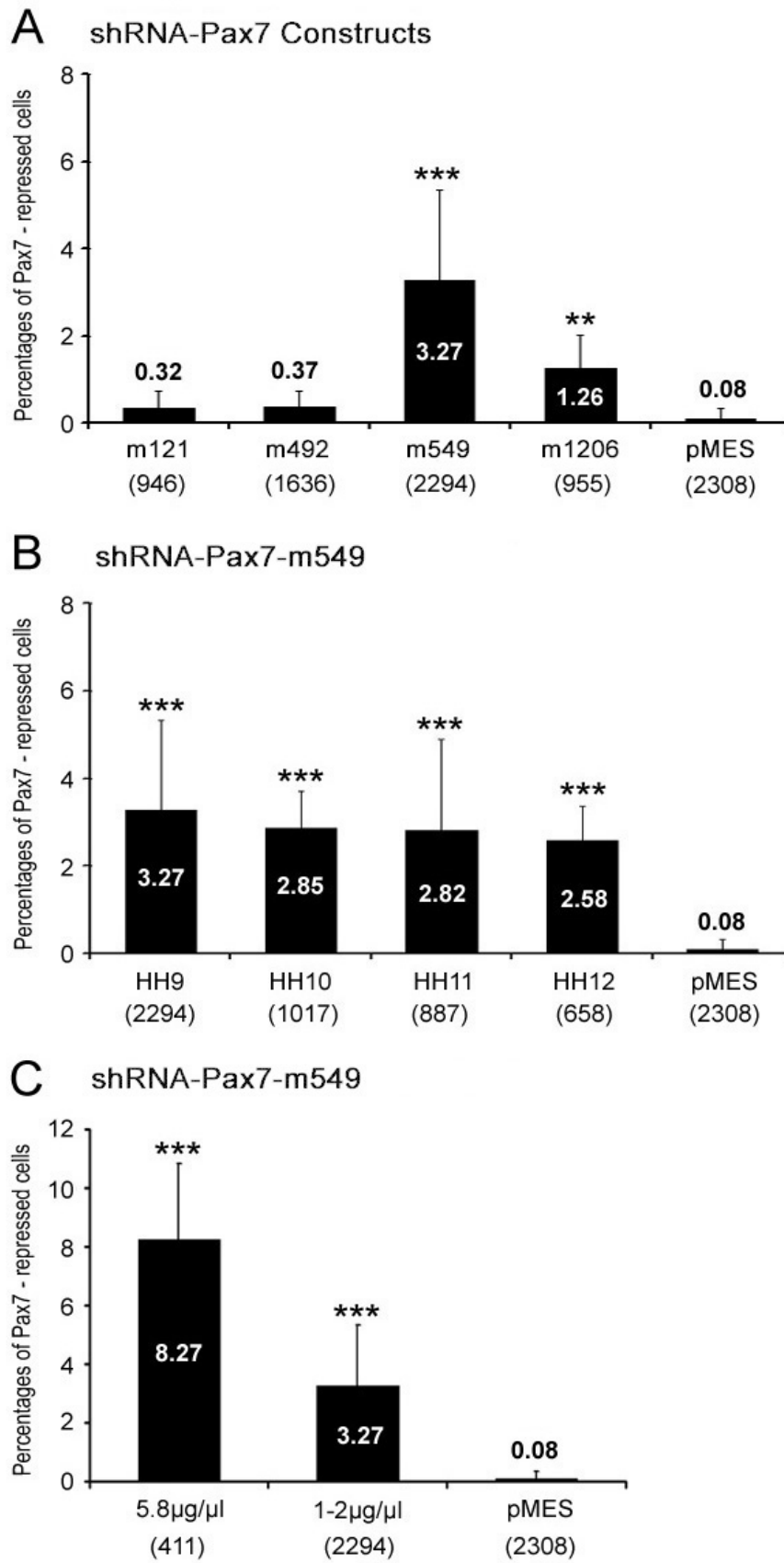


Figure 79: Quantitative analysis of the protein repression in the dorsal cells by pMES-based shRNA – Pax7 constructs

Figure 79: Quantitative analysis of the protein repression in the dorsal cells by pMES-based shRNA – Pax7 constructs

A: Chick dorsal midbrains were transfected with 1 – 2 $\mu\text{g}/\mu\text{l}$ of four pMES – based shRNA – Pax7 constructs at stage 9 and fixed in 24h. The percentage of Pax7 - repressed cells (GFP⁺/Pax7⁻) in all transfected dorsal cells (GFP positive) was evaluated. At least 900 transfected cells by each construct on 5 to 18 midbrains were analyzed. The transfection of the m549 construct resulted in most of Pax7 – repressed cells among the four constructs, and the m1206 transfection also caused Pax7 repression as well. Both ratios were significantly different with the GFP controls ($P < 0.001$ and 0.01). However, the m121 and m492 constructs did not cause significant repression of Pax7 compared to GFP controls ($P > 0.05$). The GFP midbrains transfected with pMES vector showed a neglectable amount of GFP⁺/Pax7⁻ cells (0.08 %) as controls.

B: Comparison of the midbrains transfected with m549 at stage 9 to 12 showed the reduction of Pax7 – repressed cells from 3.27 % – 2.58 % with the time, and all ratios were significantly different with GFP controls (t -test, $P < 0.001$). However, the differences among them were not significant (F -test, $P > 0.05$). 3 to 18 midbrains at each stage were analyzed.

C: The m549 transfection at stage 9 using different concentrations showed that the percentage of Pax7 - repressed cells by 5.8 $\mu\text{g}/\mu\text{l}$ was 2.5 times higher than that of the 1 – 2 $\mu\text{g}/\mu\text{l}$ transfection (t -test, $P < 0.001$). Both ratios were significantly higher than the GFP controls ($P < 0.001$).

The number of the transfected cells is indicated in the brackets.

Transfection of pSilencer 1.0-U6 – based shRNA – Pax7 Constructs

Next, two types of pSilencer 1.0-U6 – based shRNA constructs for Pax7 gene – s121 and s549 – were evaluated the effect on protein repression. The rest two pSilencer – based constructs – s492 and s1206 were not tested here, since they were assumed to produce the same short dsRNAs as m492 and m1206 constructs, respectively, which have displayed no or less efficiency on Pax7 repression. Compared to pMES – based shRNA constructs, these constructs contained a mouse U6 promoter instead of chick β – actin promoter and lacked a GFP reporter after an IRES site (Fig. 90). 2 $\mu\text{g}/\mu\text{l}$ of the each construct was transfected into the dorsal midbrains at stage 9 to 12. To visualize the transfected cells, pCA β - GFP vector was co-transfected simultaneously. This vector contains a mGFP6 downstream from CMV-IE enhancer/CAG promoter, which produces a brighter green fluorescence (Fig. 80 A, C).

In totally, the results of s549 transfection indicated that majority of embryos (76 %, $n = 62$) developed into smaller ipsilateral midbrains (Tab. 28). This morphological change in the midbrain was apparent when the transfection was performed at earlier stages, i.e. about 80 % at stage 9/10 compared to 30 - 40 % at stage 11/12. In contrast, no smaller midbrain was observed in the s121 – transfected embryos ($n = 16$). This morphological differences between the two pSilencer-based shRNA constructs also reflected in the protein level (Fig. 80). 8 out of 13 embryos displayed an obvious Pax7 repression in the midbrains when the s549 construct was transfected at stage 9/10 (Fig. 80 C and D). At the same stages, s121 transfection did not result in such a Pax7 repression in the midbrains ($n = 5$, Fig. 80 A and B). Instead, the Pax7 was still expressed symmetrically in both dorsal regions. This difference was confirmed by high resolution (Fig. 81). Nearly all of the s121 – transfected dorsal cells expressed Pax7 at a normal level (Fig. 81 A – C), however, only a small part of s549 – transfected dorsal cells still expressed Pax7 (Fig. 81 D – I), and these

expressing cells seemed to be located close to the roof plate (Fig. 80 D, Fig. 81 E). These protein – repressed cells mostly expressed strong GFP signal and their neighbor cells could keep to express Pax7 as normal, suggesting the shRNA only functioned in the transfected cells and this repression of Pax7 was not spread from cell to cell. The transfection at stage 10 (Fig. 81 G – I) also resulted in a prevailing protein repression in the dorsal midbrain, however, less Pax7 – deficient cells were observed compared to the stage 9 transfection. Statistical analysis indicated that the Pax7 was reduced or absent in over 90% of s549 - transfected cells at stage 9 (Fig. 82 A, n = 10), and this percentage was still about 50 % at one stage later when Pax7 started to be expressed normally (Fig. 82 B, n = 6). However, the ratios decreased to less than 20 % at stage 11 and 12 (Fig. 82 B, n = 4 and 3, respectively). The effect on protein repression was significantly different between at stage 9/10 and at later stages 11/12 ($P < 0.001$), however, no significant difference between stage 11 and 12 ($P > 0.05$). Compared to GFP controls, these ratios of Pax7 – repressed cells were all significant high (t -test, $P < 0.001$). In contrast, no significant effect of s121 construct on protein repression was indicated (Fig. 81 A; n = 5, $P > 0.05$).

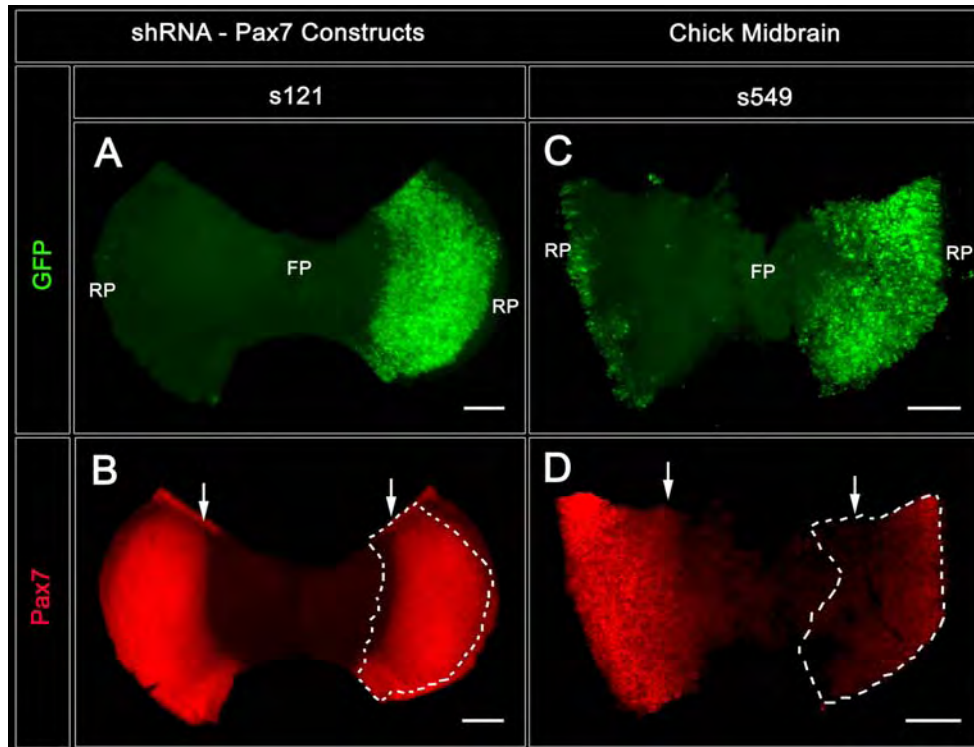


Figure 80: Protein expression in the midbrains transfected with pSilencer-based shRNA – Pax7 constructs

Chick embryos were transfected with pSilencer-based shRNA – Pax7 constructs at stage 9 and fixed in 28 (A, B) or 20 hours (C, D). pCA β -GFP vector was co-transfected as a marker simultaneously. The ‘open-book’ prepared midbrains were stained with Pax7 (red) and GFP (green). Anterior is up. Roof and floor plates are indicated.

A, B: A midbrain transfected with the s121 construct showed that the expression pattern of Pax7 was symmetrical on the transfected (right) and control sides. The transfected area was marked (B).

C, D: The s549 - transfected midbrain showed that the Pax7 was strongly repressed in the transfected region (the marked area in D) compared to the control side (left). Note: the transfected side of the midbrain was smaller.

Abbreviations: FP, floor plate; RP, roof plate. Scale bar: 100 μ m.

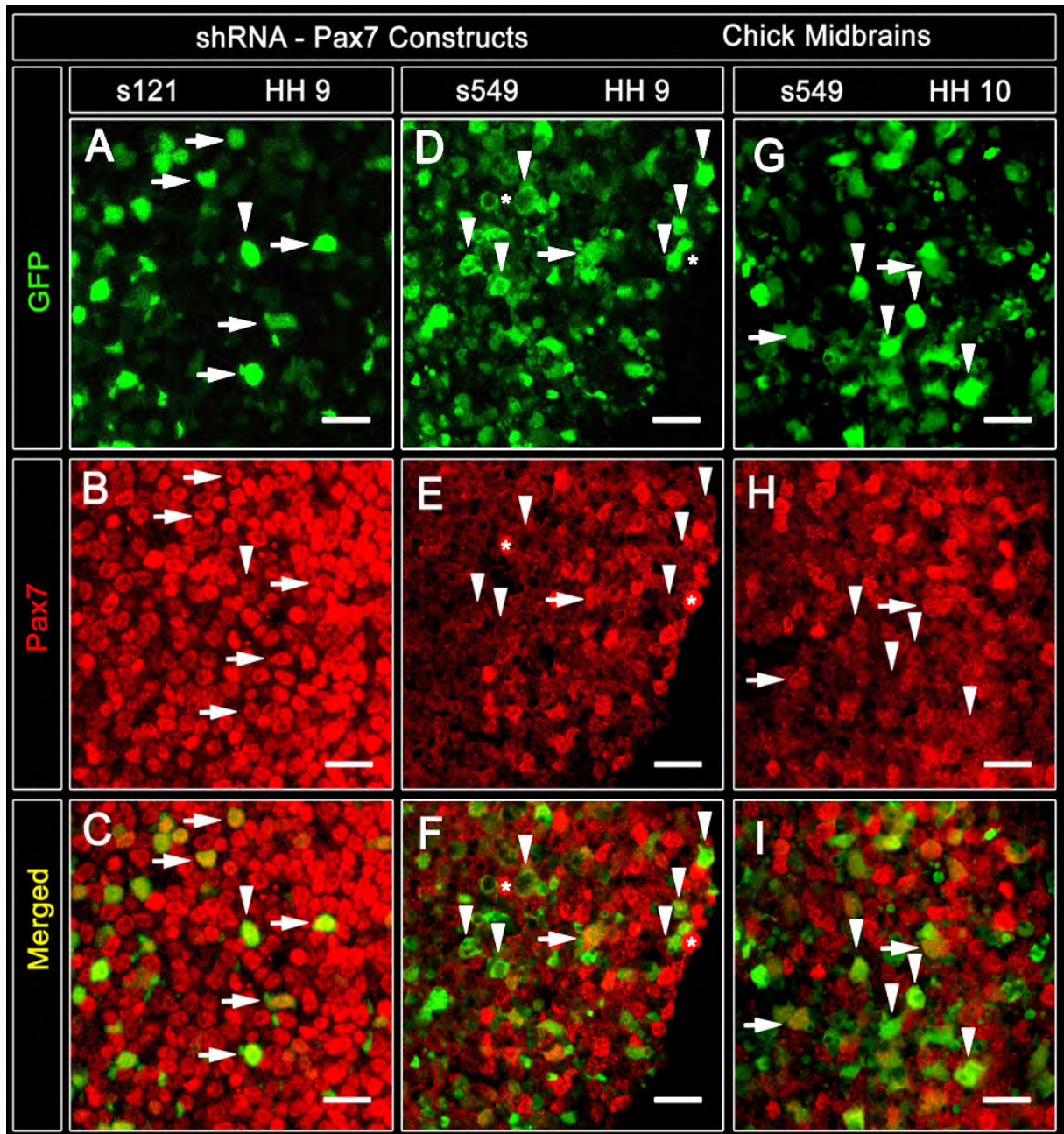


Figure 81: Protein repression in the dorsal cells transfected with p*Silencer*-based shRNA constructs

Chick embryos were transfected with p*Silencer*-based shRNA – Pax7 constructs at stage 9/10 and fixed in 24 hours. pCAB-GFP vector was co-transfected as a marker. Magnifications of a transfected area in the dorsal midbrains were illustrated with GFP (green) and Pax7 (red). Anterior is up, and dorsal to the right.

A – C: s121 transfection did result in a significant Pax7 repression in most of cells. Arrows point to the GFP positive cells, which still expressed Pax7 clearly as normal level (yellow or orange in C). However, Pax7 expression seemed to be repressed in a few transfected cells (arrowheads). C is the merged figure of A and B. Double staining of Pax7 and GFP was shown in yellow.

D – F: Transfection of s549 at stage 9 resulted in a strongly Pax7 repression in most of the transfected cells. Arrowheads represent such cells. The non – GFP expressing cells (asterisk) nearby the Pax7 – repressed cells kept to express Pax7 clearly as normal. A few of both staining cells were still found (arrows). F is the merged figure of D and E.

G – I: Transfection of s549 at stage 10 also resulted in a prevailing Pax7 repression in the dorsal midbrain. Both GFP expressing cells with (arrows) or without Pax7 co-expression (arrowheads) were detectable. I is the merged figure of G and H.

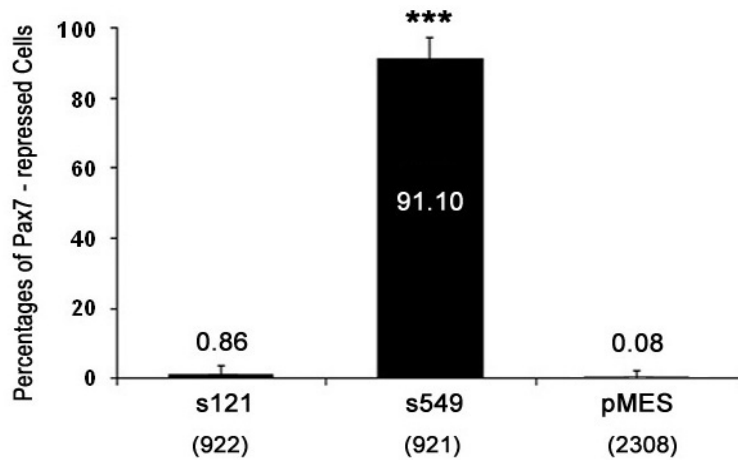
Scale bar: 25µm.

Table 28: Numbers of reduced midbrains by the transfection of p*Silencer* - based shRNA – Pax7 constructs

| shRNA – Pax7 Constructs | Reduced Midbrain (x/n) | | | | |
|----------------------------|------------------------|---------|-------|-------|---------|
| | HH 9 | HH 10 | HH 11 | HH 12 | SUM |
| s121 | 0 / 7 | 0 / 6 | 0 / 3 | - | 0 / 16 |
| s549 | 31 / 36 | 12 / 16 | 3 / 7 | 1 / 3 | 47 / 62 |

The number (x) of chick embryos showing reduced midbrains after the transfection with p*Silencer* – based shRNA – Pax7 constructs in total number of transfected embryos (n). Interestingly, the s549 displayed an apparent effect on the midbrain in size.

A shRNA - Pax7 Constructs



B shRNA - Pax7 - s549

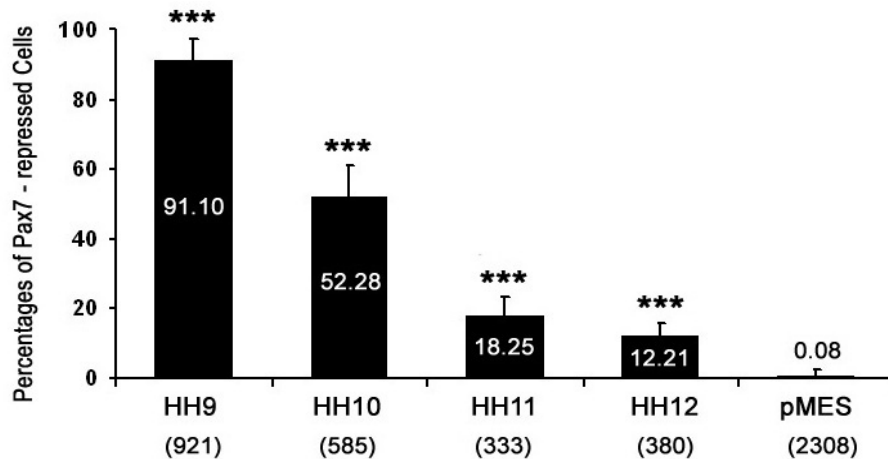


Figure 82: Quantitative analysis of protein repression in the dorsal cells by p*Silencer*-based shRNA – Pax7 constructs

A: The expression of Pax7 was largely repressed by s549 construct in chick midbrains when transfected at stage 9 ($P < 0.001$), while the s121 did not cause Pax7 reduction ($P > 0.05$). The pMES - transfected midbrains at stage 10 were used as controls.

B: The transfection of s549 showed that the ratios of Pax7 - repressed cells were decreased from 90 % to 10 % at stage 9 towards 12. The differences of this ratio among them were significant (t -test, $P < 0.001$), except the stage 11 with 12. ($P = 0.14$).

The number of the transfected cells is indicated in the brackets.

3. Antisense DNA Oligonucleotides Experiment

Nowadays the knockdown technique with antisense DNA oligonucleotides is still used in many fields (Grunweller *et al.*, 2003; Wang *et al.*, 2004; Jekerle *et al.*, 2005; Schillaci *et al.*, 2006). To investigate the effect of DNA oligos in chick embryos *in vivo*, two antisense DNA oligonucleotides (Tab. 6) were designed to be complementary to chick Pax3 and Pax7 genes, one at the beginning of the coding region (including the 1st ATG, cP3Di1/cP7Di1) and another in the middle (including the 2nd ATG, cP3Di2/cP7Di2). These antisense DNA oligonucleotides (MWG Biotech) at different concentrations (5, 2.5 and 1 $\mu\text{g}/\mu\text{l}$) were transfected into chick dorsal midbrains at stage 9 – 12 with pCA β - GFP vector simultaneously. At the same time, 2.5 $\mu\text{g}/\mu\text{l}$ of pCA β -GFP vector was transfected as control. Unfortunately, the analysis of the transfected midbrains did not show any obvious reduction of Pax3/7 expression (for Pax7, Fig. 83, for Pax3, data not shown).

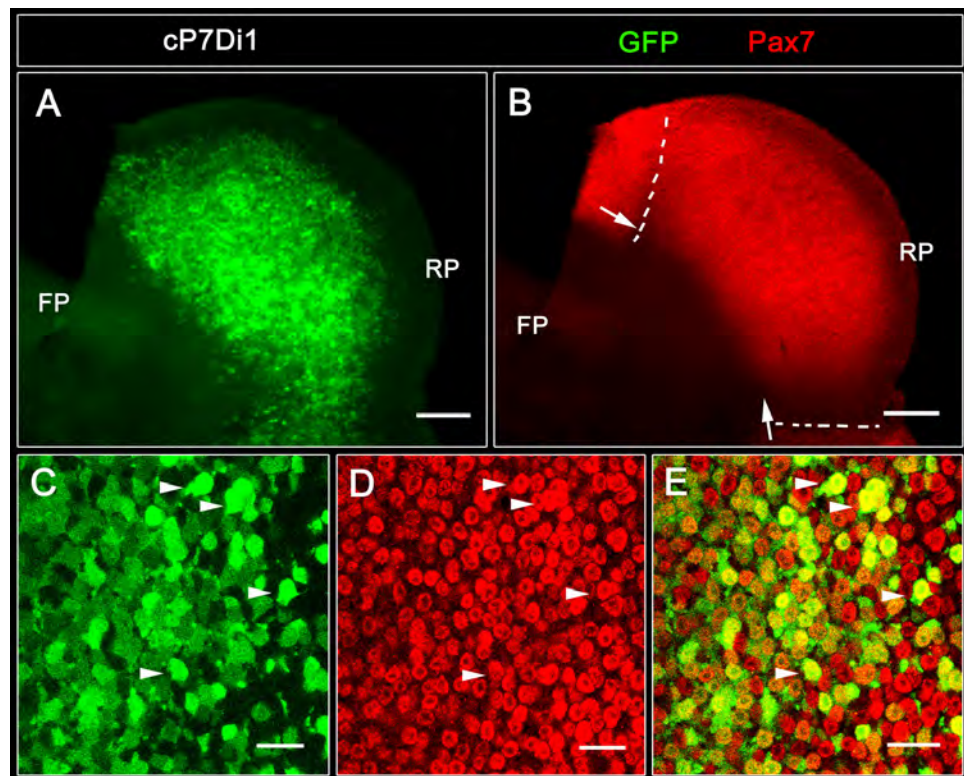


Figure 83: The protein expression in the midbrain transfected with antisense DNA oligonucleotides

Chick embryos were transfected with cP7Di1 at stage 10 and fixed in 24 (C - E) or 36 hours (A, B). Pax7 Protein (red) was stained by immunostaining and the transfected cells were marked by GFP (green). Anterior is up, and dorsal to the right.

A, B: The transfection of cP7Di1 (A) did not result in an obvious repression of Pax7 (B) in the dorsal midbrain. The boundaries of midbrain with diencephalon and hindbrain and DV border are indicated by dotted lines and arrows, respectively. The roof and floor plates are also marked.

C - E: Close view of a cP7Di1 - transfected area of a dorsal midbrain showed that nearly all transfected cells (green) still expressed Pax7 protein. Arrows indicate such double labelling cells, which was shown in yellow in the merged figure (E) of C and D.

Abbreviations: FP, floor plate; RP, roof plate. Scale bar: A, B, 100 μm ; C - E, 25 μm .

Statistical analysis clearly confirmed the above observations as the Pax3 or Pax7 - repressed cells was less than 1 % of the total transfected cells, which were not significantly different from the control midbrains with pCA β - GFP vector (Fig. 84 A, *t*-test, all *P* > 0.05). Meantime, the results also indicated that the influence of these antisense DNA oligos on Pax7 expression was not related with their concentrations (Fig. 84 B). In addition, two antisense DNA oligos (cOpbDi1/2) against Rab23 were checked without effect too (data not shown).

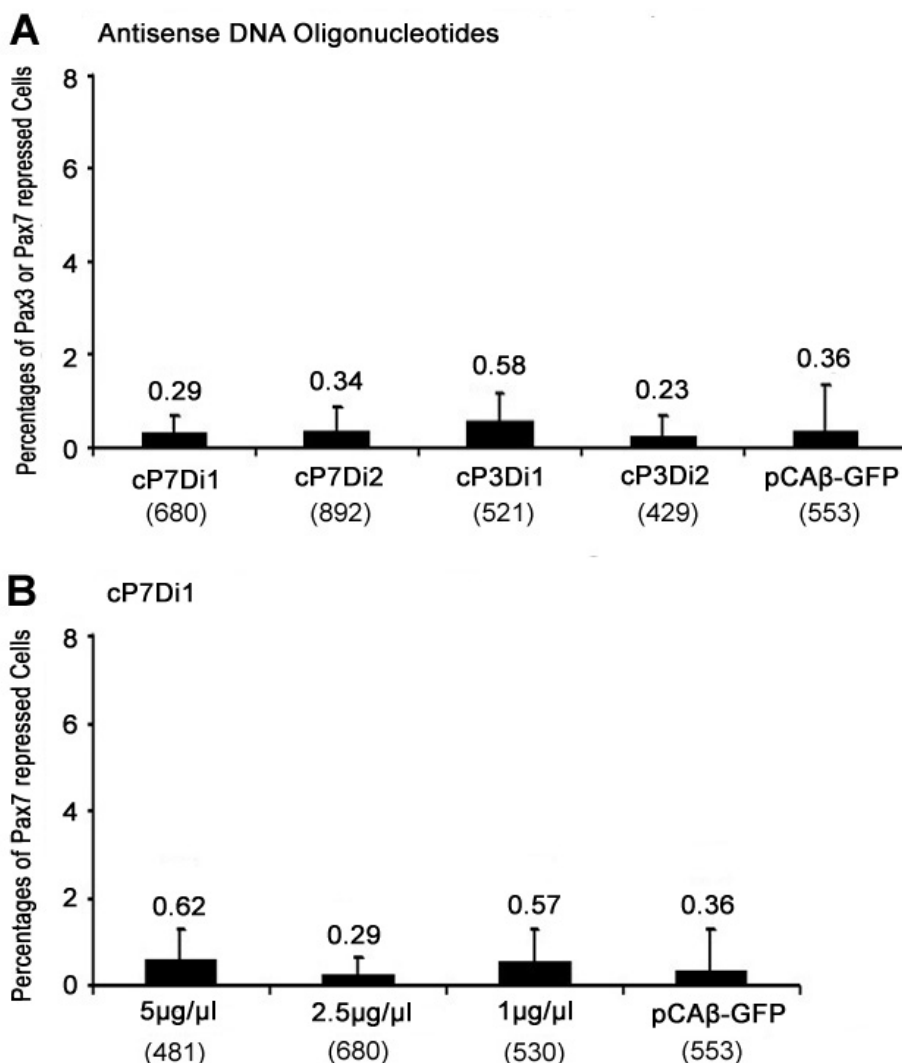


Figure 84: Quantitative analysis of protein repression by antisense DNA oligonucleotides

A: 2.5 μ g/ μ l of each antisense oligonucleotides was transfected into chick dorsal midbrains at stage 10. 4 – 6 transfected embryos in each item were evaluated. The expression of Pax7 was not obviously repressed by the antisense DNA oligonucleotides – cP7Di1 and cP7Di2, specific for chick Pax7 gene. The other 2 antisense oligonucleotides – cP3Di1 and cP3Di2 did not show any effect on Pax3 expression. Their sequences are highly similar with cP7Di1 and cP7di2, respectively. The ratios of Pax3 or Pax7 repressed cells were not significantly different from the GFP controls (*t*-test, *P* > 0.05). The expression of Pax7 in the midbrains transfected with pCA β - GFP vector was used as control (*n* = 4).

B: Comparison of different concentrations of cP7Di1 (*n* = 4, 5 and 4, respectively) at stage 10 showed no significantly difference on Pax7 repression (*P* > 0.05).

The number of the transfected cells is indicated in the brackets.

4. Morpholino Oligonucleotides Experiment

Antisense morpholino-modified oligonucleotides (morpholinos; MO) are testified to be effective and specific translational inhibitors in zebrafish, frog, mouse and other species (reviews see Summerton and Weller, 1999; Ekker and Larson, 2001; Heasman, 2002). Several authors also showed the efficacy of morpholinos in chick embryos (Tucker, 2001; Kos *et al.*, 2003; Chen *et al.*, 2004a). To compare the efficiency of the short - hairpin dsRNAs in chick embryos, antisense morpholino oligonucleotides were designed specific against Pax7 (Pax7-MO1/2, Tab. 3) and Rab23 genes (Rab23-MO1/2). These 25mer morpholinos are complementary to the 5' UTR of the target genes in principle. However, because of the high GC % content in 5' UTR of Pax7 gene, the selected sequences from this gene are a little far from the start codon. Two Pax7 morpholinos were transfected into midbrain or other brain regions at stages 9 to 12 with the pCA β -GFP vector, which marked the transfected cells. Different concentrations of the morpholinos (1.0, 0.5, 0.25 and 0.1 mM) were tested for their efficiency. After 24 hours of incubations, the embryos were fixed and stained for Pax7 and GFP proteins or *in situ* hybridisation for *Rab23* gene.

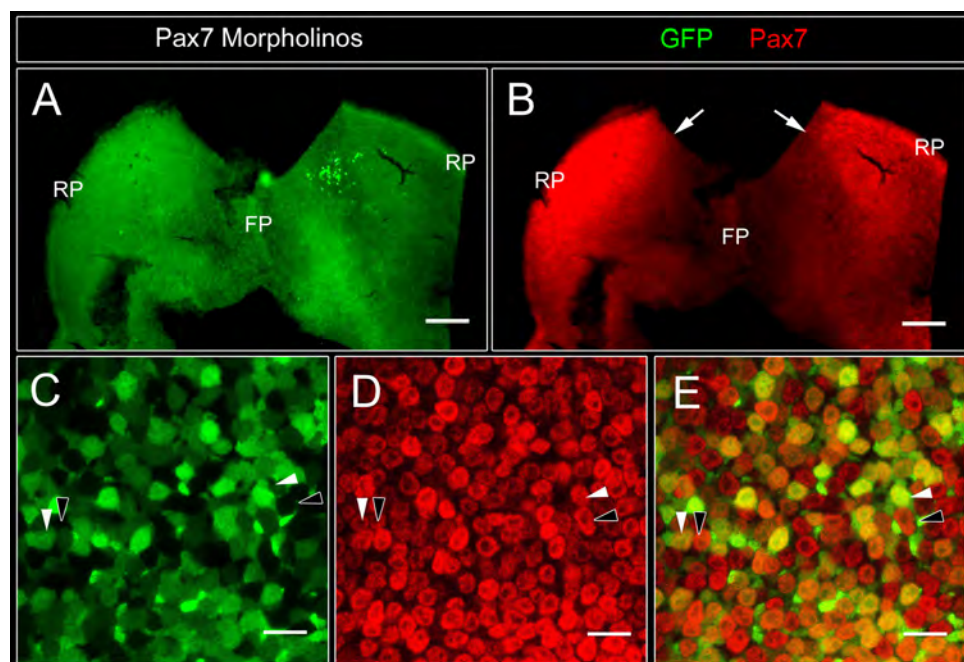


Figure 85: The protein expression in the midbrains transfected with antisense morpholinos against Pax7 gene

Chick midbrains were transfected with antisense morpholinos for Pax7 gene (0.5 mM) at stage 9, and fixed in 24 hours. pCA β -GFP vector (2.5 $\mu\text{g}/\mu\text{l}$) was co-transfected simultaneously. 'Open-book' prepared midbrains were labelled with Pax7 and GFP.

A, B: Pax7-MO2 was transfected in the right dorsal midbrain (green in A), however, no apparent effect on Pax7 expression was observed (B). Arrows indicate the DV border of the midbrain. Roof and floor plates are also marked.

C - E: A transfected area of a midbrain with Pax7-MO1 showed that Pax7 was still expressed in the GFP expressing cells (white arrowheads) at same level as their non-transfected neighbour cells (black arrowheads). E is the merge of figure C and D, where double staining is illustrated in yellow.

Abbreviations: FP, floor plate; RP, roof plate. Scale bar: A, B, 100 μm ; C - E, 25 μm .

The results showed both Pax7 morpholinos (Pax7-MO1/2) did not result in a significant repression on Pax7 protein (Fig. 85). Only the morpholinos against Rab23 (Rab23-MO1/2) resulted in a slight reduction on Rab23 expression in chick neural tubes at the concentration of 0.5 mM (n = 4/23). Interestingly, more of the analysed embryos were dead or showed morphological abnormalities after the transfection of 1.0 mM morpholinos (n = 9/14). Statistical analysis on Pax7 – MO1 transfected midbrains displayed that indeed the percentages of Pax7 – repressed cells were decreased from 2.5 - 1 % with the concentration of the solution from high to low (Fig. 86, n = 3 – 6 in each item). 0.5 mM of Pax7 - MO2 transfection (1.99 %, n = 4) resulted in a similar effect as Pax7 – MO1 with the same concentration. However, all ratios were not significantly different from the pCAβ-GFP controls (*t*-test, *P* > 0.05). In addition, the expression of several genes and proteins, like BMP4, Gli3, Nkx6.1 and Lim1/2, also did not display any significant change in the analyzed embryos (data not shown).

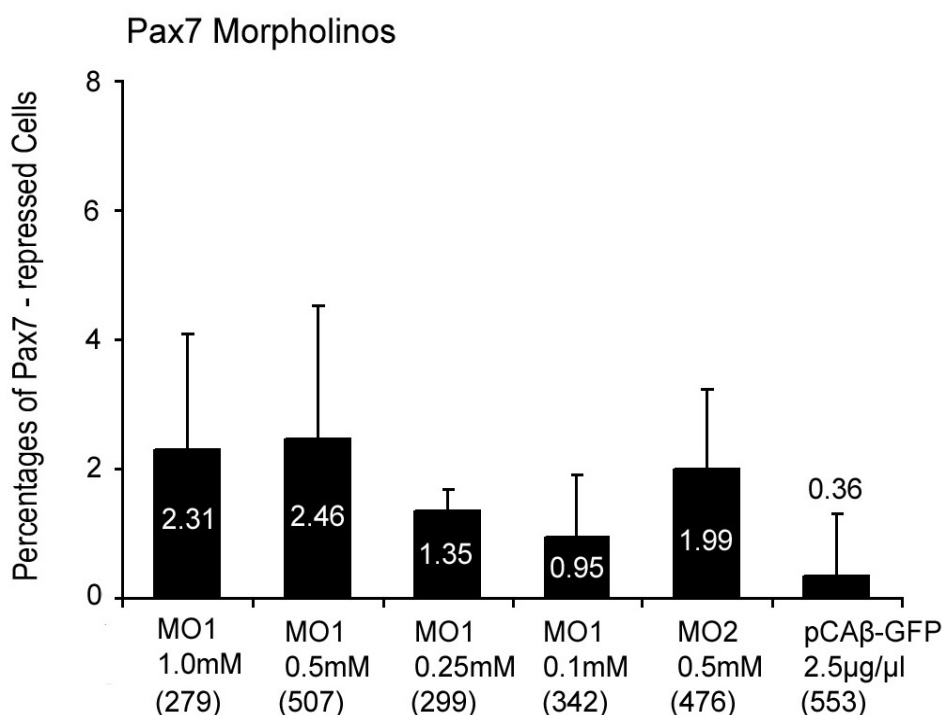


Figure 86: Quantitative analysis of protein repression by antisense morpholinos against Pax7 gene

Two antisense morpholino oligonucleotides against Pax7 gene (Pax7-MO1/2) were transfected into chick dorsal midbrains at stage 9 and fixed in 24 hours. 3 – 5 transfected embryos in each item were evaluated. The Pax7 repression by these two morpholinos was highest at the concentration of 0.5mM (2 - 2.5 %). The protein repression by Pax7-MO1 was decreased with the concentration from high to low (1.0mM – 0.1mM), however, no significant difference between them was found (*t*-test, *P* > 0.05). Compared to the pCAβ - GFP controls (0.36 %, n = 4), all transfection at different concentrations did not show a significant repression on Pax7 protein (*P* > 0.05).

The number of the transfected cells is indicated in the brackets.

5. Discussion

As a favored model for experimental developmental biology, chick embryo is easy to manipulate *in ovo*. In the past, the effect of molecular changes was studied using either transplants of secreted cells and tissues or by engrafting beads soaked with varying signaling proteins (Pagan-Westphal and Tabin, 1998; Lee *et al.*, 2001; Molle *et al.*, 2004). An approach to inject a function - blocking antibody for candidate genes has also proved to be successful to study axon guidance in nervous system (Stoeckli and Landmesser, 1995; Burstyn-Cohen *et al.*, 1999; Perrin *et al.*, 2001). Only a few years ago, a new technique of *in ovo* electroporation was introduced to misexpress or overexpress a gene in chick embryos (Muramatsu *et al.*, 1997; Itasaki *et al.*, 1999; Momose *et al.*, 1999; Inoue and Krumlauf, 2001; Swartz *et al.*, 2001). Since 2003 several laboratories tried to suppress gene expression using RNA interference (RNAi) in chick (Lee *et al.*, 2001; Hu *et al.*, 2002; Katahira and Nakamura, 2003; Pekarik *et al.*, 2003; Chesnutt and Niswander, 2004; Sato *et al.*, 2004). However, the effectiveness and reproducibility of this way of gene repression in chick embryos is still in question.

Gene Repression by Plasmid-based dsRNA in Chick Embryos

In the 90's, RNA interference (RNAi) is first discovered and used in modified plants (Napoli *et al.*, 1990; van der Krol *et al.*, 1990). From then its use spreads to simple organisms, such as the filamentous fungus *Neurospora crassa* (Romano and Macino, 1992; Cogoni *et al.*, 1996), the nematode worm *Caenorhabditis elegans* (Guo and Kemphues, 1995; Fire *et al.*, 1998) and the fruit fly *Drosophila melanogaster* (Kennerdell and Carthew, 1998; Hammond *et al.*, 2000). The use in plants and animals has shown that direct delivery of double stranded RNA (dsRNA) can result in mRNA degradation of a target gene. However, for mammalian cells, many works suggest that dsRNA cause sequence-nonspecific mRNA degradation of many genes and cell death (Clemens and Elia, 1997; Stark *et al.*, 1998; Williams, 1999; Alexopoulou *et al.*, 2001; Jackson *et al.*, 2003; Persengiev *et al.*, 2004). Although the success on repressing the expression of exogenous and endogenous genes has been reported by injections of dsRNA directly (Pekarik *et al.*, 2003), plasmids containing dsRNA transcribed sequences have the advantage that dsRNA is generated within the cells for several times (Chesnutt and Niswander, 2004). To know this, diverse dsRNA constructs were prepared with different types of expression vectors, and electroporated into chick midbrains and other brain regions to compare their effects of protein repression. These investigations illustrated that both long and short hairpin dsRNAs do destroy protein translation within the transfected cells. The effect was also obvious when the hairpin dsRNA was transcribed via the pMES vector, which has a chick actin promoter and generates a GFP protein with the help of an IRES site (Chen *et al.*, 2004b; Krull, 2004). However, the protein expression was

suppressed at a lower level compared to a U6 promotor plasmid – pSilencer 1.0-U6. This lower effect might be caused by the IRES site, which could hinder the processing of the long hairpin construct to siRNA nucleotides by the dsRNA - specific endonuclease dicer (Wang *et al.*, 2006). In many cases, the lower effect on gene downregulation, if any, accounts for the lack of morphological defects in RNAi treated embryos (Pekarik *et al.*, 2003). Fortunately, since Pax7 is a developmental gene, the effect of dsRNA constructs for this gene can be visible in this study.

Common to both sets of experiments was that not a complete downregulation of Pax7 expression took place, although cells expressed the shRNA duplex constructs. Two possibilities could be the reason. Firstly, the gene expression might not cease completely because not enough of dsRNA construct is generated to degrade Pax7 mRNA totally. This could be due to the lack of the RdRP-mediated amplification that has not been testified in vertebrates. In plants and *C. elegans*, this amplification produces the secondary RNAs (Lipardi *et al.*, 2001; Sijen *et al.*, 2001; Hoken *et al.*, 2002). In addition, most studies were performed in a time when quite a lot of cells are still proliferating. Therefore, there will be the dilution of the RNA hairpin containing plasmid in the daughter cells, which could be accompanied by an unequal allocation of the plasmid in the daughter cells. This is supported by this study as showed that the effect of gene repression depended on the concentration of the plasmid DNA. Secondly, one has to take into account the half-life of the affected proteins. dsRNA only prevents the generation of new protein, whereas the already generated proteins are not affected.

Using co-expression of two vectors – one transcribes the dsRNA and one expresses a marker protein like GFP to visualize the infected cells – should be performed with the same concentration to avoid wrongly labelled cells. This is especially important considering that a maximum of 60 % of the cells of the electroporated side are actually transfected with the reporter plasmid (Pekarik *et al.*, 2003). This handicap can be avoided using an expression vector expressing a GFP after an IRES site (like the pMES vector) or a bicistronic construct (Mangeot *et al.*, 2004).

Length of the Hairpins

Comparison of the effect of different hairpin constructs clearly showed that all of the selected long sequences (200 – 300 bp) did not result in strong effects on gene silencing (2.3 % - 5.1 %), whereas the short - hairpin dsRNAs (21 – 23 bp) expressed by the same vector displayed an obvious difference on gene downregulation. This suggests that the selectivity on the sequence is more important for short hairpin dsRNA construct than for long hairpin dsRNA. It might also convince a suggestion that the initiation of RNAi forms a specific dsRNA structure from diverse dsRNAs without requirements of sequence specificity (Collins and Cheng, 2006). However, it not only depends on the length and the position of the gene used as silencer (Brennecke *et al.*, 2005) but also on the vector. This work also

showed that shRNA duplex cloned into the - p*Silencer* vector with U6 promoter exhibited an even higher degree on gene repression than the same shRNA duplex in pMES vector. U6 promoter and H1 promoter are also used successfully by other scientists for siRNA constructs (Katahira and Nakamura, 2003; Chesnutt and Niswander, 2004; Mangeot *et al.*, 2004). This would imply that these promoters are better adapted to express shRNA duplexes than the beta-actin promoter in the pMES vector. However, as already discussed, the weaker gene repression by the pMES vector might be caused by the IRES site.

A local and Temporal Gene Silencing Available for Embryogenesis

The major vertebrate system widely used for genetic manipulations currently is by far the mouse (Muller, 1999; Jackson, 2001; Metzger and Chambon, 2001). However, since high costs, space, and time are required to produce genetically engineered mice, their usefulness as a model system is sometimes inconvenient. Thus, many genes involved in developmental or functional aspects can not be studied due to early embryonic lethality or due to compensation by other genes when ablated (Ihle, 2000). Genetic approaches are required to quickly select the functionally relevant gene from all the candidates or shut on/off gene transcription in a fixed time according to the process of embryogenesis. This study for example revealed an important time - dependent role of the gene Pax7 on the size of the tectum. RNA interference might successfully help to study the role of genes, necessary at several time points in development but with a lethal knockout mutant. In addition, with this approach it is easy to introduce specific shRNA construct at an exact time, early or later, dependent on the period of embryogenesis even in mouse embryos using in utero electroporation (Shimogori *et al.*, 2004; Saito, 2006; Okada *et al.*, 2007).. Thus, the function of a target gene can be analyzed within a defined period, which reflects an important aspect of a developmental gene. Although – as in this study showed – the delivery of dsRNA by electroporation do not cover the whole embryonic tissues, where the gene is expressed, the discrete gene silencing is an alternative advantage for embryogenetic research. This method can avoid the long-term effect of other genes up - or down - regulated by the targeted gene. In addition, since electroporating into a tissue will always result in one part being unaffected, due to the negative charge of the DNA, this part can serve as a control. Taken together, RNA interference on gene silencing in a locally and temporally manner would be a better approach on embryogenesis.

It has been suggested and shown in other systems (Clemens and Elia, 1997; Stark *et al.*, 1998; Williams, 1999; Alexopoulou *et al.*, 2001; Jackson *et al.*, 2003; Persengiev *et al.*, 2004) that dsRNA and siRNA molecules might trigger an apoptotic response in vertebrate cells that may mask or simulate RNAi effects. However, this study and Hernandez and Bueno' work (Hernandez and Bueno, 2005) did not reveal an increase in apoptosis.. Thus, shRNA - producing vectors at least seem not to increase cell apoptosis in chick embryos.

Delivery of dsRNA into Chick Embryos

Gene manipulation into cells is required for high efficiency of DNA delivery and transfection. Four principal methods for DNA transfer across the cell membrane in chick embryo have been described to date: lipofection, electroporation, retroviral-based methods, and engraftment of the infected chick cells or tissues.

Lipofection takes advantage of two properties of liposomes, their ability to bind DNA and their ability to fuse with the cell membrane. This approach of gene transfer was initially developed for transfection of cells *in vitro* and has become increasingly efficient (Brazolot *et al.*, 1991; Fraser *et al.*, 1993; Wakamatsu and Weston, 1997; Wang *et al.*, 2006). Another approach for stable and efficient gene transfer in the chicken embryo is based on retroviral vectors (Logan and Tabin, 1998; Bromberg-White *et al.*, 2004; Ishii and Mikawa, 2005; Kamihira *et al.*, 2005), which allow a fast and efficient *in vivo* infection. Two categories of retroviral vector systems - replication competent and replication defective - have been widely used for transfection of murine and avian cells in many different fields, such as developmental biology, cancer research, and human gene therapy (Coffin, 1996; Kafri, 2004; Tai *et al.*, 2005; Trajcevski *et al.*, 2005; Dalba *et al.*, 2007). Replication-incompetent retroviruses have also been used for infection of chicken embryos. They offer the major advantage of accommodating cDNA inserts of up to 4.5 kb. Various other viral vectors have been developed mainly based on adenoviruses. These accept larger inserts and can also infect nondividing cells (Nakagawa and Takeichi, 1998). More recently, the advantages of lentiviruses have been recognized and made them promising tools for gene expression (Verma and Somia, 1997; Mitta *et al.*, 2002; Chapman *et al.*, 2005). Another option is direct engraftment of the infected chick cells into the developing embryo (Verberne *et al.*, 1998; Munoz-Sanjuan *et al.*, 1999; Dettman *et al.*, 2003).

In ovo electroporation of plasmids is a safe and effective way to introduce exogenous genes into chick embryos for the analysis of the gene regulation, function and expression (Sakamoto *et al.*, 1998; Itasaki *et al.*, 1999; Matsunaga *et al.*, 2000). Electroporation is extremely efficient at enhancing uptake of DNA and RNA into vertebrate cells *in vivo* (Muramatsu *et al.*, 1997; Momose *et al.*, 1999). As this work and others have shown that the gene is already expressed after 4 – 6 h in the transfected cells and the effect of dsRNA on gene silencing can be visible at 24h after the electroporation. In comparison to electroporation for example viral infection is only visible after 8h or takes even longer. However, it is incorporated into the genome and its effect is thus as long as the cell lives. A new publication now shows that with the help of an additional vector, plasmid genes can be also incorporated into the genome (Sato *et al.*, 2007). This will open a complete new perspective of using electroporation to study the effect of different genes.

Antisense-based Approaches for Gene Silencing in Chick Embryos

Antisense single - stranded DNA oligonucleotides (DNA oligos) are used as a powerful tool for targeting genes in cells and animals over past two decades. They can bind to complementary sequence of the mRNA from a specific gene to prevent translation by degradation of the mRNA, and are dramatically successful in some instances (Zamecnik and Stephenson, 1978; Nieto *et al.*, 1994; Srivastava *et al.*, 1995; Runyan *et al.*, 1999). However, the results are often inconsistent *in vivo* due to rapid dispersal and degradation themselves, and nonspecific and toxic side - effects. Novel chemically modified nucleotides, such as phosphorothioate oligos, RNase H-independent 2'-*O*-methoxyethyl oligos (2'-*O*-MOE), peptide nucleic acids (PNA), locked nucleic acid (LNA), offer reasonable resistance to nucleases and enhance their target affinity (Matsukura *et al.*, 1987; Baker *et al.*, 1997; Kumar *et al.*, 1998; Larsen *et al.*, 1999; Tyler *et al.*, 1999; Malchere *et al.*, 2000; Pooga and Langel, 2001; Sazani *et al.*, 2002; Turner *et al.*, 2006; Boffa *et al.*, 2007). The half-life of diverse DNA oligos reported previously is shorter than 10h (Campbell *et al.*, 1990; Kurreck, 2003), however, in this study, no any obvious effect of unmodified DNA oligos on gene silencing was seen till 24 hours, whereas the effect of modified antisense DNA oligos in chick embryos need to be investigated further.

Morpholino-modified oligonucleotides (MOs) are used as an alternative antisense-based technique for target validation. Morpholinos interrupt mRNA translation by steric blocking of the translation initiation complex and display many advantages over the regular DNA oligos. They offer a high affinity for RNA and efficiently invade quite stable secondary structures of mRNAs. Especially their sequence specificity, non-toxicity and minimal nonspecific side-effects provide reliable antisense results in cell cultures and embryos (Summerton and Weller, 1997; 1999; Arora *et al.*, 2000; Heasman, 2002). Effective gene knockdown was achieved in all cells of zebrafish embryos (Nasevicius and Ekker, 2000; Agathon *et al.*, 2001; Topczewska *et al.*, 2001; Yang *et al.*, 2001; Hanaoka *et al.*, 2004). Up to now, morpholinos have been successfully used in a range of model organisms, including sea urchin, ascidian, frog, chick, mouse and human (Lacerra *et al.*, 2000; Audic *et al.*, 2001; Coonrod *et al.*, 2001; Howard *et al.*, 2001; Kos *et al.*, 2003). The successful gene knockdown is available only when morpholino antisense oligos (25 mers) are complementary to the 5' untranslated region or to the first 25 bases downstream of the start codon (Summerton and Weller, 1999; Heasman, 2002). However, sometimes this rigid sequence-specific selection is difficult for a target gene. This might be the case in this study. Although morpholino antisense oligos were designed by the company (Gene Tools, LLC), they did not exert a significant effect on gene downregulation compared to the p*Silencer* – based shRNA. Although a limited cellular uptake of morpholinos, however, at a high dose they can cause cell death or extensive repression of other genes (Imai and Talbot, 2001; Karlen and Rebagliati, 2001; Lele *et al.*, 2001), which is also observed in this study. Albeit morpholinos are a

sort of protected antisense DNA and should therefore be able to survive in the cell for some while, it might be that they are largely destroyed before they can exert an obvious effect compared to the continuously expressed shRNA. The length of the loss-of-function effect of an injected oligo depends on the transcription and translation characteristics of the targeted mRNA, as well as the dose of oligo, and will need to be determined for each gene of interest. Taken together, these experiments suggest that shRNA is a good tool to study the effect of gene loss in the developing chick embryo.

Recently, a large number of small RNA molecules called microRNAs (miRNAs) elevated the overall field of biomedical RNAi to the striking level of current recognition (Lagos-Quintana *et al.*, 2001; Lee and Ambros, 2001; Rajewsky, 2006; Scherr and Eder, 2007; Wang *et al.*, 2007). miRNAs represent a class of endogenous siRNA-like noncoding RNAs with the same size of siRNA, and coordinate many aspects of cellular function including development, differentiation, proliferation and apoptosis (Mendell, 2005). It is estimated that about 30% of all genes are regulated by miRNAs in mammals. miRNAs regulate endogenous gene expression via the RNAi-like pathway. The important RNase III-like protein, Dicer (DCR) for siRNA is also involved in the process of miRNA (Knight and Bass, 2001; Bernstein *et al.*, 2003; Lee *et al.*, 2003; Carmell and Hannon, 2004; Denli *et al.*, 2004; Tijsterman and Plasterk, 2004). These small miRNAs are processed from larger hairpin like precursors. However, they do not cleave the mRNA as siRNA action but rather bind to the targeted mRNA with complete or partial complementarity and suppress its translation into protein (Bartel, 2004). Currently, many varieties of miRNAs are widely reported in microbes, plants, and animals (Khvorova *et al.*, 2003; Collins and Cheng, 2006). Approaches to interfere with synthetic anti-miRNA oligonucleotides in vitro and in vivo expand the practice of RNAi in medical and biological fields. (Ford, 2006; Hammond, 2006; Rodriguez-Lebron and Paulson, 2006).

Summary

The chick midbrain is subdivided into functionally distinct ventral and dorsal domains, tectum and optic tectum. In the mature tectum, neurons are organized in layers, while they form discrete nuclei in the tectum. An interesting characteristic of the embryonic brain is the development of a large optic tectum, of which the growth becomes obvious at embryonic day 3 (E3). Dorsoventral (DV) specification of the early midbrain should thus play a crucial role for the organization of the neuronal circuitry in optic tectum and tectum.

In the first part of my thesis, I investigated regional commitment and establishment of cellular differences along the midbrain DV axis. I examined the commitment of gene expression patterns in isolated ventral and dorsal tissue *in vivo* and *in vitro*, and studied their cell mixing properties. Explant cultures, and grafting of dorsal midbrain into a ventral environment or vice versa, revealed a gradual increase in the autonomy of region-specific gene regulation between, which was accompanied by a gradual increase in differential adhesive properties from E2 to E3, once the DV axis polarity was fixed. These events happened at a time-point when the majority of midbrain cells are not yet differentiated. Long-term transplantation (6 - 9 days) using quail cells from ventral midbrain as grafts showed the same result. Hence, the results suggest that progressive specification of the midbrain DV axis is accompanied by progressively reduced cell mixing between dorsal and ventral precursors, leading to a partial regionalization of midbrain tissue into autonomous units of precursor cell populations.

In the second part I investigated the genes that might be involved in regulating the growth of the tectum. In particular, I focused on the role of Pax7 transcription factor, a paired domain protein. The results suggested that Pax7 was involved in regulating the medial-lateral extension of the tectum. Over expression of Pax7 in dorsal midbrain led to an enlarged tectum accompanied by a raise in cell division, while Pax7 knockdown by

shrank caused a reduction in tectum. The overall pattern of neuronal differentiation was not disturbed by an up or down regulation of Pax7. Pax7 also positively regulated Pax3, another pair-ruled gene expressed dorsally. These results suggest that Pax7 very likely together with Pax3 could facilitate or maintain neural cell proliferation in the midbrain at early stages and that a regulation of the size in that region does not influence the neuronal patterning of the developmental field.

I further checked the expression and function of a GFPase Rab 23, that was suggested to be involved in the DV patterning in mouse neural tube as a negative regulator of Shh signaling. Overexpression of Rab23 indicated that it facilitated the expression of Pax7 and Pax3 in the neural tube and suppressed ventral genes like Nkx6.1 cell autonomously, however, it did not disturb neuronal patterning. Interestingly, a thorough expression study of Rab 23 during chick early development revealed that Rab23 is already expressed very early and asymmetrically during gastrulation, suggesting a possible role of Rab23 on the left-right determination of Hensen's node. In combination with the result that Rab23 is expressed in the notochord early in development, I assume that both Rab23 and Shh exist in all neural progenitor cells initially, and when their expression patterns separate gradually the neural cells adopt a ventral or dorsal fate according to their location along the dorsoventral axis.

The avian embryo is a classic system used widely to investigate questions of vertebrate development. The easy and cheap accessibility of the embryo for *in ovo* or *ex ovo* experiments all around the year make it an ideal animal model to work with. The only recently developed method of over expressing genes in specific cells or regions in the chick embryo by electroporation enabled me to study different ways of gene suppression using this way of gene transfection. Thus, I compared the effect of long-hairpin and short hairpin dsRNA in different vectors and antisense morpholino oligonucleotides. The results revealed that all hairpin dsRNA constructs did reduce gene and protein expression often accompanied by morphological changes. Most efficiently were shRNAi constructs cloned into a siRNA-specific vector – p*Silencer* 1.0-U6. Gene silencing was already well observed 36 hours after transfection. In comparison antisense morpholino oligonucleotides did not show such big gene reduction as the shRNA in p*Silencer*. Taken together, this methodical research proposes that the shRNA in the p*Silencer* vector was a good and effective tool to reduce gene and protein expression locally.

Zusammenfassung

Das Mittelhirn des Huhns wird in funktionell unterschiedliche, ventrale und dorsale Regionen eingeteilt, nämlich das Tegmentum ventral und das optische Tectum dorsal. Im vollentwickelten Tectum bilden Nervenzellen Schichten, während das Tegmentum aus unterschiedlichen Nuclei besteht. Ein charakteristisches Merkmal des embryonalen Gehirns ist die Entwicklung eines großen optischen Tectums, die am dritten embryonalen Tag (E3) sehr deutlich zu beobachten ist. Diese unterschiedliche funktionelle und morphologische Entwicklung des Mittelhirns deutet daraufhin, dass die dorsoventrale Spezifikation des frühen Mittelhirns für die Organisation neuronaler Netzwerke im optischen Tectum und Tegmentum eine kritische Rolle spielt.

Im ersten Teil dieser Doktorarbeit wurde die regionale Bestimmung und Bildung zellulärer Unterschiede entlang der DV Achse des Mittelhirns untersucht. Dafür bestimmte ich den Zeitpunkt, an dem spezifische ventrale und dorsale Genexpressionsmuster festgelegt werden in isoliertem ventralen und dorsalem Gewebe *in vivo* und *in vitro*. Desweiteren untersuchte ich die Entwicklung unterschiedlicher adhäsiver Eigenschaften von ventralen und dorsalen Zellen *in vitro*. Explantatkulturen und Transplantationen von dorsalem Mittelhirn in eine ventrale Umgebung oder *vice versa* liessen eine schrittweise Zunahme der Autonomie der region-spezifischen Genregulation erkennen. Dies wurde von einer schrittweisen Zunahme des differentiellen Adhäsionsverhaltens von ventralen und dorsalen Mittelhirnzellen von E2 zu E3 begleitet, der Zeitspanne, in der die Polarität der DV Achse festgelegt wurde. Diese Entwicklungsprozesse fanden zu einem Zeitpunkt statt, an dem die meisten Zellen des Mittelhirns noch nicht differenziert hatten. Transplantationen, von ventralen Mittelhirnzellen der Wachtel ins dorsale Hühnertectum, die erst nach mehreren Tagen (6 - 9 Tage) untersucht wurden, zeigten das gleiche Ergebnis. Diese Ergebnisse lassen schließen, dass eine partielle Regionalisierung des Mittelhirns in autonome Einheiten von Vorläuferzellen der dorsoventralen Achse stattfindet. Dies erlaubt den Zellen eine Positionsidentität zu bewahren – unabhängig von der wachsenden Distanz zu Signalzentren.

Im zweiten Teil meiner Arbeit untersuchte ich Gene, die das Wachstum und die spezifische Entwicklung des Tectums regulieren könnten. Die Arbeit konzentrierte sich speziell auf die Rolle von Pax7, ein Mitglied der sogenannten ‚pair-ruled‘ Familie von Transkriptionsfaktoren, und auf die

Rolle von Rab23, einer GTPase, die den Shh-Signalweg im dorsalen Neuralrohr inhibiert. Dieser Versuch zeigte, dass Pax7 an der Regulation der medio-lateral Ausdehnung des Tectums beteiligt ist. Überexpression von Pax7 im dorsalen Mittelhirn führte zu einer Vergrößerung des Tectums, die von einer Zunahme der Zellteilung begleitet wurde, während Knockdown von Pax7 eine Größereduktion des Tectums verursachte. Das neuronale Differenzierungsmuster im generellen wurde nicht von der Überexpression oder Repression von Pax7 gestört. Pax7 induzierte ausserdem Pax3, ein Mitglied derselben Familie, das ebenfalls dorsal exprimiert wird und unterdrückte ventrale Gene wie Nkx6.1. Diese Ergebnisse lassen vermuten, dass Pax7, sehr wahrscheinlich zusammen mit Pax3, die neural Zellproliferation im Mittelhirn in frühen Entwicklungsstadien fördert oder auf einem konstanten Level hält und dass die Muster der neuronalen Entwicklung nicht durch der Regulation der Größe dieser Region beeinflusst wird. Außerdem förderte Rab 23, das sehr wahrscheinlich ein negativer Regulator von Shh ist, die Expression von Pax7 und Pax3 im ventralen Mittelhirn und unterdrückte ventrale Gene wie Nkx6.1. Die Überexpression von Rab 23 beeinflusste auch nicht das neuronale Differenzierungsmusterung. Interessanterweise zeigte eine genaue Analyse der Expression von Rab 23 während der frühen Entwicklungsstadien des Huhns, dass Rab 23 bereits sehr früh und asymmetrisch während der Gastrulation exprimiert wurde. Dies deutet auf eine mögliche Rolle von Rab 23 für die links-rechts Determination des Hensen's node an. Betrachtet man diese Ergebnisse zusammen, dann könnte man zu folgender Schlussfolgerung kommen, nämlich, dass sowohl Rab 23 als auch Shh früh in allen neural Progenitorzellen existieren, und dass die neuronalen Zellen jeweils nach ihrer Lage entlang der dorsoventral Achse ein ventrales oder dorsales Schicksal annehmen, wenn das sich die Expressionsmuster von Rab 23 und Shh allmählich trennen.

Der Vogelembryo ist ein klassisches und häufig benutztes System, um die Entwicklung der Vertebraten zu untersuchen. Die einfache und preiswerte Zugänglichkeit des Embryos für *in ovo* oder *ex ovo* Experiment das ganze Jahr über machen ihn zu einem idealen Tiermodell. Die in den letzten Jahren entwickelte Methode der Elektroporation eines Embryos zum Gentransfer in die Zellen, ermöglichte es mir unterschiedliche Weisen der Genunterdrückung in embryonalem Gewebe zu testen und zu vergleichen. Ich verglich in dieser Untersuchung die Wirkung von langen und kurzen Haarnadel-RNAs (hairpin RNA) in verschiedenen Vektoren mit der Wirkung von Antisense-morpholino-Oligonucleotiden verglichen. Die Ergebnisse zeigten, dass alle Haarnadel-dsRNA-Konstruktionen die Gen- und Proteinexpression reduzierten, wobei es häufig zu einer morphologischen Veränderung kam. Die kurze shRNAi-Konstruktionen, die in einen siRNA-spezifischen Vektor – pSilencer 1.0-U6 - geklont wurden war, zeigte sich dabei am effizientesten.. Die Herunterregulierung der Gene wurde bereits 36 Stunden nach der Transfektion beobachtet. Im Gegensatz dazu, zeigten die Antisense-Morpholino-Oligonucleotiden keine solche starke Reduktion wie das shRNA in pSilencer. Zusammenfassend zeigt diese methodische Untersuchung, dass die shRNA im pSilencer-Vektor ein gutes und effektives Werkzeug ist, um Gen- und Proteinexpression örtlich zu reduzieren.

Literatures

- Agarwala, S., Sanders, T. A. and Ragsdale, C. W. (2001). Sonic hedgehog control of size and shape in midbrain pattern formation. *Science* **291** (5511): 2147-50.
- Agathon, A., Thisse, B. and Thisse, C. (2001). Morpholino knock-down of *antivin1* and *antivin2* upregulates nodal signaling. *Genesis* **30** (3): 178-82.
- Aizawa, H., Sekine, Y., Takemura, R., Zhang, Z., Nangaku, M. and Hirokawa, N. (1992). Kinesin family in murine central nervous system. *J Cell Biol* **119** (5): 1287-96.
- Alcedo, J., Ayzenzon, M., Von Ohlen, T., Noll, M. and Hooper, J. E. (1996). The *Drosophila* smoothed gene encodes a seven-pass membrane protein, a putative receptor for the hedgehog signal. *Cell* **86** (2): 221-32.
- Alexopoulou, L., Holt, A. C., Medzhitov, R. and Flavell, R. A. (2001). Recognition of double-stranded RNA and activation of NF-kappaB by Toll-like receptor 3. *Nature* **413** (6857): 732-8.
- Alory, C. and Balch, W. E. (2000). Molecular basis for Rab prenylation. *J Cell Biol* **150** (1): 89-103.
- Altman, J. (1969). Autoradiographic and histological studies of postnatal neurogenesis. IV. Cell proliferation and migration in the anterior forebrain, with special reference to persisting neurogenesis in the olfactory bulb. *J Comp Neurol* **137** (4): 433-57.
- Altman, J. and Bayer, S. A. (1984). The development of the rat spinal cord. *Adv Anat Embryol Cell Biol* **85**: 1-164.
- Altmann, C. R. and Brivanlou, A. H. (2001). Neural patterning in the vertebrate embryo. *Int Rev Cytol* **203**: 447-82.
- Alvarado-Mallart, R. M. and Sotelo, C. (1984). Homotopic and heterotopic transplantations of quail tectal primordia in chick embryos: organization of the retinotectal projections in the chimeric embryos. *Dev Biol* **103** (2): 378-98.
- Alvarado-Mallart, R. M., Martinez, S. and Lance-Jones, C. C. (1990). Pluripotentiality of the 2-day-old avian germinative neuroepithelium. *Dev Biol* **139** (1): 75-88.
- Amor, J. C., Harrison, D. H., Kahn, R. A. and Ringe, D. (1994). Structure of the human ADP-ribosylation factor 1 complexed with GDP. *Nature* **372** (6507): 704-8.
- Amthor, H., Connolly, D., Patel, K., Brand-Saberi, B., Wilkinson, D. G., Cooke, J. and Christ, B. (1996). The expression and regulation of follistatin and a follistatin-like gene during avian somite

compartmentalization and myogenesis. *Dev Biol* **178** (2): 343-62.

Andrews, P. W. (1984). Retinoic acid induces neuronal differentiation of a cloned human embryonal carcinoma cell line in vitro. *Dev Biol* **103** (2): 285-93.

Andrews, P. W., Gonczol, E., Plotkin, S. A., Dignazio, M. and Oosterhuis, J. W. (1986). Differentiation of TERA-2 human embryonal carcinoma cells into neurons and HCMV permissive cells. Induction by agents other than retinoic acid. *Differentiation* **31** (2): 119-26.

Anton, E. S., Marchionni, M. A., Lee, K. F. and Rakic, P. (1997). Role of GGF/neuregulin signaling in interactions between migrating neurons and radial glia in the developing cerebral cortex. *Development* **124** (18): 3501-10.

Araki, I. and Nakamura, H. (1999). Engrailed defines the position of dorsal di-mesencephalic boundary by repressing diencephalic fate. *Development* **126** (22): 5127-35.

Arber, S., Han, B., Mendelsohn, M., Smith, M., Jessell, T. M. and Sockanathan, S. (1999). Requirement for the homeobox gene Hb9 in the consolidation of motor neuron identity. *Neuron* **23** (4): 659-74.

Arkell, R. and Beddington, R. S. (1997). BMP-7 influences pattern and growth of the developing hindbrain of mouse embryos. *Development* **124** (1): 1-12.

Arora, V., Knapp, D. C., Smith, B. L., Statfield, M. L., Stein, D. A., Reddy, M. T., Weller, D. D. and Iversen, P. L. (2000). c-Myc antisense limits rat liver regeneration and indicates role for c-Myc in regulating cytochrome P-450 3A activity. *J Pharmacol Exp Ther* **292** (3): 921-8.

Arsenijevic, Y., Weiss, S., Schneider, B. and Aebischer, P. (2001). Insulin-like growth factor-I is necessary for neural stem cell proliferation and demonstrates distinct actions of epidermal growth factor and fibroblast growth factor-2. *J Neurosci* **21** (18): 7194-202.

Audic, Y., Boyle, B., Slevin, M. and Hartley, R. S. (2001). Cyclin E morpholino delays embryogenesis in *Xenopus*. *Genesis* **30** (3): 107-9.

Avivi, C. and Goldstein, R. S. (1999). Differential expression of *Islet-1* in neural crest-derived ganglia: *Islet-1* + dorsal root ganglion cells are post-mitotic and *Islet-1* + sympathetic ganglion cells are still cycling. *Brain Res Dev Brain Res* **115** (1): 89-92.

Bachvarova, R. F., Skromne, I. and Stern, C. D. (1998). Induction of primitive streak and Hensen's node by the posterior marginal zone in the early chick embryo. *Development* **125** (17): 3521-34.

Bahadoran, P., Aberdam, E., Mantoux, F., Busca, R., Bille, K., Yalman, N., de Saint-Basile, G., Casaroli-Marano, R., Ortonne, J. P. and Ballotti, R. (2001). *Rab27a*: A key to melanosome transport in human melanocytes. *J Cell Biol* **152** (4): 843-50.

Bai, C. B., Stephen, D. and Joyner, A. L. (2004). All mouse ventral spinal cord patterning by hedgehog is *Gli* dependent and involves an activator function of *Gli3*. *Dev Cell* **6** (1): 103-15.

Baird, D. H., Hatten, M. E. and Mason, C. A. (1992). Cerebellar target neurons provide a stop signal for afferent neurite extension in vitro. *J Neurosci* **12** (2): 619-34.

Baker, B. F., Lot, S. S., Condon, T. P., Cheng-Flournoy, S., Lesnik, E. A., Sasmor, H. M. and Bennett, C. F. (1997). 2'-O-(2-Methoxy)ethyl-modified anti-intercellular adhesion molecule 1 (ICAM-1) oligonucleotides selectively increase the ICAM-1 mRNA level and inhibit formation of the ICAM-1 translation initiation complex in human umbilical vein endothelial cells. *J Biol Chem* **272** (18): 11994-2000.

Baldini, G., Hohl, T., Lin, H. Y. and Lodish, H. F. (1992). Cloning of a *Rab3* isotype predominantly expressed in adipocytes. *Proc Natl Acad Sci U S A* **89** (11): 5049-52.

Banerjee, A., Roach, M. C., Trcka, P. and Luduena, R. F. (1990). Increased microtubule assembly in

- bovine brain tubulin lacking the type III isotype of beta-tubulin. *J Biol Chem* **265** (3): 1794-9.
- Bang, A. G. and Goulding, M. D. (1996). Regulation of vertebrate neural cell fate by transcription factors. *Curr Opin Neurobiol* **6** (1): 25-32.
- Barbero, P., Bittova, L. and Pfeffer, S. R. (2002). Visualization of Rab9-mediated vesicle transport from endosomes to the trans-Golgi in living cells. *J Cell Biol* **156** (3): 511-8.
- Barlow, A. J. and Francis-West, P. H. (1997). Ectopic application of recombinant BMP-2 and BMP-4 can change patterning of developing chick facial primordia. *Development* **124** (2): 391-8.
- Bartel, D. P. (2004). MicroRNAs: genomics, biogenesis, mechanism, and function. *Cell* **116** (2): 281-97.
- Barth, K. A., Kishimoto, Y., Rohr, K. B., Seydler, C., Schulte-Merker, S. and Wilson, S. W. (1999). Bmp activity establishes a gradient of positional information throughout the entire neural plate. *Development* **126** (22): 4977-87.
- Bayer, S. A. and Altman, J. (1991). Development of the endopiriform nucleus and the claustrum in the rat brain. *Neuroscience* **45**: 391-412.
- Beachy, P. A., Cooper, M. K., Young, K. E., von Kessler, D. P., Park, W. J., Hall, T. M., Leahy, D. J. and Porter, J. A. (1997). Multiple roles of cholesterol in hedgehog protein biogenesis and signaling. *Cold Spring Harb Symp Quant Biol* **62**: 191-204.
- Becker, N., Gilardi-Hebenstreit, P., Seitanidou, T., Wilkinson, D. and Charnay, P. (1995). Characterisation of the Sek-1 receptor tyrosine kinase. *FEBS Lett* **368** (2): 353-7.
- Bermingham, N. A., Hassan, B. A., Wang, V. Y., Fernandez, M., Banfi, S., Bellen, H. J., Fritzsche, B. and Zoghbi, H. Y. (2001). Proprioceptor pathway development is dependent on Math1. *Neuron* **30** (2): 411-22.
- Bernstein, E., Caudy, A. A., Hammond, S. M. and Hannon, G. J. (2001). Role for a bidentate ribonuclease in the initiation step of RNA interference. *Nature* **409** (6818): 363-6.
- Bernstein, E., Kim, S. Y., Carmell, M. A., Murchison, E. P., Alcorn, H., Li, M. Z., Mills, A. A., Elledge, S. J., Anderson, K. V. and Hannon, G. J. (2003). Corrigendum: Dicer is essential for mouse development. *Nat Genet* **35** (3): 287.
- Bierhuizen, M. F., Westerman, Y., Visser, T. P., Dimjati, W., Wognum, A. W. and Wagemaker, G. (1997). Enhanced green fluorescent protein as selectable marker of retroviral-mediated gene transfer in immature hematopoietic bone marrow cells. *Blood* **90** (9): 3304-15.
- Bijlsma, M. F., Spek, C. A. and Peppelenbosch, M. P. (2004). Hedgehog: an unusual signal transducer. *Bioessays* **26** (4): 387-94.
- Blaess, S., Corrales, J. D. and Joyner, A. L. (2006). Sonic hedgehog regulates Gli activator and repressor functions with spatial and temporal precision in the mid/hindbrain region. *Development* **133** (9): 1799-809.
- Blair, S. S. (2003). Developmental biology: boundary lines. *Nature* **424** (6947): 379-81.
- Boardman, P. E., Sanz-Ezquerro, J., Overton, I. M., Burt, D. W., Bosch, E., Fong, W. T., Tickle, C., Brown, W. R., Wilson, S. A. and Hubbard, S. J. (2002). A comprehensive collection of chicken cDNAs. *Curr Biol* **12** (22): 1965-9.
- Boettger, T., Wittler, L. and Kessel, M. (1999). FGF8 functions in the specification of the right body side of the chick. *Curr Biol* **9** (5): 277-80.
- Boffa, L. C., Cutrona, G., Cilli, M., Matis, S., Damonte, G., Mariani, M. R., Millo, E., Moroni, M., Roncella, S., Fedeli, F. and Ferrarini, M. (2007). Inhibition of Burkitt's lymphoma cells growth in SCID

mice by a PNA specific for a regulatory sequence of the translocated c-myc. *Cancer Gene Ther* **14** (2): 220-6.

Boleti, H., Ojcius, D. M. and Dautry-Varsat, A. (2000). Fluorescent labelling of intracellular bacteria in living host cells. *J Microbiol Methods* **40** (3): 265-74.

Bopp, D., Burri, M., Baumgartner, S., Frigerio, G. and Noll, M. (1986). Conservation of a large protein domain in the segmentation gene paired and in functionally related genes of *Drosophila*. *Cell* **47** (6): 1033-40.

Borycki, A. G., Li, J., Jin, F., Emerson, C. P. and Epstein, J. A. (1999). Pax3 functions in cell survival and in pax7 regulation. *Development* **126** (8): 1665-74.

Bourikas, D. and Stoeckli, E. T. (2003). New tools for gene manipulation in chicken embryos. *Oligonucleotides* **13** (5): 411-9.

Bourne, H. R., Sanders, D. A. and McCormick, F. (1991). The GTPase superfamily: conserved structure and molecular mechanism. *Nature* **349** (6305): 117-27.

Bray, D. (1992). *In Cell Movements*. Garland Publishing Inc., New York.

Brazolot, C. L., Petite, J. N., Etches, R. J. and Verrinder Gibbins, A. M. (1991). Efficient transfection of chicken cells by lipofection, and introduction of transfected blastodermal cells into the embryo. *Mol Reprod Dev* **30** (4): 304-12.

Brennecke, J., Stark, A., Russell, R. B. and Cohen, S. M. (2005). Principles of microRNA-target recognition. *PLoS Biol* **3** (3): e85.

Briscoe, J. and Ericson, J. (1999). The specification of neuronal identity by graded Sonic Hedgehog signalling. *Semin Cell Dev Biol* **10** (3): 353-62.

Briscoe, J., Sussel, L., Serup, P., Hartigan-O'Connor, D., Jessell, T. M., Rubenstein, J. L. and Ericson, J. (1999). Homeobox gene Nkx2.2 and specification of neuronal identity by graded Sonic hedgehog signalling. *Nature* **398** (6728): 622-7.

Briscoe, J., Pierani, A., Jessell, T. M. and Ericson, J. (2000). A homeodomain protein code specifies progenitor cell identity and neuronal fate in the ventral neural tube. *Cell* **101** (4): 435-45.

Briscoe, J., Pierani, A., Jessell, T. M. and Ericson, J. (2000). A homeodomain protein code specifies progenitor cell identity and neuronal fate in the ventral neural tube. *Cell* **101**: 435-45.

Briscoe, J. and Ericson, J. (2001). Specification of neuronal fates in the ventral neural tube. *Curr Opin Neurobiol* **11** (1): 43-9.

Briscoe, J., Chen, Y., Jessell, T. M. and Struhl, G. (2001). A hedgehog-insensitive form of patched provides evidence for direct long-range morphogen activity of sonic hedgehog in the neural tube. *Mol Cell* **7** (6): 1279-91.

Bromberg-White, J. L., Webb, C. P., Patacsil, V. S., Miranti, C. K., Williams, B. O. and Holmen, S. L. (2004). Delivery of short hairpin RNA sequences by using a replication-competent avian retroviral vector. *J Virol* **78** (9): 4914-6.

Brown, A. (1981). *Organization in the Spinal Cord*. Springer-Verlag, Berlin.

Buckingham, M. (2003). How the community effect orchestrates muscle differentiation. *Bioessays* **25** (1): 13-6.

Burnett, S. L. and Beuchat, L. R. (2002). Comparison of methods for fluorescent detection of viable, dead, and total *Escherichia coli* O157:H7 cells in suspensions and on apples using confocal scanning laser microscopy following treatment with sanitizers. *Int J Food Microbiol* **74** (1-2): 37-45.

- Burstyn-Cohen, T., Tzarfaty, V., Frumkin, A., Feinstein, Y., Stoeckli, E. and Klar, A. (1999). F-Spondin is required for accurate pathfinding of commissural axons at the floor plate. *Neuron* **23** (2): 233-46.
- Cahana, A., Escamez, T., Nowakowski, R. S., Hayes, N. L., Giacobini, M., von Holst, A., Shmueli, O., Sapir, T., McConnell, S. K., Wurst, W., Martinez, S. and Reiner, O. (2001). Targeted mutagenesis of Lis1 disrupts cortical development and LIS1 homodimerization. *Proc Natl Acad Sci U S A* **98** (11): 6429-34.
- Campbell, J. M., Bacon, T. A. and Wickstrom, E. (1990). Oligodeoxynucleoside phosphorothioate stability in subcellular extracts, culture media, sera and cerebrospinal fluid. *J Biochem Biophys Methods* **20** (3): 259-67.
- Capdevila, J., Vogan, K. J., Tabin, C. J. and Izpisua Belmonte, J. C. (2000). Mechanisms of left-right determination in vertebrates. *Cell* **101** (1): 9-21.
- Caplen, N. J. (2004). Gene therapy progress and prospects. Downregulating gene expression: the impact of RNA interference. *Gene Ther* **11** (16): 1241-8.
- Carmell, M. A. and Hannon, G. J. (2004). RNase III enzymes and the initiation of gene silencing. *Nat Struct Mol Biol* **11** (3): 214-8.
- Carpenter, D., Stone, D. M., Brush, J., Ryan, A., Armanini, M., Frantz, G., Rosenthal, A. and de Sauvage, F. J. (1998). Characterization of two patched receptors for the vertebrate hedgehog protein family. *Proc Natl Acad Sci U S A* **95** (23): 13630-4.
- Caspary, T. and Anderson, K. V. (2003). Patterning cell types in the dorsal spinal cord: what the mouse mutants say. *Nat Rev Neurosci* **4** (4): 289-97.
- Catala, M., Teillet, M. A. and Le Douarin, N. M. (1995). Organization and development of the tail bud analyzed with the quail-chick chimaera system. *Mech Dev* **51** (1): 51-65.
- Catala, M. (2002). Genetic control of caudal development. *Clin Genet* **61** (2): 89-96.
- Catalanotto, C., Azzalin, G., Macino, G. and Cogoni, C. (2002). Involvement of small RNAs and role of the qde genes in the gene silencing pathway in *Neurospora*. *Genes Dev* **16** (7): 790-5.
- Cayuso, J., Ulloa, F., Cox, B., Briscoe, J. and Marti, E. (2006). The Sonic hedgehog pathway independently controls the patterning, proliferation and survival of neuroepithelial cells by regulating Gli activity. *Development* **133** (3): 517-28.
- Chalepakis, G. and Gruss, P. (1995). Identification of DNA recognition sequences for the Pax3 paired domain. *Gene* **162** (2): 267-70.
- Chandran, S., Compston, A., Jauniaux, E., Gilson, J., Blakemore, W. and Svendsen, C. (2004). Differential generation of oligodendrocytes from human and rodent embryonic spinal cord neural precursors. *Glia* **47** (4): 314-24.
- Chapman, S. C., Schubert, F. R., Schoenwolf, G. C. and Lumsden, A. (2002). Analysis of spatial and temporal gene expression patterns in blastula and gastrula stage chick embryos. *Dev Biol* **245** (1): 187-99.
- Chapman, S. C., Lawson, A., Macarthur, W. C., Wiese, R. J., Loechel, R. H., Burgos-Trinidad, M., Wakefield, J. K., Ramabhadran, R., Mauch, T. J. and Schoenwolf, G. C. (2005). Ubiquitous GFP expression in transgenic chickens using a lentiviral vector. *Development* **132** (5): 935-40.
- Charrier, J. B., Lapointe, F., Le Douarin, N. M. and Teillet, M. A. (2001). Anti-apoptotic role of Sonic hedgehog protein at the early stages of nervous system organogenesis. *Development* **128** (20): 4011-20.
- Chavrier, P., Gorvel, J. P., Stelzer, E., Simons, K., Gruenberg, J. and Zerial, M. (1991). Hypervariable C-terminal domain of rab proteins acts as a targeting signal. *Nature* **353** (6346): 769-72.

- Chedotal, A., Pourquie, O. and Sotelo, C. (1995). Initial tract formation in the brain of the chick embryo: selective expression of the BEN/SC1/DM-GRASP cell adhesion molecule. *Eur J Neurosci* **7** (2): 198-212.
- Chen, J., Knowles, H. J., Hebert, J. L. and Hackett, B. P. (1998). Mutation of the mouse hepatocyte nuclear factor/forkhead homologue 4 gene results in an absence of cilia and random left-right asymmetry. *J Clin Invest* **102** (6): 1077-82.
- Chen, Y., Cardinaux, J. R., Goodman, R. H. and Smolik, S. M. (1999). Mutants of cubitus interruptus that are independent of PKA regulation are independent of hedgehog signaling. *Development* **126** (16): 3607-16.
- Chen, H. H., Maeda, T., Mullett, S. J. and Stewart, A. F. (2004). Transcription cofactor Vgl-2 is required for skeletal muscle differentiation. *Genesis* **39** (4): 273-9.
- Chen, Y. X., Krull, C. E. and Reneker, L. W. (2004). Targeted gene expression in the chicken eye by in ovo electroporation. *Mol Vis* **10**: 874-83.
- Chenn, A. and Walsh, C. A. (2002). Regulation of cerebral cortical size by control of cell cycle exit in neural precursors. *Science* **297** (5580): 365-9.
- Chesnutt, C. and Niswander, L. (2004). Plasmid-based short-hairpin RNA interference in the chicken embryo. *Genesis* **39** (2): 73-8.
- Chi, N. and Epstein, J. A. (2002). Getting your Pax straight: Pax proteins in development and disease. *Trends Genet* **18** (1): 41-7.
- Chiang, C., Litingtung, Y., Lee, E., Young, K. E., Corden, J. L., Westphal, H. and Beachy, P. A. (1996). Cyclopia and defective axial patterning in mice lacking Sonic hedgehog gene function. *Nature* **383** (6599): 407-13.
- Chilton, J. K. and Guthrie, S. (2004). Development of oculomotor axon projections in the chick embryo. *J Comp Neurol* **472** (3): 308-17.
- Chisholm, A. D. and Horvitz, H. R. (1995). Patterning of the *Caenorhabditis elegans* head region by the Pax-6 family member *vab-3*. *Nature* **377** (6544): 52-5.
- Chizhikov, V. V. and Millen, K. J. (2005). Roof plate-dependent patterning of the vertebrate dorsal central nervous system. *Dev Biol* **277** (2): 287-95.
- Chuang, P. T. and Kornberg, T. B. (2000). On the range of hedgehog signaling. *Curr Opin Genet Dev* **10** (5): 515-22.
- Clarke, J. D., Erskine, L. and Lumsden, A. (1998). Differential progenitor dispersal and the spatial origin of early neurons can explain the predominance of single-phenotype clones in the chick hindbrain. *Dev Dyn* **212** (1): 14-26.
- Clarke, J. D. and Tickle, C. (1999). Fate maps old and new. *Nat Cell Biol* **1** (4): E103-9.
- Clemens, M. J. and Elia, A. (1997). The double-stranded RNA-dependent protein kinase PKR: structure and function. *J Interferon Cytokine Res* **17** (9): 503-24.
- Cobos, I., Shimamura, K., Rubenstein, J. L., Martinez, S. and Puelles, L. (2001). Fate map of the avian anterior forebrain at the four-somite stage, based on the analysis of quail-chick chimeras. *Dev Biol* **239** (1): 46-67.
- Coffin, J. M. (1996). Retrovirus restriction revealed. *Nature* **382** (6594): 762-3.
- Cogoni, C., Irelan, J. T., Schumacher, M., Schmidhauser, T. J., Selker, E. U. and Macino, G. (1996). Transgene silencing of the *al-1* gene in vegetative cells of *Neurospora* is mediated by a cytoplasmic

- effector and does not depend on DNA-DNA interactions or DNA methylation. *Embo J* **15** (12): 3153-63.
- Cogoni, C. and Macino, G. (1999). Gene silencing in *Neurospora crassa* requires a protein homologous to RNA-dependent RNA polymerase. *Nature* **399** (6732): 166-9.
- Cohen, M. M., Jr. (2003). The hedgehog signaling network. *Am J Med Genet* **123A** (1): 5-28.
- Collins, R. E. and Cheng, X. (2006). Structural and biochemical advances in mammalian RNAi. *J Cell Biochem* **99** (5): 1251-66.
- Connolly, D. J., Patel, K., Withington, S. and Cooke, J. (2000). Effects of follistatin and BMP4 proteins on early dorso-ventral patterning in chick. *Int J Dev Biol* **44** (1): 129-40.
- Conway, S. J., Henderson, D. J. and Copp, A. J. (1997). Pax3 is required for cardiac neural crest migration in the mouse: evidence from the splotch (Sp2H) mutant. *Development* **124** (2): 505-14.
- Coonrod, S. A., Bolling, L. C., Wright, P. W., Visconti, P. E. and Herr, J. C. (2001). A morpholino phenocopy of the mouse *mos* mutation. *Genesis* **30** (3): 198-200.
- Cotten, M., Baker, A., Saltik, M., Wagner, E. and Buschle, M. (1994). Lipopolysaccharide is a frequent contaminant of plasmid DNA preparations and can be toxic to primary human cells in the presence of adenovirus. *Gene Ther* **1** (4): 239-46.
- Couly, G. F., Coltey, P. M. and Le Douarin, N. M. (1993). The triple origin of skull in higher vertebrates: a study in quail-chick chimeras. *Development* **117** (2): 409-29.
- Crossley, P. H., Martinez, S. and Martin, G. R. (1996). Midbrain development induced by FGF8 in the chick embryo. *Nature* **380** (6569): 66-8.
- Curran, T. and D'Arcangelo, G. (1998). Role of reelin in the control of brain development. *Brain Res Brain Res Rev* **26** (2-3): 285-94.
- Czerny, T., Schaffner, G. and Busslinger, M. (1993). DNA sequence recognition by Pax proteins: bipartite structure of the paired domain and its binding site. *Genes Dev* **7** (10): 2048-61.
- Dalba, C., Bellier, B., Kasahara, N. and Klatzmann, D. (2007). Replication-competent Vectors and Empty Virus-like Particles: New Retroviral Vector Designs for Cancer Gene Therapy or Vaccines. *Mol Ther* **15** (3): 457-66.
- Dale, K., Sattar, N., Heemskerk, J., Clarke, J. D., Placzek, M. and Dodd, J. (1999). Differential patterning of ventral midline cells by axial mesoderm is regulated by BMP7 and chordin. *Development* **126** (2): 397-408.
- Dalmay, T., Hamilton, A., Rudd, S., Angell, S. and Baulcombe, D. C. (2000). An RNA-dependent RNA polymerase gene in *Arabidopsis* is required for posttranscriptional gene silencing mediated by a transgene but not by a virus. *Cell* **101** (5): 543-53.
- Dathe, V., Gamel, A., Manner, J., Brand-Saberi, B. and Christ, B. (2002). Morphological left-right asymmetry of Hensen's node precedes the asymmetric expression of Shh and Fgf8 in the chick embryo. *Anat Embryol (Berl)* **205** (5-6): 343-54.
- Dathe, V., Prols, F. and Brand-Saberi, B. (2004). Expression of kinesin kif5c during chick development. *Anat Embryol (Berl)* **207** (6): 475-80.
- Davies, J. E. and Miller, R. H. (2001). Local sonic hedgehog signaling regulates oligodendrocyte precursor appearance in multiple ventricular zone domains in the chick metencephalon. *Dev Biol* **233** (2): 513-25.
- Davy, A. and Robbins, S. M. (2000). Ephrin-A5 modulates cell adhesion and morphology in an integrin-dependent manner. *Embo J* **19** (20): 5396-405.

- Denli, A. M., Tops, B. B., Plasterk, R. H., Ketting, R. F. and Hannon, G. J. (2004). Processing of primary microRNAs by the Microprocessor complex. *Nature* **432** (7014): 231-5.
- Deretic, D., Huber, L. A., Ransom, N., Mancini, M., Simons, K. and Papermaster, D. S. (1995). rab8 in retinal photoreceptors may participate in rhodopsin transport and in rod outer segment disk morphogenesis. *J Cell Sci* **108** (Pt 1): 215-24.
- Dettman, R. W., Pae, S. H., Morabito, C. and Bristow, J. (2003). Inhibition of alpha4-integrin stimulates epicardial-mesenchymal transformation and alters migration and cell fate of epicardially derived mesenchyme. *Dev Biol* **257** (2): 315-28.
- Deutsch, U., Dressler, G. R. and Gruss, P. (1988). Pax 1, a member of a paired box homologous murine gene family, is expressed in segmented structures during development. *Cell* **53** (4): 617-25.
- Dias, M. S. and Schoenwolf, G. C. (1990). Formation of ectopic neurepithelium in chick blastoderms: age-related capacities for induction and self-differentiation following transplantation of quail Hensen's nodes. *Anat Rec* **228** (4): 437-48.
- Dickinson, M. E., Selleck, M. A., McMahon, A. P. and Bronner-Fraser, M. (1995). Dorsalization of the neural tube by the non-neural ectoderm. *Development* **121** (7): 2099-106.
- Downward, J. (2004). RNA interference. *Bmj* **328** (7450): 1245-8.
- Dudley, A. T. and Robertson, E. J. (1997). Overlapping expression domains of bone morphogenetic protein family members potentially account for limited tissue defects in BMP7 deficient embryos. *Dev Dyn* **208** (3): 349-62.
- Dutton, R., Yamada, T., Turnley, A., Bartlett, P. F. and Murphy, M. (1999). Sonic hedgehog promotes neuronal differentiation of murine spinal cord precursors and collaborates with neurotrophin 3 to induce Islet-1. *J Neurosci* **19** (7): 2601-8.
- Eagleson, G. W. and Harris, W. A. (1990). Mapping of the presumptive brain regions in the neural plate of *Xenopus laevis*. *J Neurobiol* **21** (3): 427-40.
- Easter, S. S., Jr., Ross, L. S. and Frankfurter, A. (1993). Initial tract formation in the mouse brain. *J Neurosci* **13** (1): 285-99.
- Echard, A., Jollivet, F., Martinez, O., Lacapere, J. J., Rousselet, A., Janoueix-Lerosey, I. and Goud, B. (1998). Interaction of a Golgi-associated kinesin-like protein with Rab6. *Science* **279** (5350): 580-5.
- Echelard, Y., Epstein, D. J., St-Jacques, B., Shen, L., Mohler, J., McMahon, J. A. and McMahon, A. P. (1993). Sonic hedgehog, a member of a family of putative signaling molecules, is implicated in the regulation of CNS polarity. *Cell* **75** (7): 1417-30.
- Edlund, T. and Jessell, T. M. (1999). Progression from extrinsic to intrinsic signaling in cell fate specification: a view from the nervous system. *Cell* **96** (2): 211-24.
- Eggenchwiler, J. T. and Anderson, K. V. (2000). Dorsal and lateral fates in the mouse neural tube require the cell-autonomous activity of the open brain gene. *Dev Biol* **227** (2): 648-60.
- Eggenchwiler, J. T., Espinoza, E. and Anderson, K. V. (2001). Rab23 is an essential negative regulator of the mouse Sonic hedgehog signalling pathway. *Nature* **412** (6843): 194-8.
- Eggenchwiler, J. T., Bulgakov, O. V., Qin, J., Li, T. and Anderson, K. V. (2006). Mouse Rab23 regulates hedgehog signaling from smoothed to Gli proteins. *Dev Biol* **290** (1): 1-12.
- Ekker, S. C., Ungar, A. R., Greenstein, P., von Kessler, D. P., Porter, J. A., Moon, R. T. and Beachy, P. A. (1995). Patterning activities of vertebrate hedgehog proteins in the developing eye and brain. *Curr Biol* **5** (8): 944-55.

- Ekker, S. C. and Larson, J. D. (2001). Morphant technology in model developmental systems. *Genesis* **30** (3): 89-93.
- Elbashir, S. M., Harborth, J., Lendeckel, W., Yalcin, A., Weber, K. and Tuschl, T. (2001). Duplexes of 21-nucleotide RNAs mediate RNA interference in cultured mammalian cells. *Nature* **411** (6836): 494-8.
- Elbashir, S. M., Lendeckel, W. and Tuschl, T. (2001). RNA interference is mediated by 21- and 22-nucleotide RNAs. *Genes Dev* **15** (2): 188-200.
- Elbashir, S. M., Martinez, J., Patkaniowska, A., Lendeckel, W. and Tuschl, T. (2001). Functional anatomy of siRNAs for mediating efficient RNAi in *Drosophila melanogaster* embryo lysate. *Embo J* **20** (23): 6877-88.
- Elbashir, S. M., Harborth, J., Weber, K. and Tuschl, T. (2002). Analysis of gene function in somatic mammalian cells using small interfering RNAs. *Methods* **26** (2): 199-213.
- Elferink, L. A., Anzai, K. and Scheller, R. H. (1992). rab15, a novel low molecular weight GTP-binding protein specifically expressed in rat brain. *J Biol Chem* **267** (31): 22693.
- Eng, S. R., Gratwick, K., Rhee, J. M., Fedtsova, N., Gan, L. and Turner, E. E. (2001). Defects in sensory axon growth precede neuronal death in Brn3a-deficient mice. *J Neurosci* **21** (2): 541-9.
- Eng, S. R., Kozlov, S. and Turner, E. E. (2003). Unaltered expression of Bcl-2 and TAG-1/axonin-1 precedes sensory apoptosis in Brn3a knockout mice. *Neuroreport* **14** (2): 173-6.
- Eng, S. R., Lanier, J., Fedtsova, N. and Turner, E. E. (2004). Coordinated regulation of gene expression by Brn3a in developing sensory ganglia. *Development* **131** (16): 3859-70.
- Epstein, D. J., Vekemans, M. and Gros, P. (1991). Splotch (Sp2H), a mutation affecting development of the mouse neural tube, shows a deletion within the paired homeodomain of Pax-3. *Cell* **67** (4): 767-74.
- Ericson, J., Thor, S., Edlund, T., Jessell, T. M. and Yamada, T. (1992). Early stages of motor neuron differentiation revealed by expression of homeobox gene Islet-1. *Science* **256** (5063): 1555-60.
- Ericson, J., Muhr, J., Placzek, M., Lints, T., Jessell, T. M. and Edlund, T. (1995). Sonic hedgehog induces the differentiation of ventral forebrain neurons: a common signal for ventral patterning within the neural tube. *Cell* **81** (5): 747-56.
- Ericson, J., Muhr, J., Jessell, T. M. and Edlund, T. (1995). Sonic hedgehog: a common signal for ventral patterning along the rostrocaudal axis of the neural tube. *Int J Dev Biol* **39** (5): 809-16.
- Ericson, J., Morton, S., Kawakami, A., Roelink, H. and Jessell, T. M. (1996). Two critical periods of Sonic Hedgehog signaling required for the specification of motor neuron identity. *Cell* **87** (4): 661-73.
- Ericson, J., Rashbass, P., Schedl, A., Brenner-Morton, S., Kawakami, A., van Heyningen, V., Jessell, T. M. and Briscoe, J. (1997). Pax6 controls progenitor cell identity and neuronal fate in response to graded Shh signaling. *Cell* **90** (1): 169-80.
- Ericson, J., Briscoe, J., Rashbass, P., van Heyningen, V. and Jessell, T. M. (1997). Graded sonic hedgehog signaling and the specification of cell fate in the ventral neural tube. *Cold Spring Harb Symp Quant Biol* **62**: 451-66.
- Erskine, L., Patel, K. and Clarke, J. D. (1998). Progenitor dispersal and the origin of early neuronal phenotypes in the chick embryo spinal cord. *Dev Biol* **199** (1): 26-41.
- Evans, T. M., Ferguson, C., Wainwright, B. J., Parton, R. G. and Wicking, C. (2003). Rab23, a negative regulator of hedgehog signaling, localizes to the plasma membrane and the endocytic pathway. *Traffic* **4** (12): 869-84.

- Eyal-Giladi, H., Goldberg, M., Refael, H. and Avner, O. (1994). A direct approach to the study of the effect of gravity on axis formation in birds. *Adv Space Res* **14** (8): 271-9.
- Faure, S., de Santa Barbara, P., Roberts, D. J. and Whitman, M. (2002). Endogenous patterns of BMP signaling during early chick development. *Dev Biol* **244** (1): 44-65.
- Fedtsova, N. G. and Turner, E. E. (1995). Brn-3.0 expression identifies early post-mitotic CNS neurons and sensory neural precursors. *Mech Dev* **53** (3): 291-304.
- Fedtsova, N. and Turner, E. E. (1997). Inhibitory effects of ventral signals on the development of Brn-3.0-expressing neurons in the dorsal spinal cord. *Dev Biol* **190** (1): 18-31.
- Fedtsova, N. and Turner, E. E. (2001). Signals from the ventral midline and isthmus regulate the development of Brn3.0-expressing neurons in the midbrain. *Mech Dev* **105** (1-2): 129-44.
- Feng, L., Hatten, M. E. and Heintz, N. (1994). Brain lipid-binding protein (BLBP): a novel signaling system in the developing mammalian CNS. *Neuron* **12** (4): 895-908.
- Feng, L. and Heintz, N. (1995). Differentiating neurons activate transcription of the brain lipid-binding protein gene in radial glia through a novel regulatory element. *Development* **121** (6): 1719-30.
- Feng, J., White, B., Tyurina, O. V., Guner, B., Larson, T., Lee, H. Y., Karlstrom, R. O. and Kohtz, J. D. (2004). Synergistic and antagonistic roles of the Sonic hedgehog N- and C-terminal lipids. *Development* **131** (17): 4357-70.
- Fire, A., Xu, S., Montgomery, M. K., Kostas, S. A., Driver, S. E. and Mello, C. C. (1998). Potent and specific genetic interference by double-stranded RNA in *Caenorhabditis elegans*. *Nature* **391** (6669): 806-11.
- Fire, A. (1999). RNA-triggered gene silencing. *Trends Genet* **15** (9): 358-63.
- Firnberg, N. and Neubuser, A. (2002). FGF signaling regulates expression of Tbx2, Erm, Pea3, and Pax3 in the early nasal region. *Dev Biol* **247** (2): 237-50.
- Ford, L. P. (2006). Using synthetic miRNA mimics for diverting cell fate: a possibility of miRNA-based therapeutics? *Leuk Res* **30** (5): 511-3.
- Frank-Kamenetsky, M., Zhang, X. M., Bottega, S., Guicherit, O., Wichterle, H., Dudek, H., Bumcrot, D., Wang, F. Y., Jones, S., Shulok, J., Rubin, L. L. and Porter, J. A. (2002). Small-molecule modulators of Hedgehog signaling: identification and characterization of Smoothed agonists and antagonists. *J Biol* **1** (2): 10.
- Franz, T. and Kothary, R. (1993). Characterization of the neural crest defect in Splotch (Sp1H) mutant mice using a lacZ transgene. *Brain Res Dev Brain Res* **72** (1): 99-105.
- Fraser, S., Keynes, R. and Lumsden, A. (1990). Segmentation in the chick embryo hindbrain is defined by cell lineage restrictions. *Nature* **344** (6265): 431-5.
- Fraser, R. A., Carsience, R. S., Clark, M. E., Etches, R. J. and Gibbins, A. M. (1993). Efficient incorporation of transfected blastodermal cells into chimeric chicken embryos. *Int J Dev Biol* **37** (3): 381-5.
- Fueshko, S. M., Key, S. and Wray, S. (1998). GABA inhibits migration of luteinizing hormone-releasing hormone neurons in embryonic olfactory explants. *J Neurosci* **18** (7): 2560-9.
- Funahashi, J., Okafuji, T., Ohuchi, H., Noji, S., Tanaka, H. and Nakamura, H. (1999). Role of Pax-5 in the regulation of a mid-hindbrain organizer's activity. *Dev Growth Differ* **41** (1): 59-72.
- Gage, F. H. (2000). Mammalian neural stem cells. *Science* **287** (5457): 1433-8.
- Gallera, J. (1971). Primary induction in birds. *Adv Morphog* **9**: 149-80.

- Garcia-Castro, M. I., Marcelle, C. and Bronner-Fraser, M. (2002). Ectodermal Wnt function as a neural crest inducer. *Science* **297** (5582): 848-51.
- Gavalas, A. and Krumlauf, R. (2000). Retinoid signalling and hindbrain patterning. *Curr Opin Genet Dev* **10** (4): 380-6.
- Geppert, M., Bolshakov, V. Y., Siegelbaum, S. A., Takei, K., De Camilli, P., Hammer, R. E. and Sudhof, T. C. (1994). The role of Rab3A in neurotransmitter release. *Nature* **369** (6480): 493-7.
- Gilbert, S. F. (2000). *Developmental Biology. 6th Edition*. Sinauer Associates, Inc., Sunderland, MA, U.S.A.
- Gilman, A. G. (1987). G proteins: transducers of receptor-generated signals. *Annu Rev Biochem* **56**: 615-49.
- Glaser, T., Jepeal, L., Edwards, J. G., Young, S. R., Favor, J. and Maas, R. L. (1994). PAX6 gene dosage effect in a family with congenital cataracts, aniridia, anophthalmia and central nervous system defects. *Nat Genet* **7** (4): 463-71.
- Goldman, S. A., Williams, S., Barami, K., Lemmon, V. and Nedergaard, M. (1996). Transient coupling of Ng-CAM expression to NgCAM-dependent calcium signaling during migration of new neurons in the adult songbird brain. *Mol Cell Neurosci* **7** (1): 29-45.
- Gotz, M., Wizenmann, A., Reinhardt, S., Lumsden, A. and Price, J. (1996). Selective adhesion of cells from different telencephalic regions. *Neuron* **16** (3): 551-64.
- Goulding, M. D., Chalepakis, G., Deutsch, U., Erselius, J. R. and Gruss, P. (1991). Pax-3, a novel murine DNA binding protein expressed during early neurogenesis. *Embo J* **10** (5): 1135-47.
- Goulding, M., Lumsden, A. and Paquette, A. J. (1994). Regulation of Pax-3 expression in the dermomyotome and its role in muscle development. *Development* **120** (4): 957-71.
- Gowan, K., Helms, A. W., Hunsaker, T. L., Collisson, T., Ebert, P. J., Odom, R. and Johnson, J. E. (2001). Crossinhibitory activities of Ngn1 and Math1 allow specification of distinct dorsal interneurons. *Neuron* **31** (2): 219-32.
- Grabs, D., Bergmann, M., Urban, M., Post, A. and Gratzl, M. (1996). Rab3 proteins and SNAP-25, essential components of the exocytosis machinery in conventional synapses, are absent from ribbon synapses of the mouse retina. *Eur J Neurosci* **8** (1): 162-8.
- Graham, A. and Lumsden, A. (1996). Interactions between rhombomeres modulate Krox-20 and follistatin expression in the chick embryo hindbrain. *Development* **122** (2): 473-80.
- Granata, A. and Quaderi, N. A. (2003). The Opitz syndrome gene MID1 is essential for establishing asymmetric gene expression in Hensen's node. *Dev Biol* **258** (2): 397-405.
- Gray, G. E. and Sanes, J. R. (1991). Migratory paths and phenotypic choices of clonally related cells in the avian optic tectum. *Neuron* **6** (2): 211-25.
- Grindley, J. C., Davidson, D. R. and Hill, R. E. (1995). The role of Pax-6 in eye and nasal development. *Development* **121** (5): 1433-42.
- Grishok, A., Tabara, H. and Mello, C. C. (2000). Genetic requirements for inheritance of RNAi in *C. elegans*. *Science* **287** (5462): 2494-7.
- Grishok, A., Pasquinelli, A. E., Conte, D., Li, N., Parrish, S., Ha, I., Baillie, D. L., Fire, A., Ruvkun, G. and Mello, C. C. (2001). Genes and mechanisms related to RNA interference regulate expression of the small temporal RNAs that control *C. elegans* developmental timing. *Cell* **106** (1): 23-34.
- Gross, M. K., Dottori, M. and Goulding, M. (2002). Lbx1 specifies somatosensory association

interneurons in the dorsal spinal cord. *Neuron* **34** (4): 535-49.

Grunweller, A., Wyszko, E., Bieber, B., Jahnel, R., Erdmann, V. A. and Kurreck, J. (2003). Comparison of different antisense strategies in mammalian cells using locked nucleic acids, 2'-O-methyl RNA, phosphorothioates and small interfering RNA. *Nucleic Acids Res* **31** (12): 3185-93.

Gruss, P. and Walther, C. (1992). Pax in development. *Cell* **69** (5): 719-22.

Gunther, T., Struwe, M., Aguzzi, A. and Schughart, K. (1994). Open brain, a new mouse mutant with severe neural tube defects, shows altered gene expression patterns in the developing spinal cord. *Development* **120** (11): 3119-30.

Gunther, T., Sporle, R. and Schughart, K. (1997). The open brain (opb) mutation maps to mouse chromosome 1. *Mamm Genome* **8** (8): 583-5.

Guo, S. and Kemphues, K. J. (1995). par-1, a gene required for establishing polarity in *C. elegans* embryos, encodes a putative Ser/Thr kinase that is asymmetrically distributed. *Cell* **81** (4): 611-20.

Guo, A., Wang, T., Ng, E. L., Aulia, S., Chong, K. H., Teng, F. Y., Wang, Y. and Tang, B. L. (2006). Open brain gene product Rab23: Expression pattern in the adult mouse brain and functional characterization. *J Neurosci Res* **83** (6): 1118-27.

Gupta, A. and Tsai, L. H. (2003). Cyclin-dependent kinase 5 and neuronal migration in the neocortex. *Neurosignals* **12** (4-5): 173-9.

Gurdon, J. B., Kato, K. and Lemaire, P. (1993). The community effect, dorsalization and mesoderm induction. *Curr Opin Genet Dev* **3** (4): 662-7.

Gurdon, J. B., Lemaire, P. and Kato, K. (1993). Community effects and related phenomena in development. *Cell* **75** (5): 831-4.

Guthrie, S. and Lumsden, A. (1991). Formation and regeneration of rhombomere boundaries in the developing chick hindbrain. *Development* **112** (1): 221-9.

Guthrie, S., Muchamore, I., Kuroiwa, A., Marshall, H., Krumlauf, R. and Lumsden, A. (1992). Neuroectodermal autonomy of Hox-2.9 expression revealed by rhombomere transpositions. *Nature* **356** (6365): 157-9.

Guthrie, S., Prince, V. and Lumsden, A. (1993). Selective dispersal of avian rhombomere cells in orthotopic and heterotopic grafts. *Development* **118** (2): 527-38.

Guthrie, S. (1996). Patterning the hindbrain. *Curr Opin Neurobiol* **6** (1): 41-8.

Hackett, B. P. (2002). Formation and malformation of the vertebrate left-right axis. *Curr Mol Med* **2** (1): 39-66.

Hahn, H., Wojnowski, L., Miller, G. and Zimmer, A. (1999). The patched signaling pathway in tumorigenesis and development: lessons from animal models. *J Mol Med* **77** (6): 459-68.

Hamada, H., Meno, C., Watanabe, D. and Saijoh, Y. (2002). Establishment of vertebrate left-right asymmetry. *Nat Rev Genet* **3** (2): 103-13.

Hamburger, V. and Hamilton, H. (1951). A series of normal stages in the development of the chick embryo. *J. Morphol.* **88**: 49-92.

Hamilton, A. J. and Baulcombe, D. C. (1999). A species of small antisense RNA in posttranscriptional gene silencing in plants. *Science* **286** (5441): 950-2.

Hammer, J. A., 3rd and Wu, X. S. (2002). Rabs grab motors: defining the connections between Rab GTPases and motor proteins. *Curr Opin Cell Biol* **14** (1): 69-75.

- Hammerschmidt, M., Brook, A. and McMahon, A. P. (1997). The world according to hedgehog. *Trends Genet* **13** (1): 14-21.
- Hammond, S. M., Bernstein, E., Beach, D. and Hannon, G. J. (2000). An RNA-directed nuclease mediates post-transcriptional gene silencing in *Drosophila* cells. *Nature* **404** (6775): 293-6.
- Hammond, S. M., Boettcher, S., Caudy, A. A., Kobayashi, R. and Hannon, G. J. (2001). Argonaute2, a link between genetic and biochemical analyses of RNAi. *Science* **293** (5532): 1146-50.
- Hammond, S. M. (2006). RNAi, microRNAs, and human disease. *Cancer Chemother Pharmacol* **58 Suppl 1**: s63-8.
- Han, Y. and Grierson, D. (2002). Relationship between small antisense RNAs and aberrant RNAs associated with sense transgene mediated gene silencing in tomato. *Plant J* **29** (4): 509-19.
- Hanaoka, R., Ohmori, Y., Uyemura, K., Hosoya, T., Hotta, Y., Shirao, T. and Okamoto, H. (2004). Zebrafish *gcmb* is required for pharyngeal cartilage formation. *Mech Dev* **121** (10): 1235-47.
- Hannon, G. J. (2002). RNA interference. *Nature* **418** (6894): 244-51.
- Harborth, J., Elbashir, S. M., Bechert, K., Tuschl, T. and Weber, K. (2001). Identification of essential genes in cultured mammalian cells using small interfering RNAs. *J Cell Sci* **114** (Pt 24): 4557-65.
- Hartley, R. S., Margulis, M., Fishman, P. S., Lee, V. M. and Tang, C. M. (1999). Functional synapses are formed between human NTera2 (NT2N, hNT) neurons grown on astrocytes. *J Comp Neurol* **407** (1): 1-10.
- Hatini, V. and DiNardo, S. (2001). Divide and conquer: pattern formation in *Drosophila* embryonic epidermis. *Trends Genet* **17** (10): 574-9.
- Hatten, M. E. (2002). New directions in neuronal migration. *Science* **297** (5587): 1660-3.
- Hattori, M., Adachi, H., Tsujimoto, M., Arai, H. and Inoue, K. (1994). Miller-Dieker lissencephaly gene encodes a subunit of brain platelet-activating factor acetylhydrolase [corrected]. *Nature* **370** (6486): 216-8.
- Haugland, R. P., Spence, M. T. Z. and Johnson, L. D. (1996). *Handbook of Fluorescent Probes and Research Chemicals. Sixth Edition*. Molecular Probes, Inc., Eugene.
- Hayakawa, M., Fujiki, K., Hotta, Y., Ito, R., Ohki, J., Ono, J., Saito, A., Nakayasu, K., Kanai, A., Ishidoh, K., Kominami, E., Yoshida, K., Kim, K. C. and Ohashi, H. (1999). Visual impairment and REP-1 gene mutations in Japanese choroideremia patients. *Ophthalmic Genet* **20** (2): 107-15.
- Heasman, J. (2002). Morpholino oligos: making sense of antisense? *Dev Biol* **243** (2): 209-14.
- Helms, A. W. and Johnson, J. E. (2003). Specification of dorsal spinal cord interneurons. *Curr Opin Neurobiol* **13** (1): 42-9.
- Hemond, S. G. and Glover, J. C. (1993). Clonal patterns of cell proliferation, migration, and dispersal in the brainstem of the chicken embryo. *J Neurosci* **13** (4): 1387-402.
- Hendzel, M. J., Wei, Y., Mancini, M. A., Van Hooser, A., Ranalli, T., Brinkley, B. R., Bazett-Jones, D. P. and Allis, C. D. (1997). Mitosis-specific phosphorylation of histone H3 initiates primarily within pericentromeric heterochromatin during G2 and spreads in an ordered fashion coincident with mitotic chromosome condensation. *Chromosoma* **106** (6): 348-60.
- Henrique, D., Adam, J., Myat, A., Chitnis, A., Lewis, J. and Ish-Horowicz, D. (1995). Expression of a Delta homologue in prospective neurons in the chick. *Nature* **375** (6534): 787-90.
- Hernandez, V. H. and Bueno, D. (2005). RNA interference is ineffective as a routine method for gene silencing in chick embryos as monitored by *fgf8* silencing. *Int J Biol Sci* **1** (1): 1-12.

Hertwig, O. (1902). *Lehrbuch der Entwicklungsgeschichte des Menschen und der wirbeltiere* 7. Aufl. Fisher, Jena.

Herzog, A. and Brosamle, C. (1997). 'Semifree-floating' treatment: a simple and fast method to process consecutive sections for immunohistochemistry and neuronal tracing. *J Neurosci Methods* **72** (1): 57-63.

Hill, M. E., Asa, S. L. and Drucker, D. J. (1999). Essential requirement for Pax6 in control of enteroendocrine proglucagon gene transcription. *Mol Endocrinol* **13** (9): 1474-86.

Hirokawa, N., Tanaka, Y., Okada, Y. and Takeda, S. (2006). Nodal flow and the generation of left-right asymmetry. *Cell* **125** (1): 33-45.

Hirsch, M. R., Tiveron, M. C., Guillemot, F., Brunet, J. F. and Goridis, C. (1998). Control of noradrenergic differentiation and Phox2a expression by MASH1 in the central and peripheral nervous system. *Development* **125** (4): 599-608.

Holen, T., Amarzguioui, M., Wiiger, M. T., Babaie, E. and Prydz, H. (2002). Positional effects of short interfering RNAs targeting the human coagulation trigger Tissue Factor. *Nucleic Acids Res* **30** (8): 1757-66.

Holland, L. Z., Schubert, M., Kozmik, Z. and Holland, N. D. (1999). AmphiPax3/7, an amphioxus paired box gene: insights into chordate myogenesis, neurogenesis, and the possible evolutionary precursor of definitive vertebrate neural crest. *Evol Dev* **1** (3): 153-65.

Houart, C., Westerfield, M. and Wilson, S. W. (1998). A small population of anterior cells patterns the forebrain during zebrafish gastrulation. *Nature* **391** (6669): 788-92.

Houldsworth, J., Heath, S. C., Bosl, G. J., Studer, L. and Chaganti, R. S. (2002). Expression profiling of lineage differentiation in pluripotential human embryonal carcinoma cells. *Cell Growth Differ* **13** (6): 257-64.

Howard, E. W., Newman, L. A., Oleksyn, D. W., Angerer, R. C. and Angerer, L. M. (2001). SpKrl: a direct target of beta-catenin regulation required for endoderm differentiation in sea urchin embryos. *Development* **128** (3): 365-75.

Hsu, D. R., Economides, A. N., Wang, X., Eimon, P. M. and Harland, R. M. (1998). The Xenopus dorsalizing factor Gremlin identifies a novel family of secreted proteins that antagonize BMP activities. *Mol Cell* **1** (5): 673-83.

Hu, W. Y., Myers, C. P., Kilzer, J. M., Pfaff, S. L. and Bushman, F. D. (2002). Inhibition of retroviral pathogenesis by RNA interference. *Curr Biol* **12** (15): 1301-11.

Hua, Y. and Scheller, R. H. (2001). Three SNARE complexes cooperate to mediate membrane fusion. *Proc Natl Acad Sci U S A* **98** (14): 8065-70.

Huang, E. J., Zang, K., Schmidt, A., Saulys, A., Xiang, M. and Reichardt, L. F. (1999). POU domain factor Brn-3a controls the differentiation and survival of trigeminal neurons by regulating Trk receptor expression. *Development* **126** (13): 2869-82.

Huangfu, D. and Anderson, K. V. (2005). Cilia and Hedgehog responsiveness in the mouse. *Proc Natl Acad Sci U S A* **102** (32): 11325-30.

Hunter, E., Begbie, J., Mason, I. and Graham, A. (2001). Early development of the mesencephalic trigeminal nucleus. *Dev Dyn* **222** (3): 484-93.

Hutvagner, G. and Zamore, P. D. (2002). RNAi: nature abhors a double-strand. *Curr Opin Genet Dev* **12** (2): 225-32.

Hutvagner, G. and Zamore, P. D. (2002). A microRNA in a multiple-turnover RNAi enzyme complex.

Science **297** (5589): 2056-60.

Ichijo, H. (1999). Differentiation of the chick retinotectal topographic map by remodeling in specificity and refinement in accuracy. *Brain Res Dev Brain Res* **117** (2): 199-211.

Ihle, J. N. (2000). The challenges of translating knockout phenotypes into gene function. *Cell* **102** (2): 131-4.

Ikeya, M., Lee, S. M., Johnson, J. E., McMahon, A. P. and Takada, S. (1997). Wnt signalling required for expansion of neural crest and CNS progenitors. *Nature* **389** (6654): 966-70.

Imai, Y. and Talbot, W. S. (2001). Morpholino phenocopies of the *bmp2b/swirl* and *bmp7/snailhouse* mutations. *Genesis* **30** (3): 160-3.

Ingham, P. W. and McMahon, A. P. (2001). Hedgehog signaling in animal development: paradigms and principles. *Genes Dev* **15** (23): 3059-87.

Inoue, T. and Krumlauf, R. (2001). An impulse to the brain--using in vivo electroporation. *Nat Neurosci* **4 Suppl**: 1156-8.

Ishibashi, M. and McMahon, A. P. (2002). A sonic hedgehog-dependent signaling relay regulates growth of diencephalic and mesencephalic primordia in the early mouse embryo. *Development* **129** (20): 4807-19.

Ishii, Y. and Mikawa, T. (2005). Somatic transgenesis in the avian model system. *Birth Defects Res C Embryo Today* **75** (1): 19-27.

Itasaki, N., Ichijo, H., Hama, C., Matsuno, T. and Nakamura, H. (1991). Establishment of rostrocaudal polarity in tectal primordium: engrailed expression and subsequent tectal polarity. *Development* **113** (4): 1133-44.

Itasaki, N. and Nakamura, H. (1992). Rostrocaudal polarity of the tectum in birds: correlation of en gradient and topographic order in retinotectal projection. *Neuron* **8** (4): 787-98.

Itasaki, N. and Nakamura, H. (1996). A role for gradient en expression in positional specification on the optic tectum. *Neuron* **16** (1): 55-62.

Itasaki, N., Bel-Vialar, S. and Krumlauf, R. (1999). 'Shocking' developments in chick embryology: electroporation and in ovo gene expression. *Nat Cell Biol* **1** (8): E203-7.

Jackson, I. J. (2001). Mouse mutagenesis on target. *Nat Genet* **28** (3): 198-200.

Jackson, A. L., Bartz, S. R., Schelter, J., Kobayashi, S. V., Burchard, J., Mao, M., Li, B., Cavet, G. and Linsley, P. S. (2003). Expression profiling reveals off-target gene regulation by RNAi. *Nat Biotechnol* **21** (6): 635-7.

Jacob, J. and Briscoe, J. (2003). Gli proteins and the control of spinal-cord patterning. *EMBO Rep* **4** (8): 761-5.

Jacobsen, S. E., Running, M. P. and Meyerowitz, E. M. (1999). Disruption of an RNA helicase/RNase III gene in Arabidopsis causes unregulated cell division in floral meristems. *Development* **126** (23): 5231-43.

Jacobson, A. G. and Moury, J. D. (1995). Tissue boundaries and cell behavior during neurulation. *Dev Biol* **171** (1): 98-110.

Jedrusik, M. A. and Schulze, E. (2001). A single histone H1 isoform (H1.1) is essential for chromatin silencing and germline development in *Caenorhabditis elegans*. *Development* **128** (7): 1069-80.

Jekerle, V., Kassack, M. U., Reilly, R. M., Wiese, M. and Piquette-Miller, M. (2005). Functional comparison of single- and double-stranded *mdr1* antisense oligodeoxynucleotides in human ovarian

cancer cell lines. *J Pharm Pharm Sci* **8** (3): 516-27.

Jensen, J., Serup, P., Karlsen, C., Nielsen, T. F. and Madsen, O. D. (1996). mRNA profiling of rat islet tumors reveals nkx 6.1 as a beta-cell-specific homeodomain transcription factor. *J Biol Chem* **271** (31): 18749-58.

Jeong, J. and McMahon, A. P. (2005). Growth and pattern of the mammalian neural tube are governed by partially overlapping feedback activities of the hedgehog antagonists patched 1 and Hhip1. *Development* **132** (1): 143-54.

Jessell, T. M. (2000). Neuronal specification in the spinal cord: inductive signals and transcriptional codes. *Nat Rev Genet* **1** (1): 20-9.

Jia, J., Amanai, K., Wang, G., Tang, J., Wang, B. and Jiang, J. (2002). Shaggy/GSK3 antagonizes Hedgehog signalling by regulating Cubitus interruptus. *Nature* **416** (6880): 548-52.

Johnson, R. L. and Tabin, C. (1995). The long and short of hedgehog signaling. *Cell* **81** (3): 313-6.

Jones, C. M., Kuehn, M. R., Hogan, B. L., Smith, J. C. and Wright, C. V. (1995). Nodal-related signals induce axial mesoderm and dorsalize mesoderm during gastrulation. *Development* **121** (11): 3651-62.

Jonk, L. J., de Jonge, M. E., Vervaart, J. M., Wissink, S. and Kruijer, W. (1994). Isolation and developmental expression of retinoic-acid-induced genes. *Dev Biol* **161** (2): 604-14.

Jostes, B., Walther, C. and Gruss, P. (1990). The murine paired box gene, Pax7, is expressed specifically during the development of the nervous and muscular system. *Mech Dev* **33** (1): 27-37.

Juan, G., Traganos, F. and Darzynkiewicz, Z. (1999). Histone H3 phosphorylation in human monocytes and during HL-60 cell differentiation. *Exp Cell Res* **246** (1): 212-20.

Jungbluth, S., Larsen, C., Wizenmann, A. and Lumsden, A. (2001). Cell mixing between the embryonic midbrain and hindbrain. *Curr Biol* **11** (3): 204-7.

Juriloff, D. M. and Harris, M. J. (2000). Mouse models for neural tube closure defects. *Hum Mol Genet* **9** (6): 993-1000.

Jurnak, F. (1985). Structure of the GDP domain of EF-Tu and location of the amino acids homologous to ras oncogene proteins. *Science* **230** (4721): 32-6.

Kafri, T. (2004). Gene delivery by lentivirus vectors an overview. *Methods Mol Biol* **246**: 367-90.

Kahn, R. A., Kern, F. G., Clark, J., Gelmann, E. P. and Rulka, C. (1991). Human ADP-ribosylation factors. A functionally conserved family of GTP-binding proteins. *J Biol Chem* **266** (4): 2606-14.

Kamihira, M., Ono, K., Esaka, K., Nishijima, K., Kigaku, R., Komatsu, H., Yamashita, T., Kyogoku, K. and Iijima, S. (2005). High-level expression of single-chain Fv-Fc fusion protein in serum and egg white of genetically manipulated chickens by using a retroviral vector. *J Virol* **79** (17): 10864-74.

Kanai, Y., Okada, Y., Tanaka, Y., Harada, A., Terada, S. and Hirokawa, N. (2000). KIF5C, a novel neuronal kinesin enriched in motor neurons. *J Neurosci* **20** (17): 6374-84.

Kania, A., Johnson, R. L. and Jessell, T. M. (2000). Coordinate roles for LIM homeobox genes in directing the dorsoventral trajectory of motor axons in the vertebrate limb. *Cell* **102** (2): 161-73.

Karlen, S. and Rebagliati, M. (2001). A morpholino phenocopy of the cyclops mutation. *Genesis* **30** (3): 126-8.

Karlsson, O., Thor, S., Norberg, T., Ohlsson, H. and Edlund, T. (1990). Insulin gene enhancer binding protein Isl-1 is a member of a novel class of proteins containing both a homeo- and a Cys-His domain. *Nature* **344** (6269): 879-82.

- Kasarskis, A., Manova, K. and Anderson, K. V. (1998). A phenotype-based screen for embryonic lethal mutations in the mouse. *Proc Natl Acad Sci U S A* **95** (13): 7485-90.
- Katahira, T. and Nakamura, H. (2003). Gene silencing in chick embryos with a vector-based small interfering RNA system. *Dev Growth Differ* **45** (4): 361-7.
- Kawakami, A., Kimura-Kawakami, M., Nomura, T. and Fujisawa, H. (1997). Distributions of PAX6 and PAX7 proteins suggest their involvement in both early and late phases of chick brain development. *Mech Dev* **66** (1-2): 119-30.
- Kay, P. H. and Ziman, M. R. (1999). Alternate Pax7 paired box transcripts which include a trinucleotide or a hexanucleotide are generated by use of alternate 3' intronic splice sites which are not utilized in the ancestral homologue. *Gene* **230** (1): 55-60.
- Keller, R., Shih, J., Sater, A. K. and Moreno, C. (1992). Planar induction of convergence and extension of the neural plate by the organizer of *Xenopus*. *Dev Dyn* **193** (3): 218-34.
- Kennerdell, J. R. and Carthew, R. W. (1998). Use of dsRNA-mediated genetic interference to demonstrate that frizzled and frizzled 2 act in the wingless pathway. *Cell* **95** (7): 1017-26.
- Ketting, R. F., Fischer, S. E., Bernstein, E., Sijen, T., Hannon, G. J. and Plasterk, R. H. (2001). Dicer functions in RNA interference and in synthesis of small RNA involved in developmental timing in *C. elegans*. *Genes Dev* **15** (20): 2654-9.
- Khvorova, A., Reynolds, A. and Jayasena, S. D. (2003). Functional siRNAs and miRNAs exhibit strand bias. *Cell* **115** (2): 209-16.
- Kinzler, K. W., Ruppert, J. M., Bigner, S. H. and Vogelstein, B. (1988). The GLI gene is a member of the Kruppel family of zinc finger proteins. *Nature* **332** (6162): 371-4.
- Knight, S. W. and Bass, B. L. (2001). A role for the RNase III enzyme DCR-1 in RNA interference and germ line development in *Caenorhabditis elegans*. *Science* **293** (5538): 2269-71.
- Kohtz, J. D., Baker, D. P., Corte, G. and Fishell, G. (1998). Regionalization within the mammalian telencephalon is mediated by changes in responsiveness to Sonic Hedgehog. *Development* **125** (24): 5079-89.
- Kos, R., Tucker, R. P., Hall, R., Duong, T. D. and Erickson, C. A. (2003). Methods for introducing morpholinos into the chicken embryo. *Dev Dyn* **226** (3): 470-7.
- Krull, C. E. (2004). A primer on using in ovo electroporation to analyze gene function. *Dev Dyn* **229** (3): 433-9.
- Kull, F. J. (2000). Motor proteins of the kinesin superfamily: structure and mechanism. *Essays Biochem* **35**: 61-73.
- Kumar, R., Singh, S. K., Koshkin, A. A., Rajwanshi, V. K., Meldgaard, M. and Wengel, J. (1998). The first analogues of LNA (locked nucleic acids): phosphorothioate-LNA and 2'-thio-LNA. *Bioorg Med Chem Lett* **8** (16): 2219-22.
- Kurreck, J. (2003). Antisense technologies. Improvement through novel chemical modifications. *Eur J Biochem* **270** (8): 1628-44.
- Kuznetsov, S. A., Langford, G. M. and Weiss, D. G. (1992). Actin-dependent organelle movement in squid axoplasm. *Nature* **356** (6371): 722-5.
- LaBonne, C. and Bronner-Fraser, M. (1999). Molecular mechanisms of neural crest formation. *Annu Rev Cell Dev Biol* **15**: 81-112.
- Lacerra, G., Sierakowska, H., Carestia, C., Fucharoen, S., Summerton, J., Weller, D. and Kole, R. (2000). Restoration of hemoglobin A synthesis in erythroid cells from peripheral blood of thalassemic

patients. *Proc Natl Acad Sci U S A* **97** (17): 9591-6.

Lagos-Quintana, M., Rauhut, R., Lendeckel, W. and Tuschl, T. (2001). Identification of novel genes coding for small expressed RNAs. *Science* **294** (5543): 853-8.

Lamb, T. M., Knecht, A. K., Smith, W. C., Stachel, S. E., Economides, A. N., Stahl, N., Yancopolous, G. D. and Harland, R. M. (1993). Neural induction by the secreted polypeptide noggin. *Science* **262** (5134): 713-8.

Lapierre, L. A., Kumar, R., Hales, C. M., Navarre, J., Bhartur, S. G., Burnette, J. O., Provance, D. W., Jr., Mercer, J. A., Bahler, M. and Goldenring, J. R. (2001). Myosin vb is associated with plasma membrane recycling systems. *Mol Biol Cell* **12** (6): 1843-57.

Larsen, H. J., Bentin, T. and Nielsen, P. E. (1999). Antisense properties of peptide nucleic acid. *Biochim Biophys Acta* **1489** (1): 159-66.

Latchman, D. S. (1998). The Brn-3a transcription factor. *Int J Biochem Cell Biol* **30** (11): 1153-7.

LaVail, J. H. and Gowan, W. M. (1971). The development of the chick optic tectum. I. Normal morphology and cytoarchitectonic development. *Brain Res* **28** (3): 391-419.

Lawrence, P. A., Sanson, B. and Vincent, J. P. (1996). Compartments, wingless and engrailed: patterning the ventral epidermis of Drosophila embryos. *Development* **122** (12): 4095-103.

Lawrence, P. A., Casal, J. and Struhl, G. (1999). The hedgehog morphogen and gradients of cell affinity in the abdomen of Drosophila. *Development* **126** (11): 2441-9.

Le Douarin, N. (1973). A biological cell labeling technique and its use in experimental embryology. *Dev Biol* **30** (1): 217-22.

Le Douarin, N. M. and Teillet, M. A. (1973). The migration of neural crest cells to the wall of the digestive tract in avian embryo. *J Embryol Exp Morphol* **30** (1): 31-48.

Leber, S. M. and Sanes, J. R. (1995). Migratory paths of neurons and glia in the embryonic chick spinal cord. *J. Neurosci.* **15**: 1236-1248.

Lee, V. M. and Andrews, P. W. (1986). Differentiation of NTERA-2 clonal human embryonal carcinoma cells into neurons involves the induction of all three neurofilament proteins. *J Neurosci* **6** (2): 514-21.

Lee, K. J., Mendelsohn, M. and Jessell, T. M. (1998). Neuronal patterning by BMPs: a requirement for GDF7 in the generation of a discrete class of commissural interneurons in the mouse spinal cord. *Genes Dev* **12** (21): 3394-407.

Lee, K. J. and Jessell, T. M. (1999). The specification of dorsal cell fates in the vertebrate central nervous system. *Annu Rev Neurosci* **22**: 261-94.

Lee, K. J., Dietrich, P. and Jessell, T. M. (2000). Genetic ablation reveals that the roof plate is essential for dorsal interneuron specification. *Nature* **403** (6771): 734-40.

Lee, R. C. and Ambros, V. (2001). An extensive class of small RNAs in Caenorhabditis elegans. *Science* **294** (5543): 862-4.

Lee, S. H., Fu, K. K., Hui, J. N. and Richman, J. M. (2001). Noggin and retinoic acid transform the identity of avian facial prominences. *Nature* **414** (6866): 909-12.

Lee, Y., Ahn, C., Han, J., Choi, H., Kim, J., Yim, J., Lee, J., Provost, P., Radmark, O., Kim, S. and Kim, V. N. (2003). The nuclear RNase III Drosha initiates microRNA processing. *Nature* **425** (6956): 415-9.

Lee, Y. S., Nakahara, K., Pham, J. W., Kim, K., He, Z., Sontheimer, E. J. and Carthew, R. W. (2004). Distinct roles for Drosophila Dicer-1 and Dicer-2 in the siRNA/miRNA silencing pathways. *Cell* **117** (1):

69-81.

Lei, Q., Zelman, A. K., Kuang, E., Li, S. and Matisse, M. P. (2004). Transduction of graded Hedgehog signaling by a combination of Gli2 and Gli3 activator functions in the developing spinal cord. *Development* **131** (15): 3593-604.

Lele, Z., Bakkers, J. and Hammerschmidt, M. (2001). Morpholino phenocopies of the swirl, snailhouse, somitabun, minifin, silberblick, and pipetail mutations. *Genesis* **30** (3): 190-4.

Letinic, K. and Rakic, P. (2001). Telencephalic origin of human thalamic GABAergic neurons. *Nat Neurosci* **4** (9): 931-6.

Levin, M., Johnson, R. L., Stern, C. D., Kuehn, M. and Tabin, C. (1995). A molecular pathway determining left-right asymmetry in chick embryogenesis. *Cell* **82** (5): 803-14.

Levin, M., Pagan, S., Roberts, D. J., Cooke, J., Kuehn, M. R. and Tabin, C. J. (1997). Left/right patterning signals and the independent regulation of different aspects of situs in the chick embryo. *Dev Biol* **189** (1): 57-67.

Levitan, I. B. and Kaczmarek, L. K. (2002). *The Neuron Cell and Molecular Biology. Third Edition.* Oxford Uni. Press, New York.

Lewin, B. (2000). *Genes VII.* Oxford University Press Inc., New York.

Li, J., Liu, K. C., Jin, F., Lu, M. M. and Epstein, J. A. (1999). Transgenic rescue of congenital heart disease and spina bifida in Splotch mice. *Development* **126** (11): 2495-503.

Li, N., Hornbruch, A., Klafke, R., Katzenberger, B. and Wizenmann, A. (2005). Specification of dorsoventral polarity in the embryonic chick mesencephalon and its presumptive role in midbrain morphogenesis. *Dev Dyn* **233** (3): 907-920.

Liem, K. F., Jr., Tremml, G., Roelink, H. and Jessell, T. M. (1995). Dorsal differentiation of neural plate cells induced by BMP-mediated signals from epidermal ectoderm. *Cell* **82** (6): 969-79.

Liem, K. F., Jr., Tremml, G. and Jessell, T. M. (1997). A role for the roof plate and its resident TGFbeta-related proteins in neuronal patterning in the dorsal spinal cord. *Cell* **91** (1): 127-38.

Liem, K. F., Jr., Jessell, T. M. and Briscoe, J. (2000). Regulation of the neural patterning activity of sonic hedgehog by secreted BMP inhibitors expressed by notochord and somites. *Development* **127** (22): 4855-66.

Lin, J. H., Saito, T., Anderson, D. J., Lance-Jones, C., Jessell, T. M. and Arber, S. (1998). Functionally related motor neuron pool and muscle sensory afferent subtypes defined by coordinate ETS gene expression. *Cell* **95** (3): 393-407.

Lipardi, C., Wei, Q. and Paterson, B. M. (2001). RNAi as random degradative PCR: siRNA primers convert mRNA into dsRNAs that are degraded to generate new siRNAs. *Cell* **107** (3): 297-307.

Litingtung, Y. and Chiang, C. (2000). Specification of ventral neuron types is mediated by an antagonistic interaction between Shh and Gli3. *Nat Neurosci* **3** (10): 979-85.

Liu, X., Sun, Y., Constantinescu, S. N., Karam, E., Weinberg, R. A. and Lodish, H. F. (1997). Transforming growth factor beta-induced phosphorylation of Smad3 is required for growth inhibition and transcriptional induction in epithelial cells. *Proc Natl Acad Sci U S A* **94** (20): 10669-74.

Liu, A. and Joyner, A. L. (2001). EN and GBX2 play essential roles downstream of FGF8 in patterning the mouse mid/hindbrain region. *Development* **128** (2): 181-91.

Liu, Y., Helms, A. W. and Johnson, J. E. (2004). Distinct activities of Msx1 and Msx3 in dorsal neural tube development. *Development* **131** (5): 1017-28.

- Liu, A., Wang, B. and Niswander, L. A. (2005). Mouse intraflagellar transport proteins regulate both the activator and repressor functions of Gli transcription factors. *Development* **132** (13): 3103-11.
- Lodish, H., Berk, A., Zipursky, S. L., Matsudaira, P., Baltimore, D. and Darnell, J. E. (2000). *Molecular Cell Biology. 4th edition*. W. H. Freeman & Co., New York.
- Logan, M. and Tabin, C. (1998). Targeted gene misexpression in chick limb buds using avian replication-competent retroviruses. *Methods* **14** (4): 407-20.
- Lum, L., Zhang, C., Oh, S., Mann, R. K., von Kessler, D. P., Taipale, J., Weis-Garcia, F., Gong, R., Wang, B. and Beachy, P. A. (2003). Hedgehog signal transduction via Smoothed association with a cytoplasmic complex scaffolded by the atypical kinesin, Costal-2. *Mol Cell* **12** (5): 1261-74.
- Lumsden, A. G. and Davies, A. M. (1983). Earliest sensory nerve fibres are guided to peripheral targets by attractants other than nerve growth factor. *Nature* **306** (5945): 786-8.
- Lumsden, A. and Krumlauf, R. (1996). Patterning the vertebrate neuraxis. *Science* **274** (5290): 1109-15.
- Luskin, M. B., Pearlman, A. L. and Sanes, J. R. (1988). Cell lineage in the cerebral cortex of the mouse studied in vivo and in vitro with a recombinant retrovirus. *Neuron* **1** (8): 635-47.
- Lutcke, A., Jansson, S., Parton, R. G., Chavrier, P., Valencia, A., Huber, L. A., Lehtonen, E. and Zerial, M. (1993). Rab17, a novel small GTPase, is specific for epithelial cells and is induced during cell polarization. *J Cell Biol* **121** (3): 553-64.
- Lyons, K. M., Hogan, B. L. and Robertson, E. J. (1995). Colocalization of BMP 7 and BMP 2 RNAs suggests that these factors cooperatively mediate tissue interactions during murine development. *Mech Dev* **50** (1): 71-83.
- Macdonald, R., Barth, K. A., Xu, Q., Holder, N., Mikkola, I. and Wilson, S. W. (1995). Midline signalling is required for Pax gene regulation and patterning of the eyes. *Development* **121** (10): 3267-78.
- Maden, M. (2006). Retinoids and spinal cord development. *J Neurobiol* **66** (7): 726-38.
- Maeda, R., Kobayashi, A., Sekine, R., Lin, J. J., Kung, H. and Maeno, M. (1997). Xmsx-1 modifies mesodermal tissue pattern along dorsoventral axis in *Xenopus laevis* embryo. *Development* **124** (13): 2553-60.
- Malchere, C., Verheijen, J., van der Laan, S., Bastide, L., van Boom, J., Lebleu, B. and Robbins, I. (2000). A short phosphodiester window is sufficient to direct RNase H-dependent RNA cleavage by antisense peptide nucleic acid. *Antisense Nucleic Acid Drug Dev* **10** (6): 463-8.
- Mangeot, P. E., Cosset, F. L., Colas, P. and Mikaelian, I. (2004). A universal transgene silencing method based on RNA interference. *Nucleic Acids Res* **32** (12): e102.
- Mann, R. S. and Morata, G. (2000). The developmental and molecular biology of genes that subdivide the body of *Drosophila*. *Annu Rev Cell Dev Biol* **16**: 243-71.
- Mansouri, A., Stoykova, A. and Gruss, P. (1994). Pax genes in development. *J Cell Sci Suppl* **18**: 35-42.
- Mansouri, A., Stoykova, A., Torres, M. and Gruss, P. (1996). Dysgenesis of cephalic neural crest derivatives in *Pax7*^{-/-} mutant mice. *Development* **122** (3): 831-8.
- Mansouri, A. and Gruss, P. (1998). Pax3 and Pax7 are expressed in commissural neurons and restrict ventral neuronal identity in the spinal cord. *Mech Dev* **78** (1-2): 171-8.
- Mansouri, A. (1998). The role of Pax3 and Pax7 in development and cancer. *Crit Rev Oncog* **9** (2): 141-9.

- Mansouri, A., Goudreau, G. and Gruss, P. (1999). Pax genes and their role in organogenesis. *Cancer Res* **59** (7 Suppl): 1707s-1709s; discussion 1709s-1710s.
- Mansouri, A., Pla, P., Larue, L. and Gruss, P. (2001). Pax3 acts cell autonomously in the neural tube and somites by controlling cell surface properties. *Development* **128** (11): 1995-2005.
- Marcos, I., Borrego, S. and Antinolo, G. (2003). Molecular cloning and characterization of human RAB23, a member of the group of Rab GTPases. *Int J Mol Med* **12** (6): 983-7.
- Margue, C. M., Bernasconi, M., Barr, F. G. and Schafer, B. W. (2000). Transcriptional modulation of the anti-apoptotic protein BCL-XL by the paired box transcription factors PAX3 and PAX3/FKHR. *Oncogene* **19** (25): 2921-9.
- Marigo, V., Davey, R. A., Zuo, Y., Cunningham, J. M. and Tabin, C. J. (1996). Biochemical evidence that patched is the Hedgehog receptor. *Nature* **384** (6605): 176-9.
- Maroto, M., Reshef, R., Munsterberg, A. E., Koester, S., Goulding, M. and Lassar, A. B. (1997). Ectopic Pax-3 activates MyoD and Myf-5 expression in embryonic mesoderm and neural tissue. *Cell* **89** (1): 139-48.
- Marszalek, J. R., Ruiz-Lozano, P., Roberts, E., Chien, K. R. and Goldstein, L. S. (1999). Situs inversus and embryonic ciliary morphogenesis defects in mouse mutants lacking the KIF3A subunit of kinesin-II. *Proc Natl Acad Sci U S A* **96** (9): 5043-8.
- Marti, E., Bumcrot, D. A., Takada, R. and McMahon, A. P. (1995). Requirement of 19K form of Sonic hedgehog for induction of distinct ventral cell types in CNS explants. *Nature* **375** (6529): 322-5.
- Marti, E., Takada, R., Bumcrot, D. A., Sasaki, H. and McMahon, A. P. (1995). Distribution of Sonic hedgehog peptides in the developing chick and mouse embryo. *Development* **121** (8): 2537-47.
- Martinez, S. and Alvarado-Mallart, R. M. (1989). Transplanted mesencephalic quail cells colonize selectively all primary visual nuclei of chick diencephalon: a study using heterotopic transplants. *Brain Res Dev Brain Res* **47** (2): 263-74.
- Martinez, S., Wassef, M. and Alvarado-Mallart, R. M. (1991). Induction of a mesencephalic phenotype in the 2-day-old chick prosencephalon is preceded by the early expression of the homeobox gene en. *Neuron* **6** (6): 971-81.
- Matsukura, M., Shinozuka, K., Zon, G., Mitsuya, H., Reitz, M., Cohen, J. S. and Broder, S. (1987). Phosphorothioate analogs of oligodeoxynucleotides: inhibitors of replication and cytopathic effects of human immunodeficiency virus. *Proc Natl Acad Sci U S A* **84** (21): 7706-10.
- Matsunaga, E., Araki, I. and Nakamura, H. (2000). Pax6 defines the di-mesencephalic boundary by repressing En1 and Pax2. *Development* **127** (11): 2357-65.
- Matsunaga, E., Araki, I. and Nakamura, H. (2001). Role of Pax3/7 in the tectum regionalization. *Development* **128** (20): 4069-77.
- Matsuno, T., Ichijo, H. and Nakamura, H. (1991). Regulation of the rostrocaudal axis of the optic tectum: histological study after rostrocaudal rotation in quail-chick chimeras. *Brain Res Dev Brain Res* **58** (2): 265-70.
- Matsuno, T. and Nakamura, H. (1993). Plasticity of avian mesencephalic polarity revealed by trajectories of tectofugal axons. *Brain Res Dev Brain Res* **75** (1): 39-44.
- Matsuno, T. and Nakamura, H. (1994). Plasticity in mesencephalic and retinal polarity formation in avian embryos. *Neurosci Res* **19** (1): 1-8.
- Matzuk, M. M., Kumar, T. R. and Bradley, A. (1995). Different phenotypes for mice deficient in either activins or activin receptor type II. *Nature* **374** (6520): 356-60.

- McBurney, M. W., Jones-Villeneuve, E. M., Edwards, M. K. and Anderson, P. J. (1982). Control of muscle and neuronal differentiation in a cultured embryonal carcinoma cell line. *Nature* **299** (5879): 165-7.
- McEvelly, R. J., Erkman, L., Luo, L., Sawchenko, P. E., Ryan, A. F. and Rosenfeld, M. G. (1996). Requirement for Brn-3.0 in differentiation and survival of sensory and motor neurons. *Nature* **384** (6609): 574-7.
- McKay, R. (1997). Stem cells in the central nervous system. *Science* **276** (5309): 66-71.
- McMahon, A. P. and Bradley, A. (1990). The Wnt-1 (int-1) proto-oncogene is required for development of a large region of the mouse brain. *Cell* **62** (6): 1073-85.
- McMahon, J. A., Takada, S., Zimmerman, L. B., Fan, C. M., Harland, R. M. and McMahon, A. P. (1998). Noggin-mediated antagonism of BMP signaling is required for growth and patterning of the neural tube and somite. *Genes Dev* **12** (10): 1438-52.
- McMahon, A. P. (2000). More surprises in the Hedgehog signaling pathway. *Cell* **100** (2): 185-8.
- McMahon, A. P., Ingham, P. W. and Tabin, C. J. (2003). Developmental roles and clinical significance of hedgehog signaling. *Curr Top Dev Biol* **53**: 1-114.
- Megason, S. G. and McMahon, A. P. (2002). A mitogen gradient of dorsal midline Wnts organizes growth in the CNS. *Development* **129** (9): 2087-98.
- Megjorni, F., Mora, B., Indovina, P. and Mazzilli, M. C. (2005). Expression of neuronal markers during Ntera2/cloned1 differentiation by cell aggregation method. *Neurosci Lett* **373** (2): 105-9.
- Mendell, J. T. (2005). MicroRNAs: critical regulators of development, cellular physiology and malignancy. *Cell Cycle* **4** (9): 1179-84.
- Metzger, D. and Chambon, P. (2001). Site- and time-specific gene targeting in the mouse. *Methods* **24** (1): 71-80.
- Meyer, N. P. and Roelink, H. (2003). The amino-terminal region of Gli3 antagonizes the Shh response and acts in dorsoventral fate specification in the developing spinal cord. *Dev Biol* **257** (2): 343-55.
- Meyers, E. N., Lewandoski, M. and Martin, G. R. (1998). An Fgf8 mutant allelic series generated by Cre- and Flp-mediated recombination. *Nat Genet* **18** (2): 136-41.
- Miaczynska, M., Christoforidis, S., Giner, A., Shevchenko, A., Uttenweiler-Joseph, S., Habermann, B., Wilm, M., Parton, R. G. and Zerial, M. (2004). APPL proteins link Rab5 to nuclear signal transduction via an endosomal compartment. *Cell* **116** (3): 445-56.
- Millen, K. J., Millonig, J. H. and Hatten, M. E. (2004). Roof plate and dorsal spinal cord dl1 interneuron development in the dreher mutant mouse. *Dev Biol* **270** (2): 382-92.
- Millonig, J. H., Millen, K. J. and Hatten, M. E. (2000). The mouse Dreher gene Lmx1a controls formation of the roof plate in the vertebrate CNS. *Nature* **403** (6771): 764-9.
- Ming, J. E., Roessler, E. and Muenke, M. (1998). Human developmental disorders and the Sonic hedgehog pathway. *Mol Med Today* **4** (8): 343-9.
- Mitta, B., Rimann, M., Ehrenguber, M. U., Ehrbar, M., Djonov, V., Kelm, J. and Fussenegger, M. (2002). Advanced modular self-inactivating lentiviral expression vectors for multigene interventions in mammalian cells and in vivo transduction. *Nucleic Acids Res* **30** (21): e113.
- Mittal, V. (2004). Improving the efficiency of RNA interference in mammals. *Nat Rev Genet* **5** (5): 355-65.
- Miyagishi, M. and Taira, K. (2002). U6 promoter-driven siRNAs with four uridine 3' overhangs

efficiently suppress targeted gene expression in mammalian cells. *Nat Biotechnol* **20** (5): 497-500.

Mo, R., Freer, A. M., Zinyk, D. L., Crackower, M. A., Michaud, J., Heng, H. H., Chik, K. W., Shi, X. M., Tsui, L. C., Cheng, S. H., Joyner, A. L. and Hui, C. (1997). Specific and redundant functions of Gli2 and Gli3 zinc finger genes in skeletal patterning and development. *Development* **124** (1): 113-23.

Mohler, J. and Vani, K. (1992). Molecular organization and embryonic expression of the hedgehog gene involved in cell-cell communication in segmental patterning of *Drosophila*. *Development* **115** (4): 957-71.

Molle, K. D., Chedotal, A., Rao, Y., Lumsden, A. and Wizenmann, A. (2004). Local inhibition guides the trajectory of early longitudinal tracts in the developing chick brain. *Mech Dev* **121** (2): 143-56.

Momose, T., Tonegawa, A., Takeuchi, J., Ogawa, H., Umesono, K. and Yasuda, K. (1999). Efficient targeting of gene expression in chick embryos by microelectroporation. *Dev Growth Differ* **41** (3): 335-44.

Monnier, V., Ho, K. S., Sanial, M., Scott, M. P. and Plessis, A. (2002). Hedgehog signal transduction proteins: contacts of the Fused kinase and Ci transcription factor with the kinesin-related protein Costal2. *BMC Dev Biol* **2** (1): 4.

Monsoro-Burq, A. and Le Douarin, N. M. (2001). BMP4 plays a key role in left-right patterning in chick embryos by maintaining Sonic Hedgehog asymmetry. *Mol Cell* **7** (4): 789-99.

Morcos, P. A. (2001). Achieving efficient delivery of morpholino oligos in cultured cells. *Genesis* **30** (3): 94-102.

Morett, E. and Segovia, L. (1993). The sigma 54 bacterial enhancer-binding protein family: mechanism of action and phylogenetic relationship of their functional domains. *J Bacteriol* **175** (19): 6067-74.

Moritz, O. L., Tam, B. M., Hurd, L. L., Peranen, J., Deretic, D. and Papermaster, D. S. (2001). Mutant rab8 Impairs docking and fusion of rhodopsin-bearing post-Golgi membranes and causes cell death of transgenic *Xenopus* rods. *Mol Biol Cell* **12** (8): 2341-51.

Motoyama, J., Milenkovic, L., Iwama, M., Shikata, Y., Scott, M. P. and Hui, C. C. (2003). Differential requirement for Gli2 and Gli3 in ventral neural cell fate specification. *Dev Biol* **259** (1): 150-61.

Mourrain, P., Beclin, C., Elmayan, T., Feuerbach, F., Godon, C., Morel, J. B., Jouette, D., Lacombe, A. M., Nikic, S., Picault, N., Remoue, K., Sanial, M., Vo, T. A. and Vaucheret, H. (2000). Arabidopsis SGS2 and SGS3 genes are required for posttranscriptional gene silencing and natural virus resistance. *Cell* **101** (5): 533-42.

Muller, U. (1999). Ten years of gene targeting: targeted mouse mutants, from vector design to phenotype analysis. *Mech Dev* **82** (1-2): 3-21.

Muller, F., Albert, S., Blader, P., Fischer, N., Hallonet, M. and Strahle, U. (2000). Direct action of the nodal-related signal cyclops in induction of sonic hedgehog in the ventral midline of the CNS. *Development* **127** (18): 3889-97.

Muller, T., Brohmann, H., Pierani, A., Heppenstall, P. A., Lewin, G. R., Jessell, T. M. and Birchmeier, C. (2002). The homeodomain factor *lhx1* distinguishes two major programs of neuronal differentiation in the dorsal spinal cord. *Neuron* **34** (4): 551-62.

Muller, Y. L., Yueh, Y. G., Yaworsky, P. J., Salbaum, J. M. and Kappen, C. (2003). Caudal dysgenesis in *Islet-1* transgenic mice. *Faseb J* **17** (10): 1349-51.

Muller, M., Jabs, N., Lorke, D. E., Fritsch, B. and Sander, M. (2003). Nkx6.1 controls migration and axon pathfinding of cranial branchio-motoneurons. *Development* **130** (23): 5815-26.

Munoz-Sanjuan, I., Simandl, B. K., Fallon, J. F. and Nathans, J. (1999). Expression of chicken fibroblast growth factor homologous factor (FHF)-1 and of differentially spliced isoforms of FHF-2

during development and involvement of FHF-2 in chicken limb development. *Development* **126** (2): 409-21.

Muramatsu, T., Mizutani, Y., Ohmori, Y. and Okumura, J. (1997). Comparison of three nonviral transfection methods for foreign gene expression in early chicken embryos in ovo. *Biochem Biophys Res Commun* **230** (2): 376-80.

Murcia, N. S., Richards, W. G., Yoder, B. K., Mucenski, M. L., Dunlap, J. R. and Woychik, R. P. (2000). The Oak Ridge Polycystic Kidney (orpk) disease gene is required for left-right axis determination. *Development* **127** (11): 2347-55.

Muresan, V., Abramson, T., Lyass, A., Winter, D., Porro, E., Hong, F., Chamberlin, N. L. and Schnapp, B. J. (1998). KIF3C and KIF3A form a novel neuronal heteromeric kinesin that associates with membrane vesicles. *Mol Biol Cell* **9** (3): 637-52.

Murone, M., Rosenthal, A. and de Sauvage, F. J. (1999). Sonic hedgehog signaling by the patched-smoothed receptor complex. *Curr Biol* **9** (2): 76-84.

Murone, M., Luoh, S. M., Stone, D., Li, W., Gurney, A., Armanini, M., Grey, C., Rosenthal, A. and de Sauvage, F. J. (2000). Gli regulation by the opposing activities of fused and suppressor of fused. *Nat Cell Biol* **2** (5): 310-2.

Muroyama, Y., Fujihara, M., Ikeya, M., Kondoh, H. and Takada, S. (2002). Wnt signaling plays an essential role in neuronal specification of the dorsal spinal cord. *Genes Dev* **16** (5): 548-53.

Nakagawa, S. and Takeichi, M. (1998). Neural crest emigration from the neural tube depends on regulated cadherin expression. *Development* **125** (15): 2963-71.

Nakamura, H., Nakano, K. E., Igawa, H. H., Takagi, S. and Fujisawa, H. (1986). Plasticity and rigidity of differentiation of brain vesicles studied in quail-chick chimeras. *Cell Differ* **19** (3): 187-93.

Nakamura, H. and O'Leary, D. D. (1989). Inaccuracies in initial growth and arborization of chick retinotectal axons followed by course corrections and axon remodeling to develop topographic order. *J Neurosci* **9** (11): 3776-95.

Nakamura, H. and Funahashi, J. (2001). Introduction of DNA into chick embryos by in ovo electroporation. *Methods* **24** (1): 43-8.

Nakamura, H. and Watanabe, Y. (2005). Isthmus organizer and regionalization of the mesencephalon and metencephalon. *Int J Dev Biol* **49** (2-3): 231-5.

Napoli, C., Lemieux, C. and Jorgensen, R. (1990). Introduction of a Chimeric Chalcone Synthase Gene into Petunia Results in Reversible Co-Suppression of Homologous Genes in trans. *Plant Cell* **2** (4): 279-289.

Nasevicius, A. and Ekker, S. C. (2000). Effective targeted gene 'knockdown' in zebrafish. *Nat Genet* **26** (2): 216-20.

Navone, F., Consalez, G. G., Sardella, M., Caspani, E., Pozzoli, O., Frasconi, C., Morlacchi, E., Sitia, R., Sprocati, T. and Cabibbo, A. (2001). Expression of KIF3C kinesin during neural development and in vitro neuronal differentiation. *J Neurochem* **77** (3): 741-53.

Nery, S., Wichterle, H. and Fishell, G. (2001). Sonic hedgehog contributes to oligodendrocyte specification in the mammalian forebrain. *Development* **128** (4): 527-40.

Neubuser, A., Koseki, H. and Balling, R. (1995). Characterization and developmental expression of Pax9, a paired-box-containing gene related to Pax1. *Dev Biol* **170** (2): 701-16.

Newman, C. M. and Magee, A. I. (1993). Posttranslational processing of the ras superfamily of small GTP-binding proteins. *Biochim Biophys Acta* **1155** (1): 79-96.

- Nguyen, V. H., Trout, J., Connors, S. A., Andermann, P., Weinberg, E. and Mullins, M. C. (2000). Dorsal and intermediate neuronal cell types of the spinal cord are established by a BMP signaling pathway. *Development* **127** (6): 1209-20.
- Nielsen, E., Severin, F., Backer, J. M., Hyman, A. A. and Zerial, M. (1999). Rab5 regulates motility of early endosomes on microtubules. *Nat Cell Biol* **1** (6): 376-82.
- Nieto, M. A., Sargent, M. G., Wilkinson, D. G. and Cooke, J. (1994). Control of cell behavior during vertebrate development by Slug, a zinc finger gene. *Science* **264** (5160): 835-9.
- Nishimura, A., Morita, M., Nishimura, Y. and Sugino, Y. (1990). A rapid and highly efficient method for preparation of competent Escherichia coli cells. *Nucleic Acids Res* **18** (20): 6169.
- Noll, M. (1993). Evolution and role of Pax genes. *Curr Opin Genet Dev* **3** (4): 595-605.
- Nomura, T., Kawakami, A. and Fujisawa, H. (1998). Correlation between tectum formation and expression of two PAX family genes, PAX7 and PAX6, in avian brains. *Dev Growth Differ* **40** (5): 485-95.
- Nonaka, S., Tanaka, Y., Okada, Y., Takeda, S., Harada, A., Kanai, Y., Kido, M. and Hirokawa, N. (1998). Randomization of left-right asymmetry due to loss of nodal cilia generating leftward flow of extraembryonic fluid in mice lacking KIF3B motor protein. *Cell* **95** (6): 829-37.
- Nornes, H. O. and Carry, M. (1978). Neurogenesis in spinal cord of mouse: an autoradiographic analysis. *Brain Res* **159** (1): 1-6.
- Novina, C. D., Murray, M. F., Dykxhoorn, D. M., Beresford, P. J., Riess, J., Lee, S. K., Collman, R. G., Lieberman, J., Shankar, P. and Sharp, P. A. (2002). siRNA-directed inhibition of HIV-1 infection. *Nat Med* **8** (7): 681-6.
- Nusslein-Volhard, C. and Wieschaus, E. (1980). Mutations affecting segment number and polarity in Drosophila. *Nature* **287** (5785): 795-801.
- Nybakken, K. E., Turck, C. W., Robbins, D. J. and Bishop, J. M. (2002). Hedgehog-stimulated phosphorylation of the kinesin-related protein Costal2 is mediated by the serine/threonine kinase fused. *J Biol Chem* **277** (27): 24638-47.
- Nykanen, A., Haley, B. and Zamore, P. D. (2001). ATP requirements and small interfering RNA structure in the RNA interference pathway. *Cell* **107** (3): 309-21.
- O'Rourke, N. A., Dailey, M. E., Smith, S. J. and McConnell, S. K. (1992). Diverse migratory pathways in the developing cerebral cortex. *Science* **258** (5080): 299-302.
- O'Rourke, N. A., Chenn, A. and McConnell, S. K. (1997). Postmitotic neurons migrate tangentially in the cortical ventricular zone. *Development* **124** (5): 997-1005.
- Odent, S., Atti-Bitach, T., Blayau, M., Mathieu, M., Aug, J., Delezo de, A. L., Gall, J. Y., Le Marec, B., Munnich, A., David, V. and Vekemans, M. (1999). Expression of the Sonic hedgehog (SHH) gene during early human development and phenotypic expression of new mutations causing holoprosencephaly. *Hum Mol Genet* **8** (9): 1683-9.
- Ohkubo, Y., Uchida, A. O., Shin, D., Partanen, J. and Vaccarino, F. M. (2004). Fibroblast growth factor receptor 1 is required for the proliferation of hippocampal progenitor cells and for hippocampal growth in mouse. *J Neurosci* **24** (27): 6057-69.
- Okada, Y., Nonaka, S., Tanaka, Y., Saijoh, Y., Hamada, H. and Hirokawa, N. (1999). Abnormal nodal flow precedes situs inversus in iv and inv mice. *Mol Cell* **4** (4): 459-68.
- Okada, T., Keino-Masu, K. and Masu, M. (2007). Migration and nucleogenesis of mouse precerebellar neurons visualized by in utero electroporation of a green fluorescent protein gene. *Neurosci Res* **57** (1): 40-9.

Okafuji, T., Funahashi, J. and Nakamura, H. (1999). Roles of Pax-2 in initiation of the chick tectal development. *Brain Res Dev Brain Res* **116** (1): 41-9.

Olguin, H. C. and Olwin, B. B. (2004). Pax-7 up-regulation inhibits myogenesis and cell cycle progression in satellite cells: a potential mechanism for self-renewal. *Dev Biol* **275** (2): 375-88.

Olkkonen, V. M., Peterson, J. R., Dupree, P., Lutcke, A., Zerial, M. and Simons, K. (1994). Isolation of a mouse cDNA encoding Rab23, a small novel GTPase expressed predominantly in the brain. *Gene* **138** (1-2): 207-11.

Orentas, D. M., Hayes, J. E., Dyer, K. L. and Miller, R. H. (1999). Sonic hedgehog signaling is required during the appearance of spinal cord oligodendrocyte precursors. *Development* **126** (11): 2419-29.

Oustanina, S., Hause, G. and Braun, T. (2004). Pax7 directs postnatal renewal and propagation of myogenic satellite cells but not their specification. *Embo J* **23** (16): 3430-9.

Paduch, M., Jelen, F. and Otlewski, J. (2001). Structure of small G proteins and their regulators. *Acta Biochim Pol* **48** (4): 829-50.

Pagan-Westphal, S. M. and Tabin, C. J. (1998). The transfer of left-right positional information during chick embryogenesis. *Cell* **93** (1): 25-35.

Palma, V. and Ruiz i Altaba, A. (2004). Hedgehog-Gli signaling regulates the behavior of cells with stem cell properties in the developing neocortex. *Development* **131** (2): 337-45.

Panhuyzen, M., Vogt Weisenhorn, D. M., Blanquet, V., Brodski, C., Heinzmann, U., Beisker, W. and Wurst, W. (2004). Effects of Wnt1 signaling on proliferation in the developing mid-/hindbrain region. *Mol Cell Neurosci* **26** (1): 101-11.

Park, J. H., Jensen, B. C., Kifer, C. T. and Parsons, M. (2001). A novel nucleolar G-protein conserved in eukaryotes. *J Cell Sci* **114** (Pt 1): 173-185.

Pasini, A. and Wilkinson, D. G. (2002). Stabilizing the regionalisation of the developing vertebrate central nervous system. *Bioessays* **24** (5): 427-38.

Patel, K., Isaac, A. and Cooke, J. (1999). Nodal signalling and the roles of the transcription factors SnR and Pitx2 in vertebrate left-right asymmetry. *Curr Biol* **9** (11): 609-12.

Patten, I. and Placzek, M. (2000). The role of Sonic hedgehog in neural tube patterning. *Cell Mol Life Sci* **57** (12): 1695-708.

Pattyn, A., Vallstedt, A., Dias, J. M., Sander, M. and Ericson, J. (2003). Complementary roles for Nkx6 and Nkx2 class proteins in the establishment of motoneuron identity in the hindbrain. *Development* **130** (17): 4149-59.

Pearse, R. V., 2nd, Vogan, K. J. and Tabin, C. J. (2001). Ptc1 and Ptc2 transcripts provide distinct readouts of Hedgehog signaling activity during chick embryogenesis. *Dev Biol* **239** (1): 15-29.

Pekarik, V., Bourikas, D., Miglino, N., Joset, P., Preiswerk, S. and Stoeckli, E. T. (2003). Screening for gene function in chicken embryo using RNAi and electroporation. *Nat Biotechnol* **21** (1): 93-6.

Perrin, F. E., Rathjen, F. G. and Stoeckli, E. T. (2001). Distinct subpopulations of sensory afferents require F11 or axonin-1 for growth to their target layers within the spinal cord of the chick. *Neuron* **30** (3): 707-23.

Persengiev, S. P., Zhu, X. and Green, M. R. (2004). Nonspecific, concentration-dependent stimulation and repression of mammalian gene expression by small interfering RNAs (siRNAs). *Rna* **10** (1): 12-8.

Persson, M., Stamatakis, D., te Welscher, P., Andersson, E., Bose, J., Ruther, U., Ericson, J. and Briscoe, J. (2002). Dorsal-ventral patterning of the spinal cord requires Gli3 transcriptional repressor

activity. *Genes Dev* **16** (22): 2865-78.

Petersen, M. A. and Dailey, M. E. (2004). Diverse microglial motility behaviors during clearance of dead cells in hippocampal slices. *Glia* **46** (2): 195-206.

Pfaff, S. L., Mendelsohn, M., Stewart, C. L., Edlund, T. and Jessell, T. M. (1996). Requirement for LIM homeobox gene *Isl1* in motor neuron generation reveals a motor neuron-dependent step in interneuron differentiation. *Cell* **84** (2): 309-20.

Pfeffer, S. R. (1992). GTP-binding proteins in intracellular transport. *Trends Cell Biol* **2** (2): 41-6.

Pham, J. W., Pellino, J. L., Lee, Y. S., Carthew, R. W. and Sontheimer, E. J. (2004). A Dicer-2-dependent 80s complex cleaves targeted mRNAs during RNAi in *Drosophila*. *Cell* **117** (1): 83-94.

Piccolo, S., Sasai, Y., Lu, B. and De Robertis, E. M. (1996). Dorsoventral patterning in *Xenopus*: inhibition of ventral signals by direct binding of chordin to BMP-4. *Cell* **86** (4): 589-98.

Pierani, A., Brenner-Morton, S., Chiang, C. and Jessell, T. M. (1999). A sonic hedgehog-independent, retinoid-activated pathway of neurogenesis in the ventral spinal cord. *Cell* **97** (7): 903-15.

Placzek, M., Dodd, J. and Jessell, T. M. (2000). Discussion point. The case for floor plate induction by the notochord. *Curr Opin Neurobiol* **10** (1): 15-22.

Poncet, C., Soula, C., Trousse, F., Kan, P., Hirsinger, E., Pourquie, O., Duprat, A. M. and Cochard, P. (1996). Induction of oligodendrocyte progenitors in the trunk neural tube by ventralizing signals: effects of notochord and floor plate grafts, and of sonic hedgehog. *Mech Dev* **60** (1): 13-32.

Pooga, M. and Langel, U. (2001). Targeting of cancer-related proteins with PNA oligomers. *Curr Cancer Drug Targets* **1** (3): 231-9.

Prausnitz, M. R., Corbett, J. D., Gimm, J. A., Golan, D. E., Langer, R. and Weaver, J. C. (1995). Millisecond measurement of transport during and after an electroporation pulse. *Biophys J* **68** (5): 1864-70.

Price, M. A. and Kalderon, D. (2002). Proteolysis of the Hedgehog signaling effector Cubitus interruptus requires phosphorylation by Glycogen Synthase Kinase 3 and Casein Kinase 1. *Cell* **108** (6): 823-35.

Pruitt, S. C. (1992). Expression of Pax-3- and neuroectoderm-inducing activities during differentiation of P19 embryonal carcinoma cells. *Development* **116** (3): 573-83.

Przyborski, S. A., Smith, S. and Wood, A. (2003). Transcriptional profiling of neuronal differentiation by human embryonal carcinoma stem cells in vitro. *Stem Cells* **21** (4): 459-71.

Psychoyos, D. and Stern, C. D. (1996). Fates and migratory routes of primitive streak cells in the chick embryo. *Development* **122** (5): 1523-34.

Psychoyos, D. and Stern, C. D. (1996). Restoration of the organizer after radical ablation of Hensen's node and the anterior primitive streak in the chick embryo. *Development* **122** (10): 3263-73.

Puelles, L. and Rubenstein, J. L. (1993). Expression patterns of homeobox and other putative regulatory genes in the embryonic mouse forebrain suggest a neuromeric organization. *Trends Neurosci* **16** (11): 472-9.

Purves, D., Augustine, G. J., Fitzpatrick, D., Katz, L. C., LaMantia, A.-S., McNamara, J. O. and Williams, S. M. (2001). *Neuroscience. 2nd Edition*. Sinauer Associates, Inc., Sunderland (MA).

Qiu, M., Shimamura, K., Sussel, L., Chen, S. and Rubenstein, J. L. (1998). Control of anteroposterior and dorsoventral domains of *Nkx-6.1* gene expression relative to other *Nkx* genes during vertebrate CNS development. *Mech Dev* **72** (1-2): 77-88.

- Rajewsky, N. (2006). microRNA target predictions in animals. *Nat Genet* **38 Suppl**: S8-13.
- Rakic, P. (1972). Mode of cell migration to the superficial layers of fetal monkey neocortex. *J Comp Neurol* **145** (1): 61-83.
- Rakic, P. (1995). Radial versus tangential migration of neuronal clones in the developing cerebral cortex. *Proc Natl Acad Sci U S A* **92** (25): 11323-7.
- Rallu, M., Machold, R., Gaiano, N., Corbin, J. G., McMahon, A. P. and Fishell, G. (2002). Dorsoventral patterning is established in the telencephalon of mutants lacking both Gli3 and Hedgehog signaling. *Development* **129** (21): 4963-74.
- Ray, A., Lang, J. D., Golden, T. and Ray, S. (1996). SHORT INTEGUMENT (SIN1), a gene required for ovule development in Arabidopsis, also controls flowering time. *Development* **122** (9): 2631-8.
- Ray, S., Golden, T. and Ray, A. (1996). Maternal effects of the short integument mutation on embryo development in Arabidopsis. *Dev Biol* **180** (1): 365-9.
- Raya, A. and Izpisua Belmonte, J. C. (2004). Unveiling the establishment of left-right asymmetry in the chick embryo. *Mech Dev* **121** (9): 1043-54.
- Reinhart, B. J., Slack, F. J., Basson, M., Pasquinelli, A. E., Bettinger, J. C., Rougvie, A. E., Horvitz, H. R. and Ruvkun, G. (2000). The 21-nucleotide let-7 RNA regulates developmental timing in *Caenorhabditis elegans*. *Nature* **403** (6772): 901-6.
- Reiter, J. F. and Skarnes, W. C. (2006). Tectonic, a novel regulator of the Hedgehog pathway required for both activation and inhibition. *Genes Dev* **20** (1): 22-7.
- Relaix, F., Rocancourt, D., Mansouri, A. and Buckingham, M. (2004). Divergent functions of murine Pax3 and Pax7 in limb muscle development. *Genes Dev* **18** (9): 1088-105.
- Relaix, F., Rocancourt, D., Mansouri, A. and Buckingham, M. (2005). A Pax3/Pax7-dependent population of skeletal muscle progenitor cells. *Nature* **435** (7044): 948-53.
- Relaix, F., Montarras, D., Zaffran, S., Gayraud-Morel, B., Rocancourt, D., Tajbakhsh, S., Mansouri, A., Cumano, A. and Buckingham, M. (2006). Pax3 and Pax7 have distinct and overlapping functions in adult muscle progenitor cells. *J Cell Biol* **172** (1): 91-102.
- Robbins, D. J., Nybakken, K. E., Kobayashi, R., Sisson, J. C., Bishop, J. M. and Therond, P. P. (1997). Hedgehog elicits signal transduction by means of a large complex containing the kinesin-related protein costal2. *Cell* **90** (2): 225-34.
- Rodriguez Esteban, C., Capdevila, J., Economides, A. N., Pascual, J., Ortiz, A. and Izpisua Belmonte, J. C. (1999). The novel Cer-like protein Caronte mediates the establishment of embryonic left-right asymmetry. *Nature* **401** (6750): 243-51.
- Rodriguez-Esteban, C., Capdevila, J., Kawakami, Y. and Izpisua Belmonte, J. C. (2001). Wnt signaling and PKA control Nodal expression and left-right determination in the chick embryo. *Development* **128** (16): 3189-95.
- Rodriguez-Lebron, E. and Paulson, H. L. (2006). Allele-specific RNA interference for neurological disease. *Gene Ther* **13** (6): 576-81.
- Roelink, H., Augsburger, A., Heemskerk, J., Korzh, V., Norlin, S., Ruiz i Altaba, A., Tanabe, Y., Placzek, M., Edlund, T., Jessell, T. M. and et al. (1994). Floor plate and motor neuron induction by vhh-1, a vertebrate homolog of hedgehog expressed by the notochord. *Cell* **76** (4): 761-75.
- Roelink, H., Porter, J. A., Chiang, C., Tanabe, Y., Chang, D. T., Beachy, P. A. and Jessell, T. M. (1995). Floor plate and motor neuron induction by different concentrations of the amino-terminal cleavage product of sonic hedgehog autoproteolysis. *Cell* **81** (3): 445-55.

- Roessler, E., Belloni, E., Gaudenz, K., Jay, P., Berta, P., Scherer, S. W., Tsui, L. C. and Muenke, M. (1996). Mutations in the human Sonic Hedgehog gene cause holoprosencephaly. *Nat Genet* **14** (3): 357-60.
- Romano, N. and Macino, G. (1992). Quelling: transient inactivation of gene expression in *Neurospora crassa* by transformation with homologous sequences. *Mol Microbiol* **6** (22): 3343-53.
- Rubenstein, J. L. and Beachy, P. A. (1998). Patterning of the embryonic forebrain. *Curr Opin Neurobiol* **8** (1): 18-26.
- Rubenstein, J. L., Shimamura, K., Martinez, S. and Puelles, L. (1998). Regionalization of the prosencephalic neural plate. *Annu Rev Neurosci* **21**: 445-77.
- Rudnick, A., Ling, T. Y., Odagiri, H., Rutter, W. J. and German, M. S. (1994). Pancreatic beta cells express a diverse set of homeobox genes. *Proc Natl Acad Sci U S A* **91** (25): 12203-7.
- Ruiz i Altaba, A. (1998). Combinatorial Gli gene function in floor plate and neuronal inductions by Sonic hedgehog. *Development* **125** (12): 2203-12.
- Ruiz i Altaba, A., Sanchez, P. and Dahmane, N. (2002). Gli and hedgehog in cancer: tumours, embryos and stem cells. *Nat Rev Cancer* **2** (5): 361-72.
- Ruiz i Altaba, A., Nguyen, V. and Palma, V. (2003). The emergent design of the neural tube: prepattern, SHH morphogen and GLI code. *Curr Opin Genet Dev* **13** (5): 513-21.
- Ruiz i Altaba, A., Stecca, B. and Sanchez, P. (2004). Hedgehog--Gli signaling in brain tumors: stem cells and paradevelopmental programs in cancer. *Cancer Lett* **204** (2): 145-57.
- Runyan, R. B., Wendler, C. C., Romano, L. A., Boyer, A. S., Dagle, J. M. and Weeks, D. L. (1999). Utilization of antisense oligodeoxynucleotides with embryonic tissues in culture. *Methods* **18** (3): 316-21.
- Saito, T. (2006). In vivo electroporation in the embryonic mouse central nervous system. *Nat Protoc* **1** (3): 1552-8.
- Saitou, N. and Nei, M. (1987). The neighbor-joining method: a new method for reconstructing phylogenetic trees. *Mol Biol Evol* **4** (4): 406-25.
- Sakamoto, K., Nakamura, H., Takagi, M., Takeda, S. and Katsube, K. (1998). Ectopic expression of lunatic Fringe leads to downregulation of Serrate-1 in the developing chick neural tube; analysis using in ovo electroporation transfection technique. *FEBS Lett* **426** (3): 337-41.
- Sambrook, J., Fritsch, E. F. and Maniatis, T. (1989). *Molecular Cloning, A Laboratory Manual, 2nd Edition. second*. Cold Spring Harbor Laboratory Press, Plainview.
- Sander, M., Paydar, S., Ericson, J., Briscoe, J., Berber, E., German, M., Jessell, T. M. and Rubenstein, J. L. (2000). Ventral neural patterning by Nkx homeobox genes: Nkx6.1 controls somatic motor neuron and ventral interneuron fates. *Genes Dev* **14** (17): 2134-9.
- Sanger, F., Nicklen, S. and Coulson, A. R. (1977). DNA sequencing with chain-terminating inhibitors. *Proc Natl Acad Sci U S A* **74** (12): 5463-7.
- Saraste, M., Sibbald, P. R. and Wittinghofer, A. (1990). The P-loop--a common motif in ATP- and GTP-binding proteins. *Trends Biochem Sci* **15** (11): 430-4.
- Sasai, Y., Lu, B., Steinbeisser, H., Geissert, D., Gont, L. K. and De Robertis, E. M. (1994). *Xenopus* chordin: a novel dorsalizing factor activated by organizer-specific homeobox genes. *Cell* **79** (5): 779-90.
- Sato, F., Nakagawa, T., Ito, M., Kitagawa, Y. and Hattori, M. A. (2004). Application of RNA interference to chicken embryos using small interfering RNA. *J Exp Zool A Comp Exp Biol* **301** (10):

820-7.

Sato, Y., Kasai, T., Nakagawa, S., Tanabe, K., Watanabe, T., Kawakami, K. and Takahashi, Y. (2007). Stable integration and conditional expression of electroporated transgenes in chicken embryos. *Dev Biol* **305** (2): 616-24.

Saueressig, H., Burrill, J. and Goulding, M. (1999). Engrailed-1 and netrin-1 regulate axon pathfinding by association interneurons that project to motor neurons. *Development* **126** (19): 4201-12.

Sazani, P., Gemignani, F., Kang, S. H., Maier, M. A., Manoharan, M., Persmark, M., Bortner, D. and Kole, R. (2002). Systemically delivered antisense oligomers upregulate gene expression in mouse tissues. *Nat Biotechnol* **20** (12): 1228-33.

Schafer, B. W., Czerny, T., Bernasconi, M., Genini, M. and Busslinger, M. (1994). Molecular cloning and characterization of a human PAX-7 cDNA expressed in normal and neoplastic myocytes. *Nucleic Acids Res* **22** (22): 4574-82.

Schafer, B. W. (1998). Emerging roles for PAX transcription factors in cancer biology. *Gen Physiol Biophys* **17** (3): 211-24.

Schedl, A., Ross, A., Lee, M., Engelkamp, D., Rashbass, P., van Heyningen, V. and Hastie, N. D. (1996). Influence of PAX6 gene dosage on development: overexpression causes severe eye abnormalities. *Cell* **86** (1): 71-82.

Scherr, M. and Eder, M. (2007). Gene silencing by small regulatory RNAs in mammalian cells. *Cell Cycle* **6** (4): 444-9.

Schillaci, R., Salatino, M., Cassataro, J., Proietti, C. J., Giambartolomei, G. H., Rivas, M. A., Carnevale, R. P., Charreau, E. H. and Elizalde, P. V. (2006). Immunization with murine breast cancer cells treated with antisense oligodeoxynucleotides to type I insulin-like growth factor receptor induced an antitumoral effect mediated by a CD8+ response involving Fas/Fas ligand cytotoxic pathway. *J Immunol* **176** (6): 3426-37.

Schlierf, B., Fey, G. H., Hauber, J., Hocke, G. M. and Rosorius, O. (2000). Rab11b is essential for recycling of transferrin to the plasma membrane. *Exp Cell Res* **259** (1): 257-65.

Schoenwolf, G. C., Everaert, S., Bortier, H. and Vakaet, L. (1989). Neural plate- and neural tube-forming potential of isolated epiblast areas in avian embryos. *Anat Embryol (Berl)* **179** (6): 541-9.

Schoenwolf, G. C. (1991). Cell movements driving neurulation in avian embryos. *Development Suppl* **2**: 157-68.

Schoenwolf, G. C. (2001). Cutting, pasting and painting: experimental embryology and neural development. *Nat Rev Neurosci* **2** (11): 763-71.

Scholl, F. A., Kamarashev, J., Murmann, O. V., Geertsen, R., Dummer, R. and Schafer, B. W. (2001). PAX3 is expressed in human melanomas and contributes to tumor cell survival. *Cancer Res* **61** (3): 823-6.

Schubert, F. R., Dietrich, S., Mootoosamy, R. C., Chapman, S. C. and Lumsden, A. (2001). Lbx1 marks a subset of interneurons in chick hindbrain and spinal cord. *Mech Dev* **101** (1-2): 181-5.

Schulte, T. W., Toretzky, J. A., Ress, E., Helman, L. and Neckers, L. M. (1997). Expression of PAX3 in Ewing's sarcoma family of tumors. *Biochem Mol Med* **60** (2): 121-6.

Schultheiss, T. M., Burch, J. B. and Lassar, A. B. (1997). A role for bone morphogenetic proteins in the induction of cardiac myogenesis. *Genes Dev* **11** (4): 451-62.

Schweitzer, R., Vogan, K. J. and Tabin, C. J. (2000). Similar expression and regulation of Gli2 and Gli3 in the chick limb bud. *Mech Dev* **98** (1-2): 171-4.

- Seabra, M. C., Brown, M. S. and Goldstein, J. L. (1993). Retinal degeneration in choroideremia: deficiency of rab geranylgeranyl transferase. *Science* **259** (5093): 377-81.
- Seale, P., Sabourin, L. A., Girgis-Gabardo, A., Mansouri, A., Gruss, P. and Rudnicki, M. A. (2000). Pax7 is required for the specification of myogenic satellite cells. *Cell* **102** (6): 777-86.
- Seale, P., Asakura, A. and Rudnicki, M. A. (2001). The potential of muscle stem cells. *Dev Cell* **1** (3): 333-42.
- Selleck, M. A. and Bronner-Fraser, M. (1995). Origins of the avian neural crest: the role of neural plate-epidermal interactions. *Development* **121** (2): 525-38.
- Senut, M. C. and Alvarado-Mallart, R. M. (1986). Development of the retinotectal system in normal quail embryos: cytoarchitectonic development and optic fiber innervation. *Brain Res* **394** (1): 123-40.
- Senut, M. C. and Alvarado-Mallart, R. M. (1987). Cytodifferentiation of quail tectal primordium transplanted homotopically into the chick embryo. *Brain Res* **429** (2): 187-205.
- Seo, H. C., Saetre, B. O., Havik, B., Ellingsen, S. and Fjose, A. (1998). The zebrafish Pax3 and Pax7 homologues are highly conserved, encode multiple isoforms and show dynamic segment-like expression in the developing brain. *Mech Dev* **70** (1-2): 49-63.
- Shamim, H., Mahmood, R., Logan, C., Doherty, P., Lumsden, A. and Mason, I. (1999). Sequential roles for Fgf4, En1 and Fgf8 in specification and regionalisation of the midbrain. *Development* **126** (5): 945-59.
- Shetty, K. M., Kurada, P. and O'Tousa, J. E. (1998). Rab6 regulation of rhodopsin transport in *Drosophila*. *J Biol Chem* **273** (32): 20425-30.
- Shimogori, T., Banuchi, V., Ng, H. Y., Strauss, J. B. and Grove, E. A. (2004). Embryonic signaling centers expressing BMP, WNT and FGF proteins interact to pattern the cerebral cortex. *Development* **131** (22): 5639-47.
- Shuman, S. (1991). Recombination mediated by vaccinia virus DNA topoisomerase I in *Escherichia coli* is sequence specific. *Proc Natl Acad Sci U S A* **88** (22): 10104-8.
- Shuman, S. (1994). Novel approach to molecular cloning and polynucleotide synthesis using vaccinia DNA topoisomerase. *J Biol Chem* **269** (51): 32678-84.
- Sijen, T., Fleenor, J., Simmer, F., Thijssen, K. L., Parrish, S., Timmons, L., Plasterk, R. H. and Fire, A. (2001). On the role of RNA amplification in dsRNA-triggered gene silencing. *Cell* **107** (4): 465-76.
- Simeone, A. (2000). Positioning the isthmus where Otx2 and Gbx2 meet. *Trends Genet* **16** (6): 237-40.
- Simon, H. and Lumsden, A. (1993). Rhombomere-specific origin of the contralateral vestibulo-acoustic efferent neurons and their migration across the embryonic midline. *Neuron* **11** (2): 209-20.
- Simon, H., Hornbruch, A. and Lumsden, A. (1995). Independent assignment of antero-posterior and dorso-ventral positional values in the developing chick hindbrain. *Curr Biol* **5** (2): 205-14.
- Smith, W. C., Knecht, A. K., Wu, M. and Harland, R. M. (1993). Secreted noggin protein mimics the Spemann organizer in dorsalizing *Xenopus* mesoderm. *Nature* **361** (6412): 547-9.
- Smith, J. L. and Schoenwolf, G. C. (1997). Neurulation: coming to closure. *Trends Neurosci* **20** (11): 510-7.
- Solloway, M. J., Dudley, A. T., Bikoff, E. K., Lyons, K. M., Hogan, B. L. and Robertson, E. J. (1998). Mice lacking Bmp6 function. *Dev Genet* **22** (4): 321-39.
- Sommer, L. (2007). [Stem cells of the enteric nervous system: causal therapy for Hirschsprung's

disease?]. *Pathologie* **28** (2): 125-30.

Song, D. L., Chalepakis, G., Gruss, P. and Joyner, A. L. (1996). Two Pax-binding sites are required for early embryonic brain expression of an Engrailed-2 transgene. *Development* **122** (2): 627-35.

Sossey-Alaoui, K., Hartung, A. J., Guerrini, R., Manchester, D. K., Posar, A., Puche-Mira, A., Andermann, E., Dobyns, W. B. and Srivastava, A. K. (1998). Human doublecortin (DCX) and the homologous gene in mouse encode a putative Ca²⁺-dependent signaling protein which is mutated in human X-linked neuronal migration defects. *Hum Mol Genet* **7** (8): 1327-32.

Spoerner, M., Herrmann, C., Vetter, I. R., Kalbitzer, H. R. and Wittinghofer, A. (2001). Dynamic properties of the Ras switch I region and its importance for binding to effectors. *Proc Natl Acad Sci U S A* **98** (9): 4944-9.

Sporle, R., Gunther, T., Struwe, M. and Schughart, K. (1996). Severe defects in the formation of epaxial musculature in open brain (opb) mutant mouse embryos. *Development* **122** (1): 79-86.

Sporle, R. and Schughart, K. (1998). Paradox segmentation along inter- and intrasomitic borderlines is followed by dysmorphology of the axial skeleton in the open brain (opb) mouse mutant. *Dev Genet* **22** (4): 359-73.

Sprang, S. R. (1997). G protein mechanisms: insights from structural analysis. *Annu Rev Biochem* **66**: 639-78.

Srivastava, D., Cserjesi, P. and Olson, E. N. (1995). A subclass of bHLH proteins required for cardiac morphogenesis. *Science* **270** (5244): 1995-9.

Stark, H., Rodnina, M. V., Rinke-Appel, J., Brimacombe, R., Wintermeyer, W. and van Heel, M. (1997). Visualization of elongation factor Tu on the Escherichia coli ribosome. *Nature* **389** (6649): 403-6.

Stark, G. R., Kerr, I. M., Williams, B. R., Silverman, R. H. and Schreiber, R. D. (1998). How cells respond to interferons. *Annu Rev Biochem* **67**: 227-64.

Stegman, M. A., Vallance, J. E., Elangovan, G., Sosinski, J., Cheng, Y. and Robbins, D. J. (2000). Identification of a tetrameric hedgehog signaling complex. *J Biol Chem* **275** (29): 21809-12.

Stern, C. D. and Canning, D. R. (1988). Gastrulation in birds: a model system for the study of animal morphogenesis. *Experientia* **44** (8): 651-7.

Stern, C. D., Jaques, K. F., Lim, T. M., Fraser, S. E. and Keynes, R. J. (1991). Segmental lineage restrictions in the chick embryo spinal cord depend on the adjacent somites. *Development* **113** (1): 239-44.

Stoeckli, E. T. and Landmesser, L. T. (1995). Axonin-1, Nr-CAM, and Ng-CAM play different roles in the in vivo guidance of chick commissural neurons. *Neuron* **14** (6): 1165-79.

Stoykova, A. and Gruss, P. (1994). Roles of Pax-genes in developing and adult brain as suggested by expression patterns. *J Neurosci* **14** (3 Pt 2): 1395-412.

Stoykova, A., Fritsch, R., Walther, C. and Gruss, P. (1996). Forebrain patterning defects in Small eye mutant mice. *Development* **122** (11): 3453-65.

Stoykova, A., Gotz, M., Gruss, P. and Price, J. (1997). Pax6-dependent regulation of adhesive patterning, R-cadherin expression and boundary formation in developing forebrain. *Development* **124** (19): 3765-77.

Stoykova, A., Treichel, D., Hallonet, M. and Gruss, P. (2000). Pax6 modulates the dorsoventral patterning of the mammalian telencephalon. *J Neurosci* **20** (21): 8042-50.

Streit, A., Lee, K. J., Woo, I., Roberts, C., Jessell, T. M. and Stern, C. D. (1998). Chordin regulates

primitive streak development and the stability of induced neural cells, but is not sufficient for neural induction in the chick embryo. *Development* **125** (3): 507-19.

Sui, G., Soohoo, C., Affar el, B., Gay, F., Shi, Y. and Forrester, W. C. (2002). A DNA vector-based RNAi technology to suppress gene expression in mammalian cells. *Proc Natl Acad Sci U S A* **99** (8): 5515-20.

Summerbell, D. and Lewis, J. H. (1975). Time, place and positional value in the chick limb-bud. *J Embryol Exp Morphol* **33** (3): 621-43.

Summerton, J. and Weller, D. (1997). Morpholino antisense oligomers: design, preparation, and properties. *Antisense Nucleic Acid Drug Dev* **7** (3): 187-95.

Summerton, J. and Weller, D. (1999). Morpholino antisense oligomers: the case for an RNase H-independent structural type. *Biochim Biophys Acta* **1489** (1): 141-58.

Supp, D. M., Brueckner, M., Kuehn, M. R., Witte, D. P., Lowe, L. A., McGrath, J., Corrales, J. and Potter, S. S. (1999). Targeted deletion of the ATP binding domain of left-right dynein confirms its role in specifying development of left-right asymmetries. *Development* **126** (23): 5495-504.

Swartz, M. E., Eberhart, J., Pasquale, E. B. and Krull, C. E. (2001). EphA4/ephrin-A5 interactions in muscle precursor cell migration in the avian forelimb. *Development* **128** (23): 4669-80.

Swartz, M., Eberhart, J., Mastick, G. S. and Krull, C. E. (2001). Sparking new frontiers: using in vivo electroporation for genetic manipulations. *Dev Biol* **233** (1): 13-21.

Tai, C. K., Wang, W. J., Chen, T. C. and Kasahara, N. (2005). Single-shot, multicycle suicide gene therapy by replication-competent retrovirus vectors achieves long-term survival benefit in experimental glioma. *Mol Ther* **12** (5): 842-51.

Takada, S., Stark, K. L., Shea, M. J., Vassileva, G., McMahon, J. A. and McMahon, A. P. (1994). Wnt-3a regulates somite and tailbud formation in the mouse embryo. *Genes Dev* **8** (2): 174-89.

Takahashi, Y., Tonegawa, A., Matsumoto, K., Ueno, N., Kuroiwa, A., Noda, M. and Nifuji, A. (1996). BMP-4 mediates interacting signals between the neural tube and skin along the dorsal midline. *Genes Cells* **1** (8): 775-83.

Takai, Y., Kaibuchi, K., Kikuchi, A. and Kawata, M. (1992). Small GTP-binding proteins. *Int Rev Cytol* **133**: 187-230.

Takeda, S., Yonekawa, Y., Tanaka, Y., Okada, Y., Nonaka, S. and Hirokawa, N. (1999). Left-right asymmetry and kinesin superfamily protein KIF3A: new insights in determination of laterality and mesoderm induction by *kif3A*^{-/-} mice analysis. *J Cell Biol* **145** (4): 825-36.

Tanabe, Y. and Jessell, T. M. (1996). Diversity and pattern in the developing spinal cord. *Science* **274** (5290): 1115-23.

Tanaka, A., Kamiakito, T., Hakamata, Y., Fujii, A., Kuriki, K. and Fukayama, M. (2001). Extensive neuronal localization and neurotrophic function of fibroblast growth factor 8 in the nervous system. *Brain Res* **912** (2): 105-15.

Tanaka, Y., Okada, Y. and Hirokawa, N. (2005). FGF-induced vesicular release of Sonic hedgehog and retinoic acid in leftward nodal flow is critical for left-right determination. *Nature* **435** (7039): 172-7.

Teillet, M. A. and Le Douarin, N. M. (1983). Consequences of neural tube and notochord excision on the development of the peripheral nervous system in the chick embryo. *Dev Biol* **98** (1): 192-211.

Thaler, J., Harrison, K., Sharma, K., Lettieri, K., Kehrl, J. and Pfaff, S. L. (1999). Active suppression of interneuron programs within developing motor neurons revealed by analysis of homeodomain factor HB9. *Neuron* **23** (4): 675-87.

- Theisen, H., Haerry, T. E., O'Connor, M. B. and Marsh, J. L. (1996). Developmental territories created by mutual antagonism between Wingless and Decapentaplegic. *Development* **122** (12): 3939-48.
- Thomas, M., Lazic, S., Beazley, L. and Ziman, M. (2004). Expression profiles suggest a role for Pax7 in the establishment of tectal polarity and map refinement. *Exp Brain Res* **156** (3): 263-73.
- Thomas, M., Beazley, L. and Ziman, M. (2006). A multiphasic role for Pax7 in tectal development. *Exp Brain Res* **169** (2): 266-71.
- Tijsterman, M., Ketting, R. F. and Plasterk, R. H. (2002). The genetics of RNA silencing. *Annu Rev Genet* **36**: 489-519.
- Tijsterman, M. and Plasterk, R. H. (2004). Dicers at RISC; the mechanism of RNAi. *Cell* **117** (1): 1-3.
- Timmer, J. R., Wang, C. and Niswander, L. (2002). BMP signaling patterns the dorsal and intermediate neural tube via regulation of homeobox and helix-loop-helix transcription factors. *Development* **129** (10): 2459-72.
- Topczewska, J. M., Topczewski, J., Shostak, A., Kume, T., Solnica-Krezel, L. and Hogan, B. L. (2001). The winged helix transcription factor Foxc1a is essential for somitogenesis in zebrafish. *Genes Dev* **15** (18): 2483-93.
- Toresson, H., Potter, S. S. and Campbell, K. (2000). Genetic control of dorsal-ventral identity in the telencephalon: opposing roles for Pax6 and Gsh2. *Development* **127** (20): 4361-71.
- Towers, P., Patel, K., Withington, S., Isaac, A. and Cooke, J. (1999). Flik, a chick follistatin-related gene, functions in gastrular dorsalisation/neural induction and in subsequent maintenance of midline Sonic hedgehog signalling. *Dev Biol* **214** (2): 298-317.
- Trajcevski, S., Solly, S. K., Frisen, C., Trenado, A., Cosset, F. L. and Klatzmann, D. (2005). Characterization of a semi-replicative gene delivery system allowing propagation of complementary defective retroviral vectors. *J Gene Med* **7** (3): 276-87.
- Treisman, J., Harris, E. and Desplan, C. (1991). The paired box encodes a second DNA-binding domain in the paired homeo domain protein. *Genes Dev* **5** (4): 594-604.
- Tremblay, P., Pituello, F. and Gruss, P. (1996). Inhibition of floor plate differentiation by Pax3: evidence from ectopic expression in transgenic mice. *Development* **122** (8): 2555-67.
- Tsuchida, T., Ensini, M., Morton, S. B., Baldassare, M., Edlund, T., Jessell, T. M. and Pfaff, S. L. (1994). Topographic organization of embryonic motor neurons defined by expression of LIM homeobox genes. *Cell* **79** (6): 957-70.
- Tsukamoto, K., Nakamura, Y. and Niikawa, N. (1994). Isolation of two isoforms of the PAX3 gene transcripts and their tissue-specific alternative expression in human adult tissues. *Hum Genet* **93** (3): 270-4.
- Tucker, R. P. (2001). Abnormal neural crest cell migration after the in vivo knockdown of tenascin-C expression with morpholino antisense oligonucleotides. *Dev Dyn* **222** (1): 115-9.
- Tumpel, S., Sanz-Ezquerro, J. J., Isaac, A., Eblaghie, M. C., Dobson, J. and Tickle, C. (2002). Regulation of Tbx3 expression by anteroposterior signalling in vertebrate limb development. *Dev Biol* **250** (2): 251-62.
- Turner, J. J., Fabani, M., Arzumanov, A. A., Ivanova, G. and Gait, M. J. (2006). Targeting the HIV-1 RNA leader sequence with synthetic oligonucleotides and siRNA: chemistry and cell delivery. *Biochim Biophys Acta* **1758** (3): 290-300.
- Tyler, B. M., Jansen, K., McCormick, D. J., Douglas, C. L., Boules, M., Stewart, J. A., Zhao, L., Lacy, B., Cusack, B., Fauq, A. and Richelson, E. (1999). Peptide nucleic acids targeted to the neurotensin receptor and administered i.p. cross the blood-brain barrier and specifically reduce gene expression.

Proc Natl Acad Sci U S A **96** (12): 7053-8.

Tyurina, O. V., Guner, B., Popova, E., Feng, J., Schier, A. F., Kohtz, J. D. and Karlstrom, R. O. (2005). Zebrafish Gli3 functions as both an activator and a repressor in Hedgehog signaling. *Dev Biol* **277** (2): 537-56.

Underhill, D. A. and Gros, P. (1997). The paired-domain regulates DNA binding by the homeodomain within the intact Pax-3 protein. *J Biol Chem* **272** (22): 14175-82.

Vaccarino, F. M., Ganat, Y., Zhang, Y. and Zheng, W. (2001). Stem cells in neurodevelopment and plasticity. *Neuropsychopharmacology* **25** (6): 805-15.

Vainio, S., Karavanova, I., Jowett, A. and Thesleff, I. (1993). Identification of BMP-4 as a signal mediating secondary induction between epithelial and mesenchymal tissues during early tooth development. *Cell* **75** (1): 45-58.

Valencia, A., Chardin, P., Wittinghofer, A. and Sander, C. (1991). The ras protein family: evolutionary tree and role of conserved amino acids. *Biochemistry* **30** (19): 4637-48.

van der Krol, A. R., Mur, L. A., Beld, M., Mol, J. N. and Stuitje, A. R. (1990). Flavonoid genes in petunia: addition of a limited number of gene copies may lead to a suppression of gene expression. *Plant Cell* **2** (4): 291-9.

Van Hooser, A., Goodrich, D. W., Allis, C. D., Brinkley, B. R. and Mancini, M. A. (1998). Histone H3 phosphorylation is required for the initiation, but not maintenance, of mammalian chromosome condensation. *J Cell Sci* **111** (Pt 23): 3497-506.

Varela-Echavarria, A., Pfaff, S. L. and Guthrie, S. (1996). Differential expression of LIM homeobox genes among motor neuron subpopulations in the developing chick brain stem. *Mol Cell Neurosci* **8** (4): 242-57.

Verberne, M. E., Gittenberger-de Groot, A. C. and Poelmann, R. E. (1998). Lineage and development of the parasympathetic nervous system of the embryonic chick heart. *Anat Embryol (Berl)* **198** (3): 171-84.

Verberne, M. E., Gittenberger-De Groot, A. C. and Poelmann, R. E. (2000). Distribution of antigen epitopes shared by nerves and the myocardium of the embryonic chick heart using different neuronal markers. *Anat Rec* **260** (4): 335-50.

Verdel, A., Jia, S., Gerber, S., Sugiyama, T., Gygi, S., Grewal, S. I. and Moazed, D. (2004). RNAi-mediated targeting of heterochromatin by the RITS complex. *Science* **303** (5658): 672-6.

Verma, I. M. and Somia, N. (1997). Gene therapy -- promises, problems and prospects. *Nature* **389** (6648): 239-42.

Viebahn, C. (2001). Hensen's node. *Genesis* **29** (2): 96-103.

Wada, H., Holland, P. W., Sato, S., Yamamoto, H. and Satoh, N. (1997). Neural tube is partially dorsalized by overexpression of HrPax-37: the ascidian homologue of Pax-3 and Pax-7. *Dev Biol* **187** (2): 240-52.

Waddington, C. and Schmidt, G. (1933). Induction by heteroplastic grafts of the primitive streak in birds. *Wilhelm Roux Arch Entwicklungsmech* **128**: 522-563.

Wagner, J., Schmidt, C., Nikowits, W., Jr. and Christ, B. (2000). Compartmentalization of the somite and myogenesis in chick embryos are influenced by wnt expression. *Dev Biol* **228** (1): 86-94.

Wakamatsu, Y., Watanabe, Y., Nakamura, H. and Kondoh, H. (1997). Regulation of the neural crest cell fate by N-myc: promotion of ventral migration and neuronal differentiation. *Development* **124** (10): 1953-62.

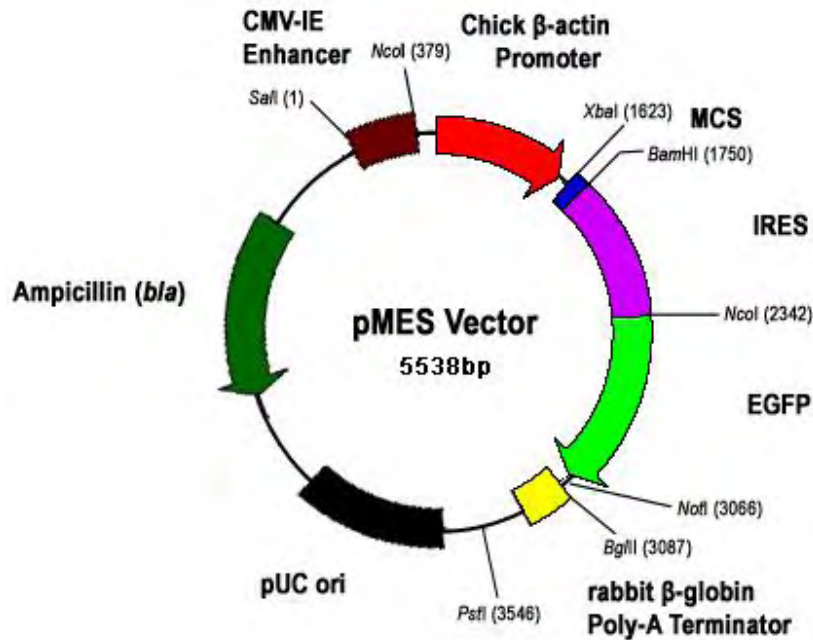
- Wakamatsu, Y. and Weston, J. A. (1997). Sequential expression and role of Hu RNA-binding proteins during neurogenesis. *Development* **124** (17): 3449-60.
- Walsh, C. and Cepko, C. L. (1993). Clonal dispersion in proliferative layers of developing cerebral cortex. *Nature* **362** (6421): 632-5.
- Wang, G., Amanai, K., Wang, B. and Jiang, J. (2000). Interactions with Costal2 and suppressor of fused regulate nuclear translocation and activity of cubitus interruptus. *Genes Dev* **14** (22): 2893-905.
- Wang, B., Fallon, J. F. and Beachy, P. A. (2000). Hedgehog-regulated processing of Gli3 produces an anterior/posterior repressor gradient in the developing vertebrate limb. *Cell* **100** (4): 423-34.
- Wang, S., Yu, X., Zhang, T., Zhang, X., Zhang, Z. and Chen, Y. (2004). Chick Pcl2 regulates the left-right asymmetry by repressing Shh expression in Hensen's node. *Development* **131** (17): 4381-91.
- Wang, X. S., Wang, K., Li, X. and Fu, S. B. (2004). Effects of phosphorothioate anti-sense oligodeoxynucleotides on colorectal cancer cell growth and telomerase activity. *World J Gastroenterol* **10** (23): 3455-8.
- Wang, Y., Kato, N., Jazag, A., Dharel, N., Otsuka, M., Taniguchi, H., Kawabe, T. and Omata, M. (2006). Hepatitis C virus core protein is a potent inhibitor of RNA silencing-based antiviral response. *Gastroenterology* **130** (3): 883-92.
- Wang, Y., Stricker, H. M., Gou, D. and Liu, L. (2007). MicroRNA: past and present. *Front Biosci* **12**: 2316-29.
- Watanabe, Y. and Nakamura, H. (2000). Control of chick tectum territory along dorsoventral axis by Sonic hedgehog. *Development* **127** (5): 1131-40.
- Waterhouse, P. M., Wang, M. B. and Lough, T. (2001). Gene silencing as an adaptive defence against viruses. *Nature* **411** (6839): 834-42.
- Wei, Y., Yu, L., Bowen, J., Gorovsky, M. A. and Allis, C. D. (1999). Phosphorylation of histone H3 is required for proper chromosome condensation and segregation. *Cell* **97** (1): 99-109.
- Weinstein, D. C. and Hemmati-Brivanlou, A. (1999). Neural induction. *Annu Rev Cell Dev Biol* **15**: 411-33.
- Wiggan, O., Fadel, M. P. and Hamel, P. A. (2002). Pax3 induces cell aggregation and regulates phenotypic mesenchymal-epithelial interconversion. *J Cell Sci* **115** (Pt 3): 517-29.
- Wijgerde, M., McMahon, J. A., Rule, M. and McMahon, A. P. (2002). A direct requirement for Hedgehog signaling for normal specification of all ventral progenitor domains in the presumptive mammalian spinal cord. *Genes Dev* **16** (22): 2849-64.
- Wildner, H., Muller, T., Cho, S. H., Brohl, D., Cepko, C. L., Guillemot, F. and Birchmeier, C. (2006). dILA neurons in the dorsal spinal cord are the product of terminal and non-terminal asymmetric progenitor cell divisions, and require Mash1 for their development. *Development* **133** (11): 2105-13.
- Williams, B. R. (1999). PKR; a sentinel kinase for cellular stress. *Oncogene* **18** (45): 6112-20.
- Wilson, S. M., Yip, R., Swing, D. A., O'Sullivan, T. N., Zhang, Y., Novak, E. K., Swank, R. T., Russell, L. B., Copeland, N. G. and Jenkins, N. A. (2000). A mutation in Rab27a causes the vesicle transport defects observed in ashen mice. *Proc Natl Acad Sci U S A* **97** (14): 7933-8.
- Wilson, S. I., Rydstrom, A., Trimborn, T., Willert, K., Nusse, R., Jessell, T. M. and Edlund, T. (2001). The status of Wnt signalling regulates neural and epidermal fates in the chick embryo. *Nature* **411** (6835): 325-30.
- Wilson, L., Gale, E. and Maden, M. (2003). The role of retinoic acid in the morphogenesis of the neural tube. *J Anat* **203** (4): 357-68.

- Wilson, L. and Maden, M. (2005). The mechanisms of dorsoventral patterning in the vertebrate neural tube. *Dev Biol* **282** (1): 1-13.
- Wingate, R. J. and Lumsden, A. (1996). Persistence of rhombomeric organisation in the postsegmental hindbrain. *Development* **122** (7): 2143-52.
- Wizenmann, A. and Lumsden, A. (1997). Segregation of rhombomeres by differential chemoaffinity. *Mol Cell Neurosci* **9** (5-6): 448-59.
- Wolpert, L., Beddington, R., Brockes, J., Jesseö, T., Lawrence, P. and Meyerowitz, E. (1998). *Principles of Development*. Current Biology, Ltd., London.
- Wu, X., Jung, G. and Hammer, J. A., 3rd (2000). Functions of unconventional myosins. *Curr Opin Cell Biol* **12** (1): 42-51.
- Wurst, W. and Bally-Cuif, L. (2001). Neural plate patterning: upstream and downstream of the isthmus organizer. *Nat Rev Neurosci* **2** (2): 99-108.
- Xiang, M., Zhou, L., Macke, J. P., Yoshioka, T., Hendry, S. H., Eddy, R. L., Shows, T. B. and Nathans, J. (1995). The Brn-3 family of POU-domain factors: primary structure, binding specificity, and expression in subsets of retinal ganglion cells and somatosensory neurons. *J Neurosci* **15** (7 Pt 1): 4762-85.
- Xiang, M., Gan, L., Zhou, L., Klein, W. H. and Nathans, J. (1996). Targeted deletion of the mouse POU domain gene Brn-3a causes selective loss of neurons in the brainstem and trigeminal ganglion, uncoordinated limb movement, and impaired suckling. *Proc Natl Acad Sci U S A* **93** (21): 11950-5.
- Xu, W., Rould, M. A., Jun, S., Desplan, C. and Pabo, C. O. (1995). Crystal structure of a paired domain-DNA complex at 2.5 Å resolution reveals structural basis for Pax developmental mutations. *Cell* **80** (4): 639-50.
- Xu, H. E., Rould, M. A., Xu, W., Epstein, J. A., Maas, R. L. and Pabo, C. O. (1999). Crystal structure of the human Pax6 paired domain-DNA complex reveals specific roles for the linker region and carboxy-terminal subdomain in DNA binding. *Genes Dev* **13** (10): 1263-75.
- Yamada, T., Placzek, M., Tanaka, H., Dodd, J. and Jessell, T. M. (1991). Control of cell pattern in the developing nervous system: polarizing activity of the floor plate and notochord. *Cell* **64** (3): 635-47.
- Yamane, H. K., Farnsworth, C. C., Xie, H. Y., Howald, W., Fung, B. K., Clarke, S., Gelb, M. H. and Glomset, J. A. (1990). Brain G protein gamma subunits contain an all-trans-geranylgeranyl cysteine methyl ester at their carboxyl termini. *Proc Natl Acad Sci U S A* **87** (15): 5868-72.
- Yang, D., Lu, H. and Erickson, J. W. (2000). Evidence that processed small dsRNAs may mediate sequence-specific mRNA degradation during RNAi in *Drosophila* embryos. *Curr Biol* **10** (19): 1191-200.
- Yang, Z., Roberts, E. A. and Goldstein, L. S. (2001). Functional analysis of mouse kinesin motor Kif3C. *Mol Cell Biol* **21** (16): 5306-11.
- Yang, Z., Liu, N. and Lin, S. (2001). A zebrafish forebrain-specific zinc finger gene can induce ectopic *dlx2* and *dlx6* expression. *Dev Biol* **231** (1): 138-48.
- Ye, W., Shimamura, K., Rubenstein, J. L., Hynes, M. A. and Rosenthal, A. (1998). FGF and Shh signals control dopaminergic and serotonergic cell fate in the anterior neural plate. *Cell* **93** (5): 755-66.
- Yokouchi, Y., Vogan, K. J., Pearse, R. V., 2nd and Tabin, C. J. (1999). Antagonistic signaling by Caronte, a novel Cerberus-related gene, establishes left-right asymmetric gene expression. *Cell* **98** (5): 573-83.
- Younkin, D. P., Tang, C. M., Hardy, M., Reddy, U. R., Shi, Q. Y., Pleasure, S. J., Lee, V. M. and

- Pleasure, D. (1993). Inducible expression of neuronal glutamate receptor channels in the NT2 human cell line. *Proc Natl Acad Sci U S A* **90** (6): 2174-8.
- Yun, K., Potter, S. and Rubenstein, J. L. (2001). Gsh2 and Pax6 play complementary roles in dorsoventral patterning of the mammalian telencephalon. *Development* **128** (2): 193-205.
- Zacchei, A. M. (1961). [The embryonal development of the Japanese quail (*Coturnix coturnix japonica* T. and S.)]. *Arch Ital Anat Embriol* **66**: 36-62.
- Zamecnik, P. C. and Stephenson, M. L. (1978). Inhibition of Rous sarcoma virus replication and cell transformation by a specific oligodeoxynucleotide. *Proc Natl Acad Sci U S A* **75** (1): 280-4.
- Zammit, P. S., Relaix, F., Nagata, Y., Perez Ruiz, A., Collins, C. A., Partridge, T. A. and Beauchamp, J. R. (2006). Pax7 and myogenic progression in skeletal muscle satellite cells. *J Cell Sci*.
- Zamore, P. D., Tuschl, T., Sharp, P. A. and Bartel, D. P. (2000). RNAi: double-stranded RNA directs the ATP-dependent cleavage of mRNA at 21 to 23 nucleotide intervals. *Cell* **101** (1): 25-33.
- Zamore, P. D. (2002). Ancient pathways programmed by small RNAs. *Science* **296** (5571): 1265-9.
- Zarembinski, T. I., Hung, L. W., Mueller-Dieckmann, H. J., Kim, K. K., Yokota, H., Kim, R. and Kim, S. H. (1998). Structure-based assignment of the biochemical function of a hypothetical protein: a test case of structural genomics. *Proc Natl Acad Sci U S A* **95** (26): 15189-93.
- Zechner, D., Muller, T., Wende, H., Walther, I., Taketo, M. M., Crenshaw, E. B., 3rd, Treier, M., Birchmeier, W. and Birchmeier, C. (2007). Bmp and Wnt/beta-catenin signals control expression of the transcription factor Olig3 and the specification of spinal cord neurons. *Dev Biol* **303** (1): 181-90.
- Zeng, X., Goetz, J. A., Suber, L. M., Scott, W. J., Jr., Schreiner, C. M. and Robbins, D. J. (2001). A freely diffusible form of Sonic hedgehog mediates long-range signalling. *Nature* **411** (6838): 716-20.
- Zerial, M. and McBride, H. (2001). Rab proteins as membrane organizers. *Nat Rev Mol Cell Biol* **2** (2): 107-17.
- Zhang, X. M. and Yang, X. J. (2001). Temporal and spatial effects of Sonic hedgehog signaling in chick eye morphogenesis. *Dev Biol* **233** (2): 271-90.
- Zhang, X., Friedman, A., Heaney, S., Purcell, P. and Maas, R. L. (2002). Meis homeoproteins directly regulate Pax6 during vertebrate lens morphogenesis. *Genes Dev* **16** (16): 2097-107.
- Zheng, J. Y., Koda, T., Fujiwara, T., Kishi, M., Ikehara, Y. and Kakinuma, M. (1998). A novel Rab GTPase, Rab33B, is ubiquitously expressed and localized to the medial Golgi cisternae. *J Cell Sci* **111** (Pt 8): 1061-9.
- Zhong, J. M., Chen-Hwang, M. C. and Hwang, Y. W. (1995). Switching nucleotide specificity of Ha-Ras p21 by a single amino acid substitution at aspartate 119. *J Biol Chem* **270** (17): 10002-7.
- Ziman, M. R. and Kay, P. H. (1998). Differential expression of four alternate Pax7 paired box transcripts is influenced by organ- and strain-specific factors in adult mice. *Gene* **217** (1-2): 77-81.
- Ziman, M. R., Pelham, J. T., Mastaglia, F. L. and Kay, P. H. (2000). Characterization of the alternate allelic forms of human PAX7. *Mamm Genome* **11** (4): 332-7.
- Ziman, M. R., Thomas, M., Jacobsen, P. and Beazley, L. (2001). A key role for Pax7 transcripts in determination of muscle and nerve cells. *Exp Cell Res* **268** (2): 220-9.
- Ziman, M., Rodger, J., Lukehurst, S., Hancock, D., Dunlop, S. and Beazley, L. (2003). A dorso-ventral gradient of Pax6 in the developing retina suggests a role in topographic map formation. *Brain Res Dev Brain Res* **140** (2): 299-302.

Appendix

A. pMES Vector



CMV-IE enhancer: 1-380
Chick β-actin promoter: 386-1621
Multiple cloning site: 1623-1755
Internal ribosome entry site: 1756-2340
enhanced green fluorescent protein: 2337-3063
rabbit β-globin Poly-A Terminator: 3087-3288
pUC origin: 3789-4376
Ampicillin (*bla*) resistance gene: 4547-5407

Sequence shown 1570-1900

```

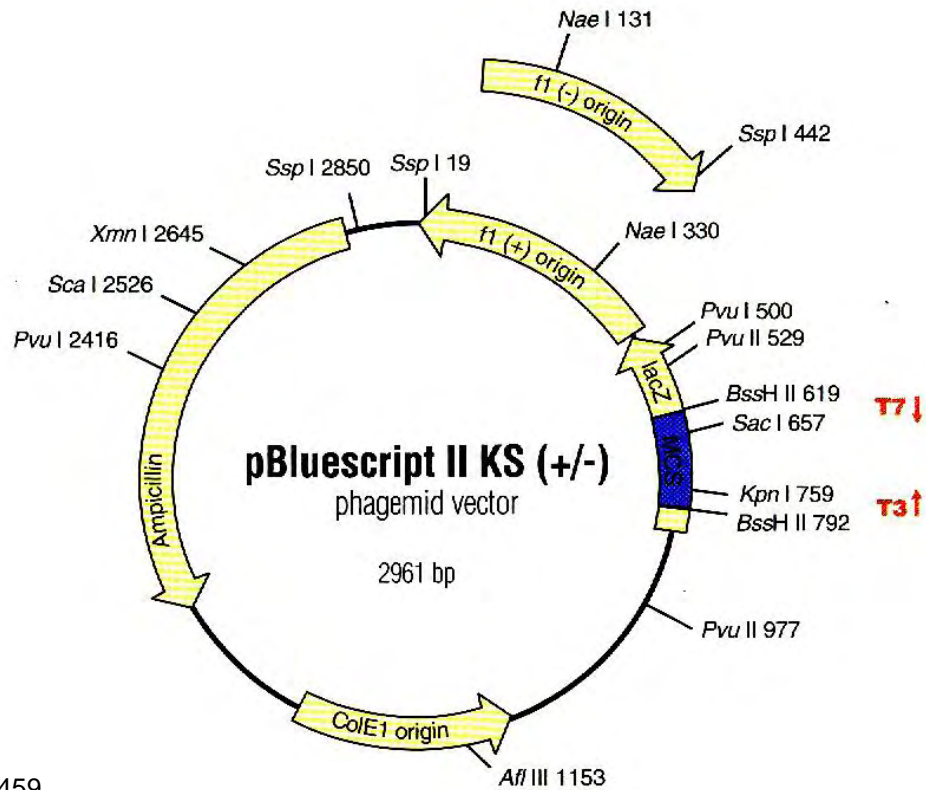
          pMESf3 primer          XbaI          pMESf1 primer
TCGGGGGGGACGGGGCAGGGCGGGGTTCTGGCTTCTGGCGTGTGACCGGCGGCTCTAGAGCCTCTGCTAACCATGTTTCATGCCTTCTTCTTT
          EcoRI          PstI HincII          KpnI SacI          SmaI BamHI
TCCTACAGCTCCTGGGCAACGTGCTGTTGTTGTGCTGTCTCATATTTGGCAAAGAATTCTGCAATCGACGGTACCGCGGGCCCGGATCC

GCCCCTCTCCCTCCCCCCCCCTAACGTTACTGGCCGAAGCCGCTTGAATAAGGCCGGTGTGCGTTTGTCTATATGTTATTTCCACCATATTG
          pMESr4 primer          pMESr1 primer
CCGTCTTTTGCAATGTGAGGGCCCGAAACCTGGCCCTGTCTTCTTGAC
    
```

Figure 87: Map of the pMES vector

Schematic map shows the various elements of pMES vector. pMES vector is 5538 bp made by moving IRES-EGFP sequence from pIRES2-EGFP (Clontech) into the pCAX vector. pIRES2 was cut with *NotI*, pCAX was cut with *NheI* and both cuts were made blunt with Klenow. Both plasmids were then cut with *EcoRI*. The IRES-EGFP sequence was ligated into the MCS of pCAX. This replaced the pCAX MCS with the 3' portion of the pIRES2 MCS. PCAX vector is derived from pCAGGS vector (Clontech). Positions of the restriction endonuclease recognition sites within MCS and sequencing primer-binding sites are provided. Positions of various elements in this vector are listed. (After Dr. Christine Krull.)

B. pBluescript® II KS (+/-) Phagemid Vector



- f1 (+/-) origin** 3-459
- ColE1 origin** 1032-1972
- β-galactosidase α-fragment** 460-816
- lacZ promoter** 816-938
- Multiple Cloning site** 657-759
- Ampicillin resistance (*bla*) ORF** 1975-2832

pBluescript II KS (+/-) Multiple Cloning Site Region (sequence shown 598–826)

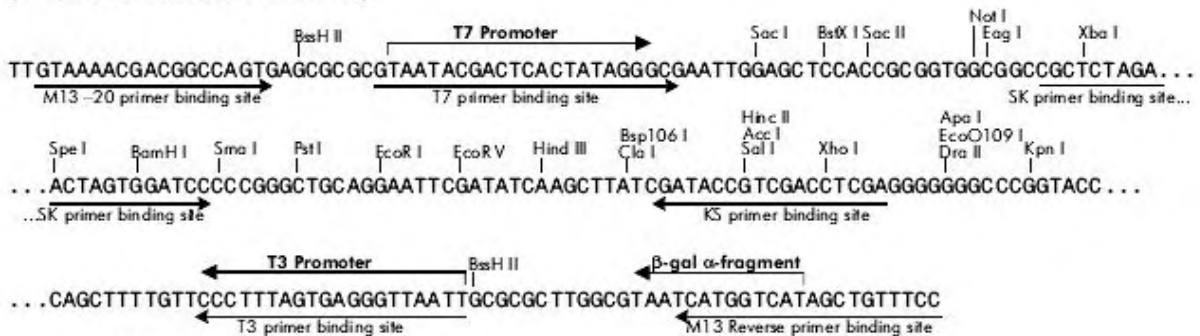


Figure 88: Map of pBluescript® II KS (+/-) phagemid

The pBluescript II KS (+/-) phagemid is 2961–bp vector derived from pUC19. The KS designation indicates the polylinker is oriented such that *lacZ* transcription proceeds from *KpnI* to *SacI*. Positions of various elements and unique restriction enzyme recognition sites in MCS are listed. (Photographs from Stratagene)

C. pCR[®]4-TOPO[®] Vector

```

                LacZα initiation codon
                |
M13 Reverse priming site | T3 priming site
201 CACACAGGAA ACAGCTAIGA CCATGATTAC GCCAAGCTCA GAATTAACCC TCACTAAAGG
    GGTGTGTCCT TGTCGATACT GGTACTAATG CGGTTCGAGT CTTAATTGGG AGTGATTTC
    Spe I      Pst I   Pme I   EcoR I
261 GACTAGTCCT GCAGGTTTAA ACGAATTGCG CCTT PCR Product AAGGGC GAATTCGGGG
    CTGATCAGGA CGTCCAAATT TGCTTAAGCG GGA TTCCCG CTTAAGCGCC
                T7 priming site
311 CCGCTAAATT CAATTCGCC TATAGTGAGT CGTATTACAA TTCACTGGCC GTCGTTTTAC
    GGCGATTTAA GTTAAGCGGG ATATCACTCA GCATAATGTT AAGTGACCGG CAGCAAAATG
    M13 Forward (-20) priming site
  
```



lac promoter region: bases 2-216
 CAP binding site: bases 95-132
 RNA polymerase binding site: bases 133-178
 Lac repressor binding site: bases 179-199
 Start of transcription: base 179
 M13 Reverse priming site: bases 205-221
 LacZα-*ccdB* gene fusion: bases 217-810
 LacZα portion of fusion: bases 217-497
 ccdB portion of fusion: bases 508-810
 T3 priming site: bases 243-262
 TOPO[®] Cloning site: bases 294-295
 T7 priming site: bases 328-347
 M13 Forward (-20) priming site: bases 355-370
 Kanamycin promoter: bases 1021-1070
 Kanamycin resistance gene: bases 1159-1953
 Ampicillin (*b/a*) resistance gene: bases 2309-3061 (c)
 Ampicillin (*b/a*) promoter: bases 3062-3158 (c)
 pUC origin: bases 3159-3832
 (c) = complementary strand

Figure 89: pCR[®]4-TOPO[®] Vector Map

PCR products with A overhangs for insertion are marked as black block in the sequence. Positions of the T7 and T3 promoter sites, the M13 forward and reverse sequencing primer binding sites, and the restriction endonuclease recognition sites on either side of the TOPO cloning site are provided. Positions of various elements in the vector are listed. (From Invitrogen life technologies)

D. p*Silencer*TM1.0-U6 siRNA Expression vector

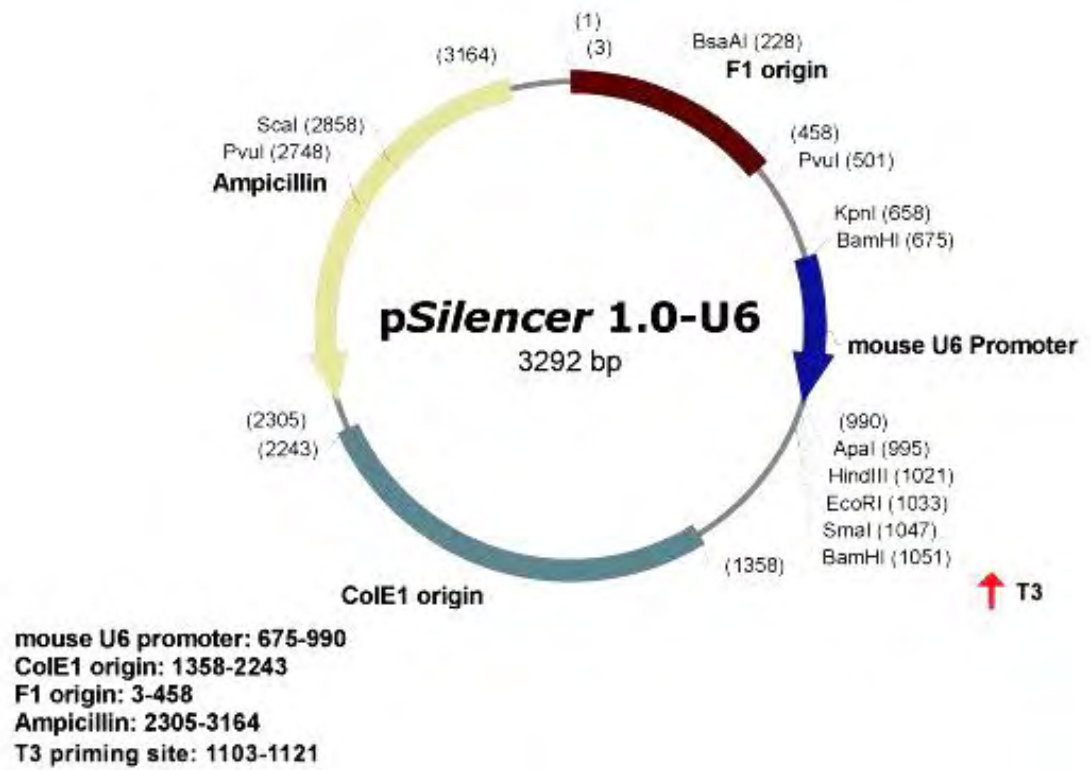


Figure 90: p*Silencer*TM1.0-U6 siRNA Expression Vector Map

The linearized p*Silencer* 1.0-U6 vectors were cut at *Apal* and *EcoRI* sites (bases 995-1033), where an oriental dsDNA can be ligated into the vector. Positions of various elements are listed, including mouse U6 promoter. The siRNA inserts can be sequenced by using T3 primer and self-designed U6m1 or U6m2 primer. (From Ambion Inc.)

| Sense | Loop | Antisense | |
|--------------------|-------------|------------------|--------------------------|
| 5'-N(19) | TTCAAGAGA | N(19) | TTTTTT-3' (53 bases) |
| 3'-CCGG N(19) | AAGTTCTCT | N(19) | AAAAAATTAA-5' (61 bases) |
| <i>Apal</i> | | | <i>EcoRI</i> |

Figure 91: Sequence and Structure of siRNA Insert

In the forward oligonucleotides, the 19 nt sense siRNA sequence is linked to the reverse complementary antisense siRNA by a 9 nt spacer (TTCAAGAGA). 5-6 Ts are added to the 3' end. In the reverse oligonucleotides, 4 nt overhangs to the *EcoRI* (AATT) and *Apal* (GGCC) restriction sites are added. Finally, the RNA transcript can fold back and form a stem-loop structure comprising 19-nt stem and 9-nt loop with 2-3 Us at the 3' end.

E. Chick Rab23 cDNA and protein sequences

| | | |
|------|---|------|
| 1 | GTTTCCTCTCGCCTCCTTTCCTCCGCCGCCGCTTCCATCCCTCCTTCCCTCCCTTCCCTCCCGCCGT | 69 |
| 70 | CTCCGAGGCGGAGCCGCCGCCGCGCCAGGGATCGGATTGATAGATTTCGTGAATAAGCCAGAGAGTCACC | 138 |
| 139 | TGAGCTGCAGAGATGTTTGGAAAGAAGACATGGAGGTGGCCATCAAGGTGGTAGTGGTAGGAAATGGAGCT | 207 |
| 1 | M L E E D M E V A I K V V V V G N G A | 19 |
| 208 | GTTGGGAAGTCCAGTATGATTCAGCGATACTGCAAGGGGATCTTTACAAAAGACTACAAGAAGACTATT | 276 |
| 20 | V G K S S M I Q R Y C K G I F T K D Y K K T I | 42 |
| 277 | GGTGTAGATTTCTGGAAAGACAAATCCAAGTTAATGATGAAGAAGTCAGGCTAATGTTATGGGACACT | 345 |
| 43 | G V D F L E R Q I Q V N D E E V R L M L W D T | 65 |
| 346 | GCAGGTCAAGAGGAATTTGATGCGATACTAAGGCCTACTACAGAGGAGCCAGGCTTGTGTTCTTGTG | 414 |
| 66 | A G Q E E F D A I T K A Y Y R G A Q A C V L V | 88 |
| 415 | TTTTCTACAACCTGACAGAGAGTCCTTCAAAGCAATCCCTACCTGGAAGGAAAAAGTGACGACTGAAGTT | 483 |
| 89 | F S T T D R E S F K A I P T W K E K V T T E V | 111 |
| 484 | GGAGACATCCCACAGTCTTGTGTCAGAATAAGATCGATCTTTGGATGACTCTTGTATAAAGAATGAA | 552 |
| 112 | G D I P T V L V Q N K I D L L D D S C I K N E | 134 |
| 553 | GAGGCAGAAGCACTGGCAAAAAAGCTGAAATTAAGGTTCTACCGAGCATCTGTGAAGGAGGACCTCAAC | 621 |
| 135 | E A E A L A K K L K L R F Y R A S V K E D L N | 157 |
| 622 | GTCACCGAAGTTTTTAAGTATTTGGCTGATAAATATCTTCAAAGGCTCAAGCAGCAAACGGCTGAAGAA | 690 |
| 158 | <u>V T E V F K Y L A D K Y L Q R L K Q Q T A E E</u> | 180 |
| 691 | CCAGAACTAGTACATACAAGCAGTAACAAGATTGGTGTTCATACAGCCATTGGAAGTCACCCCAAC | 759 |
| 181 | <u>P E L V H T S S N K I G V F N T A I G S H P N</u> | 203 |
| 760 | CAGAATCCAACACTCTTAACGGTGGAGACGTCAACCTCAGACCAAACAAACAGAGAACCAAGAAA | 828 |
| 204 | <u>Q N S N T L N G G D V I N L R P N K Q R T K K</u> | 226 |
| 829 | AGCAGAAGTCTTTTTAGCAACTGCAGCATACCTTAGGCTGCTTGGGAGGAAAAGAAAAGAGCGACCCG | 897 |
| 227 | <u>S R S L F S N</u> C S I P * | 237 |
| 898 | TGAATTGGATGAAGTTGTGCAATTGAATACAGAGTAAAGCTTTAGAGGTATTTTACCAGTGCTTTAGCA | 966 |
| 967 | AATCTTGTGCCTATGGGATCCTTGTCTGGTGGAGTTATCTAAAATTGCTGATGCGGTGTTTTTTGGTGT | 1035 |
| 1036 | GTAGAGTGAGACACCTGGTGGCAAAGCGCTGAACCGTGGCTGCCCGTGCACTTTTTTAACAATTAATA | 1104 |
| 1105 | GCAAACCTCTCCATTTTGAAGGAATTAATTACAGAGCTATGAACCAGTTTTTGCAGAATTGAGAAGCAC | 1173 |
| 1174 | <u>ATTTAAACGTAAGATAATGCACACACGTAGGTACAGACCATAACATTATGGCCCAAGATAAAGTAGCA</u> | 1242 |
| 1243 | ACCTCGTAACTAAATTTCAAAGGAAATGGTAGCATTGGTTAGCCAGGACACTAAGAAGTTAGCAGAAGA | 1311 |
| 1312 | GCAAAGTGAAGACATCACATTTTATGCCTTTCTCCGTTAGCGTGGATTCTGGTGGTTTCAGTCAGTGCAA | 1380 |
| 1381 | TATACTCGTGGTCTGTGTATGCTTGTGGAGGTCTGTATGTACATGTTGGCTATGAATACTTTTGCTAAA | 1449 |
| 1450 | TTCCGGTGTATTTCGATACGTGGAGGTGAGTACTGATTATCAGATAGCATCTGCACAAGAAATTTTCCT | 1518 |
| 1519 | TTTAAATGTTACCTTTTCAGATGAGGCTCTCCAGCTGCTGCTGTGTGTGTTGGACTCGCTATGCCTGG | 1587 |
| 1588 | GCCTAAACGCTTAGATTTAAAAATGGACAGGTGCCAAAAATGCTCCTCCTTATTACCGAAATGCTTCAT | 1656 |
| 1657 | TGCCAGATGTTTTCTAAGTTGTTTTCTCAGTCTTAACAGGTTGAACCA | 1706 |

Figure 92: Characterization of the cDNA and deduced amino acid sequence of chick *Rab23*

The mRNA transcription sequence is represented in capital letters. The start codon and stop codon are indicated by double-underlining. The AU-rich elements located in the 3'UTR are underlined. The amino acid sequence is shown in single code letters beneath the cDNA sequence, with the stop codon indicated by an asterisk. The long carboxyterminal tail is marked in underlined. The four highly conserved domains are marked in yellow. The sequence corresponding to the effector domain is marked in blue color and the post-translational modification domain is boxed.

F. Curriculum Vitae

Personal details

Name: Li, Naixin
Date of Birth: 09.05.1970
Place of Birth: Tianjin, P. R. China
Nationality: Chinese
Marital Status: Single
Address: Gräfstr. 74, 81241 Muenchen, Germany
Email: naixin_lee1@yahoo.com
Tel: +49-89-28743488

Education

PhD. in Genetics and Neurobiology

September 2000 –

Bayerische Julius-Maximilians-Universität Würzburg, Theodor Boveri Institut, Lehrstuhl für Genetik und Neurobiologie, Würzburg, Deutschland.

Betreuer: Prof. Dr. Martin Heisenberg.

Thesis title: Dorso-ventral Differentiation and Specification of Mesencephalon in Early Chick Embryos

MSc. in Neurosurgery

July 1994 – July 1995

Tianjin Medical University, Tianjin Medical University General Hospital, Department of Neurosurgery, Tianjin, P.R.China

Tutor: Prof. Dr. Shu-yuan Yang

Thesis title: Measurement of ERP-P300 on CHI Patients and Its Clinical Significance.

BSc. (MD.) in Clinic Medicine

September 1990 – July 1995

Tianjin Medical University, Clinic Medicine College, Seven-year System, Tianjin, P.R.China

September 1988 – July 1990

Nankai University, Life Science College, Premedical, Tianjin, P.R.China

G. Publication

Li, N., Hornbruch, A., Klafke, R., Katzenberger, B. and Wizenmann, A. (2005). Specification of Dorsoventral Polarity in the Embryonic Chick Mesencephalon and Its Presumptive Role in Midbrain Morphogenesis. *Dev. Dyn.* 233: 907-920

Li, N., Volff, J-N., and Wizenmann, A. (2007). Rab23 GTPase is Expressed Asymmetrically in Henson's Node and Plays a Role in Dorsoventral Pattern of Chick Neural Tube. *Dev. Dyn.* [in press]

Agoston, Z., Badde1, A., **Li, N.**, Vennemann A., Wizenmann, A., and Schulte, D. (2007). Transcriptional Control of Ephrin-B1 Expression in the Embryonic Chick Midbrain. [in press]

Li, N., Schulte, D., Wizenmann, A. Pax3/7 Function on the Expansion of Chick Dorsal Midbrain. [in preparation]

Li, N., Zahn, M., Wizenmann, A. A local and Temporal Gene Silencing by shRNAs is Available for Embryonic Chick. [in preparation]

Scientific activities

Li, N.X., Tao, H.Y., Chen, S.J., Wang, N.L., and Yang, S.Y. (2000). Clinical Significance of P300 on High Brain Function for Mild CHI Patients. *World Spine 1: First Interdisciplinary World Congress on Spinal Surgery*. Berlin, Germany

Li, N., Katzenberger, B. and Wizenmann A. (2001). Determination of the Ventral Midbrain Cells an their Behavior in an Ectopic Surround. International conference of DFG and MDC. *Cell migration in Development and Disease*. Berlin, Germany.

Li, N. and Wizenmann A. (2002). Integration of Ventral Midbrain Cells in a Dorsal Midbrain Enviroment. EMBO-FMI conference. *Organizing the Brain: Genes, Neurons and Circuits*. Ascona, Switzerland.

Li, N. and Wizenmann A. (2003). The Possible Role of Rab23 in Patterning the Dorsal Midbrain. *1st joint meeting of the British and French Societies for Development Biology*. Nice, France.

H. Acknowledgements

Since I stepped into the ‘chicken lab’, a new begun life for me. From medicine to biology, from a neurosurgeon to a scientific research person, from a medical doctor to a student, from a native to a foreigner, my role was greatly changed. However, each person in this lab showed friendship towards me. This superb atmosphere made it is easy for me to start my laboratory work and move forwards. Here, I want to express my gratitude to all people that in one or another way were part of that life. First of all, I would like to express my gratefulness to **PD Dr. Andrea Wizenmann** for believing in *me*, supporting me and pushing me. She gave me so much help on my project going on and solved several dilemmas in my life, wherever she worked in Würzburg or München. The detailed and deep discussions with her always enlighten me and solved confusions easily. Thank you for giving me the important lessons in conducting an independent and fruitful research and for the scrupulous scientific attitude. I’m also very grateful to **Prof. Dr. Martin Heisenberg**. First, I should thank you for trusting me and accepting me as your PhD student. To be honest, I am very proud of this fact. I also want to sincerely thank you for providing helps when I was in difficulties. Your friendly and gentleman demeanor left a deep impression on me. I will not forget the wonderful trip, and your precise translation in English for me. **Prof. Erich Buchner** provided me a working place when I still had to finish some experiments, and thought about my convenience. Such a friendly professor is well worth keeping in my heart. I’m deeply obliged to **Prof. Dr. Werner Göbel** for accepting me to the faculty of Biology. He was so kindly to understand my master thesis in Chinese. **Prof. Dr. Georg Krohne**, in close proximity to our group allowed us to use his instruments. I also want to thank **PD. Dr. Christoph Winkler** for offering the microinjector, **Dr. Matthias Schäfer** providing an antibody, **Ellen Fecher** performing most of the DNA sequencing in my work. I’m very thankful to **Dhananjay A. Wagh** for sharing a working room with me day and night, and teaching me how to distinguish the male and female fruit fly. During the time in München, **Thomas Hendel** helped me so much and shared an apartment with me.

I would like to thank every member in the ‘chicken lab’ for giving me the feeling to be one team. Without you my staying here wouldn’t be the same. Thank you for all those moments that I’ve shared with you. **Dr. Farshid Seif** helped me doing in situ hybridization and PCR with his good molecular biological knowledge, and shared his lunch times with me. **Klaus Molle**, now a post-doc, as a good friend invited me to join his family and birthday party. Especially, I will not forget my first skiing with you in Switzerland. I will also thank **Danila Bunsen**, **Amata Hornbruch**, **Ruth Klafke** and **Marcel Zahn** for technical supports. Here, I should remember **Babara Katzenberger**, plenty of your effective work made a simple way for my experiments, and the sunny boy, **Nils Klüver**, always joking with us. I would like to thank both of you and wish you happiness. A silent girl, **Julia**, a straight-hearted **Katharina**, a clever boy, **Stephen**, I will miss all of you, miss the time in Würzburg, and miss our memory game. It is so nice and I can find each one of you, and recall the past time. Specially thanks to the secretaries for keeping the things going on smoothly.

I cannot express in words the gratitude for my family. It would have been impossible for me to finish my study without their love and support. At last I should thank Jing. She did so much for me. Without her support this thesis would not be finished. The time will elapse; the memory will be everlasting and be kept in our memory game.

Declaration:

I hereby declare that the submitted dissertation was completed by myself and no other. I have not used any sources or materials other than those enclosed.

Moreover I declare that the following dissertation has not been submitted further in this form or any other form, and has not been used for obtaining any other equivalent qualifications at any other organisation/institution.

Additionally, I have not applied for, nor will I attempt to apply for any other degree of qualification in relation to this work.

Würzburg, den 15 Juni 2007

Naixin Li

Memory game is never out-of-date



*It is a pleasure to work in the wonderful chicken lab
and share happy days with well-loved persons.*